



University Transportation Research Center - Region 2

Final Report



Field Methods for Determining Lead Content in Bridge Paint Removal Waste

Performing Organization: New Jersey Institute of Technology



December 2013



Sponsor:
New York State Department of Transportation (NYSDOT)

University Transportation Research Center - Region 2

The Region 2 University Transportation Research Center (UTRC) is one of ten original University Transportation Centers established in 1987 by the U.S. Congress. These Centers were established with the recognition that transportation plays a key role in the nation's economy and the quality of life of its citizens. University faculty members provide a critical link in resolving our national and regional transportation problems while training the professionals who address our transportation systems and their customers on a daily basis.

The UTRC was established in order to support research, education and the transfer of technology in the field of transportation. The theme of the Center is "Planning and Managing Regional Transportation Systems in a Changing World." Presently, under the direction of Dr. Camille Kamga, the UTRC represents USDOT Region II, including New York, New Jersey, Puerto Rico and the U.S. Virgin Islands. Functioning as a consortium of twelve major Universities throughout the region, UTRC is located at the CUNY Institute for Transportation Systems at The City College of New York, the lead institution of the consortium. The Center, through its consortium, an Agency-Industry Council and its Director and Staff, supports research, education, and technology transfer under its theme. UTRC's three main goals are:

Research

The research program objectives are (1) to develop a theme based transportation research program that is responsive to the needs of regional transportation organizations and stakeholders, and (2) to conduct that program in cooperation with the partners. The program includes both studies that are identified with research partners of projects targeted to the theme, and targeted, short-term projects. The program develops competitive proposals, which are evaluated to insure the most responsive UTRC team conducts the work. The research program is responsive to the UTRC theme: "Planning and Managing Regional Transportation Systems in a Changing World." The complex transportation system of transit and infrastructure, and the rapidly changing environment impacts the nation's largest city and metropolitan area. The New York/New Jersey Metropolitan has over 19 million people, 600,000 businesses and 9 million workers. The Region's intermodal and multimodal systems must serve all customers and stakeholders within the region and globally. Under the current grant, the new research projects and the ongoing research projects concentrate the program efforts on the categories of Transportation Systems Performance and Information Infrastructure to provide needed services to the New Jersey Department of Transportation, New York City Department of Transportation, New York Metropolitan Transportation Council, New York State Department of Transportation, and the New York State Energy and Research Development Authority and others, all while enhancing the center's theme.

Education and Workforce Development

The modern professional must combine the technical skills of engineering and planning with knowledge of economics, environmental science, management, finance, and law as well as negotiation skills, psychology and sociology. And, she/he must be computer literate, wired to the web, and knowledgeable about advances in information technology. UTRC's education and training efforts provide a multidisciplinary program of course work and experiential learning to train students and provide advanced training or retraining of practitioners to plan and manage regional transportation systems. UTRC must meet the need to educate the undergraduate and graduate student with a foundation of transportation fundamentals that allows for solving complex problems in a world much more dynamic than even a decade ago. Simultaneously, the demand for continuing education is growing – either because of professional license requirements or because the workplace demands it – and provides the opportunity to combine State of Practice education with tailored ways of delivering content.

Technology Transfer

UTRC's Technology Transfer Program goes beyond what might be considered "traditional" technology transfer activities. Its main objectives are (1) to increase the awareness and level of information concerning transportation issues facing Region 2; (2) to improve the knowledge base and approach to problem solving of the region's transportation workforce, from those operating the systems to those at the most senior level of managing the system; and by doing so, to improve the overall professional capability of the transportation workforce; (3) to stimulate discussion and debate concerning the integration of new technologies into our culture, our work and our transportation systems; (4) to provide the more traditional but extremely important job of disseminating research and project reports, studies, analysis and use of tools to the education, research and practicing community both nationally and internationally; and (5) to provide unbiased information and testimony to decision-makers concerning regional transportation issues consistent with the UTRC theme.

UTRC-RF Project No: 55505-02-02

Project Date: December 2013

Project Title: Field Methods for Determining Lead Content in Bridge Paint Removal Waste

Project's Website:

<http://www.utrc2.org/research/projects/lead-content-bridge-paint-removal-waste>

Principal Investigator:

Dr. Lisa B. Axe
Professor, Civil and Environmental Engineering
Department of Civil and Environmental Engineering
New Jersey Institute of Technology
Newark, NJ 07102
Email: axe@adm.njit.edu

Performing Organizations: New Jersey Institute of Technology

Sponsor:

New York State Department of Transportation (NYSDOT)

To request a hard copy of our final reports, please send us an email at utrc@utrc2.org

Mailing Address:

University Transportation Research Center
The City College of New York
Marshak Hall, Suite 910
160 Convent Avenue
New York, NY 10031
Tel: 212-650-8051
Fax: 212-650-8374
Web: www.utrc2.org

Board of Directors

The UTRC Board of Directors consists of one or two members from each Consortium school (each school receives two votes regardless of the number of representatives on the board). The Center Director is an ex-officio member of the Board and The Center management team serves as staff to the Board.

City University of New York

Dr. Hongmian Gong - Geography
Dr. Neville A. Parker - Civil Engineering

Clarkson University

Dr. Kerop D. Janoyan - Civil Engineering

Columbia University

Dr. Raimondo Betti - Civil Engineering
Dr. Elliott Sclar - Urban and Regional Planning

Cornell University

Dr. Huaizhu (Oliver) Gao - Civil Engineering
Dr. Mark A. Turnquist - Civil Engineering

Hofstra University

Dr. Jean-Paul Rodrigue - Global Studies and Geography

Manhattan College

Dr. Anirban De - Civil & Environmental Engineering
Dominic Esposito - Research Administration

New Jersey Institute of Technology

Dr. Steven Chien - Civil Engineering
Dr. Jyoung Lee - Civil & Environmental Engineering

New York Institute of Technology

Dr. Nada Marie Anid - Engineering & Computing Sciences
Dr. Marta Panero - Engineering & Computing Sciences

New York University

Dr. Mitchell L. Moss - Urban Policy and Planning
Dr. Rae Zimmerman - Planning and Public Administration

Polytechnic Institute of NYU

Dr. John C. Falcocchio - Civil Engineering
Dr. Kaan Ozbay - Civil Engineering

Rensselaer Polytechnic Institute

Dr. José Holguín-Veras - Civil Engineering
Dr. William "Al" Wallace - Systems Engineering

Rochester Institute of Technology

Dr. J. Scott Hawker - Software Engineering
Dr. James Winebrake - Science, Technology, & Society/Public Policy

Rowan University

Dr. Yusuf Mehta - Civil Engineering
Dr. Beena Sukumaran - Civil Engineering

Rutgers University

Dr. Robert Noland - Planning and Public Policy

State University of New York

Michael M. Fancher - Nanoscience
Dr. Catherine T. Lawson - City & Regional Planning
Dr. Adel W. Sadek - Transportation Systems Engineering
Dr. Shmuel Yahalom - Economics

Stevens Institute of Technology

Dr. Sophia Hassiotis - Civil Engineering
Dr. Thomas H. Wakeman III - Civil Engineering

Syracuse University

Dr. Riyad S. Aboutaha - Civil Engineering
Dr. O. Sam Salem - Construction Engineering and Management

The College of New Jersey

Dr. Thomas M. Brennan Jr. - Civil Engineering

University of Puerto Rico - Mayagüez

Dr. Ismael Pagán-Trinidad - Civil Engineering
Dr. Didier M. Valdés-Díaz - Civil Engineering

UTRC Consortium Universities

The following universities/colleges are members of the UTRC consortium.

City University of New York (CUNY)
Clarkson University (Clarkson)
Columbia University (Columbia)
Cornell University (Cornell)
Hofstra University (Hofstra)
Manhattan College
New Jersey Institute of Technology (NJIT)
New York Institute of Technology (NYIT)
New York University (NYU)
Polytechnic Institute of NYU (Poly)
Rensselaer Polytechnic Institute (RPI)
Rochester Institute of Technology (RIT)
Rowan University (Rowan)
Rutgers University (Rutgers)*
State University of New York (SUNY)
Stevens Institute of Technology (Stevens)
Syracuse University (SU)
The College of New Jersey (TCNJ)
University of Puerto Rico - Mayagüez (UPRM)

** Member under SAFETEA-LU Legislation*

UTRC Key Staff

Dr. Camille Kamga: *Director, UTRC*
Assistant Professor of Civil Engineering, CCNY

Dr. Robert E. Paaswell: *Director Emeritus of UTRC and Distinguished Professor of Civil Engineering, The City College of New York*

Herbert Levinson: *UTRC Icon Mentor, Transportation Consultant and Professor Emeritus of Transportation*

Dr. Ellen Thorson: *Senior Research Fellow, University Transportation Research Center*

Penny Eickemeyer: *Associate Director for Research, UTRC*

Dr. Alison Conway: *Associate Director for New Initiatives and Assistant Professor of Civil Engineering*

Nadia Aslam: *Assistant Director for Technology Transfer*

Dr. Anil Yazici: *Post-doc/ Senior Researcher*

Nathalie Martinez: *Research Associate/Budget Analyst*

Final Report
for Research Project No. C-08-19
Field Methods for Determining Lead Content in Bridge Paint
Removal Waste

Zhan Shu, Lisa Axe

Department of Civil and Environmental Engineering
New Jersey Institute of Technology
Newark, NJ 07102

Submitted

to

Carl Kochersberger
Environmental Science Bureau
Hazardous Materials and Asbestos Unit
Pod 4-1
New York State Department of Transportation
50 Wolf Road
Albany, NY 12232

December 2013

DISCLAIMER

This report was funded in part through grant(s) from the Federal Highway Administration, United States Department of Transportation, under the State Planning and Research Program, Section 505 of Title 23, U.S. Code. The contents of this report do not necessarily reflect the official views or policy of the United States Department of Transportation, the Federal Highway Administration or the New York State Department of Transportation. This report does not constitute a standard, specification, regulation, product endorsement, or an endorsement of manufacturers.

Technical Report Documentation Page

| | | | |
|---|---|--|------------|
| 1. Report No.: C-08-19 | 2. Government Accession No.: | 3. Recipient's Catalog No.: | |
| 4. Title and Subtitle: Field Methods for Determining Lead Content in Bridge Paint Removal Waste | | 5. Report Date: December 2013 | |
| | | 6. Performing Organization Code: | |
| 7. Author(s): Zhan Shu, Axe Lisa | | 8. Performing Organization Report No.: 55505-02-02 | |
| 9. Performing Organization Name and Address: Department of Civil and Environmental Engineering New Jersey Institute of Technology Newark, NJ 07102 | | 10. Work Unit No.: | |
| | | 11. Contract or Grant No.: C030506 | |
| 12. Sponsoring Agency Name and Address: Environmental Science Bureau Hazardous Materials and Asbestos Unit Pod 4-1 New York State Department of Transportation 50 Wolf Road, Albany, NY 12232 | | 13. Type of Report and Period Covered: Final Report. November 2009 - December 2013 | |
| | | 14. Sponsoring Agency Code: | |
| 15. Supplementary Notes: | | | |
| 16. Abstract: The removal of paint from bridges and other structures is a significant issue facing transportation agencies because of the presence and potential for release of lead and other contaminants upon disposal. A large percentage of the bridges are reaching a critical level of deterioration, resulting in management issues for paint waste. The New York State Department of Transportation (NYSDOT) applies a conservative approach by assuming all waste generated from bridges previously painted with lead-based paint (LBP) is hazardous. Therefore, an approach that provides accurate in-situ characterization of the waste classification would be beneficial. The goal of this project is to develop a rapid and cost-effective method that can provide an accurate characterization of waste classification. With 11 Regions and 2,385 bridges rehabilitated and subsequently repainted after NYSDOT stopped using LBP on bridges (after 1988), 24 bridges from across the NYS were selected for this study based on Sampling Theory (Deliverable Task 1). The literature review demonstrated that elevated metal concentrations in paint waste have resulted in leaching that exceeds toxicity characteristic (TC) concentrations; however, models to predict leaching behavior have not been developed (Deliverable Task 2). Field portable X-ray fluorescence (FP-XRF) (Deliverable Task 3) was applied to quantify Resource Conservation and Recovery Act (RCRA) metals (i.e., As, Ba, Cr, Cd, Pb, Hg, Se, and Ag) along with iron and zinc in paint waste samples (Deliverable Task 4), while Hach DR 2800 field portable spectrophotometer (Deliverable Task 3) was employed for measuring dissolved and total lead concentrations in bridge wash water (Deliverable Task 5). Leaching behavior of the paint waste was evaluated with the U.S. Environmental Protection Agency (U.S. EPA) toxicity characteristic leaching procedure (TCLP) and multiple extraction procedure (MEP) (Deliverable Task 6). Elevated Pb (5 to 168,090 mg kg ⁻¹), Cr (21 to 10,192 mg kg ⁻¹), and other metal concentrations were observed in the paint samples. However, 48 out of 51 samples passed the TCLP test, while 19 out of 24 samples revealed concentrations less than the TC level in the MEP study. These results are attributed to the use of iron-based abrasives (steel grit) in the paint removal process. Trace metals are sequestered through interactions with the steel grit surface resulting in reduced leachable concentrations (less than the TC limit). Using the suite of analyses including sequential extraction procedure (SEP), X-ray diffraction (XRD), and field emission scanning electron microscopy (FE-SEM), iron oxides were observed on the steel grit surface and are important surfaces affecting the degree of metal leaching from the paint waste (Deliverable Task 6). Given an understanding of mechanistic processes along with a demonstrated analysis of variables through principle component analysis (PCA), statistically-based models for leaching from paint waste were developed (Deliverable Task 7). The statistical models demonstrated 96 percent of the data fall within the 95% confidence level for Pb (R^2 0.6 – 0.9, $p \leq 0.01$), Ba (R^2 0.6 – 0.7, $p \leq 0.1$), and Zn (R^2 0.6 – 0.7, $p \leq 0.01$), although the regression model was not significant for Cr leaching (R^2 0.5 – 0.7, $p \leq 0.75$). The models have applicability over a wide range of total metal concentrations. A practical advantage in applying models developed is the ability to estimate contaminant leaching from paint waste without additional laboratory studies including the U.S. EPA TCLP. Therefore, the statistically-based models developed are a powerful approach for predicting metal leaching and therefore waste classification. | | | |
| 17. Key Words: leaching, iron oxide, paint waste, lead, TCLP, MEP | | 18. Distribution Statement: | |
| 19. Security Classification (of this report): | 20. Security Classification (of this page): | 21. No of Pages: 13 | 22. Price: |

Form DOT F 1700.7 (06/98).

Table of Contents

| | |
|---|----|
| Disclaimer | i |
| Technical Report Documentation Page | ii |
| Executive Summary | iv |
| 1. Introduction..... | 1 |
| 2. Scope of Work | 2 |
| 3. Findings and Conclusions | 5 |

Attachments

Deliverable for Task 1: Identification of Sites for the Study.

Deliverable for Task 2: Literature Review.

Deliverable for Task 3: Purchase of X-Ray Fluorescence (XRF) and Field Spectrophotometer for Analyses.

Deliverable for Task 4: In-Situ Bridge Paint Analyses Using an XRF meter.

Deliverable for Task 5: Bridge Wash Water Analysis for Lead Using the Field Spectrophotometer.

Deliverable for Task 6: Collection of Samples for Laboratory Analyses.

Deliverable for Task 7: Correlation, Comparison and Interpretation of Field and Laboratory Data.

Deliverable for Task 8: Project Presentation and Outreach.

EXECUTIVE SUMMARY

The removal of paint from bridges and other structures is a significant issue facing transportation agencies because of the presence and potential for release of lead and other contaminants upon disposal. A large percentage of the bridges are reaching a critical level of deterioration, resulting in management issues for paint waste. The New York State Department of Transportation (NYSDOT) applies a conservative approach by assuming all waste generated from bridges previously painted with lead-based paint (LBP) is hazardous. Therefore, an approach that provides accurate in-situ characterization of the waste classification would be beneficial. The goal of this project is to develop a rapid and cost-effective method that can provide an accurate characterization of waste classification. With 11 Regions and 2,385 bridges rehabilitated and subsequently repainted after NYSDOT stopped using LBP on bridges (after 1988), 24 bridges from across the NYS were selected for this study based on Sampling Theory (Deliverable Task 1). The literature review demonstrated that elevated metal concentrations in paint waste have resulted in leaching that exceeds toxicity characteristic (TC) concentrations; however, models to predict leaching behavior have not been developed (Deliverable Task 2). Field portable X-ray fluorescence (FP-XRF) (Deliverable Task 3) was applied to quantify Resource Conservation and Recovery Act (RCRA) metals (i.e., As, Ba, Cr, Cd, Pb, Hg, Se, and Ag) along with iron and zinc in paint waste samples (Deliverable Task 4), while Hach DR 2800 field portable spectrophotometer (Deliverable Task 3) was employed for measuring dissolved and total lead concentrations in bridge wash water (Deliverable Task 5). Leaching behavior of the paint waste was evaluated with the U.S. Environmental Protection Agency (U.S. EPA) toxicity characteristic leaching procedure (TCLP) and multiple extraction procedure (MEP) (Deliverable Task 6).

Elevated Pb (5 to 168,090 mg kg⁻¹), Cr (21 to 10,192 mg kg⁻¹), and other metal concentrations were observed in the paint samples. However, 48 out of 51 samples passed the TCLP test, while 19 out of 24 samples revealed concentrations less than the TC level in the MEP study. These results are attributed to the use of iron-based abrasives (steel grit) in the paint removal process. Trace metals are sequestered through interactions with the steel grit surface resulting in reduced leachable concentrations (less than the TC limit). Using the suite of analyses including sequential extraction procedure (SEP), X-ray diffraction (XRD), and field emission scanning electron microscopy (FE-SEM), iron oxides were observed on the steel grit surface and are important surfaces affecting the degree of metal leaching from the paint waste (Deliverable Task 6). Given an understanding of mechanistic processes along with a demonstrated analysis of variables through principle component analysis (PCA), statistically-based models for leaching from paint waste were developed (Deliverable Task 7). The statistical models demonstrated 96 percent of the data fall within the 95% confidence level for Pb (R^2 0.6 – 0.9, $p \leq 0.01$), Ba (R^2 0.6 – 0.7, $p \leq 0.1$), and Zn (R^2 0.6 – 0.7, $p \leq 0.01$), although the regression model was not significant for Cr leaching (R^2 0.5 – 0.7, $p \leq 0.75$). The models have applicability over a wide range of total metal concentrations. A practical advantage in applying models developed is the ability to estimate contaminant leaching from paint waste without additional laboratory studies including the U.S. EPA TCLP. Therefore, the statistically-based models developed are a powerful approach for predicting metal leaching and therefore waste classification.

1. Introduction

The removal of paint from bridges and other structures is a significant issue facing transportation agencies because of the presence and potential for release of lead and/or other contaminants, and the consequent impacts to human health and the environment. Although the hazards of lead paint removal from bridges have been largely identified and advances have been made in worker protection, there is still a need to identify rapid and cost-effective methods for field detection that can provide an accurate characterization of waste classification. Currently, New York State Department of Transportation (NYSDOT) uses a conservative approach of classifying all paint waste from bridges constructed before 1989 as hazardous. This practice stems from the fact that there is no approved reliable, fast, and efficient method for classifying paint waste in-situ as non-hazardous. This conservative practice eliminates the need for extensive testing, but also results in greater expense and increased regulatory burdens than are likely required. With the advent of more accurate and sophisticated analytical equipment for in-situ field measurements, state DOTs will benefit from research focused on the reliability of such field equipment for waste characterization.

Paint waste removed from the bridges is generally stored in 55 gallon drums or roll-off containers in the field. Because the waste will not be pretreated before shipping for disposal, the field portable X-ray fluorescence (FP-XRF) analysis was conducted on the collected paint waste samples as well as through direct analysis of paint on the bridge. The main objective of this study is to develop a model that can predict the leachability of metals in paint waste generated during bridge rehabilitation. Data from FP-XRF analysis of metals were compiled and related to the associated leaching results to better understand key variables required in developing statistical

models. Mechanistic modeling further supported variables required to predict metal leaching processes. The statistical models formulated in this work are based exclusively on data collected from bridges undergoing rehabilitation where steel grit was used as the blasting material. Therefore, for other state DOTs working with similar structures and rehabilitation procedures, this research may be beneficial in supporting a field analysis for waste classification.

Between October 2010 and November 2011, 117 samples of paint waste were obtained from 24 bridges under rehabilitation in New York State. Studies were conducted to evaluate Resource Conservation and Recovery Act (RCRA) metals (i.e., Ag, As, Ba, Cd, Cr, Hg, Pb, Se), zinc as well as iron concentrations in the paint waste. Leachable and extracted metal concentrations were obtained from the toxicity characteristic leaching procedure (TCLP), multiple extraction procedure (MEP), and sequential extraction (SE). In addition, to understand the mechanism responsible for metal leaching, a suite of analyses was conducted on the paint waste samples. Mechanistic modeling (surface complexation along with precipitation/dissolution modeling) was applied to support principal component analysis (PCA) of data obtained with FP-XRF. As a result, statistically-based models for leaching from paint waste were developed. Results of this work assist in better understanding and predicting the mobility of trace metals as well as in addressing disposal and management of paint waste during bridge rehabilitation.

2. Scope of Work

This study consists of a phased approach involving nine integrated tasks:

Task 1: Identification of Sites for the Study – A Task 1 report was submitted to the NYSDOT Project Manager and Technical Working Group (TWG) to jointly identify a statistically significant number of NYSDOT bridges for this study. Approximately 4,500 bridges maintained

by NYSDOT have been previously painted with LBP. To obtain a statistically representative number of samples for the study, the report reviewed the approach of sample size estimation using hypothesis testing and stratified sampling theory. The report concluded with a recommended number of statistically representative bridges to be sampled.

Task 2: Literature Review – A Task 2 report was submitted to the NYSDOT Project Manager and TWG for review and comment. The report summarized the Task 2 activity and the findings of the literature search. The literature review demonstrates that field portable tools are effective instruments that have significant potential for characterizing paint waste as well as wash water.

Task 3: Purchase XRF and Field Spectrophotometer for Analyses – The purpose of this report is to review the types of field portable tools for assessing metal concentrations in paint and wash water. Specifically, both the FP-XRF and the field portable spectrophotometer were discussed with respect to their effectiveness in providing reliable lead and metal concentrations present in bridge paint waste and wash water. Based on the review and vendor information, the field portable equipment selected for this project was presented.

Task 4: In-Situ Bridge Paint Analyses Using XRF – In this report, the application of the NITON XLp-300 series and NITON XL3t-600 series FP-XRF was presented for quantifying RCRA metals (i.e., As, Ba, Cr, Cd, Pb, Hg, Se, and Ag) along with iron and zinc in paint waste samples. In addition, a standard operating procedure (SOP) was introduced for applying the field instrumentation in this project and for the NYSDOT personnel in general.

Task 5: Bridge Wash Water Analysis for Lead Using the Field Spectrophotometer – In this report, the application of the Hach DR 2800 field portable spectrophotometer was presented for quantifying dissolved and total lead concentrations in bridge wash water. The U.S. Environmental Protection Agency (U.S. EPA) approved Method 8033 is used for Pb analysis and is based on Standard Method 3500-Pb. A standard operating procedure (SOP) was introduced for using the Hach field portable spectrophotometer in this project and for the NYSDOT personnel. Portable spectrophotometer results were reviewed for the 14 bridges from which wash water was available for sampling and analysis in this study.

Task 6: Collection of Samples for Laboratory Analyses – In this report, results from conducting laboratory analyses on the paint waste collected were presented. To address disposal and management of paint waste, a number of leaching studies were employed. These studies included the U.S. EPA TCLP, MEP, and SEP. X-ray diffraction (XRD) and field emission scanning electron microscopy (FESEM) were applied as well for assessing mineralogy and morphology.

Task 7: Correlation, Comparison and Interpretation of Field and Laboratory Data – Data obtained from the field measurements were correlated and compared to results obtained from laboratory analyses. Interpreting the relationship(s) and validating whether a bridge waste is classified as a hazardous waste are critical in applying the field-portable XRF by NYSDOT. Based on a statistically significant number of bridges, a statistically - based model was developed to address the waste classification.

Task 8: Project Presentation and Outreach - The findings and outreach for this project were conveyed through in person meetings, conference calls, and reports. From November 2009 to December 2013, the Lisa Axe and Zhan Shu from NJIT have met with the NYSDOT Project Manager, TWG, and other interested parties, at prescheduled meetings to present project findings and provide overall outreach:

Task 9: Final Report and Disposition of Equipment – A final report was developed summarizing Task 1 through Task 8 and submit it to the NYSDOT Project Manager for review and acceptance.

3. Findings and Conclusions

XRF results indicated that although the 24 bridges studied to date have been repainted after 1989, LBP was not entirely removed. Eighty percent of paint waste samples exhibited lead concentrations greater than $5,000 \text{ mg kg}^{-1}$. The elevated iron concentrations are present from the application of steel grit used to remove paint. Other compounds of As, Ba, Cd, Hg, Se, and Ag were observed in paint as pigments and preservatives as well. Pb concentrations were observed to correlate with As ($R^2 = 0.78$), Cd ($R^2 = 0.73$), Cr ($R^2 = 0.88$), and Ag ($R^2 = 0.67$), while other relationships were observed between Hg and Se ($R^2 = 0.99$), Hg and Zn ($R^2 = 0.94$), and Se and Zn ($R^2 = 0.76$). The trends were found across all the regions in NYS indicating consistent application of these metals as pigments and extenders in paint composition.

However, although elevated metals were observed in the paint waste, leaching results from TCLP and MEP revealed only up to 22.6 mg L^{-1} for Pb and 9.52 mg L^{-1} for Cr. The relatively low concentrations observed are attributed to the use of iron-based abrasives (steel grit) in the

paint removal process. Because steel grit is used for blasting bridges in NY to remove paint, metals such as Pb in the paint waste are sequestered by the elevated iron concentrations, which ranged from 5 - 80% by wt. As a result, metal concentrations in the leachate are less than the toxicity characteristic (TC) level. Sequential extraction demonstrated that less than 6.8% of Pb, Cr, and Ba were associated with the exchangeable and carbonate forms, while greater contributions were found with iron oxides. The largest fraction, however, greater than 80%, was associated with the residual phase comprised of minerals in the paint including SiO_2 and TiO_2 . XRD analysis corroborated that iron oxides formed on the steel grit surface provided an important interface for trace metals. The presence of the iron oxides in the paint waste may have an environmental advantage in considering contaminant mobility.

Ferrihydrite was observed to be an important surface on the steel grit; spherical particle aggregates ranged from 20 to 200 nm in diameter. The diffuse layer model (DLM) described leaching of Pb and Cr in the presence of the steel grit. Adsorption/desorption is likely the main mechanism responsible for the Pb and Cr leaching. For Ba and Zn, both adsorption and precipitation are important processes supporting predictive mechanistic leaching from the waste. Nonetheless, ferrihydrite, the dominant phase on the steel grit surface, provides abundant binding sites for trace metals. Surface sorption and co-precipitation may lead to structural incorporation of sorbed metals. Consequently, removal of metals (such as Pb) by iron oxides in the environment may be permanent. The findings in this study may have positive implications for DOT agencies in addressing disposal and management of paint waste during bridge rehabilitation.

Based on an understanding of mechanistic processes along with a demonstrated analysis of variables through PCA, statistically-based models for leaching from paint waste were developed.

The statistical models developed for metal leaching demonstrated 96 percent of the data falling within the 95% confidence level for Pb (R^2 0.6 – 0.9, $p \leq 0.01$), Ba (R^2 0.6 – 0.7, $p \leq 0.1$), and Zn (R^2 0.6 – 0.7, $p \leq 0.01$). However, the regression model obtained for Cr leaching is not significant (R^2 0.5 – 0.7, $p \leq 0.75$). The results in this study indicated that the paint waste from bridges cleaned with the Society for Protective Coatings (SSPC) surface preparation standard SP-10 (Near White Blast Cleaning) is classified as non-hazardous material, while 14% of the sample set is classified as hazardous for the bridges blasted using standard SP-6 (Commercial Blast Cleaning). Therefore, results of this work may assist in better understanding and predicting the mobility of trace metals as well as in addressing disposal and management of paint waste during bridge rehabilitation.

One recommendation from this study is the need for model validation in the field. Because the models developed in this study are based on the collected samples from the 24 bridges in seven regions of NYS, bridge samples collected from other regions are suggested for model validation. The simplicity of verifying a waste to be hazardous or nonhazardous using FP-XRF and the model has significant benefits that substantiate its continued use as SSPC 10 is applied.

Deliverable for Task 1:
Identification of Sites for the Study

Submitted

to

**Carl Kochersberger
Environmental Science Bureau
Hazardous Materials and Asbestos Unit
Pod 4-1
New York State Department of Transportation
50 Wolf Road
Albany, NY 12232**

August 31, 2010

Table of Contents

| | |
|--|----|
| 1. Introduction | 1 |
| 2. Sample Size Estimation | 1 |
| 2.1 Sampling theory | 1 |
| 2.2 Sampling size | 4 |
| 3. Stratified Sampling | 7 |
| 3.1 Stratified sampling theory | 7 |
| 3.2 Stratified sampling strategies | 9 |
| 3.3 Practical example | 9 |
| 3.4 Bridge selection | 9 |
| 4. Conclusion | 10 |
| Reference | 13 |
| Appendix A | 16 |

1. Introduction

Approximately 4,500 bridges are in need of rehabilitation in the New York. To obtain a statistically representative number of samples for the study, this report reviews the approach of sample size estimation using hypothesis testing and stratified sampling theory. The report concludes with a recommended number of statistically representative bridges to be sampled.

2. Sample Size Estimation

2.1 Sampling theory

Sample size determination is an important step in planning a statistical study. One of the most popular approaches to sample-size determination involves applying hypothesis testing (Livingston and Cassidy, 2005; Belle, 2008). The approach includes the following elements:

- Type I Error (α): Probability of rejecting the null hypothesis (H_0) when it is true. A Type I Error is the probability of alpha (α) in rejecting a true null hypothesis.
- Type II Error (β): Probability of not rejecting the null hypothesis (H_0) when it is false.
- Power = $1 - \beta$: Probability of rejecting the null hypothesis when it is false.
- σ_0 and σ_1 : Variances under the null and alternative hypotheses (may be the same).
- μ_0 : Mean under the null and alternative hypotheses.
- μ_1 : Mean under the expected data.
- n : Sample size.

A Correct Decision I occurs when we fail to reject a true null hypothesis; it has a probability of $1 - \alpha$. A Correct Decision II occurs when we reject a false null hypothesis. The purpose of the experiment is to provide the occasion for this type of decision. In other words, we perform the

statistical test because we expect the sample to differ. The probability of this situation is $1 - \beta$ and is known as the power of the statistical test. In other words, the ability of a test to find a difference when there really is a difference is the power (Figure 1).

For continuous measurements, the normal distribution is the default model, the null and alternative distributions are both normal and only differ by a shift in the mean. Specifically,

$$\bar{x} \propto N(\mu_0, \frac{\sigma^2}{n}) \quad \text{Equation 1}$$

$$\bar{x} \propto N(\mu_1, \frac{\sigma^2}{n}) \quad \text{Equation 2}$$

For a given test, α is assigned by the investigator in advance of performing the test. This value is a measure of the risk acceptable in rejecting a true null hypothesis. On the other hand, β may assume one of many values. Suppose we wish to test the null hypothesis that some population parameter is equal to some specified value. If H_0 is false and we fail to reject it, we commit a Type II Error. If the hypothesized value of the parameter is not the true value, the value of β (the probability of committing a Type II Error) depends on several factors (Wayne, 2005; Livingston and Cassidy, 2005): **(1)** the true value of the parameter of interest, **(2)** the hypothesized value of the parameter, **(3)** the value of α , and **(4)** the sample size, n .

For a given hypothesis test we need to understand how well the test controls Type II Errors. If H_0 is in fact false, we would like to know the probability that we will reject it. The power of a test, designated $1 - \beta$ is the probability that we will reject a false null hypothesis; it may be computed for any alternative value of the parameter about which we are testing a hypothesis. Therefore, $1 - \beta$ is the probability that we will take the correct action when H_0 is false because the true parameter value is equal to the one for which we computed $1 - \beta$. For a given test we may

Hypothesis

| | Hypothesis | |
|----------|----------------|-----------------------|
| | H ₀ | H ₁ |
| Decision | H ₀ | Type II Error β |
| | H ₁ | Correct rejection |

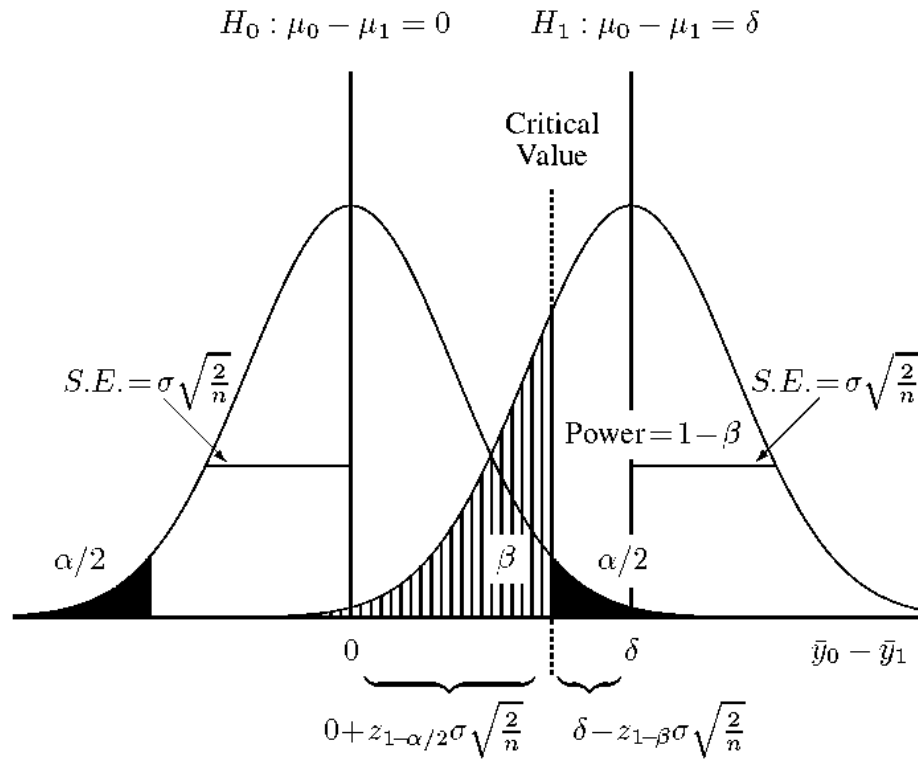


Figure 1. Type I Error (α), Type II Error (β) and sample size n (adopted from Belle, 2008)

specify any number of possible values of the parameter of interest and for each the value of $1 - \beta$ is computed. The result is called the power function.

2.2 Sampling size

For a fixed Type I error (α), the goal of constructing and testing a hypothesis is to maximize power. Anderson-Cook and Dorai-Raj (2003) show how α , β , and power are related:

$$\text{Power} = P(\text{rejecting } H_0 \mid H_0 \text{ is false}) \quad \text{Equation 3}$$

$$\begin{aligned} &= P\left(\frac{\bar{x} - \mu_0}{\sigma / \sqrt{n}} > t_a \mid \mu = \mu_1\right) \\ &= P\left(\bar{x} > \mu_0 + t_a \cdot \frac{\sigma}{\sqrt{n}} \mid \mu = \mu_1\right) \\ &= P\left(\bar{x} - \mu_1 > \mu_0 - \mu_1 + t_a \cdot \frac{\sigma}{\sqrt{n}}\right) \\ &= P\left(\frac{\bar{x} - \mu_1}{\sigma / \sqrt{n}} > \frac{\mu_0 - \mu_1 + t_a \cdot \sigma / \sqrt{n}}{\sigma / \sqrt{n}}\right) \\ &= P\left(t > t_a - \frac{\mu_0 - \mu_1}{\sigma / \sqrt{n}}\right) \\ &= P\left(t > t_a - \frac{\Delta}{\sigma / \sqrt{n}}\right) \end{aligned}$$

Power is affected by the following:

- Δ is the difference in means between the null and alternative distributions.
- n is the sample size.
- α is the probability (Type I error).

Based on the literature review developed earlier for this NYSDOT project (Shu and Axe, 2010), most bridges built before 1978 applied lead based paint (Montgomery and Mathee, 2005; Falk et al., 2005; Kyger et al., 1999; Choe et al., 2002). Although the majority of the steel bridges in the New York State were constructed between 1950 and 1980, approximately 53% of these bridges have been rehabilitated and subsequently repainted after 1989 (Kochersberger, 2010; Appendix A). As a result, lead concentrations in the paint waste are expected to be reduced. For wastes originating from abatement of non-residential structures, the U. S. EPA (1992) toxicity characteristic leaching procedure (TCLP) is used to determine waste classification based on toxicity characteristic (TC) concentrations (U. S. EPA, 1991b; U.S. EPA, 1998). In this project, bridge sampling will be conducted to study metal concentrations in paint waste from bridges repainted after 1989 using field portable x-ray fluorescence (FP-XRF) and comparing the results to TC concentrations (Kochersberger, 2010). These field results will be correlated with TCLP data, where for example, Pb concentrations greater than or equal to 5 mg/L indicate the waste is classified as hazardous. Based on resulting correlations, an objective of the project is predicting waste classification from the field data. For the purpose of determining a sample size, the following assumption is used:

Bridges repainted after 1989 are tested with a one-sided test of $H_0: \mu_0 < 5 \text{ mg/L}$ versus $H_1: \mu_0 \geq 5 \text{ mg/L}$ (the mean of TCLP results is less than 5 mg/L versus greater than or equal to 5 mg/L). The hypothesis of interest will be the right-tailed hypothesis, which indicates to reject null hypothesis, enough sample size is needed to control the probability (power) $1 - \beta$ that we will take the correct action when H_0 is false. The purpose is to know how large a sample (n) we need in order to realize that H_0 is false. The parameters include:

- N is $4,500 \times 53\% = 2,385$ bridges (based on the data from NYSDOT, 53% of the bridges have been rehabilitated and subsequently repainted after 1989), large enough for continuous measurements in a Gaussian distribution (Navidi, 2006).
- Confidence intervals are typically stated at the 95% confidence level in applied practice. (Zar, 1984) However, when presented graphically, confidence intervals can be shown at several confidence levels, for example 50%, 95% and 99%. In related statistical studies (Livingston and Cassidy, 2005; Lenth, 2001), the confidence level is generally targeted for 95%, which is therefore applied in this project.
- Type I Error is α , where $\alpha = 1 - \text{confidence level}$, which is 0.05 resulting in $t_{n,1-\alpha} = t_{n,0.95}$.
- To evaluate the lead-based paint removal waste stabilization technology, Daniels et al. (2001) apply the TCLP to assess the effectiveness of the technologies. In the study, the lead concentrations in the paint were greatly reduced by the stabilization technology: the TCLP the lead concentrations for the stabilized paint residue ranged from 0.2 – 52 mg/L. In our project, most bridges have been rehabilitated and subsequently repainted after 1989 (Kochersberger, 2010; Appendix A), as such lead concentrations in the paint waste are expected to be reduced. Because of the similar work in this project, we assume a sample mean equivalent to that of the Daniels et al. study (2001), $\mu_1 = 13 \text{ mg/L}$.
- The studies (Daniels et al., 2001; Wadanambi et al., 2008) have shown standard deviations (SD) in the TCLP concentration ranging from 2.1 – 17.6. The average standard deviations (SD) of the each series of data were calculated as 8.6 and 13.4 mg/L, respectively. In this project, 11 mg/L (average of 8.6 and 13.4) is assumed as the SD.
- For a given test we may specify any number of possible values of the parameter of interest and for each the value of $1 - \beta$ is computed. Lenth (2001) applied a range of β

values to obtain a series of sample sizes. In this report, sample values of β are proposed to be 1%, 2.5%, 5%, 10%, and 20% resulting in powers, $1-\beta$, of 80%, 90%, 95%, 97.5%, and 99%.

Because $\Delta = \mu_1 - \mu_0$, which is determined by the data (for the null hypothesis $\mu_0 < 5$ mg/L, we assume $\mu_0 = 4$ mg/L; $\mu_1 = 13$ mg/L) obtained from previous assumption and α is fixed at 0.05, we can develop a relationship between Power, $1-\beta$, and sample size, n (Table 1) based on Equation 3. Therefore, applying $\alpha = 0.05$, with varying Power = $1 - \beta$, we generate a series of sampling sizes for bridges repainted after 1989 (Table 1). The larger the power, the more likely we will take the correct action when H_0 is false.

3. Stratified Sampling

3.1 Stratified sampling theory

Stratified sampling (representative sampling, proportional sampling) is used to divide a population into homogeneous subgroups (strata) (Groves et al, 2009); each stratum is sampled individually. Sample results may be evaluated as groups or combined to estimate characteristics of the total population. When high- or low-value items are segregated into separate populations, each population is more homogeneous. A more representative sample can be derived from a relatively homogeneous population. Stratification improves the sampling process. Various audit procedures may be applied to each stratum, depending on the circumstances. The strata should be mutually exclusive: every element in the population should be assigned to only one stratum. The strata should also be collectively exhaustive: no population element can be excluded. Random or systematic sampling is applied within each stratum. This sampling often improves the representativeness of the sample by reducing sampling error (Griffith, 2008); a weighted

Table 1. Sample size for bridges repainted after 1989 (one-sided alternative hypothesis, Type I Error, $\alpha=0.05$)

| Type II Error β | Power = $1 - \beta$ | Numerator for sample size |
|-----------------------|---------------------|---------------------------|
| 0.5 | 0.5 | 8 |
| 0.2 | 0.8 | 15 |
| 0.15 | 0.85 | 17 |
| 0.1 | 0.9 | 20 |
| 0.075 | 0.925 | 22 |
| 0.05 | 0.95 | 24 |

mean that has less variability than the arithmetic mean of a simple random sample of the population is obtained.

3.2 Stratified sampling strategies

- (a) Proportional allocation uses a sampling fraction in each of the strata that is proportional to that of the total population. If the population consists of 60% in the male stratum and 40% in the female stratum, the relative size of the two samples should reflect this proportion.
- (b) Optimum allocation (or disproportionate allocation): Each stratum is proportionate to the standard deviation of the distribution of the variable. Larger samples are taken in the strata with the greatest variability to generate the least possible sampling variance.

3.3 Practical example

In general the size of the sample in each stratum is taken in proportion to the size of the stratum which is called proportional allocation. Suppose a company has a total of 180 employees, for example, where a sample of 40 is used, the resulting composition would be the following:

- % male, full time = $(90 / 180) \times 40 = 20$
- % male, part time = $(18 / 180) \times 40 = 4$
- % female, full time = $(9 / 180) \times 40 = 2$
- % female, part time = $(63 / 180) \times 40 = 14$

3.4 Bridge selection

Analogously, based on bridges undergoing rehabilitation, the state is divided into 11 regions (Figure 2). However, considering the project budget, the sample size will focus on the bridges that are closer to New Jersey Institute of Technology (bridges in regions 8, 9, 10 and 11). From

the bridges repainted after 1989 available to be sampled (Kochersberger, 2010; Appendix A), 18 bridges are in Region 8, 19 bridges are in Regions 10 and 11, 11 bridges are in Region 9. With the power equal to 0.99 and applying the theory of stratified sampling, a total of 24 sampling sites from these 48 bridges result in

- $18/48 \times 24 = 9$ bridges from Region 8
- $19/48 \times 24 = 10$ bridges from Regions 10 and 11
- $11/48 \times 24 = 5$ bridges from Region 9

For a given power, sample size distributions are obtained (Table 2).

4. Conclusion

A sample size is acceptable when the power is greater than or equal to 0.9 (Lenth, 2001). Based on sample size estimation, stratified sampling theory, and the project budget for travel, the sample size recommended is 24. To best meet the goal of the study, the bridge should be chosen from those have been repainted after 1989.

Table 2. The distribution of samples

| Sample size | 13 (1 – β =0.9) | 17 (1 – β =0.95) | 20 (1– β =0.975) | 24 (1– β =0.99) |
|-------------------|--------------------------|---------------------------|---------------------------|--------------------------|
| Region 8 | 5 | 7 | 8 | 9 |
| Regions 10 and 11 | 5 | 7 | 8 | 10 |
| Region 9 | 3 | 3 | 4 | 5 |

Bridge Painting Overview 7/30/2010

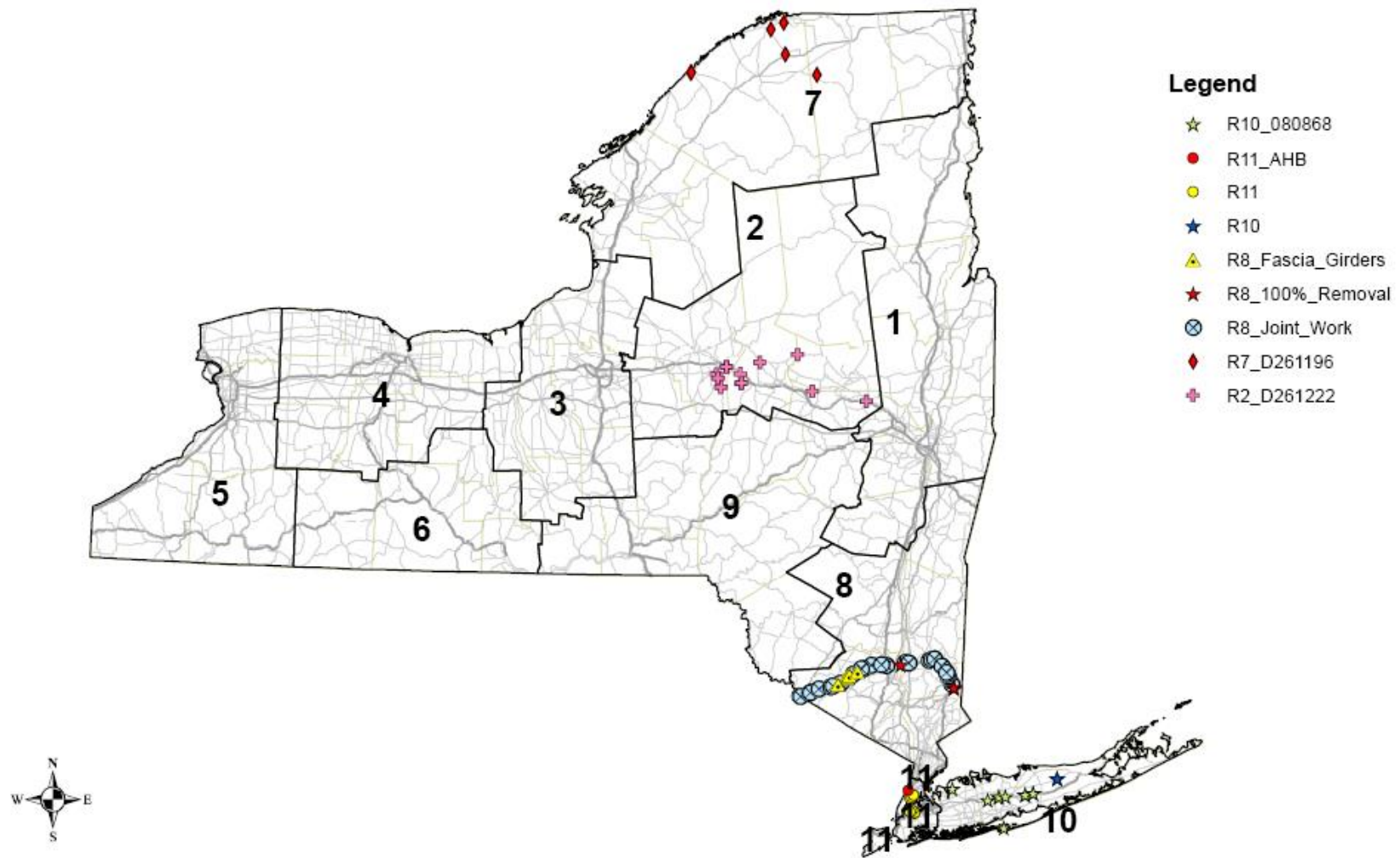


Figure 2. Bridge painting overview

Reference

Anderson-Cook, C. M., and Dorai-Raj, S. (2003) Making the concepts of power and sample size relevant and accessible to students in introductory statistics courses using applets, *Journal of Statistics Education*, 11(3).

Belle, G. V. (2008) *Statistical Rules of Thumb*, the second edition, University of Washington, Seattle, WA.

Binstock, D. A., Gutknecht, W. F., McWilliams, A. C. (2009) Lead in Soil - An Examination of Paired XRF Analysis Performed in the Field and Laboratory ICP-AES Results, *International Journal of Soil, Sediment and Water*. 2(2):1-8.

Choe T. K., Trunov M., Menrath W., Succop P., Grinshpun A. S. (2002) Relationship between lead levels on painted surfaces and percent lead in the particles aerosolized during lead abatement, *Applied Occupational and Environmental Hygiene*, 17(8): 573–579.

Daniels, A. E., Kominsky, J. R., Clark, P. J. (2001) Evaluation of two lead-based paint removal and waste stabilization technology combinations on typical exterior surfaces, *Journal of Hazardous Materials*, B87: 117–126.

Falk, R. H., Janowiak, J. J., Cosper, S. D., Drozd, S. A. (2005) Remilling of salvaged wood siding coated with lead-based paint Part I. Lead exposure, *Forest Products Journal*, 55(7/8): 76-80.

Groves, R. M., Fowler, F. J., Couper, M. P., Lepkowski, J.M., Singer, E., Tourangeau, R., (2009) *Survey methodology*, Second Edition.

Griffith, D.A. (2008), Geographic sampling of urban soils for contaminant mapping: How many samples and from where, *Environmental Geochemistry and Health*, 30 (6): 495-509.

Jing, C. Y., Meng, X. G., Korfiatis, G. P. (2004) Lead leachability in stabilized/solidified soil samples evaluated with different leaching tests, *Journal of Hazardous Materials B114*: 101–110.

Kyger, J. R., Rinke, S. D., Biagioni, R. N., Sheets, R. W. (1999) Soil contamination from paint on highway bridge, *Symposia Papers Presented Before the Division of Environmental Chemistry* American Chemical Society, Anaheim, CA.

Kochersberger, C., Bridge history data, NYSDOT, August 5, 2010.

Livingston, E. H., Cassidy, L. (2005) Statistical power and estimation of the number of required subjects for a study based on the t-test: A surgeon's primer, *Journal of Surgical Research*, 128(2) : 207-217.

Lenth, R. V. (2001) Some Practical Guidelines for Effective Sample Size Determination, *The American Statistician*, 55 (3): 187-193.

Mucha, A. P., Stites, N., Evens, A., MacRoy, P. M, Persky, V. W, Jacobs, D. E. (2009) Lead dust fall from demolition of scattered site family housing: Developing a sampling methodology, *Environmental Research*, 109: 143–148.

Montgomery, M., Mathee, A. (2005) A preliminary study of residential paint lead concentrations in Johannesburg, *Environmental Research*, 98: 279-283.

Navidi, W. (2006) *Statistics for engineers scientists*, First Edition, Colorado School of Mines.

Shu, Z., Axe, L. (2010) *Field Methods for Determining Lead Content in Bridge Paint Removal Waste*, (2009) Final Scope, Schedule & Budget for Research Project No. C-08-19.

U.S. Environmental Protection Agency (U.S. EPA) (1998) Federal Register, FR 63(243), 70190–70233, Washington, DC.

U. S. EPA (1991b) Toxicity characteristic leaching procedure (TCLP), SW-846 Method 1311 Federal Register, 55(March 29), Washington, DC.

Wayne, W. D. (2005) Biostatistics: A foundation for analysis in the health sciences, 8th Edition, Georgia State University.

Wadanambi, L., Dubey, B., Townsend, T. (2008) The leaching of lead from lead-based paint in landfill environments, Journal of Hazardous Materials, 157: 194-200.

Zar, J. H. (1984) Biostatistical Analysis. Prentice Hall International, New Jersey, 43–45.

Appendix A

Bridges rehabilitation history

| Region | Bin | Carried | Crossed | Year Built | Painted | Blasted |
|--------|---------|------------------|-------------------|------------|------------------------|---------|
| 2 | 1002390 | 5 5 23111035 | STERLING CREEK | 1929 | 1988, 1996 | NA |
| 2 | 1002960 | 5S 5S25032010 | 30 30 25042004 | 1960 | 1977, 1987, | 1977 |
| 2 | 1009890 | Route 12B | Oriskany Creek | 1928 | 1990, 1999 | NA |
| 2 | 1020110 | 28 28 23041206 | WEST CANADA CREEK | 1936 | 1977, 1996 | 1977 |
| 2 | 1020620 | Bridge Street | Route 29 | 1957 | 1977, 1996 | 1977 |
| 2 | 1020740 | 29A 29A21021000 | EAST CANADA CREEK | 1931 | 1977, 1988, 1991, 1996 | 1977 |
| 2 | 1039100 | 171 171 23011028 | MOYER CREEK | 1993 | NA | NA |
| 2 | 1039120 | 171 171 23011037 | MOYER CREEK | 1992 | NA | NA |
| 2 | 1051170 | Route 29 | EAST CANADA CREEK | 1932 | 1993 | NA |
| 2 | 1051471 | 8 8 26071100 | PINNACLE RD- CR 9 | 1969 | 1985, 1996 | NA |
| 2 | 1051472 | 8 8 26071100 | PINNACLE RD- CR 9 | 1969 | 1985, 1996 | NA |
| 2 | 1051511 | 8 8 26071136 | KELLOGG ROAD-CR26 | 1969 | 1985, 1996 | NA |
| 2 | 1051512 | 8 8 26071136 | KELLOGG ROAD-CR26 | 1969 | 1985, 1996 | NA |
| 2 | 1051530 | 8 8 26076000 | 921E 921E26011010 | 1967 | 1990, 1999 | NA |
| 2 | 1053810 | 67 X | CAROGA CRK | 1937 | 1977, 1992 | 1977 |
| 2 | 1073600 | 790I X | 921C X | 1989 | 1997 | NA |
| 2 | 1073670 | 790I X | NORTH GENESEE ST. | 1989 | 1997 | NA |
| 2 | 4426040 | Mill St. | NYS Barge Canal | 1992 | NA | NA |
| 3 | 1049610 | Pedestrian walk | State Fair Blvd | 1959 | 2007 (railing) | NA |
| 3 | 1050759 | I-690 | N. Geddes Ave. | 1968 | 1989 | NA |
| 3 | 1053870 | I-81 | N. Townsend St. | 1968 | 1992 | NA |
| 3 | 1053931 | I-690 | Bear St. Ext. | 1968 | 1989 | NA |
| 3 | 1053932 | I-690 | Bear St. Ext. | 1968 | 1989 | NA |
| 3 | 1093390 | NYS Route 5 | Roadway A | 1975 | 1991, 1999 | NA |
| 3 | 1093400 | Roadway C | Roadway A | 1975 | 1991, 1999 | NA |

| Region | Bin | Carried | Crossed | Year Built | Painted | Blasted |
|--------|---------|-------------------|-------------------|------------|----------------------------|---------|
| 3 | 1093430 | NYS Route 5 | NYS Route 174 | 1977 | 1991, 1999 | NA |
| 7 | 1023820 | 37 37 75021279 | OSWEGATCHIE RIVER | 1958 | 1998 | NA |
| 7 | 1023830 | 37 37 75021283 | 970E 970E75011001 | 1958 | 1998 | NA |
| 7 | 1024020 | 37C 37C75011005 | RAQUETTE RIVER | 1930 | 1998 | NA |
| 7 | 1029600 | 458 458 72021040 | ST REGIS RIVER | 1929 | 1988, 1998 | NA |
| 7 | 1048260 | 420 420 75011115 | RAQUETTE RIVER | 1966 | 1986, 1998, 2003 (railing) | NA |
| 7 | 3341950 | 420 420 75011004 | E BR ST REGIS RVR | 1965 | 1997, 2008 | NA |
| 8 | 1003081 | 84I 84I83011044 | 6 6 83012039 | 1964 | 1987, 1993 | NA |
| 8 | 1003082 | 84I 84I83011044 | 6 6 83012039 | 1964 | 1987, 1993 | NA |
| 8 | 1006360 | 9D 9D82033001 | 84I 84I82021014 | 1964 | 1987 | NA |
| 8 | 1026821 | 84I 84I82021031 | CR36-RED SCHLHS R | 1964 | NA | NA |
| 8 | 1026822 | 84I 84I82021031 | CR36-RED SCHLHS R | 1964 | NA | NA |
| 8 | 1026831 | 84I 84I82021045 | 52 52 8242036 | 1963 | NA | NA |
| 8 | 1026832 | 84I 84I82021045 | 52 52 82042036 | 1963 | NA | NA |
| 8 | 1032441 | 84I 84I83011007 | COUNTY RD 15 | 1965 | 1987, 1993 | NA |
| 8 | 1032442 | 84I 84I83011007 | COUNTY RD 15 | 1965 | 1987, 1992 | NA |
| 8 | 1032451 | 84I 84I83011048 | COUNTY ROAD 35U | 1966 | 1987, 1993 | NA |
| 8 | 1032452 | 84I 84I83011048 | COUNTY ROAD 35U | 1966 | 1987, 1993 | NA |
| 8 | 1032571 | 84I 84I82021124 | 987G TSP 82031029 | 1963 | 1989 | NA |
| 8 | 1032572 | 84I 84I82021124 | 987G TSP 82031029 | 1963 | 1989 | NA |
| 8 | 1032580 | 84I 84I84203H01 | 84I 84I84031097 | 1967 | 1978, 1986, 1993 | 1986 |
| 8 | 1032591 | 684I 684I84021032 | 84I X | 1967 | 1986 | 1986 |
| 8 | 1032592 | 684I 684I84021032 | 84I X | 1967 | 1986 | 1986 |
| 8 | 1052351 | 84I 84I82021134 | HOSNER MTN ROAD | 1968 | 1993 | NA |
| 8 | 1052352 | 84I 84I82021134 | HOSNER MTN ROAD | 1968 | 1993 | NA |

| Region | Bin | Carried | Crossed | Year Built | Painted | Blasted |
|--------|---------|-----------------|--------------------|------------|------------------|---------|
| 8 | 1052361 | 84I 84I82021146 | RTE 52 | 1968 | 1986, 1993 | 1986 |
| 8 | 1052362 | 84I 84I82021146 | RTE 52 | 1968 | 1986, 1993 | 1986 |
| 8 | 1052411 | 84I 84I83011003 | COUNTY ROAD 16 | 1967 | 1987 | NA |
| 8 | 1052412 | 84I 84I83011003 | COUNTY ROAD 16 | 1967 | 1987 | NA |
| 8 | 1052421 | 84I 84I83011081 | CR70- ETONTOWN RD | 1967 | 1987, 1993 | NA |
| 8 | 1052422 | 84I 84I83011081 | CR70- ETONTOWN RD | 1967 | 1987 | NA |
| 8 | 1052461 | 84I X | COUNTY ROAD 49 | 1967 | 1987 | NA |
| 8 | 1052462 | 84I X | COUNTY ROAD 49 | 1967 | NA | NA |
| 8 | 1052471 | 84I 84I83011136 | EX-MDDL TN & NJ RR | 1967 | 1984 | 1984 |
| 8 | 1052472 | 84I 84I83011136 | EX-MDDL TN & NJ RR | 1967 | 1984 | 1984 |
| 8 | 1052490 | 6 6 83012158 | 84I 84I83011154 | 1968 | 1987 | NA |
| 8 | 1052501 | 84I 84I83011165 | MCVEIGH ROAD | 1967 | 1984, 1995 | 1984 |
| 8 | 1052502 | 84I 84I83011165 | MCVEIGH ROAD | 1967 | 1984, 1993, 1995 | 1984 |
| 8 | 1052511 | 84I 84I83011167 | MONHAGEN CREEK | 1967 | 1995 | NA |
| 8 | 1052512 | 84I 84I83011167 | MONHAGEN CREEK | 1967 | 1995 | NA |
| 8 | 1052559 | 17 17 83101083 | 84I 84I83011192 | 1968 | NA | NA |
| 8 | 1052562 | Ballard Rd. | I-84 | 1969 | NA | NA |
| 8 | 1052570 | GOSHEN TURNPIKE | 84I 84I83011208 | 1969 | 1984, 1993 | 1984 |
| 8 | 1052601 | 84I 84I83011227 | CR 53-OHAIRE ROAD | 1969 | NA | NA |
| 8 | 1052602 | 84I 84I83011227 | CR53- OHAIRE ROAD | 1969 | NA | NA |
| 8 | 1052610 | BART BULL ROAD | 84I 84I83011243 | 1969 | NA | NA |
| 8 | 1052621 | 84I 84I83011262 | 416 416 83011033 | 1969 | NA | NA |
| 8 | 1052641 | 84I 84I83011272 | BEAVER DAM ROAD | 1969 | 1988 | NA |
| 8 | 1052642 | 84I 84I83011272 | BEAVER DAM RD | 1969 | 1988, 1993 | NA |
| 8 | 1052671 | 84I 84I83011302 | BARRON ROAD | 1968 | 1988 | NA |

| Region | Bin | Carried | Crossed | Year Built | Painted | Blasted |
|--------|---------|------------------|-------------------|------------|------------------|---------|
| 8 | 1052672 | 84I 84I83011302 | BARRON ROAD | 1968 | 1988 | NA |
| 8 | 1052701 | 84I 84I83011341 | 17K 17K83011175 | 1968 | 1988 | NA |
| 8 | 1052702 | 84I 84I83011341 | 17K 17K83011175 | 1968 | 1988 | NA |
| 8 | 1052721 | 84I 84I83011361 | 87I X | 1968 | 1984 | 1984 |
| 8 | 1052722 | 84I 84I83011361 | 87I X | 1971 | 1984 | 1984 |
| 8 | 1052741 | 84I X | LUDNGTNVL RD-CR43 | 1969 | 1986 | 1986 |
| 8 | 1052742 | 84I MM 58.84 | LUDINGTONVILLE RD | 1969 | 1986 | 1986 |
| 8 | 1052771 | 84I 84I84031033 | 311 311 84011010 | 1968 | 1986 | 1986 |
| 8 | 1052772 | 84I 84I84031033 | 311 311 84011010 | 1968 | 1986 | 1986 |
| 8 | 1052781 | 84I MM 62.48 | FAIR STREET-CR 30 | 1968 | 1986 | 1986 |
| 8 | 1052782 | 84I MM 62.46 | FAIR STREET-CR 60 | 1968 | 1986 | 1986 |
| 8 | 1052791 | 84I 84I84031049 | BULLET HOLE ROAD | 1968 | NA | NA |
| 8 | 1052792 | 84I 84I84031049 | BULLET HOLE ROAD | 1968 | NA | NA |
| 8 | 1052831 | 84I 84I84031081 | COUNTY ROAD 58 | 1968 | 1986 | NA |
| 8 | 1052832 | 84I 84I84031081 | COUNTY ROAD 58 | 1968 | 1986 | NA |
| 9 | 1003620 | Rte 7 | Susquehanna River | 1930 | 1896, 2000 | NA |
| 9 | 1012999 | Rte 26 | Rte 434 | 1964 | 2000 | NA |
| 9 | 1013010 | Pennsylvania Ave | Rte 434 | 1954 | 1986, 2000 | NA |
| 9 | 1018580 | Rte 26 | I-81 | 1965 | 1986, 1996, 2000 | NA |
| 9 | 1018590 | Rte 26 | NY Susq. & W RR | 1965 | 1986, 2000 | NA |
| 9 | 1054781 | Rte 17 | Castle Gardens Rd | 1969 | 1989, 2000 | NA |
| 9 | 1054782 | Rte 17 | Castle Gardens Rd | 1969 | 1989, 2000 | NA |
| 9 | 1054791 | Rte 17 | Choconut Creek | 1969 | 1989, 2000 | NA |
| 9 | 1054792 | Rte 17 | Choconut Creek | 1969 | 1989, 2000 | NA |
| 9 | 1054801 | Rte 17 | North Main Street | 1969 | 1989, 2000 | NA |

| Region | Bin | Carried | Crossed | Year Built | Painted | Blasted |
|--------|---------|-------------------|-----------------------|------------|------------------------|---------|
| 9 | 1054802 | Rte 17 | North Main Street | 1969 | 1989, 2000 | NA |
| 10 | 1018281 | 25 25 07041316 | CR46-WM FLOYD PKY | 1966 | 1995 | NA |
| 10 | 1018282 | 25 25 07041316 | CR46-WM FLOYD PKY | 1966 | 1995 | NA |
| 10 | 1036889 | 107 10703012000 | Seacliff Ave | 1953 | 1995 | NA |
| 10 | 1049320 | Bagatelle Rd | 495I 495I07031039 | 1963 | 1977, 1997 | NA |
| 10 | 1049361 | 495I 495I07031082 | CR4 Commack Rd | 1963 | 1978, 1989, 1993, 1994 | NA |
| 10 | 1049362 | 495I 495I07031082 | CR4 Commack Rd | 1963 | 1978, 1992, 1994, 1995 | NA |
| 10 | 1049400 | Washington Ave | 495I 495I07031106 | 1964 | 1986, 1989 | NA |
| 10 | 1049489 | Ronkonkoma Ave | 495I 495I07031178 | 1967 | 1999 | NA |
| 10 | 1049509 | Hawkins Ave | 495I 495I07031180 | 1967 | 1985, 1999 | NA |
| 10 | 1058780 | 908J 908J07021010 | 909D 909D07021038 | 1963 | 1995 | NA |
| 10 | 1064560 | 906A 906A07041209 | CR97 Nicholls Rd | 1970 | 1979, 1986, 1999 | NA |
| 10 | 1064570 | 906B 906B07041209 | CR97 Nicholls Rd | 1970 | 1979, 1986, 1999 | NA |
| 11 | 1055009 | 495I 495IX5M13025 | 495I 495IX5C13A04 | 1969 | 1994 | NA |
| 11 | 1065569 | 278I 278IX5M33006 | 495I 495IX5M14023 | 1969 | 1990 | NA |
| 11 | 1065871 | 495I 495IX5C14B14 | CSX TRANS/CPR&P&W | 1988 | NA | NA |
| 11 | 1065872 | 495I 495IX5M13044 | CSX TRANS/CPR&P&W | 1954 | NA | NA |
| 11 | 1065873 | 495I 495IX5C13B02 | CSX TRANS/CPR&P&W | 1988 | NA | NA |
| 11 | 1066669 | 278I 278IX1M53003 | BRUCKNER BLVD-143 | 1962 | 1997 | NA |
| 11 | 1066889 | I-95 | I-87 and Harlem River | 1962 | 1977 | NA |
| 11 | 1075910 | 278I278IX5MR02F1 | WB LAUREL HILL BD | 1969 | 1990 | NA |
| 11 | 2065971 | 495I 495IX5C14B15 | 74TH STREET | 1988 | NA | NA |
| 11 | 2065972 | 495I 495IX5M13043 | 74TH STREET | 1955 | 1992, 1995 | NA |
| 11 | 2065973 | LIE EB COLL DIST | 74TH STREET | 1988 | NA | NA |
| 11 | 2065981 | 495I 495IX5C14D12 | 80TH STREET | 1991 | NA | NA |

| Region | Bin | Carried | Crossed | Year Built | Painted | Blasted |
|--------|---------|-------------------|-------------------|------------|---------|---------|
| 11 | 2065982 | 495I 495IX5M14046 | 80TH STREET | 1955 | 1995 | 1995 |
| 11 | 2065983 | 495I 495IX5C13B02 | 80TH STREET | 1988 | NA | NA |
| 11 | 106666B | 278I 278IX1M54006 | BRUCKNER BLVD | 1959 | 1997 | NA |
| 11 | 106666C | 278I 278IX1M54004 | RAMP AG@CYPRESSAV | 1959 | 1996 | NA |
| 11 | 106666E | 278I 278IX1MR02B1 | RELIEF | 1962 | NA | NA |
| 11 | 106666F | 278I 278IX1M54022 | HUNTS POINT AVE | 1960 | NA | NA |

Deliverable for Task 2: Literature Review

Submitted

to

**Carl Kochersberger
Environmental Science Bureau
Hazardous Materials and Asbestos Unit
Pod 4-1
New York State Department of Transportation
50 Wolf Road
Albany, NY 12232**

May 30, 2010

Abstract

NYSDOT uses a conservative approach of classifying all paint waste from bridges constructed before 1989 as hazardous. The objective of this project is to investigate the effectiveness of using field-portable x-ray fluorescence (FP-XRF) instruments and field spectrophotometers to reliably characterize the hazardous nature of metal contaminated waste, namely paint and wash water, resulting from bridge rehabilitation. Studies of paints on bridges, buildings, and houses indicate that: 1. Lead often exceeds 5,000 ppm (mg/kg); 2. Mercury and zinc have been observed at elevated concentrations as great as 955 and 10,580 ppm, respectively; 3. Cadmium and chromium are not routinely observed at detectable concentrations; and, 4. Selenium, silver, and barium were not generally used. During aging and weathering, paints tend to chalk, chip, flake, and otherwise deteriorate, resulting in an accumulation of lead pigment material on and within soils or surface water surrounding painted structures. Furthermore, during maintenance, reconstruction, and demolition of bridges and other steel structures, solid waste and paint wash-water are generated on-site. The literature review demonstrates that field portable tools are effective instruments that have significant potential for characterizing paint waste as well as wash water.

Table of Contents

| | |
|--|----|
| Abstract | ii |
| 1. Introduction | 1 |
| 2. Metal distribution and behavior | 2 |
| 2.1 Metals distribution in paints | 2 |
| 2.2 Characteristics of paint and waste classification | 9 |
| 2.2.1 Characteristics of paint..... | 9 |
| 2.2.2 Paint removal methods and waste classification | 10 |
| 2.2.2.1 Paint removal method | 10 |
| 2.2.2.2 Waste classification | 12 |
| 2.3 Metal release and behavior in the environment..... | 13 |
| 2.3.1 Metals found in the soil and surface water..... | 15 |
| 2.3.2 Metals released into air | 21 |
| 3. Characteristic and classification of paint waste | 24 |
| 3.1 Classification of wastewater generated on site | 25 |
| 3.2 Leaching studies and waste classification | 26 |
| 3.2.1 Paint waste classification with TCLP..... | 29 |
| 3.2.2 Correlations observed between XRF results and TCLP or SPLP Analysis..... | 30 |
| 4. Conclusions | 32 |
| 5. References | 35 |
| Appendices | 42 |

1. Introduction

The removal of paint from bridges and other structures is a significant issue facing transportation agencies because of the presence and potential for release of lead and/or other contaminants, and the consequent impacts to human health and the environment. Although the hazards of lead paint removal from bridges have been largely identified and advances have been made in worker protection, there is still a need to identify rapid and cost-effective methods for field detection that can provide an accurate characterization of waste classification. Currently, NYSDOT uses a conservative approach of classifying all paint waste from bridges constructed before 1989 as hazardous. This practice stems from the fact that there is no approved reliable, fast, and efficient method for classifying paint waste in situ as non-hazardous. This conservative practice eliminates the need for extensive testing, but also results in greater expense and increased regulatory burdens than are likely required. With the advent of more accurate and sophisticated analytical equipment for in-situ field measurements, state DOTs will benefit from research focused on the reliability of such field equipment for waste characterization.

The objective of the project is to investigate the effectiveness of field-portable x-ray fluorescence (FP-XRF) instruments and field spectrophotometers in providing reliable characterization of paint waste and wash water generated during bridge rehabilitation. These measurements, if reliable, can then be used to determine if the waste is hazardous or not. Accuracy of the field measurements can be assessed by comparing results to laboratory analyses. Such analyses are conducted on wash water and digested paint waste using inductively coupled plasma mass spectroscopy (ICP-MS) or atomic absorption spectroscopy

(AA). Further tests include the U.S. Environmental Protection Agency (U.S. EPA) toxicity leaching characteristic procedure (TCLP) (U.S. EPA, 1992) for addressing whether the paint waste is classified as hazardous. Field and laboratory results can then be correlated to develop a model that a state DOT can use to determine if hazardous waste will be generated or not during bridge rehabilitation and painting projects.

In this report, studies on metal distribution and behavior are presented in terms of paint composition and contaminant release into the environment during bridge rehabilitation. The report continues with a review of literature related to characterizing and classifying paint waste. The report also concludes with a summary of studies reviewed.

2. Metal distribution and behavior

2.1 Metals distribution in paints

Prior to the 1960's (The National Paint & Coatings Association [NPCA], 1992), paints generally contained pigments using lead and/or chromium compounds as corrosion inhibitors. Lead based paint (LBP) functioned very well and was used in practically all painting applications, from bridges to sign trusses, from light poles to fire hydrants. The primary lead compound used in paints was lead carbonate (white lead $2\text{PbCO}_3 \cdot \text{Pb(OH)}_2$) with concentrations as great as 40% dry paint. Lead chromate (chrome yellow) was used in (colored) paint at 5 to 7%, while lead tetraoxide (red lead Pb_3O_4 , Pb_2O_4 , $\text{PbO}_2 \cdot 2\text{PbO}$) was also a component of paints (Gooch, 1993; Oil and Color Chemists Association, 1983) (Table 1). Because lead is poisonous and a carcinogen, in the early 1970's it became apparent there were worker health and safety problems associated with LBP. In 1977, the Consumer Product Safety Commission (CPSC) banned residential use of paint containing greater than 0.06%

Table 1. Lead compound used in paints^{a, b}

| Pigment | Color | Chemical Formula | Dates Used ^{c,d} |
|---------------------------------|--------|--|--|
| Lead acetate | White | $\text{Pb}(\text{CH}_3\text{COO})_2$ | 1900's – 1960's |
| Dry white lead, basic carbonate | White | $2\text{PbCO}_3 \cdot \text{Pb}(\text{OH})_2$ | 1900's – 1970's |
| Dry white lead, basic sulfate | White | $\text{PbSO}_4 \cdot \text{PbO}$ | Widely used as a primer and in building finishes. First introduced between 1855 and 1866, leaded zinc oxide form introduced in 1896. |
| | Yellow | PbO – yellow | |
| Litharge (lead oxides) | Black | Pb_2O (sub-oxide) | 1940's – 1970's |
| | Red | Pb_2O_4 – red | |
| Lead tetraoxide (red lead) | Orange | Pb_3O_4 ($\text{PbO}_2 \cdot 2\text{PbO}$) | Primer coating |
| Lead chromate/oxide | Orange | $\text{PbCrO}_4 \cdot \text{PbO}$ | 1935 – 1970's |
| Basic lead chromate | Red | $\text{Pb}_2(\text{OH})_2\text{CrO}_4$ | Discovered 1809 |
| Lead chromate | Yellow | PbCrO_4 | 1910's – 1970's |

^aWeast, 1987^bGooch, 1993^cCrown, 1968^dAlphen, M., 1998

lead (U.S. CPSC, 1977) . At the same time (1978), The Department of Housing and Urban Development (HUD) banned the use of paint with greater than 5,000 ppm or 1.0 mg/cm² lead concentrations (HUD, 1978). Since then, LBP has been phased-out of residential, commercial, and industrial use (Gooch, 1993).

As the use of lead paint declined, substantial quantities of zinc rich paint was used in bridge paint. Mixtures of zinc oxide and lead sulfate based paint grew in the market between 1920's and 1970's. Beginning about the same time, lithophone (a mixture of 30% zinc sulfide and 70% barium sulfate) exceeded the use of lead in interior paint as the primary pigment. However, lithophone lacked durability and therefore its use declined. During the time between the mid and late 1970's, zinc chromate was used in primers along with a vinyl topcoat; in the late 1980's (International Agency for Research on Cancer [IARC], 1987) this compound was found to be toxic and was phased out. Beginning in the late 1970's zinc silicate was applied as a primer for shop and field paint; experience suggests resulting wastes are not hazardous. Other metal based compounds were used as well including rutile, titanium dioxide, which was more effective and less costly than other pigments (NPCA, 1992; Ferlauto, 1994). Titanium dioxide continues to be used today for bridge paint.

In addition to the metals discussed above, other elemental compounds of arsenic, barium, cadmium, chromium, mercury, selenium, and silver, were used in paint as pigments and preservatives as well (see Appendix A). Since the 1950's, arsenic was used as a pigment; however, because of the risk of poisoning, the actual use of the associated compounds was for the most part restricted to that of insecticides (Alphen, 1998). Barium was also used as a pigment and a corrosion inhibitor (NPCA, 1992) from the 1950's, as was cadmium (after

1920's) which is as a pigment that produces bright colors in paint. As mentioned above, zinc chromate was used for a short period of time and because of its toxicity it was an effective barrier to microorganisms. Prior to 1992, the mercury compound phenylmercuric acetate (PMA) was added to some latex paints as a preservative to control bacteria, mildew, and other fungi (U.S. EPA, 1990; 2000). Selenium and silver were rarely used in the paint (Alphen, 1998).

As a consequence of their use, RCRA metals along with Zn are now found in paints on older buildings and surface structures (Table 2, Appendix A) (Boxall and von Frauhoffer, 1980; Crown, 1968). With aging and weathering, paints tend to chalk, chip, flake, and otherwise deteriorate, resulting in an accumulation of pigment material on and within soils or surface water surrounding painted structures. Subsequently, humans and the environment are exposed to heavy metals when dust and fumes are inhaled and when contaminants are ingested via contaminated hands, food, water, cigarettes, and clothing (National Institute for Occupational Safety and Health [NIOSH], 1997). For example, once in the bloodstream, lead replaces other useful elements (e.g., calcium, iron) and adversely affects oxygen transport to a number of organs including the liver, kidneys, reproductive system, and the brain (Tong et al., 2000). Lead is also a carcinogen. The effects of lead are the same whether it enters the body through inhalation or ingestion, and can affect almost every organ and system in the body. Exposure to high lead levels can damage the nervous system especially in young children, cause disorders in the blood and brain systems, and ultimately result in death. Long-term exposure to lead or its salts (especially soluble salts or the strong oxidant PbO_2) can cause nephropathy, and colic-like abdominal pains. For other metals such as hexavalent

Table 2. Typical pigment levels in liquid paints^a

| White | | Protective | |
|--|--------|--|--------|
| Titanium dioxide [TiO ₂] | 15-20% | Basic lead silichromate [4(PbCrO ₄ PbO) + 12(SiO ₂ PbO)] | 25-35% |
| Zinc oxide [ZnO] | 15-20% | Basic lead sulfate [PbO PbSO ₄] | 15-20% |
| Antimony oxide [Sb ₂ O ₃] | 15-20% | Calcium plumbate [Ca ₂ PbO ₄] | 30-40% |
| White lead [2PbCO ₃ Pb(OH) ₂] | 15-20% | Red lead [Pb ₃ O ₄] | 30-35% |
| | | Zinc phosphate [Zn ₃ (PO ₄) ₂] | 25-30% |
| | | Zinc tetroxychromate [ZnCrO ₄ 4Zn(OH) ₂] | 20-25% |
| | | Zinc chromate [ZnCrO ₄] | 30-40% |
| Green | | Blue | |
| Chromium oxide [Cr ₂ O ₃] | 10-15% | Prussian blue ^b [MFeFe(CN) ₆ H ₂ O] | 5-10% |
| Lead chrome green [PbCrO ₄] | 10-15% | Ultramarine blue [Na _{6,9} Al _{5,6} Si _{6,4} O ₂₄ S _{4,2}] | 10-15% |
| Black | | Metallic | |
| Black iron oxide [Fe ₂ O ₃ +MnO ₂] | 10-15% | Zinc | 60-70% |
| Carbon black | 1-5% | Lead | 40-50% |
| Yellow | | | |
| Lead chromates [Pb(Cr,S)O ₄] | 10-15% | | |
| Zinc chromates [ZnCrO ₄] | 10-15% | | |
| Cadmium sulfide [CdS] | 5-10% | | |

a: Boxall and von Frauhoffer (1980)

b: M could include K, Na or CH₃

chromium, inhalation can cause damage to the nose, throat, and lungs (respiratory tract); it too can lead to lung cancer and death. Chronic exposure to mercury can cause disruption of the nervous system, damage to DNA and the chromosomal system, as well as result in allergic reactions (Clarkson, 1988). Mercury is a carcinogen. Long-term exposure to mercury can lead to damage of the brain, kidney, and lungs. Damaged brain functions may result in learning abilities, personality changes, tremors, vision changes, and deafness. Dermal exposure may also result in skin rashes, tiredness, and headaches (U.S. EPA, 2009). Mercury poisoning can result in several diseases, including acrodynia (pink disease), Hunter-Russell syndrome, and Minamata disease.

In response to these health concerns, the federal government has promulgated a series of regulations to reduce exposure to these metals. In 1977, CPSC banned residential use of paint containing greater than 0.06% lead (U.S. CPSC, 1977) (Table 3). HUD (1978) set up the regulation that banned the use of paint with greater than 5,000 ppm or 1.0 mg/cm² lead concentrations. In 1993, OSHA reduced permissible exposure limit (PEL) for workers to 50 µg/dL of blood (OSHA, 1993). In 1996, U.S. EPA and HUD together enacted requirements for disclosure of known LBP used in housing (CFR 61(45), 1996). In 2001, the U.S. EPA (CFR 66(4), 2001) announced the final rule for lead levels in dust on floors, windowsills, and play areas as potential hazards. The U.S. EPA (CFR 66(4), 2001) has established 400 ppm of lead in bare soil as the maximum allowable level for children's play areas and an average of 1,200 ppm as the maximum concentration allowed in a residential yard. In 2009, lead concentration in paint for residential application was lowered to 90 ppm (Consumer Product Safety Improvement Act [CPSIA], 2009). However, auto exhaust from leaded gasoline used

Table 3. Regulations related to metals in paint

| Date | Hazardous Materials Used in Paint | References |
|-----------|---|--|
| 1972 | The Lead Based Paint Poisoning Prevention Act established the level of 0.5% in house paints. | U.S. CPSC (1972) |
| 1972 | Mercury compounds were banned by the U.S. EPA from use in marine paint. | U.S. EPA (1972) |
| 1977-1978 | The final 1977 LBP Poisoning Prevention Act regulation set the maximum allowable level at 0.06% became effective by U.S. CPSC, and it is 1.0 mg/cm ² or 5,000 ppm set by HUD (1978), as such greater concentrations were banned from consumer paints. | U.S. CPSC (1977) HUD (1978) |
| 1990 | Mercury in interior latex paint was banned by the U.S. EPA. Most buildings constructed before 1990 contain mercury in their paint. | U.S. EPA (1990) |
| 1992 | Mercury in interior paint was banned although its use had been reduced. | U.S. EPA (1992) |
| 1993 | A CPSC study of consumer paint samples found that lead in paints on the market meet the standard and are actually below the 0.06 % level. | U.S. CPSC (1993) |
| 1996 | Lead was not banned from gasoline used in transportation until December 1995. U.S. EPA and HUD together enacted requirements for disclosure of known LBP used in housing (CFR 61(45), 1996). | HUD, FR 61(45), (1996) |
| 2001 | The U.S. EPA has established 400 ppm of lead in bare soil as the maximum allowable level for children's play areas and an average of 1,200 ppm as the maximum concentration allowed in a residential yard. | U.S. EPA (2001) |
| 2006 | Work practice standards proposed to reduce lead exposure during residential renovation activities in 40 CFR Part 745 | TSCA, 40 CFR Part 745, revised in April 22, 2009 |
| 2008 | EPA finalized Toxic Substances Control Act (TSCA) regulations in 40 CFR Part 745. The rule addressed LBP hazards during residential renovation, repair, and painting activities. | |
| 2009 | The lead concentration in paint was lowered to 90 ppm, it applied to (i) paint and other similar surface coatings; (ii) toys and other articles intended for use by children; and (iii) certain furniture articles that are not otherwise exempt under our regulations. | CPSIA (2008), effective in August 14, 2009 |

as an octane-booster and anti-knock compound has been another source of lead in the environment. Between 1940 and 1989, twice as much lead in the form of lead oxide and tetraethyl lead was used in leaded gasoline as compared to that used in white lead paints from 1910 to 1989 (Weaver, 1989). Seventy-five percent of lead associated with auto exhaust mobilized into the environment and settled in soil and on structures (Ferlauto, 1994). Other metals also pose potential risk from release. For example, because of exposure concerns regarding mercury in interior paints, limits were placed on PMA additives in 1990 (U.S. EPA, 1990); subsequently these were banned in 1991 (ATSDR, 1999).

2.2 Characteristics of paint and waste classification

2.2.1 Characteristics of paint

Paint can be classified based on its primary type of solvent: waterborne, organic solvent-borne, and powder (dry, without solvent). Waterborne paints include aqueous emulsions (latex), colloidal dispersions, and water-reducible coatings. Many conventional paints are organic solvent-borne. Powder coatings are comprised of resins, pigments, curing agents, catalysts, reinforcing fillers, flow control agents, and other minor ingredients (Illinois department of Natural Resources, 1992). Organic solvent-borne paint was conventionally used for bridges until recently, when the Tellus Institute (1993) recommended waterborne paint.

Lead-based paint (LBP) is technically defined as having a minimum of 0.5% (5,000 ppm) by weight lead or when assessing surfaces greater than 1.0 mg/cm^2 (U.S. EPA, 1995). Lead concentrations in the paint depend on many factors such as age of the structure, paint film

thickness, paint film condition, and type of substrate. With aging and weathering, lead contaminated paint has been released into the environment, accumulating in soils and surface water surrounding painted structures. Because of potentially serious consequences of metal poisoning and environmental contamination, painted surfaces are tested before starting a maintenance or restoration project. Studies (Table 4) of paints on bridges, buildings, and houses indicate that 1. Lead in many of the existing painted surfaces exceeds 5,000 ppm (mg/kg) (Mielke and Gonzales, 2008; Mielke et al., 2001; Huanga et al., 2010); 2. Zinc and mercury have been observed at elevated concentrations as great as 10,580 and 955 ppm, respectively (U.S. EPA, 1990; Huanga et al., 2010); 3. Cadmium and chromium are not routinely observed at detectable concentrations (Huanga et al., 2010; Boxall and Fraunhofer, 1980); and, 4. Selenium, silver, and barium were not generally used (Boxall and Fraunhofer, 1977).

2.2.2 Paint removal methods and waste classification

During maintenance, reconstruction, and demolition of bridges and other steel structures, solid waste and paint wash-water are generated on-site.

2.2.2.1 Paint removal method

The most effective and productive method for removing paint and rust from steel has been abrasive blasting (Appleman, 1992). In this method, abrasive particles are propelled against the surface using a concentrated stream of compressed air. Dust, abrasive, and paint debris are vacuumed simultaneously with the blasting operation. Debris is separated for

Table 4. Metal concentrations in paint used on surface structures

| Sources | Concentration of Metals in paint by dry weight (ppm) | | | | | | | | | Reference |
|----------------------|--|-----------|--------------|----------------|---------|----|----|----|--------------------|----------------------------|
| | Pb | Hg | As | Cd | Cr | Se | Ag | Ba | Zn | |
| Exterior house paint | 464 – 317,151 | 0.8–214.0 | – | – ^b | – | – | – | – | – | Mielke and Gonzales (2008) |
| Interior house paint | 24 – 63,313 | 0.03–39.2 | – | – | – | – | – | – | – | |
| New Orleans houses | 112 – 256.797 | – | – | 7 - 439 | 2 - 417 | – | – | – | 52 – 98.056 | Mielke et al. (2001) |
| Interior latex paint | – | 930-955 | – | – | – | – | – | – | – | U.S. EPA (1990) |
| Solvent-based paint | 15,680 ± 11,780.00 | – | 100 ± 20.00 | ND | ND | – | – | – | 30,460 ± 10,580.00 | Huanga et al. (2010) |
| Water-based paint | 57.46 ± 22.42 | – | 20.65 ± 6.11 | ND | ND | – | – | – | 1,660 ± 1,260 | |
| ND not detected | | | | | | | | | | |
| – not measured | | | | | | | | | | |

disposal and the abrasive is returned for reuse. Typically, hard metallic abrasives are used in these systems, where for example, magnetic particles can be easily separated (Appleman, 1992). This approach can effectively remove paint from crevices and other hard-to-reach areas. Generally, a complete containment (which is negative pressure and has a vacuum system) is constructed around the work area to control emissions of dust and debris (New York State Department of Transportation [NYSDOT], 2008).

Another commonly used method is power tool cleaning (Appleman, 1992), where electric and/or air operated impact grinding or brushing tools are applied and include power chippers, needle guns, descenders, power wire brushes, and grinding wheels. Power tool cleaning produces dust and can generate airborne debris. In contrast to using abrasive particles, power tool cleaning does not require a medium. As a result, essentially the only debris generated is the material being removed (paint, rust, mill scale, and other surface debris). Often the power tool is surrounded with its own shroud that is equipped with a vacuum. This method creates a miniature containment around the tool for collecting waste as it is generated, transporting it from the work area through hoses. Prior to paint removal, high pressure water (about 3000 psi) is used to get all salt, bird droppings, etc. off the bridge so that it doesn't get impinged into the steel while blasting (NYSDOT, 2008).

2.2.2.2 Waste classification

To accelerate LBP removal from residences and control the hazardous waste produced, the U.S. EPA (2003) published the Final Rule for Disposal of Residential Lead-Based Paint Waste, which allows residential LBP waste to be exempt from hazardous waste management requirements as household waste. This document (U.S. EPA, 2003) applies to residential LBP

debris, chips, dust, and sludge, and includes LBP removed from a painted surface by sanding, scraping, or using chemical strippers. Residential LBP waste refers to waste containing LBP, which is generated as a result of activities such as abatement, rehabilitation, renovation, and remodeling in homes and other residences. As such, it can be disposed in construction and demolition landfills for facilities accepting residential LBP waste and no other household waste, and is not a municipal solid waste landfill unit. On the other hand, for the non-residential LBP waste, the U.S. EPA toxicity characteristic leaching procedure (TCLP) (U.S. EPA, 1992) must be conducted on a representative sample to determine if the wastes are characteristically hazardous (Table 5). Specifically, wastes with a TCLP concentration less than the lead toxicity characteristic (TC) limit of 5 mg/L may be disposed at a Class I or II Municipal Solid Waste Landfill (MSWLF) or a construction and demolition (C&D) landfill. On the other hand, wastes with TC lead concentrations greater than 5 mg/L must be managed as a hazardous waste and disposed at an U.S. EPA RCRA permitted treatment, storage, and disposal (TSD) facility (U.S. EPA, 1998).

The toxicity characteristic limits are based on the metal release and behavior once in the environment. The concern with contaminated paints would be the subsequent release to the environment through weathering, aging, and bridge rehabilitation.

2.3 Metal release and behavior in the environment

The majority of steel bridges in the interstate system were constructed between 1950 and 1980. As infrastructure ages, undergoes weathering, and paint coatings degrade, a large percentage of the existing steel bridges are reaching a critical level of deterioration, and

Table 5. Different types of landfills^a

| Types of landfill | Description of landfill | Acceptable waste | Determination of lead level |
|-------------------------|--|--|---|
| C&D | Construction, demolition, and land-clearing debris landfill; least protective landfill; no liners, and no groundwater monitoring | Residential LBP waste | Analyze paint using digestion for total lead analysis or by XRF |
| MSWLF (Subtitle D) | Municipal solid waste landfill; synthetic liner and leachate collection system | Residential LBP waste. Hazardous wastes from “conditionally exempt small quantity generators” if acceptable under their special waste plan. | TCLP |
| Subtitle C ^b | Hazardous waste landfill | Paint residue with toxicity concentration >5.0 mg/l for Lead (Table 11) | TCLP |

a: U.S. EPA, (2003) Disposal of Residential Lead-Based Paint Waste, Final Rule
<http://www.epa.gov/wastes/nonhaz/municipal/landfill/pb-paint.htm>

b: Disposal in a Subtitle C landfill does not apply to waste generated by construction or demolition activities conducted on a household or residence.

release of metal contaminants into the environment becomes an issue. In this section, metal release into surrounding soils and surface water along with infiltration into groundwater are discussed. Furthermore, during rehabilitation, particles can be aerosolized and dispersed as well as released into soils and surface water; this mode of transport is also reviewed in this section.

2.3.1 Metals found in the soil and surface water

Because lead concentrations in paint far exceed that of other metals (Boxall and Fraunhofer, 1977; Boxall and Fraunhofer, 1980), the following discussion is focused on lead. The elevated concentrations of lead observed in the environment originate from deteriorating exterior lead-based paint (Allen et al., 1999; Binstock et al., 2009) results in leaching through soil around the foundation of a bridge or building and into groundwater (Binstock et al., 2009) as well as transport into surface waters (Allen et al., 1999).

Decades of peeling exterior paint as along with remodeling and renovation activities, give rise to dust and debris that contribute to further dispersal of elevated lead concentrations in soil (U.S. EPA 1996; 1999a, b). Once lead as well as other metals are released from painted structures, they can be attenuated via interactions with surrounding soil. Studies (Francek, 1992; Francek et al., 1994) indicate lead sorption and attenuation in soils can be significant, residing in systems potentially for several thousand years. For example, lead concentrations in soil surrounding buildings constructed after 1978 revealed background levels, whereas prior to 1978 concentrations greater than 1,000 ppm were found (Francek, 1992; Francek et al., 1994). Binstock et al. (2009) observed lead concentrations as great as 2,540 ppm during an evaluation of soil around housing with LPB applied to exterior surfaces. Caravanos et al.

(2006) studied deposition of lead in ambient dust for the boroughs of New York City from 2003–2004 and observed concentrations ranging from 175 $\mu\text{g}/\text{ft}^2$ to 730 $\mu\text{g}/\text{ft}^2$. When compared to the HUD/EPA dust standard of 40 $\mu\text{g}/\text{ft}^2$ (U.S. EPA/HUD, 2003), they reported that in Manhattan and Queens areas, renovations at bridges and other construction/demolition activities are potential lead sources and may in part explain the lead deposited in this area.

Markey et al. (2008) found that lead concentrations in soil obtained by field-portable X-ray fluorescence (FP-XRF) protocol Method 6200 (U.S. EPA, 1998) (Appendix B) are highly correlated ($r^2 = 0.9764 - 0.992$) with laboratory results using digestion followed by atomic absorption spectrophotometry (AAS) (Table 6). One reason strong correlations were observed was that samples were homogenous, fine-grained, and dry; good correlations are generally observed for such samples (Kirtay et al., 1998; Clark et al., 1999). Kilbride et al. (2006) compared metal concentrations in contaminated soil by using FP-XRF versus aqua regia acid digestion followed by AAS and found that both the dual isotope and the X-ray tube based FP-XRF instruments are effective tools for rapid, quantitative assessment of soil metal contamination. Binstock et al. (2009) evaluated the lead concentrations in soil with FP-XRF and digested samples followed by ICP-AES around housing where LBP was applied to exterior surfaces. Statistical analysis (i.e. sign test, Wilcoxon signed rank test, and paired t-test) indicated no difference ($r^2 = 0.98 - 1.00$) between the measurements.

In paved areas, dissolved lead and lead contaminated paint particulates are transported either directly or indirectly to surface water through storm drains. Specifically, metals may be mobilized through rainfall, and urban stormwater runoff is considered to be a major source of heavy metals to surface waters. Lead contaminated paint particles will continue to dissolve as

Table 6. Correlation between metal concentrations in soil measured by FP-XRF and that found through digestion followed by AA and ICP

| Sample Type | Metal concentration by XRF (ppm) | | | | Metal concentration by AA or ICP (ppm) | | | | r ² value | Reference |
|-----------------------------|----------------------------------|-----------|-------------|----------|--|-----------|------------|---------|----------------------|------------------------------|
| | Pb | As | Zn | Cd | Pb | As | Zn | Cd | | |
| Marine sediment | 0.70 | – | 0.87 | – | – | – | – | – | – | Kirtay et al. (1998) |
| Soil | 750 - 882 | – | – | – | 920 – 1,124 | – | – | – | 0.9764 – 0.992 | Markey et al. (2008) |
| Soil | 5,300 ± 300 | 370 ± 30 | 1,040 ± 60 | – | 5,000 ± 300 | 860 ± 60 | 930 ± 60 | – | 0.843 – 0.996 | Radu and Diamond (2009) |
| Soil in the industrial land | 2 – 74,356 | 2 – 3,920 | 35 – 60,820 | 12 - 613 | 5 – 40,398 | 2 – 5,646 | 3 – 25,389 | 0 - 447 | 0.26 – 0.93 | Kilbride et al. (2006) |

– not measured

they are being transported, releasing lead into solution. The dissolution rate can be enhanced by complexing agents commonly found in natural waters, such as humic acid (Guy and Chakrabarth, 1976) and chloride (Barnes and Davis, 1996). The mobility of metals in the environment is a function of their speciation. While metals in general prefer to be bound to surfaces, cations will desorb as the pH decreases and anions are released as the pH increases. Actually, a number of factors affect metal behavior including sorbents present in the subsurface, pH, ionic strength, complexing ligands, reduction oxidation potential, competing ions, and time.

In addition, as mentioned earlier, LBP removal projects may generate wastewater from cleaning painted surfaces, wet abrasive blasting, or decontamination of personnel or equipment. Although wastewater containing lead or paint solids must be collected, properly treated, and discharged to a permitted location to prevent water pollution, some may inadvertently flow into the surface water sources. Lead distribution in the rain water and wash water from paint has been investigated (Table 7). Many of these results reveal concentrations greater than the U.S. EPA fresh water chronic and acute criteria of 2.5 and 65 $\mu\text{g/L}$, respectively (U.S. EPA, 2009) (Table 8). To assess the effect of acid rain on LBP structures, Davis and Burns (1999) used synthetic rain water with a pH range of 4.2 to 4.4 and composed of 23 mM NaCl, 18 mM HNO_3 , and 18 mM H_2SO_4 . Results revealed that the total lead concentrations (Table 7) in the runoff were a function of paint age ($> 10 \text{ y}$) $>$ (5-10 y) $>$ (0-5 y); the older the structure the greater the concentration observed. Additionally, the authors found the structure type was important where concentrations followed the trend of wood $>$ brick $>$ block. Yet, 69 – 84% of lead was associated with particulates. Concentrations in the

Table 7. Lead concentrations observed in wastewater and rain water

| Sample type | Total lead (mg/L) | Reference |
|---|---|---|
| Wastewater obtained by high pressure wash | 2.3 – 130 (without filtration) 2.0 – 220 (with filtration) | Hopwood et al. (2003) |
| Runoff obtained from synthetic rain water | Block 0 - 0.59 Wood 0 - 1.9 Brick 0 - 28 | Davis and Burns (1999) |
| Storm water runoff | 140 | Granier et al. (1990) |
| Storm water runoff from residential areas | 9 – 72 (composite) 0 – 62 (grab) | Maryland Department of Environmental Resources (1993) |
| Storm water runoff from commercial land use areas | 14 ± 39 (composite) 54 ± 230 (grab) | |

Table 8. Water Quality Criteria for the protection of aquatic life and human health in surface water^[1]

| Contaminant | Freshwater | | Saltwater | | Human Health for the consumption of | |
|----------------|-------------|---------------|-------------|---------------|-------------------------------------|---------------|
| | CMC (acute) | CCC (chronic) | CMC (acute) | CCC (chronic) | Water + Organism | Organism Only |
| | (µg/L) | (µg/L) | (µg/L) | (µg/L) | (µg/L) | (µg/L) |
| Arsenic | 340 | 150 | 69 | 36 | 0.018 | 0.14 |
| Barium | NA | NA | NA | NA | 1,000 | NA |
| Cadmium | 2 | 0.25 | 40 | 8.8 | A | NA |
| Chromium (III) | 570 | 74 | NA | NA | A | NA |
| Chromium (VI) | 16 | 11 | 1,100 | 50 | | NA |
| Lead | 65 | 2.5 | 210 | 8.1 | NA | NA |
| Mercury | 1.4 | 0.77 | 1.8 | 0.94 | NA | 0.3 mg/kg |
| Selenium | NA | 5 | 290 | 71 | 170A | 4,200 |
| Silver | 3.2 | NA | 1.9 | NA | NA | NA |
| Zinc | 120 | 120 | 90 | 81 | 7,400 | 26,000 |

[1] National Recommended Water Quality Criteria, United States Environmental Protection Agency, Office of Water Office of Science and Technology, (4304T) 2006.

NA: Not Applicable

A: A more stringent MCL has been issued by U.S. EPA. Refer to drinking water regulations (40 CFR 141) or Safe Drinking Water Hotline (1-800-426-4791) for values.

CMC: The Criteria Maximum Concentration (CMC) is an estimate of the highest concentration of a material in surface water to which an aquatic community can be exposed briefly without resulting in an unacceptable effect.

CCC: The Criterion Continuous Concentration (CCC) is an estimate of the highest concentration of a material in surface water to which an aquatic community can be exposed indefinitely without resulting in an unacceptable effect.

runoff were dependent on the intensity (flow rate/spray area) of the synthetic rain water applied, the greater the ratio the greater the concentration. The first flush of the painted structures revealed greater lead concentrations than the wash water generated during subsequent contact. As the lead concentration in the peeling paint chips increased, concentrations in the runoff increased as well. Similarly, air contamination may result from aerosolized paint particles during rehabilitation.

2.3.2 Metals released into air

Lead contaminated particles are aerosolized during abatement, and as a result pose a potential health hazard. The National Institute for Occupational Safety and Health (NIOSH, 1992) evaluated eight bridge construction sites where abrasive blasting occurred and showed airborne lead concentrations ranged from 2 to 29,400 $\mu\text{g}/\text{m}^3$. Furthermore, worker blood levels ranged from 51 to 160 $\mu\text{g}/\text{dl}$ (NIOSH, 1992). OSHA (1993) promulgated an interim final rule for lead exposure in construction (29 CFR 1926.62); the standard reduced the permissible exposure limit (PEL) from 200 $\mu\text{g}/\text{m}^3$ of air as an eight-hour time weighted average (TWA) to 50 $\mu\text{g}/\text{m}^3$ of air (Table 9). This regulation also set air action levels for workers without respirators to 30 $\mu\text{g lead}/\text{m}^3$ of air (Table 9) (OSHA, 1993). Sullivan et al. (1996) studied whether concentrations of lead, cadmium, and chromium in air during abrasive blasting exceeded the OSHA standards. Airborne lead and cadmium concentrations measured at several locations inside the containment structure as well as near the workers' breathing zones did exceed OSHA PEL (Table 10) by factors of 219 and 3.1, respectively.

Air quality monitoring has involved traditional high-volume air sampling for particulates and volatilized lead when studying LBP removal from bridges with abrasive blasting. To

Table 9. Lead exposure limits

| Environment | Lead limits | Reference |
|-------------------------------|---|-----------------------|
| Paint | 600 ppm | U.S. CPSC (1977) |
| | 1.0 mg/cm ² or 5,000 ppm | HUD (1978) |
| Dust | 40 µg /ft ² – clearance for floors | U.S. EPA / HUD (2003) |
| | 250 µg /ft ² –clearance for window sills | |
| | 400 µg /ft ² –clearance for window wells | |
| Dust lead hazard screens only | 25 µg /ft ² – floors | U.S. EPA / HUD (2003) |
| | 125 µg /ft ² –window sills | |
| Soil | 500-1,000 ppm- superfund limit | U.S. EPA (2001) |
| | 400 ppm– high contact play areas (communicate) | |
| | 1,200 ppm – other residential yard areas (average) | |
| | 5,000 ppm – require permanent abatement | |
| | Background or < 400ppm –replacement soil | |
| Air | 1.5 µg /m ³ - EPA national air quality standard (quarterly) | OSHA (1993) |
| | 30 µg /m ³ – OSHA action level ^[1] | |
| | 50 µg /m ³ – OSHA permit exposure limit (PEL) (8 hour average) | |
| Blood | 10 µg /dl (CDC) level of concern for children | OSHA (1993) |
| | 40 µg /dl permissible blood lead level | |
| | 50 µg /dl worker removal – lead level | |

[1] Action level: means employee exposure, without regard to the use of respirators, to an airborne concentration of lead of 30 micrograms per cubic meter of air (30 µg /m³) averaged over an 8-hour period.

Table 10. Permissible exposure limit (PEL) for different metals

| Metal | Permissible exposure limit (PEL) ($\mu\text{g}/\text{m}^3$) | Reference |
|---|---|--|
| As | 10.0 | CFR 29, 1910.1018 |
| Ba | | |
| Soluble compounds | 0.5 | |
| Barium sulfate | | CFR 29, 1910.1000 Table Z-1 ^[1] |
| Total dust | 15.0 | |
| Respirable fraction | 5.0 | |
| Cd | 5.0 | CFR 29, 1910.1027 |
| Cr | | |
| Chromic acid and chromates (as CrO_3) | 2.0 | |
| Chromium (II) compounds | 0.5 | CFR 29, 1910.1000 Table Z-1 |
| Chromium (III) compounds | 0.5 | CFR 29, 1910.1026 |
| Chromium (VI) compounds | 5.0 | |
| Chromium metal and insoluble salts | 1.0 | |
| Pb | 50.0 | CFR 29, 1910.1025 |
| Hg | | |
| Aryl and inorganic | 2.0 | CFR 29, 1910.1000 Table Z-1 |
| Organo alkyl compounds | 2.0 | |
| Vapor | 2.0 | |
| Se | | |
| Selenium compounds | 0.2 | CFR 29, 1910.1000 Table Z-1 |
| Selenium hexafluoride | 0.4 | |
| Ag | 0.01 | CFR 29, 1910.1000 Table Z-1 |
| Zn | | |
| Zinc chloride fume | 1.0 | |
| Zinc oxide fume | 5.0 | |
| Zinc oxide | | |
| Total dust | 15.0 | CFR 29, 1910.1000 Table Z-1 |
| Respirable fraction | 5.0 | |
| Zinc stearate | | |
| Total dust | 15.0 | |
| Respirable fraction | 5.0 | |

[1] http://www.osha.gov/pls/oshaweb/owadisp.show_document?p_table=STANDARDS&p_id=9992

determine the airborne lead concentration in a worker's breathing zone at a lead abatement site, Morley et al. (1997) used closed-faced, 37-mm cassettes with pre-loaded 0.8 micron pore size filters to sample aerosolized particles during blasting. A FP-XRF was used for analysis and compared with that of digested samples measured with the graphite furnace AAS. No significant difference was reported between the lead concentrations obtained by the two methods (p-value 0.72). As a result, NIOSH (1998) developed Method 7702 (Appendix C) for the FP-XRF analysis of air samples on filters. In another similar study, Zamurs et al. (1998) compared results of traditional laboratory filter analysis for lead by using ICP versus FP-XRF; results indicated that the latter effectively measured concentrations. In fact, a linear relationship between XRF and ICP measurements of digested samples was developed for air samples ($\text{XRF } \mu\text{g} / \text{filter} = 0.6478 \times \text{total suspended particulates [TSP]} \mu\text{g} / \text{filter} + 193.06$), and the results showed a strong correlation ($r^2 = 0.95$). Such a relationship can be used to compare lead concentrations determined by FP-XRF analysis with lead limits established for workers in bridge-cleaning activities.

Overall, XRF has been widely applied in such applications as air monitoring of particles (Morley et al., 1997; Zamurs et al., 1998), dust samples (Herman et al., 2006), soil samples (Clark et al., 1999; Sterling et al., 2004), and paint (Ashley et al., 1998; Daniels et al., 2001). XRF has been proven effective in on site analysis as demonstrated by correlations between field and laboratory results. However, based on the literature, studies to date have not been conducted on correlating field results to lab analyses evaluating whether a paint waste is a hazardous waste using the U.S. EPA TCLP (U.S. EPA, 1992).

3. Characteristic and classification of paint waste

3.1 Classification of wastewater generated on site

During rehabilitation or after paint has been removed, substrates are typically power-rinsed with high pressure water to ensure that all material is removed (Hopwood et al., 2003). Wash water also referred to as wastewater contaminated with lead paint debris as well as any metal dissolved during the removal process are generated. Regardless of the source, wastewater containing lead or paint solids must be collected, properly treated, and discharged to a permitted location to prevent water pollution. Wastewater may either be collected into drums or other containers and transported to a permitted disposal facility, or discharged in an appropriate location at or near the project site. If it is possible to discharge the wastewater to an on-site sanitary sewer, the requirements of the city or sanitary district which owns the sewer must be followed.

Hopwood et al. (2003) attempted to apply geotextile fabric to filter wastewater from bridges undergoing maintenance prior to its release. Lead concentrations both dissolved and total generated by high pressure (3,000 to 10,000 psi) washing ranged from 0 – 5.5 mg/l and 2.3 – 130 mg/l, respectively; after filtration, concentrations were 0 – 4.1 mg/l and 2.0 – 220 mg/l, respectively. These results demonstrated that the filter was ineffective in removing suspended fines or dissolved metals ions. One possible explanation for the inefficiency may be attributed to the pore size of the filter. Hopwood et al. also analyzed the water pressure, nozzle type, as well as paint parameters (thickness, adhesion, and lead content). No significant correlations were observed between the lead concentration in wash water and the factors associated with the high pressure washing. Davis and Burns (1999) found that concentrations in the runoff were a function of the intensity (flow rate/spray area) of the

synthetic rain water applied, the greater the ratio the greater the concentration.

A number of studies (Ingole and Bhole, 2003; Kucukbay et al., 2007; Pehlivan and Cetin, 2009) have relied on laboratory UV-visible spectrophotometer for evaluating metals. One method (Hach Method 8033) (Appendix D) which has been approved by the U.S. EPA (SM 3500-Pb D, Appendix E) (U. S. EPA, 1996; Eaton, et al., 2005) is a portable UV-visible spectrophotometer for total lead analysis. In this procedure, the DithiVer metals reagent (a stable powder form of dithizone, $C_{13}H_{12}N_4S$) reacts with lead ions in an alkaline solution to form a pink to red lead-dithizonate complex, which is extracted with chloroform. Extracted samples are then measured in the spectrophotometer at 515 nm. The portable spectrophotometer is an effective and convenient method for field measurements of Pb in wash water.

3.2 Leaching studies and waste classification

Environmental risk assessment of heavy metals in the solid waste involves testing leachability rather than simply measuring the total metal concentrations (Hartley et al., 2004). Hazardous wastes in a landfill run the risk of contaminating groundwater as well run off (Roussat et al., 2008). The U.S. EPA (1992) leaching tests include the TCLP and synthetic precipitation leaching procedure (SPLP) (U.S. EPA, 1994). The TCLP test is intended to mimic the worst-case scenario for disposal of waste (U.S. EPA, 1992) by simulating lower pH in a landfill environment. Briefly, the solid waste is applied at a ratio of 20:1 (liquid: solid). After mixing for 18 hours, a sample of solution is filtered and acidified (Standard Methods 3120 and 3110) (Eaton, et al., 2005) prior to metal analysis by ICP or AA. Results are compared with toxicity characteristic (TC) concentrations to determine if the

solidified/stabilized waste can be landfilled. Failure to pass TC levels (Table 11) requires treatment prior to disposal of wastes. On the other hand, the U.S. EPA SPLP was proposed to simulate conditions caused by acid rain and considers the subsequent infiltration of contaminants into groundwater (Alforque, 1996). For conditions in which leaching to groundwater is a concern (e.g., land application of waste), the SPLP leachate concentrations are generally compared to drinking water standards or some other guideline based on state regulations (e.g., New Jersey Department of Environmental Protection [NJDEP], 2008; Florida Department of Environmental Protection [FDEP], 2009).

Based on the leaching test, risk-based decision making for solid waste management is a four steps process (Townsend et al. 2003). The first step involves the classification of solid waste with regard to TC based on the TCLP leaching test. If the concentration exceeds the TC levels, a waste is hazardous and subject to RCRA Subtitle C (hazardous waste regulations). If a waste is not hazardous as defined by RCRA, the potential risk to human health and the environment, through such routes as groundwater contamination, must be evaluated when disposal and reuse options of the waste are considered. In this step, the leaching results of the SPLP test for waste materials may be compared to risk-based water quality standards or guidelines (Table 11) (NJDEP, 2008; FDEP, 2009). If the concentrations of contaminants in the SPLP leachate are greater than the standards, the waste may be disposed at an U.S. EPA authorized treatment, storage, and disposal (TSD) facility (U.S. EPA, 1998). On the other hand, if concentrations are less than the criteria, possible direct exposure should be considered for reuse options based on total concentrations of the waste (Townsend et al., 2003).

Table 11. Related waste characterization limits for the RCRA metals and zinc in wastes

| Metal | Waste code | MCL ^[3] (µg/l) | New Jersey ground water quality criterion ^[1] (µg/L) | New Jersey default leachate criteria for ground water ^[2] (µg /L) | Ground water quality standard in New York State ^[4] (µg /L) | TC ^[5] (mg/l) |
|-------|------------|------------------------------------|---|--|--|--------------------------|
| As | D004 | 10 | 0.02 | 3 ^d | 25 | 5 |
| Ba | D005 | 2000 | 6000 ^c | 78000 | 1,000 | 100 |
| Cd | D006 | 5 | 4 | 52 | 5 | 1 |
| Cr | D007 | 100 | 70 | NA | 50 | 5 |
| Pb | D008 | TT ^b Action Level=15 | 5 | 65 | 25 | 5 |
| Hg | D009 | 2 | 2 | 26 | 0.7 | 0.2 |
| Se | D010 | 50 | 40 | 520 | 10 | 1 |
| Ag | D011 | 100 ^a | 40 | 520 | 50 | 5 |
| Zn | | 5000 ^a | 2000 | 26,000 | NA | NA |

[1] New Jersey Department of Environmental Protection (NJDEP) (2008) N.J.A.C. 7: 9C. Ground water quality standard.

[2] New Jersey default leachate criteria for ground water: higher of the health-based leachate criteria or aqueous practical quantitation Levels (PQLs).

NJDEP, (June 2, 2008) Guidance for the use of the Synthetic Precipitation Leaching Procedure to Develop Site-Specific Impact to Ground Water Remediation Standards.

[3] U.S. EPA (updated to May 2009), List of contaminants & their MCLs

<http://www.epa.gov/safewater/contaminants/index.html#mcls>

MCL: Maximum Contaminant Level, the highest level of a contaminant that is allowed in drinking water.

[4] New York States Department of Environmental Conservation (NYSDEC), Regulations, Chapter X - Division of Water, Part 703: Surface water and groundwater quality standards. The text reflects revisions filed January 17, 2008 and effective February 16, 2008. <http://www.dec.ny.gov/regs/4590.html>

[5] TC level: Maximum Concentration of Contaminants for the Toxicity Characteristic.

U. S. EPA (1991b), Toxicity characteristic leaching procedure (TCLP), SW-846 Method 1311 Federal Register, 55(March 29), Washington, DC.

a. SDWR: Secondary drinking water regulations.

b. Lead and copper are regulated by a treatment technique that requires systems to control the corrosiveness of their water. If more than 10% of tap water samples exceed the action level, water systems must take additional steps. For copper, the action level is 1.3 mg/L, and for lead is 0.015 mg/L.

c. Revised via administrative change (see 39 N.J.R. 3538(a)).

d. Based on aqueous practical quantization limit (PQLs).

3.2.1 Paint waste classification with TCLP

The TCLP test is used to determine whether a material is considered a hazardous waste or non-hazardous waste. The results provided by the test determine whether the material, if placed in landfill, will possibly leach into the groundwater system. In 2004, Minnesota Department of Transportation (Mn/DOT, 2004) designed guidelines and procedures to comply with Minnesota Air Quality and Waste Management regulations for the removal of paint on steel bridge structures. Specifically, XRF was designated as an effective technique to determine the presence of lead in paint for steel bridge structures prior to blasting. For paint with greater than or equal to 0.5% (5,000 ppm) by weight or 0.5 mg/cm^2 , the blasting residue will be sent to a laboratory and analyzed with the TCLP to determine waste classification. The residue can then be transported to an appropriate TSD facility. Daniels et al. (2001) studied the effectiveness of two stabilization technologies, Blastox and PreTox 2000 fast dry, on paint waste generated from a wet abrasive blasting technology. Even with the stabilization technology, paint debris was still classified as a hazardous waste based on the TCLP test ($[\text{Pb}] > 5 \text{ mg/L}$).

As discussed earlier, a number of factors affect contaminant behavior which in turn affects leaching. Wadanambi et al. (2008) used the TCLP and the SPLP to examine leaching from LBP, where samples were obtained from a military barrack at Fort Ord, California (LBP-A) and a can of metal primer that contained red lead pigment (LBP-B). Results revealed that leached concentrations were dependent on pH as using the TCLP ($\text{pH} \leq 5.51$) they were 5–25 times greater than those observed using the SPLP ($\text{pH} \geq 5.65$). In addition, the substrate impacted the degree to which leaching occurred: drywall > wood > steel > concrete. Yet, the

average lead concentration leached for all substrate conditions except concrete exceeded the TC limit for Pb (5 mg/L); the most significant factor was that of pH.

With TCLP, wastes are classified as hazardous or non-hazardous. However, this procedure requires collecting representative samples in the field, conducting the TCLP study in the lab, and analyzing samples with either ICP-MS or AAS. Therefore this method requires lengthy periods of time and effort. Should an onsite classification method be feasible, significant time and costs may be saved.

3.2.2 Correlations observed between XRF results and TCLP or SPLP Analysis

A number of studies have found correlations between the TCLP test results and total concentrations of lead (Cao et al., 2003; Sun et al., 2006; Isaacs, 2007). Cao et al. (2003) found a linear relationship between total Pb (from digestion) and TCLP-Pb when studying the weathering of lead bullets and their environmental effect at outdoor shooting ranges. To assess the toxicity of heavy metals in contaminated soils located in a lead–zinc mine, Sun et al. (2006) measured concentrations of Cu, Zn, Pb, and Cd in soils. The resulting correlation between extractable Pb by TCLP test and total Pb measured by ICP-MS on digested samples was statistically significant ($r^2 > 0.96$). Isaacs (2007) studied lead leaching from soils and observed a significant correlation between TCLP results and total lead measured by ICP-MS on digested soil samples less than 75 μm ($r^2 = 0.82$, $P < 0.001$, $n = 13$).

Recently, NJDEP (2008) provided guidance for the use of the SPLP procedure to develop site-specific impact to ground water soil remediation standards (Figure 1). A linear regression was developed between contaminant concentrations in soil and leachate. Similarly, Florida Department of Environmental Protection (FDEP) (2009) provided guidance intended to

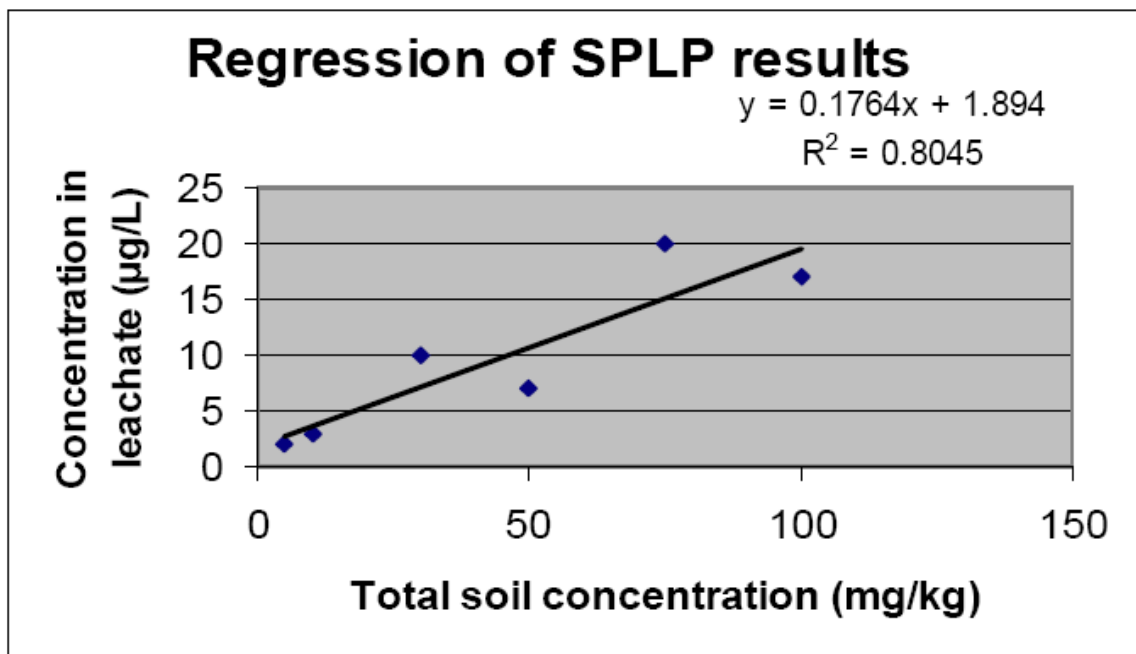


Figure 1. Relationship between contaminant concentration in soil and in leachate (NJDEP, 2008)

address application of SPLP results in establishing site-specific regulatory limits for lead in soil. Specifically, paired results for total soil contaminant concentrations versus SPLP for each sampling location were obtained. To ensure lead concentrations would be below the groundwater cleanup target level (GCTL) (drinking water standard), which is 15 µg/L in Florida, the estimated threshold based on the set of soil sampling data was approximately 250 mg/kg (Figure 2). This limit has since (FDEP, 2009) been recommended to guide remedial actions or design a risk-based approach to prevent groundwater contamination above drinking water standards. Clearly, because reliable correlations have been found between the total and leachable metal concentrations, the potential to perform direct, in situ hazardous waste classification of paint waste exists. As such, leaching studies may not be necessary and use of the FP-XRF instruments may be further advanced. In this work, a correlation between concentrations measured with FP-XRF and TCLP will be investigated to achieve in situ hazardous waste classification.

4. Conclusions

Studies of paints on bridges, buildings, and houses indicate that: 1. Lead in many of the existing paints exceed 5,000 ppm (mg/kg); 2. Zinc and mercury have been observed at elevated concentrations as great as 10,580 and 955 ppm, respectively; 3. Cadmium and chromium are not routinely observed at detectable concentrations; and, 4. Selenium, silver, and barium were not generally used. During aging and weathering, paints tend to chalk, chip, flake, and otherwise deteriorate, resulting in an accumulation of lead and other contaminants in soils or surface water surrounding painted structures. Furthermore, during maintenance, reconstruction, and demolition of bridges and other steel structures, solid waste and paint

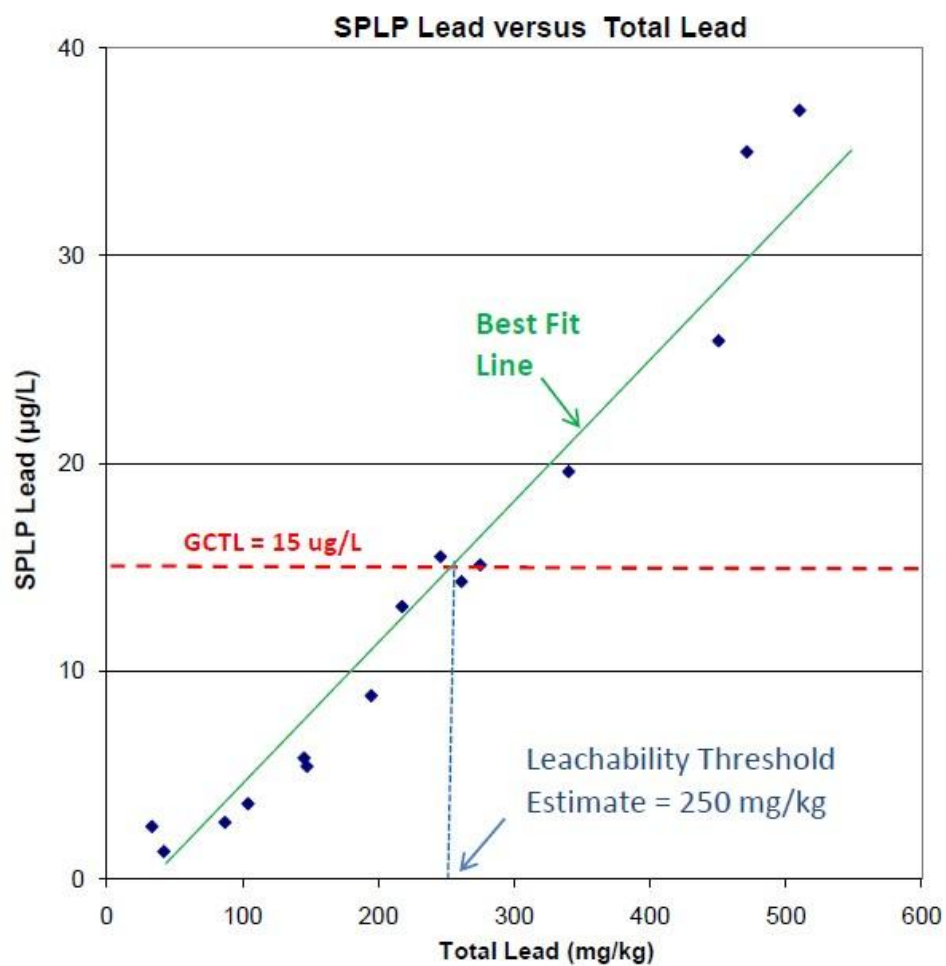


Figure 2. Relationship between the SPLP lead and total lead in the soil (FDEP, 2009).

wash water are generated on-site. FP-XRF and portable spectrophotometers are effective tools for assessing metal concentrations in bridge paint waste and wash water.

Based on the literature review, reliable correlations have been found between the total and leachable metal concentrations, the potential to perform direct, in situ hazardous classification of paint wastes exists. As such, leaching studies may not be necessary and use of the FP-XRF instruments may be further advanced. A statistical model will be developed between XRF results and TCLP to address in situ hazardous waste classification.

5. References

Alforque, M. (1996) The Newsletter of the U.S.EPA Region 10 Laboratory.

Alphen, M. (1998) Paint film components, *National Environmental Health Forum Monographs*, General Series No. 2.

Agocs, M. M., Etzel, R. A., Parrish, R. G., Paschal, D. C., Campagna, P. R., Cohen, D. S., Kilbourne, E. M., Hesse, J. L. (1990) Mercury exposure from interior latex paint, *The New England Journal of Medicine*, 323 (16): 1096–1101.

Agency for Toxic Substances and Disease Registry (ATSDR) (1999) Toxicological Profile for Mercury, U.S. Department of Health and Human Services, Public Health Service, Agency for Toxic Substances and Disease Registry. Atlanta, Georgia, 376.

Appleman, B. R. (1992) Bridge paint: removal, containment, and disposal, *Transportation Research Board*, Washington, DC.

Beusterien, K. M., Etzel, R. A., Agocs, M. M., Egeland, G. M., Socie, E. M., Rouse, M. A., Mortensen, B. K. (1991) Indoor air mercury concentrations following application of interior latex paint, *Archives of Environmental Contamination and Toxicology*, 21 (1): 62–64.

Binstock, D. A., Gutknecht, W. F., McWilliams, A. C. (2009) Lead in soil - an examination of paired XRF analysis performed in the field and laboratory ICP-AES results, *International Journal of Soil, Sediment and Water*, 2(2): 1-6.

Boxall, J., Von Fraunhofer (1977) Concise paint technology. New York: Chemical Publishing.

Boxall, J., Von Fraunhofer (1980) Paint Formulation: principles and practice. George Goodwin Limited, London.

Boyle, T.J., Fitzgerald, J. (2004) A comparison of FPXRF data with ICP/AA Data, *The Annual International Conference on Soils, Sediments and Water*, Amherst, MA.

Consumer Product Safety Improvement Act (CPSIA) (2008), Public Law 110–314, Section 101-2008.

<http://www.cpsc.gov/cpsia.Pdf>

Caravanosa, J., Weiss, A. L., Blaise, M. J., Jaeger, R. J. (2006) A survey of spatially distributed exterior dust lead loadings in New York City, *Environmental Research*, 100: 165–172.

Cao, X., Ma, L. Q., Chen, M., Hardison, Jr., D. W., & Harris, W. G. (2003) Weathering of lead bullets and their environmental effects at outdoor shooting ranges. *Journal of Environmental Quality*, 32, 526–534.

Cao, X. Dermatas, D. (2008) Evaluating the applicability of regulatory leaching tests for

assessing lead leachability in contaminated shooting range soils, *Environmental Monitoring and Assessment*, 139:1–13.

Clarkson, T. W., Friberg, L., Nordberg, G. F., Sager, P.R., eds, (1988) Biological monitoring of toxic metals. New York: Plenum Press.

Clark C. S., Menrath W., Chen M., Roda S., Succop P. (1999) Use of a field portable X-ray fluorescence analyzer to determine the concentration of lead and other metals in soil samples, *Annals of Agricultural and Environmental Medicine*, 6: 27–32.

Choe T. K., Trunov M., Menrath W., Succop P., Grinshpun A. S. (2002) Relationship between lead levels on painted surfaces and percent lead in the particles aerosolized during lead abatement, *Applied Occupational and Environmental Hygiene*, 17(8): 573–579.

Conroy, L. M., Menezes-Lindsay, R. M., Sullivan, P. M., Cali, S., Forst, L. (1996) Lead, chromium, and cadmium exposure during abrasive blasting, *Archives of Environmental Health*, 51 (2): 95-99.

Clark, C. S., Thuppil, V., Clark, R., Sinha, S., Menezes, G., D'Souza, H., Nayak, N., Kuruvilla, A., Law, T., Dave, P., Shah, S. (2005) lead in paint and soil in Karnataka and Gujarat, India, *Journal of Occupational and Environmental Hygiene*, 2 (1): 38-44.

Clark, C. S., Rampal, K.G., Thuppil, V., Chend, C.K., Clark, R., Roda, S. (2006) The lead content of currently available new residential paint in several Asian countries, *Environmental Research*, 102: 9–12.

Crown, D. A. (1968) Forensic examination of paints and pigments, Table II, Charles C Thomas, Publisher, Ltd., Springfield, Illinois.

Davis, A. P., Burns, M. (1999) Evaluation of lead concentration in runoff from painted structures, *Water Resource*, 33 (13): 2949-2958.

Daniels, A. E., Kominsky, J. R., Clark, P. J. (2001) Evaluation of two lead-based paint removal and waste stabilization technology combinations on typical exterior surfaces, *Journal of Hazardous Materials*, B87: 117–126.

Department of Environmental Resources, (1993) Water Quality Sampling and Monitoring, Prince George's County, Maryland, Prince Georges County Government, Watershed Protection Branch, Largo MD.

Eaton, A. D., Clesceri, L. S., Rice, E. W., Greenberg, A. E. (2005) Standard methods for the examination of water and wastewater, 21st edition, 3: 79-81.

Falk, R. H., Janowiak, J.J., Cosper, S. D., Drozd, S. A., (2005) Remilling of salvaged wood

siding coated with lead-based paint, Part I. Lead exposure, *Forest Products Journal*, 55 (7/8): 76-80.

FHWA (1991) *Lead-Containing Paint Removal, Containment, and Disposal*, Publication No.FHWA-RD-91-100, Federal Highway Administration, Washington, D.C.

Francek M. A. (1992) Soil lead levels in a small town environment: a case study from Mt. Pleasant, Michigan. *Environmental Pollution*, 76(3): 251-257.

Ferlauto, E. C. (1994) Lead based paint and the lead abatement issue in the United States, *Journal of Coatings Technology*, 66 (834): 69-74.

Florida Department of Environmental Protection (FDEP), Bureau of Waste Cleanup (2009) Guidance for determining leachability by analysis of SPLP results, Tallahassee, FL.

Gooch, J. W., *Lead-Based Paint Handbook*, Plenum Press, New York, 1993.

Hirschman, S. Z., Feingold, M., Boylen, G. (1963) Mercury in house paint as a cause of acrodynia. *The New England Journal of Medicine*, 269: 889–893.

Huang, S. L., Yin, C. Y., Yap S. Y. (2010) Particle size and metals concentrations of dust from a paint manufacturing plant, *Journal of Hazardous Materials*, 174: 839–842.

Hopwood, T., Palle, S., Younce, R. (2003) Environmental impacts of bridge cleaning operations, *Research Report*, University of Kentucky.

Hartley, W., Edwards, R., Lepp, N. W. (2004) Arsenic and heavy metal mobility in iron oxide-amended contaminated soils as evaluated by short- and long-term leaching tests, *Environmental Pollution*, 131: 495–504.

Isaacs, L. K. (2007) Lead leaching from soils and in storm waters at twelve military shooting ranges, *Journal for Hazardous Substance Research*, 6: 1-30.

Ingole, N.W., Bhole, A.G.(2003) Removal of heavy metals from aqueous solution by water hyacinth (*Eichhornia crassipes*), *Journal of Water Supply: Research and Technology - AQUA*, 52 (2): 119-128.

International Agency for Research on Cancer (IARC) (1987) monographs on the evaluation of carcinogenic risk of chemicals to man, Supplement 7, Lyon, France: World Health Organization, International Agency for Research on Cancer.

Kilbride, C., Poole, J. Hutchings, T. R. (2006) A comparison of Cu, Pb, As, Cd, Zn, Fe, Ni and Mn determined by acid extraction/ICP-OES and ex situ field portable X-ray fluorescence analyses, *Environmental Pollution*, 143: 16-23.

Kucukbay, F. Z. (2007) Investigation of some chemical and physical parameters in water and

sediment samples of Karakaya dam lake (Malatya-Turkey), *International Journal of Pure & Applied Chemistry*, 2(3): 303-308.

Levin, S. M., Goldberg, M., Doucette, J. T. (1997) The effect of the OSHA lead exposure in construction standard on blood lead levels among iron workers employed in bridge rehabilitation, *American of Industrial Medicine*, 31: 303–309.

Marra, C., Kopmann, J. (2009) Field methods for determining lead content in bridge paint removal waste, Final Progress and Literature Review, Rowan University.

Markey, M. A., Clark, C.S., Succop, A. P., Roda, S. (2008) Determination of the feasibility of using a portable X-Ray fluorescence (XRF) analyzer in the field for measurement of lead content of sieved soil, *Journal of Environmental Health*, 70 (7): 24-29.

Mielke, H. W., Powell, E., Shah, A., Gonzales, C., Mielke, P.W. (2001) Multiple metal contamination from house paints: consequences of power sanding and paint scraping in New Orleans, *Environmental Health Perspectives*, 109, (9): 973–978.

Mielke, W. H., Gonzales, C. (2008) Mercury (Hg) and lead (Pb) in interior and exterior New Orleans house paint films, *Chemosphere*, 72: 882–885.

Morley, J. C. (1997) Evaluation of a portable x-ray fluorescence instrument for the determination of lead in workplace air samples [Thesis], Cincinnati, OH: University of Cincinnati, Department of Environmental Health, College of Medicine.

Morley, J. C., Clark, C. S., Deddens, J. A., Ashley, K, Roda S. (1999) Evaluation of a portable X-Ray fluorescence instrument for the determination of lead in work place air samples, *Applied Occupational and Environmental Hygiene*, 14:306–316.

Morbidity and Mortality Weekly Report (MMWR), (1990) Mercury exposure from interior latex paint–Michigan, 39 (8): 125–126.

National Paint and Coatings Association (1992) Preventing childhood lead exposure: putting the issues in perspective.

National Institute for Occupational Safety and Health (1992) Health Hazard Evaluation Report: HUD Lead-Based Paint Abatement Demonstration Project, DHHS (NIOSH) Pub. No. 90-070-2181. NIOSH, Cincinnati, OH.

National Institute for Occupational Safety and Health (1998) NIOSH Manual of Analytical Methods, 4th ed., DHHS (NIOSH) Pub. No. 94-113. NIOSH, Cincinnati, OH.

New Jersey Department of Environmental Protection (NJDEP), (2008) Guidance for the use of the Synthetic Precipitation Leaching Procedure to develop site-specific impact to ground

water remediation standards.

New York State Department of Transportation (2008) Standard Specifications of May 1, 2008, Section 550 Structures.

<https://www.nysdot.gov/main/business-center/engineering/specifications/english-spec-repository/section550.pdf>

Occupational Safety and Health Administration: 58 Federal Register 26590, Lead Exposure in Construction, Interim rule (1993 revised in 1999).

Oil and Color Chemists Association, Australia, (1983) Surface Coating: Raw Materials and Their Usage, second ed., Chapman and Hall, New York, 1: 299–300.

Pehlivan, E., Cetin, S. (2009) Sorption of Cr(VI) ions on two Lewatit-anion exchange resins and their quantitative determination using UV-visible spectrophotometer, *Journal of Hazardous Materials*, 163(1): 448-453.

Roussat, N., Me hu, J., Abdelghafour, M., Brula, P. (2008) Leaching behavior of hazardous demolition waste, *Waste Management*, 28: 2032–2040.

Radu, T., Diamond, D. (2009) Comparison of soil pollution concentrations determined using AAS and portable XRF techniques, *Journal of Hazardous Materials*, 171 (1-3): 1168-1171.

Saaco, A. M., Bass, J. (2000) Application of a portable XRF instrument for field measurement of lead on TSP filters, in: *Proceedings of the Eighth International Conference on On-Site Analysis — the Lab Comes to the Field*, Lake Las Vegas, NV.

Sun, Y. F., Xie, Z. M., Li, J., Xu, J. M., Chen, Z. L., Naidu, R. (2006) Assessment of toxicity of heavy metal contaminated soils by the toxicity characteristic leaching procedure, *Environmental Geochemistry and Health*, 28: 73-78.

Sussell, A., M.P.H., C.I.H. (1997) Protecting workers exposed to lead-based paint hazards, A Report to Congress.

Tellus Institute (1993) Alternatives to solvent-based paints, Technical Report No. 4. Prepared for The Toxics Use Reduction Institute, University of Massachusetts Lowell

Townsend, T., Jang, Y. C., Tolaymat, T. (2003) A guide to the use of leaching tests in solid waste management decision making, Department of Environmental Engineering Sciences University of Florida.

[http://www.hinkleycenter.com/publications/0301\(A\)_A%20Guide%20to%20Leaching%20Tests-Final.pdf](http://www.hinkleycenter.com/publications/0301(A)_A%20Guide%20to%20Leaching%20Tests-Final.pdf)

The Society for Protective Coatings (SSPC), (1993) Lead Paint Bulletin-special issue.

U.S. Environmental Protection Agency (U.S. EPA) Phenyl mercuric acetate listing

background document for the inorganic chemical listing determination. August, 2000.

<http://www.epa.gov/waste/hazard/wastetypes/wasteid/inorchem/docs/phenyl.pdf>

U.S. Environmental Protection Agency (U.S. EPA) Mercury; Consumer Products Containing Mercury, Table <http://www.epa.gov/osw/hazard/tsd/mercury/con-prod.htm>

U.S. Environmental Protection Agency (U.S. EPA) (1998) *Federal Register*, FR 63(243), 70190–70233, Washington, DC.

U.S. Environmental Protection Agency (U.S. EPA) (1996) *Federal Register*, FR 61(45), 9064–9088, Washington, DC.

U.S. Environmental Protection Agency (U.S. EPA) (2001) *Federal Register*, FR 66(4) Rules and Regulations, Residential Lead Hazard Standards - TSCA Section 403, Washington, DC. <http://www.epa.gov/lead/pubs/leadhaz.htm>

U.S. Environmental Protection Agency (U.S. EPA) (2009) List of Contaminants & their MCLs <http://www.epa.gov/safewater/contaminants/index.html>

U.S. Environmental Protection Agency (U.S. EPA) (2003) Test Methods for Evaluating Solid Waste, SW-846, third ed., Office of Solid Waste and Emergency Response, EPA, Washington, DC.

<http://www.epa.gov/epawaste/hazard/testmethods/sw846/pdfs/3050b.pdf>

U.S. Environmental Protection Agency (U.S. EPA) (1996) Approved/Accepted Hach Methods, Cincinnati, OH.

U.S. Environmental Protection Agency (U.S. EPA) (1998) Method 6200, Field portable X-ray fluorescence spectrometry for the determination of elemental concentrations in soil and sediment (EPA/600/R-97/150, Revision 0), Retrieved November 1, 2007.

U.S. Environmental Protection Agency (U.S. EPA) (1992) Toxicity Characteristic Leaching Procedure (TCLP), SW-846 Method 1311, *Federal Register*, 55(March 29), Washington, DC.

U.S. Environmental Protection Agency (U.S. EPA) (1995) A field test of Lead-Based Paint testing technologies: *Summary Report*, EPA-747-R-95-002a, Washington, DC.

U.S. Environmental Protection Agency (U.S. EPA) (1998) *Federal Register*, 63(243), 70190–70233, Washington, DC.

U.S. Environmental Protection Agency (U.S. EPA) (1994) SW-846 Method 1312 Update 1: Synthetic Precipitation Leaching Procedure (SPLP), Office of Solid Waste, EPA: Washington, DC.

U.S. Environmental Protection Agency (U.S. EPA) (1996) Lead exposure associated with renovation and remodeling activities: *Summary Report*, EPA-747-R-96e005, Washington, DC.

U.S. Environmental Protection Agency (U.S. EPA) (1999a) Lead exposure associated with renovation and remodeling activities: Phase III, Wisconsin Childhood Blood-Lead Study, EPA-747-R-99e002, Washington, DC.

U.S. Environmental Protection Agency (U.S. EPA) (2001) Economic analysis of EPA's direct final rule amending, *Federal Register*, 40CFR, part 257 and 258.

U.S. Environmental Protection Agency (U.S. EPA) (2001) Federal Register, FR 66(4), 1205–1240, Washington, DC.

U.S. Occupational Safety and Health Administration (1993) Lead exposure in construction: interim final rule (29 CFR 1926.62). *Federal Register* 58: 26590-26649. Washington, DC.

U.S. Consumer Products Safety Commission (U. S. CPSC), (1977) Notice reducing allowable levels of lead. *Final Rule*, *Federal Register* 42 (1): 44199.

Wadanambi, L., Dubey, B., Townsend, T. (2008) The leaching of lead from lead-based paint in landfill environments, *Journal of Hazardous Materials*, 157: 194-200.

Weast, R.C. (1978) CRC Handbook of Chemistry and Physics, 59th ed. Chemical rubber Company Press, Boca Ration, Florida.

Weaver, J. C. (1989) A white paper on white lead. Why whitewash dirty lead dust from gasoline? *ASTM Standardization News*.

Zamurs, J., Bass, J., Williams, B., Fritsch, R., Sackett, D., Heman, R. (1998) Real-time measurement of lead in ambient air during bridge paint removal. *Transportation Research Record*, 1641:29-38.

Appendices

A. Inorganic pigments

B. U.S. EPA Method 6200

C. NIOSH Method 7702

D. Hach Method 8033

E. Proved/Accepted Hach Methods letter from U. S. EPA

Appendix A

Inorganic pigments

Inorganic pigments

| Name | Formula | Comments | Pigment |
|--------------------------------------|--|--|------------------------------------|
| Aluminosilicates | | Muscovite mica Phlogopite mica Pyrophyllite Talc Lepidolite Biotite | |
| Antimony Black | Sb_2S_3 | Some use in camouflage paints. | C. I. # 77050 |
| Antimony Vermillion | Sb_2S_3 or Sb_2S_5 or Sb_2O_3 | Discovered 1842, produced after 1847, minor use by artists | Pigment Red 107 C. I. # 77060 |
| Antimony White | Sb_2O_3 | Introduced 1919, widely used between 1930 and 1942 for buildings and vehicles | Pigment White 11 C. I. # 77052 |
| Azurite | $2\text{CuCO}_3 \cdot \text{Cu}(\text{OH})_2$ | Minor use | Pigment Blue 30 C. I. # 77420 |
| Barium Carbonate | BaCO_3 | | Pigment White 10 C. I. # 77099 |
| Barium Potassium Chromate | $\text{BaK}_2 (\text{CrO}_4)_2$ | Used as a metal primer. Produced after 1945. | Pigment Yellow 31 C. I. # 77103 |
| Barium White mixtures and white lead | BaSO_4 Dutch White 80:20 Hamburg White 65:35 Venetian White 50:50 | | Pigment White 21, 22 |
| Basic Lead Silicate | SiO_2 with rind of PbSiO_3 and $2\text{PbSO}_4 \cdot \text{PbO}$ | First available 1947. | |
| Basic Lead Silico Chromate | $\text{PbO} \cdot \text{SiO}_2 \cdot \text{CrO}_3$ 47:47:6 | Used for primer and finishing coat for steel | |

| Name | Formula | Comments | Pigment |
|--------------------------|--|--|---|
| Basic Lead Sulfate | $5\text{PbSO}_4 \cdot \text{PbO}$ or $2\text{PbSO}_4 \cdot \text{PbO}$ or $\text{PbSO}_4 \cdot \text{PbO}$ | Widely used as a primer and in building finishes. First introduced between 1855 and 1866, leaded zinc oxide form introduced in 1896. | Pigment White 2 C. I. # 77633 |
| Black Iron Oxide | $\text{FeO} \cdot \text{Fe}_2\text{O}_3$ or $\text{Fe}(\text{OH})_2 \cdot \text{Fe}_2\text{O}_3$ | Traces of SiO_2 and Al_2O_3 in natural forms | Pigment Black 11 C. I. # 77499 |
| Brunswick Green | Chrome Yellow, Iron Blue and Barium White | | |
| Cadmium Green | Cadmium Yellow and Cobalt Blue | | Pigment Green 14 C. I. # 77199, 77436 |
| Cadmium Orange | CdS | Commercially available in 1846 | Pigment Orange 20 C. I. # 77199 |
| Cadmium Orange Lithopone | $\text{CdS} \cdot \text{CdSe}$ and BaSO_4 plus ZnS possibly | First used around 1926 | |
| Cadmium Red | $3\text{CdS} \cdot 2\text{CdSe}$ | First produced commercially around 1910 | Pigment Red 108, Pigment Yellow 37 C. I. # 77196, 77199 |
| Cadmium Red Selenide | CdSe | Became available around 1925 | Pigment Red 108 C. I. # 77196 |
| Cadmium Selenide Orange | $\text{CdS} \cdot \text{CdSe}$ | First commercial production after 1910 | Pigment Yellow 37, 108 |
| Cadmium Yellow | CdS plus ZnS usually | Discovered 1817, commercially available after 1846. | Pigment Yellow 37 C. I. # 77199 |
| Cadmium Yellow Lithopone | Cadmium yellow, barium white and zinc sulfide or cadmium yellow and barium white | First used in 1926. | Pigment Yellow 35 C. I. # 77117 |
| Calcium Plumbate | Ca_2PbO_4 | Minor current use in primers. | Pigment Brown 10 C. I. # 77227 |
| Carbon Black | 80-95% carbon | Traces of S and organic matter. | Pigment Black, 6, 7, 8 C. I. # 77266, 77268. |

| Name | Formula | Comments | Pigment |
|--------------------------|--|--|--|
| Cerulean Blue | $\text{CoO} \cdot n\text{SnO}_2$ plus CaSO_4 | Introduced in 1860. Used by artists. | Pigment Blue 35 C. I. # 77368. |
| Chrome Green | PbCrO_4 and $\text{Fe}_4(\text{Fe}(\text{CN})_6)_3$ coprecipitated | Probably first used around 1825 | Pigment Green 15 C. I. # 77520 , 77600 ,77601 or 77603 |
| Chrome Orange | PbCrO_4 and $\text{Pb}(\text{OH})_2$ or $\text{PbCrO}_4 \cdot \text{PbO}$ and PbSO_4 sometimes | Discovered 1809, commercial production began in 1818 | Pigment Orange 21 C. I. # 77601 |
| Chrome Red | $\text{PbCrO}_4 \cdot \text{Pb}(\text{OH})_2$ and PbSO_4 possibly | Discovered 1809 | Pigment Red 103 C. I. # 77601 |
| Chrome Yellow | $\text{PbCrO}_4 + \text{PbSO}_4$ with $\text{Al}(\text{OH})_3$ sometimes | Discovered 1809, commercially available after 1818. | Pigment Yellow 34 C. I. # 77600, 77603 |
| Chromium Green | Cr_2O_3 | Discovered 1797, first used by artists in 1862 | Pigment Green 17 C. I. # 77288 |
| Cobalt Blue | $\text{CoO} \cdot \text{Al}_2\text{O}_3$ or $\text{Co}_3\text{O}_4 \cdot 2\text{Al}_2\text{O}_3$ | Discovered 1802. | Pigment Blue 28 C. I. # 77346 |
| Cobalt Green | $\text{CoO} \cdot \text{ZnO}$ | Discovered in 1780, first mentioned in the literature in 1835 | Pigment Green 19 C. I. # 77335 |
| Copper Blue | CuS | Minor current use | Pigment Blue 34 C. I. # 77450 |
| Copper Maroon | $\text{CuK} \cdot \text{Fe}(\text{CN})_6$ | Relatively recent product | |
| Copper Red | Cu_2O | Now obsolete | C. I. # 77402 |
| Cuprous Sulphide | Cu_2S | Used in antifouling paints. | C. I. # 77449 |
| English Vermillion | HgI_2 | Now obsolete | |
| Florentine Brown | $\text{Cu}_2\text{Fe}(\text{CN})_6 \cdot x\text{H}_2\text{O}$ | First mentioned in literature 1849. | Pigment Brown 9 C. I. # 77430 |
| Gypsum | $\text{CaSO}_4 \cdot 2\text{H}_2\text{O}$ or CaSO_4 | Not used on iron and steel surfaces | Pigment White 25 C. I. # 77231 |
| Hydrated Cupric Oxide | $4\text{CuO} \cdot \text{H}_2\text{O}$ | Some current use as a primer. | |

| Name | Formula | Comments | Pigment |
|-------------------|---|---|---|
| Iron Blue | $\text{Fe}_4(\text{Fe}(\text{CN})_6)_3$ plus K, Na and NH_4 salts. | Discovered 1704. Widely used. Also known as Prussian Blue | Pigment Blue 27 C. I. # 77510, 77520 |
| Iron Titanate | FeTiO_3 | First introduced 1865. | Pigment Black 12 C. I. # 77543 |
| Lead Cyanamide | $\text{Pb}(\text{CN})_2$ | Currently used in primer coatings. First produced in Germany 1928. | Pigment Yellow 48 C. I. # 77610 |
| Lead Sulphate | PbSO_4 | | Pigment White 3 C. I. # 77630 |
| Lead Titanate | PbTiO_3 or PbTiO_3 plus $\text{PbSO}_4 \cdot \text{PbO}$ | Commonly used in the Netherlands as a primer and in architectural finishes. Minor use in USA. First mentioned in the literature in 1936 | Pigment Yellow 47 C. I. # 77645 |
| Lithopone | ZnS plus BaSO_4 | First discovered 1847, commercially produced 1874, lightfast varieties since the 1920's. | Pigment White 5 C. I. # 77115 |
| Magnesite | MgCO_3 | Some use in some English flat finish paints. | Pigment White 18 C. I. # 77713 |
| Magnesium Ferrite | $\text{Fe}_2\text{O}_3 \cdot \text{MgO}$ | A recent development. | |
| Manganese Black | MnO_2 | | Pigment Black 14 C. I. # 77728 |
| Manganese Blue | $\text{BaMnO}_4 \cdot \text{BaSO}_4$ 11:89 | Fist mentioned in literature 1935. Minor use by artists. | Pigment Blue 33 C. I. # 77112 |
| Manganese White | MnCO_3 | Minor use | C. I. # 77723 |
| Mercadium Orange | CdS plus HgS | First offered commercially January 1956 | Pigment Orange 23 C. I. # 77201 |
| Mercadium Red | $\text{HgS} \cdot \text{CdS}$ | First offered commercially after 1956 | Pigment Red 113 C. I. # 77201 |
| Mercuric Arsenate | HgHAsO_4 | Minor use in waterproofing and anti-fouling paints | C. I. # 77762 |
| Mineral Black | $\text{AlHSi}_2\text{O}_6 \cdot \text{C}$ | | Pigment Black 18 C. I. # 77011 |

| Name | Formula | Comments | Pigment |
|---------------------|--|--|---|
| Mineral Grey | AlHSi_2O_6 | | Pigment Black 19 C. I. # 77017 |
| Mineral Orange | Pb_4O_5 or Pb_3O_4 | Minor use | |
| Mineral Yellow | $\text{PbCl}_2 \cdot 5\text{-}7\text{PbO}$ | Patented in 1871. Used by artists. | Pigment Yellow 30 C. I. # 77592 |
| Molybdate Orange | PbCrO_4 , PbMoO_4 and PbSO_4 | First produced commercially after 1935 | Pigment Red 104 C. I. # 77605 |
| Naples Yellow | PbSb_2O_6 or $\text{Pb}_3(\text{SbO}_4)_2$ or $\text{PbO} \cdot \text{Sb}_2\text{O}_5$ sometimes with ZnO and BiO | Used by artists. | Pigment Yellow 41 C. I. # 77588, 77589 |
| Nickle Iron Blue | $\text{Ni}_2\text{Fe}_2(\text{Fe}(\text{CN})_6)_3$ | Available after 1938 | |
| Orpiment | As_2S_3 or As_2S_2 | Used by artists to the end of the 18th century. | Pigment Yellow 39 C. I. # 77085, 77086 |
| Paris Green | $\text{CuOAs}_2\text{O}_3 \cdot \text{Cu}(\text{C}_2\text{H}_3\text{O}_2)_2$ or $\text{Cu}(\text{C}_2\text{H}_3\text{O}_2)_2 \cdot 3\text{CuAs}_2\text{O}_4$ | Still used in anti-fouling paints. First produced 1814, once used in architectural finishes | Pigment Green 21 C. I. # 77410 |
| Plessy's Green | $\text{CrPO}_4 \cdot 4\text{H}_2\text{O}$ | Common in primer coatings and vehicle finishes. Formerly used by artists, now obsolete. | Pigment Green 17 C. I. # 77298 |
| Prussian Green | $\text{FeCo}_2(\text{CN})_6 \cdot x\text{H}_2\text{O}$ | Minor use, now obsolete | |
| Realgar | As_2S_2 or AsS | An artist pigment | |
| Red Iron Oxide | $\text{Fe}_2\text{O}_3 \cdot \text{Al}_2\text{O}_3 \cdot \text{SiO}_2$, CaSO_4 and MgCO_3 possibility | Artificial forms available since 1850's | Pigment Red 101, 102 C. I. # 77015, 77491, 77538 |
| Red Lead | Pb_3O_4 or $\text{PbO}_2 \cdot 2\text{PbO}$ | Primer coating | Pigment Red 105 C. I. # 77578 |
| Scarlet Chrome | $\text{PbCrO}_4 \cdot \text{PbSO}_4 \cdot \text{PbMoO}_4$ | First produced commercially 1935 | |
| Scheele's Green | CuHAsO_3 or $3\text{CuAs}_2\text{O}_3 \cdot x\text{H}_2\text{O}$ | First prepared 1778, now obsolete in architectural finishes, some use in anti- fouling paints. | Pigment Green 22 C. I. # 77412 |

| Name | Formula | Comments | Pigment |
|--------------------|--|---|---|
| Sienna | $\text{Fe}_2\text{O}_3 \cdot \text{Al}_2\text{O}_3 \cdot \text{SiO}_2 \cdot 2\text{H}_2\text{O}$ | | |
| Umber | $\text{Fe}_2\text{O}_3 \cdot \text{Al}_2\text{O}_3 \cdot \text{SiO}_2 \cdot 2\text{H}_2\text{O} \cdot \text{MnO}_2$ | | |
| Silicon Nitride | Si_3N_4 | | C. I. # 77811 |
| Strontium White | SrSO_4 | Only minor use prior to 1927 | C. I. # 77845 |
| Strontium Yellow | SrCrO_4 | Declining use in primers and building paints. | Pigment Yellow 32 C. I. # 77839 |
| Sublimed Blue Lead | $\text{PbSO}_4 \cdot \text{PbO} \cdot \text{PbS} \cdot \text{PbSO}_3 \cdot \text{ZnO} \cdot \text{C}$ | Used in primer coatings. Was in use around turn of the 20th century | |
| Titanated Barytes | $\text{TiO}_2 + \text{BaSO}_4$ | First produced between 1918 and 1920 | |
| Titanated Gypsum | $\text{TiO}_2 + \text{CaSO}_4$ | Commonly used. 50%:50% mixtures marketed after 1952 | |
| Titanium Green | Co_2TiO_4 | Discovered in 1934, minor use. | |
| Verdigris | $\text{Cu}(\text{C}_2\text{H}_3\text{O}_2)_2 \cdot \text{H}_2\text{O}$ or $\text{Cu}_3(\text{OH})_2(\text{C}_2\text{H}_3\text{O}_2)_4$ | Used in anti-fouling paints. Former use in artists paints. | |
| Vermilion | HgS | Use declining | Pigment Red 106 C. I. # 77766 |
| Viridian | $\text{Cr}_2\text{O}_3 \cdot 2\text{H}_2\text{O}$ | Introduced 1838, patented 1859, marketed as an artist's color 1862 | Pigment Green 18 C. I. # 77289 |
| White Lead | $3\text{-}6\text{PbCO}_3 \cdot \text{Pb}(\text{OH})_2$ $2 \text{ PbCO}_3 \cdot \text{Pb}(\text{OH})_2$ or $4 \text{ PbCO}_3 \cdot \text{Pb}(\text{OH})_2 - \text{PbO}$ | | Pigment White 1 C. I. # 77597 |
| Yellow Ochre | $\text{Fe}(\text{OH})_2$ and $\text{Al}_2\text{O}_3 \cdot \text{SiO}_2$ plus trace CaSO_4 and Mg occasionally. Artificial form $\text{Fe}_2\text{O}_3 \cdot \text{H}_2\text{O}$ | | Pigment Yellow 42 , 43 C. I. # 77492 |

| Name | Formula | Comments | Pigment |
|----------------|---|---|--|
| Zinc Green | ZnCrO_4 plus $\text{Fe}_4(\text{Fe}(\text{CN})_6)_3$ | | Pigment Green 16 C. I. # 77955 plus 77525 or 77607 |
| Zinc Sulfide | ZnS or $\text{ZnS} \cdot \text{H}_2\text{O}$. | First used ca 1852, major use after 1927 | Pigment White 7 C. I. # 77975 |
| Zinc White | ZnO | First produced on a commercial scale around 1835 | Pigment White 4 C. I. # 77947 |
| Zinc-Iron Blue | $\text{Zn}_2\text{Fe}_2(\text{Fe}(\text{CN})_6)_3$ | Minor use | C. I. # 77530 |

[1] Crown (1968) The Forensic Examination of Paints and Pigments Table II, Courtesy of Charles C Thomas, Publisher, Ltd., Springfield, Illinois.

Appendix B

U.S. EPA Method 6200

METHOD 6200

FIELD PORTABLE X-RAY FLUORESCENCE SPECTROMETRY FOR THE DETERMINATION OF ELEMENTAL CONCENTRATIONS IN SOIL AND SEDIMENT

SW-846 is not intended to be an analytical training manual. Therefore, method procedures are written based on the assumption that they will be performed by analysts who are formally trained in at least the basic principles of chemical analysis and in the use of the subject technology.

In addition, SW-846 methods, with the exception of required method use for the analysis of method-defined parameters, are intended to be guidance methods which contain general information on how to perform an analytical procedure or technique which a laboratory can use as a basic starting point for generating its own detailed Standard Operating Procedure (SOP), either for its own general use or for a specific project application. The performance data included in this method are for guidance purposes only, and are not intended to be and must not be used as absolute QC acceptance criteria for purposes of laboratory accreditation.

1.0 SCOPE AND APPLICATION

1.1 This method is applicable to the in situ and intrusive analysis of the 26 analytes listed below for soil and sediment samples. Some common elements are not listed in this method because they are considered "light" elements that cannot be detected by field portable x-ray fluorescence (FPXRF). These light elements are: lithium, beryllium, sodium, magnesium, aluminum, silicon, and phosphorus. Most of the analytes listed below are of environmental concern, while a few others have interference effects or change the elemental composition of the matrix, affecting quantitation of the analytes of interest. Generally elements of atomic number 16 or greater can be detected and quantitated by FPXRF. The following RCRA analytes have been determined by this method:

| Analytes | CAS Registry No. |
|---------------|------------------|
| Antimony (Sb) | 7440-36-0 |
| Arsenic (As) | 7440-38-0 |
| Barium (Ba) | 7440-39-3 |
| Cadmium (Cd) | 7440-43-9 |
| Chromium (Cr) | 7440-47-3 |
| Cobalt (Co) | 7440-48-4 |
| Copper (Cu) | 7440-50-8 |
| Lead (Pb) | 7439-92-1 |
| Mercury (Hg) | 7439-97-6 |
| Nickel (Ni) | 7440-02-0 |
| Selenium (Se) | 7782-49-2 |
| Silver (Ag) | 7440-22-4 |
| Thallium (Tl) | 7440-28-0 |
| Tin (Sn) | 7440-31-5 |

| Analytes | CAS Registry No. |
|--------------|------------------|
| Vanadium (V) | 7440-62-2 |
| Zinc (Zn) | 7440-66-6 |

In addition, the following non-RCRA analytes have been determined by this method:

| Analytes | CAS Registry No. |
|-----------------|------------------|
| Calcium (Ca) | 7440-70-2 |
| Iron (Fe) | 7439-89-6 |
| Manganese (Mn) | 7439-96-5 |
| Molybdenum (Mo) | 7439-93-7 |
| Potassium (K) | 7440-09-7 |
| Rubidium (Rb) | 7440-17-7 |
| Strontium (Sr) | 7440-24-6 |
| Thorium (Th) | 7440-29-1 |
| Titanium (Ti) | 7440-32-6 |
| Zirconium (Zr) | 7440-67-7 |

1.2 This method is a screening method to be used with confirmatory analysis using other techniques (e.g., flame atomic absorption spectrometry (FLAA), graphite furnace atomic absorption spectrometry (GFAA), inductively coupled plasma-atomic emission spectrometry, (ICP-AES), or inductively coupled plasma-mass spectrometry, (ICP-MS)). This method's main strength is that it is a rapid field screening procedure. The method's lower limits of detection are typically above the toxicity characteristic regulatory level for most RCRA analytes. However, when the obtainable values for precision, accuracy, and laboratory-established sensitivity of this method meet project-specific data quality objectives (DQOs), FPXRF is a fast, powerful, cost effective technology for site characterization.

1.3 The method sensitivity or lower limit of detection depends on several factors, including the analyte of interest, the type of detector used, the type of excitation source, the strength of the excitation source, count times used to irradiate the sample, physical matrix effects, chemical matrix effects, and interelement spectral interferences. Example lower limits of detection for analytes of interest in environmental applications are shown in Table 1. These limits apply to a clean spiked matrix of quartz sand (silicon dioxide) free of interelement spectral interferences using long (100 -600 second) count times. These sensitivity values are given for guidance only and may not always be achievable, since they will vary depending on the sample matrix, which instrument is used, and operating conditions. A discussion of performance-based sensitivity is presented in Sec. 9.6.

1.4 Analysts should consult the disclaimer statement at the front of the manual and the information in Chapter Two for guidance on the intended flexibility in the choice of methods, apparatus, materials, reagents, and supplies, and on the responsibilities of the analyst for demonstrating that the techniques employed are appropriate for the analytes of interest, in the matrix of interest, and at the levels of concern.

In addition, analysts and data users are advised that, except where explicitly specified in a regulation, the use of SW-846 methods is *not* mandatory in response to Federal testing requirements. The information contained in this method is provided by EPA as guidance to be used by the analyst and the regulated community in making judgments necessary to generate results that meet the data quality objectives for the intended application.

1.5 Use of this method is restricted to use by, or under supervision of, personnel appropriately experienced and trained in the use and operation of an XRF instrument. Each analyst must demonstrate the ability to generate acceptable results with this method.

2.0 SUMMARY OF METHOD

2.1 The FPXRF technologies described in this method use either sealed radioisotope sources or x-ray tubes to irradiate samples with x-rays. When a sample is irradiated with x-rays, the source x-rays may undergo either scattering or absorption by sample atoms. This latter process is known as the photoelectric effect. When an atom absorbs the source x-rays, the incident radiation dislodges electrons from the innermost shells of the atom, creating vacancies. The electron vacancies are filled by electrons cascading in from outer electron shells. Electrons in outer shells have higher energy states than inner shell electrons, and the outer shell electrons give off energy as they cascade down into the inner shell vacancies. This rearrangement of electrons results in emission of x-rays characteristic of the given atom. The emission of x-rays, in this manner, is termed x-ray fluorescence.

Three electron shells are generally involved in emission of x-rays during FPXRF analysis of environmental samples. The three electron shells include the K, L, and M shells. A typical emission pattern, also called an emission spectrum, for a given metal has multiple intensity peaks generated from the emission of K, L, or M shell electrons. The most commonly measured x-ray emissions are from the K and L shells; only metals with an atomic number greater than 57 have measurable M shell emissions.

Each characteristic x-ray line is defined with the letter K, L, or M, which signifies which shell had the original vacancy and by a subscript alpha (α), beta (β), or gamma (γ) etc., which indicates the higher shell from which electrons fell to fill the vacancy and produce the x-ray. For example, a K_α line is produced by a vacancy in the K shell filled by an L shell electron, whereas a K_β line is produced by a vacancy in the K shell filled by an M shell electron. The K_α transition is on average 6 to 7 times more probable than the K_β transition; therefore, the K_α line is approximately 7 times more intense than the K_β line for a given element, making the K_α line the choice for quantitation purposes.

The K lines for a given element are the most energetic lines and are the preferred lines for analysis. For a given atom, the x-rays emitted from L transitions are always less energetic than those emitted from K transitions. Unlike the K lines, the main L emission lines (L_α and L_β) for an element are of nearly equal intensity. The choice of one or the other depends on what interfering element lines might be present. The L emission lines are useful for analyses involving elements of atomic number (Z) 58 (cerium) through 92 (uranium).

An x-ray source can excite characteristic x-rays from an element only if the source energy is greater than the absorption edge energy for the particular line group of the element, that is, the K absorption edge, L absorption edge, or M absorption edge energy. The absorption edge energy is somewhat greater than the corresponding line energy. Actually, the K absorption edge energy is approximately the sum of the K, L, and M line energies of the particular element, and the L absorption edge energy is approximately the sum of the L and M line energies. FPXRF is more sensitive to an element with an absorption edge energy close to but less than

the excitation energy of the source. For example, when using a cadmium-109 source, which has an excitation energy of 22.1 kiloelectron volts (keV), FPXRF would exhibit better sensitivity for zirconium which has a K line energy of 15.77 keV than to chromium, which has a K line energy of 5.41 keV.

2.2 Under this method, inorganic analytes of interest are identified and quantitated using a field portable energy-dispersive x-ray fluorescence spectrometer. Radiation from one or more radioisotope sources or an electrically excited x-ray tube is used to generate characteristic x-ray emissions from elements in a sample. Up to three sources may be used to irradiate a sample. Each source emits a specific set of primary x-rays that excite a corresponding range of elements in a sample. When more than one source can excite the element of interest, the source is selected according to its excitation efficiency for the element of interest.

For measurement, the sample is positioned in front of the probe window. This can be done in two manners using FPXRF instruments, specifically, in situ or intrusive. If operated in the in situ mode, the probe window is placed in direct contact with the soil surface to be analyzed. When an FPXRF instrument is operated in the intrusive mode, a soil or sediment sample must be collected, prepared, and placed in a sample cup. The sample cup is then placed on top of the window inside a protective cover for analysis.

Sample analysis is then initiated by exposing the sample to primary radiation from the source. Fluorescent and backscattered x-rays from the sample enter through the detector window and are converted into electric pulses in the detector. The detector in FPXRF instruments is usually either a solid-state detector or a gas-filled proportional counter. Within the detector, energies of the characteristic x-rays are converted into a train of electric pulses, the amplitudes of which are linearly proportional to the energy of the x-rays. An electronic multichannel analyzer (MCA) measures the pulse amplitudes, which is the basis of qualitative x-ray analysis. The number of counts at a given energy per unit of time is representative of the element concentration in a sample and is the basis for quantitative analysis. Most FPXRF instruments are menu-driven from software built into the units or from personal computers (PC).

The measurement time of each source is user-selectable. Shorter source measurement times (30 seconds) are generally used for initial screening and hot spot delineation, and longer measurement times (up to 300 seconds) are typically used to meet higher precision and accuracy requirements.

FPXRF instruments can be calibrated using the following methods: internally using fundamental parameters determined by the manufacturer, empirically based on site-specific calibration standards (SSCS), or based on Compton peak ratios. The Compton peak is produced by backscattering of the source radiation. Some FPXRF instruments can be calibrated using multiple methods.

3.0 DEFINITIONS

3.1 FPXRF -- Field portable x-ray fluorescence.

3.2 MCA -- Multichannel analyzer for measuring pulse amplitude.

3.3 SSCS -- Site-specific calibration standards.

3.4 FP -- Fundamental parameter.

3.5 ROI -- Region of interest.

3.6 SRM -- Standard reference material; a standard containing certified amounts of metals in soil or sediment.

3.7 eV -- Electron volt; a unit of energy equivalent to the amount of energy gained by an electron passing through a potential difference of one volt.

3.8 Refer to Chapter One, Chapter Three, and the manufacturer's instructions for other definitions that may be relevant to this procedure.

4.0 INTERFERENCES

4.1 The total method error for FPXRF analysis is defined as the square root of the sum of squares of both instrument precision and user- or application-related error. Generally, instrument precision is the least significant source of error in FPXRF analysis. User- or application-related error is generally more significant and varies with each site and method used. Some sources of interference can be minimized or controlled by the instrument operator, but others cannot. Common sources of user- or application-related error are discussed below.

4.2 Physical matrix effects result from variations in the physical character of the sample. These variations may include such parameters as particle size, uniformity, homogeneity, and surface condition. For example, if any analyte exists in the form of very fine particles in a coarser-grained matrix, the analyte's concentration measured by the FPXRF will vary depending on how fine particles are distributed within the coarser-grained matrix. If the fine particles "settle" to the bottom of the sample cup (i.e., against the cup window), the analyte concentration measurement will be higher than if the fine particles are not mixed in well and stay on top of the coarser-grained particles in the sample cup. One way to reduce such error is to grind and sieve all soil samples to a uniform particle size thus reducing sample-to-sample particle size variability. Homogeneity is always a concern when dealing with soil samples. Every effort should be made to thoroughly mix and homogenize soil samples before analysis. Field studies have shown heterogeneity of the sample generally has the largest impact on comparability with confirmatory samples.

4.3 Moisture content may affect the accuracy of analysis of soil and sediment sample analyses. When the moisture content is between 5 and 20 percent, the overall error from moisture may be minimal. However, moisture content may be a major source of error when analyzing samples of surface soil or sediment that are saturated with water. This error can be minimized by drying the samples in a convection or toaster oven. Microwave drying is not recommended because field studies have shown that microwave drying can increase variability between FPXRF data and confirmatory analysis and because metal fragments in the sample can cause arcing to occur in a microwave.

4.4 Inconsistent positioning of samples in front of the probe window is a potential source of error because the x-ray signal decreases as the distance from the radioactive source increases. This error is minimized by maintaining the same distance between the window and each sample. For the best results, the window of the probe should be in direct contact with the sample, which means that the sample should be flat and smooth to provide a good contact surface.

4.5 Chemical matrix effects result from differences in the concentrations of interfering elements. These effects occur as either spectral interferences (peak overlaps) or as x-ray absorption and enhancement phenomena. Both effects are common in soils contaminated with heavy metals. As examples of absorption and enhancement effects; iron (Fe) tends to absorb copper (Cu) x-rays, reducing the intensity of the Cu measured by the detector, while chromium (Cr) will be enhanced at the expense of Fe because the absorption edge of Cr is slightly lower in energy than the fluorescent peak of iron. The effects can be corrected mathematically through the use of fundamental parameter (FP) coefficients. The effects also can be compensated for using SSCS, which contain all the elements present on site that can interfere with one another.

4.6 When present in a sample, certain x-ray lines from different elements can be very close in energy and, therefore, can cause interference by producing a severely overlapped spectrum. The degree to which a detector can resolve the two different peaks depends on the energy resolution of the detector. If the energy difference between the two peaks in electron volts is less than the resolution of the detector in electron volts, then the detector will not be able to fully resolve the peaks.

The most common spectrum overlaps involve the K_{β} line of element Z-1 with the K_{α} line of element Z. This is called the K_{α}/K_{β} interference. Because the $K_{\alpha}:K_{\beta}$ intensity ratio for a given element usually is about 7:1, the interfering element, Z-1, must be present at large concentrations to cause a problem. Two examples of this type of spectral interference involve the presence of large concentrations of vanadium (V) when attempting to measure Cr or the presence of large concentrations of Fe when attempting to measure cobalt (Co). The V K_{α} and K_{β} energies are 4.95 and 5.43 keV, respectively, and the Cr K_{α} energy is 5.41 keV. The Fe K_{α} and K_{β} energies are 6.40 and 7.06 keV, respectively, and the Co K_{α} energy is 6.92 keV. The difference between the V K_{β} and Cr K_{α} energies is 20 eV, and the difference between the Fe K_{β} and the Co K_{α} energies is 140 eV. The resolution of the highest-resolution detectors in FPXRF instruments is 170 eV. Therefore, large amounts of V and Fe will interfere with quantitation of Cr or Co, respectively. The presence of Fe is a frequent problem because it is often found in soils at tens of thousands of parts per million (ppm).

4.7 Other interferences can arise from K/L, K/M, and L/M line overlaps, although these overlaps are less common. Examples of such overlap involve arsenic (As) K_{α} /lead (Pb) L_{α} and sulfur (S) K_{α} /Pb M_{α} . In the As/Pb case, Pb can be measured from the Pb L_{β} line, and As can be measured from either the As K_{α} or the As K_{β} line; in this way the interference can be corrected. If the As K_{β} line is used, sensitivity will be decreased by a factor of two to five times because it is a less intense line than the As K_{α} line. If the As K_{α} line is used in the presence of Pb, mathematical corrections within the instrument software can be used to subtract out the Pb interference. However, because of the limits of mathematical corrections, As concentrations cannot be efficiently calculated for samples with Pb:As ratios of 10:1 or more. This high ratio of Pb to As may result in reporting of a "nondetect" or a "less than" value (e.g., <300 ppm) for As, regardless of the actual concentration present.

No instrument can fully compensate for this interference. It is important for an operator to understand this limitation of FPXRF instruments and consult with the manufacturer of the FPXRF instrument to evaluate options to minimize this limitation. The operator's decision will be based on action levels for metals in soil established for the site, matrix effects, capabilities of the instrument, data quality objectives, and the ratio of lead to arsenic known to be present at the site. If a site is encountered that contains lead at concentrations greater than ten times the concentration of arsenic it is advisable that all critical soil samples be sent off site for confirmatory analysis using other techniques (e.g., flame atomic absorption spectrometry (FLAA), graphite furnace atomic absorption spectrometry (GFAA), inductively coupled plasma-

atomic emission spectrometry, (ICP-AES), or inductively coupled plasma-mass spectrometry, (ICP-MS)).

4.8 If SSCS are used to calibrate an FPXRF instrument, the samples collected must be representative of the site under investigation. Representative soil sampling ensures that a sample or group of samples accurately reflects the concentrations of the contaminants of concern at a given time and location. Analytical results for representative samples reflect variations in the presence and concentration ranges of contaminants throughout a site. Variables affecting sample representativeness include differences in soil type, contaminant concentration variability, sample collection and preparation variability, and analytical variability, all of which should be minimized as much as possible.

4.9 Soil physical and chemical effects may be corrected using SSCS that have been analyzed by inductively coupled plasma (ICP) or atomic absorption (AA) methods. However, a major source of error can be introduced if these samples are not representative of the site or if the analytical error is large. Another concern is the type of digestion procedure used to prepare the soil samples for the reference analysis. Analytical results for the confirmatory method will vary depending on whether a partial digestion procedure, such as Method 3050, or a total digestion procedure, such as Method 3052, is used. It is known that depending on the nature of the soil or sediment, Method 3050 will achieve differing extraction efficiencies for different analytes of interest. The confirmatory method should meet the project-specific data quality objectives (DQOs).

XRF measures the total concentration of an element; therefore, to achieve the greatest comparability of this method with the reference method (reduced bias), a total digestion procedure should be used for sample preparation. However, in the study used to generate the performance data for this method (see Table 8), the confirmatory method used was Method 3050, and the FPXRF data compared very well with regression correlation coefficients (r often exceeding 0.95, except for barium and chromium). The critical factor is that the digestion procedure and analytical reference method used should meet the DQOs of the project and match the method used for confirmation analysis.

4.10 Ambient temperature changes can affect the gain of the amplifiers producing instrument drift. Gain or drift is primarily a function of the electronics (amplifier or preamplifier) and not the detector as most instrument detectors are cooled to a constant temperature. Most FPXRF instruments have a built-in automatic gain control. If the automatic gain control is allowed to make periodic adjustments, the instrument will compensate for the influence of temperature changes on its energy scale. If the FPXRF instrument has an automatic gain control function, the operator will not have to adjust the instrument's gain unless an error message appears. If an error message appears, the operator should follow the manufacturer's procedures for troubleshooting the problem. Often, this involves performing a new energy calibration. The performance of an energy calibration check to assess drift is a quality control measure discussed in Sec. 9.2.

If the operator is instructed by the manufacturer to manually conduct a gain check because of increasing or decreasing ambient temperature, it is standard to perform a gain check after every 10 to 20 sample measurements or once an hour whichever is more frequent. It is also suggested that a gain check be performed if the temperature fluctuates more than 10° F. The operator should follow the manufacturer's recommendations for gain check frequency.

5.0 SAFETY

5.1 This method does not address all safety issues associated with its use. The user is responsible for maintaining a safe work environment and a current awareness file of OSHA regulations regarding the safe handling of the chemicals listed in this method. A reference file of material safety data sheets (MSDSs) should be available to all personnel involved in these analyses.

NOTE: No MSDS applies directly to the radiation-producing instrument because that is covered under the Nuclear Regulatory Commission (NRC) or applicable state regulations.

5.2 Proper training for the safe operation of the instrument and radiation training should be completed by the analyst prior to analysis. Radiation safety for each specific instrument can be found in the operator's manual. Protective shielding should never be removed by the analyst or any personnel other than the manufacturer. The analyst should be aware of the local state and national regulations that pertain to the use of radiation-producing equipment and radioactive materials with which compliance is required. There should be a person appointed within the organization that is solely responsible for properly instructing all personnel, maintaining inspection records, and monitoring x-ray equipment at regular intervals.

Licenses for radioactive materials are of two types, specifically: (1) a general license which is usually initiated by the manufacturer for receiving, acquiring, owning, possessing, using, and transferring radioactive material incorporated in a device or equipment, and (2) a specific license which is issued to named persons for the operation of radioactive instruments as required by local, state, or federal agencies. A copy of the radioactive material license (for specific licenses only) and leak tests should be present with the instrument at all times and available to local and national authorities upon request.

X-ray tubes do not require radioactive material licenses or leak tests, but do require approvals and licenses which vary from state to state. In addition, fail-safe x-ray warning lights should be illuminated whenever an x-ray tube is energized. Provisions listed above concerning radiation safety regulations, shielding, training, and responsible personnel apply to x-ray tubes just as to radioactive sources. In addition, a log of the times and operating conditions should be kept whenever an x-ray tube is energized. An additional hazard present with x-ray tubes is the danger of electric shock from the high voltage supply, however, if the tube is properly positioned within the instrument, this is only a negligible risk. Any instrument (x-ray tube or radioisotope based) is capable of delivering an electric shock from the basic circuitry when the system is inappropriately opened.

5.3 Radiation monitoring equipment should be used with the handling and operation of the instrument. The operator and the surrounding environment should be monitored continually for analyst exposure to radiation. Thermal luminescent detectors (TLD) in the form of badges and rings are used to monitor operator radiation exposure. The TLDs or badges should be worn in the area of maximum exposure. The maximum permissible whole-body dose from occupational exposure is 5 Roentgen Equivalent Man (REM) per year. Possible exposure pathways for radiation to enter the body are ingestion, inhaling, and absorption. The best precaution to prevent radiation exposure is distance and shielding.

6.0 EQUIPMENT AND SUPPLIES

The mention of trade names or commercial products in this manual is for illustrative purposes only, and does not constitute an EPA endorsement or exclusive recommendation for

use. The products and instrument settings cited in SW-846 methods represent those products and settings used during method development or subsequently evaluated by the Agency. Glassware, reagents, supplies, equipment, and settings other than those listed in this manual may be employed provided that method performance appropriate for the intended application has been demonstrated and documented.

6.1 FPXRF spectrometer -- An FPXRF spectrometer consists of four major components: (1) a source that provides x-rays; (2) a sample presentation device; (3) a detector that converts x-ray-generated photons emitted from the sample into measurable electronic signals; and (4) a data processing unit that contains an emission or fluorescence energy analyzer, such as an MCA, that processes the signals into an x-ray energy spectrum from which elemental concentrations in the sample may be calculated, and a data display and storage system. These components and additional, optional items, are discussed below.

6.1.1 Excitation sources -- FPXRF instruments use either a sealed radioisotope source or an x-ray tube to provide the excitation source. Many FPXRF instruments use sealed radioisotope sources to produce x-rays in order to irradiate samples. The FPXRF instrument may contain between one and three radioisotope sources. Common radioisotope sources used for analysis for metals in soils are iron Fe-55 (^{55}Fe), cadmium Cd-109 (^{109}Cd), americium Am-241 (^{241}Am), and curium Cm-244 (^{244}Cm). These sources may be contained in a probe along with a window and the detector; the probe may be connected to a data reduction and handling system by means of a flexible cable. Alternatively, the sources, window, and detector may be included in the same unit as the data reduction and handling system.

The relative strength of the radioisotope sources is measured in units of millicuries (mCi). All other components of the FPXRF system being equal, the stronger the source, the greater the sensitivity and precision of a given instrument. Radioisotope sources undergo constant decay. In fact, it is this decay process that emits the primary x-rays used to excite samples for FPXRF analysis. The decay of radioisotopes is measured in "half-lives." The half-life of a radioisotope is defined as the length of time required to reduce the radioisotopes strength or activity by half. Developers of FPXRF technologies recommend source replacement at regular intervals based on the source's half-life. This is due to the ever increasing time required for the analysis rather than a decrease in instrument performance. The characteristic x-rays emitted from each of the different sources have energies capable of exciting a certain range of analytes in a sample. Table 2 summarizes the characteristics of four common radioisotope sources.

X-ray tubes have higher radiation output, no intrinsic lifetime limit, produce constant output over their lifetime, and do not have the disposal problems of radioactive sources but are just now appearing in FPXRF instruments. An electrically-excited x-ray tube operates by bombarding an anode with electrons accelerated by a high voltage. The electrons gain an energy in electron volts equal to the accelerating voltage and can excite atomic transitions in the anode, which then produces characteristic x-rays. These characteristic x-rays are emitted through a window which contains the vacuum necessary for the electron acceleration. An important difference between x-ray tubes and radioactive sources is that the electrons which bombard the anode also produce a continuum of x-rays across a broad range of energies in addition to the characteristic x-rays. This continuum is weak compared to the characteristic x-rays but can provide substantial excitation since it covers a broad energy range. It has the undesired property of producing background in the spectrum near the analyte x-ray lines when it is scattered by the sample. For this reason a filter is often used between the x-ray tube and the sample to suppress the continuum radiation while passing the characteristic x-rays from the anode. This filter is sometimes incorporated into the window of the x-ray tube. The choice of

accelerating voltage is governed both by the anode material, since the electrons must have sufficient energy to excite the anode, which requires a voltage greater than the absorption edge of the anode material and by the instrument's ability to cool the x-ray tube. The anode is most efficiently excited by voltages 2 to 2.5 times the edge energy (most x-rays per unit power to the tube), although voltages as low as 1.5 times the absorption edge energy will work. The characteristic x-rays emitted by the anode are capable of exciting a range of elements in the sample just as with a radioactive source. Table 3 gives the recommended operating voltages and the sample elements excited for some common anodes.

6.1.2 Sample presentation device -- FPXRF instruments can be operated in two modes: in situ and intrusive. If operated in the in situ mode, the probe window is placed in direct contact with the soil surface to be analyzed. When an FPXRF instrument is operated in the intrusive mode, a soil or sediment sample must be collected, prepared, and placed in a sample cup. For FPXRF instruments operated in the intrusive mode, the probe may be rotated so that the window faces either upward or downward. A protective sample cover is placed over the window, and the sample cup is placed on top of the window inside the protective sample cover for analysis.

6.1.3 Detectors -- The detectors in the FPXRF instruments can be either solid-state detectors or gas-filled, proportional counter detectors. Common solid-state detectors include mercuric iodide (HgI_2), silicon pin diode and lithium-drifted silicon $\text{Si}(\text{Li})$. The HgI_2 detector is operated at a moderately subambient temperature controlled by a low power thermoelectric cooler. The silicon pin diode detector also is cooled via the thermoelectric Peltier effect. The $\text{Si}(\text{Li})$ detector must be cooled to at least -90°C either with liquid nitrogen or by thermoelectric cooling via the Peltier effect. Instruments with a $\text{Si}(\text{Li})$ detector have an internal liquid nitrogen dewar with a capacity of 0.5 to 1.0 L. Proportional counter detectors are rugged and lightweight, which are important features of a field portable detector. However, the resolution of a proportional counter detector is not as good as that of a solid-state detector. The energy resolution of a detector for characteristic x-rays is usually expressed in terms of full width at half-maximum (FWHM) height of the manganese K_α peak at 5.89 keV. The typical resolutions of the above mentioned detectors are as follows: HgI_2 –270 eV; silicon pin diode–250 eV; $\text{Si}(\text{Li})$ –170 eV; and gas-filled, proportional counter–750 eV.

During operation of a solid-state detector, an x-ray photon strikes a biased, solid-state crystal and loses energy in the crystal by producing electron-hole pairs. The electric charge produced is collected and provides a current pulse that is directly proportional to the energy of the x-ray photon absorbed by the crystal of the detector. A gas-filled, proportional counter detector is an ionization chamber filled with a mixture of noble and other gases. An x-ray photon entering the chamber ionizes the gas atoms. The electric charge produced is collected and provides an electric signal that is directly proportional to the energy of the x-ray photon absorbed by the gas in the detector.

6.1.4 Data processing units -- The key component in the data processing unit of an FPXRF instrument is the MCA. The MCA receives pulses from the detector and sorts them by their amplitudes (energy level). The MCA counts pulses per second to determine the height of the peak in a spectrum, which is indicative of the target analyte's concentration. The spectrum of element peaks are built on the MCA. The MCAs in FPXRF instruments have from 256 to 2,048 channels. The concentrations of target analytes are usually shown in ppm on a liquid crystal display (LCD) in the instrument. FPXRF instruments can store both spectra and from 3,000 to 5,000 sets of numerical analytical results. Most FPXRF instruments are menu-driven from software built into the

units or from PCs. Once the data-storage memory of an FPXRF unit is full or at any other time, data can be downloaded by means of an RS-232 port and cable to a PC.

6.2 Spare battery and battery charger.

6.3 Polyethylene sample cups -- 31 to 40 mm in diameter with collar, or equivalent (appropriate for FPXRF instrument).

6.4 X-ray window film -- Mylar™, Kapton™, Spectrolene™, polypropylene, or equivalent; 2.5 to 6.0 µm thick.

6.5 Mortar and pestle -- Glass, agate, or aluminum oxide; for grinding soil and sediment samples.

6.6 Containers -- Glass or plastic to store samples.

6.7 Sieves -- 60-mesh (0.25 mm), stainless-steel, Nylon, or equivalent for preparing soil and sediment samples.

6.8 Trowels -- For smoothing soil surfaces and collecting soil samples.

6.9 Plastic bags -- Used for collection and homogenization of soil samples.

6.10 Drying oven -- Standard convection or toaster oven, for soil and sediment samples that require drying.

7.0 REAGENTS AND STANDARDS

7.1 Reagent grade chemicals must be used in all tests. Unless otherwise indicated, it is intended that all reagents conform to the specifications of the Committee on Analytical Reagents of the American Chemical Society, where such specifications are available. Other grades may be used, provided it is first ascertained that the reagent is of sufficiently high purity to permit its use without lessening the accuracy of the determination.

7.2 Pure element standards -- Each pure, single-element standard is intended to produce strong characteristic x-ray peaks of the element of interest only. Other elements present must not contribute to the fluorescence spectrum. A set of pure element standards for commonly sought analytes is supplied by the instrument manufacturer, if designated for the instrument; not all instruments require the pure element standards. The standards are used to set the region of interest (ROI) for each element. They also can be used as energy calibration and resolution check samples.

7.3 Site-specific calibration standards -- Instruments that employ fundamental parameters (FP) or similar mathematical models in minimizing matrix effects may not require SSCS. If the FP calibration model is to be optimized or if empirical calibration is necessary, then SSCSs must be collected, prepared, and analyzed.

7.3.1 The SSCS must be representative of the matrix to be analyzed by FPXRF. These samples must be well homogenized. A minimum of 10 samples spanning the concentration ranges of the analytes of interest and of the interfering elements must be obtained from the site. A sample size of 4 to 8 ounces is recommended, and standard glass sampling jars should be used.

7.3.2 Each sample should be oven-dried for 2 to 4 hr at a temperature of less than 150 °C. If mercury is to be analyzed, a separate sample portion should be dried at ambient temperature as heating may volatilize the mercury. When the sample is dry, all large, organic debris and nonrepresentative material, such as twigs, leaves, roots, insects, asphalt, and rock should be removed. The sample should be homogenized (see Sec. 7.3.3) and then a representative portion ground with a mortar and pestle or other mechanical means, prior to passing through a 60-mesh sieve. Only the coarse rock fraction should remain on the screen.

7.3.3 The sample should be homogenized by using a riffle splitter or by placing 150 to 200 g of the dried, sieved sample on a piece of kraft or butcher paper about 1.5 by 1.5 feet in size. Each corner of the paper should be lifted alternately, rolling the soil over on itself and toward the opposite corner. The soil should be rolled on itself 20 times. Approximately 5 g of the sample should then be removed and placed in a sample cup for FPXRF analysis. The rest of the prepared sample should be sent off site for ICP or AA analysis. The method use for confirmatory analysis should meet the data quality objectives of the project.

7.4 Blank samples -- The blank samples should be from a "clean" quartz or silicon dioxide matrix that is free of any analytes at concentrations above the established lower limit of detection. These samples are used to monitor for cross-contamination and laboratory-induced contaminants or interferences.

7.5 Standard reference materials -- Standard reference materials (SRMs) are standards containing certified amounts of metals in soil or sediment. These standards are used for accuracy and performance checks of FPXRF analyses. SRMs can be obtained from the National Institute of Standards and Technology (NIST), the U.S. Geological Survey (USGS), the Canadian National Research Council, and the national bureau of standards in foreign nations. Pertinent NIST SRMs for FPXRF analysis include 2704, Buffalo River Sediment; 2709, San Joaquin Soil; and 2710 and 2711, Montana Soil. These SRMs contain soil or sediment from actual sites that has been analyzed using independent inorganic analytical methods by many different laboratories. When these SRMs are unavailable, alternate standards may be used (e.g., NIST 2702).

8.0 SAMPLE COLLECTION, PRESERVATION, AND STORAGE

Sample handling and preservation procedures used in FPXRF analyses should follow the guidelines in Chapter Three, "Inorganic Analytes."

9.0 QUALITY CONTROL

9.1 Follow the manufacturer's instructions for the quality control procedures specific to use of the testing product. Refer to Chapter One for additional guidance on quality assurance (QA) and quality control (QC) protocols. Any effort involving the collection of analytical data should include development of a structured and systematic planning document, such as a Quality Assurance Project Plan (QAPP) or a Sampling and Analysis Plan (SAP), which translates project objectives and specifications into directions for those that will implement the project and assess the results.

9.2 Energy calibration check -- To determine whether an FPXRF instrument is operating within resolution and stability tolerances, an energy calibration check should be run. The energy calibration check determines whether the characteristic x-ray lines are shifting,

which would indicate drift within the instrument. As discussed in Sec. 4.10, this check also serves as a gain check in the event that ambient temperatures are fluctuating greatly (more than 10 °F).

9.2.1 The energy calibration check should be run at a frequency consistent with manufacturer's recommendations. Generally, this would be at the beginning of each working day, after the batteries are changed or the instrument is shut off, at the end of each working day, and at any other time when the instrument operator believes that drift is occurring during analysis. A pure element such as iron, manganese, copper, or lead is often used for the energy calibration check. A manufacturer-recommended count time per source should be used for the check.

9.2.2 The instrument manufacturer's manual specifies the channel or kiloelectron volt level at which a pure element peak should appear and the expected intensity of the peak. The intensity and channel number of the pure element as measured using the source should be checked and compared to the manufacturer's recommendation. If the energy calibration check does not meet the manufacturer's criteria, then the pure element sample should be repositioned and reanalyzed. If the criteria are still not met, then an energy calibration should be performed as described in the manufacturer's manual. With some FPXRF instruments, once a spectrum is acquired from the energy calibration check, the peak can be optimized and realigned to the manufacturer's specifications using their software.

9.3 Blank samples -- Two types of blank samples should be analyzed for FPXRF analysis, specifically, instrument blanks and method blanks.

9.3.1 An instrument blank is used to verify that no contamination exists in the spectrometer or on the probe window. The instrument blank can be silicon dioxide, a polytetrafluoroethylene (PTFE) block, a quartz block, "clean" sand, or lithium carbonate. This instrument blank should be analyzed on each working day before and after analyses are conducted and once per every twenty samples. An instrument blank should also be analyzed whenever contamination is suspected by the analyst. The frequency of analysis will vary with the data quality objectives of the project. A manufacturer-recommended count time per source should be used for the blank analysis. No element concentrations above the established lower limit of detection should be found in the instrument blank. If concentrations exceed these limits, then the probe window and the check sample should be checked for contamination. If contamination is not a problem, then the instrument must be "zeroed" by following the manufacturer's instructions.

9.3.2 A method blank is used to monitor for laboratory-induced contaminants or interferences. The method blank can be "clean" silica sand or lithium carbonate that undergoes the same preparation procedure as the samples. A method blank must be analyzed at least daily. The frequency of analysis will depend on the data quality objectives of the project. If the method blank does not contain the target analyte at a level that interferes with the project-specific data quality objectives then the method blank would be considered acceptable. In the absence of project-specific data quality objectives, if the blank is less than the lowest level of detection or less than 10% of the lowest sample concentration for the analyte, whichever is greater, then the method blank would be considered acceptable. If the method blank cannot be considered acceptable, the cause of the problem must be identified, and all samples analyzed with the method blank must be reanalyzed.

9.4 Calibration verification checks -- A calibration verification check sample is used to check the accuracy of the instrument and to assess the stability and consistency of the analysis for the analytes of interest. A check sample should be analyzed at the beginning of each working day, during active sample analyses, and at the end of each working day. The frequency of calibration checks during active analysis will depend on the data quality objectives of the project. The check sample should be a well characterized soil sample from the site that is representative of site samples in terms of particle size and degree of homogeneity and that contains contaminants at concentrations near the action levels. If a site-specific sample is not available, then an NIST or other SRM that contains the analytes of interest can be used to verify the accuracy of the instrument. The measured value for each target analyte should be within ± 20 percent (%D) of the true value for the calibration verification check to be acceptable. If a measured value falls outside this range, then the check sample should be reanalyzed. If the value continues to fall outside the acceptance range, the instrument should be recalibrated, and the batch of samples analyzed before the unacceptable calibration verification check must be reanalyzed.

9.5 Precision measurements -- The precision of the method is monitored by analyzing a sample with low, moderate, or high concentrations of target analytes. The frequency of precision measurements will depend on the data quality objectives for the data. A minimum of one precision sample should be run per day. Each precision sample should be analyzed 7 times in replicate. It is recommended that precision measurements be obtained for samples with varying concentration ranges to assess the effect of concentration on method precision. Determining method precision for analytes at concentrations near the site action levels can be extremely important if the FPXRF results are to be used in an enforcement action; therefore, selection of at least one sample with target analyte concentrations at or near the site action levels or levels of concern is recommended. A precision sample is analyzed by the instrument for the same field analysis time as used for other project samples. The relative standard deviation (RSD) of the sample mean is used to assess method precision. For FPXRF data to be considered adequately precise, the RSD should not be greater than 20 percent with the exception of chromium. RSD values for chromium should not be greater than 30 percent. If both in situ and intrusive analytical techniques are used during the course of one day, it is recommended that separate precision calculations be performed for each analysis type.

The equation for calculating RSD is as follows:

$$\text{RSD} = (\text{SD}/\text{Mean Concentration}) \times 100$$

where:

| | | |
|--------------------|---|---|
| RSD | = | Relative standard deviation for the precision measurement for the analyte |
| SD | = | Standard deviation of the concentration for the analyte |
| Mean concentration | = | Mean concentration for the analyte |

The precision or reproducibility of a measurement will improve with increasing count time, however, increasing the count time by a factor of 4 will provide only 2 times better precision, so there is a point of diminishing return. Increasing the count time also improves the sensitivity, but decreases sample throughput.

9.6 The lower limits of detection should be established from actual measured performance based on spike recoveries in the matrix of concern or from acceptable method performance on a certified reference material of the appropriate matrix and within the appropriate calibration range for the application. This is considered the best estimate of the true method sensitivity as opposed to a statistical determination based on the standard deviation of

replicate analyses of a low-concentration sample. While the statistical approach demonstrates the potential data variability for a given sample matrix at one point in time, it does not represent what can be detected or most importantly the lowest concentration that can be calibrated. For this reason the sensitivity should be established as the lowest point of detection based on acceptable target analyte recovery in the desired sample matrix.

9.7 Confirmatory samples -- The comparability of the FPXRF analysis is determined by submitting FPXRF-analyzed samples for analysis at a laboratory. The method of confirmatory analysis must meet the project and XRF measurement data quality objectives. The confirmatory samples must be splits of the well homogenized sample material. In some cases the prepared sample cups can be submitted. A minimum of 1 sample for each 20 FPXRF-analyzed samples should be submitted for confirmatory analysis. This frequency will depend on project-specific data quality objectives. The confirmatory analyses can also be used to verify the quality of the FPXRF data. The confirmatory samples should be selected from the lower, middle, and upper range of concentrations measured by the FPXRF. They should also include samples with analyte concentrations at or near the site action levels. The results of the confirmatory analysis and FPXRF analyses should be evaluated with a least squares linear regression analysis. If the measured concentrations span more than one order of magnitude, the data should be log-transformed to standardize variance which is proportional to the magnitude of measurement. The correlation coefficient (r) for the results should be 0.7 or greater for the FPXRF data to be considered screening level data. If the r is 0.9 or greater and inferential statistics indicate the FPXRF data and the confirmatory data are statistically equivalent at a 99 percent confidence level, the data could potentially meet definitive level data criteria.

10.0 CALIBRATION AND STANDARDIZATION

10.1 Instrument calibration -- Instrument calibration procedures vary among FPXRF instruments. Users of this method should follow the calibration procedures outlined in the operator's manual for each specific FPXRF instrument. Generally, however, three types of calibration procedures exist for FPXRF instruments, namely: FP calibration, empirical calibration, and the Compton peak ratio or normalization method. These three types of calibration are discussed below.

10.2 Fundamental parameters calibration -- FP calibration procedures are extremely variable. An FP calibration provides the analyst with a "standardless" calibration. The advantages of FP calibrations over empirical calibrations include the following:

- No previously collected site-specific samples are necessary, although site-specific samples with confirmed and validated analytical results for all elements present could be used.
- Cost is reduced because fewer confirmatory laboratory results or calibration standards are necessary.

However, the analyst should be aware of the limitations imposed on FP calibration by particle size and matrix effects. These limitations can be minimized by adhering to the preparation procedure described in Sec. 7.3. The two FP calibration processes discussed below are based on an effective energy FP routine and a back scatter with FP (BFP) routine. Each FPXRF FP calibration process is based on a different iterative algorithmic method. The calibration procedure for each routine is explained in detail in the manufacturer's user manual for each FPXRF instrument; in addition, training courses are offered for each instrument.

10.2.1 Effective energy FP calibration -- The effective energy FP calibration is performed by the manufacturer before an instrument is sent to the analyst. Although SSCS can be used, the calibration relies on pure element standards or SRMs such as those obtained from NIST for the FP calibration. The effective energy routine relies on the spectrometer response to pure elements and FP iterative algorithms to compensate for various matrix effects.

Alpha coefficients are calculated using a variation of the Sherman equation, which calculates theoretical intensities from the measurement of pure element samples. These coefficients indicate the quantitative effect of each matrix element on an analyte's measured x-ray intensity. Next, the Lachance Traill algorithm is solved as a set of simultaneous equations based on the theoretical intensities. The alpha coefficients are then downloaded into the specific instrument.

The working effective energy FP calibration curve must be verified before sample analysis begins on each working day, after every 20 samples are analyzed, and at the end of sampling. This verification is performed by analyzing either an NIST SRM or an SSCS that is representative of the site-specific samples. This SRM or SSCS serves as a calibration check. A manufacturer-recommended count time per source should be used for the calibration check. The analyst must then adjust the y-intercept and slope of the calibration curve to best fit the known concentrations of target analytes in the SRM or SSCS.

A percent difference (%D) is then calculated for each target analyte. The %D should be within ± 20 percent of the certified value for each analyte. If the %D falls outside this acceptance range, then the calibration curve should be adjusted by varying the slope of the line or the y-intercept value for the analyte. The SRM or SSCS is reanalyzed until the %D falls within ± 20 percent. The group of 20 samples analyzed before an out-of-control calibration check should be reanalyzed.

The equation to calibrate %D is as follows:

$$\%D = ((C_s - C_k) / C_k) \times 100$$

where:

%D = Percent difference

C_k = Certified concentration of standard sample

C_s = Measured concentration of standard sample

10.2.2 BFP calibration -- BFP calibration relies on the ability of the liquid nitrogen-cooled, Si(Li) solid-state detector to separate the coherent (Compton) and incoherent (Rayleigh) backscatter peaks of primary radiation. These peak intensities are known to be a function of sample composition, and the ratio of the Compton to Rayleigh peak is a function of the mass absorption of the sample. The calibration procedure is explained in detail in the instrument manufacturer's manual. Following is a general description of the BFP calibration procedure.

The concentrations of all detected and quantified elements are entered into the computer software system. Certified element results for an NIST SRM or confirmed and validated results for an SSCS can be used. In addition, the concentrations of oxygen and silicon must be entered; these two concentrations are not found in standard metals analyses. The manufacturer provides silicon and oxygen concentrations for typical soil types. Pure element standards are then analyzed using a manufacturer-recommended

count time per source. The results are used to calculate correction factors in order to adjust for spectrum overlap of elements.

The working BFP calibration curve must be verified before sample analysis begins on each working day, after every 20 samples are analyzed, and at the end of the analysis. This verification is performed by analyzing either an NIST SRM or an SSCS that is representative of the site-specific samples. This SRM or SSCS serves as a calibration check. The standard sample is analyzed using a manufacturer-recommended count time per source to check the calibration curve. The analyst must then adjust the y-intercept and slope of the calibration curve to best fit the known concentrations of target analytes in the SRM or SSCS.

A %D is then calculated for each target analyte. The %D should fall within ± 20 percent of the certified value for each analyte. If the %D falls outside this acceptance range, then the calibration curve should be adjusted by varying the slope of the line the y-intercept value for the analyte. The standard sample is reanalyzed until the %D falls within ± 20 percent. The group of 20 samples analyzed before an out-of-control calibration check should be reanalyzed.

10.3 Empirical calibration -- An empirical calibration can be performed with SSCS, site-typical standards, or standards prepared from metal oxides. A discussion of SSCS is included in Sec. 7.3; if no previously characterized samples exist for a specific site, site-typical standards can be used. Site-typical standards may be selected from commercially available characterized soils or from SSCS prepared for another site. The site-typical standards should closely approximate the site's soil matrix with respect to particle size distribution, mineralogy, and contaminant analytes. If neither SSCS nor site-typical standards are available, it is possible to make gravimetric standards by adding metal oxides to a "clean" sand or silicon dioxide matrix that simulates soil. Metal oxides can be purchased from various chemical vendors. If standards are made on site, a balance capable of weighing items to at least two decimal places is necessary. Concentrated ICP or AA standard solutions can also be used to make standards. These solutions are available in concentrations of 10,000 parts per million, thus only small volumes have to be added to the soil.

An empirical calibration using SSCS involves analysis of SSCS by the FPXRF instrument and by a conventional analytical method such as ICP or AA. A total acid digestion procedure should be used by the laboratory for sample preparation. Generally, a minimum of 10 and a maximum of 30 well characterized SSCS, site-typical standards, or prepared metal oxide standards are necessary to perform an adequate empirical calibration. The exact number of standards depends on the number of analytes of interest and interfering elements. Theoretically, an empirical calibration with SSCS should provide the most accurate data for a site because the calibration compensates for site-specific matrix effects.

The first step in an empirical calibration is to analyze the pure element standards for the elements of interest. This enables the instrument to set channel limits for each element for spectral deconvolution. Next the SSCS, site-typical standards, or prepared metal oxide standards are analyzed using a count time of 200 seconds per source or a count time recommended by the manufacturer. This will produce a spectrum and net intensity of each analyte in each standard. The analyte concentrations for each standard are then entered into the instrument software; these concentrations are those obtained from the laboratory, the certified results, or the gravimetrically determined concentrations of the prepared standards. This gives the instrument analyte values to regress against corresponding intensities during the modeling stage. The regression equation correlates the concentrations of an analyte with its net intensity.

The calibration equation is developed using a least squares fit regression analysis. After the regression terms to be used in the equation are defined, a mathematical equation can be developed to calculate the analyte concentration in an unknown sample. In some FPXRF instruments, the software of the instrument calculates the regression equation. The software uses calculated intercept and slope values to form a multiterm equation. In conjunction with the software in the instrument, the operator can adjust the multiterm equation to minimize interelement interferences and optimize the intensity calibration curve.

It is possible to define up to six linear or nonlinear terms in the regression equation. Terms can be added and deleted to optimize the equation. The goal is to produce an equation with the smallest regression error and the highest correlation coefficient. These values are automatically computed by the software as the regression terms are added, deleted, or modified. It is also possible to delete data points from the regression line if these points are significant outliers or if they are heavily weighing the data. Once the regression equation has been selected for an analyte, the equation can be entered into the software for quantitation of analytes in subsequent samples. For an empirical calibration to be acceptable, the regression equation for a specific analyte should have a correlation coefficient of 0.98 or greater or meet the DQOs of the project.

In an empirical calibration, one must apply the DQOs of the project and ascertain critical or action levels for the analytes of interest. It is within these concentration ranges or around these action levels that the FPXRF instrument should be calibrated most accurately. It may not be possible to develop a good regression equation over several orders of analyte concentration.

10.4 Compton normalization method -- The Compton normalization method is based on analysis of a single, certified standard and normalization for the Compton peak. The Compton peak is produced from incoherent backscattering of x-ray radiation from the excitation source and is present in the spectrum of every sample. The Compton peak intensity changes with differing matrices. Generally, matrices dominated by lighter elements produce a larger Compton peak, and those dominated by heavier elements produce a smaller Compton peak. Normalizing to the Compton peak can reduce problems with varying matrix effects among samples. Compton normalization is similar to the use of internal standards in organics analysis. The Compton normalization method may not be effective when analyte concentrations exceed a few percent.

The certified standard used for this type of calibration could be an NIST SRM such as 2710 or 2711. The SRM must be a matrix similar to the samples and must contain the analytes of interests at concentrations near those expected in the samples. First, a response factor has to be determined for each analyte. This factor is calculated by dividing the net peak intensity by the analyte concentration. The net peak intensity is gross intensity corrected for baseline reading. Concentrations of analytes in samples are then determined by multiplying the baseline corrected analyte signal intensity by the normalization factor and by the response factor. The normalization factor is the quotient of the baseline corrected Compton K_{α} peak intensity of the SRM divided by that of the samples. Depending on the FPXRF instrument used, these calculations may be done manually or by the instrument software.

11.0 PROCEDURE

11.1 Operation of the various FPXRF instruments will vary according to the manufacturers' protocols. Before operating any FPXRF instrument, one should consult the manufacturer's manual. Most manufacturers recommend that their instruments be allowed to warm up for 15 to 30 minutes before analysis of samples. This will help alleviate drift or energy calibration problems later during analysis.

11.2 Each FPXRF instrument should be operated according to the manufacturer's recommendations. There are two modes in which FPXRF instruments can be operated: in situ and intrusive. The in situ mode involves analysis of an undisturbed soil sediment or sample. Intrusive analysis involves collection and preparation of a soil or sediment sample before analysis. Some FPXRF instruments can operate in both modes of analysis, while others are designed to operate in only one mode. The two modes of analysis are discussed below.

11.3 For in situ analysis, remove any large or nonrepresentative debris from the soil surface before analysis. This debris includes rocks, pebbles, leaves, vegetation, roots, and concrete. Also, the soil surface must be as smooth as possible so that the probe window will have good contact with the surface. This may require some leveling of the surface with a stainless-steel trowel. During the study conducted to provide example performance data for this method, this modest amount of sample preparation was found to take less than 5 min per sample location. The last requirement is that the soil or sediment not be saturated with water. Manufacturers state that their FPXRF instruments will perform adequately for soils with moisture contents of 5 to 20 percent but will not perform well for saturated soils, especially if ponded water exists on the surface. Another recommended technique for in situ analysis is to tamp the soil to increase soil density and compactness for better repeatability and representativeness. This condition is especially important for heavy element analysis, such as barium. Source count times for in situ analysis usually range from 30 to 120 seconds, but source count times will vary among instruments and depending on the desired method sensitivity. Due to the heterogeneous nature of the soil sample, in situ analysis can provide only "screening" type data.

11.4 For intrusive analysis of surface or sediment, it is recommended that a sample be collected from a 4- by 4-inch square that is 1 inch deep. This will produce a soil sample of approximately 375 g or 250 cm³, which is enough soil to fill an 8-ounce jar. However, the exact dimensions and sample depth should take into consideration the heterogeneous deposition of contaminants and will ultimately depend on the desired project-specific data quality objectives. The sample should be homogenized, dried, and ground before analysis. The sample can be homogenized before or after drying. The homogenization technique to be used after drying is discussed in Sec. 4.2. If the sample is homogenized before drying, it should be thoroughly mixed in a beaker or similar container, or if the sample is moist and has a high clay content, it can be kneaded in a plastic bag. One way to monitor homogenization when the sample is kneaded in a plastic bag is to add sodium fluorescein dye to the sample. After the moist sample has been homogenized, it is examined under an ultraviolet light to assess the distribution of sodium fluorescein throughout the sample. If the fluorescent dye is evenly distributed in the sample, homogenization is considered complete; if the dye is not evenly distributed, mixing should continue until the sample has been thoroughly homogenized. During the study conducted to provide data for this method, the time necessary for homogenization procedure using the fluorescein dye ranged from 3 to 5 min per sample. As demonstrated in Secs. 13.5 and 13.7, homogenization has the greatest impact on the reduction of sampling variability. It produces little or no contamination. Often, the direct analysis through the plastic bag is possible without the more labor intensive steps of drying, grinding, and sieving given in Secs. 11.5 and 11.6. Of course, to achieve the best data quality possible all four steps should be followed.

11.5 Once the soil or sediment sample has been homogenized, it should be dried. This can be accomplished with a toaster oven or convection oven. A small aliquot of the sample (20 to 50 g) is placed in a suitable container for drying. The sample should be dried for 2 to 4 hr in the convection or toaster oven at a temperature not greater than 150 °C. Samples may also be air dried under ambient temperature conditions using a 10- to 20-g portion. Regardless of what drying mechanism is used, the drying process is considered complete when a constant sample weight can be obtained. Care should be taken to avoid sample cross-contamination and these measures can be evaluated by including an appropriate method blank sample along with any sample preparation process.

CAUTION: Microwave drying is not a recommended procedure. Field studies have shown that microwave drying can increase variability between the FPXRF data and confirmatory analysis. High levels of metals in a sample can cause arcing in the microwave oven, and sometimes slag forms in the sample. Microwave oven drying can also melt plastic containers used to hold the sample.

11.6 The homogenized dried sample material should be ground with a mortar and pestle and passed through a 60-mesh sieve to achieve a uniform particle size. Sample grinding should continue until at least 90 percent of the original sample passes through the sieve. The grinding step normally takes an average of 10 min per sample. An aliquot of the sieved sample should then be placed in a 31.0-mm polyethylene sample cup (or equivalent) for analysis. The sample cup should be one-half to three-quarters full at a minimum. The sample cup should be covered with a 2.5 μm Mylar (or equivalent) film for analysis. The rest of the soil sample should be placed in a jar, labeled, and archived for possible confirmation analysis. All equipment including the mortar, pestle, and sieves must be thoroughly cleaned so that any cross-contamination is below the established lower limit of detection of the procedure or DQOs of the analysis. If all recommended sample preparation steps are followed, there is a high probability the desired laboratory data quality may be obtained.

12.0 DATA ANALYSIS AND CALCULATIONS

Most FPXRF instruments have software capable of storing all analytical results and spectra. The results are displayed in ppm and can be downloaded to a personal computer, which can be used to provide a hard copy printout. Individual measurements that are smaller than three times their associated SD should not be used for quantitation. See the manufacturer's instructions regarding data analysis and calculations.

13.0 METHOD PERFORMANCE

13.1 Performance data and related information are provided in SW-846 methods only as examples and guidance. The data do not represent required performance criteria for users of the methods. Instead, performance criteria should be developed on a project-specific basis, and the laboratory should establish in-house QC performance criteria for the application of this method. These performance data are not intended to be and must not be used as absolute QC acceptance criteria for purposes of laboratory accreditation.

13.2 The sections to follow discuss three performance evaluation factors; namely, precision, accuracy, and comparability. The example data presented in Tables 4 through 8 were generated from results obtained from six FPXRF instruments (see Sec. 13.3). The soil samples analyzed by the six FPXRF instruments were collected from two sites in the United States. The soil samples contained several of the target analytes at concentrations ranging from "nondetect" to tens of thousands of mg/kg. These data are provided for guidance purposes only.

13.3 The six FPXRF instruments included the TN 9000 and TN Lead Analyzer manufactured by TN Spectrace; the X-MET 920 with a SiLi detector and X-MET 920 with a gas-filled proportional detector manufactured by Metorex, Inc.; the XL Spectrum Analyzer manufactured by Niton; and the MAP Spectrum Analyzer manufactured by Scitec. The TN 9000 and TN Lead Analyzer both have a HgI_2 detector. The TN 9000 utilized an Fe-55, Cd-109, and Am-241 source. The TN Lead Analyzer had only a Cd-109 source. The X-Met 920 with the SiLi detector had a Cd-109 and Am-241 source. The X-MET 920 with the gas-filled proportional detector had only a Cd-109 source. The XL Spectrum Analyzer utilized a silicon pin-diode

detector and a Cd-109 source. The MAP Spectrum Analyzer utilized a solid-state silicon detector and a Cd-109 source.

13.4 All example data presented in Tables 4 through 8 were generated using the following calibrations and source count times. The TN 9000 and TN Lead Analyzer were calibrated using fundamental parameters using NIST SRM 2710 as a calibration check sample. The TN 9000 was operated using 100, 60, and 60 second count times for the Cd-109, Fe-55, and Am-241 sources, respectively. The TN Lead analyzer was operated using a 60 second count time for the Cd-109 source. The X-MET 920 with the Si(Li) detector was calibrated using fundamental parameters and one well characterized site-specific soil standard as a calibration check. It used 140 and 100 second count times for the Cd-109 and Am-241 sources, respectively. The X-MET 920 with the gas-filled proportional detector was calibrated empirically using between 10 and 20 well characterized site-specific soil standards. It used 120 second times for the Cd-109 source. The XL Spectrum Analyzer utilized NIST SRM 2710 for calibration and the Compton peak normalization procedure for quantitation based on 60 second count times for the Cd-109 source. The MAP Spectrum Analyzer was internally calibrated by the manufacturer. The calibration was checked using a well-characterized site-specific soil standard. It used 240 second times for the Cd-109 source.

13.5 Precision measurements -- The example precision data are presented in Table 4. These data are provided for guidance purposes only. Each of the six FPXRF instruments performed 10 replicate measurements on 12 soil samples that had analyte concentrations ranging from "nondetects" to thousands of mg/kg. Each of the 12 soil samples underwent 4 different preparation techniques from in situ (no preparation) to dried and ground in a sample cup. Therefore, there were 48 precision data points for five of the instruments and 24 precision points for the MAP Spectrum Analyzer. The replicate measurements were taken using the source count times discussed at the beginning of this section.

For each detectable analyte in each precision sample a mean concentration, standard deviation, and RSD was calculated for each analyte. The data presented in Table 4 is an average RSD for the precision samples that had analyte concentrations at 5 to 10 times the lower limit of detection for that analyte for each instrument. Some analytes such as mercury, selenium, silver, and thorium were not detected in any of the precision samples so these analytes are not listed in Table 4. Some analytes such as cadmium, nickel, and tin were only detected at concentrations near the lower limit of detection so that an RSD value calculated at 5 to 10 times this limit was not possible.

One FPXRF instrument collected replicate measurements on an additional nine soil samples to provide a better assessment of the effect of sample preparation on precision. Table 5 shows these results. These data are provided for guidance purposes only. The additional nine soil samples were comprised of three from each texture and had analyte concentrations ranging from near the lower limit of detection for the FPXRF analyzer to thousands of mg/kg. The FPXRF analyzer only collected replicate measurements from three of the preparation methods; no measurements were collected from the in situ homogenized samples. The FPXRF analyzer conducted five replicate measurements of the in situ field samples by taking measurements at five different points within the 4-inch by 4-inch sample square. Ten replicate measurements were collected for both the intrusive undried and unground and intrusive dried and ground samples contained in cups. The cups were shaken between each replicate measurement.

Table 5 shows that the precision dramatically improved from the in situ to the intrusive measurements. In general there was a slight improvement in precision when the sample was dried and ground. Two factors caused the precision for the in situ measurements to be poorer. The major factor is soil heterogeneity. By moving the probe within the 4-inch by 4-inch square,

measurements of different soil samples were actually taking place within the square. Table 5 illustrates the dominant effect of soil heterogeneity. It overwhelmed instrument precision when the FPXRF analyzer was used in this mode. The second factor that caused the RSD values to be higher for the in situ measurements is the fact that only five instead of ten replicates were taken. A lesser number of measurements caused the standard deviation to be larger which in turn elevated the RSD values.

13.6 Accuracy measurements -- Five of the FPXRF instruments (not including the MAP Spectrum Analyzer) analyzed 18 SRMs using the source count times and calibration methods given at the beginning of this section. The 18 SRMs included 9 soil SRMs, 4 stream or river sediment SRMs, 2 sludge SRMs, and 3 ash SRMs. Each of the SRMs contained known concentrations of certain target analytes. A percent recovery was calculated for each analyte in each SRM for each FPXRF instrument. Table 6 presents a summary of this data. With the exception of cadmium, chromium, and nickel, the values presented in Table 6 were generated from the 13 soil and sediment SRMs only. The 2 sludge and 3 ash SRMs were included for cadmium, chromium, and nickel because of the low or nondetectable concentrations of these three analytes in the soil and sediment SRMs.

Only 12 analytes are presented in Table 6. These are the analytes that are of environmental concern and provided a significant number of detections in the SRMs for an accuracy assessment. No data is presented for the X-MET 920 with the gas-filled proportional detector. This FPXRF instrument was calibrated empirically using site-specific soil samples. The percent recovery values from this instrument were very sporadic and the data did not lend itself to presentation in Table 6.

Table 7 provides a more detailed summary of accuracy data for one particular FPXRF instrument (TN 9000) for the 9 soil SRMs and 4 sediment SRMs. These data are provided for guidance purposes only. Table 7 shows the certified value, measured value, and percent recovery for five analytes. These analytes were chosen because they are of environmental concern and were most prevalently certified for in the SRM and detected by the FPXRF instrument. The first nine SRMs are soil and the last 4 SRMs are sediment. Percent recoveries for the four NIST SRMs were often between 90 and 110 percent for all analytes.

13.7 Comparability -- Comparability refers to the confidence with which one data set can be compared to another. In this case, FPXRF data generated from a large study of six FPXRF instruments was compared to SW-846 Methods 3050 and 6010 which are the standard soil extraction for metals and analysis by inductively coupled plasma. An evaluation of comparability was conducted by using linear regression analysis. Three factors were determined using the linear regression. These factors were the y-intercept, the slope of the line, and the coefficient of determination (r^2).

As part of the comparability assessment, the effects of soil type and preparation methods were studied. Three soil types (textures) and four preparation methods were examined during the study. The preparation methods evaluated the cumulative effect of particle size, moisture, and homogenization on comparability. Due to the large volume of data produced during this study, linear regression data for six analytes from only one FPXRF instrument is presented in Table 8. Similar trends in the data were seen for all instruments. These data are provided for guidance purposes only.

Table 8 shows the regression parameters for the whole data set, broken out by soil type, and by preparation method. These data are provided for guidance purposes only. The soil types are as follows: soil 1--sand; soil 2--loam; and soil 3--silty clay. The preparation methods are as follows: preparation 1--in situ in the field; preparation 2--intrusive, sample collected and homogenized; preparation 3--intrusive, with sample in a sample cup but sample still wet and not

ground; and preparation 4—intrusive, with sample dried, ground, passed through a 40-mesh sieve, and placed in sample cup.

For arsenic, copper, lead, and zinc, the comparability to the confirmatory laboratory was excellent with r^2 values ranging from 0.80 to 0.99 for all six FPXRF instruments. The slopes of the regression lines for arsenic, copper, lead, and zinc, were generally between 0.90 and 1.00 indicating the data would need to be corrected very little or not at all to match the confirmatory laboratory data. The r^2 values and slopes of the regression lines for barium and chromium were not as good as for the other for analytes, indicating the data would have to be corrected to match the confirmatory laboratory.

Table 8 demonstrates that there was little effect of soil type on the regression parameters for any of the six analytes. The only exceptions were for barium in soil 1 and copper in soil 3. In both of these cases, however, it is actually a concentration effect and not a soil effect causing the poorer comparability. All barium and copper concentrations in soil 1 and 3, respectively, were less than 350 mg/kg.

Table 8 shows there was a preparation effect on the regression parameters for all six analytes. With the exception of chromium, the regression parameters were primarily improved going from preparation 1 to preparation 2. In this step, the sample was removed from the soil surface, all large debris was removed, and the sample was thoroughly homogenized. The additional two preparation methods did little to improve the regression parameters. This data indicates that homogenization is the most critical factor when comparing the results. It is essential that the sample sent to the confirmatory laboratory match the FPXRF sample as closely as possible.

Sec. 11.0 of this method discusses the time necessary for each of the sample preparation techniques. Based on the data quality objectives for the project, an analyst must decide if it is worth the extra time necessary to dry and grind the sample for small improvements in comparability. Homogenization requires 3 to 5 min. Drying the sample requires one to two hours. Grinding and sieving requires another 10 to 15 min per sample. Lastly, when grinding and sieving is conducted, time has to be allotted to decontaminate the mortars, pestles, and sieves. Drying and grinding the samples and decontamination procedures will often dictate that an extra person be on site so that the analyst can keep up with the sample collection crew. The cost of requiring an extra person on site to prepare samples must be balanced with the gain in data quality and sample throughput.

13.8 The following documents may provide additional guidance and insight on this method and technique:

13.8.1 A. D. Hewitt, "Screening for Metals by X-ray Fluorescence Spectrometry/Response Factor/Compton K_α Peak Normalization Analysis," American Environmental Laboratory, pp 24-32, 1994.

13.8.2 S. Piorek and J. R. Pasmore, "Standardless, In Situ Analysis of Metallic Contaminants in the Natural Environment With a PC-Based, High Resolution Portable X-Ray Analyzer," Third International Symposium on Field Screening Methods for Hazardous Waste and Toxic Chemicals, Las Vegas, Nevada, February 24-26, 1993, Vol 2, pp 1135-1151, 1993.

13.8.3 S. Shefsky, "Sample Handling Strategies for Accurate Lead-in-soil Measurements in the Field and Laboratory," *International Symposium of Field Screening Methods for Hazardous Waste and Toxic Chemicals*, Las Vegas, NV, January 29-31, 1997.

14.0 POLLUTION PREVENTION

14.1 Pollution prevention encompasses any technique that reduces or eliminates the quantity and/or toxicity of waste at the point of generation. Numerous opportunities for pollution prevention exist in laboratory operation. The EPA has established a preferred hierarchy of environmental management techniques that places pollution prevention as the management option of first choice. Whenever feasible, laboratory personnel should use pollution prevention techniques to address their waste generation. When wastes cannot be feasibly reduced at the source, the Agency recommends recycling as the next best option.

14.2 For information about pollution prevention that may be applicable to laboratories and research institutions consult *Less is Better: Laboratory Chemical Management for Waste Reduction* available from the American Chemical Society's Department of Government Relations and Science Policy, 1155 16th St., N.W. Washington, D.C. 20036, <http://www.acs.org>.

15.0 WASTE MANAGEMENT

The Environmental Protection Agency requires that laboratory waste management practices be conducted consistent with all applicable rules and regulations. The Agency urges laboratories to protect the air, water, and land by minimizing and controlling all releases from hoods and bench operations, complying with the letter and spirit of any sewer discharge permits and regulations, and by complying with all solid and hazardous waste regulations, particularly the hazardous waste identification rules and land disposal restrictions. For further information on waste management, consult *The Waste Management Manual for Laboratory Personnel* available from the American Chemical Society at the address listed in Sec. 14.2.

16.0 REFERENCES

1. Metorex, X-MET 920 User's Manual.
2. Spectrace Instruments, "Energy Dispersive X-ray Fluorescence Spectrometry: An Introduction," 1994.
3. TN Spectrace, Spectrace 9000 Field Portable/Benchtop XRF Training and Applications Manual.
4. Unpublished SITE data, received from PRC Environment Management, Inc.

17.0 TABLES, DIAGRAMS, FLOWCHARTS, AND VALIDATION DATA

The following pages contain the tables referenced by this method. A flow diagram of the procedure follows the tables.

TABLE 1

EXAMPLE INTERFERENCE FREE LOWER LIMITS OF DETECTION

| Analyte | Chemical Abstract Series Number | Lower Limit of Detection in Quartz Sand (milligrams per kilogram) |
|-----------------|---------------------------------------|---|
| Antimony (Sb) | 7440-36-0 | 40 |
| Arsenic (As) | 7440-38-0 | 40 |
| Barium (Ba) | 7440-39-3 | 20 |
| Cadmium (Cd) | 7440-43-9 | 100 |
| Calcium (Ca) | 7440-70-2 | 70 |
| Chromium (Cr) | 7440-47-3 | 150 |
| Cobalt (Co) | 7440-48-4 | 60 |
| Copper (Cu) | 7440-50-8 | 50 |
| Iron (Fe) | 7439-89-6 | 60 |
| Lead (Pb) | 7439-92-1 | 20 |
| Manganese (Mn) | 7439-96-5 | 70 |
| Mercury (Hg) | 7439-97-6 | 30 |
| Molybdenum (Mo) | 7439-93-7 | 10 |
| Nickel (Ni) | 7440-02-0 | 50 |
| Potassium (K) | 7440-09-7 | 200 |
| Rubidium (Rb) | 7440-17-7 | 10 |
| Selenium (Se) | 7782-49-2 | 40 |
| Silver (Ag) | 7440-22-4 | 70 |
| Strontium (Sr) | 7440-24-6 | 10 |
| Thallium (Tl) | 7440-28-0 | 20 |
| Thorium (Th) | 7440-29-1 | 10 |
| Tin (Sn) | 7440-31-5 | 60 |
| Titanium (Ti) | 7440-32-6 | 50 |
| Vanadium (V) | 7440-62-2 | 50 |
| Zinc (Zn) | 7440-66-6 | 50 |
| Zirconium (Zr) | 7440-67-7 | 10 |

Source: Refs. 1, 2, and 3

These data are provided for guidance purposes only.

TABLE 2
SUMMARY OF RADIOISOTOPE SOURCE CHARACTERISTICS

| Source | Activity (mCi) | Half-Life (Years) | Excitation Energy (keV) | Elemental Analysis Range | |
|--------|-------------------|----------------------|----------------------------|---|-------------------------------|
| Fe-55 | 20-50 | 2.7 | 5.9 | Sulfur to Chromium Molybdenum to Barium | K Lines L Lines |
| Cd-109 | 5-30 | 1.3 | 22.1 and 87.9 | Calcium to Rhodium Tantalum to Lead Barium to Uranium | K Lines K Lines L Lines |
| Am-241 | 5-30 | 432 | 26.4 and 59.6 | Copper to Thulium Tungsten to Uranium | K Lines L Lines |
| Cm-244 | 60-100 | 17.8 | 14.2 | Titanium to Selenium Lanthanum to Lead | K Lines L Lines |

Source: Refs. 1, 2, and 3

TABLE 3
SUMMARY OF X-RAY TUBE SOURCE CHARACTERISTICS

| Anode Material | Recommended Voltage Range (kV) | K-alpha Emission (keV) | Elemental Analysis Range | |
|-------------------|--------------------------------------|------------------------------|--|--------------------|
| Cu | 18-22 | 8.04 | Potassium to Cobalt Silver to Gadolinium | K Lines L Lines |
| Mo | 40-50 | 17.4 | Cobalt to Yttrium Europium to Radon | K Lines L Lines |
| Ag | 50-65 | 22.1 | Zinc to Technicium Ytterbium to Neptunium | K Lines L Lines |

Source: Ref. 4

Notes: The sample elements excited are chosen by taking as the lower limit the same ratio of excitation line energy to element absorption edge as in Table 2 (approximately 0.45) and the requirement that the excitation line energy be above the element absorption edge as the upper limit (L2 edges used for L lines). K-beta excitation lines were ignored.

TABLE 4
EXAMPLE PRECISION VALUES

| Analyte | Average Relative Standard Deviation for Each Instrument at 5 to 10 Times the Lower Limit of Detection | | | | | |
|------------|--|---------------------|---------------------------------|---------------------------------------|----------------------------|-----------------------------|
| | TN 9000 | TN Lead Analyzer | X-MET 920 (SiLi Detector) | X-MET 920 (Gas-Filled Detector) | XL Spectrum Analyzer | MAP Spectrum Analyzer |
| Antimony | 6.54 | NR | NR | NR | NR | NR |
| Arsenic | 5.33 | 4.11 | 3.23 | 1.91 | 12.47 | 6.68 |
| Barium | 4.02 | NR | 3.31 | 5.91 | NR | NR |
| Cadmium | 29.84 ^a | NR | 24.80 ^a | NR | NR | NR |
| Calcium | 2.16 | NR | NR | NR | NR | NR |
| Chromium | 22.25 | 25.78 | 22.72 | 3.91 | 30.25 | NR |
| Cobalt | 33.90 | NR | NR | NR | NR | NR |
| Copper | 7.03 | 9.11 | 8.49 | 9.12 | 12.77 | 14.86 |
| Iron | 1.78 | 1.67 | 1.55 | NR | 2.30 | NR |
| Lead | 6.45 | 5.93 | 5.05 | 7.56 | 6.97 | 12.16 |
| Manganese | 27.04 | 24.75 | NR | NR | NR | NR |
| Molybdenum | 6.95 | NR | NR | NR | 12.60 | NR |
| Nickel | 30.85 ^a | NR | 24.92 ^a | 20.92 ^a | NA | NR |
| Potassium | 3.90 | NR | NR | NR | NR | NR |
| Rubidium | 13.06 | NR | NR | NR | 32.69 ^a | NR |
| Strontium | 4.28 | NR | NR | NR | 8.86 | NR |
| Tin | 24.32 ^a | NR | NR | NR | NR | NR |
| Titanium | 4.87 | NR | NR | NR | NR | NR |
| Zinc | 7.27 | 7.48 | 4.26 | 2.28 | 10.95 | 0.83 |
| Zirconium | 3.58 | NR | NR | NR | 6.49 | NR |

These data are provided for guidance purposes only.

Source: Ref. 4

^a These values are biased high because the concentration of these analytes in the soil samples was near the lower limit of detection for that particular FPXRF instrument.

NR Not reported.

NA Not applicable; analyte was reported but was below the established lower limit detection.

TABLE 5

EXAMPLES OF PRECISION AS AFFECTED BY SAMPLE PREPARATION

| Analyte | Average Relative Standard Deviation for Each Preparation Method | | |
|----------------------|---|------------------------------------|--------------------------------|
| | In Situ-Field | Intrusive- Undried and Unground | Intrusive- Dried and Ground |
| Antimony | 30.1 | 15.0 | 14.4 |
| Arsenic | 22.5 | 5.36 | 3.76 |
| Barium | 17.3 | 3.38 | 2.90 |
| Cadmium ^a | 41.2 | 30.8 | 28.3 |
| Calcium | 17.5 | 1.68 | 1.24 |
| Chromium | 17.6 | 28.5 | 21.9 |
| Cobalt | 28.4 | 31.1 | 28.4 |
| Copper | 26.4 | 10.2 | 7.90 |
| Iron | 10.3 | 1.67 | 1.57 |
| Lead | 25.1 | 8.55 | 6.03 |
| Manganese | 40.5 | 12.3 | 13.0 |
| Mercury | ND | ND | ND |
| Molybdenum | 21.6 | 20.1 | 19.2 |
| Nickel ^a | 29.8 | 20.4 | 18.2 |
| Potassium | 18.6 | 3.04 | 2.57 |
| Rubidium | 29.8 | 16.2 | 18.9 |
| Selenium | ND | 20.2 | 19.5 |
| Silver ^a | 31.9 | 31.0 | 29.2 |
| Strontium | 15.2 | 3.38 | 3.98 |
| Thallium | 39.0 | 16.0 | 19.5 |
| Thorium | NR | NR | NR |
| Tin | ND | 14.1 | 15.3 |
| Titanium | 13.3 | 4.15 | 3.74 |
| Vanadium | NR | NR | NR |
| Zinc | 26.6 | 13.3 | 11.1 |
| Zirconium | 20.2 | 5.63 | 5.18 |

These data are provided for guidance purposes only.

Source: Ref. 4

^a These values may be biased high because the concentration of these analytes in the soil samples was near the lower limit of detection.

ND Not detected.

NR Not reported.

TABLE 6
EXAMPLE ACCURACY VALUES

| Analyte | Instrument | | | | | | | | | | | | | | | |
|---------|------------|-----------------|-------------|------|------------------|-----------------|-------------|------|---------------------------|-----------------|-------------|------|----------------------|-----------------|-------------|------|
| | TN 9000 | | | | TN Lead Analyzer | | | | X-MET 920 (SiLi Detector) | | | | XL Spectrum Analyzer | | | |
| | n | Range of % Rec. | Mean % Rec. | SD | n | Range of % Rec. | Mean % Rec. | SD | n | Range of % Rec. | Mean % Rec. | SD | n | Range of % Rec. | Mean % Rec. | SD |
| Sb | 2 | 100-149 | 124.3 | NA | -- | -- | -- | -- | -- | -- | -- | -- | -- | -- | -- | -- |
| As | 5 | 68-115 | 92.8 | 17.3 | 5 | 44-105 | 83.4 | 23.2 | 4 | 9.7-91 | 47.7 | 39.7 | 5 | 38-535 | 189.8 | 206 |
| Ba | 9 | 98-198 | 135.3 | 36.9 | -- | -- | -- | -- | 9 | 18-848 | 168.2 | 262 | -- | -- | -- | -- |
| Cd | 2 | 99-129 | 114.3 | NA | -- | -- | -- | -- | 6 | 81-202 | 110.5 | 45.7 | -- | -- | -- | -- |
| Cr | 2 | 99-178 | 138.4 | NA | -- | -- | -- | -- | 7 | 22-273 | 143.1 | 93.8 | 3 | 98-625 | 279.2 | 300 |
| Cu | 8 | 61-140 | 95.0 | 28.8 | 6 | 38-107 | 79.1 | 27.0 | 11 | 10-210 | 111.8 | 72.1 | 8 | 95-480 | 203.0 | 147 |
| Fe | 6 | 78-155 | 103.7 | 26.1 | 6 | 89-159 | 102.3 | 28.6 | 6 | 48-94 | 80.4 | 16.2 | 6 | 26-187 | 108.6 | 52.9 |
| Pb | 11 | 66-138 | 98.9 | 19.2 | 11 | 68-131 | 97.4 | 18.4 | 12 | 23-94 | 72.7 | 20.9 | 13 | 80-234 | 107.3 | 39.9 |
| Mn | 4 | 81-104 | 93.1 | 9.70 | 3 | 92-152 | 113.1 | 33.8 | -- | -- | -- | -- | -- | -- | -- | -- |
| Ni | 3 | 99-122 | 109.8 | 12.0 | -- | -- | -- | -- | -- | -- | -- | -- | 3 | 57-123 | 87.5 | 33.5 |
| Sr | 8 | 110-178 | 132.6 | 23.8 | -- | -- | -- | -- | -- | -- | -- | -- | 7 | 86-209 | 125.1 | 39.5 |
| Zn | 11 | 41-130 | 94.3 | 24.0 | 10 | 81-133 | 100.0 | 19.7 | 12 | 46-181 | 106.6 | 34.7 | 11 | 31-199 | 94.6 | 42.5 |

Source: Ref. 4. These data are provided for guidance purposes only.

n: Number of samples that contained a certified value for the analyte and produced a detectable concentration from the FPXRF instrument.

SD: Standard deviation; NA: Not applicable; only two data points, therefore, a SD was not calculated.

%Rec.: Percent recovery.

-- No data.

TABLE 7
EXAMPLE ACCURACY FOR TN 9000^a

| Standard Reference Material | Arsenic | | | Barium | | | Copper | | | Lead | | | Zinc | | |
|-----------------------------|-------------|-------------|-------|-------------|-------------|-------|-------------|-------------|-------|-------------|-------------|-------|-------------|-------------|-------|
| | Cert. Conc. | Meas. Conc. | %Rec. | Cert. Conc. | Meas. Conc. | %Rec. | Cert. Conc. | Meas. Conc. | %Rec. | Cert. Conc. | Meas. Conc. | %Rec. | Cert. Conc. | Meas. Conc. | %Rec. |
| RTC CRM-021 | 24.8 | ND | NA | 586 | 1135 | 193.5 | 4792 | 2908 | 60.7 | 144742 | 149947 | 103.6 | 546 | 224 | 40.9 |
| RTC CRM-020 | 397 | 429 | 92.5 | 22.3 | ND | NA | 753 | 583 | 77.4 | 5195 | 3444 | 66.3 | 3022 | 3916 | 129.6 |
| BCR CRM 143R | -- | -- | -- | -- | -- | -- | 131 | 105 | 80.5 | 180 | 206 | 114.8 | 1055 | 1043 | 99.0 |
| BCR CRM 141 | -- | -- | -- | -- | -- | -- | 32.6 | ND | NA | 29.4 | ND | NA | 81.3 | ND | NA |
| USGS GXR-2 | 25.0 | ND | NA | 2240 | 2946 | 131.5 | 76.0 | 106 | 140.2 | 690 | 742 | 107.6 | 530 | 596 | 112.4 |
| USGS GXR-6 | 330 | 294 | 88.9 | 1300 | 2581 | 198.5 | 66.0 | ND | NA | 101 | 80.9 | 80.1 | 118 | ND | NA |
| NIST 2711 | 105 | 104 | 99.3 | 726 | 801 | 110.3 | 114 | ND | NA | 1162 | 1172 | 100.9 | 350 | 333 | 94.9 |
| NIST 2710 | 626 | 722 | 115.4 | 707 | 782 | 110.6 | 2950 | 2834 | 96.1 | 5532 | 5420 | 98.0 | 6952 | 6476 | 93.2 |
| NIST 2709 | 17.7 | ND | NA | 968 | 950 | 98.1 | 34.6 | ND | NA | 18.9 | ND | NA | 106 | 98.5 | 93.0 |
| NIST 2704 | 23.4 | ND | NA | 414 | 443 | 107.0 | 98.6 | 105 | 106.2 | 161 | 167 | 103.5 | 438 | 427 | 97.4 |
| CNRC PACS-1 | 211 | 143 | 67.7 | -- | 772 | NA | 452 | 302 | 66.9 | 404 | 332 | 82.3 | 824 | 611 | 74.2 |
| SARM-51 | -- | -- | -- | 335 | 466 | 139.1 | 268 | 373 | 139.2 | 5200 | 7199 | 138.4 | 2200 | 2676 | 121.6 |
| SARM-52 | -- | -- | -- | 410 | 527 | 128.5 | 219 | 193 | 88.1 | 1200 | 1107 | 92.2 | 264 | 215 | 81.4 |

Source: Ref. 4. These data are provided for guidance purposes only.

^a All concentrations in milligrams per kilogram.

%Rec.: Percent recovery; ND: Not detected; NA: Not applicable.

-- No data.

TABLE 8

EXAMPLE REGRESSION PARAMETERS FOR COMPARABILITY¹

| | Arsenic | | | | Barium | | | | Copper | | | |
|----------|---------|----------------|------|-------|--------|----------------|------|-------|--------|----------------|-------|-------|
| | n | r ² | Int. | Slope | n | r ² | Int. | Slope | n | r ² | Int. | Slope |
| All Data | 824 | 0.94 | 1.62 | 0.94 | 1255 | 0.71 | 60.3 | 0.54 | 984 | 0.93 | 2.19 | 0.93 |
| Soil 1 | 368 | 0.96 | 1.41 | 0.95 | 393 | 0.05 | 42.6 | 0.11 | 385 | 0.94 | 1.26 | 0.99 |
| Soil 2 | 453 | 0.94 | 1.51 | 0.96 | 462 | 0.56 | 30.2 | 0.66 | 463 | 0.92 | 2.09 | 0.95 |
| Soil 3 | — | — | — | — | 400 | 0.85 | 44.7 | 0.59 | 136 | 0.46 | 16.60 | 0.57 |
| Prep 1 | 207 | 0.87 | 2.69 | 0.85 | 312 | 0.64 | 53.7 | 0.55 | 256 | 0.87 | 3.89 | 0.87 |
| Prep 2 | 208 | 0.97 | 1.38 | 0.95 | 315 | 0.67 | 64.6 | 0.52 | 246 | 0.96 | 2.04 | 0.93 |
| Prep 3 | 204 | 0.96 | 1.20 | 0.99 | 315 | 0.78 | 64.6 | 0.53 | 236 | 0.97 | 1.45 | 0.99 |
| Prep 4 | 205 | 0.96 | 1.45 | 0.98 | 313 | 0.81 | 58.9 | 0.55 | 246 | 0.96 | 1.99 | 0.96 |

| | Lead | | | | Zinc | | | | Chromium | | | |
|----------|------|----------------|------|-------|------|----------------|------|-------|----------|----------------|------|-------|
| | n | r ² | Int. | Slope | n | r ² | Int. | Slope | n | r ² | Int. | Slope |
| All Data | 1205 | 0.92 | 1.66 | 0.95 | 1103 | 0.89 | 1.86 | 0.95 | 280 | 0.70 | 64.6 | 0.42 |
| Soil 1 | 357 | 0.94 | 1.41 | 0.96 | 329 | 0.93 | 1.78 | 0.93 | — | — | — | — |
| Soil 2 | 451 | 0.93 | 1.62 | 0.97 | 423 | 0.85 | 2.57 | 0.90 | — | — | — | — |
| Soil 3 | 397 | 0.90 | 2.40 | 0.90 | 351 | 0.90 | 1.70 | 0.98 | 186 | 0.66 | 38.9 | 0.50 |
| Prep 1 | 305 | 0.80 | 2.88 | 0.86 | 286 | 0.79 | 3.16 | 0.87 | 105 | 0.80 | 66.1 | 0.43 |
| Prep 2 | 298 | 0.97 | 1.41 | 0.96 | 272 | 0.95 | 1.86 | 0.93 | 77 | 0.51 | 81.3 | 0.36 |
| Prep 3 | 302 | 0.98 | 1.26 | 0.99 | 274 | 0.93 | 1.32 | 1.00 | 49 | 0.73 | 53.7 | 0.45 |
| Prep 4 | 300 | 0.96 | 1.38 | 1.00 | 271 | 0.94 | 1.41 | 1.01 | 49 | 0.75 | 31.6 | 0.56 |

Source: Ref. 4. These data are provided for guidance purposes only.

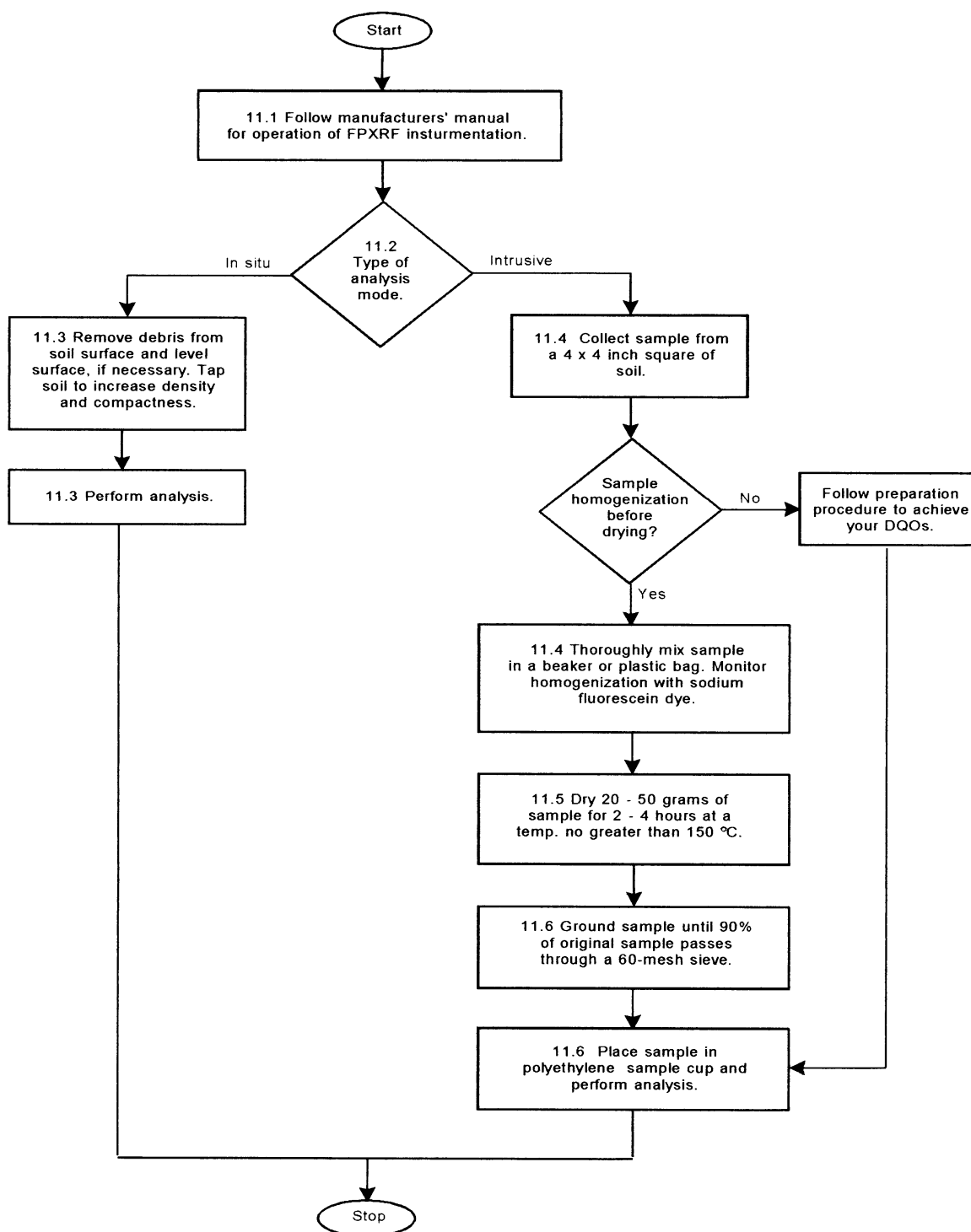
¹ Log-transformed data

n: Number of data points; r²: Coefficient of determination; Int.: Y-intercept

— No applicable data

METHOD 6200

FIELD PORTABLE X-RAY FLUORESCENCE SPECTROMETRY FOR THE DETERMINATION OF ELEMENTAL CONCENTRATIONS IN SOIL AND SEDIMENT



Appendix C

NIOSH Method 7702

LEAD BY FIELD PORTABLE XRF

7702

Pb MW: 207.19 (Pb) CAS: 7439-92-1 (Pb) RTECS: OF7525000 (Pb)
223.19 (PbO) 1317-3608 (PbO) OG1750000 (PbO)

METHOD: 7702, Issue 1

EVALUATION: FULL

Issue 1: 15 January 1998

OSHA: 0.05 mg/m³
NIOSH: <0.1 mg/m³; blood lead ≤ 60 µg/100 g
ACGIH: 0.05 mg/m³; BEI blood 30 µg/ 100 mL

PROPERTIES: soft metal; d 11.3 g/mL @ 20 °C; MP 327.5°C; BP 1740°C; valences +2, +4 in salts

SYNONYMS: elemental lead and lead compounds except alkyl lead

| SAMPLING | | MEASUREMENT | |
|------------------------------------|--|-----------------------|---|
| SAMPLER: | FILTER (0.8-µm, 37-mm, mixed cellulose ester membrane) | TECHNIQUE: | X-RAY FLUORESCENCE (XRF), PORTABLE, L-SHELL EXCITATION (e.g., ¹⁰⁹ Cd source) |
| FLOW RATE: | 1 to 4 L/min | | NOTE: Performance parameters are based upon research conducted with the NITON® 700 XRF [1]. |
| VOL-MIN: | 570 L @ 30.0 µg/m ³ [1] | | |
| -MAX: | 1900 L @ 9.0 µg/m ³ | | |
| SHIPMENT: | routine | ANALYTE: | lead |
| SAMPLE STABILITY: | stable | CALIBRATION: | lead thin-film standards (Micromatter Co., or equivalent); internal instrument calibration |
| BLANKS: | 2 to 10 field blanks per set | RANGE: | 17 to 1500 µg of Pb per sample [1] |
| ACCURACY | | ESTIMATED LOD: | 6 µg of Pb per sample [1] |
| RANGE STUDIED: | 0.1 to 1514.6 µg/m ³ (as Pb) (based upon lead mass loadings) | | |
| BIAS: | 0.069 [1] | | |
| PRECISION (S_{rT}): | 0.054 @ 10.3 to 612 µg Pb per sample | | |
| ACCURACY: | ±16.4% | | |

APPLICABILITY: This method was evaluated for air samples on filters only. The working range of this method is 0.017 mg/m³ to 1.5 mg/m³. This is a field portable analytical method, particularly useful for the analysis of initial exposure assessment samples, or for applications where laboratory analysis is impractical. Additionally, the method is non-destructive; samples analyzed in the field can later be analyzed in a laboratory. The method is applicable to all elemental lead forms, including lead fume, and all other aerosols containing lead.

INTERFERENCES: The presence of bromine will cause XRF readings for lead to be elevated, resulting in a positive bias error. Other interferences may exist in other XRF instruments.

OTHER METHODS: Laboratory-based methods include atomic spectrophotometric methods following hot plate acid digestion: NIOSH methods 7082 (flame atomic absorption spectrophotometry) [2], 7105 (graphite furnace atomic absorption spectrophotometry) [3], and 7300 (inductively coupled plasma atomic emission spectrophotometry) [4]. A field-portable analytical method for lead air filter samples using ultrasound/ASV has been developed, NIOSH Method 7701[5]. A field-portable screening method by spot test kit has been developed, NIOSH Method 7700 [6].

REAGENTS:

1. None

EQUIPMENT:

1. Sampler: Mixed cellulose ester filter, 0.8- μ m pore size, 37-mm diameter, with cellulose back-up pad, in a closed-faced cassette filter holder.
2. Personal sampling pump, 1 to 4 L/min, with flexible connecting tubing.
3. Field portable, L-shell X-Ray Fluorescence (XRF) instrument with a Cadmium-109 source.
4. Filter sleeve: thin cardboard with 37-mm dia. cut out, and covered with a light adhesive between two pieces of acetate (Mylar™) (NITON, Bedford, MA, or equivalent).
NOTE: Material must be transparent to X-ray.
5. Filter test platform to hold the filter (specific to instrument).
6. Forceps
7. Thin film standard reference materials from 15 μ g/cm² to 150 μ g/cm² (Micromatter Co., Deer Harbor, WA), or equivalent [7,8].

SPECIAL PRECAUTIONS: None

SAMPLING:

1. Calibrate each sampling pump with a representative sampler in line.
2. Sample at an accurately known flow rate (1 to 4 L/min) for a total sample size of approximately 1000 L. Do not exceed a filter loading of 2 mg total dust.

SAMPLE PREPARATION:

3. With forceps, transfer the MCE filter without the backup pad to a filter sleeve. The sleeve material must be transparent to X-rays (see EQUIPMENT, Item 4).
NOTE: Take special care when removing the filter from the backup pad to avoid loss of lead-containing dust.
4. Place the filter into 37-mm opening and seal with Mylar™ film to prevent losses and allow undisturbed analysis of the filter.
5. Place the sealed filter onto the filter test platform of the instrument for analysis.
NOTE: The NITON® 700 Series XRF has a filter test platform that allows for three readings with no substrate effect.

CALIBRATION AND QUALITY CONTROL:

6. Start XRF and allow a 30-minute warm-up period. The instrument will conduct an internal self-calibration.
7. Using thin film standards [8], verify the internal calibration to within 5% of the calibration standard. Use a minimum of three standards at concentrations of 15 μ g/cm², 150 μ g/cm², and one standard concentration between these two values.
8. Restart the instrument as needed to assure instrument accuracy prior to sample analysis.
NOTE: When the thin film standard measurements are not within the specified parameters, the instrument may need to be recalibrated at the factory.
9. Analyze one thin film standard every 2 hours to check for instrument drift.
10. Repeat step 7 when all analyses are completed as a post-calibration check.

MEASUREMENT:

11. Set instrument parameters and analyze filter samples as specified by the manufacturer. The following measurement technique is based upon the NITON® 700 XRF.
 - a. Analyze the middle of the sample filter first (see Figure 1, M).
 - b. Allow the instrument to take a one source-minute reading (This may take longer than one real-time minute, depending upon the source strength). A one source-minute reading will assure the accurate L-shell reading necessary for the analysis of lead air filter samples.
 - c. Analyze the filter sample at the top of the filter for one source minute (see Figure 1, T).
 - d. Analyze the filter sample at the bottom of the filter for one source minute (see Figure 1, B).
 - e. The instrument software uses an algorithm that converts the three readings in $\mu\text{g}/\text{cm}^2$ to an analytical result in μg of lead per sample. This result will be displayed following the third filter reading [1].
 - f. Analyze one standard every 2 hours (step 8).
 - g. Repeat three-reading calibration check following completion of analyses (step 8).

CALCULATIONS:

12. Using the measured lead concentration, W (μg), calculate the concentration, C (mg/m^3), of lead in the air volume sampled, V (L):

$$C = \frac{W}{V}, \text{ mg}/\text{m}^3$$

NOTE: $\mu\text{g}/\text{L} \equiv \text{mg}/\text{m}^3$

EVALUATION OF METHOD:

This method was validated on field samples [1] by collecting lead particulate samples from bridge lead abatement projects. Airborne concentrations of lead within the containment of a sand blasting bridge lead abatement project ranged from 1 to 10 mg/m^3 . Area samples were collected for periods of time ranging from 15 seconds to 2 hours. This sampling protocol yielded 61 filter samples with lead loadings ranging between 0.1 to 1514.6 μg of lead per sample. Four personal samples were collected from a hand-scraping bridge lead abatement project for a total sample size of 65. The samples were first analyzed using a non-destructive, field portable XRF method. Samples subsequently were subjected to confirmatory analysis by the laboratory based NIOSH method 7105, Lead by GFAAS [3]. The method was statistically evaluated according to the NIOSH Guidelines for Air Sampling and Analytical Method Development and Evaluation [9]. The overall precision (\hat{S}_{RT}) of the XRF method was calculated at 0.054 with a 95% confidence interval (CI) of 0.035 to 0.073, and the bias was 0.069 with a 95% CI of 0.006 to 1.515. The XRF method accuracy was determined to be $\pm 16\%$; however, at the upper 90% CI, the accuracy is $\pm 27\%$. Since the confidence interval includes the $\pm 25\%$, meeting the NIOSH accuracy criteria of $\pm 25\%$ is inconclusive. However, the samples used to evaluate this method were field samples. Laboratory prepared aerosol samples would be expected to give better precision. Additionally, the XRF method is non-destructive; samples analyzed in the field can subsequently be analyzed in a laboratory using a method with greater accuracy, as needed. The filter sleeve used with the NITON® 700 Series XRF used a Mylar film to cover and seal the 37-mm filter. The lead particulate on the surface of the filter came into contact with the Mylar™ film. Both the Mylar™ film and the filter were digested with nitric acid and hydrogen peroxide as is specified in NIOSH Method 7105 [3].

REFERENCES:

- [1] Morley JC [1997]. Evaluation of a portable x-ray fluorescence instrument for the determination of lead in workplace air samples [Thesis]. Cincinnati, OH: University of Cincinnati, Department of Environmental Health, College of Medicine.
- [2] NIOSH [1994]. Lead by FAAS: Method 7082. In: Eller PM, Cassinelli ME, eds. NIOSH Manual of Analytical Methods (NMAM), 4th ed. Cincinnati, OH: National Institute for Occupational Safety and Health.

- Health, DHHS (NIOSH) Publication No. 94-113.
- [3] NIOSH [1994]. Lead by GFAAS: Method 7105. In: Eller PM, Cassinelli ME, eds. NIOSH Manual of Analytical Methods (NMAM), 4th ed. Cincinnati, OH: National Institute for Occupational Safety and Health, DHHS (NIOSH) Publication No. 94-113.
- [4] NIOSH [1994]. Elements: Method 7300. In: Eller PM, Cassinelli ME, eds. NIOSH Manual of Analytical Methods (NMAM), 4th ed. Cincinnati, OH: National Institute for Occupational Safety and Health, DHHS (NIOSH) Publication No. 94-113.
- [5] NIOSH [1994]. Lead by ultrasound/ASV: Method 7701 (supplement issued 1/15/98). In: Eller PM, Cassinelli ME, eds. NIOSH Manual of Analytical Methods (NMAM), 4th ed. Cincinnati, OH: National Institute for Occupational Safety and Health, DHHS (NIOSH) Publication No. 98-119.
- [6] NIOSH [1994]. Lead in air by chemical spot test: Method 7700 (supplement issued 5/15/96). In: Eller PM, Cassinelli ME, eds. NIOSH Manual of Analytical Methods (NMAM), 4th ed. Cincinnati, OH: National Institute for Occupational Safety and Health, DHHS (NIOSH) Publication No. 96-135.
- [7] National Institute of Standards and Technology, Standard Reference Material Program, Standard Reference Material 2579, Lead paint film on Mylar sheet for portable X-ray fluorescence analyzers, Gaithersburg, MD 20899.
- [8] Micromatter Co., XRF Calibration Standards, P.O. Box 123, Deer Harbor, Washington, 98243, Phone (360) 3 76-4007.
- [9] NIOSH [1995]. Kennedy, E.R., Fishbach, T.J., Song, R., Eller, P.M., Shulman, S.S.. Guidelines for Air Sampling and Analytical Method Development and Evaluation. Cincinnati, Ohio: National Institute for Occupational Safety and Health, DHHS (NIOSH) Publication No. 95-117.

METHOD WRITTEN BY: J. Clinton Morley, MS, NIOSH/DSHEFS

,

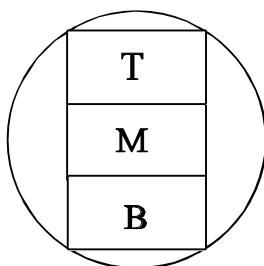


Figure 1: Analysis of a 37-mm filter
(XRF windows identified as M, T,

using XRF
and B are 2 cm x 1 cm)

Appendix D

Hach Method 8033

★Method 8033

Dithizone Method¹

Powder Pillows

(3 to 300 µg/L)

Scope and Application: For water and wastewater; USEPA accepted for reporting for wastewater analysis (digestion is required).²

¹ Adapted from Snyder, L. J., Analytical Chemistry, 19 684 (1947).

² Procedure is equivalent to Standard Method 3500-Pb D for wastewater analysis.



Test Preparation

Before starting the test:

For more accurate results, determine a reagent blank value for each new lot of reagent. Follow the procedure using deionized water instead of the sample.

Clean all glassware with a 1:1 Nitric Acid Solution. Rinse with deionized water.

Cloudy and turbid samples may require filtering before running the test. Report results as µg/L soluble lead. Use glass membrane type filter to avoid loss of lead by adsorption onto the filter paper.

If samples cannot be analyzed immediately, see [Sample Collection, Preservation, and Storage on page 5](#). Adjust the pH of preserved samples before analysis.

For more accurate results, adjust the sample to pH 11.0–11.5 using a pH meter in step 10. Omit the five additional drops of Sodium Hydroxide Standard Solution in step 11

The DithiVer powder will not completely dissolve in the chloroform. For further notes see [DithiVer Solution Preparation, Storage, and Reagent Blank on page 5](#).

Read the MSDS before testing. Spilled reagent will affect test accuracy and is hazardous to skin and other materials.

In bright light conditions (e.g. direct sunlight) it may be necessary to close the cell compartment with the protective cover during measurements.

Collect the following items:**Quantity**

| | |
|---|--------|
| Citrate Buffer Powder Pillows | 1 |
| Chloroform | 500 mL |
| DithiVer Metals Reagent Powder Pillows | 1 |
| Lead Reagent Set | 1 |
| Potassium Cyanide | 2 g |
| Sodium Hydroxide solution, 5.0 N | 5 mL |
| Sodium Hydroxide Standard Solution, 5.0 N | varies |
| Cotton Balls | 1 |
| Clippers | 1 |
| Cylinder, 50-mL graduated mixing | 1 |
| Cylinder, 5-mL graduated | 1 |
| Cylinder, 50-mL graduated | 1 |
| Cylinder, 250-mL graduated | 1 |
| Funnel, 500-mL separatory | 1 |
| Sample Cells, 1-inch square, 25-mL | 2 |
| Spoon, measuring, 1.0-g | 1 |
| Support Ring (4-inch) and Stand (5 x 8-inch base) | 1 |

Note: Reorder information for consumables and replacement items is on page 6.

Powder Pillows

Method 8033

DANGER

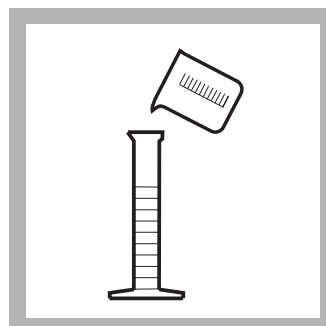
Cyanide is a deadly poison. Use a fume hood. Maintain cyanide solutions at pH 11 or greater to prevent formation of cyanide gas.



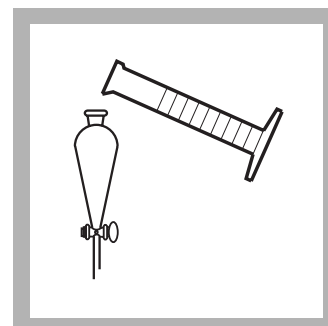
1. Press **STORED PROGRAMS**.



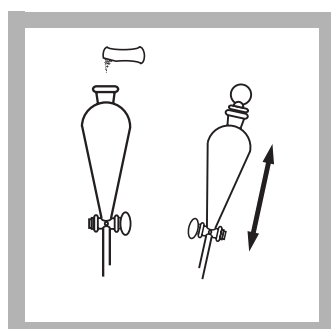
2. Select the test.



3. Fill a 250-mL graduated cylinder to the 250-mL mark with sample.

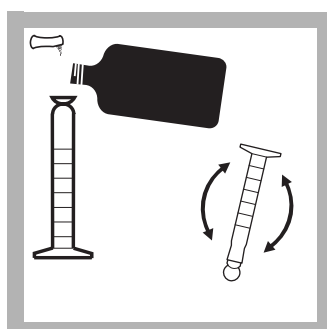


4. Transfer the sample into 500-mL separatory funnel.



5. Add the contents of one Buffer Powder Pillow for heavy metals, citrate type.

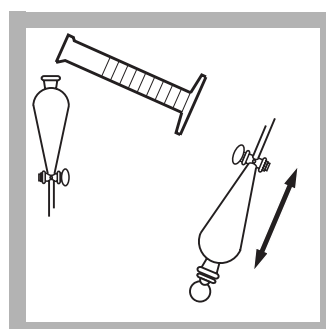
Stopper the funnel and shake to dissolve.



6. DithiVer Solution Preparation:

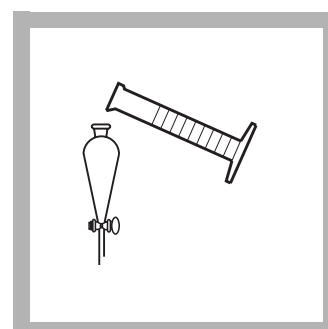
Add 50 mL of chloroform to a 50-mL mixing graduated cylinder. Add the contents of one DithiVer Metals Reagent Powder Pillow.

Stopper the cylinder. Invert several times to mix.

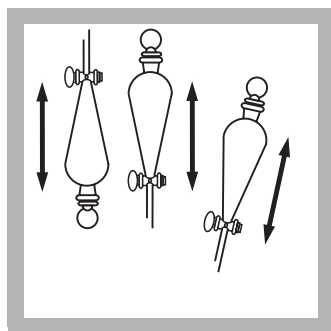


7. Measure 30 mL of the prepared dithizone solution with a second graduated cylinder and add to the separatory funnel.

Stopper and invert to mix. Open stopcock to vent. Close the stopcock.

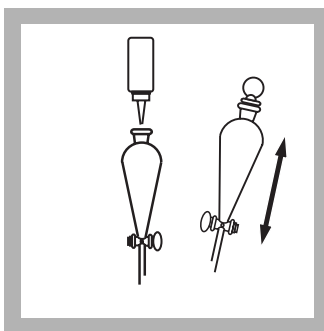


8. Add 5 mL of 5.0 N Sodium Hydroxide Standard Solution.



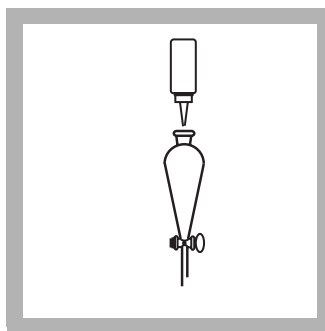
9. Stopper. Invert. Open stopcock to vent. Close the stopcock and shake the funnel once or twice and vent again.

Note: Add a few drops of 5.25 N Sulfuric Acid Standard Solution if the solution turns orange on shaking. The blue-green color will reappear. To avoid higher blanks, repeat procedure on new sample and use less sodium hydroxide in step 8.



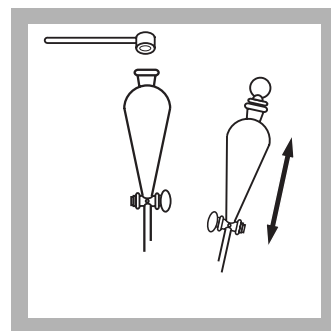
10. Continue adding 5.0 N Sodium Hydroxide Standard Solution dropwise and shaking the funnel after every few drops until the color of the solution being shaken changes from blue-green to orange.

Large amounts of zinc cause the color transition at the end point to be indistinct.



11. Add 5 more drops of 5.0 N Sodium Hydroxide Standard Solution.

A pink color in the bottom (chloroform) layer at this point does not necessarily indicate lead is present. Only after adding the potassium cyanide in the next step will the presence of lead be confirmed by a pink color.

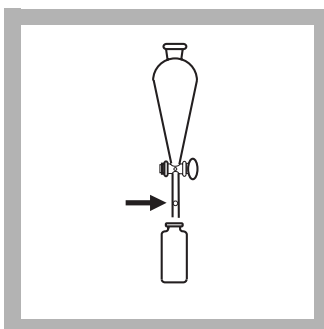


12. Add 2 heaping 1.0-g scoops of potassium cyanide to the funnel. Stopper.

Shake vigorously until the potassium cyanide is all dissolved (about 15 seconds).



13. Wait one minute for the layers to separate. The bottom (chloroform) layer will be pink if lead is present.



14. Prepared Sample: Insert a cotton plug the size of a pea into the delivery tube of the funnel and slowly drain the bottom (chloroform) layer into a dry 25-mL square sample cell. Stopper.

The lead-dithizone complex is stable for at least thirty minutes if the sample cell is kept tightly capped and out of direct sunlight.



15. Blank Preparation: Fill another 25-mL square sample cell with chloroform. Stopper.



16. Insert the blank into the cell holder with the fill line facing right.



17. Press ZERO.

The display will show:

0 µg/L Pb²⁺

18. Insert the prepared sample into the cell holder with the fill line facing right.

19. Press READ.

Results are in µg/L Pb²⁺.

Interferences

Table 1 Interfering Substances and Levels

| Interfering Substance | Interference Levels and Treatments |
|--|------------------------------------|
| Highly buffered samples or extreme sample pH | All levels. See procedure below. |
| Bismuth | All levels. See procedure below. |
| Copper | All levels. See procedure below. |
| Mercury | All levels. See procedure below. |
| Silver | All levels. See procedure below. |
| Tin | All levels. See procedure below. |

Table 2 Substances That Do Not Interfere

| | |
|----------|-----------|
| Aluminum | Lead |
| Antimony | Magnesium |
| Arsenic | Manganese |
| Calcium | Nickel |
| Chromium | Tin |
| Cobalt | Zinc |
| Iron | |

Eliminate interference from the metals in [Table 1](#) by the following treatment, beginning after [step 6](#).

1. Measure about 5-mL of the DithiVer solution into the separatory funnel. Stopper the funnel, invert and open the stopcock to vent. Close the stopcock and shake the solution vigorously for 15 seconds. Allow the funnel to stand undisturbed until the layers separate (about 30 seconds). A yellow, red, or bronze color in the bottom (chloroform) layer confirms the presence of interfering metals. Draw off and collect the bottom (chloroform) layer for proper disposal.

2. Repeat extraction with fresh 5-mL portions of prepared dithizone solution (collecting the bottom layer each time in appropriate waste collection vessel) until the bottom layer shows a pure dark green color for three successive extracts. Extractions can be repeated a number of times without appreciably affecting the amount of lead in the sample.
3. Extract the solution with several 2 or 3 mL portions of pure chloroform to remove any remaining dithizone, again collecting the bottom layer each time for proper disposal.
4. Continue the procedure, substituting 28.5 mL of prepared dithizone solution for the 30 mL in step 7.

DithiVer Solution Preparation, Storage, and Reagent Blank

Store DithiVer Powder Pillows away from light and heat. A convenient way to prepare this solution is to add the contents of 10 DithiVer Metals Reagent Powder Pillows to a 500-mL bottle of chloroform and invert several times until well mixed (carrier powder may not dissolve). Store dithizone solution in an amber glass bottle. This solution is stable for 24 hours.

A reagent blank using deionized water should be carried out through the entire method to obtain the most accurate results.

Sample Collection, Preservation, and Storage

Collect samples in an acid-washed glass or plastic containers. Adjust the pH to 2 or less with nitric acid (about 2 mL per liter). Store preserved samples up to six months at room temperature. Adjust the pH to 2.5 with 5.0 N sodium hydroxide before analysis. Correct the test result for volume additions.

Accuracy Check

1. Leave the unspiked sample in the sample cell compartment. Verify that the units displayed are in µg/L.
2. Press **OPTIONS>MORE**. Press **STANDARD ADDITIONS**. A summary of the standard additions procedure will appear.
3. Press **OK** to accept the default values for standard concentration, sample volume, and spike volumes. Press **EDIT** to change these values. After values are accepted, the unspiked sample reading will appear in top row. See the user manual for more information.
4. Snap the neck off a Lead Voluette Ampule Standard, 50-mg/L Pb.
5. Use the TenSette® Pipet (do not use a glass pipet) to add 0.1 mL, 0.2 mL, and 0.3 mL of standard, respectively to three 250-mL samples and mix each thoroughly.
6. Analyze each standard addition sample as described above. Accept the standard additions reading by pressing the soft key under **READ** each time. Each addition should reflect approximately 100% recovery.
7. After completing the sequence, press **GRAPH** to view the best-fit line through the standard additions data points, accounting for the matrix interferences. Press **IDEAL LINE** to view the relationship between the sample spikes and the "Ideal Line" of 100% recovery.

Standard Solution Method

1. Prepare a 10-mg/L lead standard solution by pipetting 10.00 mL of Lead Standard Solution, 100-mg/L, into a 100-mL volumetric flask.
2. Add 0.2 mL of concentrated nitric acid using a TenSette Pipet to prevent the adsorption of lead onto the container walls. Dilute to the mark with deionized water and mix thoroughly.
3. To make a 200-µg/L standard, pipet 5.00 mL of the 10.0-mg/L standard into 245 mL of deionized water in the 500-mL separatory funnel in step 4 of the Dithizone procedure. Prepare these solutions daily. Perform the lead procedure as described above.
4. To adjust the calibration curve using the reading obtained with the standard solution, press **OPTIONS>MORE** on the current program menu. Press **STANDARD ADJUST**.
5. Press **ON**. Press **ADJUST** to accept the displayed concentration. If an alternate concentration is used, press the number in the box to enter the actual concentration, then press **OK**. Press **ADJUST**.

Summary of Method

The dithizone method is designed for the determination of lead in water and wastewater. The DithiVer Metals Reagent is a stable powder form of dithizone. Lead ions in basic solution react with dithizone to form a pink to red lead-dithizonate complex, which is extracted with chloroform. Test results are measured at 515 nm.

Consumables and Replacement Items

Required Reagents

| Description | Quantity/Test | Unit | Cat. No. |
|--|---------------|----------|----------|
| Lead Reagent Set (100 Tests) | — | — | 22431-00 |
| Includes: (1) 14202-99, (2) 14458-17, (1) 12616-99, (2) 767-14, (1) 2450-53, (2) 2450-26 | | | |
| Buffer Powder Pillows, citrate | 1 | 100/pkg | 14202-99 |
| Chloroform, ACS | 30 mL | 4 L | 14458-17 |
| DithiVer Metals Reagent Powder Pillows | 1 | 100/pkg | 12616-99 |
| Potassium Cyanide | 0.1 g | 125 g | 767-14 |
| Sodium Hydroxide Solution, 5.0 N | 5 mL | 1000 mL | 2450-53 |
| Sodium Hydroxide Standard Solution, 5.0 N | varies | 59 mL DB | 2450-26 |

Required Apparatus

| Description | Quantity/Test | Unit | Cat. No. |
|--|---------------|---------|----------|
| Clippers, for opening powder pillows | 1 | each | 968-00 |
| Cotton Balls, absorbent | 1 | 100/pkg | 2572-01 |
| Cylinder, graduated, 5-mL | 1 | each | 508-37 |
| Cylinder, graduated, 50-mL | 1 | each | 508-41 |
| Cylinder, graduated, 250-mL | 1 | each | 508-46 |
| Cylinder, graduated, mixing, 50-mL | 1 | each | 1896-41 |
| Funnel, separatory, 500-mL | 1 | each | 520-49 |
| pH Meter, sens ^{ion} ™1, portable, with electrode | 1 | each | 51700-10 |
| Sample Cell, 1-inch square, 25 mL with cap | 2 | 2/pkg | 26126-02 |

Required Apparatus (continued)

| Description | Quantity/Test | Unit | Cat. No. |
|----------------------------------|---------------|------|----------|
| Spoon, measuring, 1-g | 1 | each | 510-00 |
| Support Ring, 4" | 1 | each | 580-01 |
| Support Ring Stand, 5" x 8" base | 1 | each | 563-00 |

Recommended Standards

| Description | Unit | Cat. No. |
|--|--------|----------|
| Lead Standard Solution, 100 mg/L Pb | 100 mL | 12617-42 |
| Lead Standard Solution, 10-mL Voluette Ampules, 50-mg/L Pb | 16/pkg | 14262-10 |

Optional Reagents and Apparatus

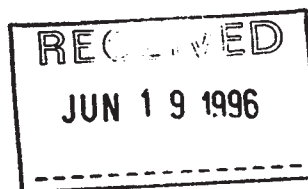
| Description | Unit | Cat. No. |
|---|-------------|----------|
| Ampule Breaker Kit | each | 21968-00 |
| Chloroform, ACS | 500 mL | 14458-49 |
| Filter Discs, glass, 47 mm | 100/pkg | 2530-00 |
| Filter Holder, glass, for 47-mm filter | each | 2340-00 |
| Flask, Erlenmeyer, 500-mL | each | 505-49 |
| Flask, filtering, 500-mL | each | 546-49 |
| Flask, volumetric, Class A, 100-mL | each | 14574-42 |
| Nitric Acid Solution, 1:1 | 500 mL | 2540-49 |
| Nitric Acid, ACS | 500 mL | 152-49 |
| pH Paper, pH 1.0 to 11.0 | 5 rolls/pkg | 391-33 |
| Pipet, serological, 2-mL | each | 532-36 |
| Pipet, TenSette®, 0.1 to 1.0 mL | each | 19700-01 |
| Pipet Tips, for TenSette Pipet 19700-01 | 50/pkg | 21856-96 |
| Pipet, volumetric, 5.00-mL, Class A | each | 14515-37 |
| Pipet, volumetric, 10.00-mL, Class A | each | 14515-38 |
| Pipet Filler, safety bulb | each | 14651-00 |
| Sulfuric Acid, 5.25 N | 100 mL MDB | 2449-32 |
| Water, deionized | 4 liters | 272-56 |

Appendix E

Approved/Accepted Hach Methods letter from U. S.
EPA



UNITED STATES ENVIRONMENTAL PROTECTION AGENCY
NATIONAL EXPOSURE RESEARCH LABORATORY
CINCINNATI, OH 45268



DATE: June 17, 1996

SUBJECT: Approved/Accepted Hach Methods

OFFICE OF
RESEARCH AND DEVELOPMENT

FROM: James W. O'Dell, Jr.
ATP Coordinator
Alternate Test Procedure Program
National Water Quality Assurance Programs Branch

TO: Addressee

This is in response to a number of requests concerning the approval/acceptance of Hach Company methods used for USEPA required compliance monitoring.

The following Hach methods are cited in Table 1A of 40 CFR Part 136.3 as approved for NPDES compliance monitoring.

| Parameter | Method | Approval Date |
|------------------------------|--------|----------------|
| Chemical Oxygen Demand (COD) | 8000 | April 21, 1980 |
| Copper--Total | 8506 | May 29, 1980 |
| Iron--Total | 8008 | June 27, 1980 |
| Manganese--Total | 8034 | June 14, 1979 |
| Nitrite (as N) | 8507 | May 1, 1979 |
| Zinc--Total | 8009 | May 29, 1980 |

The following Hach methods were reviewed by the Alternate Test Procedure (ATP) program and recommended as acceptable for NPDES compliance monitoring.

| Parameter | Method | Review Date |
|---------------------------------|--------|-------------------|
| Acidity, as CaCO ₃ | 8010 | February 17, 1983 |
| Ammonia, (as N) | 8038 | February 17, 1983 |
| Arsenic--Total | 8013 | February 17, 1983 |
| Biochemical Oxygen Demand (BOD) | 8043 | July 7, 1994 |
| Calcium--Total | 8222 | February 17, 1983 |
| Chemical Oxygen Demand (COD) | 8230 | December 24, 1985 |
| Chloride | 8224 | January 4, 1988 |
| Chloride | 8225 | December 3, 1987 |
| Chlorine--Total residual | 8167 | April 28, 1995 |
| Chlorine--Total residual | 8168 | February 17, 1983 |
| Chlorine--Total residual | 10014 | June 29, 1994 |
| Chromium VI dissolved | 8023 | February 17, 1983 |
| Fluoride--Total | 8029 | February 17, 1983 |
| Hardness--Total | 8226 | February 17, 1983 |
| Hydrogen Ion (pH) | 8156 | February 17, 1983 |

| | | |
|-----------------------------------|------|-------------------|
| Lead--Total | 8033 | May 27, 1987 |
| Nickel--Total | 8037 | December 4, 1985 |
| Oil and Grease--Total recoverable | 8005 | February 17, 1983 |
| Orthophosphate (as P) | 8048 | February 17, 1983 |
| Oxygen, Dissolved | 8157 | February 17, 1983 |
| Oxygen--Dissolved | 8229 | February 17, 1983 |
| Phenols | 8047 | January 5, 1987 |
| Phosphorous--Total | 8190 | February 17, 1983 |
| Residue--Nonfilterable (TSS) | 8158 | February 17, 1983 |
| Specific Conductance | 8160 | February 17, 1983 |
| Sulfate (as SO ₄) | 8051 | February 17, 1983 |
| Sulfide (as S) | 8131 | May 29, 1987 |
| Sulfite (as SO ₃) | 8071 | February 17, 1983 |

The following Hach methods were reviewed by the ATP program and recommended as acceptable for Drinking Water compliance monitoring.

| Contaminant | Method | Review Date |
|--------------|--------|-------------------|
| Conductivity | 8160 | February 17, 1983 |
| Fluoride | 8029 | February 17, 1983 |
| pH | 8156 | February 17, 1983 |

| Residual | Method | Review Date |
|----------------|--------|-------------------|
| Free Chlorine | 8021 | January 20, 1987 |
| Total Chlorine | 8167 | April 28, 1995 |
| Total Chlorine | 8168 | February 17, 1983 |
| Total Chlorine | 8370 | June 29, 1994 |

| Organism | Method | Review Date |
|----------------|--------|-------------------|
| Total Coliform | 8001 | February 17, 1983 |
| Fecal Coliform | 8001 | February 17, 1983 |

EPA approval/acceptance applies to the method version and reagent formulations specified at the time of review. Additional quality control procedures may be required to meet specific program monitoring requirements.

Addressees:

Arthur Clark, USEPA, Region I
 John Bourbon, USEPA, Region II
 Charles Jones, Jr., USEPA, Region III
 Wayne Turnbull, USEPA, Region IV
 Dennis Wesolowski, USEPA, Region V
 Charles Ritchey, USEPA, Region VI
 Doug Brune, USEPA, Region VII
 Rick Edmonds, USEPA, Region VIII
 Roscenne Sakamoto, USEPA, Region IX
 Bruce Woods, USEPA, Region X
 William Telliard, OW, OST
 Richard Reding, OGW & DW, TSD

**Deliverable for Task 3:
Purchase X-ray Fluorescence and
Field Spectrophotometer for Field Analyses**

Submitted

to

**Carl Kochersberger
Environmental Science Bureau
Hazardous Materials and Asbestos Unit
Pod 4-1
New York State Department of Transportation
50 Wolf Road
Albany, NY 12232**

August 02, 2012

Table of Contents

| | |
|---|----|
| 1. Introduction..... | 1 |
| 2. Field portable tools for metal analysis in paint and wash water | 2 |
| 2.1 Field Portable X-ray Fluorescence (FP-XRF) | 2 |
| 2.1.1 Comparison of FP-XRF Tools | 2 |
| 2.1.2 Selected FP-XRF: X-ray tube analyzers and NITON XLp 300 Series analyzers | 8 |
| 2.2 Field Portable Spectrophotometer..... | 11 |
| 3. Conclusion | 13 |
| 4 References..... | 14 |
| 5. Appendice | 17 |

1. Introduction

The removal of paint from bridges and other structures is a significant issue facing transportation agencies because of the potential presence of lead, as well as other metals, and potential impacts to human health and the environment that may be caused by a release of those metals. Although the hazards of lead paint removal from bridges have been largely identified, and advances have been made in worker protection, there is still a need to identify rapid and cost-effective methods for metal detection in-situ that can provide an accurate characterization of the waste classification. Currently, NYSDOT uses a conservative approach of classifying all bridge paint waste from the bridges constructed before 1989 as hazardous. This practice stems from the fact that there is no approved reliable, fast, and efficient method for classifying paint waste in situ as non-hazardous. This conservative practice eliminates the need for extensive testing, but also results in greater expense and increased regulatory burdens than are likely required. With the advent of more accurate and sophisticated analytical equipment for in-situ field measurements, state DOTs may benefit from research focused on the reliability of such field equipment for waste characterization.

The purpose of this report is to review the types of field portable tools for assessing metal concentrations in paint and wash water. Specifically, both the field portable X-ray fluorescence (FP-XRF) and the field portable spectrophotometer are discussed with respect to their effectiveness in providing reliable lead and metal concentrations present in bridge paint waste and wash water. Based on the review and vendor information, the field portable equipment selected for this project is presented.

2. Field portable tools for metal analysis in paint and wash water

Solid waste and paint wash-water are generated on-site whenever lead-based paint (LBP) is disturbed during maintenance, reconstruction, and demolition of bridges and other steel structures. FP-XRF meters and portable spectrophotometers are field tools used in providing lead and metal concentrations present in bridge paint waste and wash water. While these measurements have been found to be reliable, their effectiveness in classifying a waste or wash water as hazardous or not requires investigation.

2.1 Field Portable X-ray Fluorescence (FP-XRF)

Protocols for testing LBP with an XRF analyzer have been established by U.S. Environmental Protection Agency (U.S. EPA, 2001) and the U.S. Department of Housing and Urban Development (HUD, 1995). Several methods such as the U.S. EPA Method 6200 (U.S. EPA, 1998) and National Institute for Occupational Safety and Health (NIOSH) Method 7702 (NIOSH, 1998) involve the use of portable XRF technology. During the past several years, there has been a marked improvement in the technology of the FP-XRF, which has resulted in increased sensitivity and allowed for their use in such applications as air monitoring of particles (Morley et al., 1999; Zamurs et al., 1998), dust samples (Herman et al., 2006), soil samples (Clark et al., 1999; Sterling et al., 2004), and paint (Ashley et al., 1998; Daniels et al., 2001)

2.1.1 Comparison of FP-XRF Tools (X-ray tube vs isotope sources FP-XRF)

FP-XRF instruments use either a sealed radioisotope source or an X-ray tube to provide

the excitation energy. Radioisotope sources for irradiating samples include Fe^{55} , Co^{57} , Cd^{109} , Am^{241} , and Cm^{244} (Table 1); these sources undergo decay typically described with the half-life, which can be as short as 270 days (Co^{57}). As such, manufacturers of FP-XRF technology recommend source replacement at regular intervals based on the half-life and activity (Kalnicky and Singhvi, 2001).

Table 2 lists representative isotope and X-ray tube sources for FP-XRF instrumentation. Isotope sources give off radiation at specific energy levels and, therefore, efficiently excite elements within a specific atomic number range (L line or K line or both). As a result, no single radioisotope source is sufficient for exciting the entire range of elements of interest in environmental analysis. Some instruments provide dedicated element analysis (e.g., Pb in paint), while others provide a variety of elemental analyses depending on source and detector configuration. These units generally are readily adaptable to field operations, though they may be limited by the capacity of the battery. Units evaluated provide a minimum of 8 h of field use with rechargeable and replacement batteries.

Miniature X-ray tubes have become available since 2002 (Martin and Sackett, 2005), allowing their incorporation into portable XRFs. An important difference between X-ray tubes and radioactive sources is that X-ray tubes produce a continuum of X-rays across a broad range of energies. This continuum is weak compared to the characteristic X-rays, but can provide substantial excitation since it covers a broad energy range. However, one issue in

Table 1. Commonly used radioisotope source characteristics for XRF ^a

| Source | Activity(mCi) | Half Life (years) | Excitation Energy (keV) | Elemental Analysis Range | |
|-------------------|---------------|----------------------|----------------------------|--------------------------|---------|
| Fe ⁵⁵ | 20 – 50 | 2.7 | 5.9 | Sulfur to chromium | K Lines |
| | | | | Molybdenum to barium | L Lines |
| Co ⁵⁷ | 40 | 0.75 | 121.9 and 136 | Cobalt to cerium | K Lines |
| | | | | Barium to lead | L Lines |
| Cd ¹⁰⁹ | 5 – 30 | 1.3 | 22.1 and 87.9 | Calcium to rhodium | K Lines |
| | | | | Tantalum to lead | K Lines |
| | | | | Barium to uranium | L Lines |
| Am ²⁴¹ | 5 – 30 | 432 | 26.4 and 59.6 | Copper to thalium | K Lines |
| | | | | Tungsten to uranium | L Lines |
| Cm ²⁴⁴ | 60 – 100 | 17.8 | 14.2 | Titanium to selenium | K Lines |
| | | | | Lanthanum to lead | L Lines |

^aKalnicky and Singhvi (2001).

Table 2. Isotope and tube based sources for FP-XRF

| Developer | Technology | Element range | Excitation Source: | Cost of the instrument |
|-------------------------|-------------------------|------------------|--------------------------|------------------------------|
| Oxford | HorizonPbi ^a | Pb | Cd ¹⁰⁹ 20 mCi | Only available in France |
| Niton | Xli/p 300 | Pb | Cd ¹⁰⁹ 40 mCi | \$17,000 ^b |
| Oxford | XMET 5000/5100 | S–U | Ag anode, ≤ 45 keV | \$30,000-40,000 ^c |
| Niton | Niton XL3t 600 | K–U | Au anode, ≤ 50 keV | \$37,000 ^b |
| Innov-X Systems, Inc | LBP4000 | Pb | Ag anode, 10-25 keV | \$23, 220 ^d |
| Spectro | SPECTRO xSORT | S–U | W anode, ≤ 40 keV | \$34,536 ^e |

^a: Only available in France

^b The quotation from Niton

^c The quotation from Oxford

^d The quotation from Innov-X Systems, Inc

^e The quotation from Spectro

using an X-ray tube source is the resulting background in the spectrum near the analytic X-ray lines from scatter by the sample. For this reason a filter is often used between the X-ray tube and the sample to suppress the continuum radiation while passing the characteristic X-rays from the anode; these filters are incorporated into the XRF unit. Miniature X-ray tubes permit simultaneous analysis of 20 to 25 elements; they also generally provide lower detection limits as compared to isotope systems for most metals. Additionally, the testing time does not increase with an X-ray tube, because the source does not decay. Typically, the testing speed after 4 or 5 years is the same as when the analyzer's tube was new. While, in addition to the loss in analytic capabilities, radioisotope based units must eventually be replaced for sources. However, with a maximum output of 50 keV (Table 2), none of the handheld X-ray tube instruments found for this work can produce X-rays with sufficient energy to excite the K shell X-rays of lead. This K shell excitation is needed for lead-based paint buried beneath more recent coatings (Martin and Sackett, 2005). Because of the inconclusive range of X-ray tube-based XRF analyzers at and around the lead concentration of 1.0 mg cm^{-2} – the Federal standard for residential or occupied properties (U.S. EPA, 2003) – users run the risk of getting an inconclusive lead concentration in lead-based paint. With the ability to measure both L and K shell fluorescent lead X-rays, a radioisotope-based instrument can reliably test the lead even in the densest substrates and deeply buried or shielded paint. Given HUD's determination (HUD, 2003) that X-ray tube-based instruments provide inconclusive results as often as 16% of all samples and that these instruments can provide results with a false-positive rate of 2.5% and a false-negative rate of 1.9%, radioisotope-based instruments are needed to accurately identify and quantify lead in

lead-based paint.

With the exception of Pb, X-ray tube sources are appropriate for all Resource Conservation and Recovery Act (RCRA) metals and Zn, as these have the capability of providing faster results in detecting a wider range of metals in the sample. While, a radioisotope-based instrument can provides deeper and multilayer detection for Pb.

Isotope based FP-XRF has been used by a number of researchers for determining Pb in paint. A study was conducted by Daniels et al. (2001) to demonstrate the effectiveness of a wet abrasive blasting technology to remove lead-based paint from exterior wood siding and brick substrates as well as to evaluate the effectiveness of two waste stabilization technologies to treat the resulting blast media (coal slag and mineral sand) paint debris. The technology efficacy was determined by the use of an XRF analyzer with the capability of both L- and K-shell excitation for Pb using a radioisotope source. To detect the relationship between lead levels on painted surfaces and percent lead in the particles aerosolized during lead abatement, Choe et al. (2002) used a FP-XRF instrument (NITON-700, NITON Inc., Bedford, MA) to measure lead levels. Experiments were performed in the University of Cincinnati Environmental Test Chamber using wood doors painted with lead-based paint. While a good relationship ($r^2 = 0.83$) was found between the XRF readings and the percent lead in the particles aerosolized during dry scraping, no significant relationship was found for wet scraping ($r^2 = 0.09$) or dry machine sanding ($r^2 = 0.002$). The correlation was dependent on the paint removal method. Clark et al. (2005) used FP-XRF to determine environmental lead levels and its overall distribution in the environment by studying Pb concentrations in paint, dust, air, soil, and other bulk samples near several industries that used lead and in the

residential environments of children with very high blood lead levels.

Field investigations have benefited from the XRF instrument in various modes from safety monitoring to site screening. Kilbride and Poole (2006) detected total concentrations of Cu, Pb, As, Cd, Zn, Fe, Ni, and Mn for 81 soil samples using two types of FP-XRF systems: isotope (Niton Xli with sources Cd^{109} and Am^{241}) and an X-ray tube source (Niton XLt 700 series). Metal concentrations were statistically compared with analytical results from aqua regia digestion followed by inductively coupled plasma optical emission spectrometry (ICP-OES) analysis. The ability of each FP-XRF instrument to produce comparable analytical results was assessed by linear regression, where a strong relationship was found for Fe analysis ($r^2 > 0.89$) with the X-ray tube instrument and for Fe, Cu, Pb, Zn, Cd, and Mn ($r^2 > 0.88$) with the isotope source-based instrument. Particle size did not influence the FP-XRF analyzer performance. Radu and Diamond (2009) used the XLp 703 Cd^{109} source analyzer and the XLt 793 miniaturized X-ray tube for thin sample and bulk homogenized (soil) sample analysis. A good correlation between total metals from digested samples analyzed by flame atomic absorption spectroscopy (AAS) and the tube-based XRF technique was achieved (r^2 values for Pb, As, Cu, and Zn were 0.995, 0.991, 0.959, and 0.843, respectively). The results indicate that both the isotope and the X-ray tube FP-XRF instruments are effective tools for rapid, quantitative assessment of soil metal contamination and for monitoring the efficacy of remediation strategies. However, each type of unit has its applicability; namely, a radioisotope source is optimum for Pb in paint, while the X-ray tube is effective for the other RCRA metals and Zn.

2.1.2 Selected FP-XRF: Niton XL3t and XLp 300 Series analyzers

The Niton XL3t Series of instruments, combining advanced electronics and a 50 keV (which is the greatest X-ray energy used in tube technology) X-ray tube developed for handheld XRF instruments, provides greater analytical range, speed, and precision than the X-ray tube-based technology found for other manufacturers (Table 2). This line of instruments provides both qualitative and quantitative data for elements ranging from Mg through U, including RCRA metals, 12 priority pollutants (U.S. EPA, 2003), and 19 U.S. EPA target analytes (U.S. EPA, 2003). Specifically, the XL3t 600 is an effective analyzer to detect a wide range of the metal concentrations (in ppm) in soils, sediments, painted surfaces, dust wipes, and air filters for ambient and personal air monitoring (Table 3). These analyzers can be placed directly on the surface for in-situ analysis to perform trend analysis or quickly delineate the boundaries of contamination. Placing samples in plastic bags roughly homogenizes the sample for semi-quantitative results, while drying, grinding and sifting the sample provides a more uniform composition, making quantitative analysis possible; these two methods are also known as ex-situ analysis.

The FP-XRF NITON XLp 300A analyzer is designed to quantify only lead in paint using a sealed, 40 mCi cadmium-109 radioisotope source to excite characteristic X-rays of the test sample. Source replacement is needed after 4 year as opposed to other manufacturers where sources may require replacement as earlier as 1.2 year after use (Niton, 1998). X-ray emission from a ^{109}Cd source occurs at approximately 22.5 and 88.1 keV, which therefore excites the K shell fluorescent X-rays of lead. Since the excitation energy is about four times greater than the low energy L shell X-ray, the resulting

Table 3. NITON XRF- XL3t 600 limits of detection^b for contaminants in soil (ppm)

| Metal | SiO ₂ ^a | SRM ^a |
|----------|-------------------------------|-----------------------|
| | (interference free) | (typical soil matrix) |
| Arsenic | 9 | 11 |
| Barium | 90 | 100 |
| Cadmium | 10 | 12 |
| Chromium | 65 | 85 |
| Lead | 8 | 13 |
| Mercury | 7 | 10 |
| Selenium | 6 | 20 |
| Silver | 10 | 10 |
| Zinc | 15 | 25 |

^aThe chart above details the sensitivity, or limits of detection (LOD) of the XL3t 600 Series analyzer, specified for both SiO₂ matrix and a typical Standard Reference Material (SRM). With a 50 keV miniature X-ray tube and multiple primary filters

^bDetection limits are specified following the U.S. EPA protocol of 99.7% confidence level. Individual limits of detection (LOD) improve as a function of the square root of the testing time. The LODs are averages of those obtained using bulk analysis mode on NITON XL3t 600 analyzers at testing times of 60 seconds per sample.

penetration through overlying paint layers is much greater. This enables measurement of X-rays generated by lead from deep within the paint matrix, which otherwise may be missed by the lower-energy L shell X-rays. Using an algorithm that combines both the L shell and K shell readings provides users with both accuracy and precision, eliminating the chances of false negative readings from a thicker or metallic paint matrix. The Thermo Scientific NITON XLp 300 Series analyzers are not only used for lead paint inspection and risk assessment, but they are also routinely used as multifunctional tools to measure lead in other types of samples. Because of the ^{109}Cd source, they can effectively measure lead in paint as well as assess the Pb L shell fluorescent X-rays to measure dust wipes, soil samples, and air filters. With no need for substrate correction and no false positives/false negatives, the NITON XLp 300 Series of isotope-based analyzers is recommended for measuring lead (Table 4).

2.2 Field Portable Spectrophotometer

UV-visible spectrophotometry is commonly used for lead Pb(II) analysis because of its simplicity, precision, accuracy, low cost, and sensitivity (Stokinger, 1981). The Standard Method (SM) 3500-Pb D (Andrew et al., 2005) is a dithizone method initially developed for wastewater analysis using a spectrophotometer. Specifically, the dithizone method is

Table 4. Parameter for two types of FP-XRF^[1]

| Type of XRF | Isotope-based FP-XRF | X-ray tube-based FP-XRF |
|------------------------|---|--|
| | XLp 300A | XL3t 600 |
| Metals detected | Pb in paint mode | Ba, Sb, Sn, Cd, Ag, Mo, Zr, Sr, U, Rb, Th, Pb, Se, As, Tl, Hg, Zn, Cu, Ni, Co, Fe, Mn, Cr, V, Ti, Sc, Ca, K, Cl, S, P, I |
| Excitation energy | 22.5 keV and 88.1 keV | ≤ 50 keV |
| Excitated shell | Both L and K shells | L shell only |
| Incorrect result | | 20.4% for lead |
| Source | ¹⁰⁹ Cd (22.5 KeV, 88.1 KeV) | 50 keV Miniature Au Anode X-ray tube |
| Precision | | False negative result for Pb |
| Limits of detection | | See Table 3 |
| Cost of the instrument | 17,000.00 | 37,000.00 |
| | 41,000.00 (bundled price) (appendix A) | |

[1] Thermo Fisher Scientific, The Importance of excitation sources for X-ray fluorescence (XRF) analyzers in lead paint measurement.

designed for determining lead in water and wastewater. The DithiVer Metals Reagent is a stable powder form of dithizone. Lead ions in basic solution react with dithizone is used to form a pink to red lead-dithizonate complex, which is extracted with chloroform. Extracted samples are then measured in the spectrophotometer at 515 nm. While a number of companies manufacture spectrophotometers for lead analyses, the Hach DR 2800 is the only field portable instrument that meets the U.S. EPA approved Method 8033 (Andrew et al., 2005; appendices B and C) (which is equivalent to the SM 3500-Pb D). As a result, field detection of lead concentrations in wash water or wastewater is possible. Hach DR 2800 can detect lead concentrations as low as 3 to 300 $\mu\text{g L}^{-1}$.

The Hach portable spectrophotometer has been used for on-site applications as a field portable tool. Kucukbay et al. (2007) investigated chemical and physical parameters of the water and sediment samples taken from Karakaya Dam Lake during the four seasons. Constituents measured included Fe, Cu, Pb, Mn, Cd, Ca, NO_2^- -N, NH_3 -N, PO_4^{3-} , organic substances, and total filterable residues using standard reagents kits for the HACH DR 2010 spectrophotometer.

3. Conclusion

After a thorough review coupled with vendor information, the selected portable analytical equipment are NITON XRF- XL3t 600 X-ray tube analyzer, NITON XLp 300A analyzer (appendix D), and the HACH DR 2800 portable spectrophotometer (appendix E).

4 References

- Ashley, K., Hunter, M., Tait, L. H., Dozier, J., Lee, S. J., Berry, P. F. (1998) Field investigation of on-site techniques for the measurement of lead paint films, *Field Analytical Chemistry and Technology*, 2(1): 39-50.
- Asano, T., Yabusaki, K., Wang, P. C., Iwasaki, A. (2010) Determination of lead(II) in fly ash leachate using a newly developed simple spectrophotometric method *Spectrochimica Acta - Part A, Molecular and Biomolecular Spectroscopy*, 75(2) Pages 819-824.
- Clark, S., Menrath, W., Chen, M., Roda, S., Succop, P. (1999) Use of a field portable X-ray fluorescence analyzer to determine the concentration of lead and other metals in soil samples, *Annals of Agricultural and Environmental Medicine*, 1999, 6: 27–32.
- Clark, C.S., Thuppil, V., Clark, R., Sinha, S., Menezes, G., D'Souza, H., Nayak, N., Kuruvilla, A., Law, T., Dave, P., Shah, S. (2005) lead in paint and soil in Karnataka and Gujarat, India, *Journal of Occupational and Environmental Hygiene*, 2 (1): 38-44.
- Choe, T. K., Trunov, M., Menrath, W., Succop, P., Grinshpun, A. S. (2002) Relationship between lead levels on painted surfaces and percent lead in the particles aerosolized during lead abatement, *Applied Occupational and Environmental Hygiene*, 17(8): 573–579.
- Daniels, A. E., Kominsky, J. R., Clark, P. J. (2001) Evaluation of two lead-based paint removal and waste stabilization technology combinations on typical exterior surfaces, *Journal of Hazardous Materials*, B87: 117–126.
- Eaton, A. D., Clesceri, L. S., Rice, E. W., Greenberg, A. E. (2005) Standard methods for the examination of water and wastewater, 21st edition. 3: 79-81.
- Herman, D. S., Geraldine, M., Scott, C. C., Venkatesh, T. (2006) Health hazards by lead exposure: evaluation using ASV and XRF, *Toxicology and Industrial Health*, 22(6): 249-254.
- Kucukbay, F. Z. (2007) Investigation of some chemical and physical parameters in water and sediment samples of Karakaya dam lake (Malatya-Turkey), *International Journal of Pure & Applied Chemistry*, 2(3): 303-308.

Kalnicky, D. J., Singhvi, R. (2001) Field portable XRF analysis of environmental samples, *Journal of Hazardous Materials*, 83: 93–122.

Kilbride, C., Poole, J. Hutchings, T.R. (2006) A comparison of Cu, Pb, As, Cd, Zn, Fe, Ni and Mn determined by acid extraction/ICP-OES and ex situ field portable X-ray fluorescence analyses, *Environmental Pollution*, 143: 16-23.

Martin, J., Sackett, D. (2005) X-ray Fluorescence in the Field, *Advanced Materials and Processes*, 163 (11): 51-53.

Morley, J. C., Clark, C. S., Deddens, J. A., Ashley, K., Roda, S. (1999) Evaluation of a portable X-ray fluorescence instrument for the determination of lead in workplace air samples, *Applied Occupational and Environmental Hygiene*, 14(5):306-316.

National Institute for Occupational Safety and Health (1998) Lead by field portable XRF in *NIOSH Manual of Analytical Methods*, 4th ed. Cincinnati, Method Number 7702. Issue 1, Retrieved November 1, 2007.

<http://www.cdc.gov/Niosh/nmam/pdfs/7702.pdf>

NITON Corporation, (1998) “300 Series & 700 Series User’s Guide, version 5.2”.

<http://www.osha.gov/dea/lookback/lead-construction-review.html>

Nwani, C. D., Egwenike, C. G., Ude, E. F., Uneke, B. I. (2009) Heavy metal pollution status of a tropical freshwater lentic ecosystem, Nike Lake, south-east Nigeria. *Asian Journal of Microbiology, Biotechnology & Environmental Sciences*, 11(2): 253-256.

Radu, T., Diamond, D. (2009) comparison of soil pollution concentrations determination using AAS and portable XRF techniques, *Journal of Hazardous Materials*, 171(1-3): 1168-1171.

Sterling, D. A., Evans, R. G., Shadel, B. N., Serrano, F., Arndt, B., Chen, J. J., Harris, L. (2004) Effectiveness of cleaning and health education in reducing childhood lead poisoning among children residing near superfund sites in Missouri, *Archives of Environmental Health*, 59(3):121-131.

Stokinger, H. E. (1981) Patty’s Industrial Hygiene and Toxicology. Vol. 2A, (3rd Edition). New York: Wiley-Interscience, 2028.

Savvin, S. B., Petrova, T. V., Dzherayan, T. G., and Reichstat, M. M. (1991)

Spectrophotometric determination of lead in environmental objects with the new highly effective reagent HOCAC, *Fresenius' Journal of Analytical Chemistry*, 340(4): 217-219.

Thermo Fisher Scientific, Fact sheet: the importance of excitation sources for X-ray fluorescence (XRF) analyzers in lead paint measurement

http://www.niton.com/Libraries/Document_Library/Benefits_of_Isotope_XRF-Fact_Sheet_2_0071017_2.sflb.ashx

U. S. Department of Housing and Urban Development (1995). *Guidelines for the evaluation and control of lead-based paint hazards in housing*, Washington. DC: Author, Retrieved December 21, 2006.

<http://www.hud.gov/offices/lcad/guidelincs/hudguidelities/Intro.pdf>

U. S. Environmental Protection Agency (2001) Lead; Identification of Dangerous Levels of Lead; Final Rule, 40 CFR. §745.

U. S. Environmental Protection Agency (1998) Method 6200, Field portable X-ray fluorescence spectrometry for the determination of elemental concentrations in soil and sediment (FPA/600/R-97/150.Revision 0), Retrieved November 1, 2007.

<http://www.epa.gov/SW-846/pdfs/6200.pdf>

U. S. Environmental Protection Agency (2003) Environmental Technology Verification Report: Lead in Dust Wipe Measurement Technology- NITON LLC X-ray Fluorescence Spectrum Analyzer, XLt 700 Series.

U. S. Department of Housing and Urban Development (1997) Guidelines for the evaluation and control of lead-based paint hazards in housing, Chapter 7: lead-based paint inspection.

Zamurs, J. , Bass, J. , Williams, B. , Fritsch, R. , Sackett, D. , Heman, R. (1998) Real-time measurement of lead in ambient air during bridge paint removal, *Transportation Research Record*, 1641: 29-38.

5. Appendices

A Quote for Thermo Scientific NITON XRF- XL3t 600 X-ray tube analyzers and NITON XLp 300 Series analyzers

B Quote for HACH DR 2800 portable spectrophotometer

C Hach Method 8033

D Invoice and warranty for Thermo Scientific NITON XRF- XL3t 600 X-ray tube analyzers and NITON XLp 300 Series analyzers

E Invoice and warranty for HACH DR 2800 portable spectrophotometer

**A: Quote for Thermo Scientific NITON XRF-
XL3t 600 X-ray tube analyzers and NITON
XLp 300 Series analyzers**

July 17, 2009

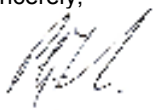
New Jersey Institute of Technology
Department of Civil and Environmental En
Newark, NJ 07102
Dr. Lisa Axe
axe@adm.njit.edu

Thank you for your interest in the NITON portable XRF Analyzer and for giving us the opportunity to earn your business; attached is the information you requested. We have worked hard to become the worldwide market leader in portable X-ray fluorescence (XRF) analysis, as well as one of the fastest growing business units in Thermo Fisher Scientific. Following are just a few of the many features and benefits which make the NITON the best value in portable XRF analyzers:

- **Outstanding Service and Support** from Thermo Fisher Scientific, the Worlds Leader in service science.
- **Exceptional balance** of size and weight.
- **Easy-to-navigate software system** with large characters for error free data input. Go from start-up to testing in three easy steps!
- **High-strength, rugged, environmentally sealed housing** to protect internal components from unwanted dirt, dust, heat, moisture, etc.
- **Proprietary operating and report generating software** which not only **protects** your data but **defies the Pocket PC fad**. Users can upgrade software package at NO Charge, often via the internet.
- **Data communication via Bluetooth wireless** to external devices such as an IPAQ PDA and portable printers if desired.
- **No reliance on "third party" software** from PDA's to operate. PDA'S are plagued with frequent "lock-ups", connections to the instruments can be interrupted, and the PDA's can be lost or stolen.
- **Fastest throughput** of any portable XRF on the market.
- **Unmatched battery use** time between charges of 8-12 hours!
- **Multiple safety features**, such as proximity buttons and count rate proximity sensors.
- **A strong commitment to Research and Development** continues to drive greater and greater reliability that smaller competitors cannot match.
- **Free Radiation Safety and Operational training** at any Thermo NITON Analyzer class for the life of the analyzer.
- **Intuitive software** to select elemental units of measure, threshold levels and display options.



I look forward to working with you, and appreciate the opportunity to present our products. Please let me know if you have any questions, or require additional information. Thank you again.

Sincerely,




Peter Faulkner
Regional Sales Manager

Thermo Fisher Scientific NITON Analyzers is pleased to provide the following quotation requested in support of our XL3t 600 Environmental series analyzer. This proposal is valid 120 days from the above date.

| Product | Standard Features | Standard Modes & Calibrations | Price |
|---|--|---|--|
| XL3t 600 Environmental Analyzer  Standard Source 50kV Au Anode X-Ray Tube | <ul style="list-style-type: none"> • Two rechargeable 6-cell Li-ion battery packs • Battery charger • AC power supply • Environmentally sealed housing • Carrying case • Shielded belt holster • SpectraView element scanner • Integrated flip-up touch screen with "virtual" keyboard • Password-protected set-up and operation with several other radiation safety features • NDT© software suite • PC connection cable • Standardization reference samples • Bluetooth Wireless Connectivity • Includes no-charge, on-site operator training • 24-month limited warranty on parts and labor • Portable Test Stand • Soil standards | Standard Calibrations <ul style="list-style-type: none"> • (D) Bulk (Soil) Analysis | Bundled Price for purchase of XL3t 600 and XLp 300A analyzers \$41,000.00 Shipping and handling \$240.00 FedEx second day fully insured |
| XLp 300A Series  Standard Source 40 mCi Cd- 109 isotope | <ul style="list-style-type: none"> ➤ Two rechargeable battery packs ➤ Battery charger ➤ Carrying case ➤ AC power supply ➤ Carrying case ➤ Shielded belt holster ➤ PC connection cable ➤ SpectraView™ element scanner ➤ Integrated touch screen display ➤ "Virtual" keyboard ➤ Integrated barcode scanner and barcode generator for sample ID input ➤ On-site operator training. ➤ NDT© software suite including remote control operation via PC, data analysis and certificate print capabilities ➤ Password-protected set-up and operations with several other radiation safety features ➤ Remote control operation via PC ➤ 24-month limited warranty on parts and labor | <ul style="list-style-type: none"> • (A) Pb in paint Mode | |

ACCESSORIES

| Product name and code | Specification | Price |
|---|---|-----------------|
|  | Folds down for transport. Allows hands-free measurement of samples. Fully shielded to protect operator from primary or scattered radiation. Use with included Niton Data Transfer (NDT) software for "remote" control, data display and download via PC connection cable or optional Bluetooth connection. Pictured PC, samples, and analyzer not included. | Included |

Included Calibrations

| | | | |
|--------------------------|----------|---|---|
| Soil Analysis "D" | XL3t 600 | X-Ray Tube | Ba, Sb, Sn, Cd, Ag, Mo, Zr, Sr, U, Rb, Th, Pb, Se, As, Tl, Hg, Zn, Cu, Ni, Co, Fe, Mn, Cr, V, Ti, Sc, Ca, K, Cl, S, P, I |
| | | Soil calibration for environmental assessments and metals in soils sediments and bulk analysis at concentrations generally < 2%. Includes soil kit (and reference standards). Calibrated for all RCRA metals. | |
| Pb in Paint "A" | XLp 300A | Cd-109 40mCi | Pb in paint mode (dual detector system with both L and K shell analysis) |

Delivery: 3 weeks ARO

Please apply applicable Taxes – If tax exempt please supply certificate with purchase order.

Terms: **CIA** (Cash in advance) or **Net 30**. Net 30 terms are **subject to credit approval**; please fill out the attached credit application and fax it to (978) 670-7430 Diana Garcia.

If you should have any questions, or require additional information, please call me at the above number. Thank you for your interest in NITON Analyzers. We look forward to working with you in the near future.

Sincerely,

 Christian Balotescu
 Authorized Representative

Agreed and Accepted By: _____

Signature of authorized company representative _____ Date _____

Print Name _____ Title _____

Model # _____ Amount _____ PO Number _____

Should we charge Sales Tax?

☐

Yes

☐

No

If no, you must provide a copy of your Tax Exemption Certificate.

**B: Quote for HACH DR 2800 portable
spectrophotometer**

Quotation/ProForma Invoice

Page 1 of 5
Date 01/26/2010



HACH COMPANY

Headquarters
P.O. Box 389
5600 Lindbergh Drive,
Loveland, CO 80539-0389

Purchase Orders
PO Box 608
Loveland, CO 80539-0608
Web Site: www.hach.com

U.S.A.
Phone: 800-227-4224
Fax: 970-669-2932
Email: orders@hach.com
quotes@hach.com
techhelp@hach.com

Export
Phone: 970-669-3050
Fax: 970-461-3939
Email: intl@hach.com

Remittance
2207, Collections Center Drive
Chicago, IL 60693

Wire Transfers
Bank of America
231 S. LaSalle St.
Chicago, IL 60604
Account 8765602385
Routing (ABA) : 026009593

Quote Number 309013255

Version Number

0

(USE QUOTE Number at time of order to ensure you receive prices quoted).

Customer Ref RFQ METHOD 8033
Second Customer Ref
Third Customer Ref
Payment Terms Net 30 Days From Invoice Date
Currency USD
Freight Terms Prepay And Bill Customer
Ship Method RPS-RPS**FedEx- -Ground
Quote Date 01/26/2010
Expiration Date 03/29/2010
Hach Sales Contact
Customer Number 008530
Quote Contact LISA AXE
Phone 9735962477
Fax
E-Mail axe@adm.njit.edu

Bill-To Account

697253
NEW JERSEY INST OF TECH
FINANCE OFFICE
323 MARTIN LUTHER KING JR BLVD

NEWARK,NJ,07102-1982
United States

Ship-To Account

759669
NEW JERSEY INST OF TECH
FINANCE OFFICE
323 MARTIN LUTHER KING JR BLVD

NEWARK,NJ,07102-1982
United States

Deliver-To Account

| Line | Item No | Description | Quantity | Unit Price | Extended Amount |
|------|-----------|---|----------|------------|-----------------|
| 1.1 | DR2800-01 | aa db DR2800 SPECTRO W/O BATTERY PACK | 1 | 2,407.50 | 2,407.50 |
| 2.1 | LZY274 | DATATRANS SOFTWARE PACK | 1 | 231.00 | 231.00 |
| 3.1 | 2243100 | Lead Reagent Set, 0-80, 0-160, 0-300 ug/L, 90 tests, Dithizone Method | 1 | 396.00 | 396.00 |
| 4.1 | 1420299 | Buffer, Citrate, pk/100 Powder Pillows | 1 | 43.04 | 43.04 |

Quotation/ProForma Invoice

Page 2 of 5
Date 01/26/2010

| | | | | | |
|------|---------|--|---|--------|--------|
| 5.1 | 1445817 | Chloroform, ACS Grade 4 L, CAS No. 67 66 3 | 1 | 126.75 | 126.75 |
| 6.1 | 1261699 | DithiVer Metals Reagent, pk/100 Powder Pillows | 1 | 58.72 | 58.72 |
| 7.1 | 76714 | Potassium cyanide, 125g | 1 | 21.26 | 21.26 |
| 8.1 | 245053 | Sodium hydroxide 5.0n 1l | 1 | 14.77 | 14.77 |
| 9.1 | 245026 | Sodium hydroxide 5.0n 50ml scdb | 1 | 7.61 | 7.61 |
| 10.1 | 96800 | Clipper, for Medium Powder Pillows | 1 | 2.69 | 2.69 |
| 11.1 | 257201 | Cotton Balls, Absorbent 100/pk | 1 | 5.47 | 5.47 |
| 12.1 | 50837 | Cylinder, Graduated Capacity 5mL, Subdivisions 0.1 mL, Tolerance +- 0.1 mL | 1 | 13.64 | 13.64 |
| 13.1 | 50841 | Cylinder, Graduated Capacity 50ML Subdivisions 1.0 mL, Tolerance +- 0.4 mL | 1 | 12.41 | 12.41 |
| 14.1 | 50846 | Cylinder, Graduated Capacity 250mL, Subdivisions 2.0 mL, Tolerance +- 1.4 mL | 1 | 21.29 | 21.29 |
| 15.1 | 189641 | Cylinder, mixing, Capacity 50mL, Subdivisions 1.0mL, Tolerance +-0.4 mL, Stopper Number 16- Tall Form Glass | 1 | 22.16 | 22.16 |
| 16.1 | 52049 | Funnel, Separatory, Squibb, 500 mL, glass pear-shape with Teflon stopcock plug, HDPE bottom, stopcock size 4 mm, fits stopper 27. Corning. | 1 | 84.75 | 84.75 |
| 17.1 | 5170010 | sensION1 Portable pH Meter with Platinum pH Electrode (-2.00 to 19.99 pH, +/- 2000 mV, -10 to 110 C. Includes 4.01 and 7.00 pH buffers, beakers, manual, and batteries. Three-year warranty) | 1 | 363.75 | 363.75 |
| 18.1 | 51000 | Measuring Spoon, 1.0 g (NaCl weight), molded plastic | 1 | 1.61 | 1.61 |
| 19.1 | 58001 | Support Ring, 4-inch, cast iron with cadmium-plate finish. Center of ring to center of clamp: 4.25 inches. Humboldt. | 1 | 8.51 | 8.51 |
| 20.1 | 56300 | Ring Stand Support, 5x8 inch black enamel cast iron base, 0.3x20 inch | 1 | 11.74 | 11.74 |

Quotation/ProForma InvoicePage 3 of 5
Date 01/26/2010

| | | | | | |
|------|---------|--|---|--------|--------|
| | | zinc-plated rod. Humboldt. | | | |
| 21.1 | 2612602 | Sample Cells, 1-inch glass, 25 mL with stopper, matched pair | 1 | 97.50 | 97.50 |
| 22.1 | 1261742 | Lead Standard, 100mg/L as Pb,100mL (NIST) | 1 | 15.94 | 15.94 |
| 23.1 | 2196800 | Ampule Breaker Kit with Holder and Instructions | 1 | 10.50 | 10.50 |
| 24.1 | 1445849 | Chloroform, ACS Grade 500 mL, CAS No . 67 66 3 | 1 | 31.69 | 31.69 |
| 25.1 | 253000 | Filter Paper,Diameter 47mm,Pore Size 1.5 um, 100/pk, Glass Fiber, Quantitative | 1 | 25.04 | 25.04 |
| 26.1 | 234000 | Filter Holder, Glass, 47mm for Vacuum Filtration | 1 | 298.50 | 298.50 |
| 27.1 | 50549 | Flask, Erlenmeyer, Capacity 500mL, Subdivision 50mL, Stopper 7, Glass | 1 | 5.06 | 5.06 |
| 28.1 | 54649 | Flask, Filtering, Capacity 500mL, Subdivision 50mL, Stopper 7, each | 1 | 18.04 | 18.04 |
| 29.1 | 1457442 | Flask, Volumetric Class A, Diameter 100mL, Tolerance +-0.08mL, #13 glass stopper. Optional poly stopper is Hach catalog number 20955-13, pk/6. | 1 | 19.76 | 19.76 |
| 30.1 | 254049 | Nitric Acid Solution, 1:1 500mL | 1 | 17.99 | 17.99 |
| 31.1 | 15249 | Nitric Acid, 500 mL ACS | 1 | 29.59 | 29.59 |
| 32.1 | 39133 | pH Paper, 1.0-11.0 pH, 5 15-ft rolls (not recommended for finished water, may be used with dispenser 2611000). Hydrion. | 1 | 7.31 | 7.31 |
| 33.1 | 53236 | Pipet, Serological, Glass, 2.00 mL, 0.01 mL divisions, +/- 0.02 mL. Calibrated to deliver/blow out. Corning. | 1 | 5.77 | 5.77 |
| 34.1 | 1970001 | TenSette Pipet, 0.1-1.0 ml dispensing range. Complete with instructions and 100 disposable pipeting tips. | 1 | 165.75 | 165.75 |
| 35.1 | 2185696 | Pipet Tips, for TenSette Pipet 19700-01, 0.1-1.0 mL, pk/50 | 1 | 8.24 | 8.24 |

Quotation/ProForma InvoicePage 4 of 5
Date 01/26/2010

| | | | | | |
|------|---------|--|---|-------|-------|
| 36.1 | 1451537 | Pipet, Volumetric, Class A, 5.00 mL, +/- 0.01 mL, designed to NNN-P-395 Type 1, ASTM Standard E694, calibrated to deliver. Corning. | 1 | 6.82 | 6.82 |
| 37.1 | 1451538 | Pipet, Volumetric, Class A, 10.00 mL, +/- 0.02 mL, designed to NNN-P-395 Type 1, ASTM Standard E694, calibrated to deliver. Corning. | 1 | 7.09 | 7.09 |
| 38.1 | 1465100 | Pipet Filler, Safety Bulb (squeeze bulb for filling glass and plastic pipets). | 1 | 21.67 | 21.67 |
| 39.1 | 244932 | Sulfuric acid 5.25n 100ml mdb | 1 | 7.49 | 7.49 |
| 40.1 | 27256 | Deionized Water, 4 L | 1 | 15.56 | 15.56 |

Merchandise Total: \$4,669.98
Total : \$4,669.98

NOTES :

Shipping and/or handling charges are applicable only if routed through carriers and /or forwarders selected by Hach Company.
Additional charges may be added for certain heavy/large items shipping to US Destinations.

E

THANK YOU FOR YOUR QUOTE REQUEST. PLEASE NOTE:

=====

MOST ITEMS ARE AVAILABLE WITHIN 30 DAYS AFTER RECEIPT OF PURCHASE ORDER. ITEMS IN STOCK WILL SHIP WITHIN 48 HOURS.

=====

PRICES QUOTED ARE VALID ONLY FOR ORDERS BILLING-SHIPPING WITHING THE USA, NOT ULTIMATE EXPORT.

=====

THIS QUOTATION DOES NOT INCLUDE FREIGHT CHARGES. PLEASE REFER TO THE ENCLOSED FREIGHT SCHEDULE, WHICH IS BASED ON THE TOTAL DOLLAR AMOUNT PER SHIPMENT.

=====

SHIPPING TERMS ARE FOB SHIPPING POINT. CUSTOMERS ARE RESPONSIBLE FOR PAYING FREIGHT CHARGES ON ORDERS. NORMALLY FREIGHT IS PREPAID AND ADDED TO YOUR INVOICE. IF YOU CHOOSE NOT TO HAVE YOUR SHIPMENT SENT PREPAID, PLEASE CONTACT CUSTOMER SERVICE AT 1-800-227-4224 SO ARRANGEMENTS CAN BE MADE TO SEND FUTURE ORDERS FREIGHT COLLECT.

=====

Due to International regulations, a U.S. Department of Commerce Export License may be required. Hach reserves the right to approve specific shipping agents. Wooden boxes suitable for ocean shipment are extra. Specify final destination to ensure proper documentation and packing suitable for International transport. In addition, Hach may require : 1). A statement of intended end-use; 2). Certification that the intended end-use does not relate to proliferation of weapons of mass destruction (prohibited nuclear end-use, chemical / biological weapons, missile technology); and 3). Certification that the goods will not be diverted contrary to U.S. law.

PAYMENT TERMS ARE SUBJECT TO CREDIT REVIEW. SALES/USE TAXES ARE SUBJECT TO CHANGE. Taxes will be added at time of order for orders shipping and used in US Destinations, unless valid resale/exemption certificate is provided. Exemption certificate can be sent to the above address or fax number.



Signed:



800-548-4381
Fax: 574-264-4533



800-949-3766
Fax: 970-461-3921



800-368-2723
Fax: 301-874-8459



800-677-0067
Fax: 505-994-3574



800-454-0263
Fax: 970-461-3919

C: Hach Method 8033

★Method 8033

Dithizone Method¹

Powder Pillows

(3 to 300 µg/L)

Scope and Application: For water and wastewater; USEPA accepted for reporting for wastewater analysis (digestion is required).²

¹ Adapted from Snyder, L. J., Analytical Chemistry, 19 684 (1947).

² Procedure is equivalent to Standard Method 3500-Pb D for wastewater analysis.



Test Preparation

Before starting the test:

For more accurate results, determine a reagent blank value for each new lot of reagent. Follow the procedure using deionized water instead of the sample.

Clean all glassware with a 1:1 Nitric Acid Solution. Rinse with deionized water.

Cloudy and turbid samples may require filtering before running the test. Report results as µg/L soluble lead. Use glass membrane type filter to avoid loss of lead by adsorption onto the filter paper.

If samples cannot be analyzed immediately, see [Sample Collection, Preservation, and Storage on page 5](#). Adjust the pH of preserved samples before analysis.

For more accurate results, adjust the sample to pH 11.0–11.5 using a pH meter in step 10. Omit the five additional drops of Sodium Hydroxide Standard Solution in step 11

The DithiVer powder will not completely dissolve in the chloroform. For further notes see [DithiVer Solution Preparation, Storage, and Reagent Blank on page 5](#).

Read the MSDS before testing. Spilled reagent will affect test accuracy and is hazardous to skin and other materials.

In bright light conditions (e.g. direct sunlight) it may be necessary to close the cell compartment with the protective cover during measurements.

Collect the following items:**Quantity**

| | |
|---|--------|
| Citrate Buffer Powder Pillows | 1 |
| Chloroform | 500 mL |
| DithiVer Metals Reagent Powder Pillows | 1 |
| Lead Reagent Set | 1 |
| Potassium Cyanide | 2 g |
| Sodium Hydroxide solution, 5.0 N | 5 mL |
| Sodium Hydroxide Standard Solution, 5.0 N | varies |
| Cotton Balls | 1 |
| Clippers | 1 |
| Cylinder, 50-mL graduated mixing | 1 |
| Cylinder, 5-mL graduated | 1 |
| Cylinder, 50-mL graduated | 1 |
| Cylinder, 250-mL graduated | 1 |
| Funnel, 500-mL separatory | 1 |
| Sample Cells, 1-inch square, 25-mL | 2 |
| Spoon, measuring, 1.0-g | 1 |
| Support Ring (4-inch) and Stand (5 x 8-inch base) | 1 |

Note: Reorder information for consumables and replacement items is on page 6.

Powder Pillows

Method 8033

DANGER

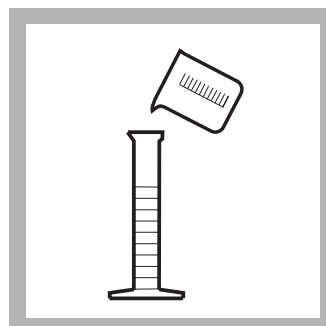
Cyanide is a deadly poison. Use a fume hood. Maintain cyanide solutions at pH 11 or greater to prevent formation of cyanide gas.



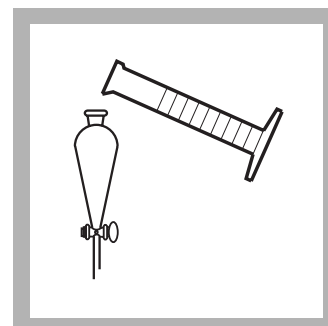
1. Press **STORED PROGRAMS**.



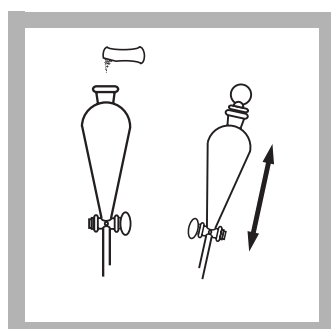
2. Select the test.



3. Fill a 250-mL graduated cylinder to the 250-mL mark with sample.

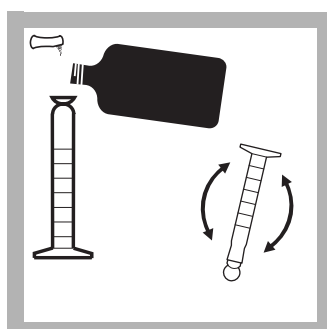


4. Transfer the sample into 500-mL separatory funnel.



5. Add the contents of one Buffer Powder Pillow for heavy metals, citrate type.

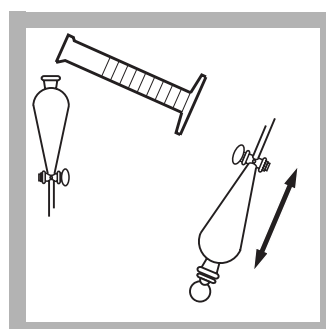
Stopper the funnel and shake to dissolve.



6. DithiVer Solution Preparation:

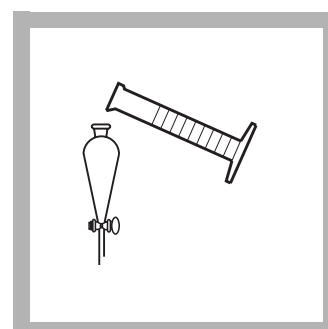
Add 50 mL of chloroform to a 50-mL mixing graduated cylinder. Add the contents of one DithiVer Metals Reagent Powder Pillow.

Stopper the cylinder. Invert several times to mix.

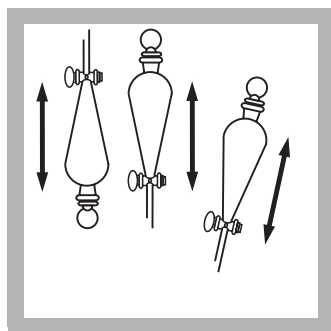


7. Measure 30 mL of the prepared dithizone solution with a second graduated cylinder and add to the separatory funnel.

Stopper and invert to mix. Open stopcock to vent. Close the stopcock.

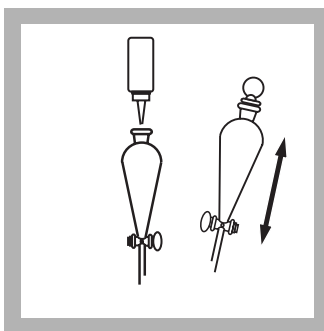


8. Add 5 mL of 5.0 N Sodium Hydroxide Standard Solution.



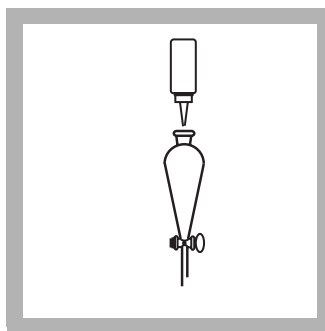
9. Stopper. Invert. Open stopcock to vent. Close the stopcock and shake the funnel once or twice and vent again.

Note: Add a few drops of 5.25 N Sulfuric Acid Standard Solution if the solution turns orange on shaking. The blue-green color will reappear. To avoid higher blanks, repeat procedure on new sample and use less sodium hydroxide in step 8.



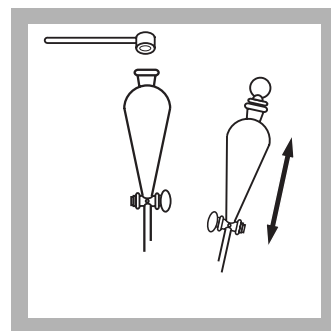
10. Continue adding 5.0 N Sodium Hydroxide Standard Solution dropwise and shaking the funnel after every few drops until the color of the solution being shaken changes from blue-green to orange.

Large amounts of zinc cause the color transition at the end point to be indistinct.



11. Add 5 more drops of 5.0 N Sodium Hydroxide Standard Solution.

A pink color in the bottom (chloroform) layer at this point does not necessarily indicate lead is present. Only after adding the potassium cyanide in the next step will the presence of lead be confirmed by a pink color.

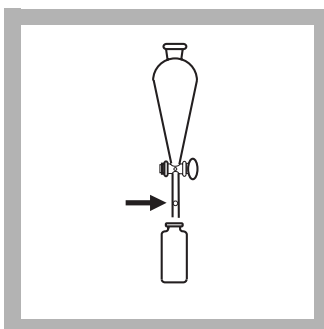


12. Add 2 heaping 1.0-g scoops of potassium cyanide to the funnel. Stopper.

Shake vigorously until the potassium cyanide is all dissolved (about 15 seconds).



13. Wait one minute for the layers to separate. The bottom (chloroform) layer will be pink if lead is present.



14. Prepared Sample: Insert a cotton plug the size of a pea into the delivery tube of the funnel and slowly drain the bottom (chloroform) layer into a dry 25-mL square sample cell. Stopper.

The lead-dithizone complex is stable for at least thirty minutes if the sample cell is kept tightly capped and out of direct sunlight.



15. Blank Preparation: Fill another 25-mL square sample cell with chloroform. Stopper.



16. Insert the blank into the cell holder with the fill line facing right.



17. Press ZERO.

The display will show:

0 µg/L Pb²⁺

18. Insert the prepared sample into the cell holder with the fill line facing right.

19. Press READ.

Results are in µg/L Pb²⁺.

Interferences

Table 1 Interfering Substances and Levels

| Interfering Substance | Interference Levels and Treatments |
|--|------------------------------------|
| Highly buffered samples or extreme sample pH | All levels. See procedure below. |
| Bismuth | All levels. See procedure below. |
| Copper | All levels. See procedure below. |
| Mercury | All levels. See procedure below. |
| Silver | All levels. See procedure below. |
| Tin | All levels. See procedure below. |

Table 2 Substances That Do Not Interfere

| | |
|----------|-----------|
| Aluminum | Lead |
| Antimony | Magnesium |
| Arsenic | Manganese |
| Calcium | Nickel |
| Chromium | Tin |
| Cobalt | Zinc |
| Iron | |

Eliminate interference from the metals in [Table 1](#) by the following treatment, beginning after [step 6](#).

1. Measure about 5-mL of the DithiVer solution into the separatory funnel. Stopper the funnel, invert and open the stopcock to vent. Close the stopcock and shake the solution vigorously for 15 seconds. Allow the funnel to stand undisturbed until the layers separate (about 30 seconds). A yellow, red, or bronze color in the bottom (chloroform) layer confirms the presence of interfering metals. Draw off and collect the bottom (chloroform) layer for proper disposal.

2. Repeat extraction with fresh 5-mL portions of prepared dithizone solution (collecting the bottom layer each time in appropriate waste collection vessel) until the bottom layer shows a pure dark green color for three successive extracts. Extractions can be repeated a number of times without appreciably affecting the amount of lead in the sample.
3. Extract the solution with several 2 or 3 mL portions of pure chloroform to remove any remaining dithizone, again collecting the bottom layer each time for proper disposal.
4. Continue the procedure, substituting 28.5 mL of prepared dithizone solution for the 30 mL in step 7.

DithiVer Solution Preparation, Storage, and Reagent Blank

Store DithiVer Powder Pillows away from light and heat. A convenient way to prepare this solution is to add the contents of 10 DithiVer Metals Reagent Powder Pillows to a 500-mL bottle of chloroform and invert several times until well mixed (carrier powder may not dissolve). Store dithizone solution in an amber glass bottle. This solution is stable for 24 hours.

A reagent blank using deionized water should be carried out through the entire method to obtain the most accurate results.

Sample Collection, Preservation, and Storage

Collect samples in an acid-washed glass or plastic containers. Adjust the pH to 2 or less with nitric acid (about 2 mL per liter). Store preserved samples up to six months at room temperature. Adjust the pH to 2.5 with 5.0 N sodium hydroxide before analysis. Correct the test result for volume additions.

Accuracy Check

1. Leave the unspiked sample in the sample cell compartment. Verify that the units displayed are in µg/L.
2. Press **OPTIONS>MORE**. Press **STANDARD ADDITIONS**. A summary of the standard additions procedure will appear.
3. Press **OK** to accept the default values for standard concentration, sample volume, and spike volumes. Press **EDIT** to change these values. After values are accepted, the unspiked sample reading will appear in top row. See the user manual for more information.
4. Snap the neck off a Lead Voluette Ampule Standard, 50-mg/L Pb.
5. Use the TenSette® Pipet (do not use a glass pipet) to add 0.1 mL, 0.2 mL, and 0.3 mL of standard, respectively to three 250-mL samples and mix each thoroughly.
6. Analyze each standard addition sample as described above. Accept the standard additions reading by pressing the soft key under **READ** each time. Each addition should reflect approximately 100% recovery.
7. After completing the sequence, press **GRAPH** to view the best-fit line through the standard additions data points, accounting for the matrix interferences. Press **IDEAL LINE** to view the relationship between the sample spikes and the "Ideal Line" of 100% recovery.

Standard Solution Method

1. Prepare a 10-mg/L lead standard solution by pipetting 10.00 mL of Lead Standard Solution, 100-mg/L, into a 100-mL volumetric flask.
2. Add 0.2 mL of concentrated nitric acid using a TenSette Pipet to prevent the adsorption of lead onto the container walls. Dilute to the mark with deionized water and mix thoroughly.
3. To make a 200-µg/L standard, pipet 5.00 mL of the 10.0-mg/L standard into 245 mL of deionized water in the 500-mL separatory funnel in step 4 of the Dithizone procedure. Prepare these solutions daily. Perform the lead procedure as described above.
4. To adjust the calibration curve using the reading obtained with the standard solution, press **OPTIONS>MORE** on the current program menu. Press **STANDARD ADJUST**.
5. Press **ON**. Press **ADJUST** to accept the displayed concentration. If an alternate concentration is used, press the number in the box to enter the actual concentration, then press **OK**. Press **ADJUST**.

Summary of Method

The dithizone method is designed for the determination of lead in water and wastewater. The DithiVer Metals Reagent is a stable powder form of dithizone. Lead ions in basic solution react with dithizone to form a pink to red lead-dithizonate complex, which is extracted with chloroform. Test results are measured at 515 nm.

Consumables and Replacement Items

Required Reagents

| Description | Quantity/Test | Unit | Cat. No. |
|--|---------------|----------|----------|
| Lead Reagent Set (100 Tests) | — | — | 22431-00 |
| Includes: (1) 14202-99, (2) 14458-17, (1) 12616-99, (2) 767-14, (1) 2450-53, (2) 2450-26 | | | |
| Buffer Powder Pillows, citrate | 1 | 100/pkg | 14202-99 |
| Chloroform, ACS | 30 mL | 4 L | 14458-17 |
| DithiVer Metals Reagent Powder Pillows | 1 | 100/pkg | 12616-99 |
| Potassium Cyanide | 0.1 g | 125 g | 767-14 |
| Sodium Hydroxide Solution, 5.0 N | 5 mL | 1000 mL | 2450-53 |
| Sodium Hydroxide Standard Solution, 5.0 N | varies | 59 mL DB | 2450-26 |

Required Apparatus

| Description | Quantity/Test | Unit | Cat. No. |
|--|---------------|---------|----------|
| Clippers, for opening powder pillows | 1 | each | 968-00 |
| Cotton Balls, absorbent | 1 | 100/pkg | 2572-01 |
| Cylinder, graduated, 5-mL | 1 | each | 508-37 |
| Cylinder, graduated, 50-mL | 1 | each | 508-41 |
| Cylinder, graduated, 250-mL | 1 | each | 508-46 |
| Cylinder, graduated, mixing, 50-mL | 1 | each | 1896-41 |
| Funnel, separatory, 500-mL | 1 | each | 520-49 |
| pH Meter, sens ^{ion} ™1, portable, with electrode | 1 | each | 51700-10 |
| Sample Cell, 1-inch square, 25 mL with cap | 2 | 2/pkg | 26126-02 |

Required Apparatus (continued)

| Description | Quantity/Test | Unit | Cat. No. |
|----------------------------------|---------------|------|----------|
| Spoon, measuring, 1-g | 1 | each | 510-00 |
| Support Ring, 4" | 1 | each | 580-01 |
| Support Ring Stand, 5" x 8" base | 1 | each | 563-00 |

Recommended Standards

| Description | Unit | Cat. No. |
|--|--------|----------|
| Lead Standard Solution, 100 mg/L Pb | 100 mL | 12617-42 |
| Lead Standard Solution, 10-mL Voluette Ampules, 50-mg/L Pb | 16/pkg | 14262-10 |

Optional Reagents and Apparatus

| Description | Unit | Cat. No. |
|---|-------------|----------|
| Ampule Breaker Kit | each | 21968-00 |
| Chloroform, ACS | 500 mL | 14458-49 |
| Filter Discs, glass, 47 mm | 100/pkg | 2530-00 |
| Filter Holder, glass, for 47-mm filter | each | 2340-00 |
| Flask, Erlenmeyer, 500-mL | each | 505-49 |
| Flask, filtering, 500-mL | each | 546-49 |
| Flask, volumetric, Class A, 100-mL | each | 14574-42 |
| Nitric Acid Solution, 1:1 | 500 mL | 2540-49 |
| Nitric Acid, ACS | 500 mL | 152-49 |
| pH Paper, pH 1.0 to 11.0 | 5 rolls/pkg | 391-33 |
| Pipet, serological, 2-mL | each | 532-36 |
| Pipet, TenSette®, 0.1 to 1.0 mL | each | 19700-01 |
| Pipet Tips, for TenSette Pipet 19700-01 | 50/pkg | 21856-96 |
| Pipet, volumetric, 5.00-mL, Class A | each | 14515-37 |
| Pipet, volumetric, 10.00-mL, Class A | each | 14515-38 |
| Pipet Filler, safety bulb | each | 14651-00 |
| Sulfuric Acid, 5.25 N | 100 mL MDB | 2449-32 |
| Water, deionized | 4 liters | 272-56 |

**D: Invoice and warranty for Thermo Scientific
NITON XRF- XL3t 600 X-ray tube analyzers
and NITON XLp 300 Series analyzers**

ORDER ACKNOWLEDGEMENT

Thermo NITON Analyzers, LLC
900 Middlesex Turnpike
Building #8
Billerica, MA 01821-3926
(978)-670-7460

BILL TO: New Jersey Institute of Technology
Fenster Hall
323 Dr. Martin Luther King, Jr. Blvd.
Newark, NJ 07102-1982
USA

| ORDER NO | CURRENT DATE | PAGE NO |
|----------|--------------|---------|
| 61427 | 3/26/2010 | 1 |

| CUSTOMER PURCHASE ORDER |
|-------------------------|
| P1007259 |

SHIP TO: New Jersey Institute of Technology
17 Summit Street
University Heights Colton Heights
Newark, NJ 07102
USA

Dear Customer,

This document acknowledges receipt of your order. Please review the information presented here and advise us of any errors you notice or disagreements you have at your earliest convenience. For fastest service, write or call us at the address and phone number printed above. Please refer to our Order Number and your P.O. Number in all correspondence.

| CUSTOMER | PAYMENT TERMS SHIP VIA | SHIP DATE PPD/COL | SHIPPING INSTRUCTIONS |
|----------|----------------------------|----------------------|---|
| N2718 | Net 30 Days FedEx 2 Day | 4/16/2010 | S/L RAD090001-507280 Exp date 2/29/12 Resp Ind Dallas Link Tel: 973 596 3070 |

| ITEM NO DESCRIPTION | QUANTITY | UOM | UNIT PRICE | CURRENCY | DISCOUNT | EXTENDED PRICE |
|---|----------|-----|---------------|----------|----------|-------------------|
| 12Months + 12Months at \$0.00 = 24 Months ----- End User: New Jersey Institute ----- Rec'd valid S/L 3/26/10 ----- | | | | | | |
| XL3T600 XL3t 600 MODEL | 1.0000 | EA | 33,995.0000 | USD | 0.00 | 33,995.00 |
| 430-010 XL3t 600 Accessory Case | 1.0000 | EA | | | | |
| D Soil Calibration | 1.0000 | EA | | | | |
| XL3TNC XL3t Hardware W/O Calibration | 1.0000 | EA | | | | |
| 183-002 Carton,Outer,RSC 1520 Case (27 x 23 1/8 x 13 1/4) | 1.0000 | EA | | | | |
| 183-008 End Cap, 1520 Case, (Grey) (Rev.Feb'08) | 2.0000 | EA | | | | |

ORDER ACKNOWLEDGEMENT

Thermo NITON Analyzers, LLC
900 Middlesex Turnpike
Building #8
Billerica, MA 01821-3926
(978)-670-7460

| ORDER NO | CURRENT DATE | PAGE NO |
|----------|--------------|---------|
| 61427 | 3/26/2010 | 2 |

| CUSTOMER PURCHASE ORDER |
|-------------------------|
| P1007259 |

BILL TO: New Jersey Institute of Technology
Fenster Hall
323 Dr. Martin Luther King, Jr. Blvd.
Newark, NJ 07102-1982
USA

SHIP TO: New Jersey Institute of Technology
17 Summit Street
University Heights Colton Heights
Newark, NJ 07102
USA

Dear Customer,

This document acknowledges receipt of your order. Please review the information presented here and advise us of any errors you notice or disagreements you have at your earliest convenience. For fastest service, write or call us at the address and phone number printed above. Please refer to our Order Number and your P.O. Number in all correspondence.

| CUSTOMER | PAYMENT TERMS SHIP VIA | SHIP DATE PPD/COL | SHIPPING INSTRUCTIONS |
|----------|----------------------------|----------------------|---|
| N2718 | Net 30 Days FedEx 2 Day | 4/16/2010 | S/L RAD090001-507280 Exp date 2/29/12 Resp Ind Dallas Link Tel: 973 596 3070 |

| ITEM NO DESCRIPTION | QUANTITY | UOM | UNIT PRICE | CURRENCY | DISCOUNT | EXTENDED PRICE |
|---|----------|-----|---------------|----------|----------|-------------------|
| 420-017 Portable Test Stand,XL3 | 1.0000 | EA | 0.0000 | USD | 0.00 | 0.00 |
| 500-649.1 Power Cord,US/JAPAN, 6' long | 1.0000 | EA | 0.0000 | USD | 0.00 | 0.00 |
| 420-014 Soil Kit, XL3 | 1.0000 | EA | 0.0000 | USD | 0.00 | 0.00 |
| 700-300AXLP XLp 300A Lead Paint Analyzer | 1.0000 | EA | 7,005.0000 | USD | 0.00 | 7,005.00 |

ORDER ACKNOWLEDGEMENT

Thermo NITON Analyzers, LLC
900 Middlesex Turnpike
Building #8
Billerica, MA 01821-3926
(978)-670-7460

| ORDER NO | CURRENT DATE | PAGE NO |
|----------|--------------|---------|
| 61427 | 3/26/2010 | 3 |

| CUSTOMER PURCHASE ORDER |
|-------------------------|
| P1007259 |

BILL TO: New Jersey Institute of Technology
Fenster Hall
323 Dr. Martin Luther King, Jr. Blvd.
Newark, NJ 07102-1982
USA

SHIP TO: New Jersey Institute of Technology
17 Summit Street
University Heights Colton Heights
Newark, NJ 07102
USA

Dear Customer,

This document acknowledges receipt of your order. Please review the information presented here and advise us of any errors you notice or disagreements you have at your earliest convenience. For fastest service, write or call us at the address and phone number printed above. Please refer to our Order Number and your P.O. Number in all correspondence.

| | PAYMENT TERMS SHIP VIA | SHIP DATE PPD/COL | SHIPPING INSTRUCTIONS |
|-------|----------------------------|----------------------|---|
| N2718 | Net 30 Days FedEx 2 Day | 4/16/2010 | S/L RAD090001-507280 Exp date 2/29/12 Resp Ind Dallas Link Tel: 973 596 3070 |

| ITEM NO DESCRIPTION | QUANTITY | UOM | UNIT PRICE | CURRENCY | DISCOUNT | EXTENDED PRICE |
|--------------------------------------|----------|-----|---------------|----------|----------|-------------------|
| 12MWE 12-Month Warranty Extension | 2.0000 | EA | 0.0000 | USD | 0.00 | 0.00 |
| FREIGHT Shipping & Handling | 1.0000 | EA | 240.0000 | USD | 0.00 | 240.00 |
| TOTAL | | | | | | 41,240.00 |

**E: Invoice and warranty for HACH DR 2800
portable spectrophotometer**



INVOICE NUMBER 6671054

DATE: 03/31/2010

Page: 1

DETACH TOP PORTION AND RETURN WITH PAYMENT TO:

TOTAL: \$4,912.43

Hach Company
2207 Collections Center Drive
Chicago, IL 60693
Phone: (800) 227-4224

Have you ordered online ?
Order at WWW.HACH.COM

66710542 000085308 00000491243 033110

DETACH HERE

Reprint

S
O
L
D

T
O

NEW JERSEY INST OF TECH

323 MARTIN LUTHER KING JR BLVD
NEWARK, NJ 07102-1982
United States

S
H
I
P

T
O

NEW JERSEY INST OF TECH

BALAVENDER, MARLON
17 SUMMIT ST
COLTON HALL
UNIVERSITY HEIGHTS
NEWARK, NJ 07102
United States

Sort Seg: 1

| | | | |
|-----------------------|-------------------------------|-------|------------|
| INVOICE NO | 6671054 | DATE: | 03/31/2010 |
| PURCHASE ORDER NUMBER | P1007504 | | |
| TERMS | Net 30 Days From Invoice Date | | |
| FREIGHT | Prepay And Bill Customer | | |
| CARRIER | MF-MF**Motor Freight- -Ground | | |
| ACCOUNT | 008530 | | |
| REF. NO. | 309013255-1 | | |

Remit to:

Hach Company
2207 Collections Center Dr
Chicago, IL 60693
Phone: (800) 227-4224

These commodities are sold, packaged, marked, and labeled for destinations in the United States. Exportation of these commodities may require special licensing, packaging, marking or labeling.

| LN# | PRODUCT DESCRIPTION | ITEM NO. | QUANTITY | UNIT PRICE | EXT. PRICE |
|-----|--|-------------|----------|------------|------------|
| 1 | aa db DR2800 SPECTROPHOTOMETER W/BATTERY | DR2800-01B1 | 1 | 2,580.00 | 2,580.00 |
| 2 | DATATRANS SOFTWARE PACK | LZY274 | 1 | 231.00 | 231.00 |
| 3 | KTO: REAGENT SET, LEAD 90 TESTS | 2243100 | 1 | 396.00 | 396.00 |
| 4 | BUFFER PWD PLW, CITRATE PK/100 | 1420299 | 1 | 43.04 | 43.04 |
| 5 | aa CHLOROFORM, ACS 4L | 1445817 | 1 | 126.75 | 126.75 |
| 6 | DITHIVER METALS RGT PP PK/100 | 1261699 | 1 | 58.72 | 58.72 |
| 7 | POTASSIUM CYANIDE, 125G | 76714 | 1 | 21.26 | 21.26 |
| 8 | SODIUM HYDROXIDE 5.0N 1L | 245053 | 1 | 14.77 | 14.77 |
| 9 | SODIUM HYDROXIDE 5.0N 50ML SCDB | 245026 | 1 | 7.61 | 7.61 |
| 10 | CLIPPER, FOR MEDIUM PWD PLWS | 96800 | 1 | 2.69 | 2.69 |
| 11 | COTTON BALLS, ABSORBENT PK/100 | 257201 | 1 | 5.47 | 5.47 |
| 12 | CYLINDER, GRADUATED 5ML TD WHITE | 50837 | 1 | 13.64 | 13.64 |
| 13 | CYLINDER, GRADUATED 50ML TD WHITE | 50841 | 1 | 12.41 | 12.41 |
| 14 | CYLINDER, GRADUATED 250ML TD WHITE | 50846 | 1 | 21.29 | 21.29 |
| 15 | CYLINDER, GRAD MIXING 50 ML | 189641 | 1 | 22.16 | 22.16 |
| 16 | FUNNEL, SEPARATORY 500ML | 52049 | 1 | 84.75 | 84.75 |

PURCHASE AND ACCEPTANCE OF PRODUCT(S) SUBJECT TO HACH COMPANY'S TERMS AND CONDITIONS OF SALE,
PUBLISHED ON HACH COMPANY'S WEBSITE AT WWW.HACH.COM/TERMS

For order discrepancies or product exchanges please call 800-227-4224 or 970-669-3050 to obtain Return Authorization.

FEDERAL TAX ID # 42-0704420



Other brands
from Hach



INVOICE NUMBER 6671054

DATE: 03/31/2010

Page: 2

| LN# | PRODUCT DESCRIPTION | ITEM NO. | QUANTITY | UNIT PRICE | EXT. PRICE |
|-----|--------------------------------------|----------|----------|------------|------------|
| 17 | KTO:SENSION1 W/PLATINUM PH ELECTRODE | 5170010 | 1 | 363.75 | 363.75 |
| 18 | SPOON, MEASURING 1.0G | 51000 | 1 | 1.61 | 1.61 |
| 19 | RING, SUPPORT 4 INCH | 58001 | 1 | 8.51 | 8.51 |
| 20 | SUPPORT, RING STAND 5X8 BASE | 56300 | 1 | 11.74 | 11.74 |
| 21 | SAMPLE CELL, W/STOPPER MATCHED PAIR | 2612602 | 1 | 97.50 | 97.50 |
| 22 | LEAD STD SOLN, 100MG/L 100ML | 1261742 | 1 | 15.94 | 15.94 |
| 23 | AMPULE BREAKER KIT | 2196800 | 1 | 10.50 | 10.50 |
| 24 | CHLOROFORM, ACS 500ML | 1445849 | 1 | 31.69 | 31.69 |
| 25 | FILTER, GLASS FBR 47MM PK/100 | 253000 | 1 | 25.04 | 25.04 |
| 26 | FILTER HOLDER, GLASS, 47MM | 234000 | 1 | 298.50 | 298.50 |
| 27 | FLASK, ERLLENMEYER 500ML | 50549 | 1 | 5.06 | 5.06 |
| 28 | FLASK, FILTERING 500ML | 54649 | 1 | 18.04 | 18.04 |
| 29 | FLASK, VOLUMETRIC CLASS A 100ML | 1457442 | 1 | 19.76 | 19.76 |
| 30 | NITRIC ACID SOLN, 1:1 500ML | 254049 | 1 | 17.99 | 17.99 |
| 31 | NITRIC ACID, ACS 500ML | 15249 | 1 | 29.59 | 29.59 |
| 32 | PH PAPER, 1.0-11.0 PK/5 | 39133 | 1 | 7.31 | 7.31 |
| 33 | PIPET, SEROLOGICAL 2ML | 53236 | 1 | 5.77 | 5.77 |
| 34 | TENSETTE PIPET 0.1-1.0 ML | 1970001 | 1 | 165.75 | 165.75 |
| 35 | PIPET TIP, FOR 19700-01 PK/50 | 2185696 | 1 | 8.24 | 8.24 |
| 36 | PIPET, VOLUMETRIC CLASS A 5ML | 1451537 | 1 | 6.82 | 6.82 |
| 37 | PIPET, VOLUMETRIC CLASS A 10ML | 1451538 | 1 | 7.09 | 7.09 |
| 38 | SAFETY BULB | 1465100 | 1 | 21.67 | 21.67 |
| 39 | SULFURIC ACID 5.25N 100ML MDB | 244932 | 1 | 7.49 | 7.49 |
| 40 | WATER, DEIONIZED 4L (DEMINERALIZED) | 27256 | 1 | 15.56 | 15.56 |

ORDER CONTACT:LISA AXE
9735962477**Notes:**

| | |
|----------------------------|----------|
| SUBTOTAL | 4,842.48 |
| FREIGHT CHARGES | 69.95 |
| TAX | 0.00 |
| INVOICE TOTAL (USD) | 4,912.43 |

PURCHASE AND ACCEPTANCE OF PRODUCT(S) SUBJECT TO HACH COMPANY'S TERMS AND CONDITIONS OF SALE,
PUBLISHED ON HACH COMPANY'S WEBSITE AT WWW.HACH.COM/TERMS

For order discrepancies or product exchanges please call 800-227-4224 or 970-669-3050 to obtain Return Authorization.

FEDERAL TAX ID # 42-0704420

**Other brands
from Hach**

Section 11 Limited Warranty

Hach Company warrants its products to the original purchaser against any defects that are due to faulty material or workmanship for a period of one year from date of shipment unless otherwise noted in the product manual.

In the event that a defect is discovered during the warranty period, Hach Company agrees that, at its option, it will repair or replace the defective product or refund the purchase price excluding original shipping and handling charges. Any product repaired or replaced under this warranty will be warranted only for the remainder of the original product warranty period.

This warranty does not apply to consumable products such as chemical reagents; or consumable components of a product, such as, but not limited to, lamps and tubing.

Contact Hach Company or your distributor to initiate warranty support. Products may not be returned without authorization from Hach Company.

Limitations

This warranty does not cover:

- Damage caused by acts of God, natural disaster, labor unrest, acts of war (declared or undeclared), terrorism, civil strife or acts of any governmental jurisdiction
- Damage caused by misuse, neglect, accident or improper application or installation
- Damage caused by any repair or attempted repair not authorized by Hach Company
- Any product not used in accordance with the instructions furnished by Hach Company
- Freight charges to return merchandise to Hach Company
- Freight charges on expedited or express shipment of warranted parts or product
- Travel fees associated with on-site warranty repair

This warranty contains the sole express warranty made by Hach Company in connection with its products. All implied warranties, including without limitation, the warranties of merchantability and fitness for a particular purpose, are expressly disclaimed.

Some states within the United States do not allow the disclaimer of implied warranties and if this is true in your state the above limitation may not apply to you. This warranty gives you specific rights, and you may also have other rights that vary from state to state.

This warranty constitutes the final, complete, and exclusive statement of warranty terms and no person is authorized to make any other warranties or representations on behalf of Hach Company.

Limitation of Remedies

The remedies of repair, replacement or refund of purchase price as stated above are the exclusive remedies for the breach of this warranty. On the basis of strict liability or under any other legal theory, in no event shall Hach Company be liable for any incidental or consequential damages of any kind for breach of warranty or negligence.

Deliverable for Task 4:
In-Situ Bridge Paint Analyses Using XRF

Submitted

to

**Carl Kochersberger
Environmental Science Bureau
Hazardous Materials and Asbestos Unit
Pod 4-1
New York State Department of Transportation
50 Wolf Road
Albany, NY 12232**

May 2013

ABSTRACT

In this report, the application of the NITON XLp-300 series and NITON XL3t-600 series field portable X-ray fluorescence (FP-XRF) is presented for quantifying Resource Conservation and Recovery Act (RCRA) metals (i.e., As, Ba, Cr, Cd, Pb, Hg, Se, and Ag) along with iron and zinc in paint waste samples. In addition, a standard operating procedure (SOP) is introduced for applying the field instrumentation in this project and for New York State Department of Transportation (NYSDOT) personnel in general. Results from applying the FP-XRF are reviewed for the 24 bridges sampled in this project. XRF results indicate that, although the 24 bridges studied to date have been repainted after 1989, lead based paint was not entirely removed. The majority paint samples exhibit lead concentrations greater than 5,000 mg/kg or 1 mg/cm². The elevated iron concentrations found in paint samples ranging from 49,367 to 799,210 mg/kg (5 to 80%), are present from the application of steel grit to remove paint. Concentrations of Pb, As, Cd, Cr, and Ag follow similar trends, while concentration trends of Zn, Hg, and Se are consistent. Because of historical application of the pigments and consequent incomplete paint removal procedure, the data reveals metal residue on the bridge structure. Pb was correlated with As ($R^2 = 0.78$), Cd ($R^2 = 0.73$), Cr ($R^2 = 0.88$) and Ag ($R^2 = 0.67$), while Zn, Se, and Hg were highly correlated with $R^2 = 0.99$ between Hg and Se, $R^2 = 0.94$ for Hg and Zn, and $R^2 = 0.76$ for Se and Zn. Correlations were not observed between Pb, Fe, and Zn concentrations ($R^2 < 0.11$) suggesting unique sources in the paint waste.

Table of Contents

| | |
|---|----|
| ABSTRACT..... | I |
| 1. Introduction..... | 1 |
| 2. Paint sample collection and analysis..... | 2 |
| 2.1 Quality Assurance/Quality Control (QA/QC)..... | 4 |
| 2.2 Paint waste sample collection | 4 |
| 2.3 Paint sample analysis | 5 |
| 2.3.1 Paint sample analysis using NITON XLp-300 FP-XRF analyzer..... | 5 |
| 2.3.2 Paint sample analysis using NITON XL3t 600 series FP-XRF analyzer..... | 5 |
| 2.3.3 Digestion followed by inductively coupled plasma mass spectroscopy (ICP-MS) | 10 |
| 3. Analytical results from the bridges in the project..... | 13 |
| 3.1 Results from HF digestion followed by ICP- MS analysis | 13 |
| 3.2 Results from FP-XRF analysis | 16 |
| 3.2.1 Comparisons of two field techniques | 16 |
| 3.2.2 Distribution of the RACA metals as well as iron and zinc..... | 20 |
| 4. Summary | 32 |
| 5. References..... | 34 |
| Appendix A Bridges sampled and details for samples | 38 |
| Appendix B Standard operating procedure (SOP) for NITON XLp-300 series analyzer | 45 |
| Appendix C Standard operating procedure (SOP) for NITON XL3t-600 series analyzer | 58 |

1. Introduction

Prior to bridge repainting, the paint removal process is referred to as bridge rehabilitation (NYSDOT, 2008). The general practice for protecting steel bridges from corrosion involves applying paint coatings (Boxall and Von Fraunhofer, 1980; Lambourne and Strivens, 1999; Gooch, 1993). Between 1950 and 1980, these paint coatings used lead and chromate for corrosion protection; however, because of the potential release of contaminants and the consequent impact to human health, the Department of Housing and Urban Development (HUD) and Consumer Product Safety Commission (CPSC) prohibited residential use of the lead-based paint (LBP) since 1978 (U.S. CPSC, 1977, HUD, 1978). In New York State, LBP has been prohibited from commercial use since 1989 (NYSDOT, 1988). Even though rehabilitation and subsequent repainting were conducted more than once since 1989, LBP may not be entirely removed. The degree to which paint remains on the bridge is based on surface preparation methods applied in the paint removal procedure (NYSDOT, 2008). One of the more effective approaches for removing paint and rust from steel bridges is through abrasive blasting (Appleman, 1992) where abrasive particles are propelled against the surface using a concentrated stream of compressed air. Dust, abrasive, and paint debris are vacuumed simultaneously in the blasting operation. Debris is separated for disposal and the abrasive particles are returned for reuse. Generally, surface preparation standard SSPC (The Society for Protective Coatings) SP-6 (Commercial Blast Cleaning) (NYSDOT, 2008) had been applied to the bridges in New York State before 2006, where paint and rust from steel were removed to a remaining residual of 33% per unit area of surface. After 2006, SSPC SP-10 (Near White Blast Cleaning) was required in the blasting procedure (NYSDOT, 2008). SP-10 restricts the visible residues and remainder on

the bridge surface to 5% per unit area. According to the rehabilitation records (Margrey and Riese, 2012), bridges from Regions 1, 3, 7, 10, 11 in this study were cleaned to SSPC SP-6 standard, while bridges in Regions 2 and 5 were rehabilitated to the SSPC SP-10 standard. Consequently, the paint waste generated from the bridges may be contaminated with lead and other Resource Conservation and Recovery Act (RCRA) metals to a greater degree in Regions 2 and 5.

In this project, the NITON XLp-300 series lead-in-paint analyzer was applied to detect and quantify lead present in the painted surface and subsurface, while the NITON XL3t-600 series analyzer was used to evaluate RCRA metals as well as iron and zinc in the paint waste. Specifically, paint sample collection, preparation, and the detailed analysis are introduced by using NITON XLp-300 series field portable X-ray fluorescence (FP-XRF) as well as NITON XL3t-600 series FP-XRF. In addition, standard operating procedures (SOP) are reviewed for applying field portable XRF equipment in this project and for New York State Department of Transportation (NYSDOT) personnel in general. Results from applying the FP-XRF are reviewed for 24 bridges in this project. Lastly, based on the statistical analysis of XRF results, correlations between RCRA metals as well as iron and zinc in the paint waste are summarized.

2. Paint sample collection and analysis

Based on the sample size estimation (Deliverable for Task 1), 24 bridges were chosen from those that have been repainted after 1989 (Figure 1, Appendix C).

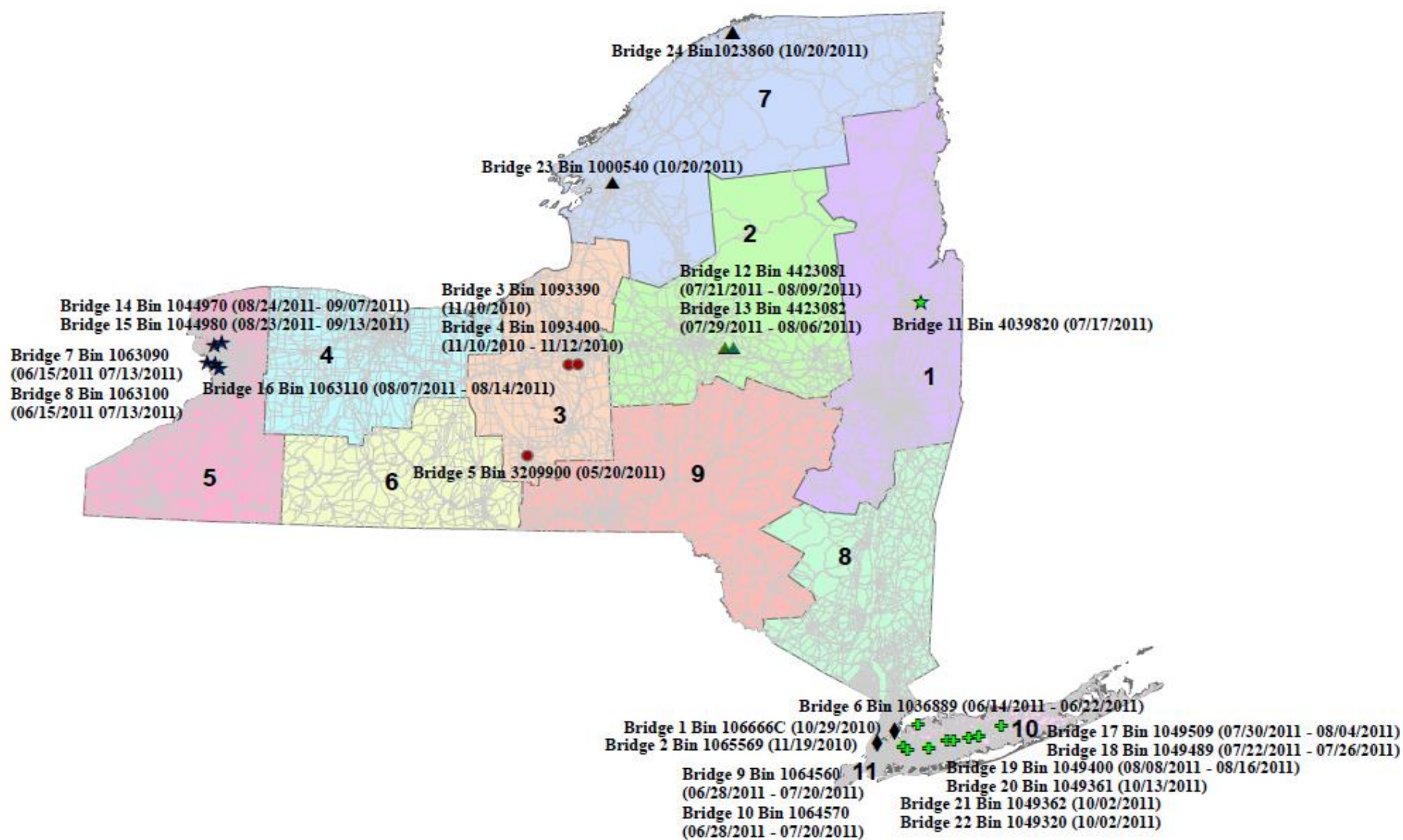


Figure 1. Bridge locations and sampling dates.

2.1 Quality Assurance/Quality Control (QA/QC)

For fieldwork, gloves, dust masks, steel-toed boots, and safety goggles are needed along with a lab coat. Because of its resistance to acids and bases, the Nalgene® HDPE high-density polyethylene containers were used for storing the bridge paint waste. All HDPE containers were cleaned with a metal-free nonionic detergent solution, rinsed with deionized water, soaked in 10% nitric acid (trace metal grade) for 24 h, and then rinsed with metal-free deionized water (ASTM, 1990; Eaton et al., 2005).

2.2 Paint waste sample collection

Duplicate (paint waste) samples were collected from five random locations/drums for each bridge under rehabilitation and evaluated in this project. Samples were evaluated in situ as well as brought back to the NJIT Metals Lab for further analysis. Specifically, the paint samples were obtained by using trowels where the sampled material was stored in HDPE containers that preserved the integrity of the sample. All sample bottles were labeled with the bridge bin number, the date, region, location, and bridge ID (e.g., Bin 106666C / 10/29/2010 / Region 11 / Bruckner Expressway / 11-1a). Samples were subsequently sealed and stored at 4 °C for transport to the NJIT Metals Lab. Preserved samples may be stored up to 6 months prior to analysis in a refrigerator at 4°C (U.S. EPA, 2007). The painted surface selected for in situ detection should be cleaned from debris with brushes to prevent contamination of the measurement and instrument. The FP-XRF is then applied on the selected surface to evaluate the lead concentrations in the paint.

2.3 Paint sample analysis

2.3.1 Paint sample analysis using NITON XLp-300 FP-XRF analyzer

The in situ analysis of bridge paint was conducted with a NITON XLp-300 FP-XRF analyzer (Appendix B), where rapid analysis was accomplished for lead assessment in units of mg/cm^2 . Briefly, after self-calibration, the Pb paint mode with K-shell and L-shell detection is selected on the analyzer. When the screening results are stable, the instrument provides the lead concentrations in units of mg/cm^2 . This analyzer has a 40 mCi cadmium-109 radioisotope source, which excites characteristic X-rays of the test sample. X-ray emission from a ^{109}Cd source occurs at approximately 22.5 and 88.1 keV (Table 1), which therefore excites the K shell fluorescent X-rays of lead. Because the excitation energy is approximately four times greater than the lower energy L shell, the resulting penetration through overlying paint layers is much greater, which enables measurement of lead in subsurface paint layers. Using an algorithm that combines both the L-shell and K-shell readings provides accuracy and precision for measuring Pb in surface or subsurface paint layers.

2.3.2 Paint sample analysis using NITON XL3t 600 series FP-XRF analyzer

All samples are loaded into 12 ml sample holders (SC-4331), sealed with transparent membranes (Figures 2 and 3), and then measured with the XRF (Appendix C).

2.3.2.1. Paint sample preparation (Figures 2 and 3)

- The container used to secure the sample may affect the accuracy of the measurement. A container with a polypropylene seal is used as it does not interfere with the analysis. Consistency and careful attention to details are important in ensuring an accurate measurement.

Table 1. Parameter for two types of FP-XRF^[1]

| Type of XRF | Isotope-based FP-XRF | X-ray tube-based FP-XRF |
|------------------------|--|---|
| | XLp 300A | XL3t 600 |
| Metals detected | Pb in paint mode | P, S, Cl, K, Ca, Sc, Ti, V, Cr, Mn, Fe, Co, Ni, Cu, Zn, As, Se, Rb, Sr, Zr, Mo, Ag, Cd, Sn, Sb, I, Ba, Hg, Tl, Pb, Th, U* |
| Excitation energy | 22.5 keV and 88.1 keV | ≤ 50 keV |
| Excited shell | Both L and K shells | L shell only |
| Incorrect result | | 20.4% for lead |
| Source | ¹⁰⁹ Cd (22.5 KeV, 88.1 KeV) | 50 keV Miniature Au Anode X-ray tube |
| Precision | | False negative result for Pb |
| Limits of detection | | See Table 2 |
| Cost of the instrument | 17,000.00 | 37,000.00 |
| | 41,000.00 (bundled price) | |

* – the elements are listed in order of increasing atomic number.

[1] Thermo Fisher Scientific, The Importance of excitation sources for X-ray fluorescence (XRF) analyzers in lead paint measurement.

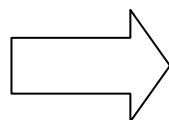
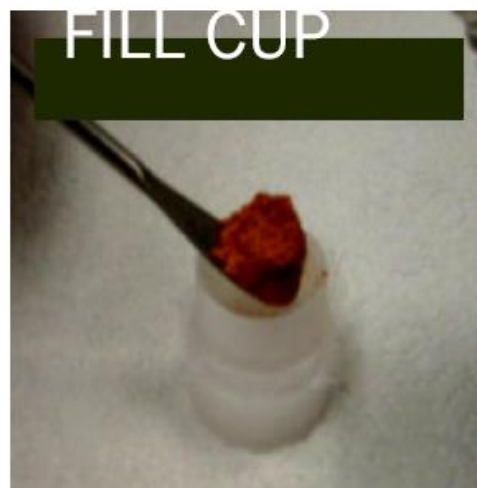
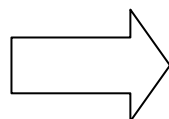
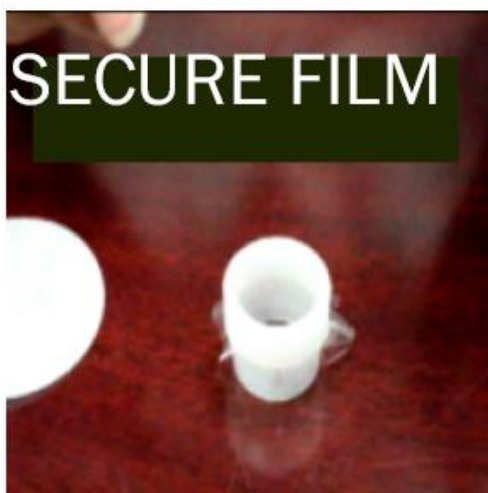
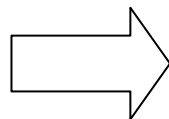


Figure 2. Setting up the XRF sample cup

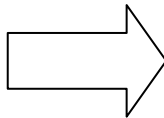
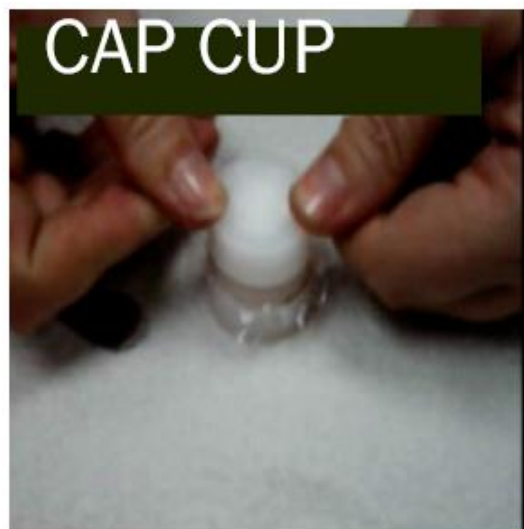
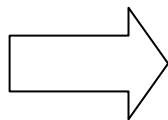


Figure 3. Setting up the XRF sample cups

- Polypropylene film is used to secure the sample in the XRF sample cup with the indented ring. Thermo Scientific recommends preparing the cup in advance, if possible.
- The film should be secured with the collar. The flange inside the collar faces down and snaps into the indented ring of the cup. Inspect the installed film window for continuity and smooth, taut appearance.
- The cup needs to be set on a flat surface film-window-side down. The cup should be filled with at least five grams of the prepared sample, making sure that no voids or uneven layers.
- The sample is tamped lightly into the cup. The end of the pestle makes a convenient tamper.
- A filter-paper disk should be placed on the sample after tamping it.
- The rest of the cup needs to be filled with polyester fiber stuffing to prevent sample movement. Aquarium filter may be used and does not interfere with the analysis. A small supply of stuffing comes with your bulk sample kit.
- The cup is capped.
- A label should be placed on the cup. Identifying information must be included with indelible ink, for example, a record of the sample designation, the site and location, the date of the sample, and any other relevant comments.
- The sample is ready for analysis.

2.3.2.2 Paint sample analysis by NITON XL3t 600 series FP-XRF

RCRA metals (i.e., As, Ba, Cr, Cd, Pb, Hg, Se, and Ag) along with iron and zinc were analyzed with the NITON XL3t-600 series FP-XRF following EPA method 6200 (U. S. EPA,

1998) by using Soil Mode (Table 2) and Mining Mode (Table 3). Briefly, after the self – calibration, sample analysis is carried out for 180 s (Appendix C). The XL3t-600 FP-XRF frame is used to hold the analyzer during the detection procedure. The instrument combines advanced electronics and a 50 keV (which is the greatest X-ray energy used in tube technology, Table 1) X-ray tube. This FP-XRF is an effective analyzer in detecting a wide range of the metal concentrations (in ppm) in soils, sediments, painted surfaces, dust wipes, and air filters for ambient and personal air monitoring. This line of instruments provides both qualitative and quantitative data for elements ranging from Mg through U, including RCRA metals, 12 priority pollutants (U.S. EPA, 2003), and 19 U.S. EPA target analytes (U.S. EPA, 2003). For the bridge paint waste samples, RCRA metals, (i.e., arsenic, barium, cadmium, chromium, lead, mercury, selenium, and silver) along with zinc were investigated.

2.3.3 Digestion followed by inductively coupled plasma mass spectroscopy (ICP-MS)

To compare the results from using the FP-XRF, hydrogen fluoride (HF) digestion followed by inductively coupled plasma mass spectroscopy (ICP-MS) analysis was conducted on paint waste samples. Specifically, eight paint samples with Pb concentrations ranged from 210 to 168093 mg/kg were digested and analyzed for metal concentrations using EPA SW-846 digestion Method 3052 (U.S. EPA, 2004) followed by ICP-MS (Method 6020A) (U.S. EPA, 2007).

Table 2. NITON XRF- XL3t 600 limits of detection for contaminants using Soil Mode (mg/kg)

| Metal | SiO ₂ ^a | SRM ^a |
|----------|-------------------------------|-----------------------|
| | (interference free) | (typical soil matrix) |
| | (mg/kg) | (mg/kg) |
| Arsenic | 9 | 11 |
| Barium | 90 | 100 |
| Cadmium | 10 | 12 |
| Chromium | 65 | 85 |
| Lead | 8 | 13 |
| Mercury | 7 | 10 |
| Selenium | 6 | 20 |
| Silver | 10 | 10 |
| Zinc | 15 | 25 |

^aThe chart above details the sensitivity, or limits of detection (LOD) of Soil Mode for the XL3t 600 Series analyzer, specified for both SiO₂ matrix and a typical Standard Reference Material (SRM). The unit has a 50 keV miniature X-ray tube and multiple primary filters.

^bDetection limits are specified following the U.S. EPA protocol of 99.7% confidence level. Individual limits of detection (LOD) improve as a function of the square root of the testing time. The LODs are averages of those obtained using bulk analysis mode on NITON XL3t 600 analyzers at testing times of 60 seconds per sample.

Table 3. NITON XRF- XL3t 600 limits of detection for contaminants using Mining Mode (mg/kg)

| Time | 60s filter | | | |
|---------------------|-----------------|-----------------|-----------------|-----------------|
| Matrix ^a | Al-based matrix | Ti-based matrix | Fe-based matrix | Cu-based matrix |
| Chromium | 200 | 500 | 110 | 100 |
| Iron | 75 | 300 | N/A | 75 |
| Pb | 20 | 20 | 75 | 50 |
| Selenium | N/A | 20 | 20 | 25 |
| Silver | N/A | N/A | N/A | N/A |
| Zinc | 30 | 40 | 60 | 300 |

N/A = Not applicable

^aThe chart above details the sensitivity, or limits of detection (LOD) of Mining Mode for the XL3t 600 Series analyzer, specified Al-based matrix, Ti-based matrix, Fe-based matrix, and Cu-based matrix. The unit has a 50 keV miniature X-ray tube and multiple primary filters.

^bDetection limits are specified following the U.S. EPA protocol of 99.7% confidence level. Individual limits of detection (LOD) improve as a function of the square root of the testing time. The LODs are averages of those obtained using bulk analysis mode on NITON XL3t 600 analyzers at testing times of 60 seconds per sample.

3. Analytical results from the bridges in the project

3.1 Results from HF digestion followed by ICP- MS analysis

A number of studies have demonstrated the accuracy of XRF analysis for contaminated soil (Binstock et al., 2009; Clark et al., 1999), paint (Zamurs et al., 1998), and glass beads (Sandhu, 2011). In this study, results from using the field portable XRF correlated ($R = 0.85$ to 0.98) with the HF digestion followed by ICP-MS analysis (Figures 4 and 5). This work demonstrates the effectiveness of using FP-XRF as a field method to analyze the RCRA metals as well as iron and zinc concentrations in bridge paint waste. Specifically, both NITON XLp-300 and NITON XL3t 600 XRF analyzer correlated ($R = 0.96$; $R = 0.95$) with the ICP-MS results. In general, results from using XRF reveal greater concentrations of zinc, lead, and chromium than from the digestion analysis. One issue in this approach is incomplete dissolution as observed by others (Pyle and Nocerino, 1996; Kilbride et al., 2006). Pyle and Nocerino,(1996) investigated the samples from a hazardous waste site contaminated with lead and cadmium by using atomic absorption spectroscopy (AAS), XRF, inductively coupled plasma-atomic emission spectroscopy (ICP-AES), and potentiometric stripping analysis (PSA). They concluded that lead and cadmium concentrations determined by XRF were lower than or equal to recoveries determined by ICP-AES and AAS. Kilbride et al. (2006) compared metal concentrations in contaminated soil by using X-ray tube based FP-XRF versus aqua regia acid digestion followed by ICP-OES. Kilbride et al. found that although the measurements were correlated ($R = 0.93$ for Zn, $R = 0.94$ For Pb), results from

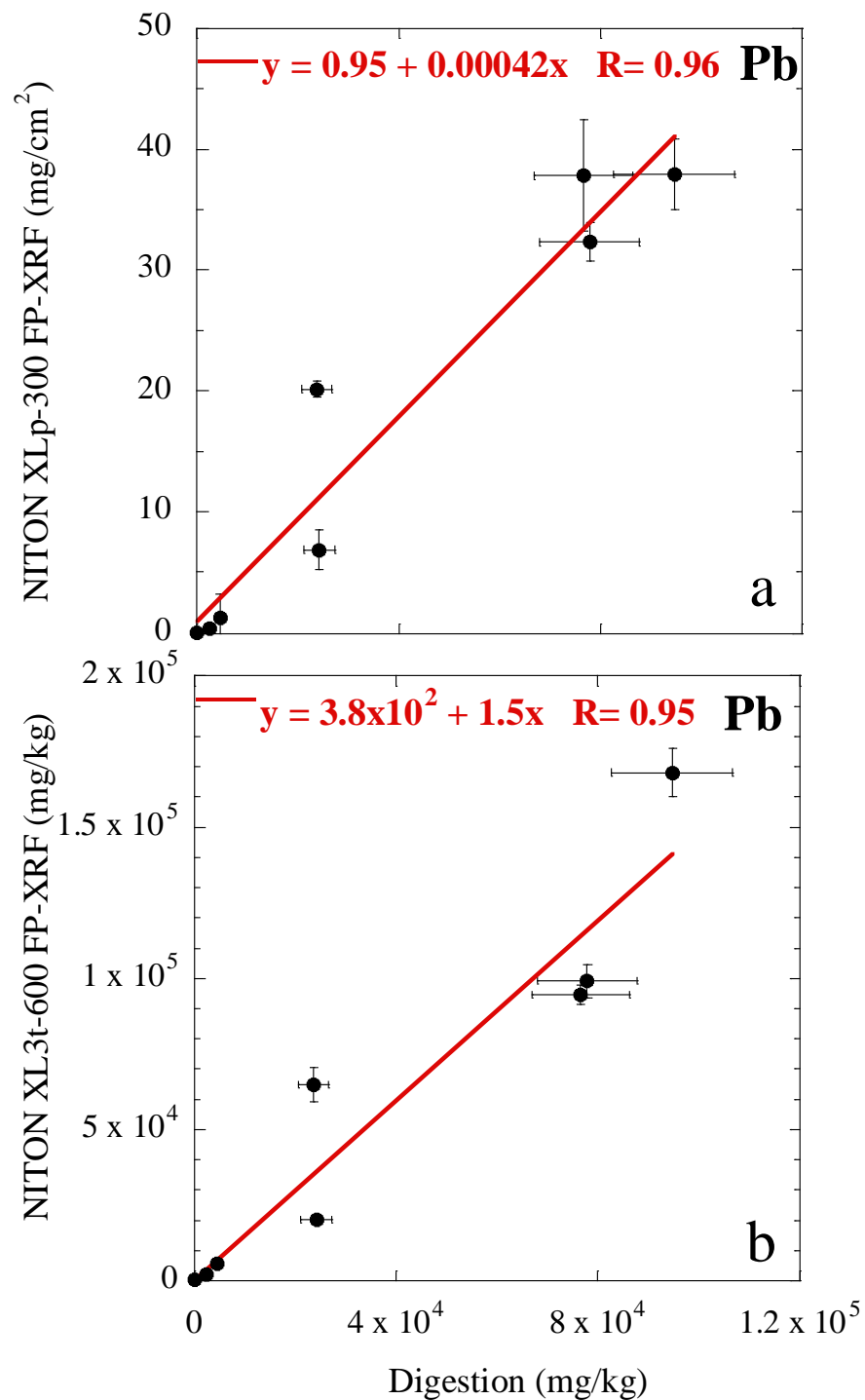


Figure 4. Results from measuring Pb concentrations in paint waste samples with (a) the NITON XLP-300 series lead-in-Paint FP-XRF and HF digestion followed by ICP-MS (b) the NITON XL3t-600 series FP-XRF and HF digestion followed by ICP-MS.

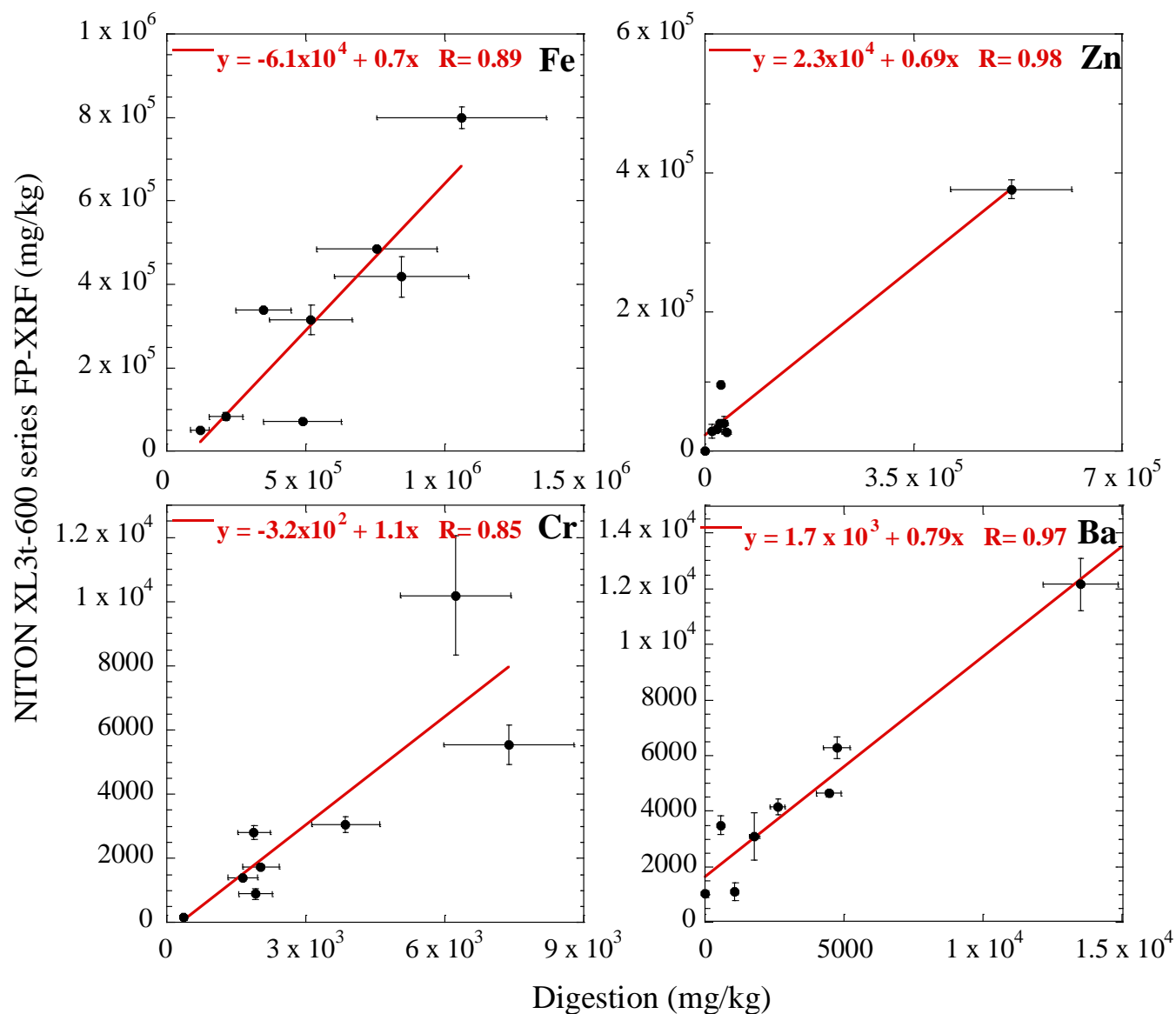


Figure 5. Results from measuring metal concentrations in paint waste samples with NITON XL3t-600 series FP-XRF and HF digestion followed by ICP-MS.

FP-XRF revealed the greater concentrations (35-60820 mg/kg for Zn, 2-74356 mg/kg for Pb) than the data from digestion analysis (3-25389 mg/kg for Zn, 5-40398 mg/kg for Pb).

3.2 Results from FP-XRF analysis

3.2.1 Comparisons of two field techniques

The in-situ analysis of lead was conducted with a NITON XLp-300 series lead-in-paint FP-XRF analyzer, while the NITON XL3t-600 series FP-XRF provided quantitative results for RCRA metals arsenic, barium, cadmium, chromium, lead, mercury, selenium, silver, and zinc along with iron. Pb concentrations in bridges using these two analyzers were highly correlated ($R=0.95$, Figure 6). Both instruments are effective for measuring metals in paint surfaces. However, the NITON XLp-300 series detects lead in subsurface paint layers as well because of the high-energy source (Cd^{109} 40 mCi, Table 1).

The calibration range for the Soil Mode using the NITON XL3t-600 XRF is up to 2% by mass (20,000 mg/kg). The results from applying the Soil Mode revealed greater Pb concentrations than those from the Mining Mode when concentrations exceeded the calibration range maximum (2%) (Figure 7). Therefore, Mining Mode was applied for the samples with metal concentrations greater than 2% (20,000 mg/kg). Specifically, 83% of results from applying the NITON XLp-300 XRF presented relative errors less than 30%, while 79% of the data from the NITON XL3t-600 XRF revealed relative errors less than 20% when operating within the calibration range (Figure 8). In addition, both of the XRF instruments revealed greater relative errors in the lower Pb concentration range (less than 1.2 mg/cm² or 1%).

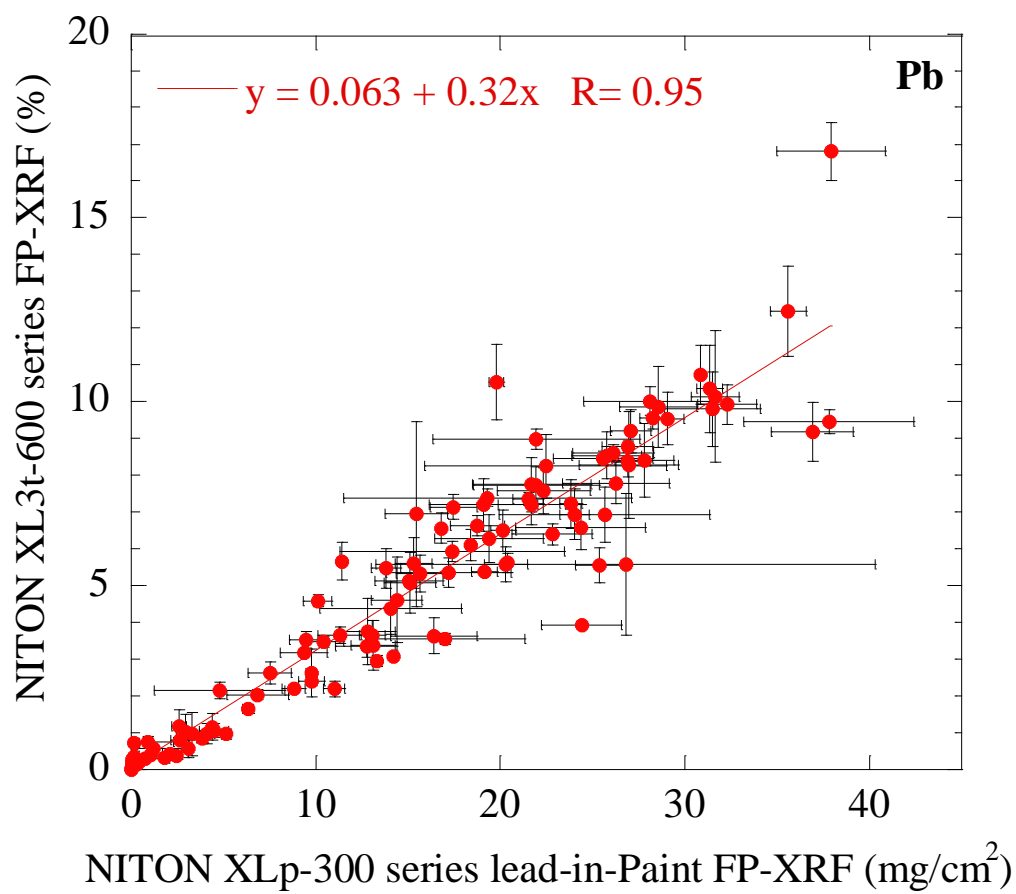


Figure 6. Results of total lead concentrations in bridge paint waste measured with the NITON XLp-300 series lead-in-Paint FP-XRF and the NITON XL3t-600 series FP-XRF. Mining Mode was used for sample with metal concentrations greater than 2%, while Soil Mode was applied for samples with metal concentrations less than 2%. Error bars represent analytical error for the two methods.

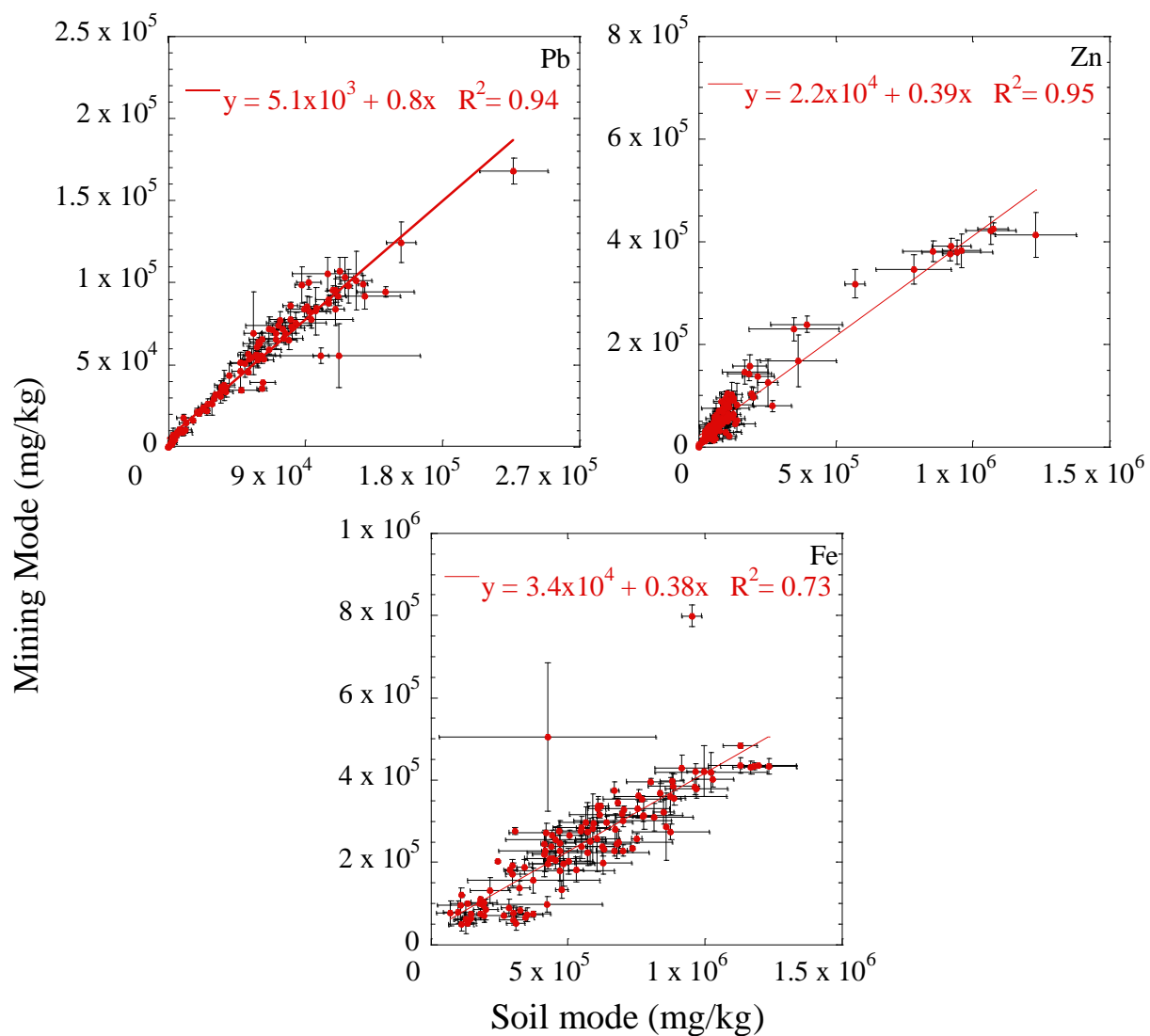


Figure 7. Results of metal concentrations in bridge paint waste measured with Soil Mode and Mining Mode in the NITON XL3t-600 series FP-XRF. Error bars represent analytical error for the two Modes.

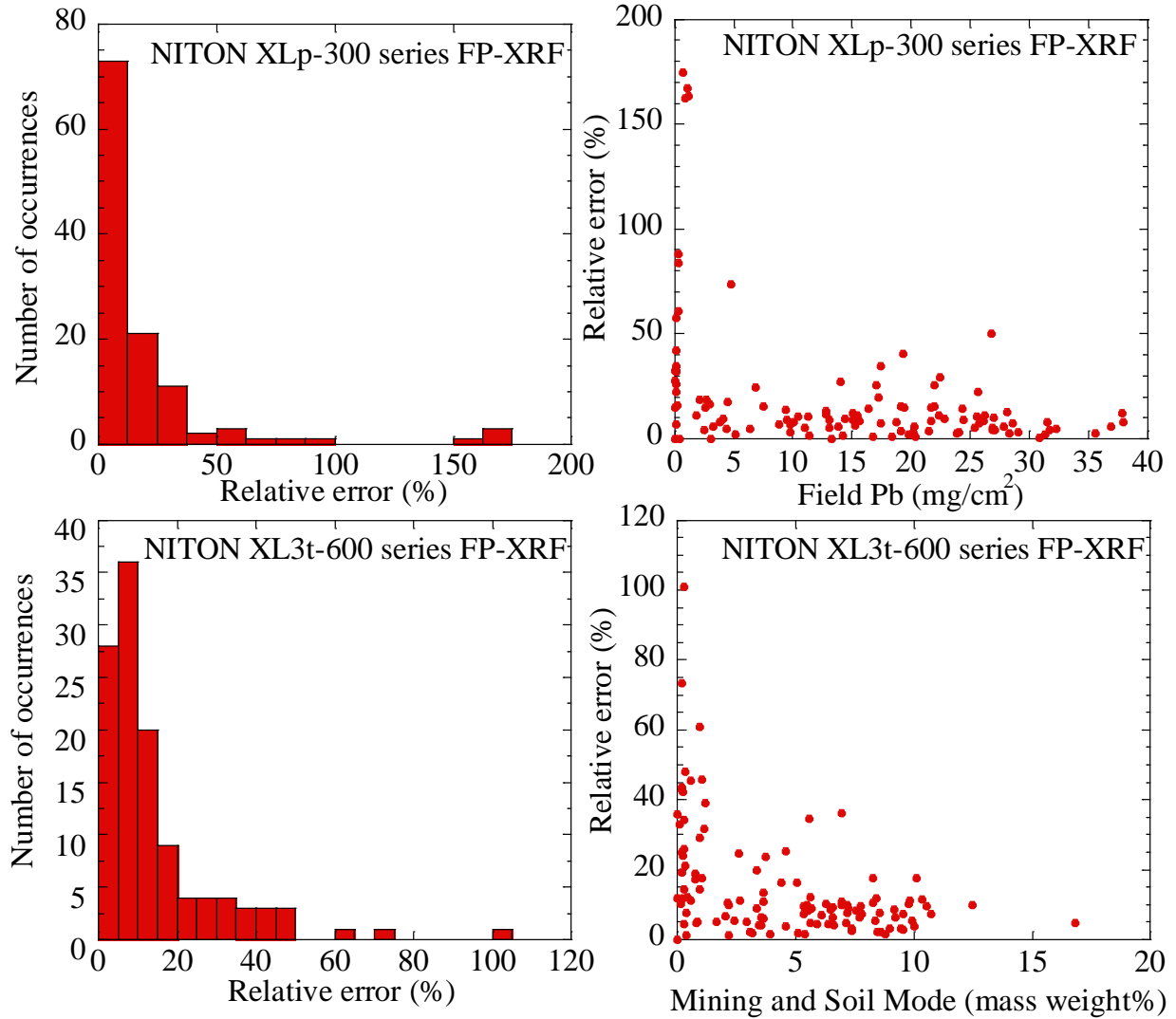


Figure 8. Relative error distribution observed in the samples using NITON XLp-300 series lead-in-Paint FP-XRF and the NITON XL3t-600 series FP-XRF. Mining Mode was used for sample with metal concentrations greater than 2%, while Soil Mode was applied for samples with metal concentrations less than 2%. Relative error = standard error/value of the measurement.

3.2.2 Distribution of the RACA metals as well as iron and zinc.

Concentrations of most metals ranged over several orders of magnitude (Figures 9 and 10): 5 to 168,090 mg/kg for Pb (0.0005 to 17%), 49,367 to 799,210 mg/kg for Fe (5 to 80%), and 27 to 425,510 mg/kg for Zn (0.003 to 43%). The observed Pb concentrations are a consequence of its wide application as a corrosion inhibitor in paint (National Paint & Coatings Association [NPCA], 1992), including lead carbonate (white lead $2\text{PbCO}_3 \cdot \text{Pb}(\text{OH})_2$), lead chromate (PbCrO_4), and lead tetraoxide (red lead Pb_3O_4 , Pb_2O_4 , $\text{PbO}_2 \cdot 2\text{PbO}$) (Gooch, 1993; Oil and Color Chemists Association, 1983). Even though rehabilitation and subsequent repainting were conducted more than once since 1989, LBP was not removed entirely. For the 24 bridges studied, 99% of the paint samples from the bridges in Regions 1, 3, 7, 10, and 11 revealed lead concentrations greater than the HUD limit (Department of Housing and Urban Development, 1978) of 5,000 mg/kg (or 1 mg/cm^2) ranging between 2,730 to 160,890 mg/kg (0.27 to 16%), while 57% of the samples from remaining seven bridges in Regions 2 and 5 exhibited lead concentrations less than 5,000 mg/kg (or 1 mg/cm^2) (Figure 9). These results can be explained by the surface preparation standard applied in New York State. Bridges in Region 2 (Syracuse area) were blast cleaned to surface preparation standard SSPC SP-10 (Margrey, 2012) during rehabilitation in 1997 (Table 4). Although it is not recorded, bridges in Region 5 are likely cleaned to SSPC SP-10 blasting standard where surfaces are cleaned to 5% of residue per unit area (Table 4). In the other regions, the SSPC SP-6 blasting standard was applied (Table 4). Specifically, SSPC SP-6 is a commercial blast cleaning method and was applied to most of the bridges in New York State (NYSDOT, 2008) before 2006, where slight shadows, streaks or discolorations caused by rust stain, mill scale oxides or residual paint or coating remained on the bridge were limited to no more than 33% per unit area of surface. After 2006, NYS required the

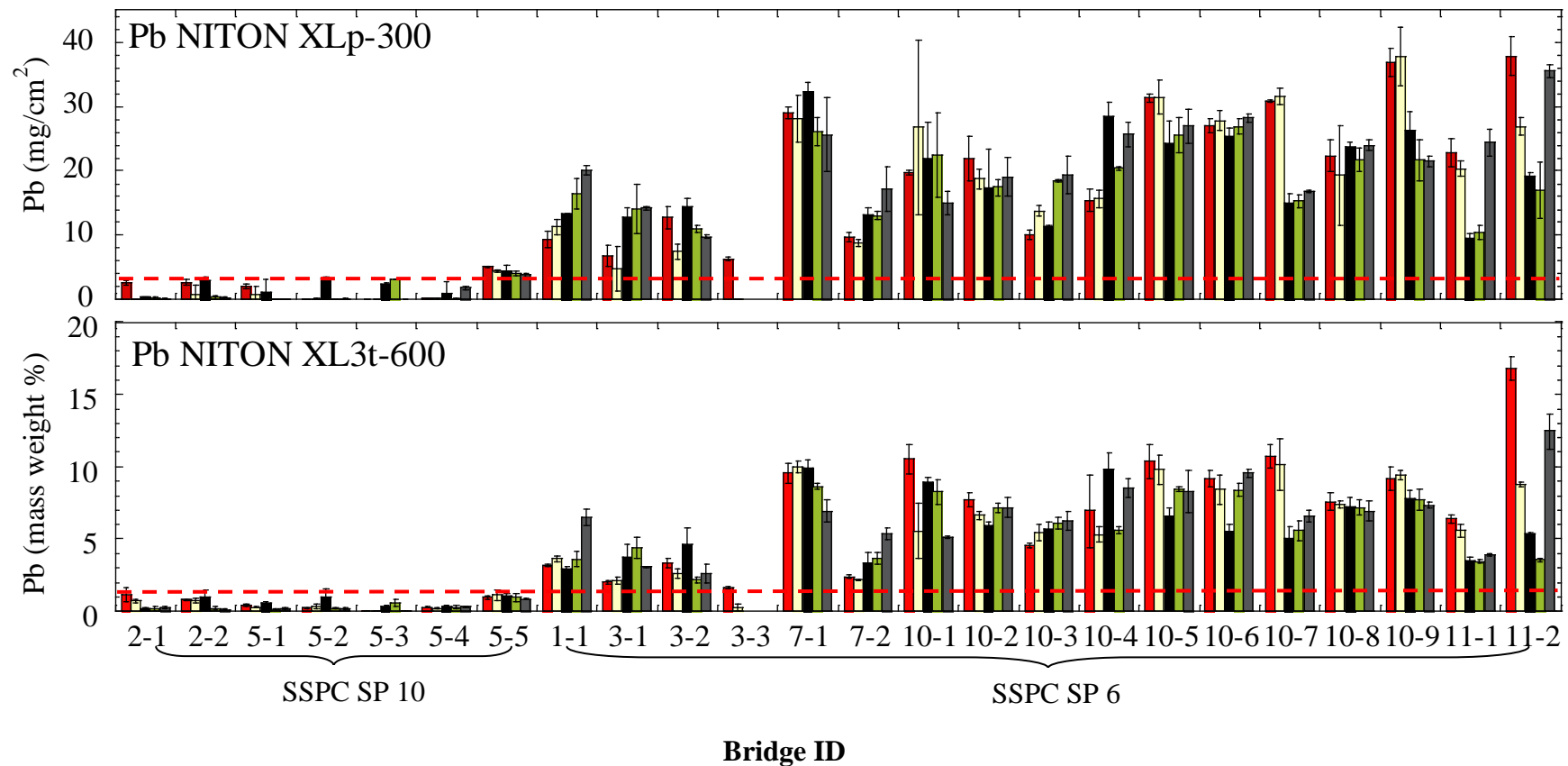


Figure 9. Pb concentrations in paint are shown as a function of the five locations for bridges in Regions 1, 2, 3, 5, 7, 10, and 11 using the NITON XLp-300 lead-in-paint FP-XRF and NITON XL3t-600 series FP-XRF. Mining Mode was used for sample with metal concentrations greater than 2%, while Soil Mode was applied for samples with metal concentrations less than 2%. Bridge ID represents the Region number and bridge sampled in this Region. All bridges sampled were rehabilitated after 1989. Blasting standard SSPC SP 10 was applied for bridges in Regions 2 and 5, while SSPC SP 6 were used for bridges in Regions 1, 3, 7, 10, and 11

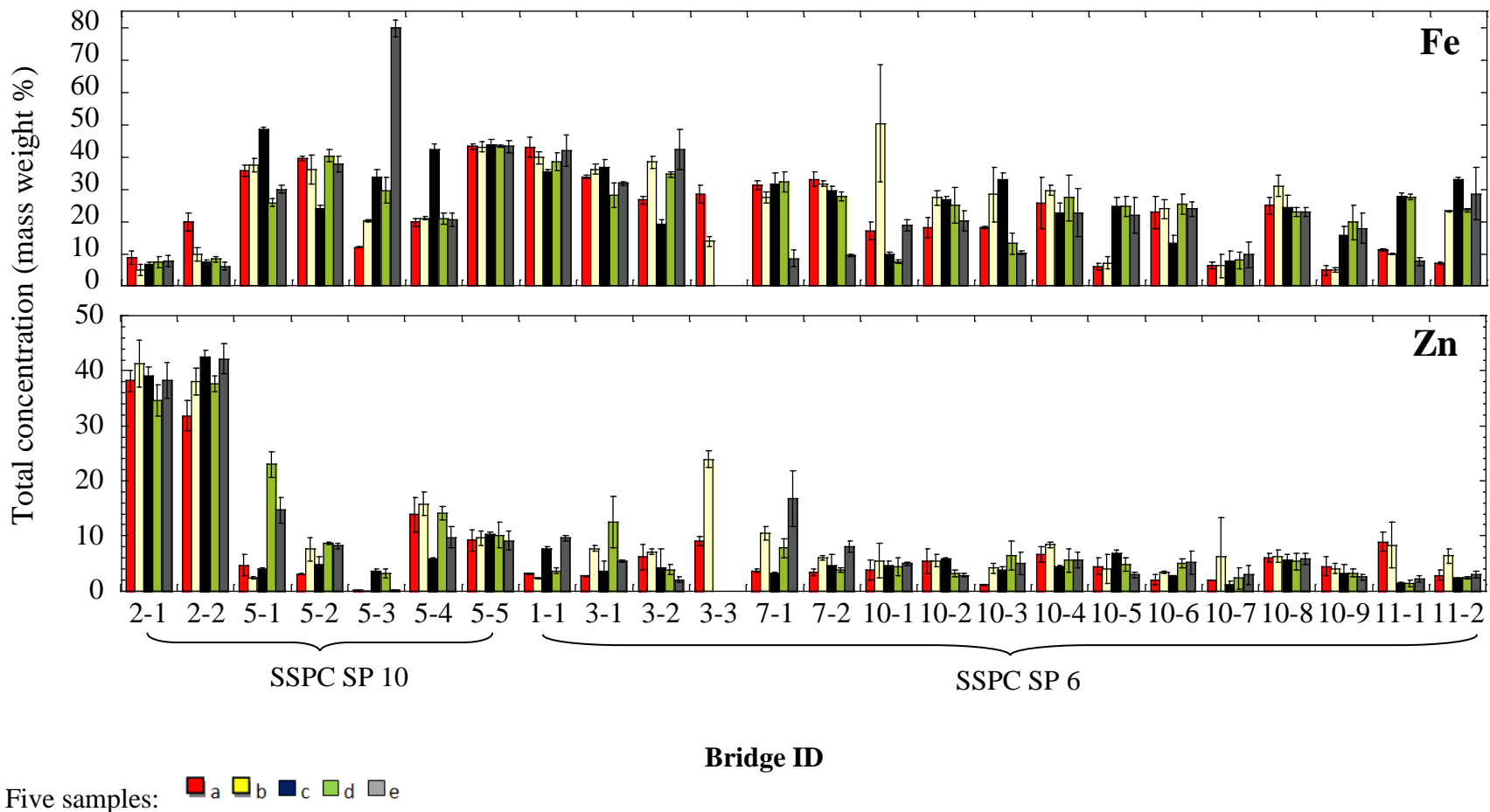


Figure 10. Iron and zinc concentrations in paint are shown as a function of the five locations for bridges in Regions 1, 2, 3, 5, 7, 10, and 11 using NITON XL3t-600 series FP-XRF. Mining Mode was used for sample with metal concentrations greater than 2%, while Soil Mode was applied for samples with metal concentrations less than 2%. Bridge ID represents the Region number and bridge sampled in this Region. All bridges sampled were rehabilitated after 1989. Blasting standard SSPC SP 10 was applied for bridges in Regions 2 and 5, while SSPC SP 6 were used for bridges in Regions 1, 3, 7, 10, and 11.

Table 4. Bridge rehabilitation information and pigments historically used*.

| Paint waste collected | Sample ID | SSPC standard applied | Year built | Year(s) repainted | Paint and pigment information |
|-----------------------|---------------------------------|-----------------------|--------------------------------------|--------------------------------------|---|
| Region 1 | 1-1 | SP 6 | 1938 | 1990,1991 | NA |
| Region 2 | 2-1 2-2 | SP 10 | 1955 | 1997 | Organic zinc primer (80% zinc dry matter content), epoxy penetration sealer second coat, epoxy third coat, and polyurethane finish coat. Manufacture was Carboline. |
| Region 3 | 3-1 3-2 3-3 | SP 6 | 1975 1940 | 1991, 1999 1991 | NA |
| Region 5 | 5-1 5-2 5-3 5-4 5-5 | SP 10 | 1972 1972 1963 1963 1972 | 2002 2002 1998 1998 1992 | Low-gloss to flat-finish, micaceous iron oxide (MIO) pigmented, one component of polyurthane top coat. Manufacture was Xymax Coatings. NA |
| Region 7 | 7-1 7-2 | SP 6 | 1948 1957 | 1997 1998 | NA |

| Paint waste collected | Sample ID | SSPC standard applied | Year built | Year(s) repainted | Paint and pigment information |
|-----------------------|-----------|-----------------------|------------|------------------------|-------------------------------|
| Region 10 | 10-1 | SP 6 | 1953 | 1995 | NA |
| | 10-2 | | 1970 | 1979, 1986, 1999 | |
| | 10-3 | | 1970 | 1979, 1986, 1999 | |
| | 10-4 | | 1967 | 1985, 1999 | |
| | 10-5 | | 1967 | 1999 | |
| | 10-6 | | 1964 | 1986, 1989 | |
| | 10-7 | | 1963 | 1978, 1989, 1993, 1994 | |
| | 10-8 | | 1963 | 1978, 1992, 1994, 1995 | |
| | 10-9 | | 1963 | 1977, 1997 | |
| Region 11 | 11-1 | SP 6 | 1959 | 1996 | NA |
| | 11-2 | | 1969 | 1990 | |

SP 6 – Commercial Blast Cleaning where paint and rust from steel were removed to a remaining residual of 33% per unit area of surface.

SP10 – Near White Blast Cleaning where paint and rust from steel were removed to a remaining residual of 5% per unit area of surface. SSPC SP-10 was required in NYS since 2006. However, some contractors have applied SP-10 to the bridges even before 2006.

NA– Historical records for the bridges are not available.

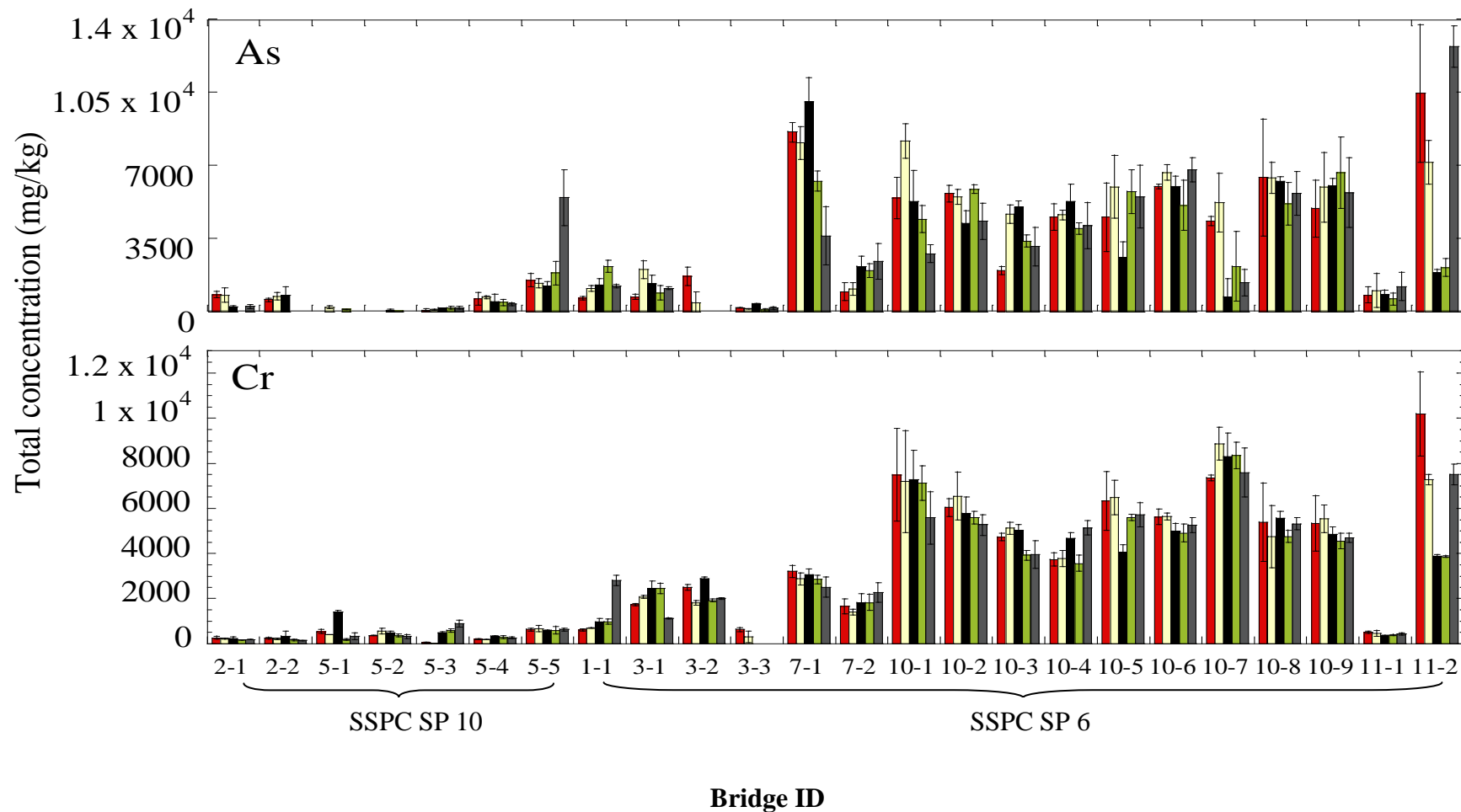
*– lead was discontinued for the bridges paint in New York State.

SSPC SP-10 (Near White Blast Cleaning) blasting procedure (NYSDOT, 2008). SP-10 is a similar method to the SP-6 except it restricts the visible residues and remainder on the bridge surface to 5% per unit area.

Iron (Figure 10), ranging from 49,367 to 799,210 mg/kg (5 to 80%), is from a number of sources: the 10 - 15% black iron oxide ($\text{Fe}_2\text{O}_3 + \text{MnO}_2$) used in the paint (Boxall and von Frauhoffer, 1980), rust formed on the bridge, as well as the blasting abrasive steel grit. Generally, sand, steel grit, steel shot, and aluminum oxide are used as abrasives during bridge rehabilitation. For bridges studied in New York State (NYSDOT, 2008), recycled steel grit is applied as blasting material. Although contractors use a magnetic separation process to remove steel grit from the paint waste, the blasting abrasive agent is not entirely separated. The percent remaining with the waste is reported to be the smallest size fraction (Feliciano and Kochersberger, 2011). Therefore, the elevated iron concentrations observed are due to the steel grit applied as a blasting agent for removing paint during bridge rehabilitation.

Samples from Region 2 (Utica site) revealed the greatest Zn concentrations ranging from 318,270 to 425,510 mg/kg (32% - 43%) (Figure 10). The data are consistent with applying an organic zinc primer (80% zinc content dry) (Table 4) to these bridges (Bridges 2-1 and 2-2), which were built in 1955 and repainted in 1997 (Margrey, 2012). Bridges in other Regions revealed Zn ranging from 27 to 239,420 mg/kg (0.0027% to 24%), as zinc sulfide and zinc chromate were applied as corrosion inhibitors between 1920 and 1970 (Boxall and von Frauhoffer, 1980). The presence of Zn in the paint waste reflects the increasing usage of zinc primer (ZnO , $\text{Zn}_3(\text{PO}_4)_2 \cdot 2\text{H}_2\text{O}$, and epoxy zinc rich primer) (80% zinc content dry) to the bridges.

Chromium (Figure 11) concentrations ranged from 21 to 10,192 mg/kg, and can be attributed to the application of a number of pigments in paint between 1920 and 1970: zinc

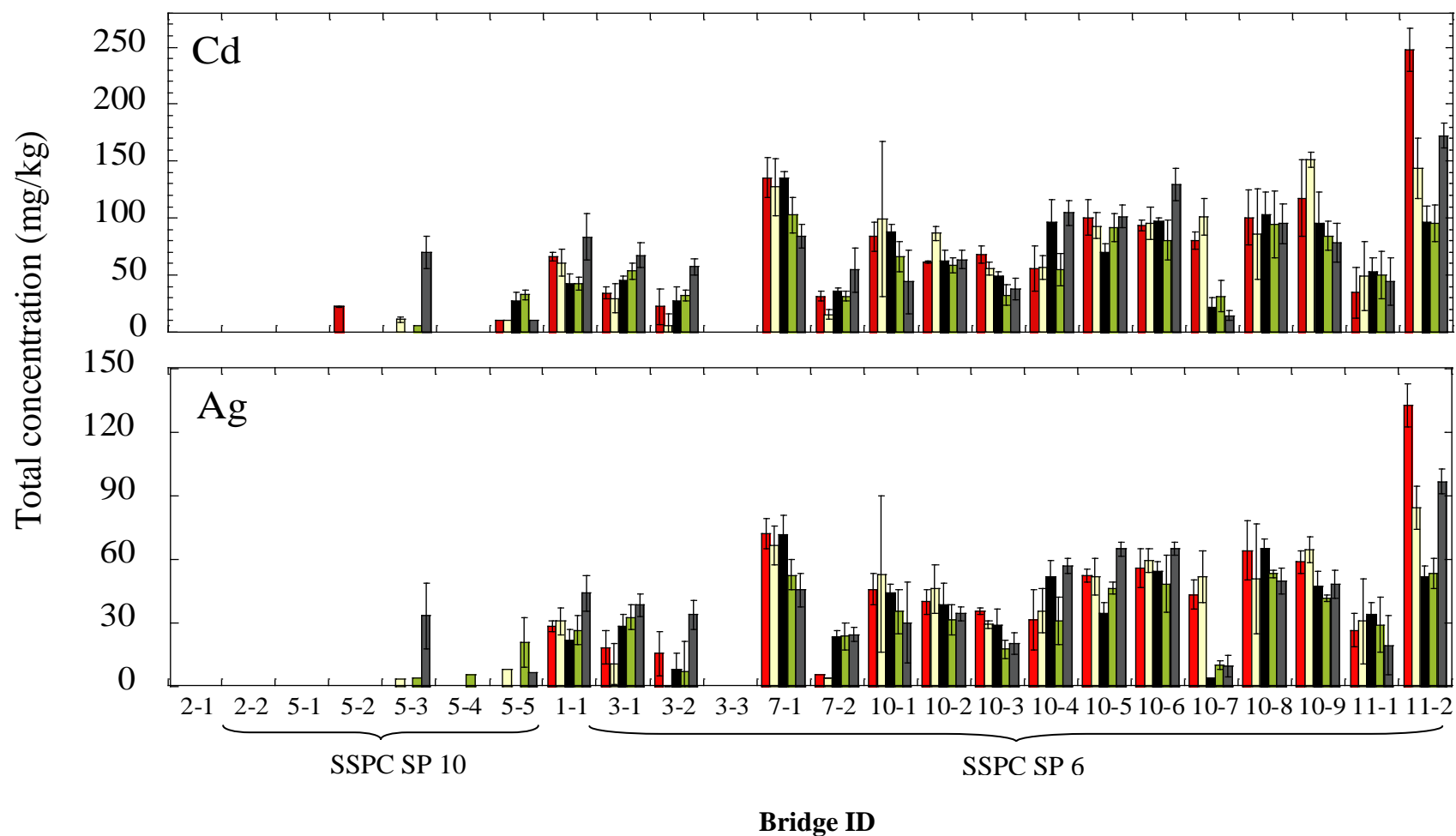


Five samples: ■ a ■ b ■ c ■ d ■ e

Figure 11. Arsenic and chromium concentrations in paint are shown as a function of the five locations for bridges in Regions 1, 2, 3, 5, 7, 10, and 11 using NITON XL3t-600 series FP-XRF. Soil Mode was applied for all samples. Bridge ID represents the Region number and bridge sampled in this Region. All bridges sampled were rehabilitated after 1989. Blasting standard SSPC SP 10 was applied for bridges in Regions 2 and 5, while SSPC SP 6 were used for bridges in Regions 1, 3, 7, 10, and 11.

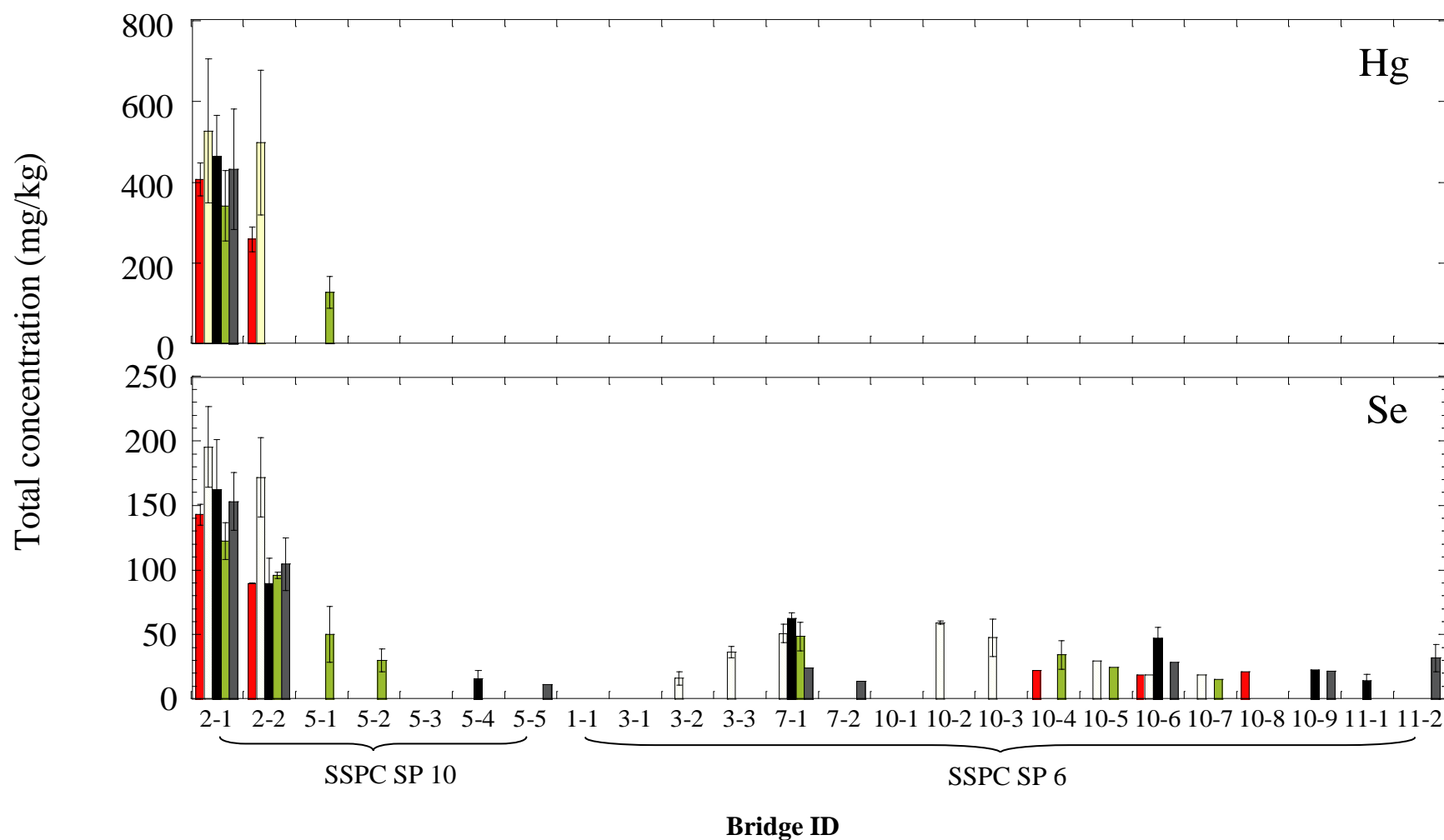
chromate (ZnCrO_4), lead chromate (PbCrO_4), and chromium oxide (Cr_2O_3) (Boxall and von Frauhoffer, 1980). Arsenic was observed in waste up to 12,678 mg/kg, resulting from its application as pigment and corrosion inhibitors in the 1950's (NPCA, 1992) (Figure 11). Because of its use as an extender (Lambourne and Strivens, 1999), barium was observed as great as 16,319 mg/kg in paint (Figure 14). Cadmium was detected up to 248 mg/kg (Figure 12), which is a consequence of its wide application between 1920 and 1970 as a pigment that produces bright colors in paint (Alphen, 1998). Because of their infrequent use in paint (Alphen, 1998), selenium and silver were detected at lower concentrations up to 195 mg/kg and 132 mg/kg, respectively (Figures 12 and 13). Although used before 1992 as a preservative to control bacteria, mildew, and other fungi for marine paint (U.S. EPA, 1990; 2000), mercury was only observed in three bridges up to 527 mg/kg: Bridge 2-1, 2-2, and 5-1 (Figure 13).

Interestingly, Pb correlated As ($R^2 = 0.78$), Cr ($R^2 = 0.73$), Cd ($R^2 = 0.88$), and Ag ($R^2 = 0.67$). These results reveal that the usage of these metals was associated with Pb. The presence of As, Cd, Cr, and Ag coincided with the observation of Pb. Similar trends with strong correlation coefficients were observed between Cd and Ag ($R^2 = 0.95$) as well as As and Cd ($R^2 = 0.72$) (Table 5). Zn, Se, and Hg were also correlated with $R^2 = 0.99$ between Hg and Se, $R^2 = 0.94$ for Hg and Zn, and $R^2 = 0.76$ for Se and Zn. These results reflect the consistent of usage of Hg, Se, and Zn in the paint coatings. Correlations were not observed between Pb, Fe, and Zn concentrations ($R^2 < 0.11$, Table 5) suggesting unique sources in the paint waste.



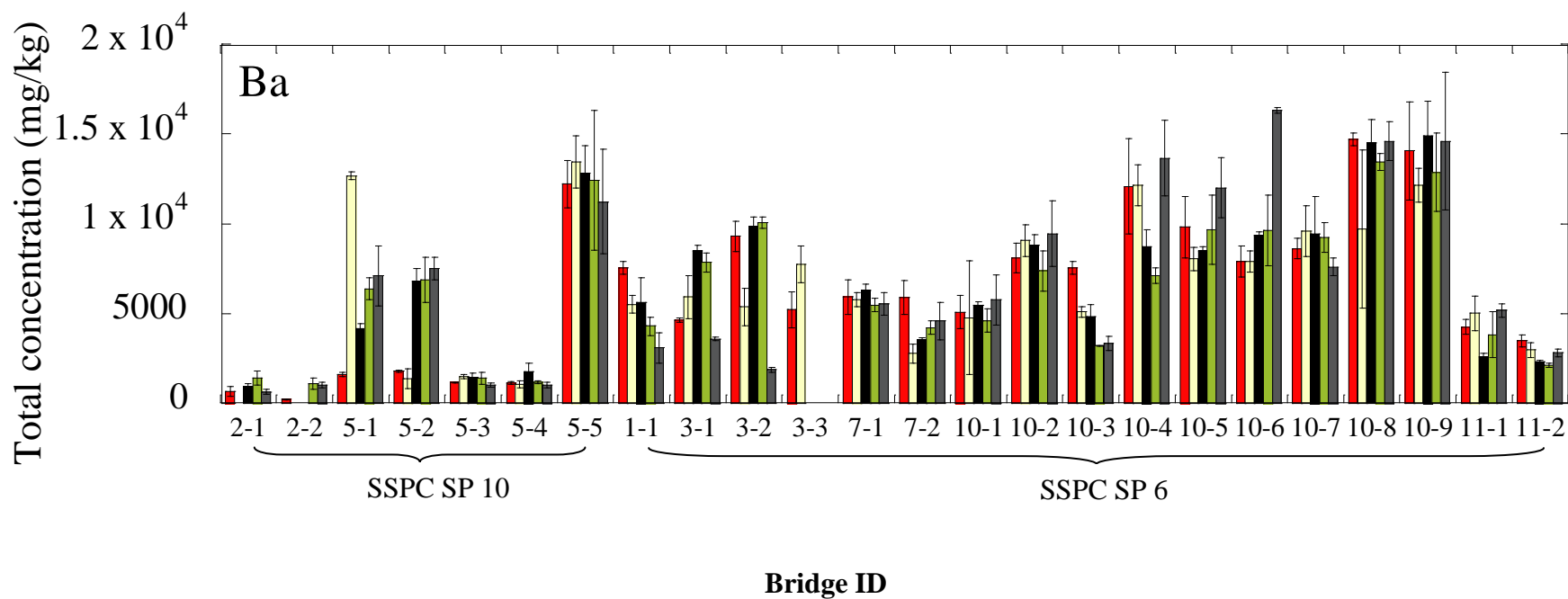
Five samples: ■ a ■ b ■ c ■ d ■ e

Figure 12. Cadmium and silver concentrations in paint are shown as a function of the five locations for bridges in Regions 1, 2, 3, 5, 7, 10, and 11 using NITON XL3t-600 series FP-XRF. Soil Mode was applied for all samples. Bridge ID represents the Region number and bridge sampled in this Region. All bridges sampled were rehabilitated after 1989. Blasting standard SSPC SP 10 was applied for bridges in Regions 2 and 5, while SSPC SP 6 were used for bridges in Regions 1, 3, 7, 10, and 11.



Five samples: ■ a ■ b ■ c ■ d ■ e

Figure 13. Mercury and selenium concentrations in paint are shown as a function of the five locations for bridges in Regions 1, 2, 3, 5, 7, 10, and 11 using NITON XL3t-600 series FP-XRF. Soil Mode was applied for all samples. Bridge ID represents the Region number and bridge sampled in this Region. All bridges sampled were rehabilitated after 1989. Blasting standard SSPC SP 10 was applied for bridges in Regions 2 and 5, while SSPC SP 6 were used for bridges in Regions 1, 3, 7, 10, and 11.



Five samples: ■ a ■ b ■ c ■ d ■ e

Figure 14. Barium concentrations in paint are shown as a function of the five locations for bridges in Regions 1, 2, 3, 5, 7, 10, and 11 using NITON XL3t-600 series FP-XRF. Soil Mode was applied for all samples. Bridge ID represents the Region number and bridge sampled in this Region. All bridges sampled were rehabilitated after 1989. Blasting standard SSPC SP 10 was applied for bridges in Regions 2 and 5, while SSPC SP 6 were used for bridges in Regions 1, 3, 7, 10, and 11.

Table 5. Coefficient of determination (R^2) for RCRA metals, as well as iron and zinc.

| | Pb | Ba | Cr | Cd | Ag | Hg | Se | As | Fe | Zn |
|----|-------------|--------|-------|-------------|-------------|-------------|-------------|-------|-------|-----|
| Pb | 1.0 | | | | | | | | | |
| Ba | 0.17 | 1.0 | | | | | | | | |
| Cr | 0.73 | 0.17 | 1.0 | | | | | | | |
| Cd | 0.68 | 0.02 | 0.33 | 1.0 | | | | | | |
| Ag | 0.67 | 0.03 | 0.31 | 0.95 | 1.0 | | | | | |
| Hg | 0.11 | 0.60 | 0.07 | 0.0 | 0.0 | 1.0 | | | | |
| Se | 0.33 | 0.40 | 0.30 | 0.10 | 0.085 | 0.99 | 1.0 | | | |
| As | 0.78 | 0.10 | 0.56 | 0.72 | 0.72 | 0.28 | 0.17 | 1.0 | | |
| Fe | 0.056 | 0.0004 | 0.091 | 0.063 | 0.033 | 0.82 | 0.29 | 0.024 | 1.0 | |
| Zn | 0.14 | 0.10 | 0.18 | 0.011 | 0.0082 | 0.94 | 0.76 | 0.11 | 0.086 | 1.0 |

4. Summary

The NITON XLp-300 FP-XRF and XL3t-600 series FP-XRF are both effective instruments for measuring RCRA metals as well as iron and zinc in paint wastes. However, the NITON XLp-300 series detects lead in subsurface paint layers as well due to the high energy source (Cd^{109} 40 mCi). 83% of the results from using the NITON XLp-300 XRF demonstrated relative errors less than 30%. Similarly, 79% of the data from the NITON XL3t-600 XRF revealed relative errors less than 20%. Both of XRF instruments revealed greater relative errors in the lower Pb concentration range (less than 1.2 mg/cm^2 or 1% by mass).

In general, results are consistent with other studies where

1. Lead often exceeds 5,000 mg/kg or 1 mg/cm^2 (Mielke and Gonzales, 2008; Mielke et al., 2001; Huang et al., 2010);
2. Zinc is observed at elevated concentrations as great as 425,510 mg/kg (42% by mass) (U.S. EPA, 1990; Huang et al., 2010);
3. Arsenic, chromium, cadmium are present at lower concentrations in paint waste as well because of their use as extenders, pigments, and preservatives (Mielke et al., 2001; Huang et al., 2010).

Additional observations included

1. The elevated iron concentrations ranging from 49,367 to 799,210 mg/kg (5 to 80% by mass) are due to the steel grit applied as a blasting agent during the paint removal procedure. Barium and silver were observed as great as 16,319 mg/kg and 132 mg/kg, respectively, because of its use as extenders and preservatives.

2. Selenium and mercury were not routinely observed at detectable concentrations as they were generally not used; mercury was just found in three bridges in Regions 2 and 5;
3. The difference in metal concentrations between Regions 2 and 5 can be attributed to the surface preparation standard applied in New York State;
4. Pb was correlated with As ($R^2 = 0.78$), Cd ($R^2 = 0.73$), Cr ($R^2 = 0.88$) and Ag ($R^2 = 0.67$), while Zn, Se, and Hg were correlated with $R^2 = 0.99$ between Hg and Se, $R^2 = 0.94$ for Hg and Zn, and $R^2 = 0.76$ for Se and Zn. The results demonstrate that the usage of these metals in paint is consistent with each other. When the paint was removed, these metals remained;
5. Correlations were not observed between Pb, Fe, and Zn concentrations ($R^2 < 0.11$) suggesting unique sources in the paint waste.

5. References

American Society for Testing and materials (ASTM), (1990) Standard practice for decontamination of field equipment used at nonradioactive waste sites, Designation D5088-90, West Conshohocken, PA.

Alphen, M. (1998) Paint film components, National Environmental Health Forum Monographs, General Series No. 2.

Appleman, B. R. (1992) Bridge paint: removal, containment, and disposal, *Transportation Research Board*, Washington, DC., Report 176

Bernecki, T. F., Nichols, G. M., Prine, D., Shubinsky, G. and Zdunek, (1995)"Chapter 4 - Evaluation of Procedures for Analysis and Disposal of Lead-Based Paint-Removal Debris," Issues Impacting Bridge Painting: An Overview, Infrastructure Technology Institute, FHWA/RD/94/098, August 1995, Northwestern University.

Boxall, J., Von Fraunhofer (1977) Concise paint technology. New York: Chemical Publishing.

Boxall, J., Von Fraunhofer (1980) Paint Formulation: principles and practice. George Goodwin Limited, London.

Binstock, D. A., Gutknecht, W. F., McWilliams, A. C. (2009) Lead in soil - an examination of paired XRF analysis performed in the field and laboratory ICP-AES results, *International Journal of Soil, Sediment and Water*, 2(2): 1-6.

Clark C. S., Menrath W., Chen M., Roda S., Succop P. (1999) Use of a field portable X-ray fluorescence analyzer to determine the concentration of lead and other metals in soil samples, *Annals of Agricultural and Environmental Medicine*, 6: 27–32.

Eaton, A. D., Clesceri, L. S., Rice, E. W., Greenberg, A. E. (2005) Standard methods for the examination of water and wastewater, 21st edition, 3: 79-81.

Environmental Canada and Alberta Environmental Centre (Testing Methods, Canada), (1986) Test methods for solidified waste characterization, Edmonton.

Feliciano, Willie; Kochersberger, Carl; Email on August 24th 2011.

Gooch, J. W., Lead-Based Paint Handbook, Plenum Press, New York, 1993

Huang, S. L., Yin, C. Y., Yap S. Y. (2010) Particle size and metals concentrations of dust from a paint manufacturing plant, Journal of Hazardous Materials, 174: 839–842.

Lambourne, R., Strivens, T., Paint and Surface Coatings: Theory and Practices, Woodhead Publishing, Cambridge, 1999.

Kochersberger, Carl; Email on June 7th 2011.

Kochersberger, Carl; Bass, Jonathan; Conference call for the preliminary results. August 9th 2011.

Kendall, S. D. (2003) Toxicity Characteristic Leaching Procedure and Iron Treatment of Brass Foundry Waste. Environmental Science and Technology, 37: 367-371.

Kilbride, C., Poole, J. Hutchings, T. R. (2006) A comparison of Cu, Pb, As, Cd, Zn, Fe, Ni and Mn determined by acid extraction/ICP-OES and ex situ field portable X-ray fluorescence analyses, Environmental Pollution, 143: 16-23.

Margrey, Kenneth W., Riese., John B.; Email on February 24th 2012.

Mielke, H. W., Powell, E., Shah, A., Gonzales, C., Mielke, P.W. (2001) Multiple metal contamination from house paints: consequences of power sanding and paint scraping in New Orleans, Environmental Health Perspectives, 109, (9): 973–978.

Mielke, W. H., Gonzales, C. (2008) Mercury (Hg) and lead (Pb) in interior and exterior New Orleans house paint films, Chemosphere, 72: 882–885.

New Jersey Department of Environmental Protection (NJDEP) (2005) Field Sampling Procedures Manual.

New York State Department of Transportation, Standard Specification, May 1, 2008.

<https://www.nysdot.gov/main/business-center/engineering/specifications/english-spec-repository/section550.pdf>

New York State Department of Transportation, (1988) Specification for bridges – removal of lead based paints – new department paint system for structural steel, Engineering instruction, EI 88-36.

National Paint and Coatings Association (1992) Preventing childhood lead exposure: putting the issues in perspective.

Oil and Color Chemists Association, Australia, (1983) Surface Coating: Raw Materials and Their Usage, second ed., Chapman and Hall, New York, 1: 299–300.

Pyle, S., Nocerino, J. (1996) Comparison of AAS, ICP-AES, PSA, and XRF in Determining Lead and Cadmium in Soil, Environmental Science and Technology. 30: 204-213.

Quevauviller, P. (1998) Operationally defined extraction procedures for soil and sediment analysis I. Standardization, Trends in Analytical Chemistry

Sandhu, N., Axe, L., Jahan, R., K. V. (2011) Heavy Metal Contamination in Highway Marking Glass Beads, NJDOT Research Study.

Thermo Scientific, NITON XL3t 600 series Analyzer User's Guide, Version 6.5

Thermo Scientific, NITON XLp 300 series Analyzer User's Guide, Version 5.2.1 P/N 500-92

U. S. Environmental Protection Agency (U.S. EPA) (1996) hazardous waste characteristics scoping study, Office of Solid Waste, EPA: Washington, DC

U. S. EPA, (2002) RCRA Waste Sampling Draft Technical Guidance-Planning, Implementation, and Assessment, EPA530-D-02-002.

U. S. Environmental Protection Agency (U.S. EPA) (1998), Method 6200, Field portable x-ray fluorescence spectrometry for the determination of elemental concentrations in soil and sediment (EPA/600/R-97/150, Revision 0), Retrieved November 1, 2007.

U. S. EPA, (1990) 55 FR 4440, Environmental Protection Agency; Amendment of Hazardous Waste Testing and Monitoring Regulation.

U. S. EPA, (2006) 40 CFR 262.11, Hazardous waste determination.

U.S. Environmental Protection Agency (U.S. EPA) (2003) Test Methods for Evaluating Solid Waste, SW-846, third ed., Office of Solid Waste and Emergency Response, EPA, Washington, DC.

U. S. Environmental Protection Agency (U.S. EPA) (2007), Method 6020A Inductively coupled plasma-mass spectrometry, SW-846 Chapter 3.

U. S. Environmental Protection Agency (U.S. EPA) (2004), Method 3052 Microwave assisted acid digestion of siliceous and organically based matrices, SW-846 Chapter 3.

U.S. Occupational Safety and Health Administration (1993) Lead exposure in construction: interim final rule (29 CFR 1926.62). Federal Register 58: 26590-26649. Washington, DC.

U.S. Consumer Products Safety Commission (U. S. CPSC), (1977) Notice reducing allowable levels of lead. Final Rule, Federal Register 42 (1): 44199.

Zamurs, J., Bass, J., Williams, B., Fritsch, R., Sackett, D., Heman, R. (1998) Real-time measurement of lead in ambient air during bridge paint removal. Transportation Research Record, 1641:29-38.

Appendix A

Bridges sampled and details for samples

Table A1. Bridges sampling and details for samples

| Bridge number | Region | Bridge name and the location | Bin | Date rehabilitated | Date sampled | Wash water sample | Paint waste sample |
|---------------|--------|---|---------|------------------------|-----------------------|-------------------|--------------------|
| 1 | 11 | Bruckner Expressway, Bronx | 106666C | | 10/29/2010 | 0 | 10 |
| 2 | 11 | Brooklyn-Queens Expressway(BQE) over Long Island Expressway (LIE), New York | 1065569 | | 11/19/2010 | 0 | 10 |
| 3 | 3 | Route 5 over Roadway A, Syracuse, | 1093390 | 10/20/2010-10/28/2010 | 11/10/2010 | 2 ^a | 10 |
| 4 | 3 | Roadway C over Roadway A, Syracuse | 1093400 | 11/03/2010-11/10/2010 | 11/10/2010-11/12/2010 | 2 ^b | 10 |
| 5 | 3 | Ithaca | 3209900 | | 05/20/2011 | 0 | 4 ^c |
| 6 | 10 | Rt 107 over Sea Cliff Ave, Sea Cliff | 1036889 | 06/13/2011-06/22/2011 | 06/14/2011-6/22/2011 | 4 | 10 |
| 7 | 5 | Virginia-Carolina ramp to I-190 Southbound, Buffalo | 1063090 | 06/02/2011-7/10/2011 | 06/15/2011-7/13/2011 | 4 | 10 |
| 8 | 5 | I-190 Southbound ramp to Virginia-Carolina, Buffalo | 1063100 | 06/02/2011-7/10/2011 | 06/15/2011-7/13/2011 | 4 | 10 |
| 9 | 10 | Rt 495 (Wesbound) Service Rd over Nicolls Rd, Queens | 1064560 | 06/27/2011-07/ 22/2011 | 6/28/2011-07/20/2011 | 4 | 10 |
| 10 | 10 | Rt 495 (Easbound) Service Rd over Nicolls Rd, Queens | 1064570 | 06/27/2011-07/ 22/2011 | 6/28/2011-07/20/2011 | 4 | 10 |

| Bridge number | Region | Bridge name and the location | Bin | Date rehabilitated | Date sampled | Wash water sample | Paint waste sample |
|---------------|--------|--|---------|-----------------------|-----------------------|-------------------|--------------------|
| 11 | 1 | Route 196 over Town Rd/Champlain Canal, Town of Kingsbury, Washington County | 4039820 | | 07/17/2011 | 0 | 10 |
| 12 | 2 | Mainline Thruway over Mohawk River (W. B.), Herkimer County | 4423081 | | 07/21/2011-08/09/2011 | 0 | 10 |
| 13 | 2 | Mainline Thruway over Mohawk River (E. B.), Herkimer County | 4423082 | | 07/29/2011-08/06/2011 | 0 | 10 |
| 14 | 5 | Two-mile creek Road over I-290, Tonawanda | 1044970 | | 08/24/011-09/07/2011 | 4 | 10 |
| 15 | 5 | East park drive over I-290, Tonawanda | 1044980 | 08/23/2011-09/12/2011 | 8/23/2011-09/13/2011 | 4 | 10 |
| 16 | 5 | Peace bridge plaza ramp to I-190 Southbound, Buffalo | 1063110 | 07/17/2011-07/26/2011 | 08/07/2011-08/14/2011 | 4 | 10 |
| 17 | 10 | Hawkins Ave over Rt 495, Ronkonkoma | 1049509 | 07/25/2011-8/02/2011 | 07/30/2011-8/04/2011 | 0 | 10 |
| 18 | 10 | Ronkonkoma Ave over Rt 495, Ronkonkoma | 1049489 | 07/18/2011-07/24/2011 | 07/22/2011-07/26/2011 | 0 | 10 |
| 19 | 10 | Washington Ave over Rt 495, Ronkonkoma | 1049400 | 08/05/2011-08/15/2011 | 08/08/2011-08/16/2011 | 4 | 10 |
| 20 | 10 | Rt 495 (Eastbound) over Commack Rd, New York | 1049361 | 10/05/2011-10/12/2011 | 10/13/2011 | 4 | 10 |

| Bridge number | Region | Bridge name and the location | Bin | Date rehabilitated | Date sampled | Wash water sample | Paint waste sample |
|---------------|--------|--|---------|--------------------|--------------|-------------------|--------------------|
| 21 | 10 | Rt 495 (Westbound) over Commack Rd, New York | 1049362 | | 10/02/2011 | 4 | 10 |
| 22 | 10 | Bagatelle Rd over Rt 495, Huntington | 1049320 | | 10/02/2011 | 4 | 10 |
| 23 | 7 | NYS Route 3 over Black River, Town of Rutland | 1000540 | 10/05/2011 | 10/20/2011 | 0 | 10 |
| 24 | 7 | NYS Route 37 over Big Sucker Brook, Village of Waddington, St. | 1023860 | 10/05/2011 | 10/20/2011 | 0 | 10 |

a, b Only one location is available for wash water sampling in the bridge working site.

c Only two locations are available for paint waste sampling in the bridge working site.

Table A2. Bridges rehabilitation detail and contact information

| Bridge number | Region | Bridge name and the location | Bin | Year built | Year(s) repainted | Contact |
|---------------|--------|---|---------|------------|-------------------|----------------------------------|
| 1 | 11 | Bruckner Expressway, Bronx | 106666C | 1959 | 1996 | Bukhari, Majid 917-807-4251 |
| 2 | 11 | Brooklyn-Queens Expressway(BQE) over Long Island Expressway (LIE), New York | 1065569 | 1969 | 1990 | Bukhari, Majid 917-807-4251 |
| 3 | 3 | Route 5 over Roadway A, Syracuse, | 1093390 | 1975 | 1991, 1999 | Nick Huffman 315-877-5585 |
| 4 | 3 | Roadway C over Roadway A, Syracuse | 1093400 | 1975 | 1991, 1999 | Nick Huffman 315-877-5585 |
| 5 | 3 | Ithaca | 3209900 | 1940 | 1991 | Dudley, Paul R. 716-289-4467 |
| 6 | 10 | Rt 107 over Sea Cliff Ave, Sea Cliff | 1036889 | 1953 | 1995 | Connor, John 917-406-9451 |
| 7 | 5 | Virginia-Carolina ramp to I-190 Southbound, Buffalo | 1063090 | 1972 | 2000 | Jakubowski, Gary 716-908-0273 |
| 8 | 5 | I-190 Southbound ramp to Virginia-Carolina, Buffalo | 1063100 | 1972 | 2000 | Jakubowski, Gary 716-908-0273 |

| Bridge number | Region | Bridge name and the location | Bin | Year built | Year(s) repainted | Contact |
|---------------|--------|--|---------|------------|-------------------|---|
| 9 | 10 | Rt 495 (Wesbound) Service Rd over Nicolls Rd, Queens | 1064560 | 1970 | 1979, 1986, 1999 | Connor, John 917-406-9451 |
| 10 | 10 | Rt 495 (Easbound) Service Rd over Nicolls Rd, Queens | 1064570 | 1970 | 1979, 1986, 1999 | Connor, John 917-406-9451 |
| 11 | 1 | Route 196 over Town Rd/Champlain Canal, Town of Kingsbury, Washington County | 4039820 | 1938 | 1990,1991 | Carl Kochersberger 518-485-5316 |
| 12 | 2 | Mainline Thruway over Mohawk River (W. B.), Herkimer County | 4423081 | 1955 | 1997 | Riese, John 315-457-5200 315-263-4567 |
| 13 | 2 | Mainline Thruway over Mohawk River (E. B.), Herkimer County | 4423082 | 1955 | 1997 | Riese, John 315-457-5200 315-263-4567 |
| 14 | 5 | Two-mile creek Road over I-290, Tonawanda | 1044970 | 1963 | 1998 | Jakubowski, Gary 716-908-0273 |
| 15 | 5 | East park drive over I-290, Tonawanda | 1044980 | 1963 | 1998 | Jakubowski, Gary 716-908-0273 |
| 16 | 5 | Peace bridge plaza ramp to I-190 Southbound, Buffalo | 1063110 | 1972 | 1992 | Jakubowski, Gary 716-908-0273 |

| Bridge number | Region | Bridge name and the location | Bin | Year built | Year(s) repainted | Contact |
|---------------|--------|---|---------|------------|---------------------------|-----------------------------------|
| 17 | 10 | Hawkins Ave over Rt 495, Ronkonkoma | 1049509 | 1967 | 1985, 1999 | Connor, John 917-406-9451 |
| 18 | 10 | Ronkonkoma Ave over Rt 495, Ronkonkoma | 1049489 | 1967 | 1999 | Connor, John 917-406-9451 |
| 19 | 10 | Washington Ave over Rt 495, Ronkonkoma | 1049400 | 1964 | 1986, 1989 | Connor, John 917-406-9451 |
| 20 | 10 | Rt 495 (Eastbound) over Commack Rd, New York | 1049361 | 1963 | 1978, 1989, 1993, 1994 | Connor, John 917-406-9451 |
| 21 | 10 | Rt 495 (Westbound) over Commack Rd, New York | 1049362 | 1963 | 1978, 1992, 1994, 1995 | Connor, John 917-406-9451 |
| 22 | 10 | Bagatelle Rd over Rt 495, Huntington | 1049320 | 1963 | 1977, 1997 | Connor, John 917-406-9451 |
| 23 | 7 | NYS Route 3 over Black River, Town of Rutland | 1000540 | 1948 | 1997 | Richard J. Gaebel 315-779-3090 |
| 24 | 7 | NYS Route 37 over Big Sucker Brook, Village of Waddington, St. | 1023860 | 1957 | 1998 | Richard J. Gaebel 315-779-3090 |

Appendix B

Standard operating procedure (SOP) for NITON XLp-300 series analyzer

Standard operating procedure (SOP) for NITON XLp-300 series analyzer

1. Log on and calibration procedures

1.1 Log on procedures

- (1) To turn on the instrument, depress on/off/escape button on the control panel for approximately 3 seconds (Figure B1), until you hear a beep.
- (2) When the Logon screen (Figure B1) present, tap anywhere on this screen to continue.
- (3) The Logon Screen will be replaced by a Warning Screen (Figure B1), advising that this analyzer produces radiation when the lights are flashing. This warning has to be acknowledged by selecting the “Yes” button before logging on (Selecting the “No” button will result in returning to the Logon Screen).
- (4) The Virtual Numeric Keypad becomes available to log onto the analyzer (Figure B1). The temporary password assigned by default is 1-2-3-4, followed by the “E” key. After the log on procedures are completed, the word "USER" will appear on the bottom of the screen, then the Main Menu (Figure B2) will appear.
- (5) After being powered on, the NITON 300 Series Analyzer will perform an internal re-calibration before an analysis is initiated. It is recommended to let the instrument warm up for ten minutes after start up, before testing is begun.

1.2 Instrument calibration

- (1) To calibrate the instrument, select the Calibrate icon from the Utilities Menu (Figure B2).
The analyzer is programmed to calibrate for a specific, predetermined period in order to ensure proper operation of the Niton XLp analyzer in the field.

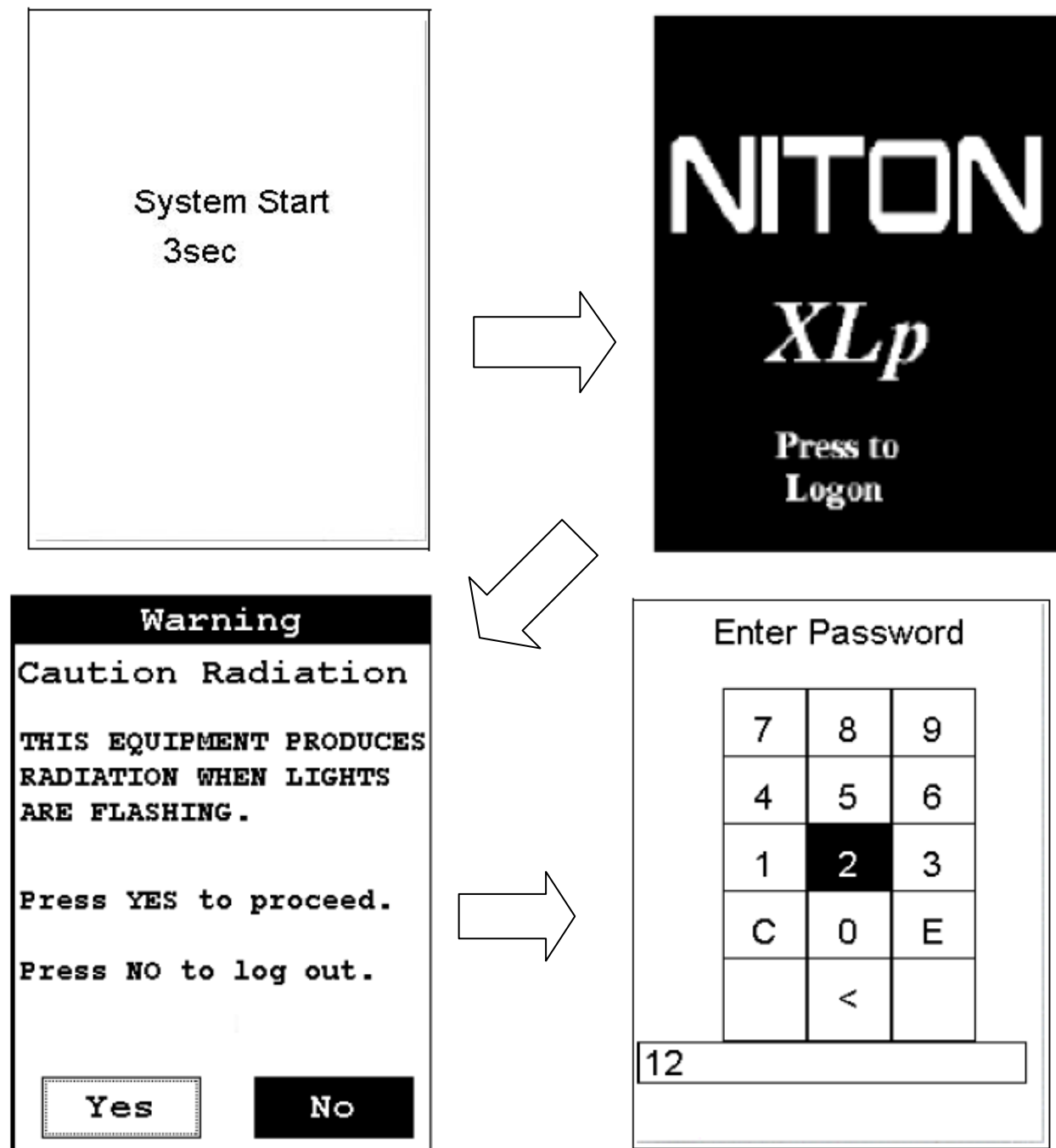


Figure B1. Log on procedure for NITON XLp-300 series analyzer

- (2) After the calibration has finished, the calibration results will be displayed. Press the on/off/escape button or the Return icon to return to the Main Menu. In order to insure good test results, it is essential to calibrate Niton XLp300 Series Lead-based-Paint Analyzer daily.
- (3) Note the “Res” figure displayed following the detector calibration. This number, usually < 500eV, is an evaluation of the detector resolution and should be consistent with past calibration results. This data will download as a stored reading if the user chooses to download readings, so it can be saved for tracking the instrument’s performance.
- (4) During analysis and detector calibrations, it is important to ensure that the analyzer is not exposed to strong electromagnetic fields, including those produced by computer monitors, hard drives, cellular telephones, walkie-talkies, etc. Keep a minimum two feet (0.7 meters) distance between the analyzer and electronic devices. Avoid any vibration, loud noise, strong electronic fields, or other possible interference when the analyzer is calibrating its detector.

2. Icon functions in the main menu

The Main menu is divided into 6 sub-menus (Figure B2):

- By selecting the **Mode** icon from the Main Menu screen, the analyzer will remember the last mode used on the analyzer, and will use that mode by default unless another mode is selected.
- By selecting the **Utilities** icon from the Main Menu screen, the Utilities Menu enables you to view analyzer specifications; set the date and time; and auto-calibrate the analyzer electronics and the touch screen display.

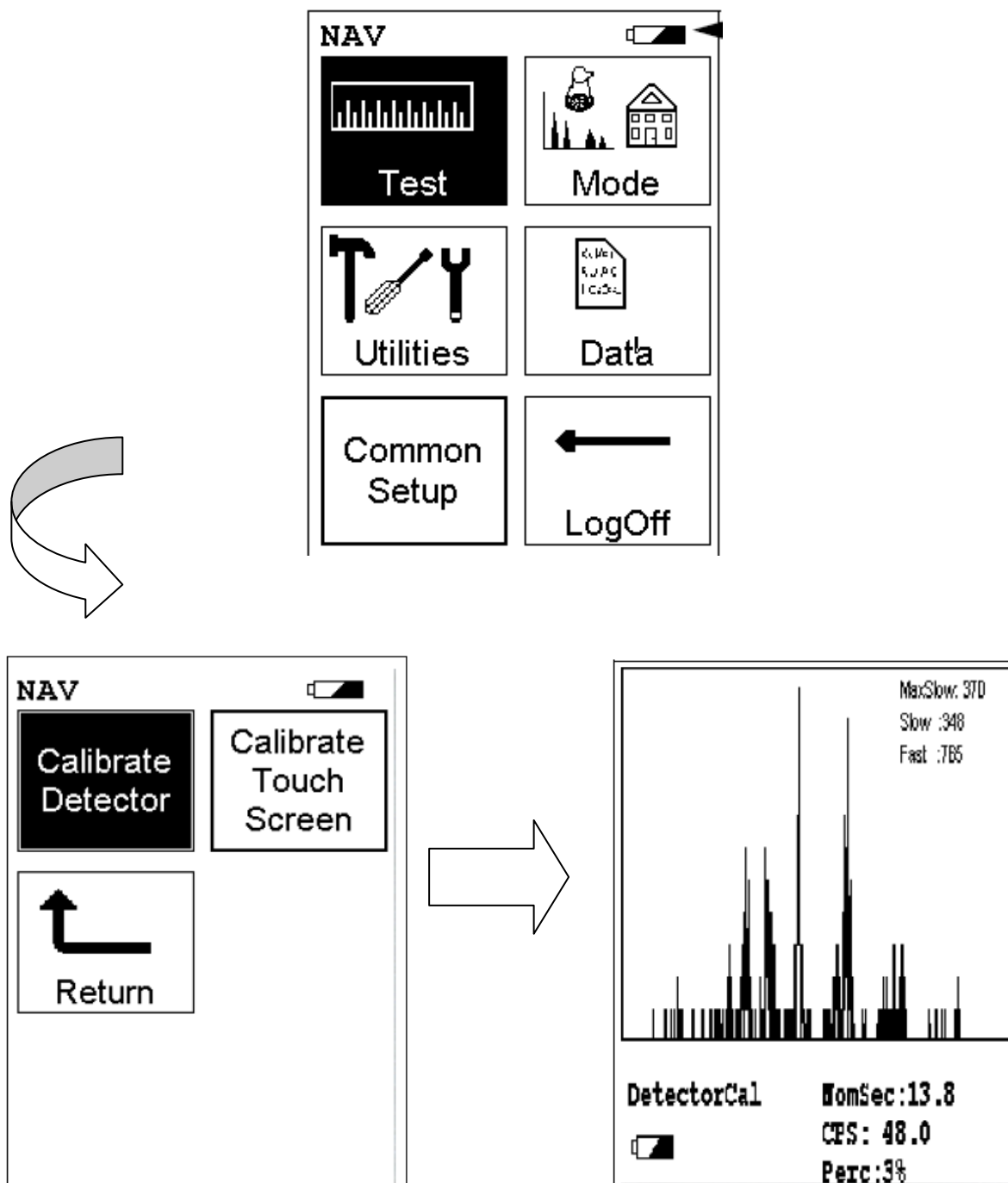


Figure B2. Main menu for NITON XLp-300 series Lead-in-Paint analyzer and the analyzer calibration.

- By selecting the **Data** icon from the Main Menu screen, the Data Menu allows you to view readings, and allows you to view the alloy library and stored signatures.
- By selecting the **Common Setup** icon from the Main Menu screen, the Common Setup Menu allows you to turn on or off the liquid crystal display backlight, turn on or off the integrated bar code scan engine, to enable and configure source utilization, and to enable or disable the printer.
- By selecting the **Logoff** icon, the Logon Screen logs you out and allows you to login again, preventing casual unauthorized access to your analyzer.

3. Two modes for lead paint detection

There are two kinds of modes can be used for lead testing: Standard Mode and K+L Mode (Figure B3). The Standard Mode is a qualitative analysis designed for 95% confidence level as to whether the sample is above or below the Action Level. This mode tends to give very fast readings, because it terminates the test as soon as 95% confidence has been achieved. The Set Action Level Screen needs to be set for Standard Mode test. To change the preset Action Level to match the Action Level set by specific locality, select the “C” key from the Virtual Numeric Keypad to clear the current Action Level value, select the new Action Level value using the numeric keys, then select “E” to enter the new Action Level value (Figure B3). The Action Level will be changed to the new value. Then new Set Action Level Screen will be displayed. K+L Mode is a quantitative analysis which allows you to determine the statistical confidence of the

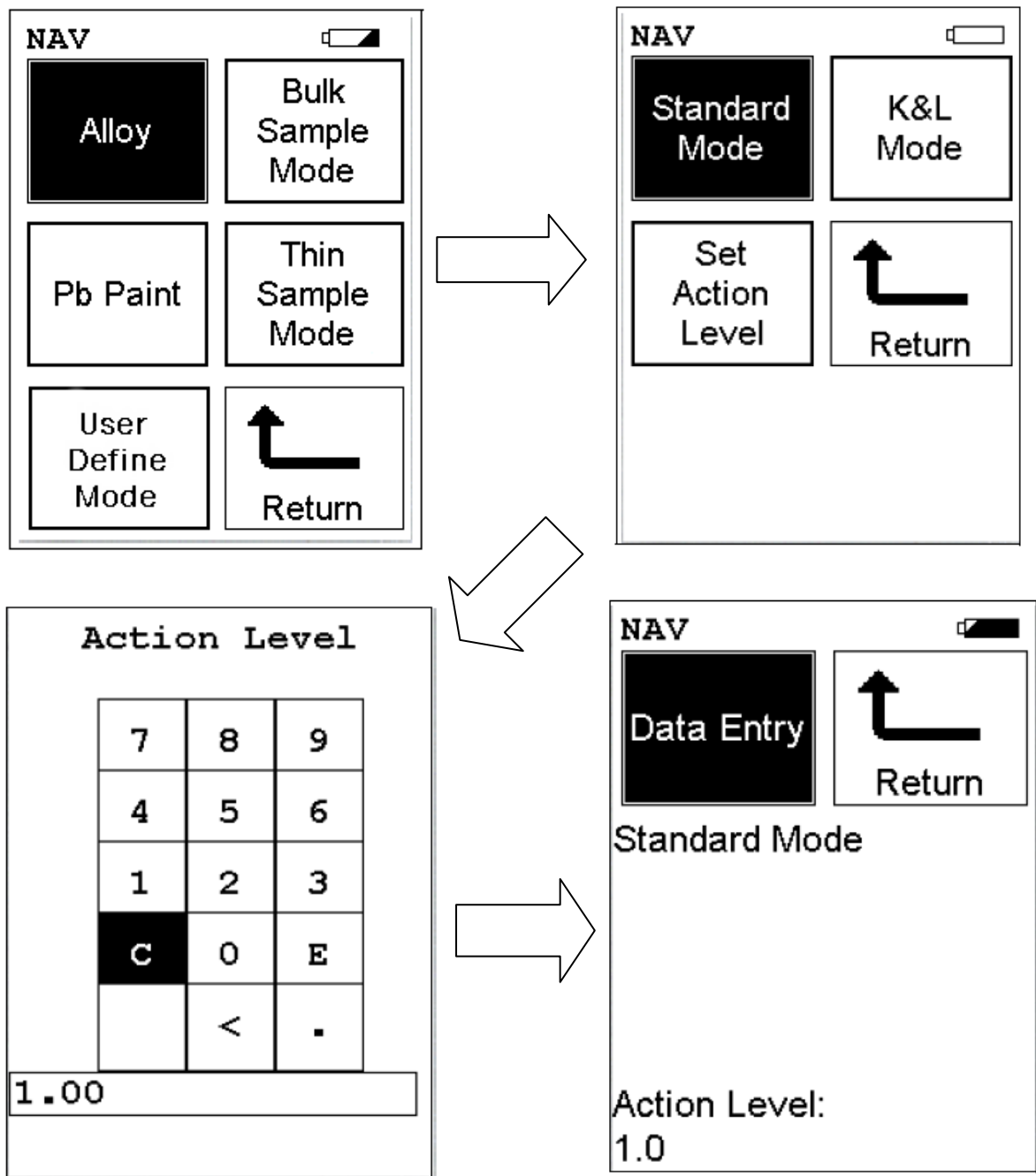
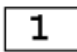




Figure B3. The Pb Paint Mode Menu and Set Action Level

reading to a 95% Confidence Level while allowing you the flexibility of continuing the test for as long as you wish up to the (user-definable) maximum test time.

4. Data entry screens

Once Standard Mode or K+L Mode is selected, a sample test can be immediately initiated using the proper preconditions for operation. The data information entered will be associated with the next sample tested. By using The Data Entry Screens (Figure B4), the values for various parameters can be tracked by the system along with the actual analysis results. The data information can be input in several different fields, or categories, concerning the sample, in several different ways:

-  • Selecting the Menu Code Number will initiate a bar code scan to input pre-printed bar code parameter values
-  • Selecting the Drop-Down Menu Button will access the particular Drop-Down Menu for that parameter, allowing you to select the parameter value from a pre-determined list.
-  • Selecting the Keyboard button allows you to input a parameter value as required using the Virtual Keyboard.

These fields are saved along with the subsequent reading, and allow you to associate important information about the sample directly with the reading, so that you have a full description of the sample tied into the reading itself. These parameters all describe the particular test target to be analyzed. The location of the target in the site, the type of target, the surface and

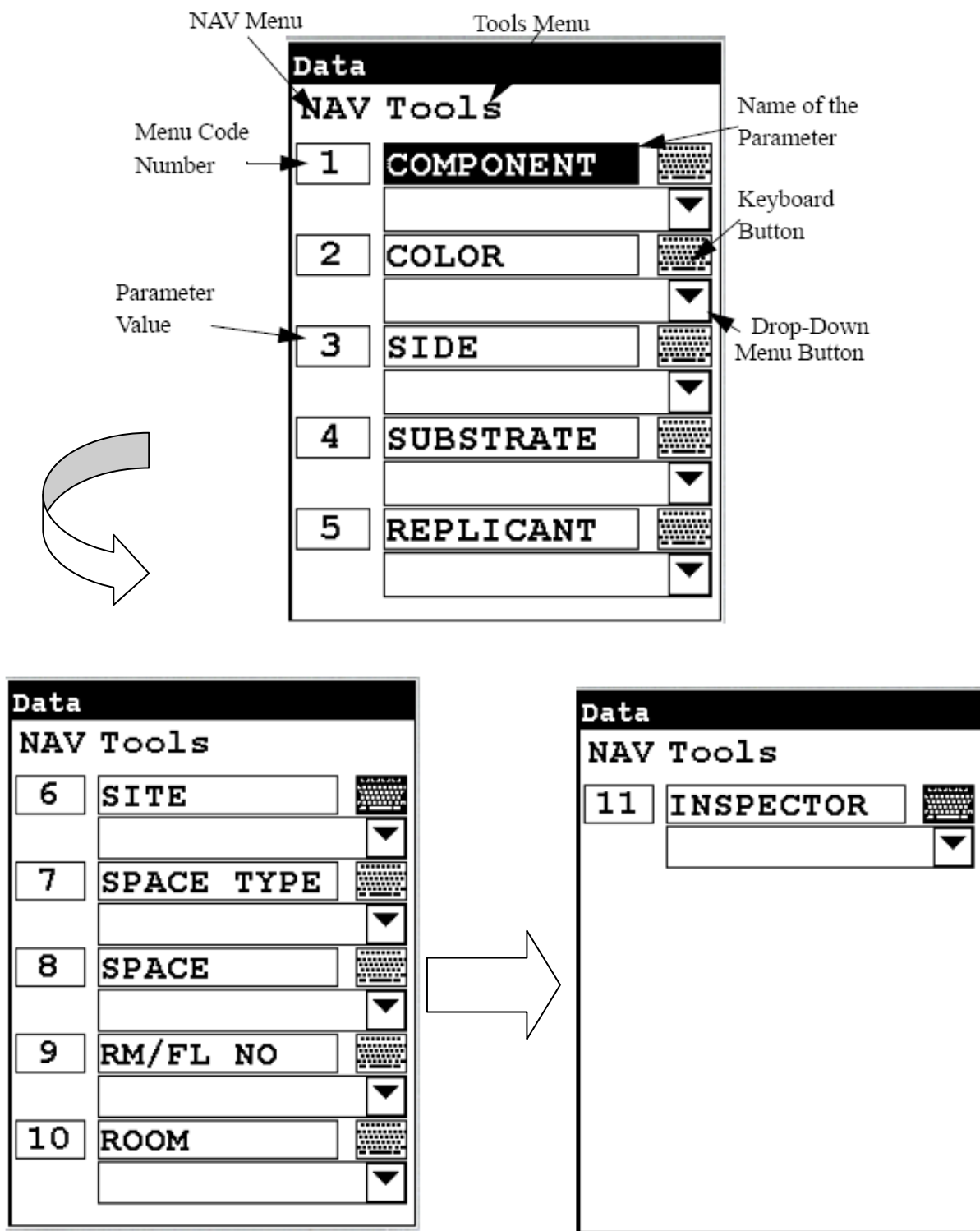


Figure B4. Data input information

substrate, the condition of the surface, and the inspector performing the test are some of the parameters tracked by the analyzer.

5. Measurements

Five different methods of operation are used for taking a sample measurement. The analyzer will be configured to use one of those methods, depending on the regulatory requirements of the specific locality.

- **Trigger-Only method.** With the Trigger-Only method, you only need to place the measurement window close to the sample to be analyzed and pull the trigger for sample analysis to be initiated.
- **Trigger-and-Proximity-Sensor method.** With the Trigger-and-Proximity-Sensor method, you must place the measurement window against the sample to be analyzed to engage the proximity sensor on the front of the instrument, then pull the trigger for sample analysis to be initiated.
- **Momentary-Trigger-Touch-and-Proximity-Sensor method.** With the Momentary-Trigger Touch-and-Proximity-Sensor method, you must place the measurement window against the surface to be analyzed to engage the proximity sensor on the front of the instrument, then pull the trigger. The trigger may be released and the reading will continue until you release the proximity button, or other criteria (such as Max Time) are reached.
- **Trigger-and-Interlock method.** With the Trigger-and-Interlock method, you need to place the measurement window close to the sample to be analyzed, press and keep pressing the interlock button at the rear of the instrument with your free hand, then pull the trigger for sample analysis to be initiated.

- Trigger-Interlock-and-Proximity-Sensor method. With the Trigger-Interlock-and-Proximity-Sensor method, you must place the measurement window against the sample to be analyzed to engage the proximity sensor on the front of the instrument, press and keep pressing the interlock button at the rear of the instrument with your free hand, then pull the trigger for sample analysis to be initiated.

With any of these methods, analysis will stop if any one of the preconditions are violated. For example, with the Trigger-Interlock-and-Proximity-Sensor method, if the trigger or the Proximity Sensor or the Interlock is released, the reading will stop immediately, and the shutters will close.

6. Results

NITON Analyzer will display the Results Screen throughout the duration of each reading. The Results Screen is updated regularly throughout the reading. When the reading is complete, a final screen update will appear, and your NITON analyzer will display the final results of the measurement which has just been completed.

6.1 Standard mode testing results

Before the analyzer has reached a determination, the result will be shown as “Inconclusive”. The analyzer will beep twice when a result is reached then terminate the reading. The display will change from “Inconclusive” to show the result, either “Positive” for lead detected above the action level, or “Negative” for no lead or lead below the action level. The lead concentration is displayed in mg/cm².

6.2 K+L Mode testing results

The K+L Mode results screen will show the same basic display throughout the reading. The analyzer will beep twice to indicate it has reached a conclusion, and the result field will change

from “Inconclusive” to “Positive” or “Negative”, but the reading will continue for as long as you the trigger continue to be hold down and the Proximity Sensor is depressed. The K+L results screen shows the reading results and error for both K and L-shell readings (Figure B5). The “Lead Detected in mg/cm² total” field (Figure B5) is the result of the judgment of the analyzer as to which reading, K or L-shell, best represents the true condition.

In the Standard mode / K+L Mode, the Depth Index (Figure B5) is a numerical value indicating the amount of non-lead paint covering the lead (if any) detected by the analyzer:

- A Depth Index of less than 1.5 indicates a reading very near the surface.
- A Depth Index between 1.6 and 4.0 indicates a moderate depth.
- A Depth Index of greater than 4.0 indicates a deeply buried reading.

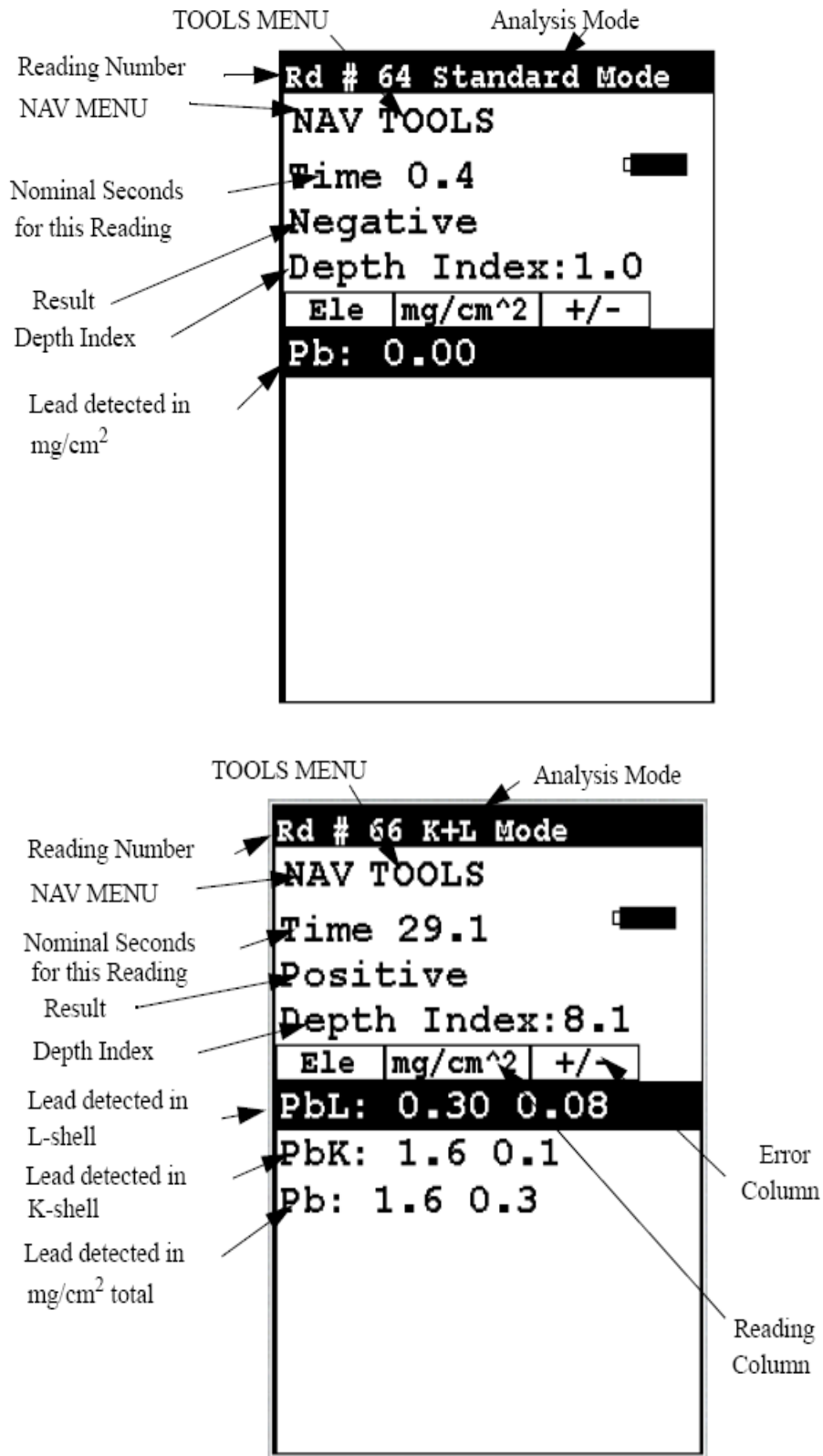


Figure B5. Testing results under the Standard Mode and K+L Mode

Appendix C

Standard operating procedure (SOP) for NITON XL3t-600 series analyzer

Standard operating procedure (SOP) for NITON XL3t-600 series analyzer

1. Log on and calibration procedures

Log on and calibration procedures for NITON XL3t-600 series analyzer (Figure C1) are the same as NITON XLp-300 series analyzer (part 1).

2. Icon functions in the main menu

Icon functions in the main menu for NITON XL3t-600 series analyzer (Figure C2) are the same as NITON XLp-300 series analyzer (part 2).

3. Standard Soil Mode or Mining Mode for the RCRA metals and zinc detection in the paint

To detect metal concentrations in the paint, simply select the Standard Soil Mode icon or Mining Mode Cu/Zn icon from the Bulk Analysis Menu (Figure C3).

4. Data entry screens

The function of the Data Entry Screens for NITON XL3t-600 series analyzer (Figure C4) is the same as NITON XLp-300 series analyzer (part 4).

5. Measurements

There are six different methods of operation for taking a sample measurement, and the analyzer will be configured to use one of those methods for samples, depending on the regulatory requirements of the specific locality.

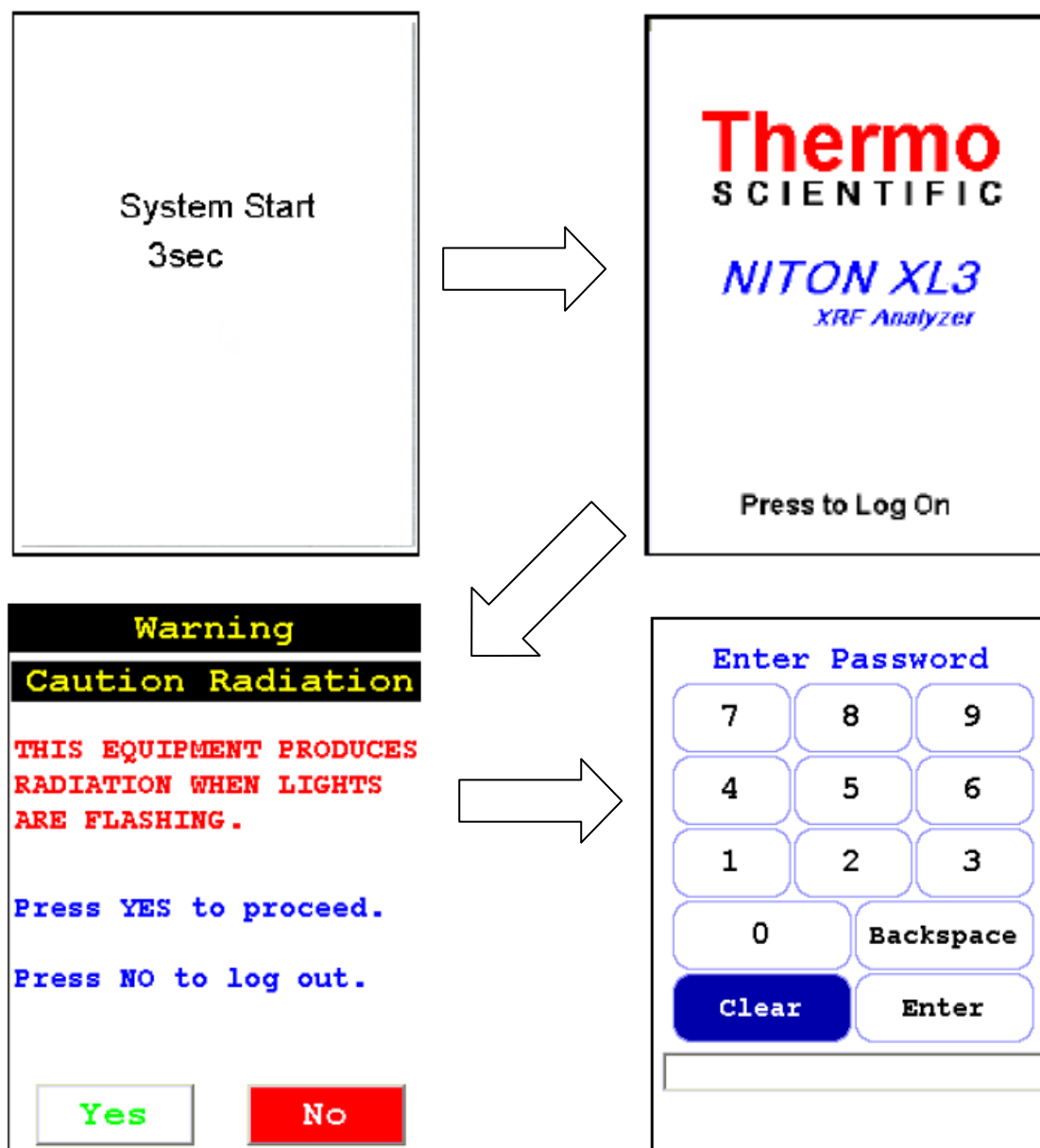


Figure C1. Log on procedure for NITON XL3t-600 series analyzer



Figure C2. Main menu for NITON XL3t-600 series analyze

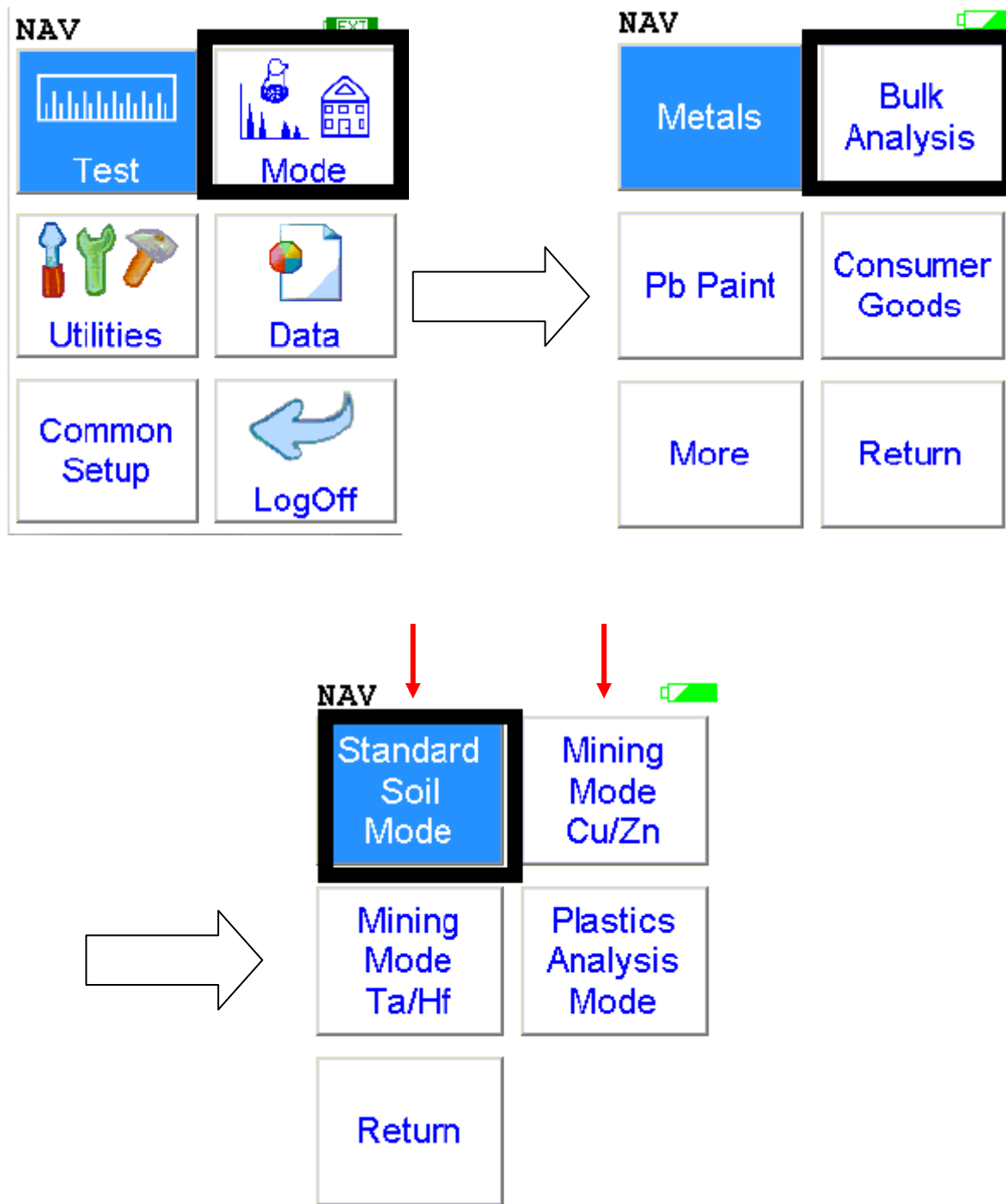






Figure C3. Standard soil analysis mode



Data


NAV Tools



SAMPLE 


 



LOCATION 


 

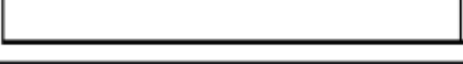

INSPECTOR 

COR 1 

COR 2 

Virtual Keyboard
Button


Parameter Field
Name



Drop-down List
Button


Parameter Field

Data

NAV Tools

MISC 

NOTE 



 

Figure C4. Data input information for NITON XL3t-600 series analyzer

- **Trigger-Only method.** With the Trigger-Only method, you only need to place the measurement window close to the sample to be analyzed and pull the trigger for sample analysis to be initiated.
- **Trigger-and-Proximity-Sensor method.** With the Trigger-and-Proximity-Sensor method, you must place the measurement window against the sample to be analyzed to engage the proximity sensor on the front of the instrument, then pull the trigger for sample analysis to be initiated.
- **Momentary-Trigger-Touch-and-Proximity-Sensor method.** With the Momentary-Trigger-Touch-and-Proximity-Sensor method, you must place the measurement window against the surface to be analyzed to engage the proximity sensor on the front of the instrument, then pull the trigger. The trigger may be released and the reading will continue until you release the proximity button, or other criteria (such as Max Time) are reached.
- **Trigger-and-Interlock method.** With the Trigger-and-Interlock method, you need to place the measurement window close to the sample to be analyzed, press and keep pressing the interlock button at the rear of the instrument with your free hand, then pull the trigger for sample analysis to be initiated.
- **Trigger-Interlock-and-Proximity-Sensor method.** With the Trigger-Interlock-and-Proximity-Sensor method, you must place the measurement window against the sample to be analyzed to engage the proximity sensor on the front of the instrument, press and keep pressing the interlock button at the rear of the instrument with your free hand, then pull the trigger for sample analysis to be initiated.
- **Easy Trigger method.** With the Easy trigger method, you need only place the measurement window against the sample area and pull the trigger once to initiate a sample analysis. Your

analyzer will continuously sample the backscatter, using a complex internal algorithm, to determine if the measurement window is against a sample or pointing to the empty air. If it finds that there is no sample directly against the measurement window, the analyzer will stop directing radiation through the window as soon as this determination is made.

With any of these methods, analysis will stop if any one of the preconditions are violated. For example, with the Trigger-Interlock-and-Proximity-Sensor method, if the trigger or the Proximity Sensor or the Interlock is released, the reading will stop immediately, and the X-ray tube will shut down.

6. Results

At the top are the elements detected in the sample; and underneath this, elements are below the detection limit (Figure C5). For an element to be detected by your analyzer in a given sample, the measured concentration of the sample must be at least three times the standard deviation of the measurement. This detection limit will depend on the composition of the sample. The measurement precision for each element displayed appears to the right of the measured concentration, under the heading “+/-“. The precision of each measurement is two times the standard deviation (sigma). An element is classified as “detected” if the measured concentration (in ppm) is at least 1.5 times the precision. Detected elements are displayed in ppm, followed by the measurement precision. Non-detected elements are shown as < the detection limit (LOD) for that sample. The detection limit for a given element varies depending on the other elements in the matrix.

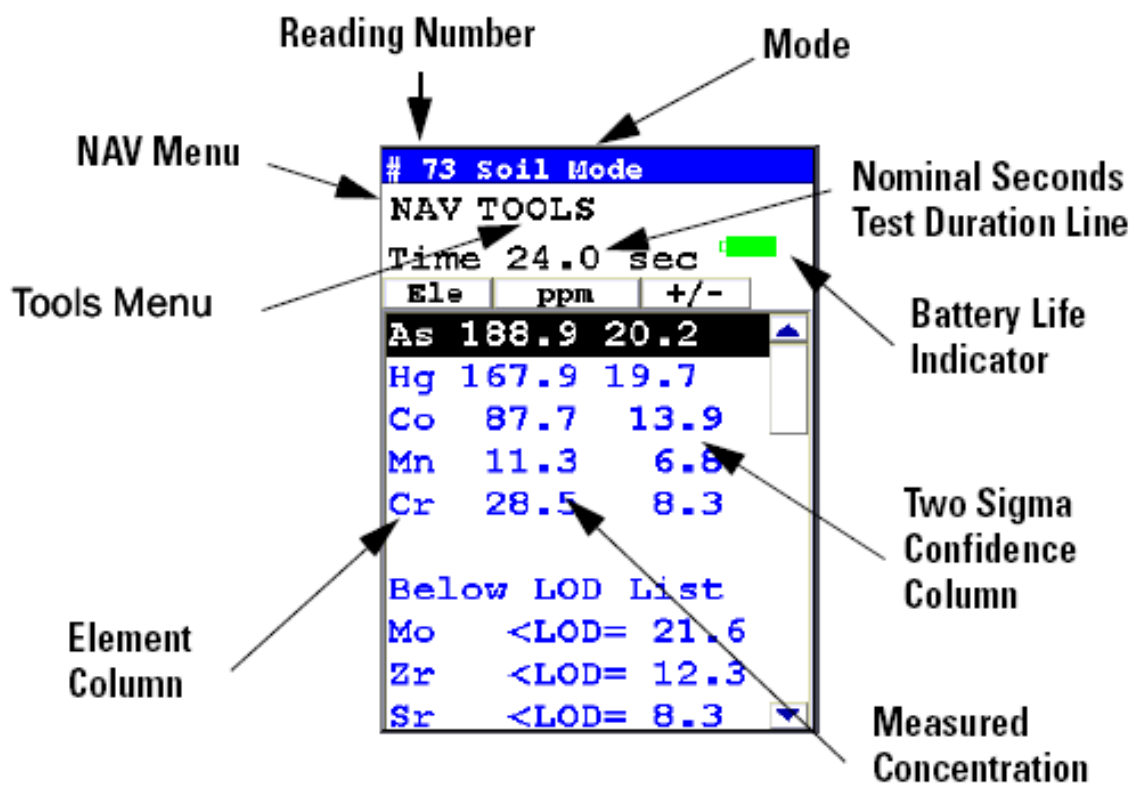


Figure C5. The standard bulk measurement result screen

Deliverable for Task 5:
Bridge Wash Water Analysis for Lead Using
the Field Spectrophotometer

Submitted

to

Carl Kochersberger
Environmental Science Bureau
Hazardous Materials and Asbestos Unit
Pod 4-1
New York State Department of Transportation
50 Wolf Road
Albany, NY 12232

May 2013

ABSTRACT

In this report, the application of the Hach DR 2800 field portable spectrophotometer is presented for quantifying dissolved and total lead concentrations in bridge wash water. The U.S. Environmental Protection Agency (U.S. EPA) approved Method 8033 is used for Pb analysis and is based on Standard Method 3500-Pb. A standard operating procedure (SOP) is introduced for using the Hach field portable spectrophotometer in this project and for New York State Department of Transportation (NYSDOT) personnel. Portable spectrophotometer results are reviewed for the 14 bridges from which wash water was available for sampling and analysis in this study. All wash water samples were collected using Nalgene® HDPE high density polyethylene containers during the rehabilitation process in New York State. Dissolved Pb concentrations ranged from 2.5 µg/L to 410 µg/L while total Pb concentrations were as great as 10 times the dissolved between 33 and 5,700 µg/L. In general, Pb concentrations in wash water samples from Region 5 were less than those from Regions 3 and 10. The results are consistent with trends found from analyzing metal concentrations in the paint waste. Although a linear correlation is between total and dissolved Pb concentrations ($R = 0.78$), Pb concentrations in wash water samples were not related to the total Pb concentrations found in the paint waste. All samples revealed dissolved lead concentrations less than 1,000 µg/L; four samples showed total lead concentrations greater than 1,000 µg/L. Based on the surface water quality standard New York State (New York State Department of Environmental Conservation [NYSDEC], 1999), the wash water generated during bridge rehabilitation may require treatment and discharge to a permitted location to prevent surface water or ground water pollution.

Table of Contents

| | |
|--|----|
| 1. Introduction..... | 1 |
| 2. Sample collection and analysis | 2 |
| 2.1 Quality Assurance/Quality Control (QA/QC)..... | 2 |
| 2.2 Wash water sampling procedure | 2 |
| 2.3 Wash water analysis | 3 |
| 3. Results from the field spectrophotometer for the bridges in the project..... | 4 |
| 3.1 Field spectrophotometer results | 4 |
| 3.2 Correlation between total and dissolved Pb in bridge wash water..... | 9 |
| 3.3 The environmental impact..... | 9 |
| 4. Summary | 12 |
| References | 14 |
| Appendix A: Bridge wash water samples information | 16 |
| Appendix B Standard operating procedure (SOP) for Hach DR 2800 Field Spectrophotometer | 19 |
| Appendix C: Consumables and replacement items | 32 |
| Appendix D: Method 3010A - Acid digestion of aqueous samples and extracts for total metals for analysis by FLAA or ICP spectroscopy | 35 |
| Appendix E: U.S. EPA approved (Hach) Methods..... | 41 |

1. Introduction

Prior to paint removal, high-pressure water (1800 to 2000 psi,) is applied to remove salt, bird droppings, and other associated debris from bridge structures (NYSDOT, 2008). General practice for protecting steel bridges from corrosion involves applying paint coatings (Boxall and Von Fraunhofer, 1980; Lambourne and Strivens, 1999; Gooch, 1993). Between 1950 and 1980, these paint coatings involved the use of lead and chromate for corrosion protection; however, because of the potential release of contaminants and the consequent impact to human health, the Department of Housing and Urban Development (HUD) and Consumer Product Safety Commission (CPSC) prohibited the residential use of lead-based paint (LBP) since 1978 (U.S. CPSC, 1977, HUD, 1978). In New York State, LBP has been prohibited from commercial use since 1989 (NYSDOT, 1988). Even though rehabilitation and subsequent repainting were conducted more than once since 1989, lead-based paint (LBP) may not be entirely removed and the residual paint on structures may be attributed to the surface preparation standard for paint removal procedures (NYSDOT, 2008). Generally, surface preparation standard SSPC SP-6 (The Society for Protective Coatings) (Commercial Blast Cleaning) (NYSDOT, 2008) was applied to most of the bridges in New York State before 2006, where slight shadows, streaks or discolorations caused by rust stain, mill scale oxides or slight, tight residues of paint or coating remained on the bridge were limited to less than 33% per unit area of surface. After 2006, SSPC SP-10 (Near White Blast Cleaning) was specified (NYSDOT, 2008), which restricts visible residue on the bridge surface to 5% per unit area. All bridges in this study were cleaned to SSPC-6 with the exception of the bridges in Regions 2 and 5, where SSPC SP-10 standard was applied. Consequently, the wash water generated may be contaminated with lead paint debris.

In this report, Hach DR 2800 field portable spectrophotometer was applied to detect and quantify dissolved and total lead concentrations present in bridge wash water. The Hach Method 8033 was used for Pb analysis based on EPA approved Method 3500-Pb (Eaton et al., 2005). Specifically, sample collection, preparation, and the detailed steps in conducting the analysis using Hach DR 2800 field portable spectrophotometer are introduced. In addition, a standard operating procedure (SOP) is reviewed for applying the Hach field portable spectrophotometer in this project and for New York State Department of Transportation (NYSDOT) personnel in general. The report also includes a list of reagents and apparatus required. Results from applying the portable spectrophotometer are reviewed for the 14 bridges from which wash water was available for sampling. Lastly, based on disposal practices, the environmental impact of generating and handling the waste is summarized.

2. Sample collection and analysis

2.1 Quality Assurance/Quality Control (QA/QC)

For the field work, gloves, dust masks, steel-toed boots, and safety goggles are needed along with a lab coat. Because of its resistance to acids and bases, the Nalgene® HDPE containers were used for the bridge wash water sampling. All glass and HDPE containers were cleaned with a metal-free nonionic detergent solution, rinsed with deionized water, soaked in 10% nitric acid (trace metal grade) for 24 h, and then rinsed with metal-free deionized water (ASTM, 1990; Eaton et al., 2005).

2.2 Wash water sampling procedure

Because some of the bridges applied the high-pressure wash during the evening, sampling wash water was prohibitive. Therefore, for the 24 bridges in this project, wash water sampling

was available for 14 bridges. Two sampling locations were selected for each bridge where two wash water samples, one filtered and one unfiltered, were collected. Only one location was available for Bridges 3-1 and 3-2. Total lead concentrations were determined in an unfiltered sample after digestion (EPA Method 3010 A), while dissolved metal represents the concentration of metal in an unacidified sample that passed through a 0.45- μm membrane filter (Eaton et al., 2005). Specifically, the samples were obtained by using the Nalgene® HDPE (1 L) containers to collect water draining off the bridge surface to a minimum of 0.75 L. The pH measurement in the field was determined with the Hach sensION 1 portable pH meter; solutions were then adjusted to a pH less than 2 with nitric acid (HNO_3) (EPA Method 3010B; Eaton et al., 2005). For dissolved lead analysis, filtration was conducted with sterilized disposable syringe filters (0.45 μm nylon membrane filters) before acid adjustment. Samples were subsequently sealed and stored at 4°C for transport to the NJIT Metals Lab. Preserved samples may be stored up to 6 months prior to analysis at 4°C (U.S. EPA, 2007).

2.3 Wash water analysis

The Standard Method 3500-Pb (Eaton et al., 2005), the dithizone method, is designed for determining lead in water and wastewater. In 1996, the Hach Method 8033 (which is equivalent to Standard Method 3500-Pb D) was approved by the U.S. Environmental Protection Agency (Appendix E) (U. S. EPA, 1996). For the dissolved lead analysis, because the sample has been filtered through the 0.45 μm glass fiber filters before acid adjustment, the subsequent analysis was conducted directly with the sample using the Hach field spectrophotometer (Appendix B). Briefly, the DithiVer metals reagent (a stable powder form of dithizone, $\text{C}_{13}\text{H}_{12}\text{N}_4\text{S}$) reacts with lead ions in an alkaline solution to form a pink to red lead-dithizonate complex, which is

extracted with chloroform. Extracted samples are then measured in the spectrophotometer at 515 nm. For total lead analysis, the samples were digested using EPA SW-846 Method 3010A (U.S. EPA, 1992; Appendix D) before filtration. Specifically, 100 ml water samples were treated with repeated addition of nitric acid and then heated until the sample was light in color or stabilized. After cooling to room temperature, 10 ml of hydrochloric acid (1:1 by volume) was added and the solution was then filtered through a 0.45 μm glass fiber filters, diluted to 100 ml with de-ionized water, and prepared for Pb analysis using the Hach field spectrophotometer (Appendix B). To compare the results from using the field spectrophotometer, inductively coupled plasma mass spectroscopy (ICP-MS) analysis was conducted as well on wash water samples.

3. Results from the field spectrophotometer for the bridges in the project

3.1 Field spectrophotometer results

Results from using the Hach field spectrophotometer correlated ($R = 0.93$) with the ICP-MS analysis (Figure 1). This work demonstrates the effectiveness of using spectrophotometer as a field method to analyze the Pb concentrations in bridge wash water. Dissolved Pb concentrations ranged from 2.5 $\mu\text{g/L}$ to 410 $\mu\text{g/L}$ (Figure 2), while total Pb concentrations were observed from 33 to 5,700 $\mu\text{g/L}$ (Figure 3). Variability in dissolved Pb and total Pb was observed throughout the regions (Figures 2 and 3), and can be attributed to a number of factors including high pressure wash intensity and duration of application. The total lead concentrations are as great as 10 times the dissolved lead concentrations. On average, 84% of total lead concentrations in bridge wash water are in the particulate form. In general, Pb concentrations in the wash water samples from Region 5 were less than those from Regions 3 and 10 (Figures 2 and 3). The results are consistent with trends found from analyzing metal concentrations in the paint waste.

Because surface preparation standard SSPC SP-6 (Commercial Blast Cleaning) (NYSDOT, 2008) was applied to the bridges, as great as 33% of paint remained on the bridge (NYSDOT, 2008). During high-pressure wash, the water impinges on the existing paint and exposed steel surfaces, removing weakly held material, which is carried off by the wash water. Therefore, the wash water generated is contaminated with lead paint debris. However, Pb concentrations observed in wash water samples were not related to the total Pb concentrations in the paint waste. The wash water concentrations are lower than those observed by Hopwood et al. (2003), where they attempted to apply a geotextile fabric to filter wash water from bridges undergoing maintenance prior to its release. Hopwood et al. reported dissolved lead concentrations ranged from less than detection to 5,500 µg/L while total lead concentrations were observed from 2,300 to 130,000 µg/L during high pressure (3,000 to 10,000 psi) washing. After filtration, dissolved lead concentrations were reduced to less than detection to 4,100 µg/L, while total lead concentrations ranged from 2,000 to 22,000 µg/L. On the other hand, results from this study are comparable with those obtained by Davis and Burns (1999) where the affect of acid rain on LBP structures was investigated. Results revealed that the total lead concentrations in the runoff from structures followed the order of wood 2.6 – 380 µg/L, brick 3.3 – 240 µg/L, and cement 2.0 – 110 µg/L. The lead concentrations depended on the age of the paint and condition of deterioration. In our study, Bridge 10-1 (Figure 2) exhibited the greatest dissolved lead concentration of 410 µg/L and total lead concentration of 5,700 µg/L. These results were consistent with the elevated lead concentrations observed using FP-XRF on the paint waste samples from Bridge 10-1.

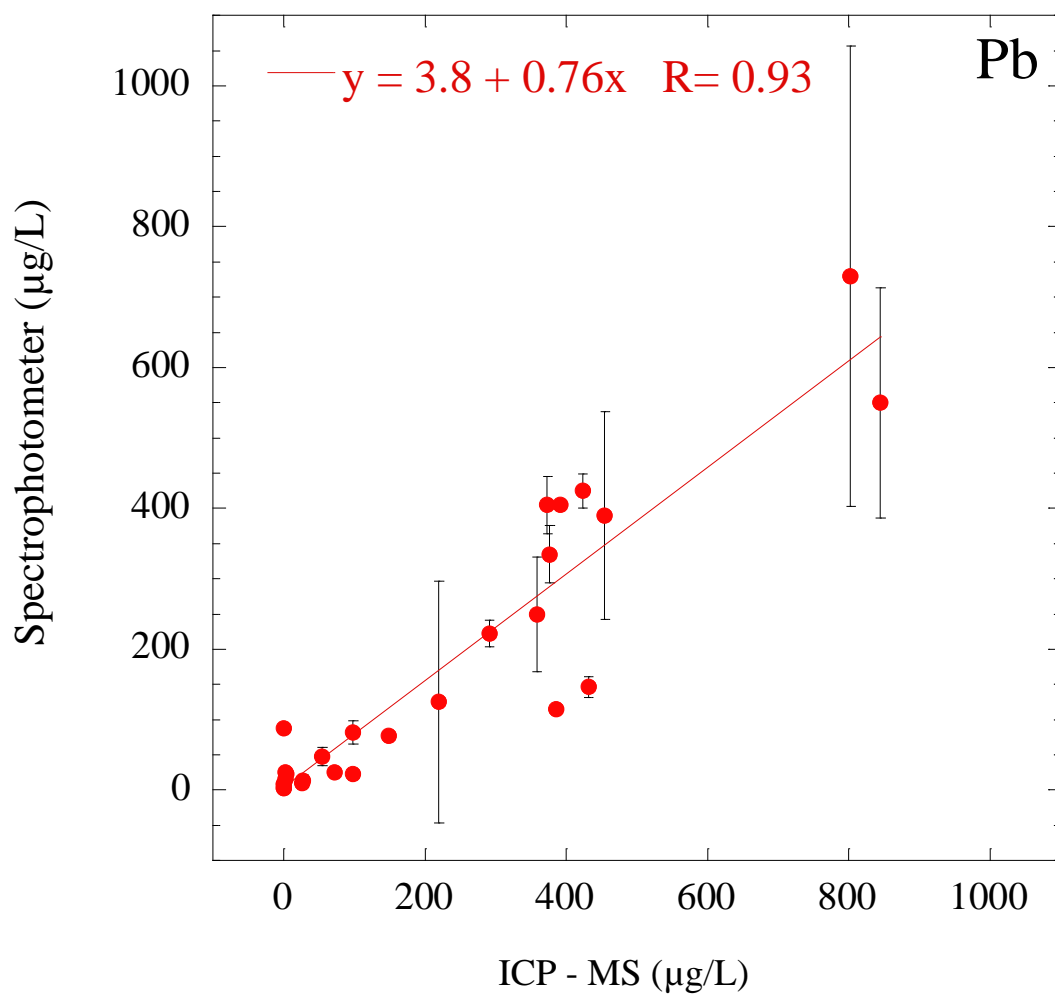
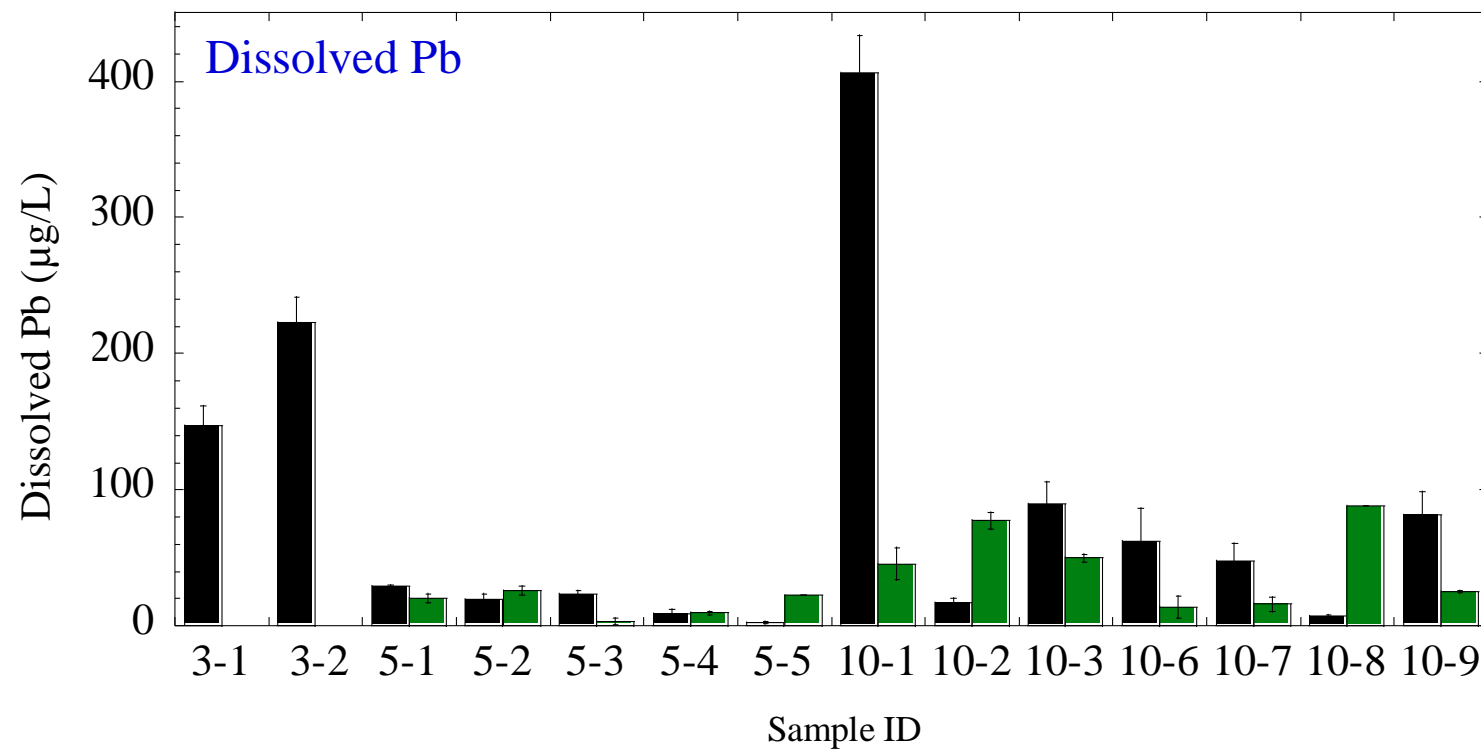
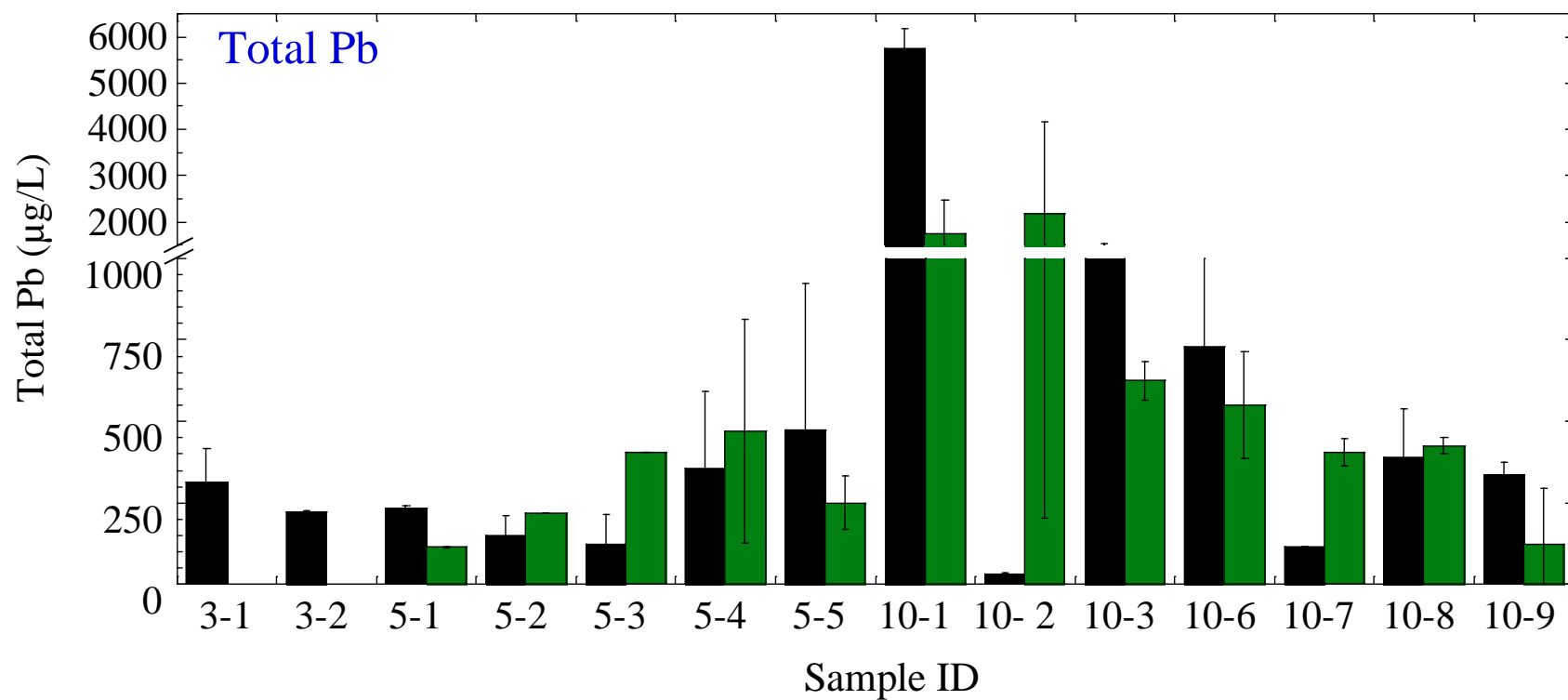


Figure 1. Results from measuring lead concentrations in bridge wash water with ICP-MS and Hach field spectrophotometer.



Two sampling locations for each bridge: ■ a ■ b

Figure 2. Dissolved Pb concentrations are shown as a function of the two locations for the 14 bridges sampled using the Hach field spectrophotometer. One sampling location was available for Bridges 3-1 and 3-2. All bridges sampled were rehabilitated after 1989.



Two sampling locations for each bridge: ■ a ■ b

Figure 3. Total Pb concentrations are shown as a function of the two locations sampled for the 14 bridges using the Hach field spectrophotometer. One sampling location was available for Bridges 3-1 and 3-2. All bridges sampled were rehabilitated after 1989.

3.2 Correlation between total and dissolved Pb in bridge wash water

Although significant variability was observed across bridges, the total and dissolved concentrations were correlated with an R of 0.78 (Figure 4). The results revealed a trend of increasing dissolved lead concentration with increasing total lead concentration in wash water. The difference in concentration between the dissolved and total lead can be attributed to the particulate collected in the wash water. Because a 0.45- μm membrane filter was applied, colloid size particles were likely present in the filtrate samples. Pb concentrations observed in wash water samples were not related to the total Pb concentrations found in the paint waste samples. This result may be due to the variable surface conditions of bridges. Paint chips that were flaking or readily removed during the high-pressure wash were collected, while bridges in relatively better condition would have less paint particles in wash water. Therefore, Pb concentration in wash water samples and the total Pb concentration in the paint waste were not correlated.

3.3 The environmental impact

Generally, wash water is filtered before discharged into a sewer or through runoff if determined hazardous (Appleman, 1997). States set their own standard for determining whether wash water is hazardous. Pennsylvania DOT requires a series of handling and disposal conditions for wash water including water collection, filtration of paint chips or particles, and water characterization; Massachusetts Turnpike set 100 ppm Pb as the criterion for wash water. In NYS, special collection requirements exist for washing a structure over a public water supply, where wash water over a body of water is required to be collected and diverted to the adjoining land mass (NYSDOT, 2008). In this study, all samples revealed dissolved lead concentrations

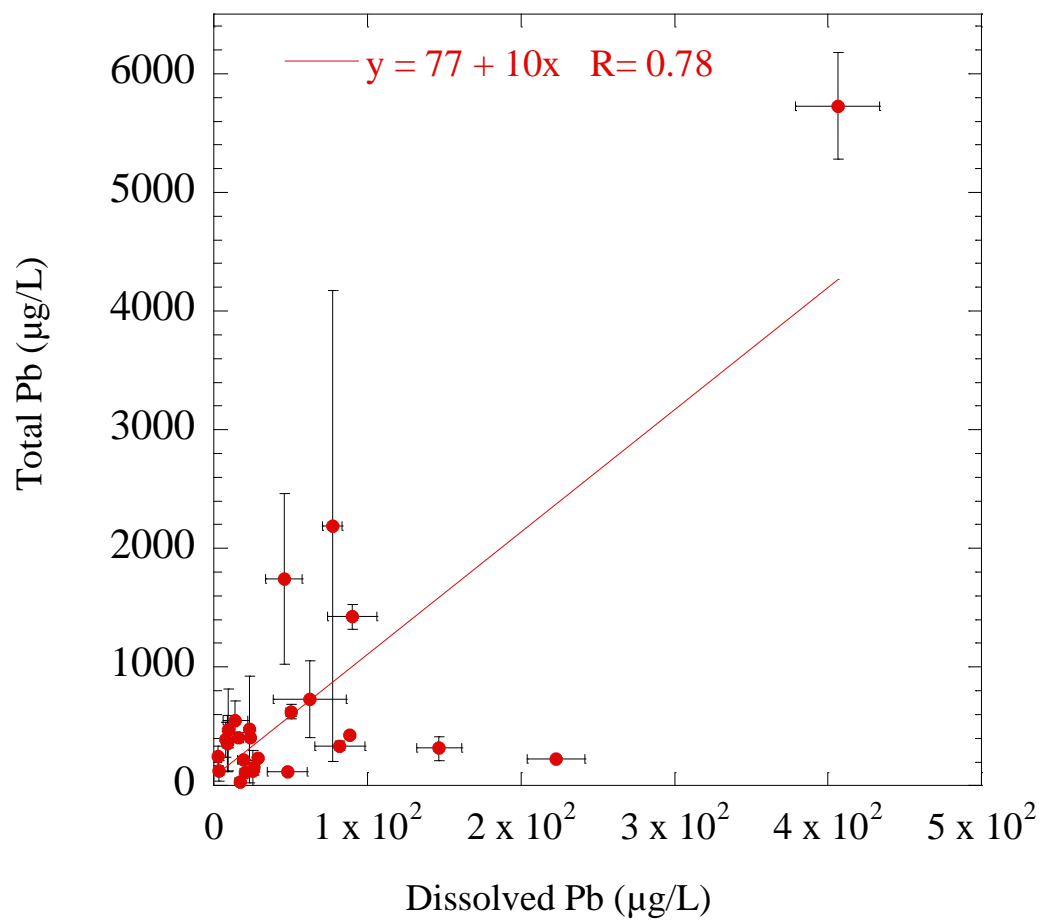


Figure 4. Results of dissolved and total Pb concentrations observed in the bridge wash water measured with the Hach field spectrophotometer. Total Pb concentrations were obtained by first digesting the sample before analysis.

less than 1,000 µg/L; 89% of the samples were observed from non-detectable to 90 µg/L (Figure 5). Four of the samples showed total lead concentrations greater than 1,000 µg/L; 85% of the samples ranged from non-detectable to 750 µg/L (Figure 5). Dissolved lead and lead contaminated paint particulates in wash water are transported either directly or indirectly to surface water through storm drains. Lead contaminated paint particles will continue to dissolve as they are being transported, releasing lead into solution. The dissolution rate can be enhanced by complexing ligands commonly found in natural waters, such as humic acid (Guy and Chakrabarth, 1976) and chloride (Davis and Barnes, 1996). The mobility of metals in the environment is a function of their speciation. In addition to the wash water, metals may be mobilized through rainfall, and urban stormwater runoff is considered to be a major source of metals to surface waters. Therefore, although lead concentrations were investigated in the bridge wash water during high pressure wash, the results suggest potential for rainwater contamination from the bridge paint surface as well.

The surface water quality standard in New York State is 50 µg/L for Pb, where the surface water used as drinking water source; as low as 8 µg/L is applied for the saline surface water where there is fish, shellfish, and wildlife propagation and survival (NYSDEC, 1999). Ground water quality standard in NYS is 25 µg/L for Pb (NYSDEC, 1999). 35% of the samples revealed dissolved lead concentrations greater than the surface water quality standard 50 µg/L, while 96% of the samples were observed total lead in wash water greater than 50 µg/L. These results suggest that bridge wash water containing lead or paint solids may be collected, properly treated, and discharged to a permitted location to prevent surface water or ground water pollution.

4. Summary

The Hach spectrophotometer is an effective method to analyze the Pb in bridge wash water samples. In this report, the portable spectrophotometer results were reviewed for the 14 bridges from which wash water was available for sampling and analysis in this study. Dissolved Pb concentrations ranged from 2.5 µg/L to 410 µg/L, while total Pb concentrations were observed from 33 to 5,700 µg/L. The total lead concentrations were as great as 10 times the dissolved lead concentrations. In general, Pb concentrations in wash water samples from Region 5 were less than those from Regions 3 and 10. The results were consistent with trends found from analyzing metal concentrations in the paint waste. Total and dissolved Pb concentrations were correlated ($R = 0.78$) for the bridge wash water samples. However, Pb concentrations observed in wash water samples were not related to the total Pb concentrations in the paint waste. Results revealed dissolved lead concentrations less than 1,000 µg/L; 89% of the samples were observed from non-detectable to 90 µg/L. Four of the samples revealed total lead concentrations greater than 1,000 µg/L; 85% of the samples ranged from non-detectable to 750 µg/L. Based on the surface water quality standards, results in this study suggest that bridge wash water containing lead or paint solids may require collection, treatment, and discharge to a permitted location to prevent surface water or ground water pollution.

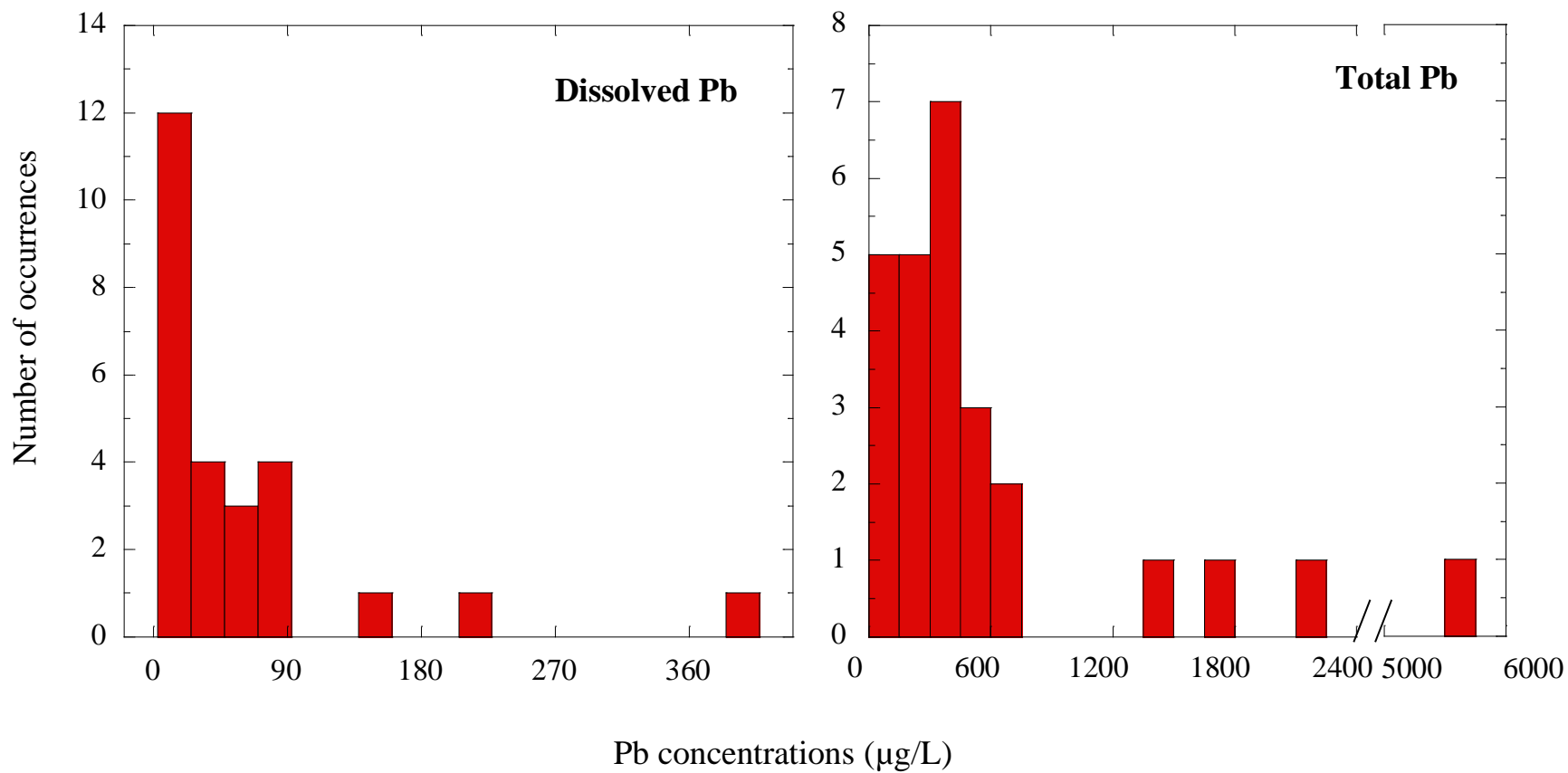


Figure 5. Dissolved and total Pb distribution observed in the wash water samples from 14 bridges.

References

Appleman, B. R. (1997) Lead-base paint removal for steel highway bridges., *Transportation Research Board*, Washington, DC., Report 1251.

American Society for Testing and materials (ASTM), (1990) Standard practice for decontamination of field equipment used at nonradioactive waste sites, Designation D5088-90, West Conshohocken, PA.

Boxall, J., Von Fraunhofer (1980) Paint Formulation: principles and practice. George Goodwin Limited, London

Davis, A. P., Burns, M. (1999) Evaluation of lead concentration in runoff from painted structures, *Water Resource*, 33 (13): 2949-2958.

Eaton, A. D., Clesceri, L. S., Rice, E. W., Greenberg, A. E. (2005) Standard methods for the examination of water and wastewater, 21st edition, 3: 79-81.

Hach Company, DR2800 User manual, January 2008, Edition 2.

Hach Company, DR 2800 Spectrophotometer procedures manual, June 2007, Edition 2.

Hopwood, T., Palle, S., Younce, R. (2003) Environmental impacts of bridge cleaning operations, Research Report, University of Kentucky.

Gooch, J. W., Lead-Based Paint Handbook, Plenum Press, New York, 1993

Lambourne, R., Strivens, T., Paint and Surface Coatings: Theory and Practices, Woodhead Publishing, Cambridge, 1999.

New York State Department of Transportation, Standard Specification, May 1, 2008. <https://www.nysdot.gov/main/business-center/engineering/specifications/english-spec-repository/section550.pdf>

New York State Department of Transportation, (1988) Specification for bridges – removal of lead based paints – new department paint system for structural steel, Engineering instruction, EI 88-36.

New York State Department of Environmental Conservation, Part 703: Surface Water and Groundwater Quality Standards and Groundwater Effluent Limitations, 1999.

<http://www.dec.ny.gov/regs/4590.html#16130>

Plumb, R., Jr., (1981) Procedures for handling and chemical analysis of sediment and water samples: Vicksburg, Miss., U.S. Army Corps of Engineers Waterways Experiment Station, Environmental Laboratory, Technical Report EPA/CE-81-1.

U.S. EPA, (1992) Method 3010A Acid digestion of aqueous samples and extracts for total metals for analysis by FLAA or ICP spectroscopy, SW-846 Chapter 3.

U.S. Occupational Safety and Health Administration (1993) Lead exposure in construction: interim final rule (29 CFR 1926.62). Federal Register 58: 26590-26649. Washington, DC.

U.S. Consumer Products Safety Commission (U. S. CPSC), (1977) Notice reducing allowable levels of lead. Final Rule, Federal Register 42 (1): 44199.

U.S. EPA, (2007) Inorganic analytes, SW-846 Chapter 3.

U.S. EPA, (2002) National Recommended Water Quality Criteria: Office of Water, Office of Science and Technology, EPA-822-R-02-047, 2002; available at:

<http://www.epa.gov/waterscience/criteria/wqcriteria.htm>.

Appendix A

Bridge wash water samples information

Table A.1 Sampling sites and contact

| Bridge ID | Collection Date | Bridge name and the location | Contact |
|-----------|------------------------|--|------------------|
| 3-1 a | 11/12/10 | Right Shoulder | Huffman, Nick |
| 3-2 a | 11/12/10 | Right Shoulder | 315-877-5585 |
| 5-1 a | 6/15/11 | I-190 SB Span 5 left and center lanes | Jakubowski, Gary |
| 5-1 b | 06/29/2011 | I-190 NB Span 6 left lane | 716-908-0273 |
| 5-2 a | 6/15/11 | I-190 SB Span 5 left and center lanes | |
| 5-2 b | 6/29/2011 | I-190 NB Span 6 left lane | |
| 5-3 a | 08/24/2011 | I-290 WB Span 3 right and center lane | |
| 5-3 b | 09/07/2011 | Span 2 I-290EB right and center lane | |
| 5-4 a | 08/23/2011 | I-290 WB right lane east park drive span 3 | |
| 5-4 b | 09/07/2011 | Span 2 I-290EB right and center lane | |
| 5-5 a | 8/1/2011 | Span 4 I-190 SB left lane | |
| 5-5 b | 8/14/2011 | Span 6 Ramp B right lane | |
| 10-1 a | 6/14/11 | NA | Connor, John |
| 10-1 b | 6/15/11 | NA | 917-406-9451 |
| 10-2 a | 6/28/2011 - 07/20/2011 | NA | |
| 10-2 b | 6/28/2011 - 07/20/2011 | NA | |

| Bridge ID | Collection Date | Bridge name and the location | Contact |
|-----------|------------------------|------------------------------|---------|
| 10-3 a | 6/28/2011 - 07/20/2011 | NA | |
| 10-3 b | 6/28/2011 - 07/20/2011 | NA | |
| 10-6 a | 08/16/2011 | South abutment | |
| 10-6 b | 08/16/2011 | North abutment | |
| 10-7 a | 10/13/2011 | Northeast abutment | |
| 10-7 b | 10/13/2011 | Northeast abutment | |
| 10-8 a | 10/02/2011 | Southwest abutment | |
| 10-8 b | 10/02/2011 | South west abutment | |
| 10-9 a | 10/02/2011 | North abutment | |
| 10-9 b | 10/02/2011 | South abutment | |

NA: not available

Appendix B

**Standard operating procedure (SOP) for Hach
DR 2800 Field Spectrophotometer**

Standard operating procedure (SOP) for Hach DR 2800 Field Spectrophotometer

1. Preparing, storing DithiVer solution and reagent blank store

The DithiVer Powder must be stored in a dark and cool location (10-25 °C). A convenient way to prepare this solution is to add the contents of 10 DithiVer Metals Reagent Powder Pillows (Hach labeled package) to a 500 ml bottle of chloroform and invert several times until well mixed (carrier powder may not dissolve). The resulting dithizone solution is then stored in an amber glass bottle. This solution is stable for 24 hours. A reagent blank using deionized water instead of the sample should be run through the entire method to obtain the most accurate results.

2. Preparing samples (Figure 1, 2, 3)

3. Running the instrument

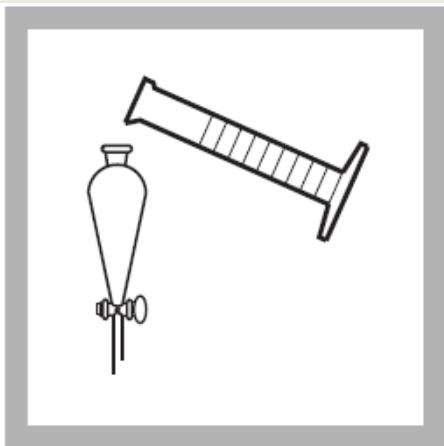
3.1 System setting (Figure 4)

3.2 Sample test

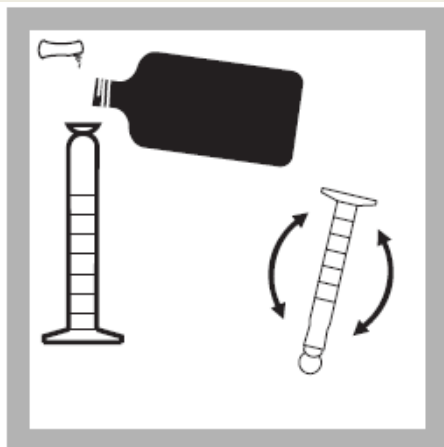
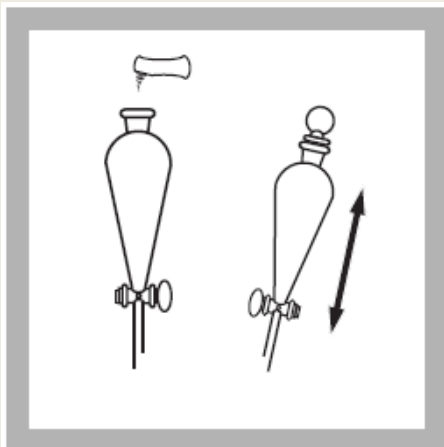
The instrument contains more than 200 programmed procedures. They can be accessed through the Stored Programs menu. 280 Lead Dithizone is the program needed for the lead analysis (Figures 5 and 6).

3.3 Recall and send data

The Data Log will store up to 500 readings. A complete record of the analysis is stored, including the date, time, results, sample ID, and operator ID.

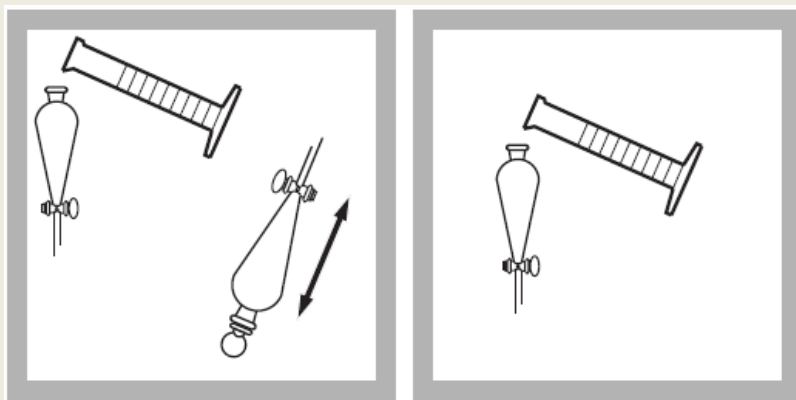


1. Fill a 250 ml graduated cylinder to the 250 ml mark with sample.
2. Transfer the sample into 500 ml separatory funnel.



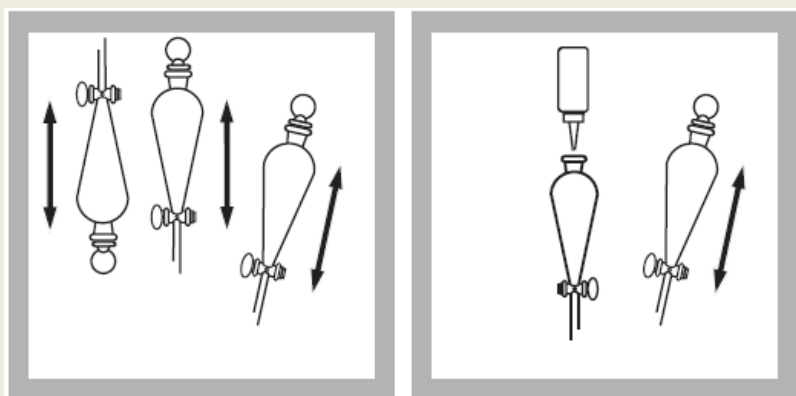
3. Add the contents of one Buffer Powder Pillow for heavy metals, citrate type. Stopper the funnel and shake to dissolve.
4. **DithiVer Solution Preparation:** Add 50 ml of chloroform to a 50 ml mixing graduated cylinder. Add the contents of one DithiVer Metals Reagent Powder Pillow. Stopper the cylinder. Invert several times to mix.

Figure 1. Steps 1 through 4 for preparing the solution for analysis.



5. Measure 30 ml of the prepared dithizone solution with a second graduated cylinder and add to the separatory funnel. Stopper and invert to mix. Open stopcock to vent. Close the stopcock.

6. Add 5 ml of 5.0 N Sodium Hydroxide Standard Solution.

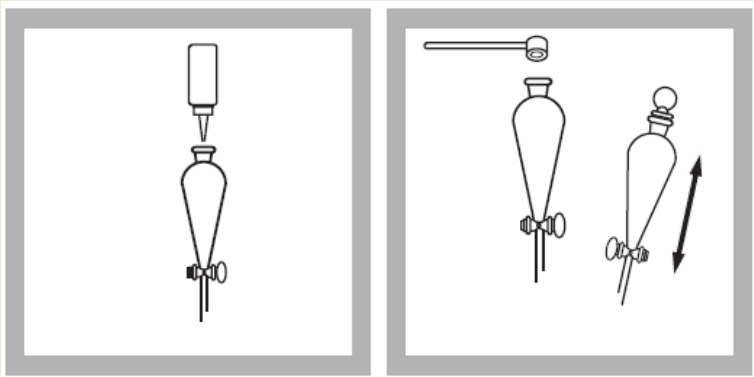


7. Stopper. Invert. Open stopcock to vent. Close the stopcock and shake the funnel once or twice and vent again.

Note: Add a few drops of 5.25 N Sulfuric Acid Standard Solution if the solution turns orange on shaking. The blue-green color will reappear. To avoid higher blanks, repeat procedure on new sample and use less sodium hydroxide in **Step 6**.

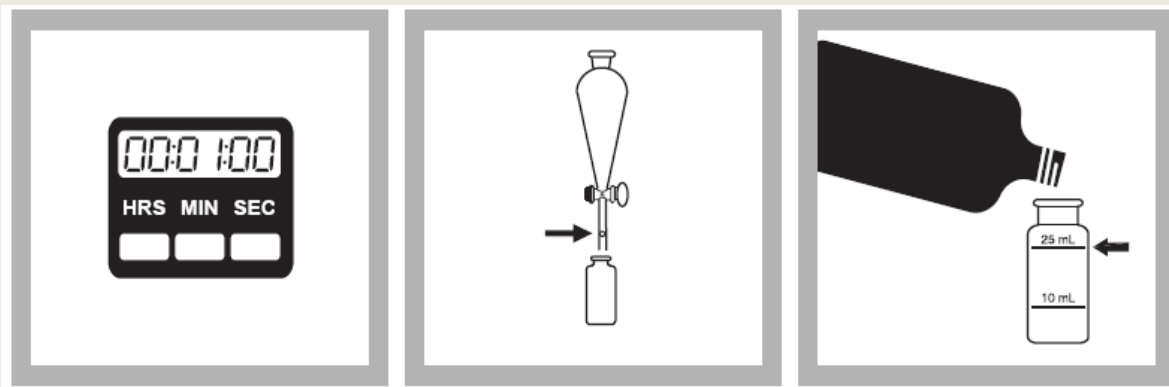
8. Continue adding 5.0 N Sodium Hydroxide Standard Solution dropwise and shaking the funnel after every few drops until the color of the solution being shaken changes from blue-green to orange. Large amounts of zinc cause the color transition at the end point to be indistinct.

Figure 2. Steps 5 through 8 for samples preparing for analysis.



9. Add 5 more drops of 5.0 N sodium hydroxide standard solution. A pink color in the bottom (chloroform) layer at this point does not necessarily indicate lead is present. Only after adding the potassium cyanide in the next step will the presence of lead be confirmed by a pink color.

10. Add 2 heaping 1.0 g scoops of potassium cyanide to the funnel. Stopper. Shake vigorously until the potassium cyanide is all dissolved (about 15 seconds).

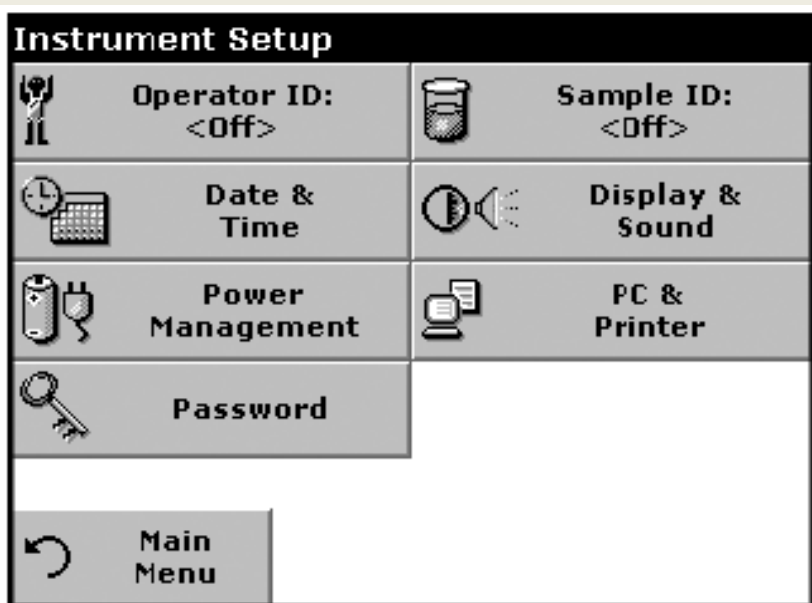


11. Wait one minute for the layers to separate. The bottom (chloroform) layer will be pink if lead is present.

Figure 3. Steps 9 through 11 for sample preparing for analysis.

12. Prepared Sample: Insert a cotton plug the size of a pea into the delivery tube of the funnel and slowly drain the bottom (chloroform) layer into a dry 25 ml square sample cell. Stopper. The lead-dithizone complex is stable for at least thirty minutes if the sample cell is kept tightly capped and out of direct sunlight.

13. Blank Preparation: Fill another 25 ml square sample cell with chloroform. Stopper.

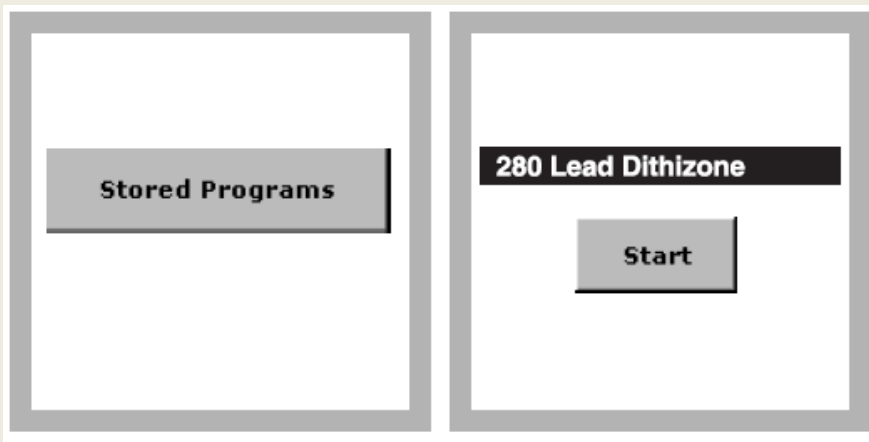


14. Select **Instrument Setup** in the **Main Menu** shown above. A selection of functions appears in order to configure the functions of the instrument.

Figure 4. Step 12 through 14 for prepared sample and instrument setup.

| Stored Programs | | |
|--|------------------|------------|
| 10 | Aluminum Alumin. | 0.800 mg/L |
| 9 | Aluminum ECR | 0.250 mg/L |
| 20 | Barium | 100 mg/L |
| 771 | Beer color | 60.0 units |
| 30 | Benzotriazole | 16.0 mg/L |
| 40 | Boron | 14.0 mg/L |
| 45 | Boron LR | 1.50 mg/L |
| 50 | Bromine | 4.50 mg/L |
| 55 | Bromine AV | 4.50 mg/L |
| 395 | CD 2 | 6.00 g/l |
| <div> <div> </div> <div> Main Menu </div> </div> <div> Select by Number </div> <div> Program Options </div> <div> Start </div> | | |

15. Press **Stored Programs** in the Main Menu to view an alphabetical list of stored programs with program numbers. The Stored Programs list will appear.



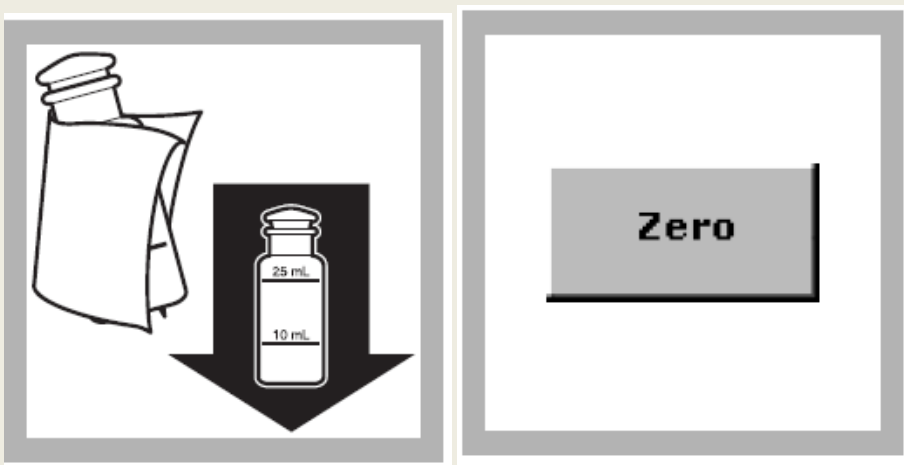
16. Highlight the required test (280 Lead Dithizone)

***Note:** Select the program number by name or use the arrow keys to scroll through the list quickly and highlight the program or press **Select by number** to search for a specific program number. Use the alphanumeric keypad to enter the test number and press **OK**.*

17. Press **Start** to run the program. After a program is selected, the screen for that parameter will appear.

***Note:** All corresponding data (wavelength, factors and constants) are already preset.*

Figure 5. Steps 15 through 17: Program selection



18. Insert the blank into the cell holder with the fill line facing right.

19. Press **ZERO**. The display will show: 0 $\mu\text{g/L Pb}^{2+}$.



20. Insert the prepared sample into the cell holder with the fill line facing right.

21. Press **READ**. Results are in $\mu\text{g/L Pb}^{2+}$.

Note: In bright light conditions (e.g., direct sunlight) it may be necessary to close the cell compartment with the protective cover during measurements.

Figure 6. Steps 18 through 21 for the sample analysis.

Recall data

The function Filter Settings is used to search for specific items (Figures 7 and 8).

Send data

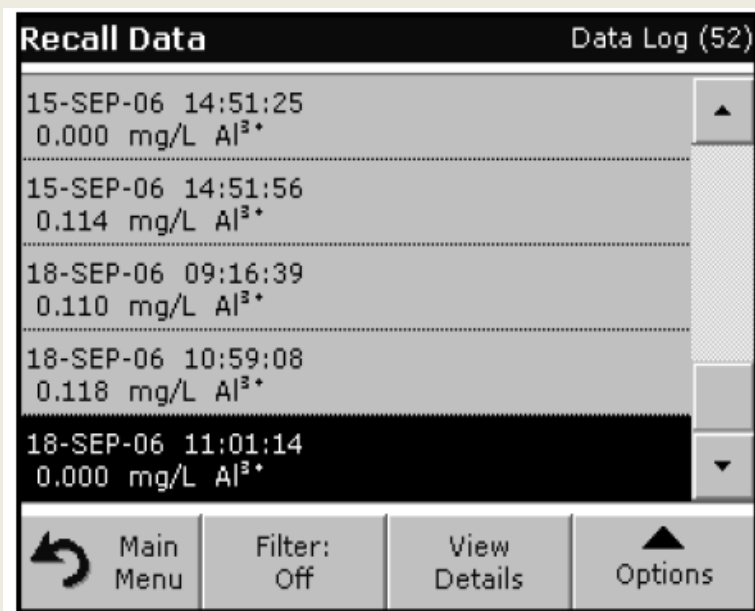
Data are sent from the data log as CSV (comma separated values) files through a USB memory stick to a file named DATALOG (Figure 9). The file can then be processed using a spreadsheet program. The file name will be formatted as:

DLYear_Month_Day_Hour_Minute_Second. CSV.

4. Cautions for accurate results

- (1) As mentioned above, for more accurate results, determine a reagent (DithiVer Metals Reagent) blank value for each new package of reagent. Follow the procedure using deionized water instead of the sample.
- (2) Results from the spectrophotometer are provided in $\mu\text{g/L}$ soluble lead.
- (3) For more accurate results, in **step 8** the sample should be adjusted to pH 11.0–11.5 using a pH meter. Omit the five additional drops of sodium hydroxide standard in **step 9**. Because in an ammoniacal cyanide solution (pH 8.5-9.5) dithizone forms colored complexes with bismuth, stannous tin, and monovalent thallium, results will produce interferences. In strong ammoniacal cyanide solution (pH 10.0-11.5), the dithizonates of these ions are unstable and are extracted only partially. This method uses a high pH, mixed color single dithizone extraction.
- (4) The DithiVer powder will not completely dissolve in the chloroform. For further notes see **Preparing, storing DithiVer solution and reagent blank**

- (5) The interfering substances include bismuth, copper, mercury, silver, tin, and highly buffered samples or extreme sample pH. To eliminate interference from these substances, the following procedure should be applied beginning after **step 4**.
- a. Measure about 5-ml of the DithiVer solution into the separatory funnel. Stopper the funnel, invert and open the stopcock to vent. Close the stopcock and shake the solution vigorously for 15 seconds. Allow the funnel to stand undisturbed until the layers separate (about 30 seconds). A yellow, red, or bronze color in the bottom (chloroform) layer confirms the presence of interfering metals. Draw off and collect the bottom (chloroform) layer for proper disposal.
 - b. Repeat extraction with fresh 5-ml portions of prepared dithizone solution (collecting the bottom layer each time in appropriate waste collection vessel) until the bottom layer shows a pure dark green color for three successive extracts. Extractions can be repeated a number of times without appreciably affecting the amount of lead in the sample.
 - c. Extract the solution with several 2 or 3 ml portions of pure chloroform to remove any remaining dithizone, again collecting the bottom layer each time for proper disposal.
 - d. Continue the procedure, substituting 28.5 ml of prepared dithizone solution for the 30 ml in **step 5**.

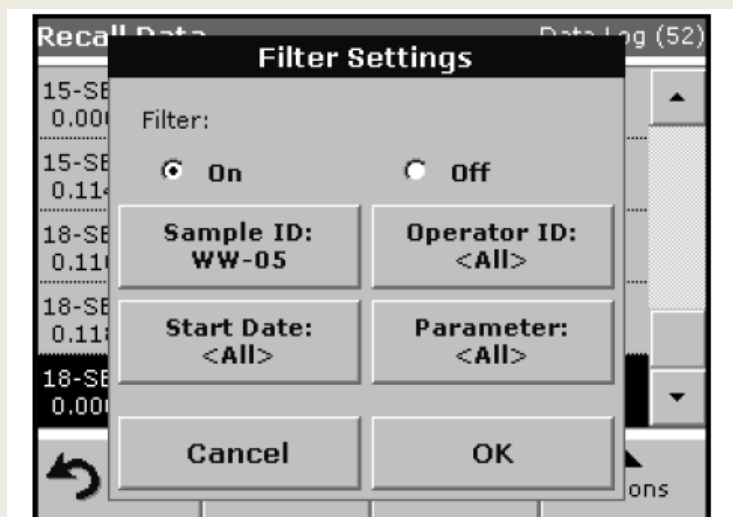


22. Press **Recall Data** in the Main Menu.

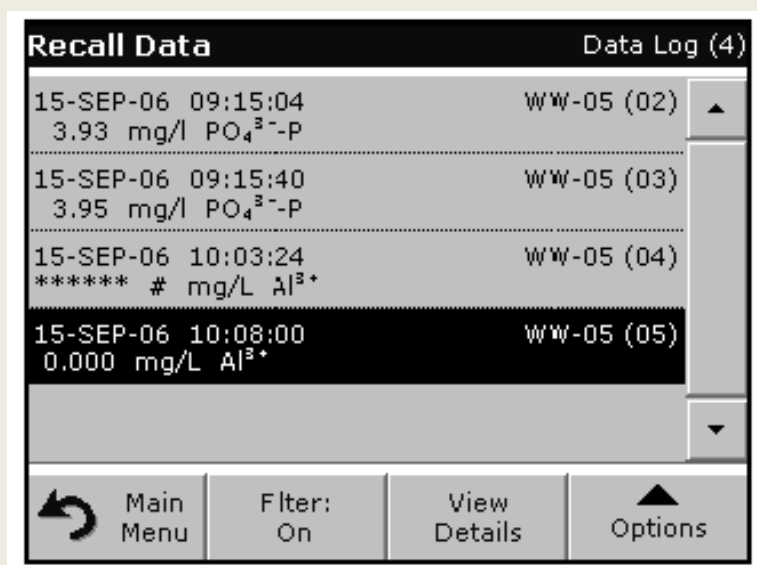
23. Press **Data Log**. A listing of the stored data is displayed.

24. Press **Filter: On/Off**. The function **Filter Settings** is used to search for specific items.

Figure 7. Steps 22 through 24 for turning on the filter settings



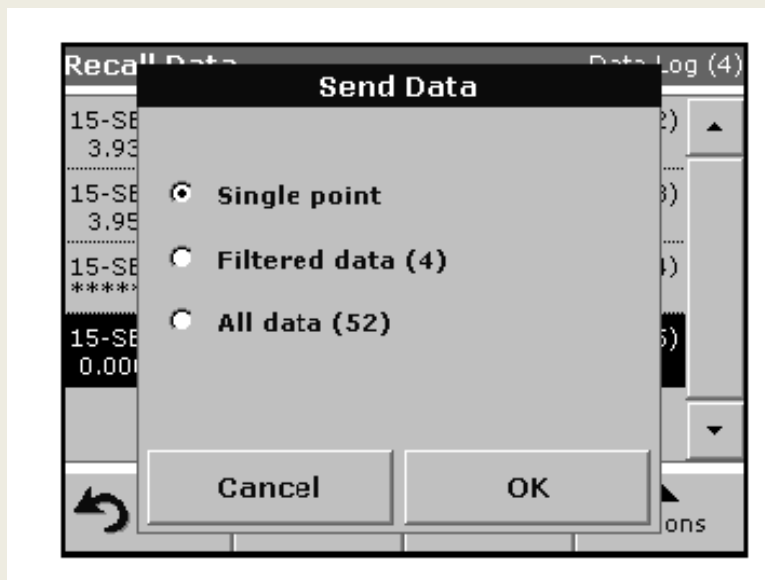
25. Highlight **On** to turn on the filters to select data by: Sample ID, Operator ID, Start Date, Parameter or any combination of the four.



26. Press **OK** to confirm the selection. The chosen items are listed.

27. Press **View Details** to get more information.

Figure 8. Steps 25 through 27 for recalling data.



28. Plug in the USB device.

29. Press **Recall Data** from the Main Menu. Press **Options** and then the **PC & Printer** icon.

30. Select the data to send to the memory stick and press **OK**.

Note: The number in parenthesis is the total number of data sets assigned to this selection.

Figure 9. Steps 28 through 30 for downloading data.

Appendix C

Consumables and replacement items

Required Reagents

| Description | Quantity/Test | Unit | Cat. No. |
|--|---------------|----------|----------|
| Lead Reagent Set (100 Tests) — | | — | 22431-00 |
| Includes: (1) 14202-99, (2) 14458-17, (1) 12616-99, (2) 767-14, (1) 2450-53, (2) 2450-26 | | | |
| Buffer Powder Pillows, citrate | 1 | 100/pkg | 14202-99 |
| Chloroform, ACS | 30 ml | 4 L | 14458-17 |
| DithiVer Metals Reagent Powder Pillows | 1 | 100/pkg | 12616-99 |
| Potassium Cyanide | 0.1 g | 125 g | 767-14 |
| Sodium Hydroxide Solution, 5.0 N | 5 ml | 1000 ml | 2450-53 |
| Sodium Hydroxide Standard Solution, 5.0 N | varies | 59 ml DB | 2450-26 |

Required Apparatus

| Description | Quantity/Test | Unit | Cat. No. |
|---|---------------|---------|----------|
| Clippers, for opening powder pillows | 1 | each | 968-00 |
| Cotton Balls, absorbent | 1 | 100/pkg | 2572-01 |
| Cylinder, graduated, 5-ml | 1 | each | 508-37 |
| Cylinder, graduated, 50-ml | 1 | each | 508-41 |
| Cylinder, graduated, 250-ml | 1 | each | 508-46 |
| Cylinder, graduated, mixing, 50-ml | 1 | each | 1896-41 |
| Funnel, separatory, 500-ml | 1 | each | 520-49 |
| pH Meter, sension™1, portable, with electrode | 1 | each | 51700-10 |
| Sample Cell, 1-inch square, 25 ml with cap | 2 | 2/pkg | 26126-02 |
| Spoon, measuring, 1-g | 1 | each | 510-00 |
| Support Ring, 4" | 1 | each | 580-01 |
| Support Ring Stand, 5" x 8" base | 1 | each | 563-00 |

Recommended Standards

| Description | Unit | Cat. No. |
|--|--------|----------|
| Lead Standard Solution, 100 mg/L Pb | 100 ml | 12617-42 |
| Lead Standard Solution, 10-ml Voluette Ampules, 50-mg/L Pb | 16/pkg | 14262-10 |

Optional Reagents and Apparatus

| Description | Unit | Cat. No. |
|---|-------------|-----------------|
| Ampule Breaker Kit | each | 21968-00 |
| Chloroform, ACS | 500 ml | 14458-49 |
| Filter Discs, glass, 47 mm | 100/pkg | 2530-00 |
| Filter Holder, glass, for 47-mm filter | each | 2340-00 |
| Flask, Erlenmeyer, 500-ml | each | 505-49 |
| Flask, filtering, 500-ml | each | 546-49 |
| Flask, volumetric, Class A, 100-ml | each | 14574-42 |
| Nitric Acid Solution, 1:1 | 500 ml | 2540-49 |
| Nitric Acid, ACS | 500 ml | 152-49 |
| pH Paper, pH 1.0 to 11.0 | 5 rolls/pkg | 391-33 |
| Pipet, serological, 2-ml | each | 532-36 |
| Pipet, TenSette®, 0.1 to 1.0 ml | each | 19700-01 |
| Pipet Tips, for TenSette Pipet 19700-01 | 50/pkg | 21856-96 |
| Pipet, volumetric, 5.00-ml, Class A | each | 14515-37 |
| Pipet, volumetric, 10.00-ml, Class A | each | 14515-38 |
| Pipet Filler, safety bulb | each | 14651-00 |
| Sulfuric Acid, 5.25 N | 100 ml MDB | 2449-32 |
| Water, deionized | 4 liters | 272-56 |

Appendix D:

Method 3010A

**Acid digestion of aqueous samples and extracts
for total metals for analysis by FLAA or ICP
spectroscopy**

METHOD 3010A

ACID DIGESTION OF AQUEOUS SAMPLES AND EXTRACTS FOR TOTAL METALS FOR ANALYSIS BY FLAA OR ICP SPECTROSCOPY

1.0 SCOPE AND APPLICATION

1.1 This digestion procedure is used for the preparation of aqueous samples, EP and mobility-procedure extracts, and wastes that contain suspended solids for analysis, by flame atomic absorption spectroscopy (FLAA) or inductively coupled argon plasma spectroscopy (ICP). The procedure is used to determine total metals.

1.2 Samples prepared by Method 3010 may be analyzed by FLAA or ICP for the following:

| | |
|-----------|------------|
| Aluminum | Magnesium |
| *Arsenic | Manganese |
| Barium | Molybdenum |
| Beryllium | Nickel |
| Cadmium | Potassium |
| Calcium | *Selenium |
| Chromium | Sodium |
| Cobalt | Thallium |
| Copper | Vanadium |
| Iron | Zinc |
| Lead | |

* Analysis by ICP

NOTE: See Method 7760 for the digestion and FLAA analysis of Silver.

1.3 This digestion procedure is not suitable for samples which will be analyzed by graphite furnace atomic absorption spectroscopy because hydrochloric acid can cause interferences during furnace atomization. Consult Method 3020A for samples requiring graphite furnace analysis.

2.0 SUMMARY OF METHOD

2.1 A mixture of nitric acid and the material to be analyzed is refluxed in a covered Griffin beaker. This step is repeated with additional portions of nitric acid until the digestate is light in color or until its color has stabilized. After the digestate has been brought to a low volume, it is refluxed with hydrochloric acid and brought up to volume. If sample should go to dryness, it must be discarded and the sample reprepared.

3.0 INTERFERENCES

3.1 Interferences are discussed in the referring analytical method.

4.0 APPARATUS AND MATERIALS

4.1 Griffin beakers - 150-mL or equivalent.

4.2 Watch glasses - Ribbed and plain or equivalent.

4.3 Qualitative filter paper or centrifugation equipment.

4.4 Graduated cylinder or equivalent - 100mL.

4.5 Funnel or equivalent.

4.6 Hot plate or equivalent heating source - adjustable and capable of maintaining a temperature of 90-95°C.

5.0 REAGENTS

5.1 Reagent grade chemicals shall be used in all tests. Unless otherwise indicated, it is intended that all reagents shall conform to the specifications of the Committee on Analytical Reagents of the American Chemical Society, where such specifications are available. Other grades may be used, provided it is first ascertained that the reagent is of sufficiently high purity to permit its use without lessening the accuracy of the determination.

5.2 Reagent Water. Reagent water will be interference free. All references to water in the method refer to reagent water unless otherwise specified. Refer to Chapter One for a definition of reagent water.

5.3 Nitric acid (concentrated), HNO_3 . Acid should be analyzed to determine levels of impurities. If method blank is < MDL, the acid can be used.

5.4 Hydrochloric acid (1:1), HCl . Prepared from water and hydrochloric acid. Hydrochloric acid should be analyzed to determine level of impurities. If method blank is < MDL, the acid can be used.

6.0 SAMPLE COLLECTION, PRESERVATION, AND HANDLING

6.1 All samples must have been collected using a sampling plan that addresses the considerations discussed in Chapter Nine of this manual.

6.2 All sample containers must be prewashed with detergents, acids, and water. Plastic and glass containers are both suitable. See Chapter Three, Step 3.1.3, for further information.

6.3 Aqueous wastewaters must be acidified to a pH of < 2 with HNO_3 .

7.0 PROCEDURE

7.1 Transfer a 100-mL representative aliquot of the well-mixed sample to a 150-mL Griffin beaker and add 3 mL of concentrated HNO_3 . Cover the beaker with

a ribbed watch glass or equivalent. Place the beaker on a hot plate or equivalent heating source and cautiously evaporate to a low volume (5 mL), making certain that the sample does not boil and that no portion of the bottom of the beaker is allowed to go dry. Cool the beaker and add another 3-mL portion of concentrated HNO_3 . Cover the beaker with a nonribbed watch glass and return to the hot plate. Increase the temperature of the hot plate so that a gentle reflux action occurs.

NOTE: If a sample is allowed to go to dryness, low recoveries will result. Should this occur, discard the sample and reprepare.

7.2 Continue heating, adding additional acid as necessary, until the digestion is complete (generally indicated when the digestate is light in color or does not change in appearance with continued refluxing). Again, uncover the beaker or use a ribbed watch glass, and evaporate to a low volume (3 mL), not allowing any portion of the bottom of the beaker to go dry. Cool the beaker. Add a small quantity of 1:1 HCl (10 mL/100 mL of final solution), cover the beaker, and reflux for an additional 15 minutes to dissolve any precipitate or residue resulting from evaporation.

7.3 Wash down the beaker walls and watch glass with water and, when necessary, filter or centrifuge the sample to remove silicates and other insoluble material that could clog the nebulizer. Filtration should be done only if there is concern that insoluble materials may clog the nebulizer. This additional step can cause sample contamination unless the filter and filtering apparatus are thoroughly cleaned. Rinse the filter and filter apparatus with dilute nitric acid and discard the rinsate. Filter the sample and adjust the final volume to 100 mL with reagent water and the final acid concentration to 10%. The sample is now ready for analysis.

8.0 QUALITY CONTROL

8.1 All quality control measures described in Chapter One should be followed.

8.2 For each analytical batch of samples processed, blanks should be carried throughout the entire sample-preparation and analytical process. These blanks will be useful in determining if samples are being contaminated. Refer to Chapter One for the proper protocol when analyzing blanks.

8.3 Replicate samples should be processed on a routine basis. A replicate sample is a sample brought through the whole sample preparation and analytical process. A replicate sample should be processed with each analytical batch or every 20 samples, whichever is greater. Refer to Chapter One for the proper protocol when analyzing replicates.

8.4 Spiked samples or standard reference materials should be employed to determine accuracy. A spiked sample should be included with each batch of samples processed and whenever a new sample matrix is being analyzed. Refer to Chapter One for the proper protocol when analyzing spikes.

8.5 The method of standard addition shall be used for the analysis of all EP extracts and delisting petitions (see Method 7000, Step 8.7). Although not

required, use of the method of standard addition is recommended for any sample that is suspected of having an interference.

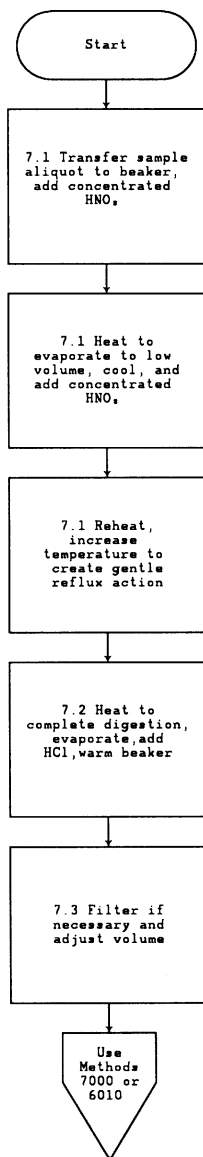
9.0 METHOD PERFORMANCE

9.1 No data provided.

10.0 REFERENCES

1. Rohrbough, W.G.; et al. Reagent Chemicals, American Chemical Society Specifications, 7th ed.; American Chemical Society: Washington, DC, 1986.
2. 1985 Annual Book of ASTM Standards, Vol. 11.01; "Standard Specification for Reagent Water"; ASTM: Philadelphia, PA, 1985; D1193-77.

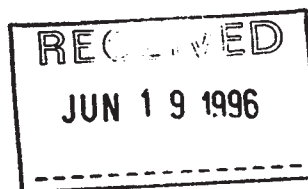
METHOD 3010A
ACID DIGESTION OF AQUEOUS SAMPLES AND EXTRACTS
FOR TOTAL METALS ANALYSIS BY FLAA OR ICP SPECTROSCOPY



Appendix E:
U.S. EPA approved (Hach) Methods



UNITED STATES ENVIRONMENTAL PROTECTION AGENCY
NATIONAL EXPOSURE RESEARCH LABORATORY
CINCINNATI, OH 45268



DATE: June 17, 1996

SUBJECT: Approved/Accepted Hach Methods

OFFICE OF
RESEARCH AND DEVELOPMENT

FROM: James W. O'Dell, Jr.
ATP Coordinator
Alternate Test Procedure Program
National Water Quality Assurance Programs Branch

TO: Addressee

This is in response to a number of requests concerning the approval/acceptance of Hach Company methods used for USEPA required compliance monitoring.

The following Hach methods are cited in Table 1A of 40 CFR Part 136.3 as approved for NPDES compliance monitoring.

| Parameter | Method | Approval Date |
|------------------------------|--------|----------------|
| Chemical Oxygen Demand (COD) | 8000 | April 21, 1980 |
| Copper--Total | 8506 | May 29, 1980 |
| Iron--Total | 8008 | June 27, 1980 |
| Manganese--Total | 8034 | June 14, 1979 |
| Nitrite (as N) | 8507 | May 1, 1979 |
| Zinc--Total | 8009 | May 29, 1980 |

The following Hach methods were reviewed by the Alternate Test Procedure (ATP) program and recommended as acceptable for NPDES compliance monitoring.

| Parameter | Method | Review Date |
|---------------------------------|--------|-------------------|
| Acidity, as CaCO ₃ | 8010 | February 17, 1983 |
| Ammonia, (as N) | 8038 | February 17, 1983 |
| Arsenic--Total | 8013 | February 17, 1983 |
| Biochemical Oxygen Demand (BOD) | 8043 | July 7, 1994 |
| Calcium--Total | 8222 | February 17, 1983 |
| Chemical Oxygen Demand (COD) | 8230 | December 24, 1985 |
| Chloride | 8224 | January 4, 1988 |
| Chloride | 8225 | December 3, 1987 |
| Chlorine--Total residual | 8167 | April 28, 1995 |
| Chlorine--Total residual | 8168 | February 17, 1983 |
| Chlorine--Total residual | 10014 | June 29, 1994 |
| Chromium VI dissolved | 8023 | February 17, 1983 |
| Fluoride--Total | 8029 | February 17, 1983 |
| Hardness--Total | 8226 | February 17, 1983 |
| Hydrogen Ion (pH) | 8156 | February 17, 1983 |

| | | |
|-----------------------------------|------|-------------------|
| Lead--Total | 8033 | May 27, 1987 |
| Nickel--Total | 8037 | December 4, 1985 |
| Oil and Grease--Total recoverable | 8005 | February 17, 1983 |
| Orthophosphate (as P) | 8048 | February 17, 1983 |
| Oxygen, Dissolved | 8157 | February 17, 1983 |
| Oxygen--Dissolved | 8229 | February 17, 1983 |
| Phenols | 8047 | January 5, 1987 |
| Phosphorous--Total | 8190 | February 17, 1983 |
| Residue--Nonfilterable (TSS) | 8158 | February 17, 1983 |
| Specific Conductance | 8160 | February 17, 1983 |
| Sulfate (as SO4) | 8051 | February 17, 1983 |
| Sulfide (as S) | 8131 | May 29, 1987 |
| Sulfite (as SO3) | 8071 | February 17, 1983 |

The following Hach methods were reviewed by the ATP program and recommended as acceptable for Drinking Water compliance monitoring.

| Contaminant | Method | Review Date |
|--------------|--------|-------------------|
| Conductivity | 8160 | February 17, 1983 |
| Fluoride | 8029 | February 17, 1983 |
| pH | 8156 | February 17, 1983 |

| Residual | Method | Review Date |
|----------------|--------|-------------------|
| Free Chlorine | 8021 | January 20, 1987 |
| Total Chlorine | 8167 | April 28, 1995 |
| Total Chlorine | 8168 | February 17, 1983 |
| Total Chlorine | 8370 | June 29, 1994 |

| Organism | Method | Review Date |
|----------------|--------|-------------------|
| Total Coliform | 8001 | February 17, 1983 |
| Fecal Coliform | 8001 | February 17, 1983 |

EPA approval/acceptance applies to the method version and reagent formulations specified at the time of review. Additional quality control procedures may be required to meet specific program monitoring requirements.

Addressees:

Arthur Clark, USEPA, Region I
 John Bourbon, USEPA, Region II
 Charles Jones, Jr., USEPA, Region III
 Wayne Turnbull, USEPA, Region IV
 Dennis Wesolowski, USEPA, Region V
 Charles Ritchey, USEPA, Region VI
 Doug Brune, USEPA, Region VII
 Rick Edmonds, USEPA, Region VIII
 Roscenne Sakamoto, USEPA, Region IX
 Bruce Woods, USEPA, Region X
 William Telliard, OW, OST
 Richard Reding, OGW & DW, TSD

Deliverable for Task 6:
Collection of samples for laboratory analyses

Submitted

to

**Carl Kochersberger
Environmental Science Bureau
Hazardous Materials and Asbestos Unit
Pod 4-1
New York State Department of Transportation
50 Wolf Road
Albany, NY 12232**

June 2013

ABSTRACT

In this report, results from conducting laboratory analyses on the paint waste collected are presented. To address disposal and management of paint waste, a number of leaching studies were employed. These studies included the United States Environmental Protection Agency (U.S. EPA) toxicity characteristic leaching procedure (TCLP), multiple extraction procedure (MEP), and sequential extraction procedure (SEP). X-ray diffraction (XRD) and field emission scanning electron microscopy (FESEM) were applied as well for assessing mineralogy and morphology. The TCLP results revealed metal leaching from less than 0.0005 (detection limit) to 1.46 mg L⁻¹ for Pb, less than 0.0007 (detection limit) to 9.52 mg L⁻¹ for Cr, and less than 0.0004 (detection limit) to 9.60 mg L⁻¹ for Ba. Concentrations observed were less than the toxicity characteristics (TC) levels with the exception of three samples exhibiting Cr concentrations greater than the TC of 5 mg L⁻¹. With 10 days of extraction in the MEP studies, the greatest leached concentrations were detected in the first day, and the metal release was reduced in the following days. Five of the 24 bridge paint samples revealed Pb concentrations were greater than the TC level of 5 mg L⁻¹, while other leached metals including Cr and Ba were much less than the TC levels (for Cr 5 mg L⁻¹ and Ba is 100 mg L⁻¹). SEP was conducted to better understand the phases metals are associated with in the paint waste. Lower fractions of Pb, Cr, and Ba were extracted in exchangeable and carbonate forms, while greater contributions of these metals were associated with iron oxides. Yet, the largest fraction, greater than 50%, was associated with the residual phase. FESEM along with energy dispersive x-ray analysis (EDX) revealed the surface morphology of the steel grit was consistent with iron oxide coatings. XRD further corroborated the presence of iron oxide minerals. Using the suite of analyses, iron oxides were observed to be important surfaces for controlling the degree of metal leaching from the paint waste.

TABLE OF CONTENTS

| | |
|--|-----|
| ABSTRACT _____ | ii |
| 1. Introduction _____ | 1 |
| 2. Leaching procedure and characterization techniques _____ | 2 |
| 3. Lab methodology _____ | 7 |
| 3.1 Quality assurance and quality control (QA/QC) procedures _____ | 7 |
| 3.2 Toxicity characteristic leaching procedure (TCLP) _____ | 7 |
| 3.3 Multiple extraction procedure (MEP) _____ | 8 |
| 3.4 Sequential extraction procedure (SEP) _____ | 10 |
| 3.5 X-ray diffraction (XRD) _____ | 14 |
| 3.6 Field emission scanning electron microscopy with energy dispersive x-ray analysis (FESEM/EDX) _____ | 14 |
| 4. Laboratory results and discussion _____ | 15 |
| 4.1 TCLP results _____ | 15 |
| 4.2 Multiple extraction procedure _____ | 31 |
| 4.3 Sequential extraction results _____ | 46 |
| 4.4 XRD results _____ | 52 |
| 4.5 FESEM/EDX analysis _____ | 60 |
| 5. Conclusions _____ | 64 |
| 6. References _____ | 67 |
| Appendix A TCLP, and MEP results for the 24 bridges _____ | 80 |
| Appendix B Material Safety Data Sheet for steel grit used in Region 10 _____ | 109 |
| Appendix C Solubility and speciation of RCRA metals as well as Fe and Zn _____ | 112 |
| Appendix D XRD analysis data _____ | 133 |

TABLE OF FIGURES

| | |
|---|----|
| Figure 1. Flow Chart of the TCLP Test procedure (Method 1311) (U. S. EPA, 1992)..... | 9 |
| Figure 2. Flow Chart of the MEP Test Procedure (Method1320) (U. S. EPA, 1986)..... | 11 |
| Figure 3. Leaching results from TCLP for Pb and Cr as a function of pH after 18 hours with 0.05 M ionic strength. Samples are extracted using Fluid #1 (0.1 N CH ₃ COOH, which has been adjusted with NaOH to an initial pH of 4.93 ± 0.05) or Fluid #2 (0.1 N CH ₃ COOH, which has an initial pH of 2.88 ± 0.05) based on the alkalinity of the waste material. | 16 |
| Figure 4. Leaching results from TCLP for Ba and Zn as a function of pH after 18 hours with 0.05 M ionic strength. Samples are extracted using Fluid #1 (0.1 N CH ₃ COOH, which has been adjusted with NaOH to an initial pH of 4.93 ± 0.05) or Fluid #2 (0.1 N CH ₃ COOH, which has an initial pH of 2.88 ± 0.05) based on the alkalinity of the waste material. | 17 |
| Figure 5. Leaching results from TCLP for Fe as a function of pH after 18 hours with 0.05 M ionic strength. Samples are extracted using Fluid #1 (0.1 N CH ₃ COOH, which has been adjusted with NaOH to an initial pH of 4.93 ± 0.05) or Fluid #2 (0.1 N CH ₃ COOH, which has an initial pH of 2.88 ± 0.05) based on the alkalinity of the waste material. | 18 |
| Figure 6. Schematic diagram of the pH-dependent charge on an amphoteric metal oxide surface (Haynes, 1982; Zhou and Haynes, 2010)..... | 23 |
| Figure 7. Potential – pH equilibrium diagram of iron or steel considering four concentrations of soluble species (10^0 , 10^{-2} , 10^{-4} , 10^{-6} M), four soluble species (Fe ³⁺ , Fe ²⁺ , FeO ₄ ²⁻ , HFeO ₂ ⁻), and corrosion material ferrihydrite [Fe(OH) ₃] at 298 K..... | 25 |
| Figure 8. Fe ²⁺ solubility in equilibrium with Fe(OH) ₂ and FeCO ₃ , CH ₃ COOH at 0.1 M, 298 K and open to atmosphere. All the speciation was computed using MINEQL ⁺ | 26 |
| Figure 9. Fe ³⁺ solubility in equilibrium with Ferrihydrite [Fe(OH) ₃], CH ₃ COOH at 0.1 M, 298 K and open to atmosphere. All the speciation was computed using MINEQL ⁺ | 27 |

| | |
|--|----|
| Figure 10. pH from MEP are shown as a function of 10 days of extractions. The first extraction is performed with a pH of 5.0 followed by the subsequent nine successive extractions using the initial pH of 3.0 ± 0.2 that simulate acid rain conditions..... | 32 |
| Figure 11. Leaching concentrations of Ba from MEP are shown as a function of pH. The first extraction is performed with a pH of 5.0 followed by the subsequent nine successive extractions using the initial pH of 3.0 ± 0.2 that simulate acid rain conditions. Toxicity characteristic Pb = 5 mg L^{-1} | 34 |
| Figure 12. Leaching concentrations of Pb from MEP are shown as a function of 10 days of extractions. The first extraction is performed with a pH of 5.0 followed by the subsequent nine successive extractions using the initial pH of 3.0 ± 0.2 that simulate acid rain conditions. Toxicity characteristic Pb = 5 mg L^{-1} | 35 |
| Figure 13. Leaching concentrations of Cr from MEP are shown as a function of pH. The first extraction is performed with a pH of 5.0 followed by the subsequent nine successive extractions using the initial pH of 3.0 ± 0.2 that simulate acid rain conditions. Toxicity characteristic Cr = 5 mg L^{-1} | 36 |
| Figure 14. Leaching concentrations of Cr from MEP are shown as a function of 10 days of extractions. The first extraction is performed with a pH of 5.0 followed by the subsequent nine successive extractions using the initial pH of 3.0 ± 0.2 that simulate acid rain conditions. Toxicity characteristic Cr = 5 mg L^{-1} | 37 |
| Figure 15. Leaching concentrations of Ba from MEP are shown as a function of pH. The first extraction is performed with a pH of 5.0 followed by the subsequent nine successive extractions using the initial pH of 3.0 ± 0.2 that simulate acid rain conditions. Toxicity characteristic Ba = 100 mg L^{-1} | 38 |
| Figure 16. Leaching concentrations of Ba from MEP are shown as a function of 10 days of extractions. The first extraction is performed with a pH of 5.0 followed by the subsequent nine successive extractions using the initial pH of 3.0 ± 0.2 that simulate acid rain conditions. Toxicity characteristic Ba = 100 mg L^{-1} | 39 |

| | |
|---|----|
| Figure 17. Leaching concentrations of Zn from MEP are shown as a function of pH. The first extraction is performed with a pH of 5.0 followed by the subsequent nine successive extractions using the initial pH of 3.0 ± 0.2 that simulate acid rain conditions. | 40 |
| Figure 18. Leaching concentrations of Zn from MEP are shown as a function of 10 days of extractions. The first extraction is performed with a pH of 5.0 followed by the subsequent nine successive extractions using the initial pH of 3.0 ± 0.2 that simulate acid rain conditions..... | 41 |
| Figure 19. Leaching concentrations of Fe from MEP are shown as a function of pH. The first extraction is performed with a pH of 5.0 followed by the subsequent nine successive extractions using the initial pH of 3.0 ± 0.2 that simulate acid rain conditions. | 42 |
| Figure 20. Leaching concentrations of Zn from MEP are shown as a function of 10 days of extractions. The first extraction is performed with a pH of 5.0 followed by the subsequent nine successive extractions using the initial pH of 3.0 ± 0.2 that simulate acid rain conditions..... | 43 |
| Figure 21. Mass balances of selective sequential extraction fractions for Pb, Cr, Zn, and Ba. | 48 |
| Figure 22. XRD analysis of the possible minerals in paint samples from Regions 3, 5, 10, and 11. | 53 |
| Figure 23. XRD patterns of lead and chromium in paint samples from Regions 3, 10, and 11. ... | 55 |
| Figure 24. XRD patterns of iron and iron oxide in paint waste samples from Region 5..... | 57 |
| Figure 25. Schematic representation of formation and transformation pathways of common iron oxides, together with the approximate transformation conditions (Schwertmann and Cornell, 1991; Jambor and Dutrizac, 1998)..... | 59 |
| Figure 26. FE-SEM images and EDX mapping on the paint waste sample. (a) FE-SEM image; (b) Blue particles represent the steel grit; green particles present the paint in the paint waste; (c) EDX mapping on paint waste sample from Region 7 (color images in mapping represent the corresponding elements). | 61 |
| Figure 27. FE-SEM images on the steel grit surface of the paint waste sample from Region 7. . | 63 |

LIST OF TABLES

| | |
|--|----|
| Table 1. Chemical Extraction Protocol (Rauret et al., 1999)..... | 13 |
| Table 2. TCLP (mg L^{-1}) results from Lead-Based Paint (LBP) or other waste studies..... | 19 |
| Table 3. Zero point of charge (ZPC) for different iron oxides | 29 |
| Table 4. Semi- quantitative information from using XRD analysis on paint waste samples. | 54 |
| Table 5. Typical pigment and associated compounds in liquid paints ^a | 62 |

1. Introduction

Lead and chromium based pigments along with other metals have been used in paint coatings for protecting bridges from corrosion between 1950 and 1980 (Federal Highway Administration [FHWA], 1989). The resulting paint waste generated during paint removal is a significant issue for New York State Department of Transportation. Although magnetic separation is used on the paint waste, a fraction of abrasive blasting material remains. In New York, steel grit is typically used as the blasting abrasive (Kochersberger, 2011). Other abrasives used throughout the country include black beauty (a mixture of Fe oxide, Al oxide, Ca oxide, and silicon dioxide), boiler slag, sand, furnace slag, aluminum oxide, and garnet (Minnesota Department of Transportation [MnDOT], 2004; Iowa Department of Transportation [IADOT], 2009; United States Environmental Protection Agency [U.S. EPA], 1997). A hypothesis in this work is that the fraction of steel grit remaining affects the leaching behavior of trace metals in paint waste, and consequently changes the hazardous nature of the waste. A number of studies (Appleman, 1992; Smith, 1993; Bernecki et al., 1995; Kendall; 2003) observed reduced leaching in the presence of iron-based abrasive material. However, there has been no systematic study to investigate the mechanism responsible for leaching when abrasive blasting material, steel grit, is present. Because the paint waste will not be pretreated before disposal in landfill, it is necessary to assess the potential risk of the waste. Therefore, the purpose of this study is to evaluate metal leachability, the forms metals are associated with, and the mechanism(s) responsible for reduced leaching. The results obtained can be used for understanding transport of lead and other metals in paint waste as well as in developing a model to simulate and predict metal leachability.

In this project, the U.S. EPA standard method toxicity characteristic leaching procedure (TCLP) was applied to characterize the paint waste as hazardous or not. Long-term mobility of

trace metals was then evaluated with the U.S. EPA multiple extraction procedure (MEP). Sequential extraction procedure (SEP) was conducted to investigate the phases metals are associated with in the paint waste. X-ray diffraction (XRD) and field emission scanning electron microscopy with energy dispersive x-ray analysis (FESEM/EDX) were applied to further identify phases in the paint waste. Overall, results from these studies support the delineation of possible mechanisms responsible for metal mobility observed in the leaching procedures.

2. Leaching procedure and characterization techniques

The U.S. EPA standard leaching test for characterizing whether a waste is hazardous involves applying the TCLP (U.S. EPA, 1992). This procedure is used to simulate landfill conditions where the pH is lowered and volatile fatty acids (acetic acid, propionic acid, and butyric acid) (Martel et al., 1997) are generated. However, a number of studies (U. S. EPA, 1991; Smith, 1993; Bernecki et al., 1995) have reported that the presence of iron reduced the degree of metal leaching from paint waste. Smith (1993) reported TCLP (U.S. EPA, 1992) results from lead-based paints (LBP) where leached concentrations of Pb averaged 70 mg L^{-1} . After the steel grit was physically added, results from the TCLP revealed concentrations reduced to less than 5 mg L^{-1} (U.S. EPA, 1992). In another study, Bernecki et al. (1995) reviewed the practice of using iron containing abrasive in stabilizing paint waste. They found that in the presence of iron blasting material, leachable lead concentrations were less than 0.1 mg L^{-1} using TCLP procedure, while Pb concentrations in the waste ranged from 996 to $1,280 \text{ mg kg}^{-1}$. Sand, steel grit, steel shot, aluminum oxide, and Black Beauty are widely used abrasives. Because of the incomplete separation process, these abrasive materials remained in the paint waste. Many researchers have investigated the metal leaching behavior from sediment, soil, fly ash, and foundry sand wastes, in the presence of steel slag, blast furnace slag, red mud, and other iron-

containing materials (Ciccu et al., 2003; Feng et al., 2004; Brunori et al., 2005a; Cornelis et al., 2008; Komarek et al., 2013). However, there has been no systematic study to assess the leaching behavior of paint waste in the presence of abrasive materials. In New York State during the paint removal procedure, recycled steel grit is applied as blasting material (Kochersberger, 2011). Although contractors use a magnetic separation process to remove steel grit from the paint waste, the blasting abrasive agent is not entirely separated. The steel grit remaining with the waste is reported to be the smallest size fraction (Feliciano, 2011). The presence of steel grit (iron) can affect the leaching of metals, where concentrations are reduced to less than the toxicity characteristic (TC) level. To address the long-term mobility of the metals and associated metalloids in the paint wastes, other leaching tests were considered.

MEP (U.S. EPA, 1986) was designed to simulate leaching of waste from repetitive events of acid rain in a landfill. The method is intended to simulate 1,000 years of freeze and thaw cycles and prolonged exposure to a leaching medium. This method involves an initial extraction with an acetic acid (CH_3COOH) solution (the pH of the solution maintained less than 5 through addition of 0.5 N CH_3COOH) (Method 1310B) (U. S. EPA, 2004) and then at least nine successive extractions with a synthetic acid rain solution (sulfuric/nitric acid [$\text{H}_2\text{SO}_4/\text{HNO}_3$] adjusted to an initial pH 3). Each extraction is conducted for 24 hours under completely mixed conditions. The repetitive extractions reveal the leachable concentrations in a simulated natural environment. One advantage of the MEP over the TCLP is that the MEP gradually removes excess alkalinity in the waste. Therefore, the leaching behavior of metal contaminants can be evaluated as a function of decreasing pH, which increases the solubility and mobility of metal cations.

A limitation of the MEP method is the lack of the mechanistic information on how the metal contaminant is associated with the solid. In a number of studies, the MEP test has been applied to

investigate the long-term mobility of the waste. Esakku et al. (2008) assessed the leaching potential of select metals comparing total acid digestion (AD) with the MEP, TCLP, and a Canadian equilibrium leach test (ELT) (Environmental Canada and Alberta Environmental Centre [ECAEC], 1986). Results from the MEP approach revealed that leaching increased one to two orders of magnitude as compared to the TCLP. In addition, the extraction efficiency decreased in the following order: MEP > TCLP > ELT. To assess the toxicity and long-term stability, Shanmugamathan et al. (2008) conducted the TCLP and MEP on copper slag samples from an Indian copper plant. Results revealed that although the leachable metal concentrations (Pb and Zn) from the MEP test are greater than those from TCLP, the leached concentrations over the nine extraction cycles did not exceed the TC levels for the target metals. Based on these results, Shanmugamathan et al. concluded that the metals in the slag are not labile and would not be expected to leach under acid rain conditions.

While MEP and TCLP simulate leaching under landfill conditions, SEP subjects a sample to an extractant where a phase is dissolved. This extraction provides an estimate of the potential phases metals may be associated within the system (Tessier et al., 1979; Quevauviller, 1998; Filgueiras et al., 2002). SEP was developed in the 1970s for studying metal behavior (Gibbs, 1973; McLaren and Crawford, 1973a; Shuman, 1979; Stover et al., 1976; Tessier et al., 1979). The number of steps and operationally defined phases in SEP schemes vary between three (Quevauviller et al., 1994; Rauret et al., 1999; Silviera and Sommers, 1977) and nine (Krishnamurti and Naidu, 2000, 2002; Miller et al., 1986b; Heron et al., 1994) according to preferences and purpose. One of the more commonly used procedures (Tessier et al., 1979) isolates how the metal is associated with the specific phases. Five fractions of increasing stability are isolated in the procedure: ion exchangeable, carbonates, sorption to iron and manganese

oxides, bound to organic matter, and residuals, with estimated uncertainties up to 10%. However, the limitation for Tessier et al. (1979) protocol is that metal sulfide analysis is not included in the extraction (Peltier et al., 2005; Hass and Fine, 2010). Another issue is that specifically adsorbed metals can be extracted in the carbonate step (Tessier et al., 1979; Ma and Uren, 1995; 1998). Another procedure is the BCR, which was developed to provide an internationally accepted SEP protocol by the Commission of the European Communities Bureau of Reference (Quevauviller et al., 1996; Quevauviller et al., 1998). The procedure isolates three metal fractions, acid extractable (exchangeable and bound to carbonates), reducible (bound to iron and manganese oxides), and oxidizable (bound to sulfides and organics) (Rauret et al., 1999; Kartal et al., 2006). The second extraction step was later amended (Rauret et al., 1999) to improve the extraction efficiency of the refractory, crystalline oxyhydroxides by raising the concentration of $\text{NH}_2\text{OH-HCl}$ to 0.5 M, and by adding more acid (Rauret et al., 1999). Sutherland and Tack (2002) found uncertainty in an optimized BCR procedure is typically 15%. The main difference between Tessier and BCR is that the former was designed to extract elements from specific phases including exchangeable, carbonates, hydroxides, and organic matter. The BCR method was not designed to attack specific phases, but rather to examine the potential for trace metal release under environmental conditions (ion exchange, reduction, and oxidation) (Kersten et al., 1997; Ho and Evans, 2000; Perez et al., 2008; Díaz-de Alba et al., 2011). Many researchers applied three-step BCR procedure to evaluate the metal association in the sediment, soil, and waste in the presence of iron oxides (Ariza et al., 2000; Tokalioglu et al., 2003; Ryan et al., 2008). To compare the results with these studies, the extractions were conducted with the modified BCR procedure (Rauret et al., 1999). To further investigate the phases in the paint waste and metal association with the steel grit, characterization techniques are considered.

Characterization techniques such as XRD and FESEM/EDX have been widely used to investigate mineralogy, surface morphology, and surface composition. Recently, many researchers have applied XRD and FESEM to identify the minerals and pigments in paint or historical paintings (Serifaki et al., 2009; Shi et al., 2011; Bonneau et al., 2012). For example, Serifaki et al. (2009) used XRD, SEM/EDX, thermo-gravimetric analysis (TGA), and laser induced breakdown spectroscopy (LIBS) for historic oil paintings characterization. They found that the paintings were composed of very thin binding and white priming layers on which the pigments were applied. Pigments used in paintings were mainly composed of green earth and red chrome. In addition, XRD is an effective tool to identify the presence of iron oxide minerals present at concentrations greater than 2% (Komárek et al., 2013; Davranche and Bollinger, 2000; Porsch et al., 2010; Johnston et al., 2010; Das and Hendry, 2011). Combined with XRD, FESEM was applied to identify the form of iron oxide on the surface of the steel grit and better understand the surface composition and surface morphology, which is a function of the surface coatings.

In summary, a systematic study is important in investigating mechanisms responsible for leaching when abrasive blasting material, steel grit, is present. Although the presence of steel grit may affect the leaching behavior of the paint waste and consequently reduce the metal leaching, long-term mobility of metals from paint waste has not been fully evaluated yet. Coupled with leaching studies, SEP can further describe the phases metals are associated with in paint waste. XRD and FESEM-EDX are effective tools to identify the presence of iron oxide minerals on the surface. Therefore, in this study a suite of analyses of TCLP, MEP, SEP, XRD, and FESEM-EDX are applied. In the next section, lab methodology is presented and followed by the associated results and discussion.

3. Lab methodology

3.1 Quality assurance and quality control (QA/QC) procedures

QA/QC procedures are based on Standard Methods for the Examination of Water and Wastewater (Eaton et al., 2005) as well as on the American Society for Testing and Materials (ASTM, 1990) methods. Milli-Q Type II de-ionized water was employed in all experiments. All reagents were of certified analytical grade or trace metal quality. Glassware, plastic-ware, and associated materials were washed initially with a detergent and rinsed with tap water and then with deionized water. For all studies, containers were soaked in a 10% HNO₃ solution for 48 hours when using glassware and 24 hours for Nalgene[®] HDPE high-density polyethylene containers. Subsequently, all material was rinsed in de-ionized water and stored in a particle-free environment. Paint samples were collected from bridge locations determined in the field. Tools were cleaned following QA/QC procedures. For each sample, new powder-free latex gloves (acid resistant) were worn to prevent cross contamination. Samples were stored in coolers maintained at a temperature of 4°C.

3.2 Toxicity characteristic leaching procedure (TCLP)

The U.S. EPA (1992) TCLP is conducted to determine whether a waste is classified as hazardous or not. Because the blasting machine is used during the paint removal procedure, the particle size of the paint waste is less than 9.5 mm. Neither crushing nor grinding is needed for the waste sample. The test is performed in triplicate following Method 1311 of the U.S. EPA SW-846 (U.S. EPA, 1992) (Figure 1). Based on the alkalinity of the waste material, extraction Fluid #1 (0.1 N acetic acid [CH₃COOH], which has been adjusted with NaOH to a pH of 4.93 ± 0.05) or Fluid #2 (0.1 N CH₃COOH, which has a pH of 2.88 ± 0.05) was used in the procedure.

Extractions were carried out with 75 grams of sample and 1.5 L of extraction fluid (20:1 extraction fluid to solid ratio) in 2 L HDPE bottles at 30 ± 2 rpm. After the standard 18 ± 2 hr leaching period, the pH was measured and a 30 mL sample was withdrawn through an acid washed $0.7 \mu\text{m}$ borosilicate filter, acidified to less than pH 2, and stored in closed Nalgene® bottles under refrigeration at 4°C until inductively coupled plasma mass spectrometry (ICP-MS) analysis (Method 6020A; U.S. EPA, 2007) was conducted for the eight Resource Conservation and Recovery Act (RCRA) metals along with Fe and Zn. Results are compared TC concentrations to determine classification of the solidified/stabilized waste. In this study, initially, only the TCLP method was considered for leachability analysis for this project. However, because the presence of iron, which is common in bridge paint waste, appears to interfere with the leaching of lead, additional analyses were conducted on the samples to investigate long-term mobility. Specifically, the number of total samples analyzed for TCLP was computed using the number of samples from the bridge multiplied by the number of bridges multiplied by three as conducted in triplicate: $5 \times 4 \times 3 + 4 \times 4 \times 3 + 1 \times 16 \times 3 = 156$.

3.3 Multiple extraction procedure (MEP)

To investigate the long-term mobility of metals from paint waste, the multiple extraction procedure (MEP) (U.S. EPA, 1986) has been applied. MEP is designed to simulate leaching of waste from repetitive events of acid rain in a landfill. In the interest of generating the most significant impacts from the five paint samples collected from each bridge, the sample with the greatest lead concentration was used. The total concentration of each metal was determined with the field portable x-ray fluorescence (FP-XRF) (Method 6200; U.S. EPA, 1998). The test was

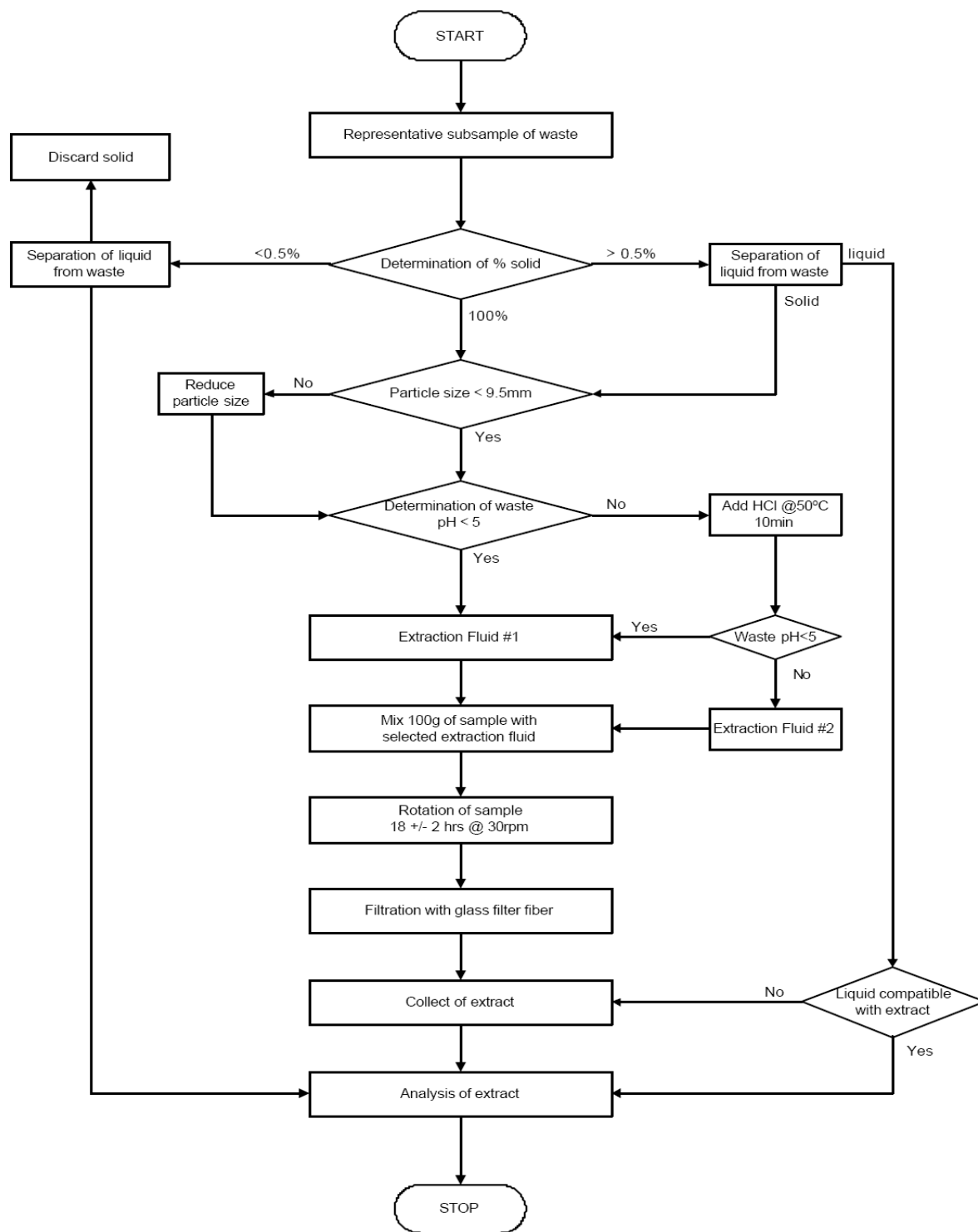


Figure 1. Flow Chart of the TCLP Test procedure (Method 1311) (U. S. EPA, 1992).

performed in duplicate following Methods 1310B and 1320 of the U.S. EPA SW-846 (U.S.EPA, 1986; U.S. EPA, 2004) (Figure 2). Specifically, MEP was conducted on duplicate samples from each of the 24 bridges with an extraction period of 10 days where samples were collected once every 24 hours resulting in $10 \times 24 \times 2 = 480$ samples. The first extraction procedure was carried out with 10 grams of sample and 160 ml of de-ionized water open to the atmosphere in 250 ml HDPE bottles. The pH of the solution was maintained less than 5 through addition of 0.5 N CH_3COOH (and the solution was adjusted to 20:1 extraction fluid to solid ratio accordingly). After the standard 24 hr leaching period, the pH was measured and the sample was withdrawn through an acid washed $0.45 \mu\text{m}$ filter. Filtrate was then acidified to less than pH 2 and stored in HDPE bottles under refrigeration at 4°C until ICP-MS analysis is conducted for the eight RCRA metals along with Zn. Remaining solids collected on the filter were used for successive extractions that simulate acid rain conditions (Method 1320) (U. S. EPA, 1986). Each extraction was carried out with the remaining solids from the previous extraction and the synthetic acid rain solution (20:1 extraction fluid to solid ratio) in 250 ml HDPE bottles. The initial pH of this solution was 3.0 ± 0.2 adjusted by addition of a 60/40 weight percent mixture of sulfuric and nitric acids ($\text{H}_2\text{SO}_4/\text{HNO}_3$) to de-ionized water. Analysis was carried out on the filtrates. If the concentration of any constituent of concern increases from the 8th to the 9th extraction, the procedure would be repeated until the concentration decreases.

3.4 Sequential extraction procedure (SEP)

The SEP was used in this study to understand the phases metals are associated with in paint waste samples. The extractions were conducted with the modified three-step sequential

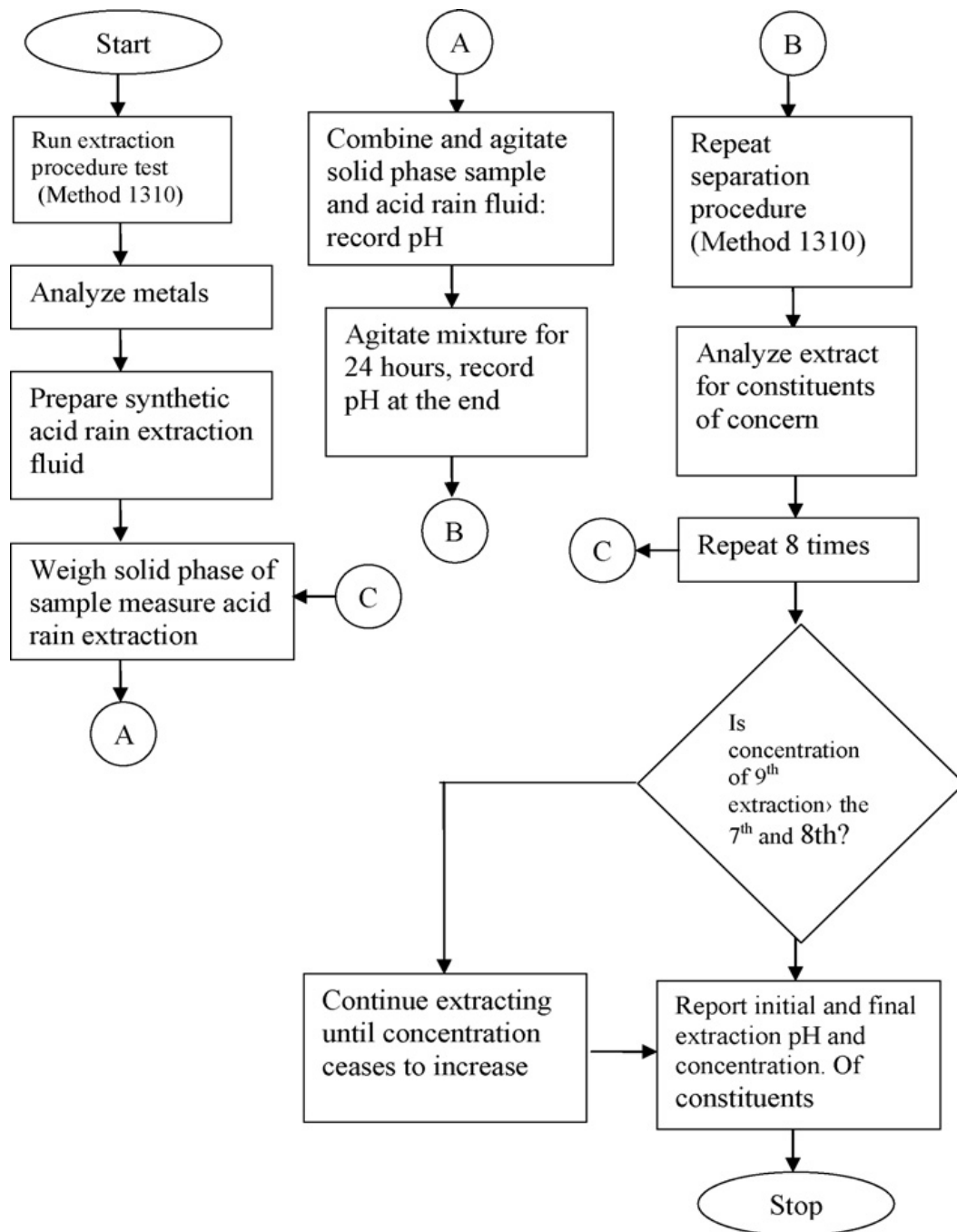


Figure 2. Flow Chart of the MEP Test Procedure (Method1320) (U. S. EPA, 1986).

extraction procedure proposed by the Commission of the European Communities Bureau of Reference (BCR) of the Standards, Measurements and Testing (SM&T) Programme (Rauret et al., 1999). Specifically, extractions were performed in 40 ml Sorvall® polypropylene centrifuge tubes using an end-over-end shaker rotated at 30 rpm. Between successive extractions, separation of extract from residue was carried out by centrifugation at 3,000g for 20 min. The supernatant was decanted into Naglene® HDPE bottles, acidified to pH less than 2, and refrigerated until analysis with ICP-MS. The residues were washed with 20 mL of deionized water, centrifuged for 20 min, and the supernatant discarded. In Step 1 (Table 1), extraction for exchangeables and carbonates involved 0.11 M acetic acid solution (CH_3COOH), while in Step 2 a 0.5 M hydroxylammonium chloride ($\text{NH}_2\text{OH}\cdot\text{HCl}$) and 0.05 M HNO_3 solution were used to extract adsorbed to iron and manganese oxide phases from remaining residue. In Step 3, residue from Step 2 was treated at 85 ± 2 °C with two sequential 10 ml portions of 30% H_2O_2 adjusted to pH 2 with HNO_3 , and then extracted with 1.0 M ammonium acetate ($\text{CH}_3\text{COONH}_4$) solution at $\text{pH } 2.0 \pm 0.1$. This step in the extraction is used for isolating the organic and sulfide fraction. The concentration associated with the residue from Step 3 was calculated using a mass balance along with concentrations found in Steps 1, 2, and 3 and the initial total concentration from FP-XRF. The residual is assumed to represent the metals associated with minerals in the paint (SiO_2 , TiO_2 , and Al), steel grit (iron) in the waste, or various constituents in the pigment matrix more difficult to digest (Barnes and Davis, 1996; Hass and Fine, 2010).

To further investigate the phases in the paint waste, XRD and FESEM-EDX was applied to evaluate the mineralogy, morphology, and surface composition.

Table 1. Chemical Extraction Protocol (Rauret et al., 1999)

| | Phases denominations | Reagents |
|-----|-----------------------------|--|
| I | Exchangeable and Carbonates | 0.11 M CH ₃ COOH |
| II | Iron and manganese oxides | 0.5 M NH ₂ OH•HCl , 0.05 M HNO ₃ |
| III | Sulfide and organic matter | HNO ₃ (0.02 M), H ₂ O ₂ (30%), NH ₄ OAc (3.2 M) |

3.5 X-ray diffraction (XRD)

Mineralogy was assessed with PANalytical Empyrean XRD system with detection limit of approximately 1% (by weight) (Quinn, 2013). Primary minerals in the paint waste were evaluated in this analysis. In the interest of assessing minerals of Pb and Cr in the paint waste and iron oxides formed on the steel grit surface, samples with the greatest concentrations of Pb, Cr, and Fe were used. The paint waste samples were placed in the sample holder with the back filling technique. Diffraction data was obtained by step-scans using Cu K- α radiation generated at 45 kV and 40 mA, scanning from 10° to 100° 2 θ . The (hkl) values corresponding to various peaks were calculated and compared with the standard powder diffraction file (PDF) (JCPDS, 1998).

3.6 Field emission scanning electron microscopy with energy dispersive x-ray analysis (FESEM/EDX)

Scanning electron microscopy (SEM) is used to visualize objects larger than 1 μ m, while FESEM has a higher resolution of 2.5 nm at 5 kV (1.2 nm at 20 kV; 3 nm at 1 kV). Because iron oxides occur as nano-sized materials, FESEM was applied for this study. The LEO 1530 FESEM equipped with an energy dispersive X-ray micro analyzer EDX (Inca series 200) was utilized to investigate the morphology and metal association with the steel grit in the paint waste. For the FESEM, samples were coated under high vacuum with a layer of carbon using an Edward's 12E6/1266 coating unit. Uncoated samples were prepared for EDX analysis to investigate the surface composition of the steel grit such as Fe, O, and C.

4. Laboratory results and discussion

4.1 TCLP results

Leached concentrations of Pb, Cr, Ba, Fe, and Zn were observed (Figures 3 and 4) in the TCLP extracts, while the other metals and metalloids analyzed, As, Se, Cd, Ag, and Hg, were not routinely detected (Appendix A; Table A1). Specifically, the TCLP results (Figures 3 and 4) revealed that leached metal concentrations in the extracts ranged from less than 0.0005 (detection limit) to 1.46 mg L⁻¹ for Pb, less than 0.0007 (detection limit) to 9.52 mg L⁻¹ for Cr, and less than 0.0004 (detection limit) to 9.60 mg L⁻¹ for Ba. Concentrations observed were less than the TC levels (for Pb 5 mg L⁻¹, Cr 5 mg L⁻¹, and Ba 100 mg L⁻¹), with the exception of three samples exhibiting Cr concentrations greater than the TC of 5 mg L⁻¹ (U. S. EPA, 1992). These results were much lower than the other similar studies (Table 2), where leaching was observed as great as 900 mg L⁻¹ for Pb and up to 44.7 mg L⁻¹ for Cr (Table 2) (Boy et al. 1995; Martel et al. 1997; U.S. EPA 1998; Halim et al. 2003; Wadanambi et al. 2008). The reduced concentrations can be attributed to the remaining steel grit in the paint waste. Elevated Zn concentrations in the extracts were observed from 20.4 to 1307 mg L⁻¹ (0.02 M) (Figure 4), while leached Fe ranged from 183 to 3,275 mg L⁻¹ (0.06 M) (Figure 5). These concentrations were greater than the other studies (Jessop and Turner, 2011; Kendall, 2003). With increasing usage of zinc primer (ZnO, Zn₃(PO₄)₂·2H₂O, and epoxy zinc rich primer) (80% zinc content dry) (Lambourne and Strivens, 1999) and steel grit (Kendall, 2003) remaining in the paint waste, elevated concentrations would be expected.

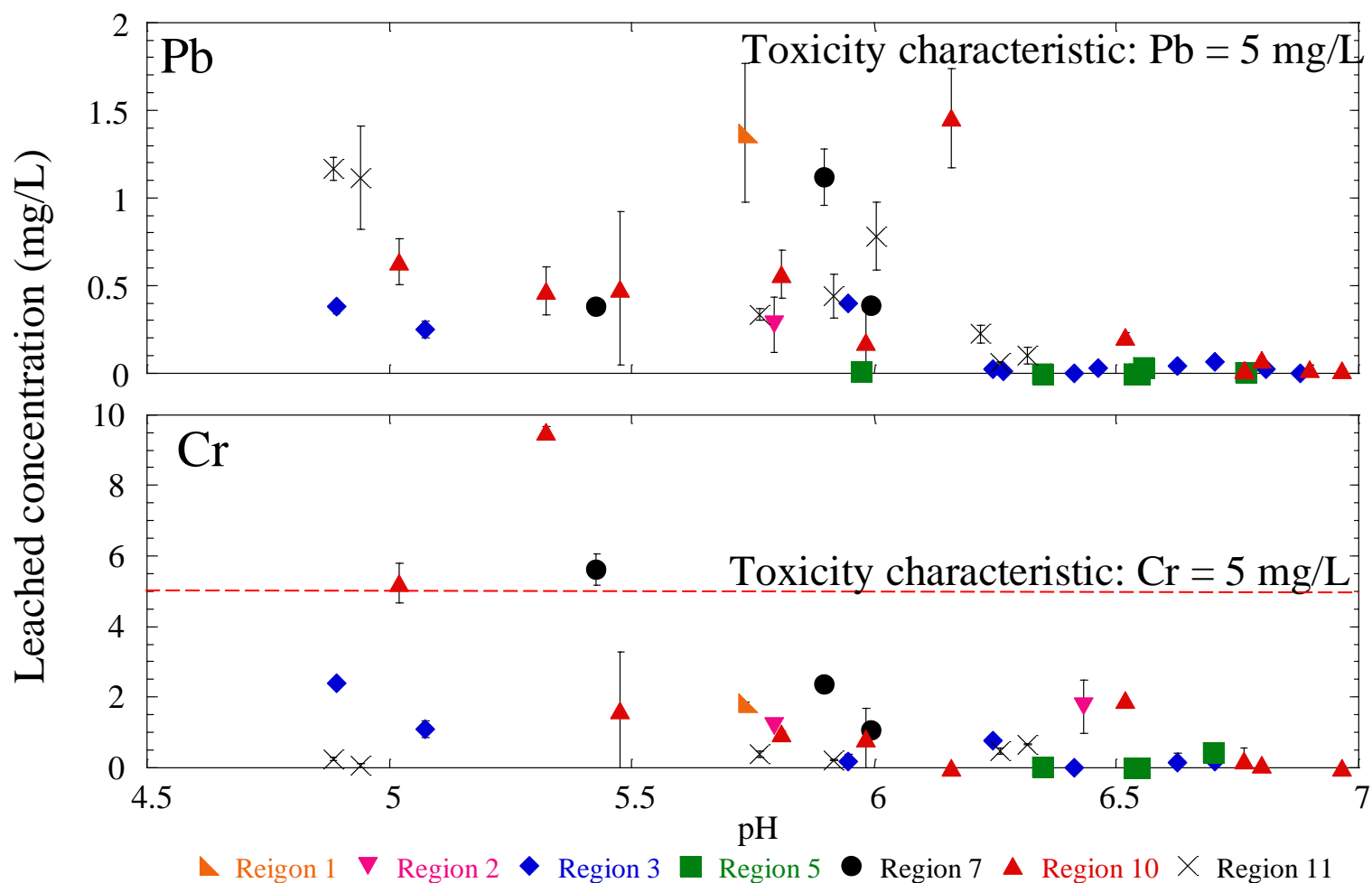


Figure 3. Leaching results from TCLP for Pb and Cr as a function of pH after 18 hours with 0.05 M ionic strength. Samples are extracted using Fluid #1 (0.1 N CH₃COOH, which has been adjusted with NaOH to an initial pH of 4.93 ± 0.05) or Fluid #2 (0.1 N CH₃COOH, which has an initial pH of 2.88 ± 0.05) based on the alkalinity of the waste material.

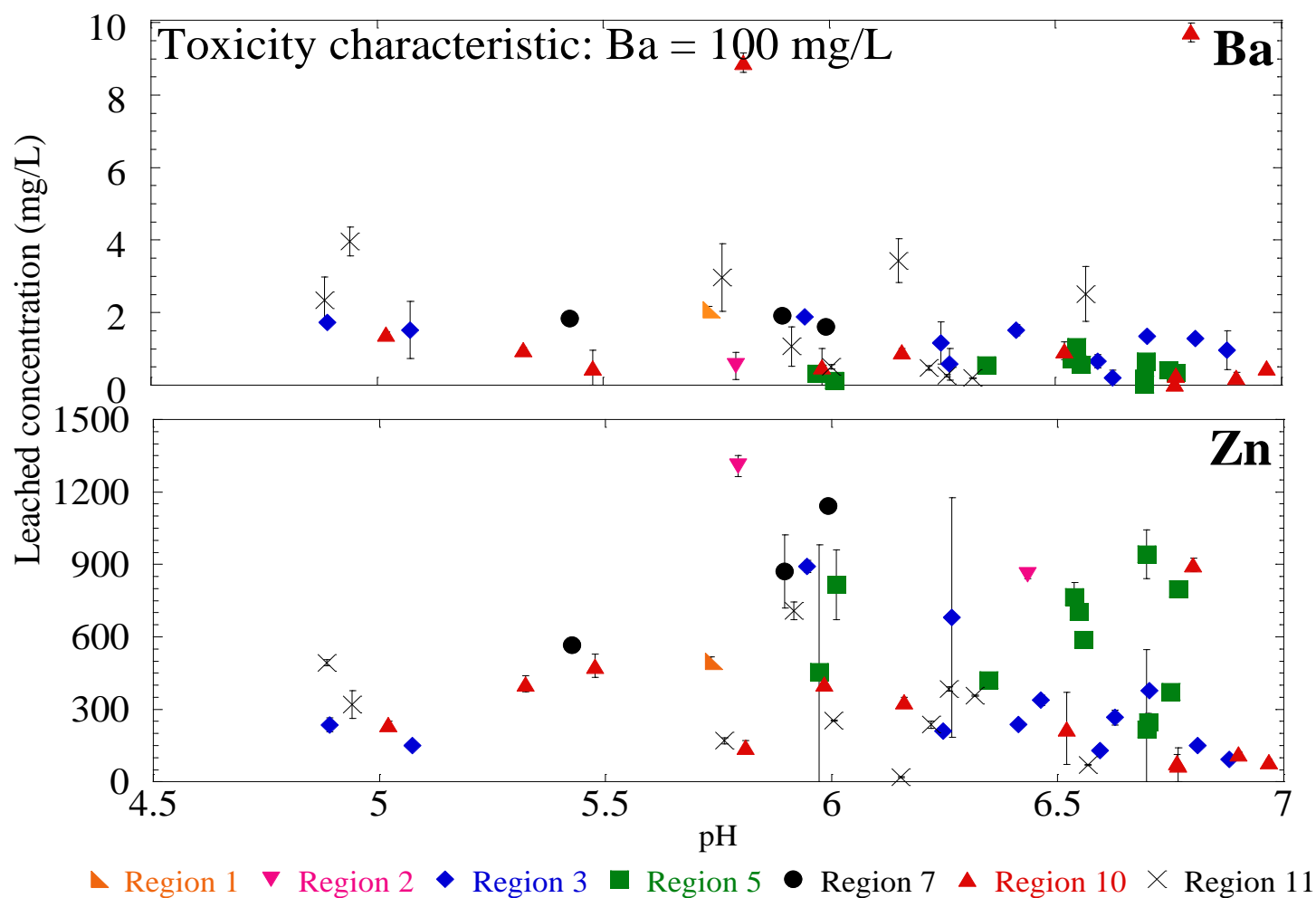


Figure 4. Leaching results from TCLP for Ba and Zn as a function of pH after 18 hours with 0.05 M ionic strength. Samples are extracted using Fluid #1 (0.1 N CH_3COOH , which has been adjusted with NaOH to an initial pH of 4.93 ± 0.05) or Fluid #2 (0.1 N CH_3COOH , which has an initial pH of 2.88 ± 0.05) based on the alkalinity of the waste material.

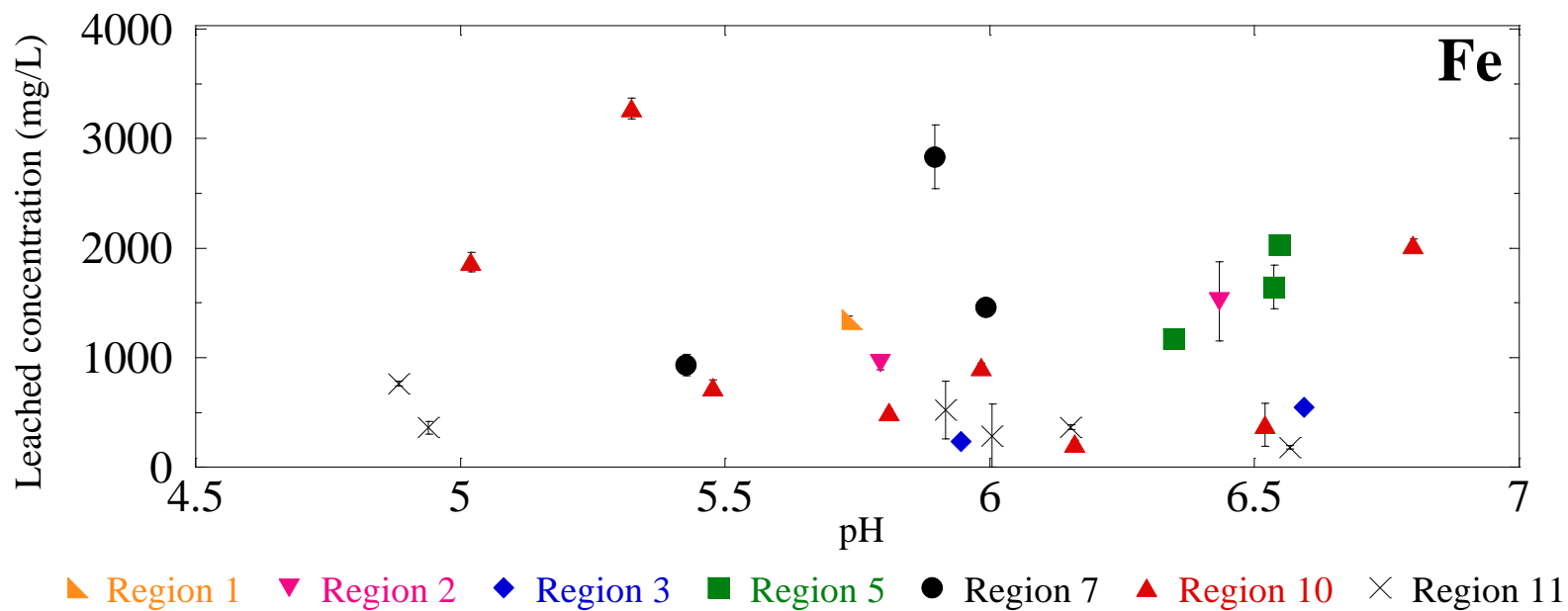


Figure 5. Leaching results from TCLP for Fe as a function of pH after 18 hours with 0.05 M ionic strength. Samples are extracted using Fluid #1 (0.1 N CH_3COOH , which has been adjusted with NaOH to an initial pH of 4.93 ± 0.05) or Fluid #2 (0.1 N CH_3COOH , which has an initial pH of 2.88 ± 0.05) based on the alkalinity of the waste material.

Table 2. TCLP (mg L⁻¹) results from Lead-Based Paint (LBP) or other waste studies.

| Sample | As | Ba | Cr | Cd | Pb | Hg | Ag | Se | Zn | Fe | reference |
|---|--------------|-------------|---------------|-------------|-------------|------|--------|-------|------------|------------|-------------------------|
| Paint wastes associated with plastic media | <0.11 – 0.14 | 0.55 – 0.74 | 16.32 – 44.73 | 1.35 – 5.15 | <0.066 | <0.1 | <0.016 | <0.18 | – | – | Boy et al. (1995) |
| LBP | – | – | – | – | 28.3 – 36.7 | – | – | – | – | – | Martel et al. (1997) |
| LBP debris | | | | | 0.05 – 72.8 | | | | | | U.S. EPA (1998) |
| Cementations wastes | – | – | – | BDL – 600 | BDL – 900 | – | – | – | – | – | Halim et al. (2003) |
| LBP | – | – | – | – | 205 – 587 | – | – | – | – | – | Wadanambi et al. (2008) |
| Paint waste with stabilizer | | | | | 0.2 – 52 | | | | | | Daniels et al.(2001) |
| Waste foundry sand associated with hydrous ferric oxide HFO | | | | | 0.4 – 9.0 | | | | 132–141 | BDL – 213 | Kendall (2003) |
| Paint waste associated with steel grit* | BDL | BDL – 9.6 | BDL – 9.52 | BDL | BDL – 1.46 | BDL | BDL | BDL | BDL – 1307 | BDL – 3275 | This study |
| BDL refers to below detection limit | | | | | | | | | | | |
| – refers to not reported | | | | | | | | | | | |
| *Detection limits (mg L ⁻¹) for this study: As = 0.0007, Ba = 0.0004, Cd = 0.0005, Cr = 0.0007, Pb = 0.0005, Se = 0.0002, Ag = 0.0003, Fe = 0.0025, Zn= 0.001, Hg=0.000002. | | | | | | | | | | | |

Several studies (Appleman, 1992; Smith, 1993; Bernecki et al., 1995; Kendall, 2003) have reported that the presence of iron greatly reduced leaching of metals from paint (Appleman, 1992; Smith, 1993; Bernecki et al., 1995) and other wastes (Kendall, 2003; Cornelis et al., 2008; Komarek et al., 2013). An example of this effect has been observed in a number of studies including one from 1992, in removal of lead-based paint from two bridges located in North Carolina (Bernecki et al., 1995). For one bridge, 10% (by weight) of steel grit was used in the abrasive blasting media (non-iron containing abrasive) while no steel was added to the blasting media (non-iron containing abrasive) for the second bridge. The debris generated from the former bridge contained 0.3 % to 3.7% total lead, but the TCLP leachate revealed only 0.3 to 6.3 mg L⁻¹. The debris where steel was not added in the blasting media (non-iron containing abrasive) contained between 0.5 and 1.5% total lead with leached concentrations ranging between 124 and 202 mg L⁻¹. Bernecki et al. (1995) reviewed the practice of using iron as an additive in stabilizing paint waste. They found that in the presence of iron blasting material, lead (996 to 1280 mg kg⁻¹) remained associated with the paint debris, with leachable lead concentrations less than 0.1 mg L⁻¹. Their hypothesis was that iron reduced the lead in the paint waste to the less soluble metallic form. However, the study did not include analyses to evaluate the presence of metallic lead. Other mechanisms may be more plausible such as sorption of Pb to iron oxides formed on the steel surfaces (Cornelis et al; 2008; Zhou and Haynes; 2010; Komarek et al. 2013). Nevertheless, Pb in the paint waste is sequestered by the steel grit, which may result in leachable concentrations less than the TC limit. Kendall (2003) found that the addition of iron filings to foundry sand wastes masked the potential leachability of Pb, Cu, and Zn. He hypothesized three processes with the addition of metallic iron filings: an oxidation/reduction reaction ($\text{Fe} + \text{Pb}^{2+} \rightarrow \text{Fe}^{2+} + \text{Pb}$), precipitation of lead hydroxide, and sorption to hydrous ferric

oxide. However, comparing precipitation and sorption modeling with the experiment data, Kendall further demonstrated that sorption is more significant over the pH range of 3 to 8. Parsa et al. (1996) and Abdel and Nowler (2004) produced compressed fly ash/contaminated waste formulations and showed that leaching of Cd, Cr, and Pb (TCLP test) were reduced to well below the TC levels. They further concluded that the mechanism responsible for reduced leaching involved metal sorption onto the amorphous ferro-aluminosilicate glass material in the fly ash (Parsa et al., 1996; Abdel and Nowler, 2004). In another study, Cornelis et al. (2008) reviewed the leaching mechanism of metal species in alkaline solid wastes including incinerator bottom ash, fly ash, and metallurgical slags. They found that adsorption to amorphous Fe oxides or Al oxides is significant in weathered wastes and consequently reduced metal concentrations in the leachate (Bernecki et al., 2008).

In our study, elevated metal concentrations were observed in the waste. For example, Pb was detected ranging from 5 (Bridge 5-3) to 168,090 mg kg⁻¹ (Bridge 11-2), Cr from 21 (Bridge 5-3) to 10,192 mg kg⁻¹ (Bridge 11-2), and Ba from 228 (Bridge 2-2) to 16,319 mg kg⁻¹ (Bridge 10-6) (Deliverable for Task 4). Yet the leached metal concentrations were less than the TC levels (Appendix A). Based on the discussion above, one explanation for the leached concentrations observed can be attributed to the use of iron-based abrasives in the paint removal process. The typical steel grit applied is composed of Fe (> 96 % by weight), C (< 1.2%), Mn (< 1.3%), Si (< 1.2%), Cr (< 0.25%), Cu (< 0.25%), and Ni (< 0.2%) (Connor, 2013; Appendix B). Earlier studies (Deliverable for Task 4) demonstrated that as great as 80% of the paint waste is comprised of steel grit. Furthermore, iron oxide coatings readily form on the surface (Meima and Comans, 1997; Jambor and Dutrizac 1998; Stipp et al. 2002; Apul, et al., 2005). Iron oxide and specifically ferrihydrite is an important sorbent for metals, because of its high surface area,

strong affinity for metals, and an abundance of binding sites. Therefore, surface interactions between metals and the oxide surface likely play an important role in metal mobility and leaching. These interactions involve potentially a number of mechanisms: (Jambor and Dutrizac 1998; Stipp et al. 2002; Apul, et al., 2005; Fan et al., 2005; Xu et al., 2006; Zhou and Haynes, 2010). Iron oxides form on the steel grit surface (Jambor and Dutrizac 1998; Stipp et al. 2002; Apul, et al., 2005). The surface charge on the iron oxide arises from deprotonation and protonation of potential determining $\text{MOH}_2^{0.5+}$ and $\text{MOH}^{0.5-}$ groups (Haynes, 1982; Zhou and Haynes, 2010) (Figure 6). This surface becomes increasingly negatively charged as the hydroxide ion activity (and pH) increases and becomes more positively charged as pH decreases; this surface charge effect is with respect to the oxide zero point of charge. A small proportion of sorbed metals will desorb (Strawn and Sparks, 1999; Swift and MaLaren, 1991) during leaching procedure. Metal sorption to iron oxide has been observed to involve a two-step process – a fast initial uptake followed by a slow surface diffusion step within the micropores of the oxide (e.g., Fan et al., 2005; Xu et al., 2006).

Given the potentially significant surface interactions between trace metals and the iron oxide surface, reduced concentrations in leaching are likely due to the presence of iron oxide. Metals sequestered through interactions with the steel grit surface would result in reduced leachable concentrations (less than the TC limit). Therefore, in this study, we hypothesize that iron oxides form on the steel grit surface. Metals in the paint waste interact with the iron oxide surface through sorption/desorption and/or dissolution/precipitation processes at the aqueous-solid interface.

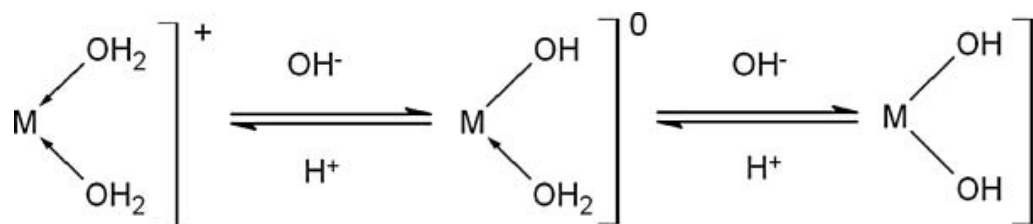
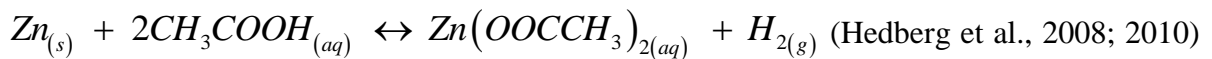
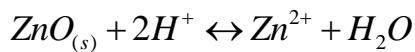


Figure 6. Schematic diagram of the pH-dependent charge on an amphoteric metal oxide surface (Haynes, 1982; Zhou and Haynes, 2010).

Although the TCLP revealed greater concentrations of Zn (20.4 to 1,307 mg L⁻¹), sorption of Zn also occurs on the steel grit surface. However, because of the relatively much greater concentrations of Zn in the paint waste, precipitation may also play an important role in the system. Given its elevated concentration (Deliverable for Task 4) in paint and its solubility (Appendix C, Figure A5), dissolution may be a more plausible mechanism responsible for Zn leaching. The presence of Zn (Figure 4) in the leachate reflects the dissolution of ZnO and the consequent dissolution (corrosion) of Zn primer with the presence of acetic acid (CH₃COOH) (Appendix C) (Hedberg et al., 2008; 2010).

The reactions are expected to proceed based on the following equations.



Interestingly, Fe concentrations were observed to range from 183 to 3,275 mg L⁻¹ (or 0.06 M) (Figure 5). Given the pourbaix diagram (Figure 7), the corrosion product iron oxide (ferrihydrite) [Fe₃HO₈·H₂O simplified as Fe(OH)₃] (Figures 8 and 9), is the dominant form under the pH conditions studied (4.5 to 7) (Liang et al., 2000). In the leaching procedure, colloidal iron oxides from the steel grit surface may release or become suspended in solution under turbulent conditions. The elevated dissolved iron observed may be attributed to organic ligands complexation with iron (Jeong et al., 2012). Nevertheless, iron oxide coatings acting as a sink for many (trace) metals, metalloids, silicates, and organic matter remain on the surface of steel grit (Davranche and Bollinger, 2000). Therefore, sorption is an important mechanism and likely reflects the reduced metal leaching (such as Pb, Cr, and Ba) observed.

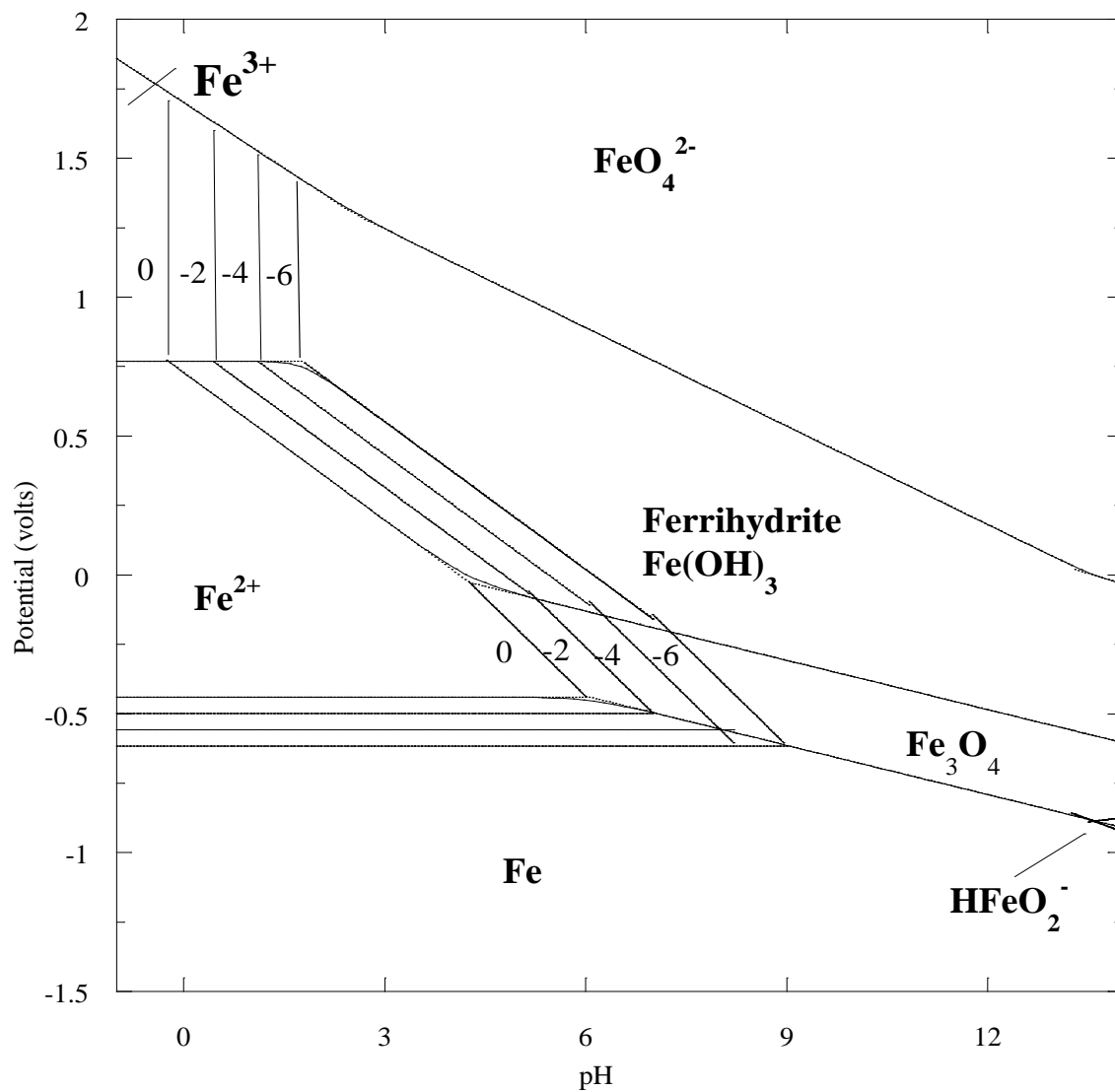


Figure 7. Potential – pH equilibrium diagram of iron or steel considering four concentrations of soluble species (10^0 , 10^{-2} , 10^{-4} , 10^{-6} M), four soluble species (Fe^{3+} , Fe^{2+} , FeO_4^{2-} , HFeO_2^-), and corrosion material ferrihydrite $[\text{Fe}(\text{OH})_3]$ at 298 K.

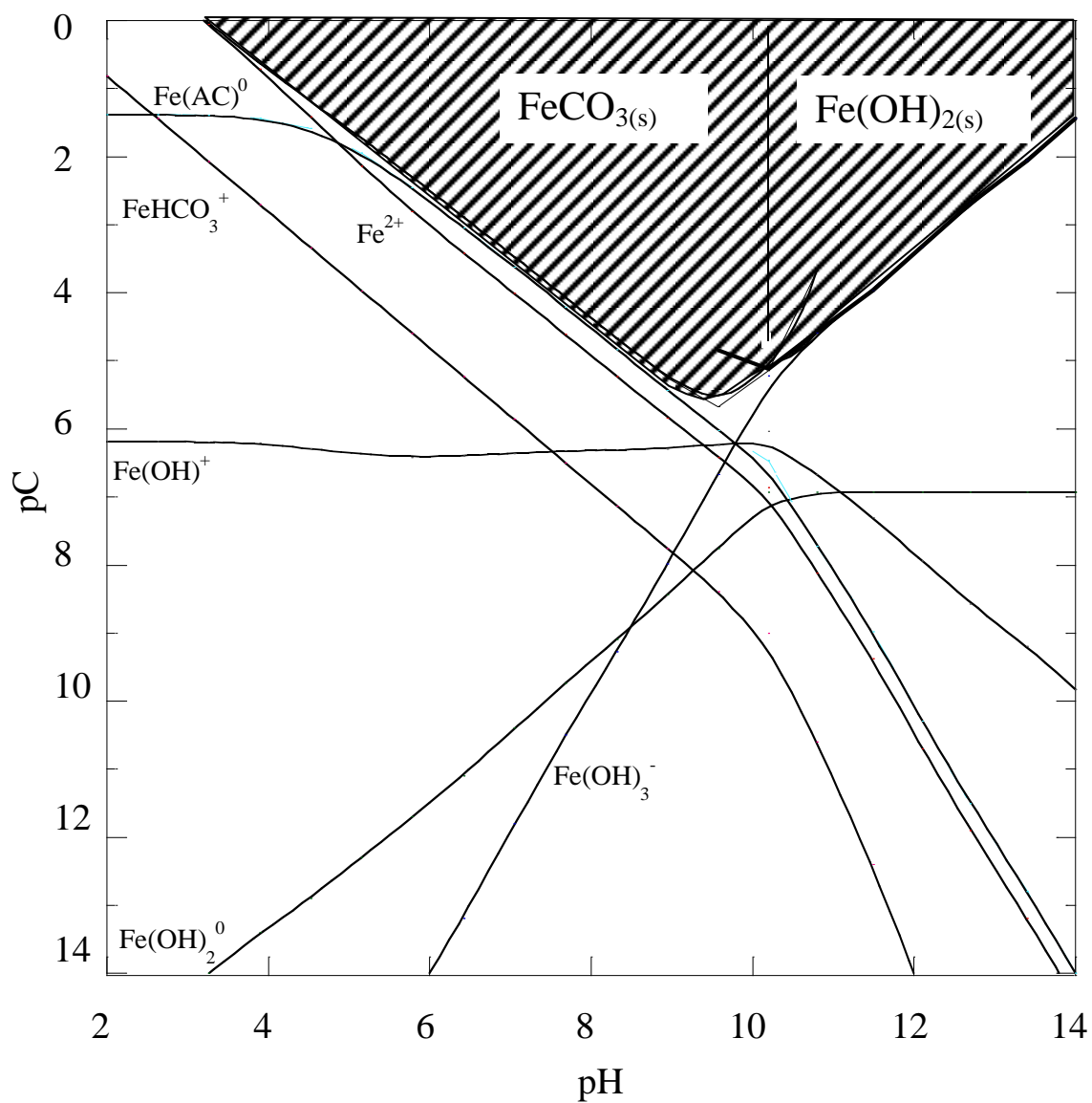


Figure 8. Fe^{2+} solubility in equilibrium with $\text{Fe}(\text{OH})_2$ and FeCO_3 , CH_3COOH at 0.1 M, 298 K and open to atmosphere. All the speciation was computed using MINEQL⁺.

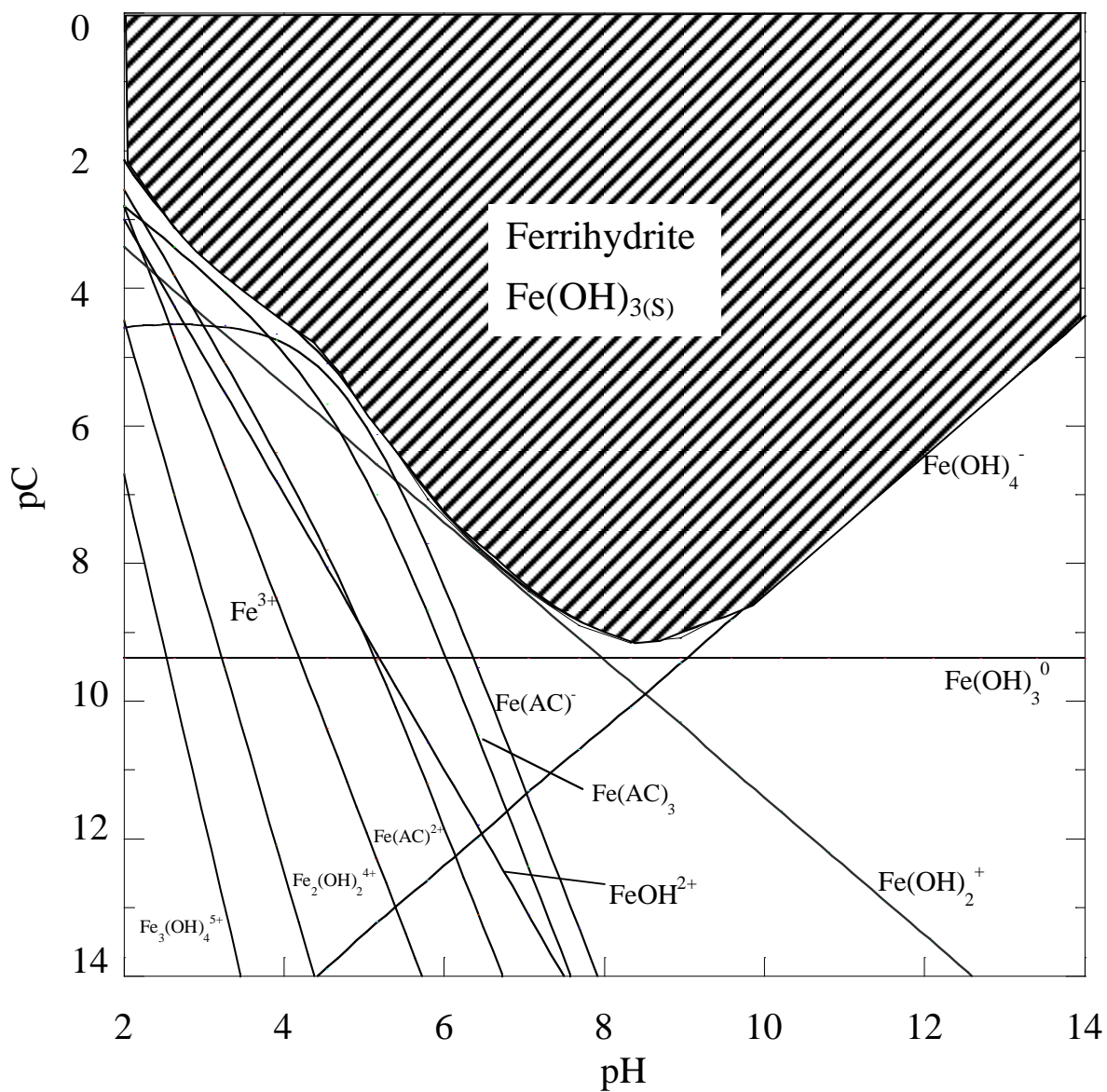


Figure 9. Fe^{3+} solubility in equilibrium with Ferrihydrite $[\text{Fe}(\text{OH})_3]$, CH_3COOH at 0.1 M, 298 K and open to atmosphere. All the speciation was computed using MINEQL⁺.

Other metals in paint waste, As, Se, Cd, Ag, and Hg, present at much lower concentrations, were only detectable in a few leaching solutions. Specifically, As and Cd were not detectable in the leaching solutions ($\leq 0.0007 \text{ mg L}^{-1}$ [detection level] for As, $\leq 0.0005 \text{ mg L}^{-1}$ [detection level] for Cd). Ag was observed in samples from Bridges 3-1, 3-2, 11-1, and 11-2 (≤ 0.0003 [detection level] to 0.44 mg L^{-1}). Se was detected in samples from Bridges 3-1, 3-2, 5-2, 11-1, and 11-2 (≤ 0.0002 [detection level] to 0.2 mg L^{-1}); Hg was found in samples from Bridges 3-1, 3-2, 10-6 and 10-8 (≤ 0.000002 [detection level] to 0.079 mg L^{-1}) (Appendix A, Table A1). Again, because of the significant surface interactions between trace metals and the iron oxide surface, these metals adsorbed onto the iron oxide resulting in reduced metal leaching.

The leaching results for Pb, Cr, and Ba (Figures 3 and 4) revealed trends as a function of pH, where the leached metal concentrations decreased as the pH increased from 4.5 to 7. Similar results have been reported by many researchers (Boy et al., 1995; Martel et al., 1997; Kendall, 2003), where metal leaching was observed to be pH dependent. The surface charge of iron oxides is a function of pH, with an increasingly net negative charge as the pH increases above the zero point of charge (Table 3). Cations desorb as the pH decreases and anions are released as the pH increases. The trend is consistent with cation sorption (Pb^{2+} , $\text{Cr}(\text{OH})^{2+}$, Ba^{2+}) to the iron oxide formed on the steel grit surface, although not observed with Zn. On the other hand, based on metal solubility (Appendix C), basic lead carbonate [$\text{Pb}_3(\text{OH})_2(\text{CO}_3)$] (Barnes and Davis, 1996), chromium (III) hydroxide [$\text{Cr}(\text{OH})_3$], BaCO_3 , ZnCO_3 , and $\text{Fe}(\text{OH})_3$ may also precipitate over this pH range (Appendix C).

Cr is among the RCRA metals and hexavalent Cr is of significant toxicity (U.S. EPA, 2008). Cr is introduced in the form of Cr_2O_3 and CrO_4^{2-} in paint (Lambourne and Strivens, 1999). Many studies (Weng et al., 1996; Peterson et al., 1996; 1997; Bidoglio et al., 1993; Deng et al., 1996;

Table 3. Zero point of charge (ZPC) for different iron oxides

| Iron oxide | formula | pH _{ZPC} | Solubility product log K _{so} | References |
|---------------|--|-------------------|---|---|
| Ferrihydrite | Fe ₃ HO ₈ ·H ₂ O [simplified as Fe(OH) ₃] | 7.8 – 8.8 | -37 to -39 ^a | Cornell and Schwertmann (1996) Langmuir (1997) Essington (2004) |
| Goethite | α-FeOOH | 7.5 – 9.4 | -44 ^a | Cornell and Schwertmann (1996) Langmuir (1997) Sposito (2008) |
| Hematite | α-Fe ₂ O ₃ | 7.5 – 9.5 | -43.9 ± 0.2 ^a | Cornell and Schwertmann (1996) Langmuir (1997) Sposito (2008) |
| Magnetite | Fe ₃ O ₄ | 6.5 – 7.9 | 12.02 ^b | Laskowski et al., (1969) Illes and Tombacz (2003) |
| Lepidocrocite | γ-FeOOH | 6.7 – 7.5 | -38.7 to -40.6 ^a | Cornell and Schwertmann (1996) Langmuir (1997) |

^a Considering the dissolution reaction written as, e.g., for goethite: FeOOH + H₂O = Fe³⁺ + 3OH⁻.

^b *K_{so} = K_{so} / K_w³

Roskovic et al., 2011; Du et al., 2012) have been conducted to investigate Cr speciation in the presence of Fe(II) or zero valent iron in soil and solid waste. Reduction of Cr(VI) to Cr(III) was observed under acidic conditions ($\text{pH} < 7$) (Weng et al., 1996; 2001) as well as with reducing agents Fe(II) or zero valent iron (Peterson et al., 1996; 1997; Du et al., 2012). Weng et al. (1996; 2001) evaluated interactions between Cr(VI) and concrete particles in synthetic groundwater. The removal of Cr(VI) and Fe(II) along with the presence of Cr(III) and Fe(III) were observed under acidic conditions. Peterson et al. (1996) investigated the redox reaction between aqueous Cr and magnetite using X-ray absorption fine structure (XAFS) spectroscopy to provide molecular-level information on Cr sorption and redox reactions. Cr(VI) reacted with freshly-synthesized magnetite with a surface coverage of 4.5 mol/m^2 where it was observed to be reduced to Cr(III), as evidenced by the Cr absorption edge position and by the absence of a $1s \rightarrow 3d$ pre-edge peak. Peterson et al. (1997) further used synchrotron-based XAFS spectroscopy to investigate the reduction of aqueous Cr(VI) to Cr(III) in magnetite-bearing soils from Cr-contaminated sites. Results indicated that mixed-valence Cr(III/VI) was reduced to Cr(III) in the presence of magnetite ($\text{Cr}^{6+} + 3\text{Fe}^{2+} \rightarrow \text{Cr}^{3+} + 3\text{Fe}^{3+}$). A recent study conducted by Du et al. (2012) reviewed reduction and immobilization of chromate in chromite ore processing residue (COPR). They found that COPR and nanoscale zero-valent iron (ZVI) with greater than 27% water (by mass) could result in a nearly complete Cr(VI) reduction with less than 0.1 mg L^{-1} Cr(VI) in the TCLP leachate. In this study, the hypothesis is that iron oxide formed on the steel grit surface. Hexavalent chromium may be reduced to trivalent chromium in the presence of ferrous iron (magnetite) or zero-valent (steel grit) iron under acidic conditions. Therefore, in this work Cr(III) is expected to be the dominant speciation in the leaching procedure.

In summary, TCLP results revealed metal concentrations of Pb, Cr and Ba were less than the toxicity characteristics (TC) levels (with the exception of three samples exhibiting Cr concentrations greater than the TC of 5 mg L^{-1} ($9.6 \times 10^{-5} \text{ M}$)). Other metals in paint waste, As, Se, Cd, Ag, and Hg, present at much lower concentrations, were only detectable in a few leaching solutions. Metal sorption onto the iron oxide surface is a plausible mechanism responsible for the reduced metal leaching. TCLP results revealed greater concentrations of Zn (20.4 to $1,307 \text{ mg L}^{-1}$), and dissolution is likely the mechanism responsible for its leaching. Elevated Fe (183 to $3,275 \text{ mg L}^{-1}$) observed can be attributed to complexation with organic ligands and colloidal iron oxide particles from the steel grit surface that may release or become suspended in solution under turbulent conditions. Cr(III) is assumed to be the dominant speciation in the leaching procedure. Although the TCLP results indicated that metal concentrations in the extracts are less than the TC levels, to understand the long-term stability of paint waste and address its disposal, multiple extraction procedure was applied in this study.

4.2 Multiple extraction procedure

With 10 days of extraction, the pH of 5 was maintained in the first day by the continuous addition of acetic acid ($0.5 \text{ N CH}_3\text{COOH}$). From the second to tenth day, a sulfuric and nitric acid solution ($\text{H}_2\text{SO}_4/\text{HNO}_3$, 60/40 weight percent mixture) was applied to adjust the initial pH of the extraction fluid to 3.0 ± 0.2 , and pH was observed to increase at the end of 24 hours of extraction (Figure 10). Specifically, in the second day, the pH was observed up to 9.6. For the following days of extraction (third day to tenth day), pH decreased from 9.6 to 5 (Figures 10b and 10c). This result demonstrates the waste has significant alkalinity (Zhou and Haynes, 2010),

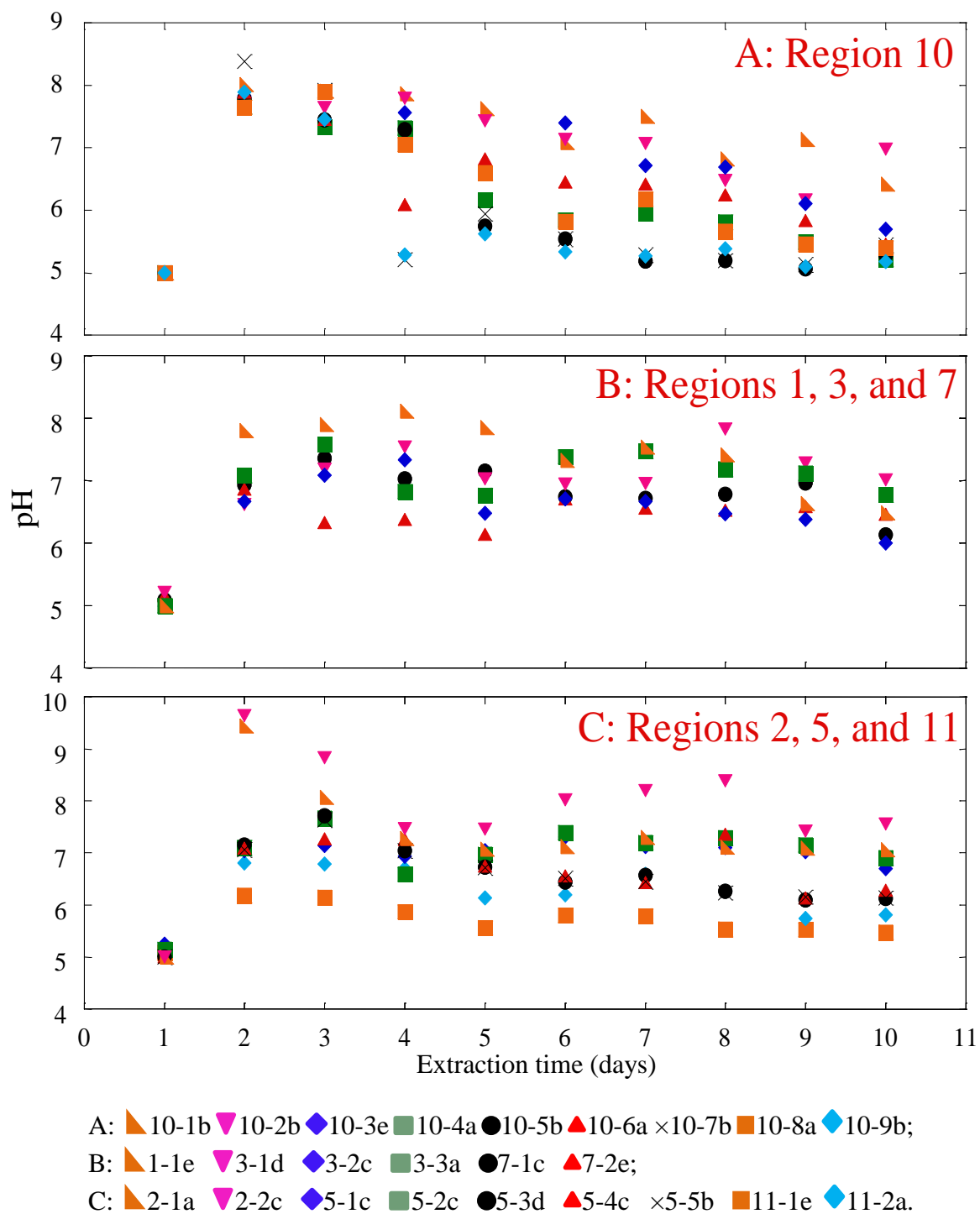


Figure 10. pH from MEP are shown as a function of 10 days of extractions. The first extraction is performed with a pH of 5.0 followed by the subsequent nine successive extractions using the initial pH of 3.0 ± 0.2 that simulate acid rain conditions.

which can be attributed to the application of calcite (CaCO_3) as an extender (supplementary pigments) in the paint.

Elevated metal concentrations were detected in extracts from the MEP experiments. In the first day of extraction (Figures 11 through 20) the greatest concentrations of metals leached were observed (Figures 11 through 20). From the second to tenth day of extraction, leached concentrations decreased as function of extraction time (Figures 12, 14, 16, 18, 20) with the exception of the metals such as Pb, Cr and Ba that revealed increased concentrations from the fourth to tenth day (These results are discussed later in this section). The first day of extraction resulted in leached concentrations as great as 22.6 mg L^{-1} for Pb, 0.064 mg L^{-1} for Cr, and up to 6.6 mg L^{-1} for Ba (Figures 11 through 16). Similar with TCLP, MEP results exhibited elevated leached concentrations for Zn (as great as 1163 mg L^{-1}) and Fe (up to 1282 mg L^{-1}) (Figures 17 through 20). From the second to tenth day of extraction, leached concentrations were observed from below detection level (BDL) (< 0.0005) to 2.04 mg L^{-1} for Pb, BDL (< 0.0007) to 0.04 mg L^{-1} for Cr, BDL (< 0.0004) to 3.00 mg L^{-1} for Ba, BDL (< 0.001) to 45.9 mg L^{-1} for Zn, and BDL (< 0.0025) to 422 mg L^{-1} for Fe. Metals and metalloids, As, Cd, Ag, Hg, and Se, were not detectable over the entire ten days of extraction (Appendix A, Table A2): less than 0.0007 (detection level) to 0.67 mg L^{-1} for As, less than 0.0005 (detection level) to 0.12 mg L^{-1} for Cd, less than 0.0003 (detection level) to 0.015 mg L^{-1} for Ag, less than 0.0002 (detection level) to 0.11 mg L^{-1} for Se, and less than 0.000002 (detection level) to 0.002 mg L^{-1} for Hg (Appendix A, Table A2). The greatest desorption or/and dissolution was observed in the first day. In fact, sorption reactions represent a continuum between specific adsorption and surface precipitation/coprecipitation:

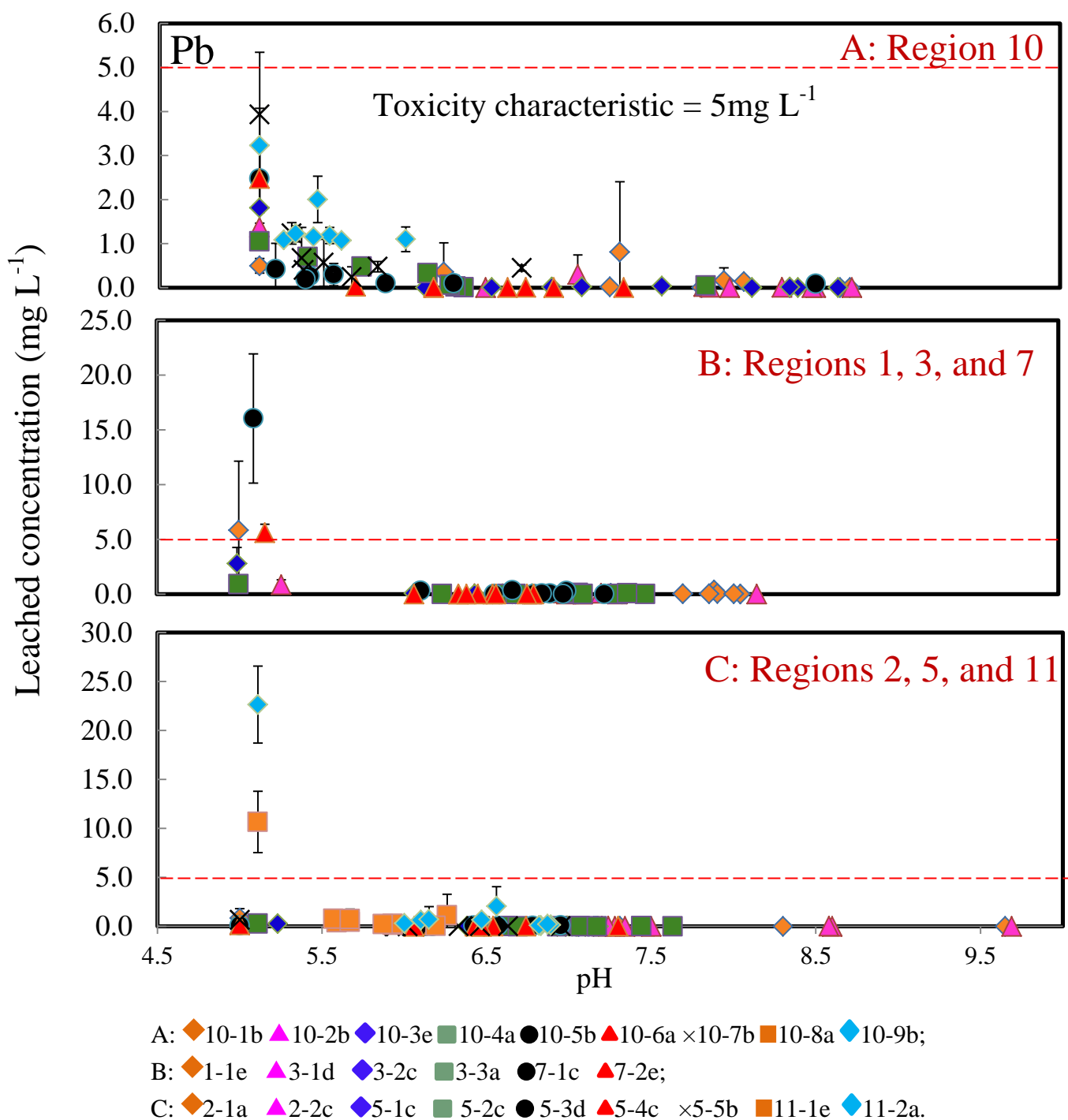


Figure 11. Leaching concentrations of Ba from MEP are shown as a function of pH. The first extraction is performed with a pH of 5.0 followed by the subsequent nine successive extractions using the initial pH of 3.0 ± 0.2 that simulate acid rain conditions. Toxicity characteristic $\text{Pb} = 5 \text{ mg L}^{-1}$.

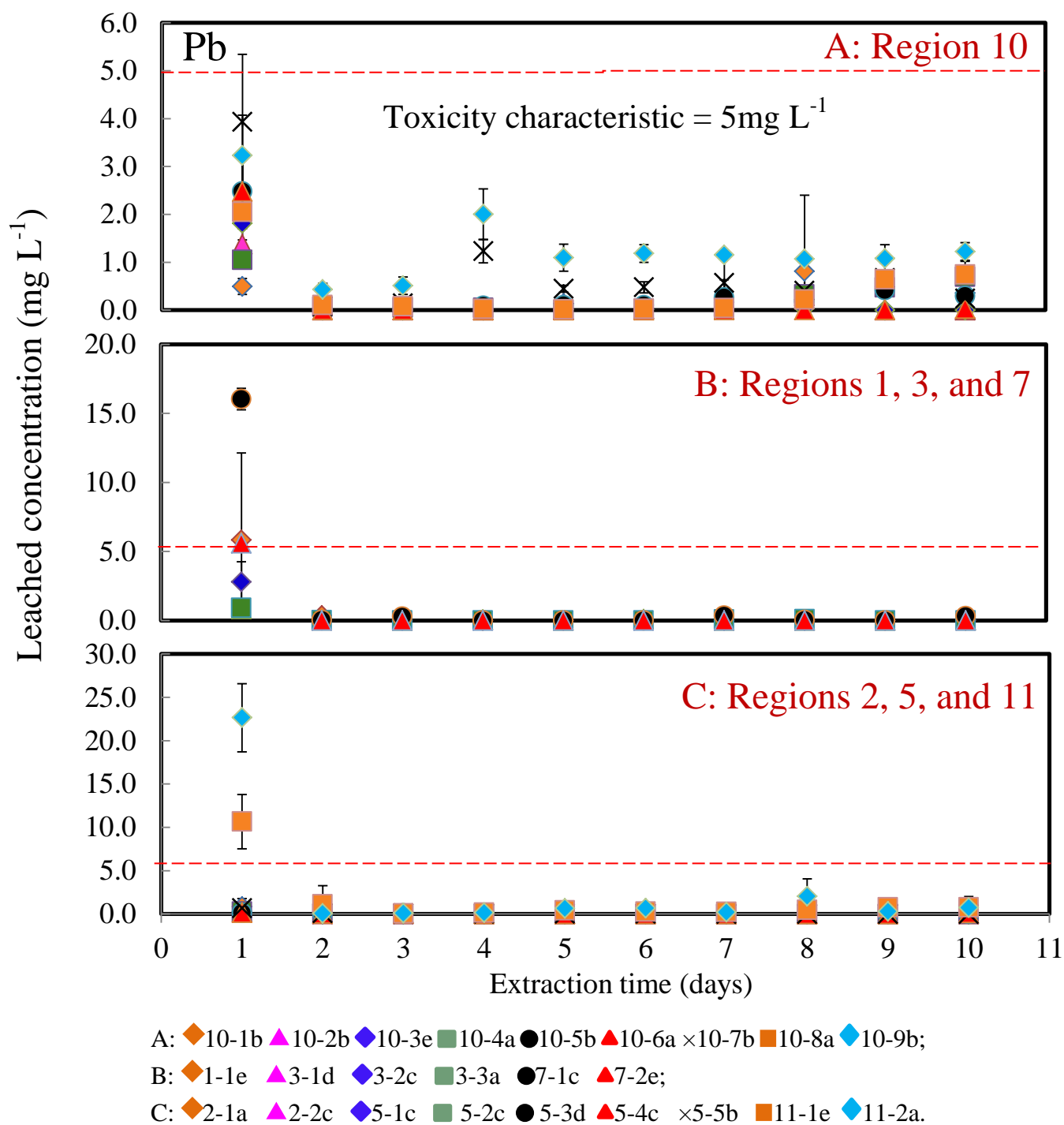


Figure 12. Leaching concentrations of Pb from MEP are shown as a function of 10 days of extractions. The first extraction is performed with a pH of 5.0 followed by the subsequent nine successive extractions using the initial pH of 3.0 ± 0.2 that simulate acid rain conditions. Toxicity characteristic Pb = 5 mg L^{-1} .

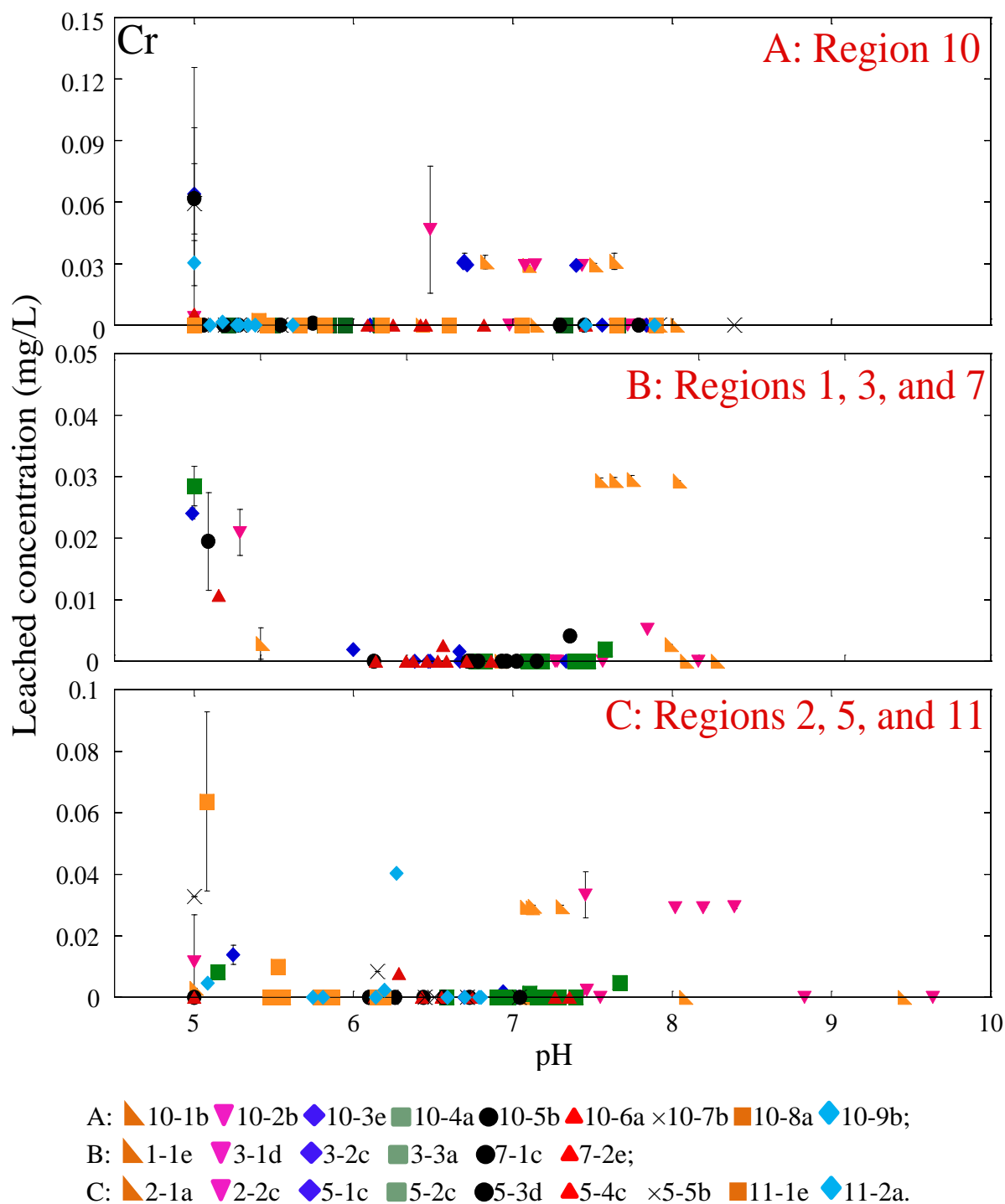


Figure 13. Leaching concentrations of Cr from MEP are shown as a function of pH. The first extraction is performed with a pH of 5.0 followed by the subsequent nine successive extractions using the initial pH of 3.0 ± 0.2 that simulate acid rain conditions. Toxicity characteristic Cr = 5 mg L^{-1} .

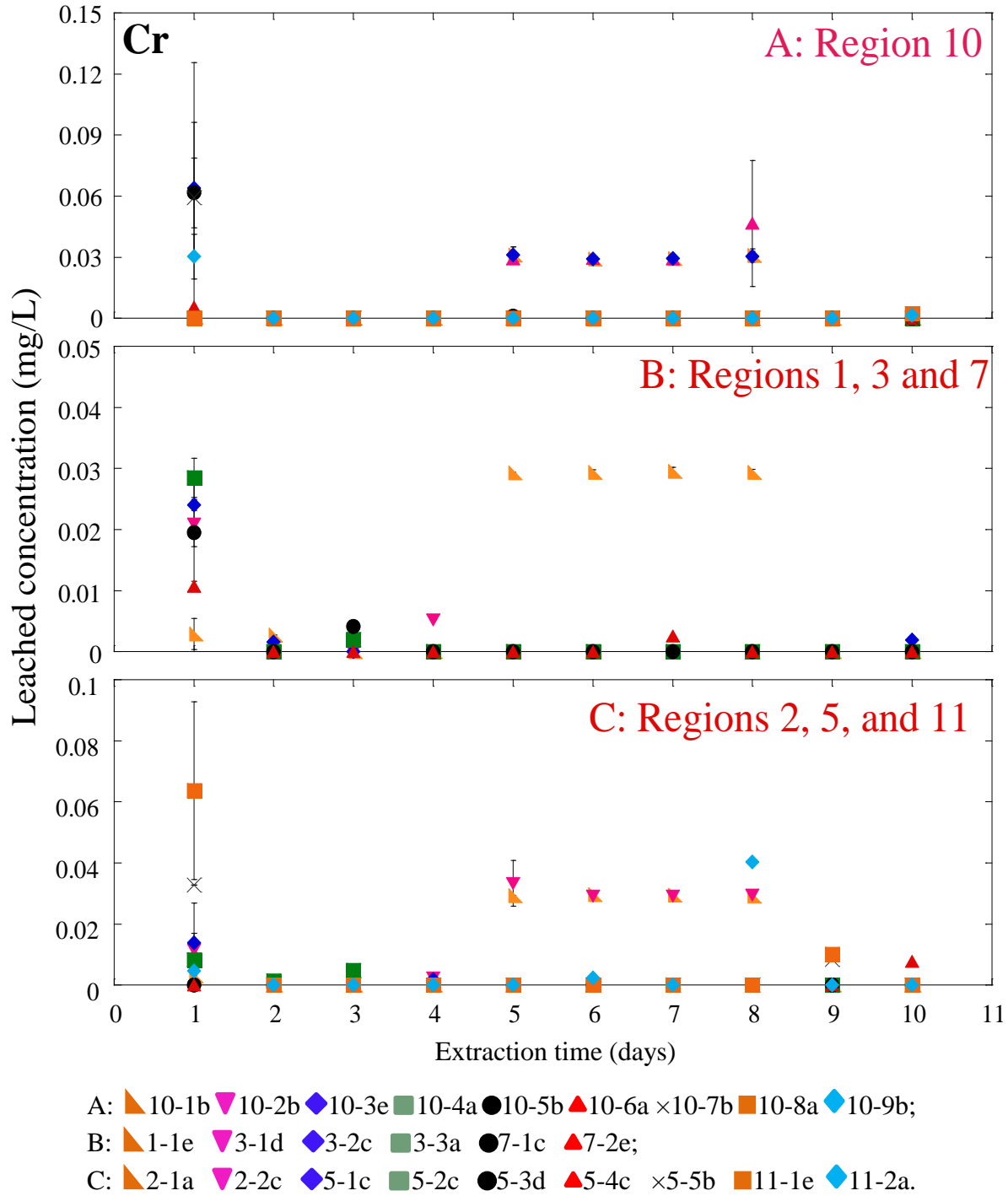


Figure 14. Leaching concentrations of Cr from MEP are shown as a function of 10 days of extractions. The first extraction is performed with a pH of 5.0 followed by the subsequent nine successive extractions using the initial pH of 3.0 ± 0.2 that simulate acid rain conditions. Toxicity characteristic Cr = 5 mg L^{-1} .

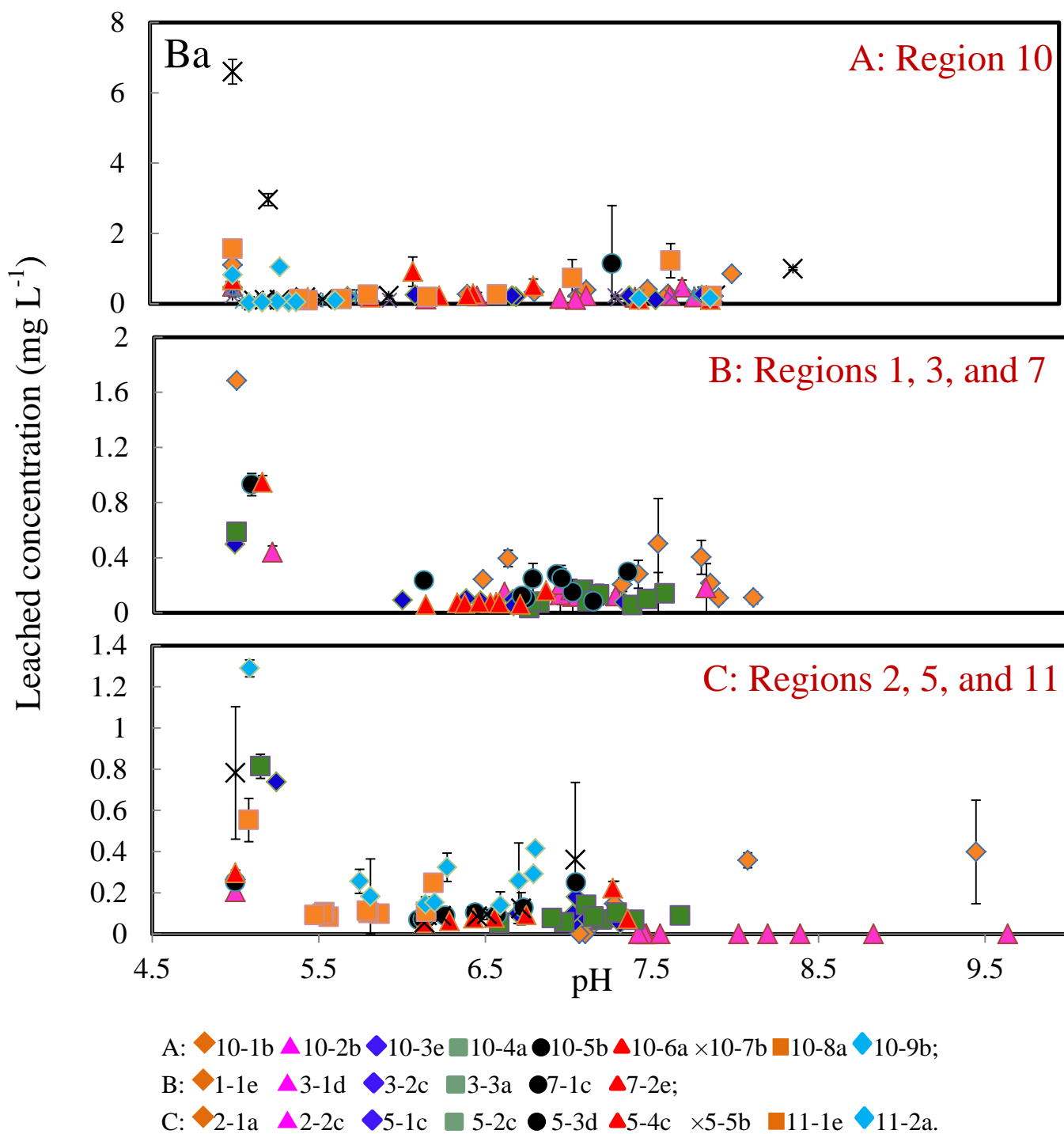


Figure 15. Leaching concentrations of Ba from MEP are shown as a function of pH. The first extraction is performed with a pH of 5.0 followed by the subsequent nine successive extractions using the initial pH of 3.0 ± 0.2 that simulate acid rain conditions. Toxicity characteristic Ba = 100 mg L^{-1} .

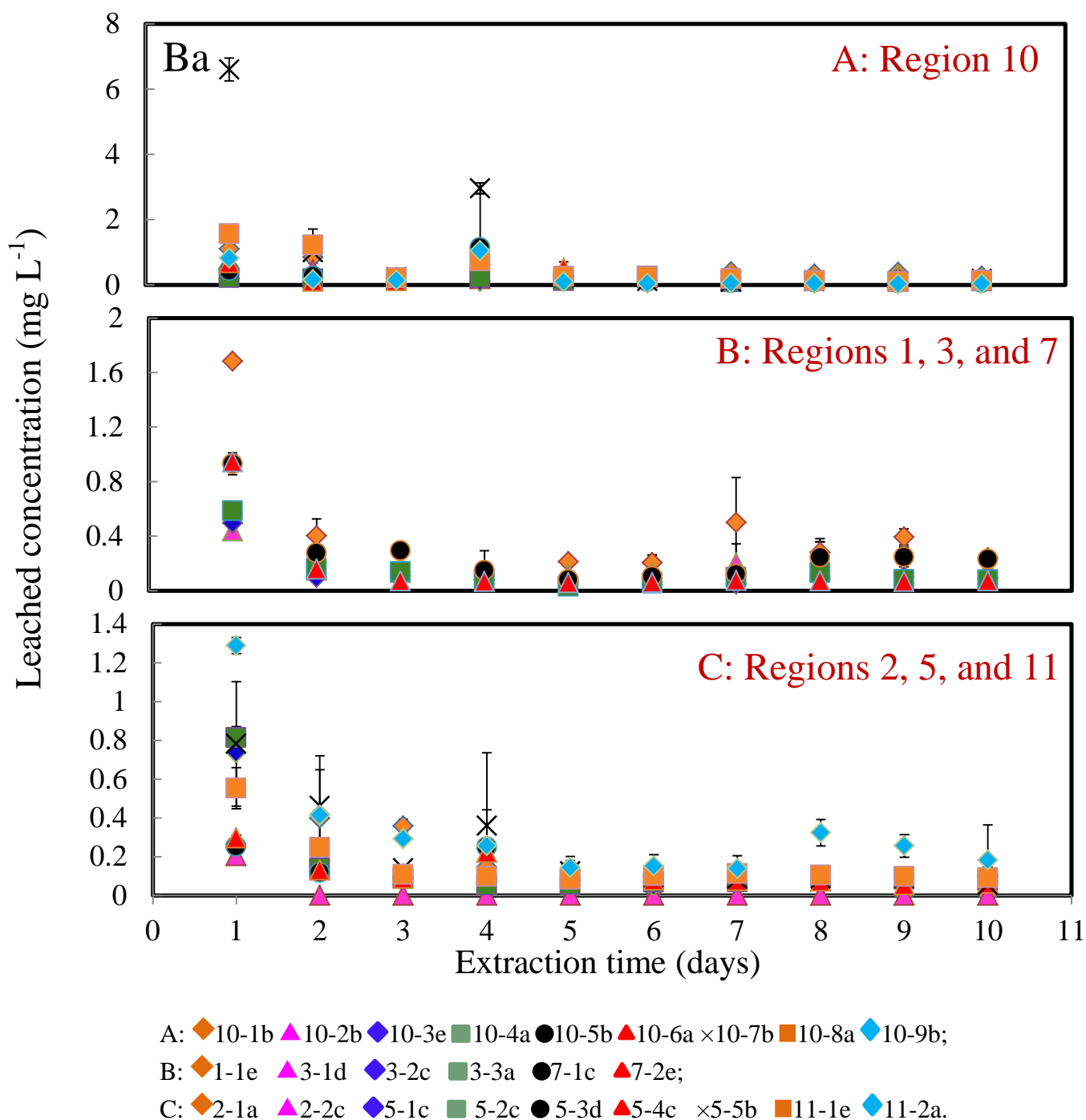


Figure 16. Leaching concentrations of Ba from MEP are shown as a function of 10 days of extractions. The first extraction is performed with a pH of 5.0 followed by the subsequent nine successive extractions using the initial pH of 3.0 ± 0.2 that simulate acid rain conditions. Toxicity characteristic Ba = 100 mg L^{-1} .

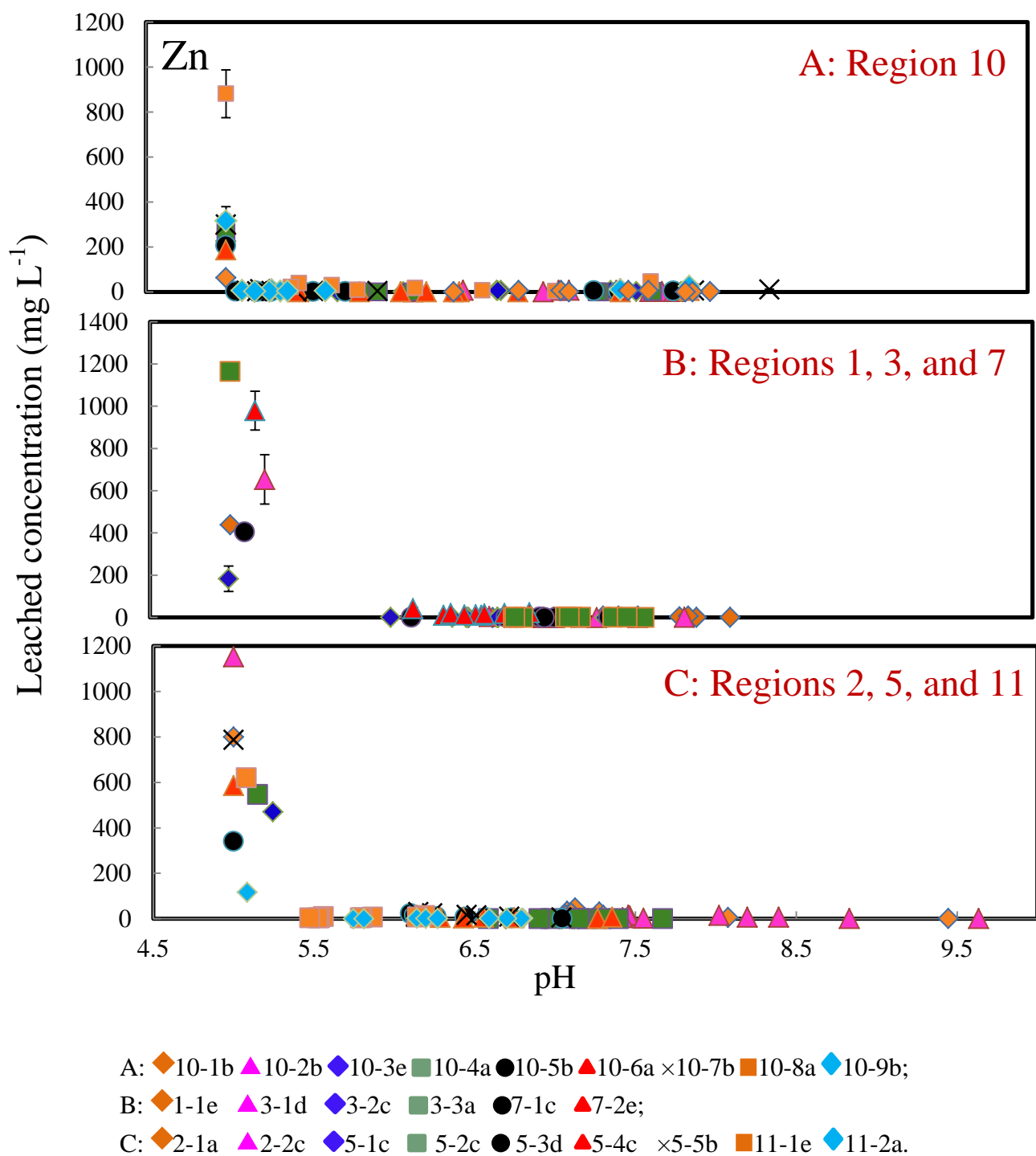


Figure 17. Leaching concentrations of Zn from MEP are shown as a function of pH. The first extraction is performed with a pH of 5.0 followed by the subsequent nine successive extractions using the initial pH of 3.0 ± 0.2 that simulate acid rain conditions.

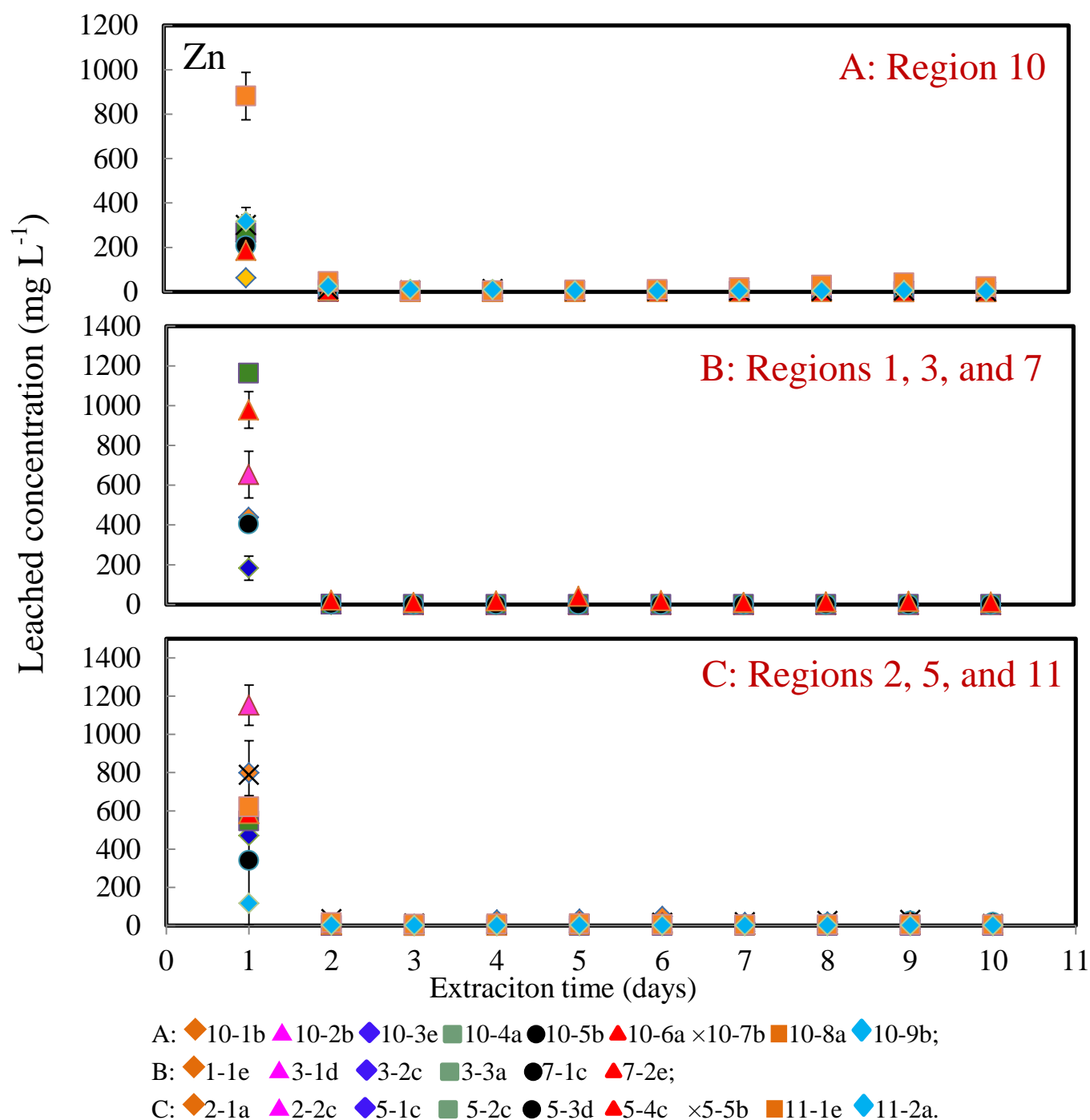


Figure 18. Leaching concentrations of Zn from MEP are shown as a function of 10 days of extractions. The first extraction is performed with a pH of 5.0 followed by the subsequent nine successive extractions using the initial pH of 3.0 ± 0.2 that simulate acid rain conditions.

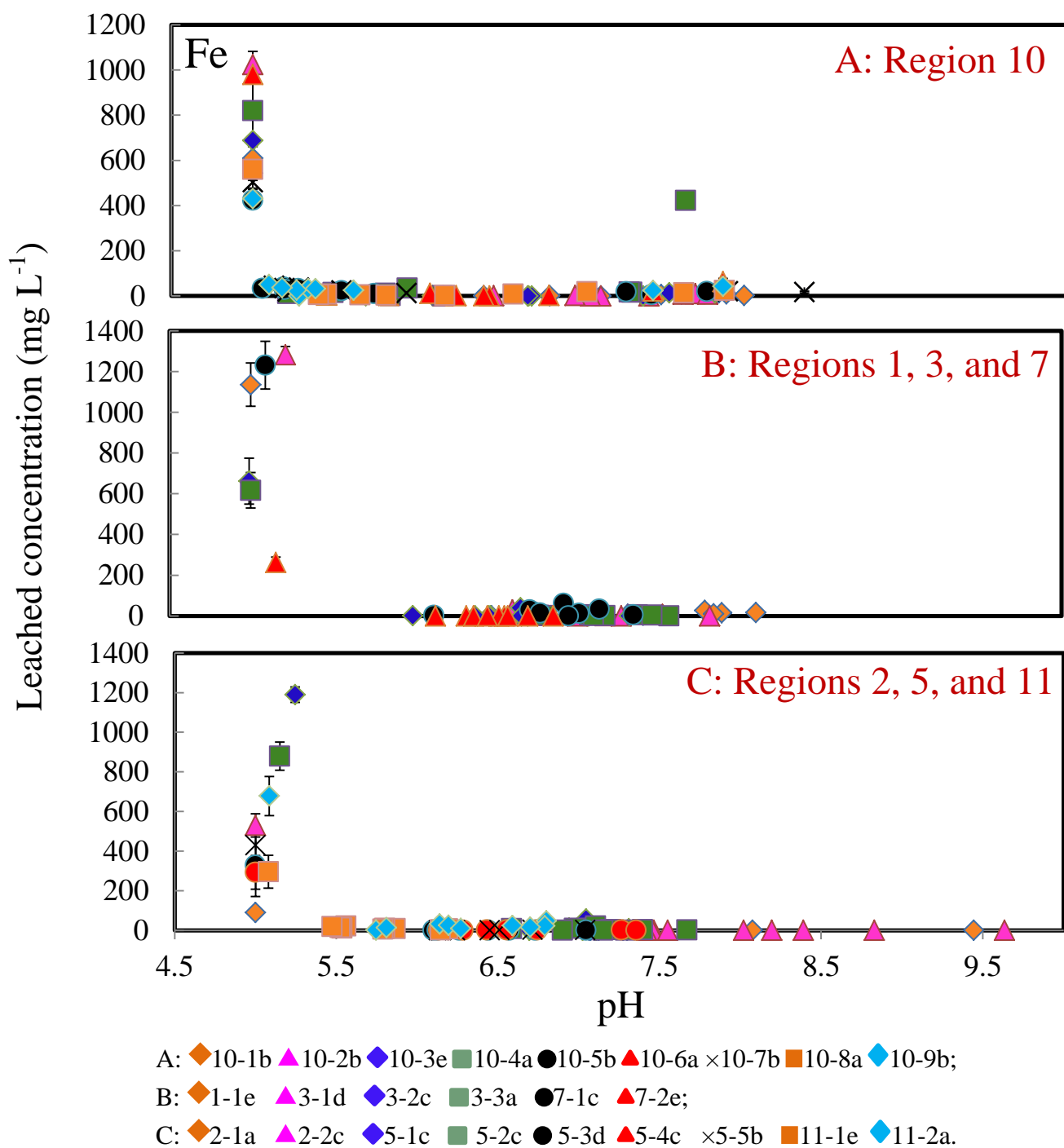


Figure 19. Leaching concentrations of Fe from MEP are shown as a function of pH. The first extraction is performed with a pH of 5.0 followed by the subsequent nine successive extractions using the initial pH of 3.0 ± 0.2 that simulate acid rain conditions.

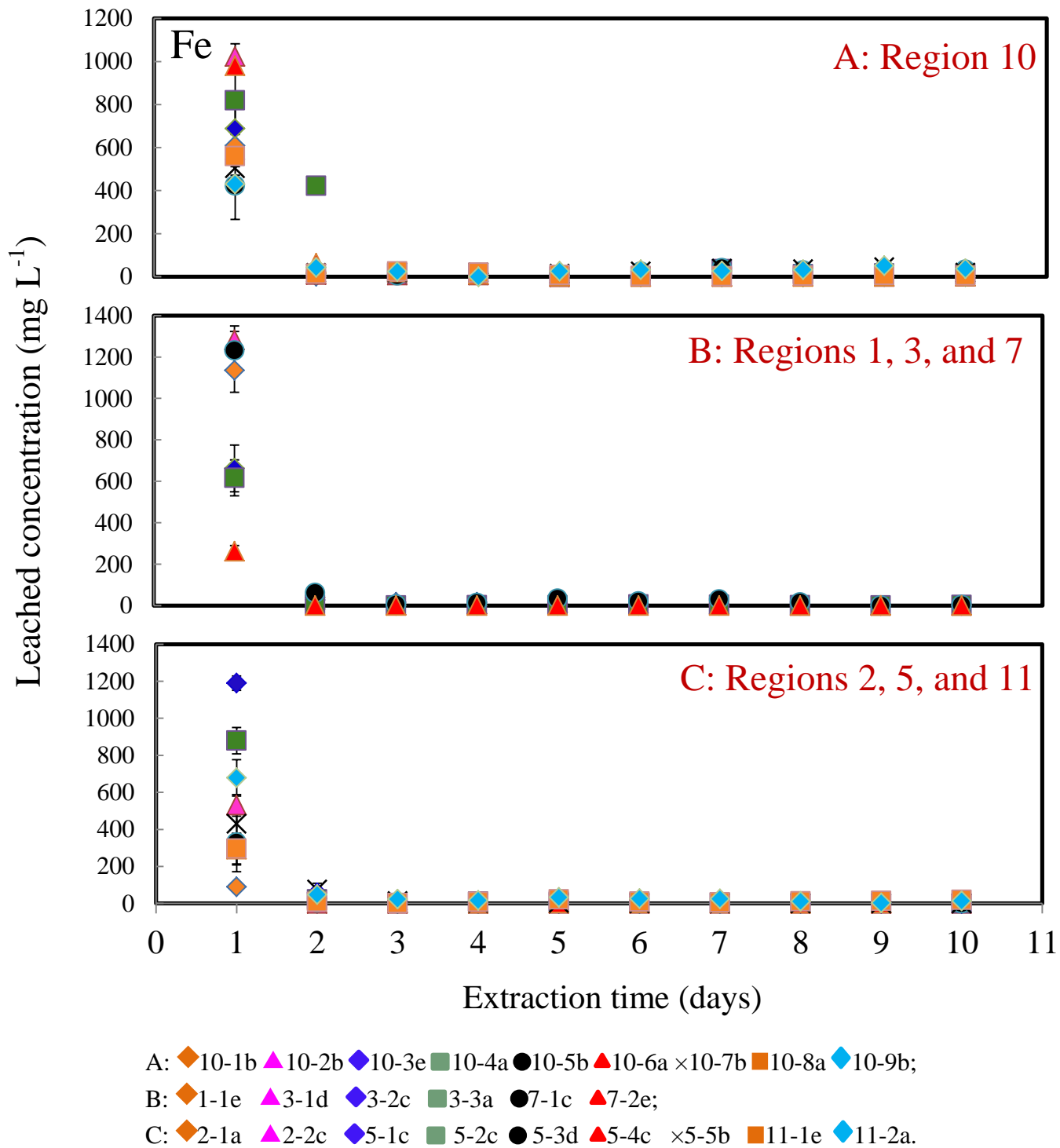
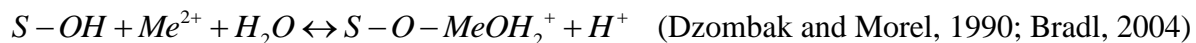


Figure 20. Leaching concentrations of Zn from MEP are shown as a function of 10 days of extractions. The first extraction is performed with a pH of 5.0 followed by the subsequent nine successive extractions using the initial pH of 3.0 ± 0.2 that simulate acid rain conditions.



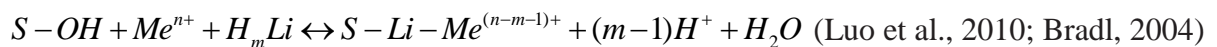
The adsorption process may be followed by surface precipitation reactions (Zhou and Haynes, 2010). In precipitation, the solid surface may exhibit a disordered lattice (amorphous) and therefore is metastable. Over time, the solid slowly converts to the more stable, less reactive, crystalline form, which has a much lower solubility. As a result, metal desorption (release) from precipitates will be greatly reduced with increasing time (Sparks, 2003).

On the other hand, metal adsorption is affected by many factors such as the solution pH, ionic strength, and inorganic and organic ligands present in the system. In this study, the higher concentration of Pb observed in the MEP study as compared to the TCLP may be attributed to the higher ionic strength (IS) in the MEP (0.5 N of CH₃COOH), where adsorption due to physical forces may decrease. Ionic strength affects metal adsorption by influencing adsorbate activity as well as the surface charge and double-layer capacitance and thickness. The effect of ionic strength on the Pb adsorption in this work is not conclusive. Generally, Pb sorption increases with increasing pH and decreasing ionic strength. Hayes and Leckie (1987) observed little ionic strength (IS) (between 10⁻¹ and 10⁰) effect on Pb and Cd adsorption on goethite, the results were best modeled as an inner-sphere surface reaction. Trivedi et al. (2003) investigated the effects of pH (4.5 to 6.5) and IS (between 10⁻³ and 10⁻¹) on Pb(II) sorption to ferrihydrite. They concluded that the change of ionic strength did not strongly influence the average local coordination environment of sorbed Pb at given pH (Trivedi et al., 2003). The modified triple layer model was developed to describe the Pb(II) sorption to the ferrihydrite as a function of pH, ionic strength, and Pb concentration (Trivedi et al., 2003).

Our experimental data also showed that the dissolved metal concentrations decreased as the pH increased from 5 to 10 (Figures 11, 13, 15, 17 and 19), which is consistent with the cation adsorption onto the iron oxide surface. The data clearly demonstrate that the use of steel grit blast media affects metal leaching. Generally, MEP results revealed five of the 24 bridge paint samples (Bridges 1-1, 7-1, 7-2, 11-1, and 11-2) exhibited Pb greater than the TC level of 5 mg L⁻¹ (Figures 11 through 12). Other leached metals including Cr and Ba were much less than the TC levels (for Cr 5 mg L⁻¹ and Ba is 100 mg L⁻¹) (Figures 13 through 16).

Interestingly, MEP results revealed increased Pb, Cr, and Ba in the leachate for pH greater than 7. Increased Pb concentrations were observed from the fourth to tenth day over pH 7.0 to 7.5; Cr leaching increased from the fifth to eighth day over pH 6.5 to 8.5, and increased Ba concentrations were observed from the eighth to tenth day over pH 6.8 to 9.5. These results are consistent with that observed by Townsend et al. (2004), where they applied MEP to evaluate the leaching of arsenic, chromium, and copper from chromated copper arsenate (CCA)-treated wood. Results may be explained in part by metal complexation with organic ligands dissolved from the paint. Trace metals such as Pb and Cr complex with both low molecular weight organic ligands (i.e., citrate, acetate, and formate) and high molecular weight organic ligands (i.e., long chain carboxylic acids). At higher pH conditions, the conjugate base of acids dominates and are released into solution binding with the metals such as Pb and Cr(III). Aqueous complexation of ligands and metals can significantly increase heavy metal mobility in the leachate for pH greater than 7 (Bowers and Huang, 1986; Bradl, 2004).

Organic ligands may form bridges between the oxide surface and the metal (Bradl, 2004; Zhou and Haynes, 2010):



Under acidic to neutral pH conditions, anionic organic ligands sorb a net positively charged iron oxide surface (Davis and Bhatnagar, 1995). Subsequently, metal adsorption onto the surface is enhanced.

In summary, significant alkalinity was observed in the paint waste. The greatest desorption was detected in the first day, while leaching was greatly reduced with increasing time (from the second day to the tenth day). MEP results revealed greater lead concentrations in the leachate than in the TCLP, and may be attributed to the higher ionic strength applied in MEP. Although the paint waste passed the TCLP test for Pb concentrations, MEP revealed five of the 24 bridge paint samples exhibited Pb greater than the TC level of 5 mg L⁻¹. Other trace metals exhibited leached concentrations much less than the TC levels. MEP results exhibited increased metal concentrations such as Pb, Cr, and Ba in the leachate for pH greater than 7. This result can be attributed to the metal complexation with organic ligands in the leaching solution. In fact, the degree of metal leaching depends on many factors including phases metals are associated within the paint waste, sorption/desorption processes with iron oxide, redox conditions, and pH (Izquierdo and Querol, 2012). To investigate the forms metals are associated with in the paint waste and further address the long-term mobility of paint waste, sequential extraction was conducted.

4.3 Sequential extraction results

SEP was conducted to investigate the forms metals are associated with in the paint waste. In the first step of sequential extraction, metals associated with exchangeable and carbonates are assessed (Figure 21) by applying 0.11 M acetic acid (CH₃COOH) at pH of 2, resulting in 0.01 to 0.02% (by weight) of Pb (% refers to the extracted concentration over the total concentration),

less than 0.0001 (detection limit) to 0.05% of Cr, 0.02 to 1.20% of Ba, and 2.35 to 6.39% of Zn. This phase represents metals and metalloids that are exchangeable and weakly bound. The metal extracted can be attributed to metal dissolution from the paint waste (i.e., PbO $pK_{SO} = 12.72$ at 25°) (Baes and Mesmer, 1976) and desorption from the steel grit surface (i.e. weak electrostatic bonding between metals and charged iron oxide surface) (Bradl, 2004). During the leaching experiments, this form is expected to be released in the aqueous phase. The relatively low concentrations of Pb, Cr, and Ba observed in this phase is consistent with other studies (Lombi et al., 2002a; Friesl et al., 2003; Hartley and Lepp, 2008b; Kumpiene et al., 2011; 2012; Lee et al., 2011) and our TCLP results. These studies involved the contaminated soils or wastes that are treated with iron oxides or other scavengers of trace metals, and the results revealed decreases of the most labile metal fractions (i.e., exchangeable) in the solids. Because steel grit is not completely separated from paint, metals in the waste may transfer from exchange sites to specific sorption sites (Hass and Fine, 2010); thereby lower concentrations of metals were extracted in this step. The extraction results revealed a relatively greater fraction (2.35 to 6.39%) of Zn, and can be attributed to the ZnO dissolution ($pK_{SO} = 11.14$ at 25°C) (Baes and Mesmer, 1976) from the paint surface in the extraction condition (CH_3COOH at pH of 2, $pK_a = 4.7$ at 20°C) (Baes and Mesmer, 1976). Surface-associated elements are more susceptible to extraction or leaching in an aqueous environment (Izquierdo and Querol, 2012) as observed with Zn in the paint particles (Kukier et al., 2003).

In the second step of the extraction (pH 3 and 0.5 M $NH_2OH \cdot HCl$), metals associated with iron and manganese oxides are considered, resulted in 7.69 to 14.38% of Pb, 3.34 to 5.26% of Cr, 1.03 to 2.75% of Ba, and 4.78% to 6.30% of Zn (Figure 21). This fraction relates to metal (Pb, Cr, Ba, and Zn) complexation with the iron oxides. The elevated metal observed (i.e., 11%

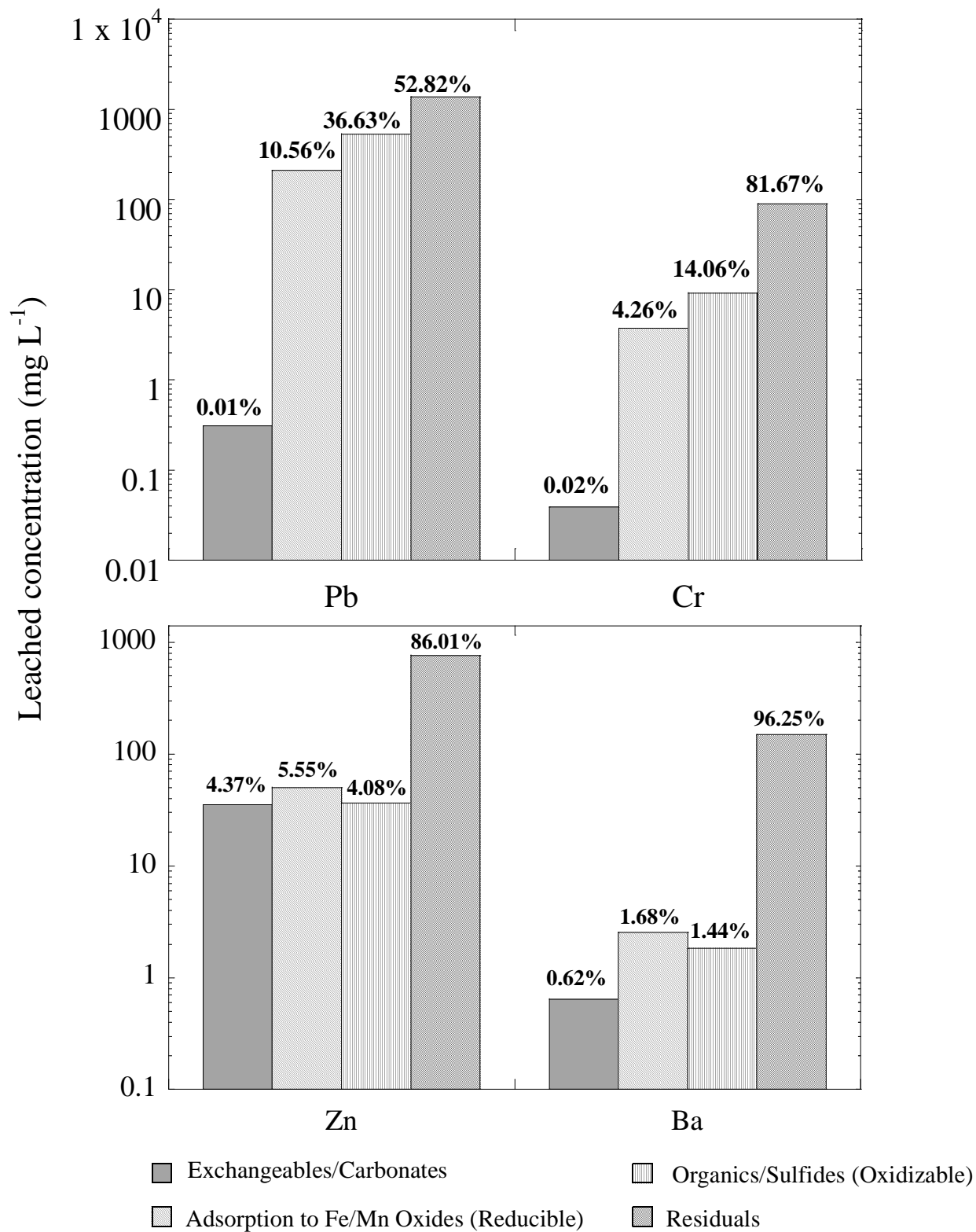


Figure 21. Mass balances of selective sequential extraction fractions for Pb, Cr, Zn, and Ba.

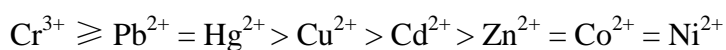
for Pb) suggests that iron oxide formed on the steel grit surface may provide a sink for the Pb and other metals (Perez et al., 2008). The degree of metal affinity for iron oxides observed in this extraction followed the trend of $Pb > Zn > Cr > Ba$. This result is consistent with metal sorption onto the iron oxide with the exception of Ba: $\log K_{MePb} = 4.65$, $K_{MeZn} = 3.49$, $\log K_{MeCr} = 2.11$, and $\log K_{MeBa} = 5.46$ (Dzombak and Morel, 1990). Pb revealed the greater affinity to the iron oxide as compared to other metals. Again, because of the presence iron oxide in the paint waste, redistribution of metals occurs from exchange sites to specific sorption sites, resulting in greater fraction of metal associated with the iron oxide phase. One limitation in this step is that $NH_2OH-HCl$ extraction efficiency for well-crystallized (or synthetic) iron oxides is less than 30% recovery (Fortin et al., 1993; La force and Fendorf, 2000). Metals extracted from this phase may re-adsorb to unextracted materials (Howard and Shu, 1996; Hass and Fine, 2010). For example, metal released from iron oxides phase can be re-adsorbed by organics that has not yet been extracted from the paint (Howard and Shu, 1996). Therefore, the extracted metals in this step may underestimate the importance of this phase.

The third extraction step using hydrogen peroxide (H_2O_2) followed by ammonium acetate (NH_4Ac) (pH 2) resulted in leaching of 36.6% of Pb, 14.1% of Cr, 1.4% of Ba, and 4.1% of Zn (Figure 21). This fraction reflects metals organically bounded. Because of the organics applied in the paint-making process (Turner, 1980; Lambourne and Strivens, 1999), this phase in the paint is expected. The composition of a paint can be summarized into two parts, carrier (continuous phase) and pigment (discontinuous phase) (Lambourne and Strivens, 1999). The former includes binders (i.e., polymer chains such as long chain carboxylic acids and alkyd resins) and solvents (i.e., ether $[-C-O-C]$ and alcohol $[-C-O-H]$), while the latter is composed of extenders (or supplementary pigment, i.e., TiO_2 and $CaCO_3$), primary pigments (fine particle organic or

inorganic, i.e., lithopone [ZnS mixed with BaSO₄], and additives (minor components) (Turner, 1980). During the paint-making process, pigments and extenders are dispersed in the organic phases (polymer) (Bentley et al., 1998). The inorganic pigment in paint is primarily composed of compounds such as Pb₃O₄ and Cr₂O₃, along with polymer to produce homogenous viscous fluid. In addition, metals exhibit affinity for organic O-containing functional groups, which include carboxyl (-COOH), enolic, and alcohols -OH and C=O (Zhou and Haynes, 2010). The order of affinity of organic groups is:

enolate > amine > carboxyl > ether > carbonyl (Sparks, 2003)

Organics applied as binders and solvents in the paint include alkyd, vinyl, acrylic, epoxy, and polyurethanes, which contain the functional groups of enolate, amine (R-NH₂), carboxylate (RCOO⁻), ether (-C-O-C), and carbonyl (C=O). The associated metal-organic interactions are complex and involve possibly chelation, adsorption, and coprecipitation (Stevenson and Vance, 1989; Zhou and Haynes, 2010). Nevertheless, trace metals such as Pb, Cr, and Ba complex with polymers in paint. The general trend of metal complexation with organics (Covelo et al., 2007; Helmke and Naidu, 1996; Jin et al., 1996; Jackson, 1998; Stevenson, 1994) follows:



The remaining or residual fraction consists of metals embedded in the mineral lattice structure of paint and steel grit (iron) in the waste. These phases are considered as the immobilized fraction. In this study, sequential extraction helps to better understand the phases that metals such as Pb and Cr may be associated with. Because total acid digestion requires the use of hydrofluoric acid (U. S. EPA Method 3052), the final step of the extraction involving HCl-HNO₃-HF (U. S. EPA Method 3052) was not conducted. Using a mass balance, approximately 53% of Pb, 82% of Cr, 96% of Ba, and 86% of Zn (Figure 21) are associated with

residual phase. These results are similar to other studies, where Pb overall exhibited greatest mobility as compared to other metals (Lee et al., 2011; Laforest and Duchesne, 2006). This fraction is not expected to be mobilized in the environment or under landfill conditions. The degree of mobilization in this extraction followed the trend of $Pb > Cr \approx Zn > Ba$. Again, the metals are potentially associated with minerals in the paint (SiO_2 , TiO_2 , and Al), steel grit (iron) in the waste, or various constituents in the pigment matrix more difficult to digest (Barnes and Davis, 1996).

In summary, the extraction revealed exchangeable and carbonate associated phases constituted 0.01 to 0.02% of Pb, less than 0.0001 (detection limit) to 0.05% of Cr, 0.02 to 1.20% of Ba, and 2.35 to 6.39% of Zn. A greater contribution of these metals (7.69 to 14.38% of Pb, 3.34 to 5.26% of Cr, 1.03 to 2.75% of Ba, and 4.78% to 6.30% of Zn) were found to be associated with iron oxides. The degree of metal affinity for iron oxides observed followed the trend of $Pb > Zn > Cr > Ba$. Inorganic pigments complex with polymer to produce homogenous viscous fluid in paint, which result in greater fraction of organically bound metals (36.6% of Pb, 14.1% of Cr, 1.4% of Ba, and 4.1% of Zn). Approximately 53% of Pb, 82% of Cr, 96% of Ba, and 86% of Zn are associated with residual phase, and Pb overall exhibited greater mobility than other metals in this extraction. The degree of mobilization in this extraction followed the trend of $Pb > Cr \approx Zn > Ba$. The hypothesis in this study is that iron oxides formed on the steel grit surface are important surfaces for trace metals. To test this hypothesis further characterization techniques such as XRD and FESEM were applied to evaluate minerals present in bulk and on iron surfaces.

4.4 XRD results

XRD was conducted to investigate the mineralogy in the paint waste. It is important to note that the detection limit for XRD is approximately 1% (by weight) (Quinn, 2013). The results from XRD revealed that primary minerals in the paint wastes are silica (SiO_2), Fe, rutile (TiO_2), Al, calcite (CaCO_3), and Zn (Figure 22, Table 4). These results are consistent with the findings from other studies (Martel et al., 1997; Serifaki et al., 2009; Bonneau et al., 2012; Franquelo et al., 2012). The presence of silica indicated the possible application of diatomaceous silica or regular silica as an extender (supplementary pigments) in paint (Martel et al., 1997). Steel grit remaining in the paint waste resulted in the presence of Fe (Kamacite) (JCPDS, 1998) (Table 4). Rutile (TiO_2 or titanium dioxide) was also observed as a consequence of its wide application as extender nowadays. Because they are more effective and less costly than other pigments, silica and calcite (or CaCO_3) are applied as extenders (supplementary pigments). The presence of Zn in the paint waste (Table 4) reflects lithopone (a mix of ZnS and BaSO_4) (NPCA, 1992; Ferlauto et al., 1994) applied since the 1990s and the increasing usage of zinc primer as a corrosion-inhibitor on metal structures (Lambourne and Strivens, 1999). Aluminum is used as an extender as well resulting from its sparkle effect in the paint.

Because of historical application of the pigments and subsequent incomplete paint removal, XRD results revealed pigments used before 1989 when lead-based paint was prohibited in NYS (NYSDOT, 1988). The primary Pb and Cr based minerals observed include Pb_3O_4 , $\text{PbCrO}_4\cdot\text{PbO}$, and Cr_2O_3 (Figure 23). Lead tetroxide (or red lead Pb_3O_4 , Pb_2O_4 , $\text{PbO}_2\cdot 2\text{PbO}$) and lead chromate ($\text{PbCrO}_4\cdot\text{PbO}$) are reported to be the most widely used corrosion-inhibiting pigments on metal structures painted before 1989 (Gooch, 1993; Oil and Color Chemists Association, 1983). The presence of Cr_2O_3 can be attributed to the application of chromium oxide green (Cr_2O_3) in paint

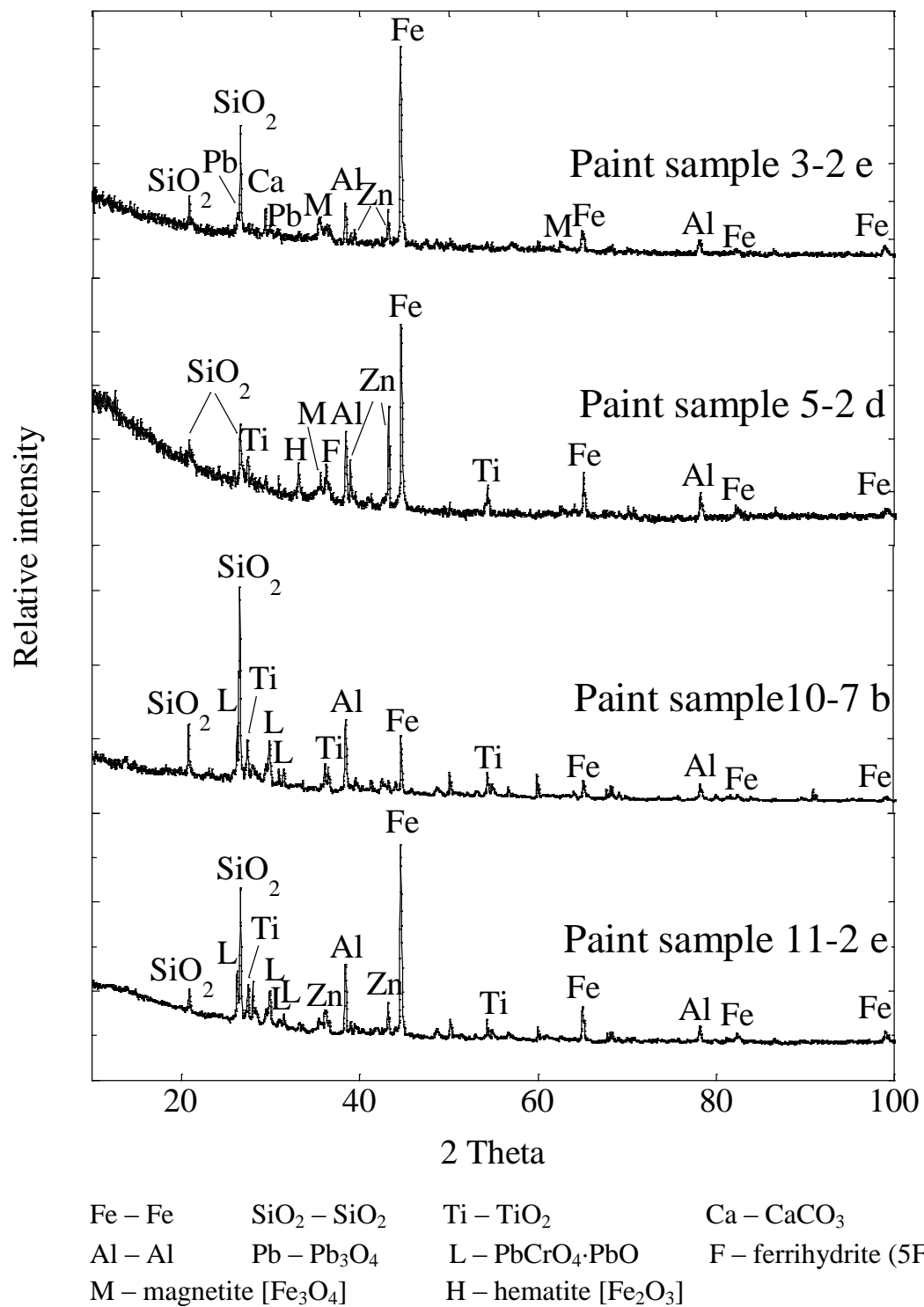


Figure 22. XRD analysis of the possible minerals in paint samples from Regions 3, 5, 10, and 11.

Table 4. Semi- quantitative information from using XRD analysis on paint waste samples.

| Bridge sample ID | Major minerals in paint waste (Wt %) | | | | |
|---------------------|--------------------------------------|---|---|--|---|
| 2-1 b | Quartz (SiO ₂) | Zinc (Zn) | Zincite (ZnO) | Al | Rutile (TiO ₂), |
| | 37 | 37 | 10 | 9 | 5 |
| 2-2 e | Quartz(SiO ₂) | Zinc(Zn) | Fe | Al | Rutile (TiO ₂), |
| | 47.5 | 27.3 | 14.1 | 8.1 | 3 |
| 3-2 e | Al | Fe | magnetite(Fe ₃ O ₄), | Quartz (SiO ₂), | CaCO ₃ |
| | 32 | 23 | 23 | 15 | 7 |
| 5-1 b | Fe | Quartz (SiO ₂) | Al | Hemetite (Fe ₂ O ₃), | Rutile (TiO ₂), |
| | 29 | 24 | 21 | 11 | 11 |
| 5-2 d | Fe | Quartz (SiO ₂) | Rutile (TiO ₂) | CaCO ₃ | Hemetite (Fe ₂ O ₃) |
| | 26 | 27 | 16 | 12 | 11 |
| 5-4 c | Quartz (SiO ₂), | CaCO ₃ | Zn | Al | Magnetite(Fe ₃ O ₄), |
| | 59.6 | 12.1 | 8.1 | 8.1 | 7.1 |
| 5-5 d | Al | Quartz (SiO ₂), | Fe | Zn | Goethite [FeO(OH)] |
| | 40.6 | 22.8 | 14.9 | 11.9 | 9.9 |
| 10-9 | Quartz(SiO ₂) | Al | Rutile (TiO ₂) | BaSO ₄ | Phoenicochroite (Pb ₂ OCrO ₄) |
| | 77 | 12 | 4 | 4f | 3 |
| 11-2 a | Quartz (SiO ₂) | Phoenicochroite (Pb ₂ OCrO ₄) | Rutile (TiO ₂) | Cr ₂ O ₃ | |
| | 70 | 11 | 10 | 9% | |
| 11-2 e | Quartz (SiO ₂) | Al | Fe | Rutile (TiO ₂), | Phoenicochroite (Pb ₂ OCrO ₄) |
| | 37.6 | 25.7 | 14.9 | 8.9 | 5 |

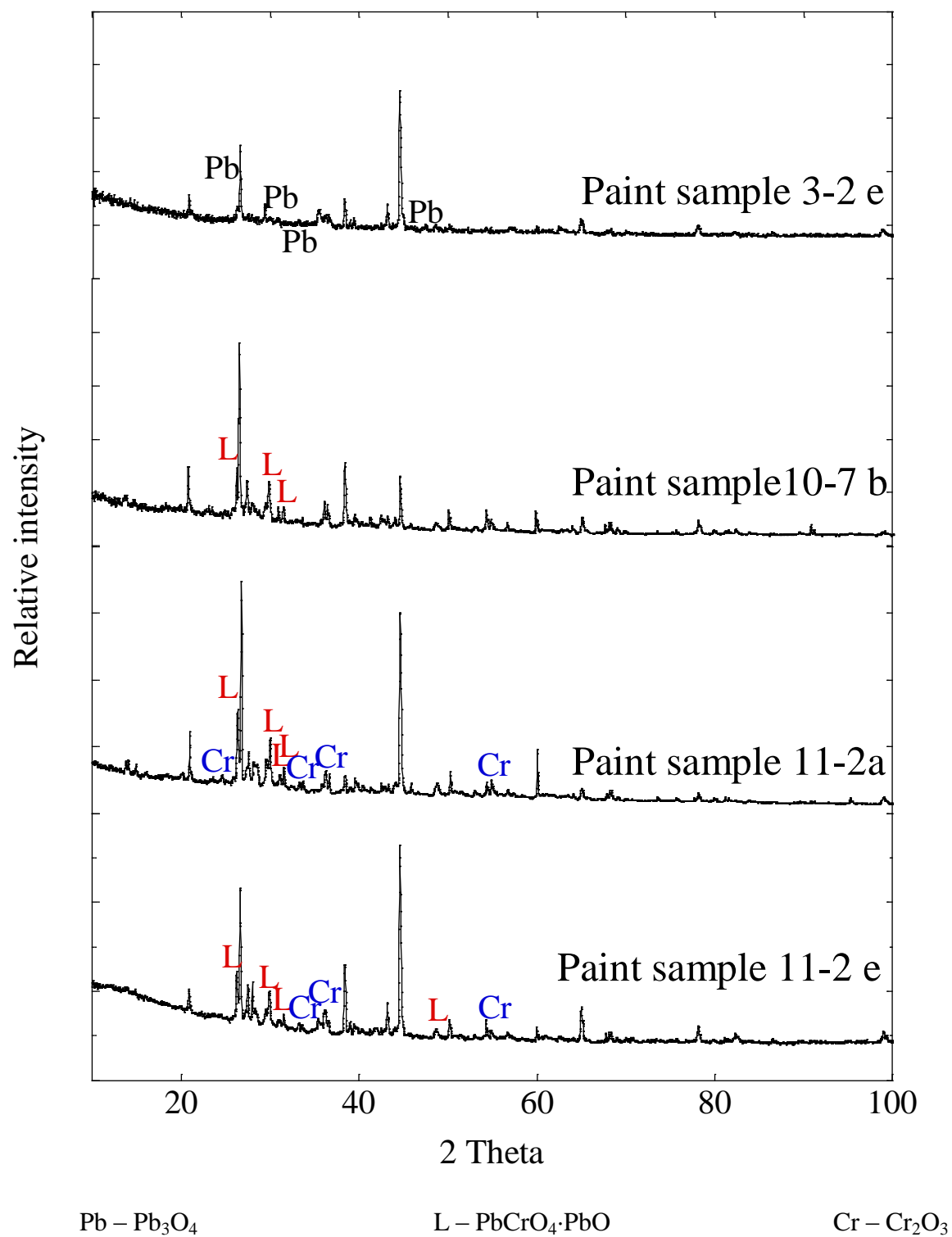


Figure 23. XRD patterns of lead and chromium in paint samples from Regions 3, 10, and 11.

as a green color pigment (Lambourne and Strivens, 1999). Another explanation for the presence of Cr_2O_3 can be attributed to the degradation (reduction) of the pigment itself. Reduction of $\text{PbCrO}_4\cdot\text{PbO}$ to the trivalent state (Cr_2O_3) in paint has been studied by several researchers (Somme-Dubru et al., 1981; Erkens et al., 2001; Monico et al., 2011). This redox process is induced by the use of heat, UV-visible light, contaminants, and SO_2 (Somme-Dubru et al., 1981; Erkens et al., 2001). A recent study from Monico et al. (2011) investigated the redox process of chromate yellow pigment ($\text{PbCrO}_4 \cdot \text{PbO}$) in paintings by using high lateral resolution spectroscopic methods such as microscopic X-ray absorption near edge (μ -XANES), X-ray fluorescence spectrometry (μ -XRF), and electron energy loss spectrometry (EELS). They found approximately two-thirds of the chromium present at the surface was reduced to Cr(III) compounds such as $\text{Cr}_2\text{O}_3\cdot 2\text{H}_2\text{O}$.

In addition to the materials discussed above, iron oxides were observed in the paint wastes as well. XRD demonstrated the presence of iron oxides which are due in part to the steel grit. Iron oxides in the paint waste are comprised of ferrihydrite [$5\text{Fe}_2\text{O}_3\cdot 9\text{H}_2\text{O}$ or $\text{Fe}_5\text{HO}_8\cdot 4\text{H}_2\text{O}$], magnetite [Fe_3O_4], goethite [$\alpha\text{-FeO}(\text{OH})$], hematite [Fe_2O_3], or a mixture of these phases (Figure 24). Ferrihydrite is one of the most widespread form in natural settings (Jambor and Dutrizac, 1998; Komarek et al., 2013) and is generally classified according to the number of X-ray diffraction lines: typically two-line ferrihydrite exhibits little crystallinity while six-line ferrihydrite is more crystalline. Specifically, two-line ferrihydrite (bulk composition $5\text{Fe}_2\text{O}_3\cdot 9\text{H}_2\text{O}$) is a poorly crystalline Fe(III) oxyhydroxide occurring as small (2-4 nm) spherical particles that aggregate in the environment (Dzombak and Morel, 1990; Jambor and Dutrizac, 1998). In this study, relatively smaller diameter (0.3 to 1 mm) (Appendix B) steel grit remained

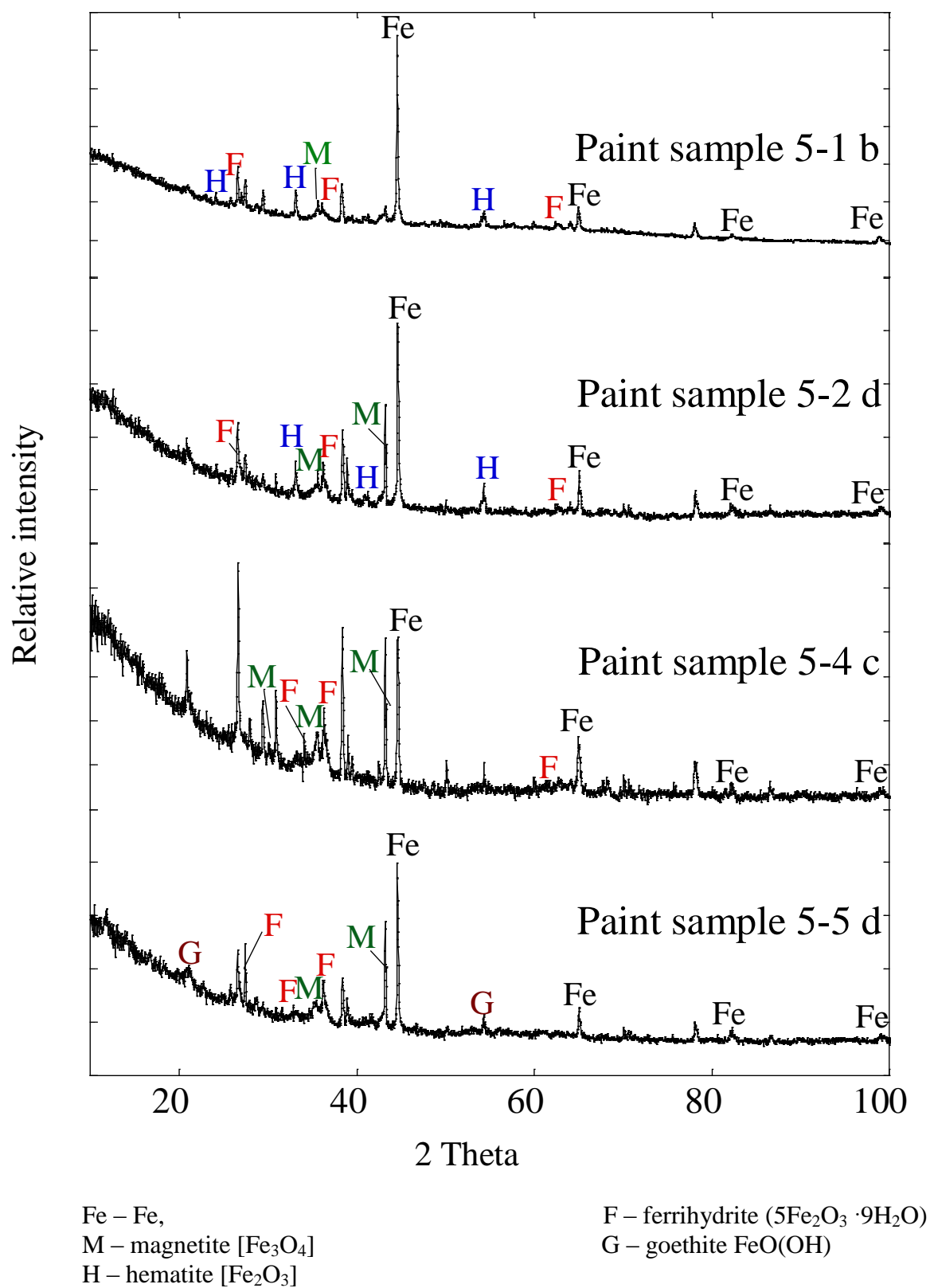


Figure 24. XRD patterns of iron and iron oxide in paint waste samples from Region 5.

in the waste. Although the mass percentage of iron oxide is not significant in the paint waste (Table 4), the large surface area of the oxide coatings provide an important sink for metals.

The formation of the iron oxide has been observed by many researchers (Stipp et al., 2002; Lu et al., 2011). Stipp et al. (2002) found that two-line ferrihydrite forms rapidly on wet samples. Atomic force microscopy (AFM) results indicated ferrihydrite particles size ranged from 0.5 to several tens of nanometers (Stipp et al., 2002). A recent study (Lu et al., 2011) showed that the size distribution of suspended ferrihydrite ranged from 2 to 6 nm diameter spheres. Lu et al. (2011) hypothesized that Pb^{2+} was first adsorbed onto the nanometer-sized, metastable, iron oxyhydroxide polymers of 2-line ferrihydrite. As these nano-particles assembled into larger particles, Pb^{2+} was trapped in the iron oxyhydroxide structure and re-arranged to form solid solutions. On the other hand, ferrihydrite may be gradually converted to the more crystalline and stable Fe(III) oxides goethite [$\alpha\text{-FeO(OH)}$; $K_{\text{SP}} = 10^{-41}$] and hematite ($\alpha\text{-Fe}_2\text{O}_3$; $K_{\text{SP}} = 10^{-43}$) at neutral pH (Das et al., 2011) (Figure 25). Nonetheless, its significant capacity and large surface area allows iron oxide to act as a sink for many (trace) metals, metalloids, and organic matter.

In summary, primary minerals in the paint wastes are silica (SiO_2), Fe, rutile (TiO_2), Al, calcite (CaCO_3), and Zn. The XRD results revealed pigments used before 1989 such as Pb_3O_4 , $\text{PbCrO}_4\cdot\text{PbO}$, and Cr_2O_3 . Iron oxides observed in paint waste included ferrihydrite [$5\text{Fe}_2\text{O}_3\cdot 9\text{H}_2\text{O}$ or $\text{Fe}_5\text{HO}_8\cdot 4\text{H}_2\text{O}$], magnetite [Fe_3O_4], goethite [$\alpha\text{-FeO(OH)}$], and hematite [Fe_2O_3]. Although the mass percentage of iron oxide is not significant in the paint waste (Table 4), the large surface area of the oxide coatings acts as a sink for Pb and other metals. While minerals and iron oxide phases in the paint waste were observed from XRD analysis, the morphology provides surface structure and surface chemical composition for the samples. Therefore, FESEM/EDX analysis

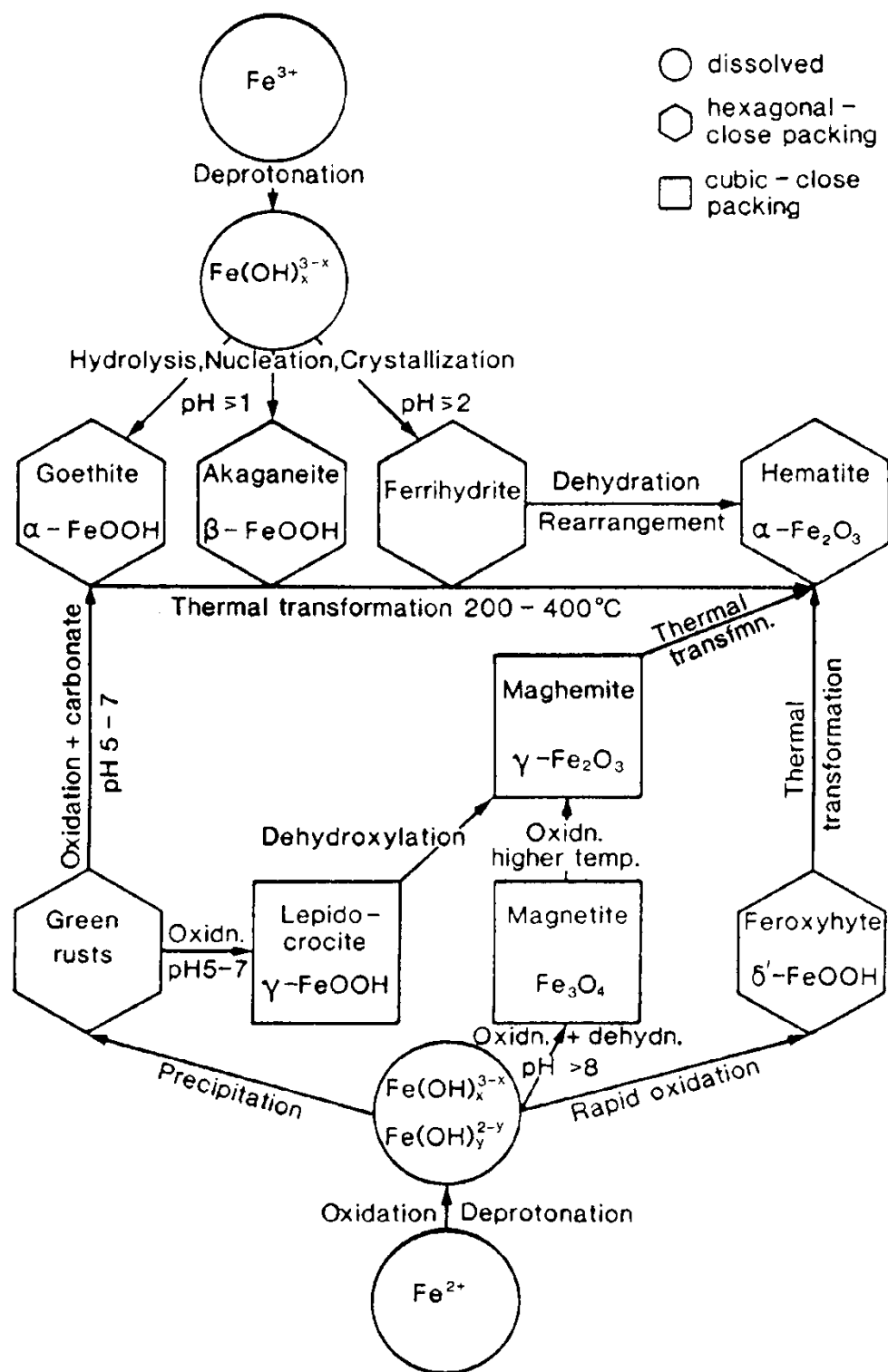


Figure 25. Schematic representation of formation and transformation pathways of common iron oxides, together with the approximate transformation conditions (Schwertmann and Cornell, 1991; Jambor and Dutrizac, 1998).

was applied to investigate the form of iron on the steel grit surface and metal association with this surface in the paint waste.

4.5 FESEM/EDX analysis

In FESEM analysis, paint waste samples were observed to be non-uniform (Figure 26a). Elemental mapping from EDX (Figure 26b) identified the distribution of paint particles (green particles, Figure 26b) and steel grit (blue particles, Figure 26b) in the paint waste. Furthermore, observation of Si, Ti, Ca, Zn, and Al being associated with Pb and Cr (Figure 26c) are indicative of the application of associated compounds in the paint (Table 5). This result is consistent with other similar studies (Walker et al., 2011; Franquelo et al. 2012) and our XRD analysis, where silica, rutile, calcite, Zn/ZnO, Al, Pb₃O₄/ PbCrO₄·PbO, and Cr₂O₃ were identified. On the other hand, elemental mapping from EDX (Figure 26c) revealed concentrated Fe in the steel particles (blue particles, Figure 26b), and is somewhat consistent with the analysis in that elevated iron in the waste is not from paint itself but from steel grit. Interestingly, the relative distribution of Pb and Cr is localized around Fe, which suggests their association with steel grit. To further investigate the metal association with the steel grit surface, FESEM was applied on the particle which is identified as steel grit by EDX (Figure 27). The surface of the steel grit exhibited non-uniform amorphous particles (Figure 27). The elevated Fe (25.81% by weight) and O (35.01%) demonstrated that iron oxide form on the steel grit surface. Iron oxides have been observed by many researchers (Stipp, et al. 2002; Equeenuddin et al., 2010; Wu et al., 2007; Lu et al., 2012; Zhang et al., 2013). Goethite was reported in the form of needle-shaped structure (Stipp, et al. 2002; Equeenuddin et al., 2010) and ferrihydrite was observed as spherical particles ranging from 13 to 30 nm (Equeenuddin et al., 2010). Magnetite was found as spherical particles as well

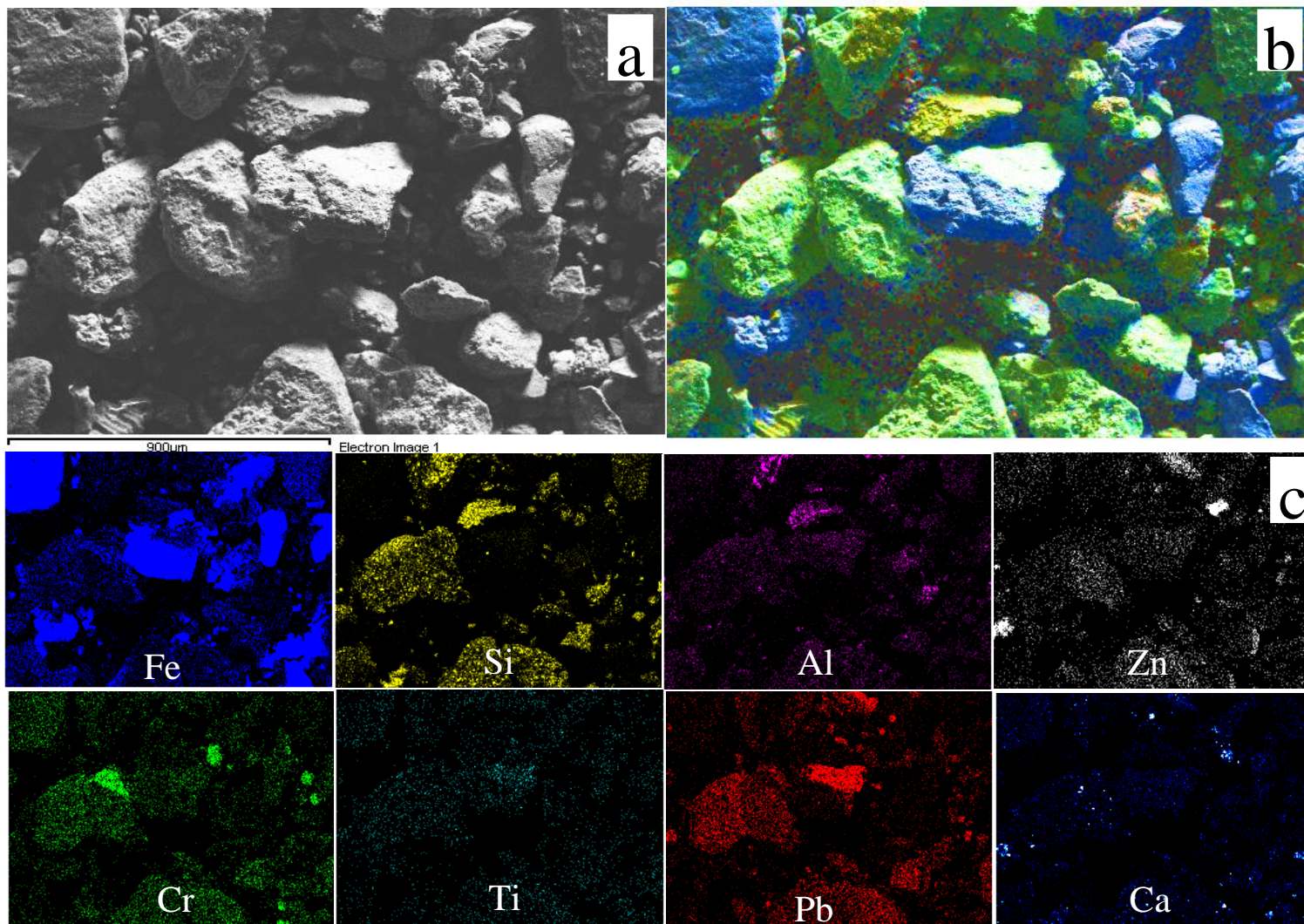


Figure 26. FE-SEM images and EDX mapping on the paint waste sample. (a) FE-SEM image; (b) Blue particles represent the steel grit; green particles present the paint in the paint waste; (c) EDX mapping on paint waste sample from Region 7 (color images in mapping represent the corresponding elements).

Table 5. Typical pigment and associated compounds in liquid paints^a

| White | | Protective | |
|--|--------|--|--------|
| Titanium dioxide [TiO ₂] | 15-20% | Basic lead silichromate [4(PbCrO ₄ ·PbO) + 12(SiO ₂ ·PbO)] | 25-35% |
| Zinc oxide [ZnO] | 15-20% | Basic lead sulfate [PbO·PbSO ₄] | 15-20% |
| Antimony oxide [Sb ₂ O ₃] | 15-20% | Calcium plumbate [Ca ₂ PbO ₄] | 30-40% |
| White lead [2PbCO ₃ ·Pb(OH) ₂] | 15-20% | Red lead [Pb ₃ O ₄] | 30-35% |
| | | Zinc phosphate [Zn ₃ (PO ₄) ₂] | 25-30% |
| | | Zinc tetroxychromate [ZnCrO ₄ ·4Zn(OH) ₂] | 20-25% |
| | | Zinc chromate [ZnCrO ₄] | 30-40% |
| Green | | Blue | |
| Chromium oxide [Cr ₂ O ₃] | 10-15% | Prussian blue ^b [MFeFe(CN) ₆ ·H ₂ O] | 5-10% |
| Lead chrome green [PbCrO ₄] | 10-15% | Ultramarine blue [Na _{6,9} Al _{5,6} Si _{6,4} O ₂₄ S _{4,2}] | 10-15% |
| Black | | Metallic | |
| Black iron oxide [Fe ₂ O ₃ +MnO ₂] | 10-15% | Zinc | 60-70% |
| Carbon black | 1-5% | Lead | 40-50% |
| Yellow | | | |
| Lead chromates [Pb(Cr,S)O ₄] | 10-15% | | |
| Zinc chromates [ZnCrO ₄] | 10-15% | | |
| Cadmium sulfide [CdS] | 5-10% | | |

a: Boxall and von Frauhoffer (1980)

b: M could include K, Na or CH₃

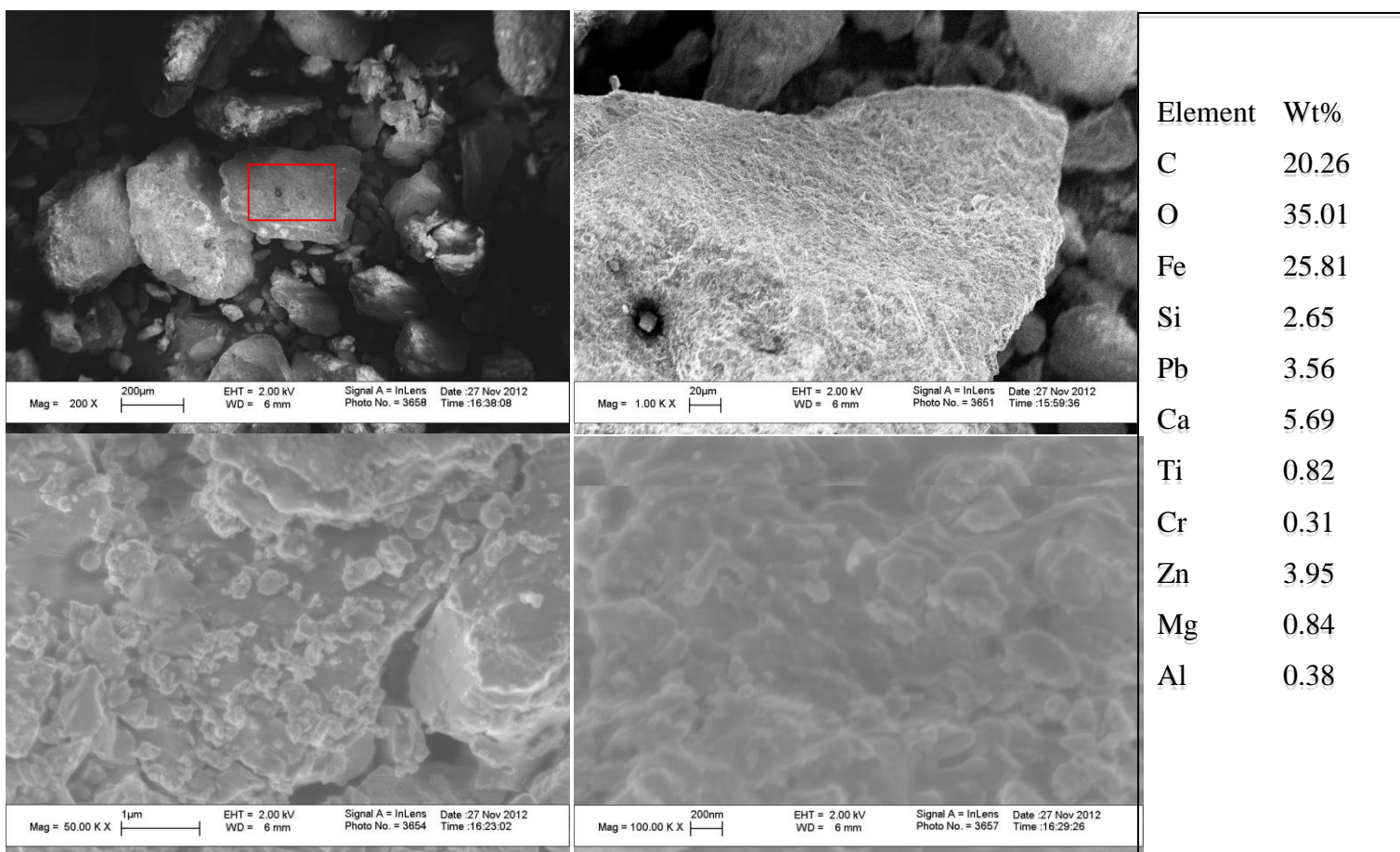


Figure 27. FE-SEM images on the steel grit surface of the paint waste sample from Region 7.

(Wu et al., 2007; Teo et al., 2012). Various structures have been reported for hematite (Zhang et al., 2013) including hexagonal pyramidal columnar (Lu et al., 2012). In this study, spherical particles indicative of ferrihydrite and needle-shaped crystals consistent with goethite were detected on steel grit surface (Figure 27). The size of the crystals observed is less than 200 nm, indicating the aggregated iron oxide formed on the steel grit surface. In addition, Pb (3.56%) and Cr (0.31%) were observed from the steel grit surface (Figure 27) suggesting the sorption of Pb and other metals to the iron oxide.

5. Conclusions

In this report, leaching studies and characterization techniques were combined to investigate possible mechanisms responsible for reduced metal mobility in paint waste. The results obtained can be used for understanding transport of lead and other metals in paint waste as well as in developing a model to simulate and predict metal leachability.

1. TCLP results revealed metal concentrations of Pb, Cr, and Ba were less than the toxicity characteristics (TC) levels (with the exception of three samples exhibiting Cr concentrations greater than the TC of 5 mg L⁻¹), while the other metals and metalloids of As, Se, Cd, Ag, and Hg, were not routinely detected. Metal sorption onto the iron oxide surface is a plausible mechanism responsible for the reduced metal leaching. TCLP results showed greater concentrations of Zn (20.4 to 1,307 mg L⁻¹), and dissolution is most likely the mechanism responsible for its leaching. Elevated Fe (183 to 3,275 mg L⁻¹) observed can be attributed to complexation with organic ligands and colloidal iron oxide particles from the steel grit surface that may release or become suspended in solution under turbulent conditions.

2. Significant alkalinity was observed in the paint waste. The greatest desorption or/and dissolution was detected in the first day. Subsequently, leaching decreased with increasing time (from the second day to then tenth day). MEP results revealed greater lead concentrations in the leachate than in the TCLP, and may be attributed to the higher ionic strength applied in MEP. Although the paint waste passed the TCLP test for Pb concentrations, MEP revealed five of the 24 bridge paint samples exhibited Pb greater than the TC level of 5 mg L^{-1} . MEP results exhibited increased metal concentrations such as Pb, Cr, and Ba in the leachate for pH greater than 7. This result can be attributed to the metal complexation with organic ligands in the leaching solution. Other trace metals exhibited leached concentrations much less than the TC levels.
3. The extraction revealed exchangeable and carbonate phases constituted 0.01 to 0.02% of Pb, less than 0.0001(detection limit) to 0.05% of Cr, 0.02 to 1.20% of Ba, and 2.35 to 6.39% of Zn. A greater contribution of these metals (7.69 to 14.38% of Pb, 3.34 to 5.26% of Cr, 1.03 to 2.75% of Ba, and 4.78% to 6.30% of Zn) were observed to be associated with iron oxides. The degree of metal affinity for iron oxides followed the trend of $\text{Pb} > \text{Zn} > \text{Cr} > \text{Ba}$. Inorganic pigments complex with polymer to produce homogenous viscous fluid in paint, which result in greater fraction of organically bound metals (36.6% of Pb, 14.1% of Cr, 1.4% of Ba, and 4.1% of Zn). Approximately 53% of Pb, 82% of Cr, 96% of Ba, and 86% of Zn are associated with residual phase involving minerals in the paint (SiO_2 , TiO_2 , and Al), steel grit (iron) in the waste, or various constituents in the pigment matrix more difficult to digest (Barnes and Davis, 1996). Pb overall exhibited greater mobility than other metals in this extraction. The degree of mobilization in this extraction followed the trend of $\text{Pb} > \text{Cr} \approx \text{Zn} > \text{Ba}$.

4. Primary minerals in the paint wastes are silica (SiO_2), Fe (Kamacite), rutile (TiO_2), Al, calcite (CaCO_3), and Zn (metal). XRD results revealed pigments used before 1989 such as Pb_3O_4 , $\text{PbCrO}_4 \cdot \text{PbO}$, and Cr_2O_3 . The iron oxides observed in paint waste included ferrihydrite [$5\text{Fe}_2\text{O}_3 \cdot 9\text{H}_2\text{O}$ or $\text{Fe}_5\text{HO}_8 \cdot 4\text{H}_2\text{O}$], magnetite [Fe_3O_4], goethite [$\alpha\text{-FeO(OH)}$], and hematite [Fe_2O_3]. Although the mass percentage of iron oxide is not significant in the paint waste, the large surface area allows oxides such as ferrihydrite to act as a sink for Pb and other metals. FESEM/EDX analysis further corroborated the presence of iron oxide on the steel grit surface. Pb and Cr were observed associated with the steel grit surface suggesting sorption of Pb and other metals to the surface.

6. References

- Apul, D., Gardner, K. H., Eighmy, T. T. (2006) Simultaneous Application of Dissolution/Precipitation and Surface Complexation/Surface Precipitation Modeling to Contaminant Leaching. *Environmental Science and Technology*, 39: 5736-5741.
- Abdel - Raouf, M. W., and Nowler, H. G. (2004) Assessment of fossil fuel fly ash formaulatations in the immobilization of hazardous wastes. *Journal of Environmental Engineering*, 130, 499–507.
- American Society for Testing and materials (ASTM) (1990) Standard practice for decontamination of field equipment used at nonradioactive waste sites, Designation D5088-90, West Conshohocken, PA.
- Ashley, K., Applegate, G. T., Marcy, A. D., Drake, P. L., Pierce, P. A., Carabin, N., Demange, M. (2009) Evaluation of sequential extraction procedures for soluble and insoluble hexavalent chromium compounds in workplace air samples. *Journal of Environmental Monitoring*, 11 (2): 318-325.
- Alphen, M. (1998) Paint film components, National Environmental Health Forum Monographs, General Series No. 2.
- Appleman, B. R. (1992) Bridge paint: removal, containment, and disposal, Transportation Research Board, Washington, DC., Report 176.
- Appleman, B. R. (1998) Lead-Based Paint removal for Steel highway Bridges, Transportation Research Board, Washington, DC., Report 251.
- Barnes G. L., Davis, A. P. (1996) Dissolution of Lead Paint in Aqueous Solutions. *Journal of Environmental Engineering*, 122 (7): 663-666.
- Bernecki, T. F., Nichols, G. M., Prine, D., Shubinsky, G. Zdunek, A. (1995) "Chapter 4 - Evaluation of Procedures for Analysis and Disposal of Lead-Based Paint-Removal Debris," Issues Impacting Bridge Painting: An Overview, Infrastructure Technology Institute, FHWA/RD/94/098, August 1995, Northwestern University.
- Boy F. H., Race, T. D., Reinbold, K. A., Bukowski, J., Zhu, X. (1995) Chromium stabilization chemistry of paint removal wastes in Portland cement and blast furnace slag, *Hazardous waste and hazardous materials*, 12 (1): 83-95.
- Boxall, J., Von Fraunhofer J. A., Paint Formulation: principles and practice. George Goodwin Limited, London, 1980.

Bradl, H. B. (2004) Adsorption of heavy metal ions on soils and soils constituents. *Journal of Colloid and Interface Science*, 277: 1–18.

Bonneau, A., Pearce, D.G., Pollard, A.M. (2012) A multi-technique characterization and provenance study of the pigments used in San rock art, South Africa. *Journal of Archaeological Science*, 39: 287-294.

Brokbartold, M., Wischermann, M., Marschner, B. (2012) Plant availability and uptake of lead, zinc, and cadmium in soils contaminated with anti-corrosion paint from pylons in comparison to heavy metal contaminated urban soils. *Water, Air, and Soil Pollution*, 223:199–213.

Brunori, C., Cremisini, C., D., Annibale, L., Massanisso, P., Pinto, V. (2005a) A kinetic study of trace element leachability from abandoned-mine-polluted soil treated with ss-msw compost and red mud, Comparison with results from sequential extraction. *Analytical Bioanalytical Chemistry*, 381: 1347–1354.

Bidoglio, G., Gibson, P. N., Gorman, M. O., Roberts, K. J. (1993) X-ray absorption spectroscopy investigation of surface redox transformations of thallium and chromium on colloidal oxides, *Geochimica et Cosmochimica Acta*, 57: 2389–2394.

Bowers, A. R., Huang, C. P. (1986) Adsorption characteristics of metal-EDTA complexes onto hydrous oxides. *Journal of colloid and interface science*, 110 (2): 575-590.

Baes, C. F., Mesmer, R. E., 1976, *The Hydrolysis of Cations*, Wiley, New York.

Bentley, J., Turner, G. P. A., Turner, G. P. (1998). *Introduction to Paint Chemistry: Principles of Paint Technology*. CRC PressI Llc.

Connor, John; Email on April 10th 2013.

Chen, F., Burnsb, P. C., Ewing, R. C. (1999) ⁷⁹Se: geochemical and crystallo-chemical retardation mechanisms. *Journal of Nuclear Materials*, 275 (1): 81–94.

Ciccu, R., Ghiani, M., Serici, A., Fadda, S., Peretti, R., Zucca, A. (2003) Heavy metal immobilization in the mining-contaminated soils using various industrial wastes. *Minerals Engineering*, 16: 187–192.

Csoban, K., Parka'nyi-Berka, M., Joo, P., Behra, P. (1998) Sorption experiments of Cr(III) onto silica. *Colloids and Surfaces A: Physicochemical and Engineering Aspects*, 141: 347–364.

Cornelis, G., Johnson, C. A., Gerven, T. V., Vandecasteele, C. (2008) Leaching mechanisms of oxyanionic metalloid and metal species in alkaline solid wastes: A review. *Applied Geochemistry*, 23: 955–976.

Cornell, R. M., Franquelo, U. (1996) *The Iron Oxides. Structure, Properties, Reactions, Occurrence and Uses*. VCH Verlagsgesellschaft mbH, Weinheim, Germany.

Cullen, W. R., Reimer, K. J. (1989) Arsenic speciation in the environment. *Chemical Reviews*, 89 (4): 713-764.

Covelo, E. F., Vega, F. A., Andrade, M. L. (2007) Competitive sorption and desorption of heavy metals by individual soil components. *Journal of Hazardous Materials*, 140(1): 308-315.

Daub, K., Zhang, X., Wang, L., Qin, Z., Noël, J. J., Wren, J. C. (2011) Oxide growth and conversion on carbon steel as a function of temperature over 25 and 80° C under ambient pressure. *Electrochimica Acta*, 56(19): 6661-6672.

Daniels, A. E., Kominsky, J. R., Clark, P. J. (2001) Evaluation of two lead-based paint removal and waste stabilization technology combinations on typical exterior surfaces, *Journal of Hazardous Materials*, B87: 117–126.

Dzombak, D. A., Morel, F. M. M., *Surface Complexation Modeling Hydrous Ferric Oxide*, Wiley: New York, 1990.

Davranche, M., Bollinger, J. C. (2000) Heavy Metal Desorption from Synthesized and Natural iron and Manganese Oxyhydroxides: Effect of Reductive Conditions. *Journal of Colloid and Interface Science*, 227: 531-539.

Davis, A. P., Bhatnagar, V. (1995) Adsorption of cadmium and humic acid onto hematite. *Chemosphere*, 30 (2): 243-256.

Deng, Y., Stjernström, M., Banwart, S. (1996) Accumulation and remobilization of aqueous chromium(VI) at iron oxide surfaces: application of a thin-film continuous flow-through reactor, *Journal of Contaminant Hydrology*, 21: 141–151.

Du, J., Lu, J. Wu, Q., Jing, C. (2012) Reduction and immobilization of chromate in chromite ore processing residue with nanoscale zero-valent iron. *Journal of Hazardous Materials*, 215– 216: 152– 158.

Environmental Canada and Alberta Environmental Centre (Testing Methods, Canada) (1986) *Test methods for solidified waste characterization*, Edmonton.

Essington, M.E., *Soil and Water Chemistry, an Integrative Approach*. CRC Press, Boca Raton, Florida, USA, 2004.

Eaton, A. D., Clesceri, L. S., Rice, E. W., Greenberg, A. E. (2005) *Standard methods for the examination of water and wastewater*, 21st edition, 3: 79-81.

Elzinga E. J., Sparks, D. (2002) X-ray Absorption Spectroscopy Study of the Effects of pH and Ionic Strength on Pb(II) Sorption to Amorphous Silica. *Environmental Science and Technology*, 36: 4352-4357.

Esakku, S., Karthikeyan, O. P., Joseph, K., Nagendran, R. (2008) Heavy metal fractionation and leachability studies on fresh and partially decomposed municipal solid waste. *Practice Periodical of Hazardous, Toxic, and Radioactive Waste Management*, 4:127-132.

Equeenuddin, S. M., Tripathy, S., Sahoo, P. K., Panigrahi, M. K. (2010) Geochemistry of ochreous precipitates from coal mine drainage in India *Environmental Earth Sciences*, 61(4): 723-731.

Erkens, L. J. H., Hamers, H., Hermans, R. J. M., Claeys, E., Bijnens, M. (2001) Lead chromates: A review of the state of the art in 2000. *Surface Coatings International Part B: Coatings Transactions*, 84(3): 169-176.

Franquelo, M. L., Duran, A., Castaing, J., Arquillo, D., Perez-Rodriguez, J. L. (2012) XRF, μ -XRD and μ -spectroscopic techniques for revealing the composition and structure of paint layers on polychrome sculptures after multiple restorations. *Talanta*, 89: 462-469.

Ferlauto, E. C., Emami, M., Galante-Fox, J., Grivna, M., Habeck, E., Jones, L., Wood, L. (1994) Selection of corrosion test methods based on mechanism principles. *JCT, Journal of coatings technology*, 66(835): 85-97.

Feng, D., Van Deventer, J. S. J., and Aldrich, C. (2004) Removal of pollutants from acid mine wastewater using metallurgical by-product slags. *Separation and Purification Technology*, 40: 61-67.

Filgueiras, A. V.; Lavilla, I.; Bendicho, C. (2002) Chemical sequential extraction for metal partitioning in environmental solid samples, *Journal of Environmental Monitoring*, 4 (6): 823-857.

Friesl, W., Lombi, E., Horak, O., Wenzel, W. W. (2003) Immobilization of heavy metals in soils using inorganic amendments in a greenhouse study. *Journal of Plant Nutrition and Soil Science* 166: 191-196.

Fortin, D., Leppard, G. G., Tessier, A. (1993) Characteristics of lacustrine diagenetic iron oxyhydroxides. *Geochimica et Cosmochimica Acta*, 57(18): 4391-4404.

Federal Highway Administration (FHWA) (1989) Performance of Alternative Coatings in the Environment (PACE), Vol. I (Publication No. FHWA-RD-89-127), Vol. II (Publication No. FHWA-RD-89-235), and Vol. III (Publication No. FHWA-RD-89-236), Washington, D.C.

Feliciano, Willie; Kochersberger, Carl; Email on August 24th 2011.

Fan, M., Boonfueng, T., Xu, Y., Axe, L., Tysonb, T. A. (2005) Modeling Pb sorption to microporous amorphous oxides as discrete particles and coatings. *Journal of Colloid and Interface Science*, 281: 39–48.

Gibbs, R.J. (1973). Mechanisms of trace metal transport in rivers. *Science*, 180, 71–73.

Gooch, J. W., *Lead-Based Paint Handbook*, Plenum Press, New York, 1993.

Hartley, W., Edwards, R., Lepp, N. W. (2004) Arsenic and heavy metal mobility in iron oxide-amended contaminated soils as evaluated by short- and long-term leaching tests. *Environmental Pollution*, 131: 495–504.

Haynes, R. J. (1982) {Haynes, 1982 #83}. A critical review in *Plant and Soil*, 68: 289–308.

Halim, C. E., Amal, R., Beydoun, D., Scott, J. A., Low, G. (2003) Evaluating the applicability of a modified toxicity characteristic leaching procedure (TCLP) for the classification of cementitious wastes containing lead and cadmium. *Journal of Hazardous Materials*, B103: 125–140.

Hass, A., Fine, P. (2010) Sequential Selective Extraction Procedures for the Study of Heavy Metals in Soils, Sediments, and Waste Materials-a Critical Review. *Critical Reviews in Environmental Science and Technology*, 40: 365–399.

Hedberg, J., Henriquez, J., Baldelli, S., Johnson, C. M., Leygraf, C. (2008) Initial Atmospheric Corrosion of Zinc Exposed to Formic Acid, Investigated by in Situ Vibrational Sum Frequency Spectroscopy and Density Functional Theory Calculations. *The Journal of Physical Chemistry C*, 113: 2088–2095.

Hedberg, J., Baldelli, S., Leygraf, C., Tyrode, E. (2010) Molecular Structural Information of the Atmospheric Corrosion of Zinc Studied by Vibrational Spectroscopy Techniques. *Journal of the Electrochemical Society*, 157 (10): C357-C362.

Helmke, P. A., Naidu, R. (1996) Fate of contaminants in the soil environment: Metal contaminants. In Naidu, R., Kookana, R. S., Oliver, D. P., Rogers, S., and McLaughlin, M. J. (eds.). *Contaminants and the soil environment in the Australasia-Pacific region*. Dordrecht: Kluwer, 69–93.

Howard, J. L., Shu, J. (1996) Sequential extraction analysis of heavy metals using a chelating agent (NTA) to counteract resorption. *Environmental Pollution*, 91(1): 89-96.

Hartley, W., Lepp, N. W. (2008) Remediation of arsenic contaminated soils by iron-oxide application, evaluated in terms of plant productivity, arsenic and phytotoxic metal uptake. *Science of the Total Environment*, 390 (1): 35-44.

Hayes, K. F., Leckie, J. O. (1987) Modeling ionic strength effects on cation adsorption at hydrous oxide/solution interfaces. *Journal of Colloid and Interface Science*, 115(2): 564-572.

Ho, M. D., Evans, G. J. (2000) Sequential extraction of metal contaminated soils with radiochemical assessment of readsorption effects, *Environmental Science and Technology*, 34(6): 1030-1035.

Illés, E., Tombácz, E. (2003) The role of variable surface charge and surface complexation in the adsorption of humic acid on magnetite. *Colloids and Surfaces A: Physicochemical and Engineering Aspects*, 230(1): 99-109.

Iowa Department of Transportation [IADOT], Chapter 10, Construction Manual, October, 2006. http://www.iowadot.gov/erl/archives/oct_2006/CM/content/10-50.htm

Izquierdo, M., Querol, X. (2012) Leaching behavior of elements from coal combustion fly ash: An overview. *International Journal of Coal Geology*, 94: 54–66.

Jing, C., Liu S., Korfiatis, G. P., Meng, X. (2006) Leaching behavior of Cr (III) in stabilized/solidified soil. *Chemosphere*, 64: 379-385.

Jambor, J. L., Dutrizac, J. E. (1998) Occurrence and constitution of natural and synthetic ferrihydrite, a widespread iron oxyhydroxide. *Chemical Review*, 98: 2549–2585.

Jessop, A., Turner A. (2011) Leaching of Cu and Zn from discarded boat paint particles into tap water and rain water. *Chemosphere*, 83: 1575–1580.

Jeong, D., Kim, K., Choi, W. (2012) Accelerated dissolution of iron oxides in ice, *Atmospheric Chemistry and Physics*, 12: 11125–11133.

JCPDS (1998) Handbook for diffraction data (PCPDFWIN ver. 2.00).

Jin, X., Bailey, G. W., Yu, Y. S., Lynch, A. T. (1996) Kinetics of single and multiple metal ion sorption processes on humic substances. *Soil science*, 161 (8): 509-520.

Jackson, T. A. (1998) The biogeochemical and ecological significance of interactions between colloidal minerals and trace elements. In Parker, A., and Rae, J. E. (eds.). *Environmental interactions of clays*. Berlin, Germany: Springer-Verlag, 93–205.

Kukier, U., Ishak, C. F., Sumner, M. E., Miller, W. P. (2003) Composition and element solubility of magnetic and non-magnetic fly ash fractions. *Environmental Pollution*, 123(2): 255-266.

Kumpiene, J., Mench, M., Bes, C. M., Fitts, J. P., (2011) Assessment of aided phytostabilization of copper-contaminated soil by X-ray absorption spectroscopy and chemical extractions. *Environmental Pollution*, 159: 1536-1542.

Kochersberger, Carl; Email on June 7th 2011.

Kochersberger, Carl; Bass, Jonathan; Conference call for the preliminary results. August 9th 2011.

Kartal, S., Aydin, Z., Tokalioglu, S. (2006) Fractionation of metals in street sediment samples by using the BCR sequential extraction procedure and multivariate statistical elucidation of the data. *Journal of Hazardous Materials*, 132: 88-89.

Karamalidis, A., Coudrias, E. A. (2008) Anion Leaching from Refinery Oily Sludge and Ash from Incineration of Oily Sludge Stabilized/Solidified with Cement, Part II. Modeling. *Environmental Science and Technology*, 42: 6124-6130.

Krishnamurti, G. S. R., Naidu, R. (2000) Speciation and phytoavailability of cadmium in selected surface soils of South Australia. *Australian Journal of Soil Research*, 38: 991–1004.

Krishnamurti, G. S. R., Naidu, R. (2002) Solid-solution speciation and phytoavailability of copper and zinc in soils. *Environmental Science and Technology*, 36: 2645–2651.

Kendall, S. D. (2003) Toxicity Characteristic Leaching Procedure and Iron Treatment of Brass Foundry Waste. *Environmental Science and Technology*, 37: 367-371.

Komarek, M., Vanek, A., Ettler, V. (2013) Chemical stabilization of metals and arsenic in contaminated soils using oxides -A review. *Environmental Pollution* 172: 9-22.

Lambourne, R., Strivens, T., *Paint and Surface Coatings: Theory and Practices*, Woodhead Publishing, Cambridge, 1999.

Lu, P., Nuhfer, N. T., Kelly, S., Li, Q., Konishi, H., Elswick, E., Zhu, C. (2011) Lead coprecipitation with iron oxyhydroxide nano-particles. *Geochimica et Cosmochimica Acta*, 75: 4547-4561.

Liang, L., Korte, N., Gu, B., Puls, R., Reeter, C. (2000) Geochemical and microbial reactions affecting the long-term performance of in situ ‘iron barriers’. *Advances in Environmental Research*, 4(4): 273-286.

Langmuir, D., *Aqueous Environmental Geochemistry*. Prentice-Hall, Upper Saddle River, New Jersey, USA, 1997.

Losi, M. E., Amrhein, C., Frankenberger, W. T. (1994) *Environmental Biochemistry of Chromium*. *Environmental Contamination and Toxicology*, 136: 91-121.

Luoma S. N., Davis, J. A. (1983) Requirement for modeling Trace Metal Partitioning in Oxidized Estuarine Sediments. *Marine Chemistry*, 12: 159-181.

Lutzenkirchen J. (1997) Ionic strength effects on cation sorption to oxides: macroscopic observations and their significance in microscopic interpretation, *Journal of Colloid and Interface Science*, 195: 149–155.

Laforest, G., Duchesne, J. (2006) Characterization and leachability of electric arc furnace dust made from remelting of stainless steel. *Journal of hazardous materials*, 135(1): 156-164.

Lu, B., Li, P., Liu, H., Zhao, L. Y., Wei, Y. (2012) Synthesis of hexagonal pyramidal columnar hematite particles by a two-step solution route and their characterization. *Powder Technology*, 215: 132-136.

Lee, S. H., Park, H., Koo, N., Hyun, S., Hwang, A., (2011) Evaluation of the effectiveness of various amendments on trace metals stabilization by chemical and biological methods. *Journal of Hazardous Materials*, 188: 44-51.

Lombi, E., Zhao, F. J., Zhang, G., Sun, B., Fitz, W., Zhang, H., McGrath, S. P. (2002) In situ fixation of metals in soils using bauxite residue: chemical assessment. *Environmental Pollution*, 118(3): 435-443.

La Force, M. J., Fendorf, S. (2000) Solid-phase iron characterization during common selective sequential extractions. *Soil Science Society of America Journal*, 64(5): 1608-1615.

Monico, L., Snickt, G. V., Janssens, K., Nolf, W. D., Miliani, C., Verbeeck, J., Tian, H., Tan, H., Dik, J., Radepon, M., Cotte, M. (2011), Degradation Process of Lead Chromate in Paintings by Vincent van Gogh Studied by Means of Synchrotron X-ray Spectromicroscopy and Related Methods. 1. Artificially Aged Model Samples, *Analytical Chemistry*, 83: 1214–1223.

Martel, C. M., Athanassopoulos, C., Marinas, B. J. Mobility of Lead from Lead-Based Paint in a Landfill. SWANA's 35th Annual International Solid Waste Exposition, Gateway to Success; St. Louis, MO; Oct 27-30, 1997.

Meima, J., Comans R. J. (1997) Geochemical Modeling of Weathering Reactions in Municipal Solid Waste Incinerator Bottom Ash. *Environmental Science and Technology*, 31 (5): 1269-1276.

Marani, D., Macchi, G., Pagano, M. (1995) Lead Precipitation in the Presence of Sulfate and Carbonate: Testing of Thermodynamic Predictions. *Water Resource*, 29 (4): 1085-1092.

McLaren, R. G., Crawford, D. V. (1973a) Studies on Soil Copper I. The fractionation of Copper in Soils. *Soil Science*, 24: 172–181.

Monico, L., Snickt, G. V., Janssens, K., Nolf, W. D., Miliani, C., Verbeeck, J., Tian, H., Tan, H., Dik, J., Radepon, M., Cotte, M. (2011) Degradation Process of Lead Chromate in Paintings by

Vincent van Gogh Studied by Means of Synchrotron X-ray Spectromicroscopy and Related Methods. 1. Artificially Aged Model Samples. *Analytical Chemistry*, 83: 1214–1223.

Minnesota Department of Transportation [MnDOT] (2004) Air quality and waste management for the removal of paint (using dry abrasive blasting) on steel bridge structures.

http://www.dot.state.mn.us/environment/pdf/bridge_manual_704.pdf

Miller, W. P., Martens, D. C., Zelazny, L. W. (1986b) Effect of sequence in extraction of trace metals from soils. *Soil Science Society of America Journal*, 50: 598–601.

Ma, Y. B., Uren, N. C. (1995) Application of anew fractionation scheme for heavy metals in soils. *Communications in Soil Science and Plant Analysis*, 26: 3291–3303.

Ma, Y. B., Uren, N. C. (1998) Transformations of heavy metals added to soil—Application of a new sequential extraction procedure. *Geoderma*, 84: 157–168.

New York State Department of Transportation, Standard Specification, May 1, 2008.

New York State Department of Transportation (1988) Specification for bridges – removal of lead based paints – new department paint system for structural steel, Engineering instruction, EI 88-36.

Parsa, J., Munson-McGee, S. H., Steiner, R. (1996) Stabilization/solidification of hazardous wastes using fly ash. *Journal of Environmental Engineering*, 122: 935–940.

Palmer, C., Puls, R. (1994) Natural attenuation of hexavalent chromium in ground water and soils, EPA/540/S-94/505. U.S. Environmental Protection Agency Ground Water Issue.

Peterson, M. L., Brown, G. E., Parks, F. A. (1996), Direct XAFS evidence for heterogeneous redox reaction at the aqueous chromium/magnetite interface, *Colloids and Surfaces A: Physicochemical and Engineering Aspects*, 107: 77-88.

Peterson, M. L., Brown, G. E., Parks, F. A., Stein, C. L. (1997) Differential redox and sorption of Cr(III/VI) on natural silicate and oxide minerals: EXAFS and XANES results, *Geochimica et Cosmochimica Acta*, 61(16): 3399-3412.

Quevauviller, P. (1998) Operationally defined extraction procedures for soil and sediment analysis I. Standardization. *Trends in Analytical Chemistry*, 17 (5): 289-298.

Quevauviller, P., Rauret, G., Muntau, H., Ure, A. M., Rubio, R., Lopez-Sanchez, J. F., Fiedler, H. D., Griepink, B. (1994) Evaluation of a sequential extraction procedure for the determination of extractable trace metal contents in sediments. *Fresenius Journal of Analytical Chemistry*, 349: 808–914.

Quinn, Julie; Email on May 6th 2013.

Rauret, G., Lopez, J. F., Sahuquillo, A., Rubio, R., Davidson, C., Ure, A., Quevauviller, P. (1999) Improvement of BCR three step sequential extraction procedure prior to the certification of new sediment and soil reference materials. *Journal of Environmental Monitoring*, 1 (1): 57-61.

Rai, D., Sass, B. M., Moore, D. A. (1987) Chromium (III) Hydrolysis Constant and Solubility of Chromium (III) Hydroxide. *Inorganic Chemistry*, 26: 345-349.

Rai, D., Eary, L. E., Zachara, J. M. (1989) Environmental chemistry of chromium. *Science of the Total Environment*, 86: 15-23.

Roskovic, R., Stipanovic Oslakovic, I., Radic, J., Serdar, M. (2011) Effects of chromium (VI) reducing agents in cement on corrosion of reinforcing steel. *Cement and Concrete Composites*, 33(10): 1020-1025.

Sparks, D. L. (2003) *Environmental soil chemistry*. Academic press.

Stevenson, F. J. 1994. *Humus chemistry, genesis, composition, reactions*, New York, New York: John Wiley.

Stevenson, F. J., Vance, G. F. 1989. Naturally occurring aluminium-organic complexes. In Sposito, G. (ed.). *The environmental chemistry of aluminium*. Boca Raton, Fla.: CRC Press,

Somme-Dubru, M. L.; Genet, M.; Mathieux, A.; Rouxhet, P. G. Rodrique, L. J. (1981) Evaluation by photoelectron spectroscopy and electron microscopy of the stabilization of chrome-yellow pigments. *Coatings Technology*, 53: 51-56.

Stumm, W., Morgan, J.J., 1981, *Aquatic Chemistry: an Introduction Emphasizing Chemical Equilibria in Natural Waters* Wiley-Interscience, Toronto.

Sposito, G. 2008, *The Chemistry of Soils*. Oxford University Press, Oxford, UK.

Shu, Z., Axe, L., Jahan, K., Ramanujachary, K. V. (2013) The distribution and the leachability of heavy metals in paint waste during bridge rehabilitation (manuscript).

Silviera, D. J., Sommers, L. E. (1977) Extractability of Copper, Zinc, Cadmium and Lead in soil incubated with sewage sludge. *Journal of Environmental Quality*, 6: 47-52.

Stover, R. C., Sommers, L. E., Silviera, D. J. (1976) Evaluation of metals in wastewater sludge. *Journal of the Water Pollution Control Federation*, 48: 2165-2175.

Shuman, L. M. (1979) Zinc, Manganese and Copper in soil fractions. *Soil Science*, 127: 10-17.

Smith, L. (1993) Oral presentation at the SSPC Sixth Annual Conference on Lead Paint removal and Abatement, March 15-17 1993, Cincinnati, Ohio USA.

Stipp, S. L. S., Hansen, M., Kristensen, R., Hochella Jr., M. F., Bennedsen, L., Dideriksen, K., Balic-Zunic, T., Leonard, D., Mathieu, H. J. (2002) Behavior of Fe-oxides relevant to contaminant uptake in the environment. *Chemical Geology*, 190: 321– 337.

Schwertmann, U., Cornell, R. M., *Iron Oxides in the Laboratory*; VCH: New York, 1991.

Shanmuganathan, P., Lakshmipathiraj, P., Srikanth, S., Nachiappan, A. L., Sumathy, A. (2008) Toxicity characterization and long-term stability studies on copper slag from the ISASMELT process. *Resources, Conservation and Recycling*, 52: 601–611.

Sutherland, R. A., Tack, F. M. G. (2002) Determination of Al, Cu, Fe, Mn, Pb and Zn in certified reference materials using the optimized BCR sequential extraction procedure. *Analytica Chimica Acta*, 454: 249-257.

Shi, H., Liu, F., Han, E. (2011) The corrosion behavior of zinc-rich paints on steel: Influence of simulated salts deposition in an offshore atmosphere at the steel/paint interface. *Surface and Coatings Technology*, 205: 4532–4539.

Serifaki, K., Boke, H., Yalcin, S., Ipekoglu, B. (2009) Characterization of materials used in the execution of historic oil paintings by XRD, SEM-EDS, TGA and LIBS analysis. *Materials Characterization*, 60: 303 – 311.

Strawn, D. G., and Sparks, D. L. (1999) Sorption kinetics of trace elements in soils and soil materials. In Selim, H. M., Iskandar, I. K. (eds.). *Fate and transport heavy metals in the Vadose Zone*. Boca Raton, Florida, Lewis Publisher, 1–28.

Swift, R. S., McLaren, R. G. (1991) Micronutrient adsorption by soils and soil colloids. In Bolt, G. H., De Boodt, M. F., Hayes, M. H. B., McBride, M. B. (eds.). *Interactions at the soil colloid-soil solution interface*. Dordrecht, Germany: Kluwer, 257–292.

Tessier, A., Campbell, P. G. C., Bisson, M. (1979) Sequential extraction procedure for the speciation of particulate trace metals. *Analytical Chemistry*, 51 (7): 844-851.

Turner, A., Sogo, Y. S. K. (2012) Concentrations and bioaccessibilities of metals in exterior urban paints, *Chemosphere*, 86: 614-618.

Trivedi, P., Dyer, J. A., Sparks, D. L. (2003) Lead sorption onto ferrihydrite. 1. A macroscopic and spectroscopic assessment. *Environmental science and technology*, 37(5): 908-914.

Townsend, T., Tolaymat, T., Solo-Gabriele, H., Dubey, B., Stook, K., Wadanambi, L. (2004) Leaching of CCA-treated wood: implications for waste disposal. *Journal of hazardous materials*, 114(1-3): 75-9.

Turan, P., Dogan, M., Alkan, M. (2007) Uptake of trivalent chromium ions from aqueous solutions using kaolinite. *Journal of Hazardous Materials*, 148: 56–63.

U. S. Environmental Protection Agency (U.S. EPA) (2004) Method 1310B Extraction Procedure (EP) Toxicity Test Method and Structural Integrity Test, Revision 2, Washington, DC.

U. S. Environmental Protection Agency (U.S. EPA) (1986) Method 1320 Multiple Extraction Procedure, Revision 0, Washington, DC.

U. S. Environmental Protection Agency (U.S. EPA) (1992) Toxicity Characteristic Leaching Procedure (TCLP), SW-846 Method 1311, Federal Register, 55 (March 29), Washington, DC.

U. S. Environmental Protection Agency (U.S. EPA) (2008), hazardous waste identification, RCRA Orientation Manual 2008: Section III: RCRA Subtitle C.

<http://www.epa.gov/wastes/inforesources/pubs/orientat/rom31.pdf>

U. S. Environmental Protection Agency (U.S. EPA) (1997) Emissions Factors & AP 42, Compilation of Air Pollutant Emission Factors, Chapter 13: Miscellaneous Sources.

U. S. Environmental Protection Agency (U.S. EPA) (2007) Method 6020A Inductively coupled plasma-mass spectrometry, SW-846 Chapter 3.

U. S. Environmental Protection Agency (U.S. EPA) (1998) Groundwater pathway analysis for lead-based paint (LBP) architectural debris, Office of Solid Waste, Washington, DC.

U. S. Environmental Protection Agency (U.S. EPA) (1998) Method 6200, Field portable x-ray fluorescence spectrometry for the determination of elemental concentrations in soil and sediment (EPA/600/R-97/150, Revision 0), Retrieved November 1, 2007.

Wadanambi, L., Dubey, B., Townsend, T. (2008) The leaching of lead from lead-based paint in landfill environments. *Journal of Hazardous Materials*, 157: 194-200.

Weng, C. H., Huang, C. P., Allen, H. E., Leavens, P. B., Sanders, P. F. (1996) Chemical interactions between Cr(VI) and hydrous concrete particles. *Environmental Science and Technology*, 30: 371-376.

Weng, C. H., Huang, C. P., Allen, H. E., Leavens, P. B., Sanders, P. F. (2001) Cr(VI) Adsorption onto Hydrous Concrete Particles from Groundwater. *Journal of Environmental Engineering*, 127: 1124-1131.

Wagman, D. D., Evans, W. H., Parker, V. B., Schumm, R. H., Halow, I., Bailey, S. M., Churney, K. L., Buttall, R. L. (1982) The NBS tables of chemical thermodynamic properties. The Journal of Physical Chemistry Ref. Data 11, Suppl. 2: 392.

Wu, T. M., Yen, S. J., Chen, E. C., Sung, T. W., Chiang, R. K. (2007) Conducting and magnetic behaviors of monodispersed iron oxide/polypyrrole nanocomposites synthesized by in situ chemical oxidative polymerization. Journal of Polymer Science Part A: Polymer Chemistry, 45(20): 4647-4655.

Xu, Y., Axe, L., Yee, N., Dyer, A. (2006) Bidentate Complexation Modeling of Heavy Metal Adsorption and Competition on Goethite. Environmental Science and Technology, 40: 2213-2218.

Zhou Y., Haynes, R. J. (2010) Sorption of Heavy Metals by Inorganic and Organic Components of Solid Wastes: Significance to Use of Wastes as Low-Cost Adsorbents and Immobilizing Agents. Critical Reviews in Environmental Science and Technology, 40: 909–977.

Appendix A

TCLP, and MEP results for the 24 bridges

Table A1. TCLP results (mg L⁻¹) for the 24 bridges from NYS.

| Sample name | pH | TCLP results (mg L ⁻¹) | | | | | | | | | |
|----------------|------|------------------------------------|------|------|------|------|-----|-----|------|------|--------|
| | | Pb | Cr | Ba | Zn | Fe | As | Cd | Ag | Se | Hg |
| 1-1 e | 5.73 | 1.37 | 1.84 | 2.08 | 501 | 1352 | BDL | BDL | BDL | BDL | BDL |
| 2-1 a | 5.79 | 0.28 | 0.98 | 0.54 | 1307 | 950 | BDL | BDL | BDL | BDL | BDL |
| 2-2 e | 6.43 | BDL* | BDL | BDL | 858 | 1515 | BDL | BDL | BDL | BDL | BDL |
| 3-1 a | 6.59 | BDL | BDL | 0.66 | 129 | 546 | BDL | BDL | 0.43 | BDL | BDL |
| 3-1 b | 6.46 | 0.03 | BDL | BDL | 338 | – | BDL | BDL | 0.43 | 0.14 | BDL |
| 3-1 c | 6.25 | 0.02 | 0.77 | 1.16 | 211 | – | BDL | BDL | 0.43 | BDL | BDL |
| 3-1 d | 6.70 | 0.06 | 0.18 | 1.35 | 378 | – | BDL | BDL | 0.44 | BDL | BDL |
| 3-1 e | 5.95 | 0.40 | 0.19 | 1.88 | 892 | 238 | BDL | BDL | 0.44 | BDL | 0.079 |
| 3-2 a | 5.07 | 0.25 | 1.10 | 1.52 | 151 | – | BDL | BDL | 0.43 | 0.17 | BDL |
| 3-2 b | 6.88 | BDL | BDL | 0.96 | 93 | – | BDL | BDL | 0.43 | BDL | BDL |
| 3-2 c | 4.89 | 0.38 | 2.40 | 1.72 | 236 | – | BDL | BDL | 0.43 | BDL | BDL |
| 3-2 d | 6.41 | 0.00 | 0.00 | 1.52 | 237 | – | BDL | BDL | 0.43 | BDL | BDL |
| 3-2 e | 6.81 | 0.03 | BDL | 1.30 | 152 | – | BDL | BDL | 0.44 | BDL | 0.0056 |
| 3-3 a | 6.63 | 0.04 | 0.14 | 0.20 | 267 | – | BDL | BDL | BDL | BDL | BDL |
| 3-3 b | 6.27 | 0.01 | BDL | 0.58 | 681 | – | BDL | BDL | BDL | BDL | BDL |

| Sample name | pH | TCLP results (mg L ⁻¹) | | | | | | | | | |
|----------------|------|------------------------------------|------|------|------|------|-----|-----|-----|------|-----|
| | | Pb | Cr | Ba | Zn | Fe | As | Cd | Ag | Se | Hg |
| 5-1 a | 5.97 | 0.01 | BDL | 0.32 | 456 | – | BDL | BDL | BDL | BDL | BDL |
| 5-1 b | 6.70 | BDL | BDL | 0.02 | 216 | – | BDL | BDL | BDL | BDL | BDL |
| 5-1 c | 6.75 | BDL | BDL | 0.41 | 373 | – | BDL | BDL | BDL | BDL | BDL |
| 5-1 d | 6.70 | BDL | BDL | 0.18 | 943 | – | BDL | BDL | BDL | BDL | BDL |
| 5-2 a | 6.01 | BDL | BDL | 0.12 | 816 | – | BDL | BDL | BDL | BDL | BDL |
| 5-2 b | 6.70 | BDL | 0.43 | 0.66 | 248 | – | BDL | BDL | BDL | BDL | BDL |
| 5-2 c | 6.56 | 0.04 | BDL | 0.57 | 588 | – | BDL | BDL | BDL | BDL | BDL |
| 5-2 d | 6.77 | 0.00 | BDL | 0.33 | 798 | – | BDL | BDL | BDL | 0.05 | BDL |
| 5-3d | 6.35 | 0.00 | 0.02 | 0.55 | 421 | 1173 | BDL | BDL | BDL | BDL | BDL |
| 5-4c | 6.54 | 0.00 | 0.00 | 0.73 | 766 | 1646 | BDL | BDL | BDL | BDL | BDL |
| 5-5b | 6.55 | 0.00 | 0.00 | 1.06 | 704 | 2029 | BDL | BDL | BDL | BDL | BDL |
| 7-1c | 5.43 | 0.38 | 5.62 | 1.92 | 565 | 935 | BDL | BDL | BDL | BDL | BDL |
| 7-1e | 5.90 | 1.12 | 2.37 | 1.83 | 872 | 2833 | BDL | BDL | BDL | BDL | BDL |
| 7-2e | 5.99 | 0.38 | 1.06 | 1.61 | 1141 | 1461 | BDL | BDL | BDL | BDL | BDL |
| 10-1 a | 6.97 | 0.02 | 0.01 | 0.47 | 84 | – | BDL | BDL | BDL | BDL | BDL |
| 10-1 b | 6.77 | 0.02 | BDL | 0.27 | 71 | – | BDL | BDL | BDL | BDL | BDL |

| Sample name | pH | TCLP results (mg L ⁻¹) | | | | | | | | | |
|----------------|------|------------------------------------|------|------|-----|------|-----|-----|------|-------|--------|
| | | Pb | Cr | Ba | Zn | Fe | As | Cd | Ag | Se | Hg |
| 10-1 c | 6.76 | 0.02 | 0.19 | 0.03 | 80 | – | BDL | BDL | BDL | BDL | BDL |
| 10-1 d | 6.90 | 0.03 | BDL | 0.22 | 115 | – | BDL | BDL | BDL | BDL | BDL |
| 10-2 b | 5.98 | 0.18 | 1.00 | 0.50 | 405 | 914 | BDL | BDL | BDL | BDL | BDL |
| 10-3 e | 5.48 | 0.48 | 2.47 | 0.48 | 480 | 732 | BDL | BDL | BDL | BDL | BDL |
| 10-4e | 5.32 | 0.47 | 9.52 | 0.99 | 406 | 3275 | BDL | BDL | BDL | BDL | BDL |
| 10-5b | 6.52 | 2.10 | 1.91 | 0.95 | 221 | 388 | BDL | BDL | BDL | BDL | BDL |
| 10-6a | 5.02 | 0.63 | 5.24 | 1.41 | 237 | 1876 | BDL | BDL | BDL | BDL | 0.014 |
| 10-7b | 5.81 | 0.56 | 0.97 | 8.89 | 144 | 507 | BDL | BDL | BDL | BDL | BDL |
| 10-8a | 6.80 | 0.08 | 0.09 | 9.74 | 898 | 2029 | BDL | BDL | BDL | BDL | 0.0054 |
| 10-9b | 6.16 | 1.46 | 0.00 | 0.92 | 331 | 218 | BDL | BDL | BDL | BDL | BDL |
| 11-1 A | 6.57 | BDL | BDL | 2.52 | 70 | 183 | BDL | BDL | 0.43 | BDL | BDL |
| 11-1 B | 4.88 | 1.17 | 0.24 | 2.35 | 493 | 766 | BDL | BDL | 0.43 | 0.035 | BDL |
| 11-1 C | 6.22 | 0.22 | BDL | 0.48 | 236 | – | BDL | BDL | 0.43 | BDL | BDL |
| 11-1 D | 6.01 | 0.78 | BDL | 0.50 | 254 | 288 | BDL | BDL | 0.43 | BDL | BDL |
| 11-1 E | 4.94 | 1.12 | 0.07 | 3.96 | 320 | 362 | BDL | BDL | 0.44 | BDL | BDL |
| 11-2 A | 6.15 | BDL | BDL | 3.43 | 20 | 365 | BDL | BDL | 0.43 | BDL | BDL |
| 11-2 B | 5.92 | 0.44 | 0.22 | 1.07 | 708 | 526 | BDL | BDL | 0.43 | 0.20 | BDL |

| Sample name | pH | TCLP results (mg L ⁻¹) | | | | | | | | | |
|----------------|------|------------------------------------|------|------|-----|----|-----|-----|------|-----|-----|
| | | Pb | Cr | Ba | Zn | Fe | As | Cd | Ag | Se | Hg |
| 11-2 C | 6.26 | 0.06 | 0.47 | 0.26 | 384 | – | BDL | BDL | 0.43 | BDL | BDL |
| 11-2 D | 6.32 | 0.10 | 0.66 | 0.19 | 356 | – | BDL | BDL | 0.43 | BDL | BDL |
| 11-2 E | 5.76 | 0.33 | 0.39 | 2.97 | 170 | – | BDL | BDL | 0.44 | BDL | BDL |

BDL refers to below detection limit.

*Detection limits (mg L⁻¹) for this study: As = 0.0007, Ba = 0.0004, Cd = 0.0005, Cr = 0.0007, Pb = 0.0005, Se = 0.0002, Ag = 0.0003, Fe = 0.0025, Zn = 0.001, Hg = 0.000002.

– refers to not measured.

Table A2. MEP results (mg L⁻¹) for the 24 bridges from NYS.

| Sample 1-1e | Pb | Cr | Ba | Zn | Fe | As | Cd | Ag | Se | Hg |
|----------------------|------|--------|------|--------|---------|------|-----|-------|-------|-----|
| 1 st day | 5.84 | 0.0029 | 1.68 | 439.20 | 1136.00 | 0.67 | BDL | BDL | BDL | BDL |
| 2 nd day | 0.37 | 0.0028 | 0.40 | 2.78 | 26.90 | 0.67 | BDL | BDL | BDL | BDL |
| 3 rd day | 0.05 | BDL | 0.11 | 1.35 | 16.00 | 0.66 | BDL | BDL | BDL | BDL |
| 4 th day | BDL | BDL | 0.11 | 0.94 | 16.25 | 0.66 | BDL | BDL | BDL | BDL |
| 5 th day | 0.02 | 0.0293 | 0.21 | 6.42 | 10.45 | 0.43 | BDL | 0.014 | 0.103 | BDL |
| 6 th day | 0.07 | 0.0294 | 0.21 | 6.81 | 7.34 | 0.43 | BDL | 0.015 | 0.103 | BDL |
| 7 th day | 0.02 | 0.0295 | 0.50 | 6.38 | 4.86 | 0.43 | BDL | 0.014 | 0.103 | BDL |
| 8 th day | 0.02 | 0.0294 | 0.28 | 6.60 | 4.54 | 0.43 | BDL | 0.01 | 0.103 | BDL |
| 9 th day | BDL | BDL | 0.39 | BDL | 0.91 | 0.66 | BDL | BDL | BDL | BDL |
| 10 th day | BDL | BDL | 0.24 | BDL | 0.28 | 0.66 | BDL | BDL | BDL | BDL |

BDL refers to below detection limit.

– refers to not measured.

| Sample 2-1 a | Pb | Cr | Ba | Zn | Fe | As | Cd | Ag | Se | Hg |
|----------------------|------|--------|------|--------|-------|------|-----|-------|-------|-------|
| 1 st day | 0.83 | 0.0030 | 0.26 | 799.00 | 89.75 | 0.06 | BDL | BDL | BDL | BDL |
| 2 nd day | BDL | BDL | 0.40 | 0.93 | 0.13 | 0.12 | BDL | BDL | BDL | BDL |
| 3 rd day | BDL | BDL | 0.36 | 5.90 | 0.01 | 0.12 | BDL | BDL | BDL | BDL |
| 4 th day | BDL | BDL | 0.15 | 29.06 | BDL | 0.12 | BDL | BDL | BDL | BDL |
| 5 th day | 0.01 | 0.0293 | 0.05 | 32.33 | BDL | 0.08 | BDL | 0.015 | 0.104 | 0.002 |
| 6 th day | 0.02 | 0.0297 | 0.03 | 47.12 | 0.01 | 0.08 | BDL | 0.014 | 0.105 | BDL |
| 7 th day | 0.01 | 0.0295 | 0.08 | 15.05 | BDL | 0.08 | BDL | 0.014 | 0.103 | BDL |
| 8 th day | 0.01 | 0.0291 | 0.05 | 18.02 | BDL | 0.08 | BDL | 0.015 | 0.103 | BDL |
| 9 th day | BDL | BDL | BDL | 24.81 | BDL | 0.12 | BDL | BDL | BDL | BDL |
| 10 th day | BDL | BDL | BDL | 15.87 | BDL | 0.12 | BDL | BDL | BDL | BDL |

BDL refers to below detection limit.

– refers to not measured.

| Sample 2-2 c | Pb | Cr | Ba | Zn | Fe | As | Cd | Ag | Se | Hg |
|----------------------|------|--------|------|---------|--------|------|-----|-------|-------|-----|
| 1 st day | 0.21 | 0.0116 | 0.20 | 1152.50 | 529.85 | 0.12 | BDL | BDL | BDL | BDL |
| 2 nd day | BDL | BDL | BDL | 1.07 | 0.06 | 0.12 | BDL | BDL | BDL | BDL |
| 3 rd day | BDL | BDL | BDL | 1.02 | 0.31 | 0.12 | BDL | BDL | BDL | BDL |
| 4 th day | BDL | 0.0024 | BDL | 10.56 | BDL | 0.12 | BDL | BDL | BDL | BDL |
| 5 th day | 0.01 | 0.0333 | BDL | 15.86 | BDL | 0.08 | BDL | 0.014 | 0.104 | BDL |
| 6 th day | 0.01 | 0.0292 | BDL | 14.00 | BDL | 0.08 | BDL | 0.014 | 0.103 | BDL |
| 7 th day | 0.01 | 0.0292 | BDL | 6.52 | BDL | 0.08 | BDL | 0.014 | 0.103 | BDL |
| 8 th day | 0.01 | 0.0296 | BDL | 6.65 | BDL | 0.08 | BDL | 0.015 | 0.103 | BDL |
| 9 th day | BDL | BDL | BDL | 4.52 | BDL | 0.12 | BDL | BDL | BDL | BDL |
| 10 th day | BDL | BDL | BDL | 2.24 | BDL | 0.12 | BDL | BDL | BDL | BDL |

BDL refers to below detection limit.

– refers to not measured.

| Sample 3-1 d | Pb | Cr | Ba | Zn | Fe | As | Cd | Ag | Se | Hg |
|----------------------|------|--------|------|--------|---------|--------|-----|--------|--------|----|
| 1 st day | 0.85 | 0.021 | 0.44 | 653.40 | 1282.60 | 0.0089 | BDL | 0.0091 | 0.0289 | – |
| 2 nd day | 0.02 | BDL | 0.15 | 4.06 | 29.74 | BDL | BDL | BDL | BDL | – |
| 3 rd day | 0.01 | BDL | 0.13 | 0.25 | 1.49 | BDL | BDL | BDL | BDL | – |
| 4 th day | 0.07 | 0.0052 | 0.15 | BDL | 7.54 | BDL | BDL | BDL | BDL | – |
| 5 th day | BDL | BDL | 0.12 | BDL | 13.25 | BDL | BDL | BDL | BDL | – |
| 6 th day | 0.09 | BDL | 0.13 | 0.12 | 9.56 | BDL | BDL | BDL | BDL | – |
| 7 th day | 0.01 | BDL | 0.20 | 0.26 | 4.72 | BDL | BDL | BDL | BDL | – |
| 8 th day | BDL | BDL | 0.18 | 0.22 | 0.32 | BDL | BDL | BDL | BDL | – |
| 9 th day | BDL | BDL | 0.12 | 0.10 | 0.16 | BDL | BDL | BDL | BDL | – |
| 10 th day | 0.01 | BDL | 0.16 | 0.56 | 0.26 | BDL | BDL | BDL | BDL | – |

BDL refers to below detection limit.

– refers to not measured.

| Sample 3-2 c | Pb | Cr | Ba | Zn | Fe | As | Cd | Ag | Se | Hg |
|----------------------|------|--------|------|--------|--------|-------|-----|-------|-------|----|
| 1 st day | 2.80 | 0.0240 | 0.50 | 182.99 | 662.22 | BDL | BDL | 0.002 | 0.000 | – |
| 2 nd day | 0.02 | 0.0016 | 0.10 | 0.76 | 39.63 | BDL | BDL | 0.000 | 0.013 | – |
| 3 rd day | BDL | BDL | 0.11 | BDL | 0.08 | BDL | BDL | BDL | BDL | – |
| 4 th day | BDL | BDL | 0.08 | BDL | 0.30 | BDL | BDL | BDL | BDL | – |
| 5 th day | BDL | BDL | 0.07 | 0.20 | 0.60 | BDL | BDL | BDL | BDL | – |
| 6 th day | 0.02 | BDL | 0.06 | 0.14 | 0.64 | BDL | BDL | BDL | BDL | – |
| 7 th day | BDL | BDL | 0.05 | 0.04 | 0.10 | 0.006 | BDL | 0.006 | 0.016 | – |
| 8 th day | BDL | BDL | 0.09 | 0.17 | 0.32 | BDL | BDL | BDL | BDL | – |
| 9 th day | BDL | BDL | 0.10 | 0.35 | 0.23 | BDL | BDL | BDL | BDL | – |
| 10 th day | 0.07 | 0.0019 | 0.09 | 0.80 | 1.66 | BDL | BDL | BDL | BDL | – |

BDL refers to below detection limit.

– refers to not measured.

| Sample 3-3 a | Pb | Cr | Ba | Zn | Fe | As | Cd | Ag | Se | Hg |
|----------------------|------|--------|------|---------|--------|-----|-----|-------|-------|----|
| 1 st day | 0.91 | 0.0285 | 0.59 | 1163.61 | 617.10 | BDL | BDL | BDL | BDL | – |
| 2 nd day | 0.02 | BDL | 0.16 | 1.87 | 5.48 | BDL | BDL | BDL | BDL | – |
| 3 rd day | 0.01 | 0.0020 | 0.14 | BDL | 0.39 | BDL | BDL | BDL | 0.016 | – |
| 4 th day | BDL | BDL | 0.07 | BDL | 1.15 | BDL | BDL | BDL | BDL | – |
| 5 th day | BDL | BDL | 0.03 | 0.14 | 1.67 | BDL | BDL | BDL | BDL | – |
| 6 th day | BDL | BDL | 0.05 | 0.62 | 5.56 | BDL | BDL | BDL | BDL | – |
| 7 th day | 0.07 | BDL | 0.10 | 0.41 | 3.98 | BDL | BDL | 0.003 | 0.007 | – |
| 8 th day | 0.09 | BDL | 0.13 | 0.55 | 1.71 | BDL | BDL | BDL | BDL | – |
| 9 th day | BDL | BDL | 0.08 | 0.28 | 0.95 | BDL | BDL | BDL | BDL | – |
| 10 th day | BDL | BDL | 0.08 | 0.45 | 2.79 | BDL | BDL | BDL | BDL | – |

BDL refers to below detection limit.

– refers to not measured.

| Sample 5-1 c | Pb | Cr | Ba | Zn | Fe | As | Cd | Ag | Se | Hg |
|----------------------|------|--------|------|--------|---------|-----|-------|-----|-------|----|
| 1 st day | 0.26 | 0.014 | 0.74 | 470.23 | 1189.58 | BDL | 0.010 | BDL | 0.012 | – |
| 2 nd day | 0.01 | BDL | 0.18 | 0.80 | 56.67 | BDL | BDL | BDL | BDL | – |
| 3 rd day | 0.01 | BDL | 0.09 | 0.09 | 11.54 | BDL | BDL | BDL | BDL | – |
| 4 th day | 0.03 | 0.0019 | 0.07 | BDL | 10.58 | BDL | BDL | BDL | 0.007 | – |
| 5 th day | BDL | BDL | 0.06 | BDL | 9.95 | BDL | BDL | BDL | BDL | – |
| 6 th day | BDL | BDL | 0.05 | BDL | 8.19 | BDL | BDL | BDL | BDL | – |
| 7 th day | BDL | BDL | 0.08 | 0.06 | 5.45 | BDL | BDL | BDL | BDL | – |
| 8 th day | BDL | BDL | 0.08 | 0.02 | 1.48 | BDL | BDL | BDL | BDL | – |
| 9 th day | BDL | BDL | 0.10 | BDL | 0.43 | BDL | BDL | BDL | BDL | – |
| 10 th day | BDL | BDL | 0.10 | 0.02 | 0.26 | BDL | BDL | BDL | BDL | – |

BDL refers to below detection limit.

– refers to not measured.

| Sample 5-2 c | Pb | Cr | Ba | Zn | Fe | As | Cd | Ag | Se | Hg |
|----------------------|------|--------|------|--------|--------|-----|-------|-----|-------|----|
| 1 st day | 0.27 | 0.0082 | 0.81 | 546.51 | 879.26 | BDL | 0.032 | BDL | 0.006 | – |
| 2 nd day | 0.02 | 0.0013 | 0.14 | 0.58 | 21.81 | BDL | BDL | BDL | BDL | – |
| 3 rd day | BDL | 0.0048 | 0.09 | 0.06 | 1.70 | BDL | BDL | BDL | BDL | – |
| 4 th day | BDL | BDL | 0.05 | BDL | 8.78 | BDL | BDL | BDL | BDL | – |
| 5 th day | BDL | BDL | 0.06 | 0.10 | 8.92 | BDL | BDL | BDL | BDL | – |
| 6 th day | BDL | BDL | 0.07 | BDL | 3.47 | BDL | BDL | BDL | BDL | – |
| 7 th day | BDL | BDL | 0.07 | 0.03 | 3.55 | BDL | BDL | BDL | BDL | – |
| 8 th day | BDL | BDL | 0.10 | 0.06 | 0.93 | BDL | BDL | BDL | BDL | – |
| 9 th day | BDL | BDL | 0.08 | 0.05 | 0.51 | BDL | BDL | BDL | BDL | – |
| 10 th day | BDL | BDL | 0.08 | 0.03 | 0.04 | BDL | BDL | BDL | BDL | – |

BDL refers to below detection limit.

– refers to not measured.

| Sample 5-3 d | Pb | Cr | Ba | Zn | Fe | As | Cd | Ag | Se | Hg |
|----------------------|------|-----|------|--------|--------|-------|-------|-----|-------|----|
| 1 st day | 0.11 | BDL | 0.25 | 340.11 | 327.76 | BDL | 0.012 | BDL | BDL | – |
| 2 nd day | 0.06 | BDL | 0.12 | 5.17 | 5.09 | BDL | BDL | BDL | BDL | – |
| 3 rd day | 0.05 | BDL | 0.09 | 0.69 | 0.13 | BDL | BDL | BDL | BDL | – |
| 4 th day | 0.08 | BDL | 0.25 | 0.64 | 0.17 | BDL | BDL | BDL | BDL | – |
| 5 th day | 0.05 | BDL | 0.13 | 2.94 | 0.19 | BDL | BDL | BDL | BDL | – |
| 6 th day | 0.06 | BDL | 0.10 | 6.35 | 0.23 | 0.006 | BDL | BDL | 0.006 | – |
| 7 th day | 0.01 | BDL | 0.09 | 4.79 | 0.19 | 0.005 | BDL | BDL | 0.005 | – |
| 8 th day | 0.01 | BDL | 0.09 | 8.58 | 0.25 | 0.004 | BDL | BDL | 0.004 | – |
| 9 th day | BDL | BDL | 0.07 | 22.63 | 0.50 | BDL | BDL | BDL | BDL | – |
| 10 th day | 0.01 | BDL | 0.07 | 15.33 | 0.33 | BDL | BDL | BDL | BDL | – |

BDL refers to below detection limit.

– refers to not measured.

| Sample 5-4 c | Pb | Cr | Ba | Zn | Fe | As | Cd | Ag | Se | Hg |
|----------------------|------|--------|------|--------|--------|-------|-------|-------|-------|----|
| 1 st day | 0.15 | BDL | 0.30 | 585.13 | 292.87 | BDL | BDL | BDL | BDL | – |
| 2 nd day | 0.05 | BDL | 0.13 | 6.32 | 19.22 | BDL | 0.004 | BDL | BDL | – |
| 3 rd day | 0.05 | BDL | 0.09 | 0.84 | 4.48 | BDL | BDL | BDL | BDL | – |
| 4 th day | 0.01 | BDL | 0.22 | 0.62 | 1.28 | BDL | BDL | BDL | BDL | – |
| 5 th day | 0.01 | BDL | 0.09 | 4.42 | 1.81 | BDL | BDL | BDL | BDL | – |
| 6 th day | 0.01 | BDL | 0.08 | 6.09 | 1.76 | BDL | BDL | BDL | BDL | – |
| 7 th day | BDL | BDL | 0.08 | 3.60 | 2.29 | 0.004 | BDL | BDL | 0.017 | – |
| 8 th day | BDL | BDL | 0.07 | 6.01 | 0.87 | 0.004 | BDL | BDL | 0.018 | – |
| 9 th day | BDL | BDL | 0.05 | 15.24 | 1.95 | BDL | BDL | 0.005 | BDL | – |
| 10 th day | 0.13 | 0.0078 | 0.06 | 5.96 | BDL | BDL | BDL | BDL | BDL | – |

BDL refers to below detection limit.

– refers to not measured.

| Sample 5-5 b | Pb | Cr | Ba | Zn | Fe | As | Cd | Ag | Se | Hg |
|----------------------|------|--------|------|--------|--------|-------|-------|-------|-------|----|
| 1 st day | 0.67 | 0.033 | 0.78 | 787.51 | 429.65 | BDL | BDL | BDL | BDL | – |
| 2 nd day | 0.09 | BDL | 0.46 | 33.43 | 73.87 | BDL | BDL | BDL | BDL | – |
| 3 rd day | 0.05 | BDL | 0.14 | 9.71 | 12.21 | BDL | BDL | BDL | BDL | – |
| 4 th day | 0.03 | BDL | 0.36 | 5.56 | 2.01 | BDL | BDL | BDL | BDL | – |
| 5 th day | 0.01 | BDL | 0.12 | 9.14 | 2.97 | BDL | BDL | BDL | BDL | – |
| 6 th day | 0.02 | BDL | 0.09 | 14.20 | 1.46 | 0.004 | BDL | BDL | 0.018 | – |
| 7 th day | 0.01 | BDL | 0.09 | 16.66 | 0.79 | 0.005 | BDL | BDL | 0.020 | – |
| 8 th day | BDL | BDL | 0.09 | 23.35 | 0.21 | BDL | BDL | BDL | BDL | – |
| 9 th day | BDL | 0.0085 | 0.09 | 29.49 | 0.18 | 0.013 | 0.005 | 0.013 | 0.023 | – |
| 10 th day | BDL | BDL | 0.05 | 7.66 | BDL | BDL | BDL | BDL | BDL | – |

BDL refers to below detection limit.

– refers to not measured.

| Sample 7-1 c | Pb | Cr | Ba | Zn | Fe | As | Cd | Ag | Se | Hg |
|----------------------|-------|--------|------|--------|---------|-----|-------|-------|-----|----|
| 1 st day | 16.04 | 0.0195 | 0.93 | 404.57 | 1231.93 | BDL | 0.121 | BDL | BDL | – |
| 2 nd day | 0.05 | BDL | 0.28 | 2.57 | 61.64 | BDL | BDL | BDL | BDL | – |
| 3 rd day | 0.27 | 0.0041 | 0.29 | 0.23 | 5.27 | BDL | BDL | BDL | BDL | – |
| 4 th day | 0.01 | BDL | 0.15 | BDL | 12.77 | BDL | BDL | BDL | BDL | – |
| 5 th day | BDL | BDL | 0.08 | 0.19 | 33.62 | BDL | BDL | BDL | BDL | – |
| 6 th day | 0.01 | BDL | 0.10 | 0.13 | 19.90 | BDL | BDL | 0.002 | BDL | – |
| 7 th day | 0.35 | BDL | 0.12 | 0.46 | 28.96 | BDL | BDL | BDL | BDL | – |
| 8 th day | 0.04 | BDL | 0.25 | 0.23 | 14.70 | BDL | BDL | BDL | BDL | – |
| 9 th day | BDL | BDL | 0.25 | 0.07 | 0.48 | BDL | BDL | BDL | BDL | – |
| 10 th day | 0.31 | BDL | 0.23 | 0.18 | 2.94 | BDL | BDL | BDL | BDL | – |

BDL refers to below detection limit.

– refers to not measured.

| Sample 7-2 e | Pb | Cr | Ba | Zn | Fe | As | Cd | Ag | Se | Hg |
|----------------------|------|--------|------|--------|--------|-----|-----|-------|-------|----|
| 1 st day | 5.60 | 0.0107 | 0.95 | 978.58 | 262.42 | BDL | BDL | BDL | BDL | – |
| 2 nd day | 0.01 | BDL | 0.16 | 22.46 | 0.52 | BDL | BDL | BDL | BDL | – |
| 3 rd day | BDL | BDL | 0.07 | 11.04 | 0.15 | BDL | BDL | BDL | BDL | – |
| 4 th day | 0.01 | BDL | 0.07 | 18.73 | 0.24 | BDL | BDL | BDL | BDL | – |
| 5 th day | 0.01 | BDL | 0.06 | 41.78 | 0.46 | BDL | BDL | BDL | BDL | – |
| 6 th day | BDL | BDL | 0.06 | 19.29 | 0.29 | BDL | BDL | 0.002 | BDL | – |
| 7 th day | BDL | 0.0026 | 0.07 | 10.81 | 0.18 | BDL | BDL | 0.002 | 0.014 | – |
| 8 th day | BDL | BDL | 0.07 | 12.87 | 0.08 | BDL | BDL | BDL | BDL | – |
| 9 th day | 0.01 | BDL | 0.07 | 16.01 | 0.08 | BDL | BDL | BDL | BDL | – |
| 10 th day | BDL | BDL | 0.07 | 12.19 | 0.05 | BDL | BDL | BDL | BDL | – |

BDL refers to below detection limit.

– refers to not measured.

| Sample 10-1 b | Pb | Cr | Ba | Zn | Fe | As | Cd | Ag | Se | Hg |
|----------------------|------|--------|------|-------|--------|------|-----|-------|-------|-----|
| 1 st day | 0.50 | 0.0006 | 1.11 | 62.92 | 609.45 | 0.12 | BDL | BDL | BDL | BDL |
| 2 nd day | BDL | BDL | 0.85 | 1.05 | 1.83 | 0.12 | BDL | BDL | BDL | BDL |
| 3 rd day | BDL | BDL | 0.22 | 0.78 | 8.88 | 0.12 | BDL | BDL | BDL | BDL |
| 4 th day | BDL | BDL | 0.11 | 0.83 | 13.31 | 0.08 | BDL | BDL | BDL | BDL |
| 5 th day | 0.14 | 0.0312 | 0.28 | 6.56 | 9.06 | 0.08 | BDL | 0.015 | 0.103 | BDL |
| 6 th day | 0.02 | 0.0293 | 0.23 | 6.39 | 5.80 | 0.08 | BDL | 0.014 | 0.103 | BDL |
| 7 th day | 0.16 | 0.0295 | 0.40 | 6.37 | 5.92 | 0.08 | BDL | 0.015 | 0.103 | BDL |
| 8 th day | 0.81 | 0.0309 | 0.33 | 6.54 | 1.13 | 0.12 | BDL | 0.014 | 0.103 | BDL |
| 9 th day | BDL | BDL | 0.39 | 0.76 | 0.18 | 0.12 | BDL | BDL | BDL | BDL |
| 10 th day | 0.36 | BDL | 0.27 | BDL | 0.58 | 0.12 | BDL | BDL | BDL | BDL |

BDL refers to below detection limit.

– refers to not measured.

| Sample 10-2 b | Pb | Cr | Ba | Zn | Fe | As | Cd | Ag | Se | Hg |
|----------------------|------|--------|------|--------|---------|------|-----|-------|-------|-----|
| 1 st day | 1.37 | 0.0038 | 0.49 | 300.25 | 1023.65 | 0.12 | BDL | BDL | BDL | BDL |
| 2 nd day | BDL | BDL | 0.47 | 1.93 | 10.24 | 0.12 | BDL | BDL | BDL | BDL |
| 3 rd day | BDL | BDL | 0.23 | 1.00 | 7.61 | 0.12 | BDL | BDL | BDL | BDL |
| 4 th day | BDL | BDL | 0.19 | 1.32 | 7.73 | 0.12 | BDL | BDL | BDL | BDL |
| 5 th day | 0.01 | 0.0292 | 0.18 | 6.49 | BDL | 0.08 | BDL | 0.014 | 0.103 | BDL |
| 6 th day | 0.02 | 0.0294 | 0.22 | 6.92 | 0.23 | 0.08 | BDL | 0.014 | 0.103 | BDL |
| 7 th day | 0.01 | 0.0291 | 0.12 | 6.74 | 0.23 | 0.08 | BDL | 0.014 | 0.103 | BDL |
| 8 th day | 0.30 | 0.0466 | 0.22 | 6.94 | 1.24 | 0.08 | BDL | 0.014 | 0.103 | BDL |
| 9 th day | BDL | BDL | 0.13 | BDL | 1.14 | 0.12 | BDL | BDL | BDL | BDL |
| 10 th day | BDL | BDL | 0.15 | BDL | 1.43 | 0.12 | BDL | BDL | BDL | BDL |

BDL refers to below detection limit.

– refers to not measured.

| Sample 10-3 e | Pb | Cr | Ba | Zn | Fe | As | Cd | Ag | Se | Hg |
|----------------------|------|--------|------|--------|--------|------|-----|-------|-------|-----|
| 1 st day | 1.81 | 0.0640 | 0.47 | 225.30 | 688.10 | 0.12 | BDL | BDL | BDL | BDL |
| 2 nd day | BDL | BDL | 0.25 | 1.71 | 13.39 | 0.12 | BDL | BDL | BDL | BDL |
| 3 rd day | BDL | BDL | 0.12 | 0.98 | 10.94 | 0.12 | BDL | BDL | BDL | BDL |
| 4 th day | BDL | BDL | 0.11 | 1.01 | 14.09 | 0.12 | BDL | BDL | BDL | BDL |
| 5 th day | 0.01 | 0.0313 | 0.22 | 6.52 | 0.26 | 0.08 | BDL | 0.014 | 0.103 | BDL |
| 6 th day | 0.01 | 0.0291 | 0.23 | 6.49 | 0.05 | 0.08 | BDL | 0.014 | 0.103 | BDL |
| 7 th day | 0.02 | 0.0296 | 0.20 | 6.45 | 0.04 | 0.08 | BDL | 0.014 | 0.103 | BDL |
| 8 th day | 0.04 | 0.0303 | 0.22 | 6.80 | 0.03 | 0.08 | BDL | 0.015 | 0.103 | BDL |
| 9 th day | BDL | BDL | 0.25 | BDL | 0.55 | 0.12 | BDL | BDL | BDL | BDL |
| 10 th day | BDL | BDL | 0.21 | BDL | 1.02 | 0.12 | BDL | BDL | BDL | BDL |

BDL refers to below detection limit.

– refers to not measured.

| Sample 10-4 e | Pb | Cr | Ba | Zn | Fe | As | Cd | Ag | Se | Hg |
|----------------------|------|-----|------|--------|--------|-------|-----|-----|-------|----|
| 1 st day | 1.05 | BDL | 0.22 | 265.85 | 819.22 | BDL | BDL | BDL | BDL | – |
| 2 nd day | 0.07 | BDL | 0.18 | 2.34 | 422.34 | BDL | BDL | BDL | BDL | – |
| 3 rd day | 0.05 | BDL | 0.13 | BDL | 16.24 | BDL | BDL | BDL | BDL | – |
| 4 th day | 0.05 | BDL | 0.22 | BDL | 17.34 | BDL | BDL | BDL | BDL | – |
| 5 th day | 0.01 | BDL | 0.13 | 0.05 | 0.95 | BDL | BDL | BDL | BDL | – |
| 6 th day | 0.03 | BDL | 0.26 | 0.00 | 0.52 | BDL | BDL | BDL | BDL | – |
| 7 th day | 0.06 | BDL | 0.09 | 0.44 | 34.87 | 0.004 | BDL | BDL | 0.017 | – |
| 8 th day | 0.33 | BDL | 0.13 | 0.37 | 11.70 | 0.004 | BDL | BDL | 0.019 | – |
| 9 th day | 0.48 | BDL | 0.11 | 0.68 | 14.23 | BDL | BDL | BDL | BDL | – |
| 10 th day | 0.69 | BDL | 0.12 | 0.44 | 10.44 | BDL | BDL | BDL | BDL | – |

BDL refers to below detection limit.

– refers to not measured.

| Sample 10-5 b | Pb | Cr | Ba | Zn | Fe | As | Cd | Ag | Se | Hg |
|----------------------|------|--------|------|--------|--------|-------|-------|-------|-------|----|
| 1 st day | 2.48 | 0.0617 | 0.43 | 206.66 | 423.15 | BDL | 0.007 | BDL | BDL | – |
| 2 nd day | 0.02 | BDL | 0.27 | 3.71 | 18.89 | BDL | BDL | BDL | BDL | – |
| 3 rd day | 0.03 | BDL | 0.20 | 0.96 | 5.06 | BDL | BDL | BDL | BDL | – |
| 4 th day | 0.09 | BDL | 1.14 | 4.39 | 17.72 | 0.002 | 0.002 | 0.015 | BDL | – |
| 5 th day | 0.10 | 0.0010 | 0.20 | 1.88 | 10.37 | BDL | BDL | BDL | BDL | – |
| 6 th day | 0.10 | BDL | 0.09 | 1.40 | 22.98 | BDL | BDL | BDL | BDL | – |
| 7 th day | 0.26 | BDL | 0.06 | 2.71 | 39.42 | 0.004 | BDL | BDL | 0.018 | – |
| 8 th day | 0.19 | BDL | 0.08 | 1.57 | 29.02 | 0.005 | BDL | BDL | 0.020 | – |
| 9 th day | 0.42 | BDL | 0.07 | 2.49 | 33.25 | BDL | BDL | BDL | BDL | – |
| 10 th day | 0.30 | BDL | 0.06 | 1.45 | 31.84 | BDL | BDL | BDL | BDL | – |

BDL refers to below detection limit.

– refers to not measured.

| Sample 10-6 b | Pb | Cr | Ba | Zn | Fe | As | Cd | Ag | Se | Hg |
|----------------------|------|--------|------|--------|--------|-------|-------|-------|-------|----|
| 1 st day | 2.48 | 0.0056 | 0.68 | 186.74 | 980.20 | BDL | 0.034 | BDL | 0.014 | – |
| 2 nd day | 0.01 | BDL | 0.11 | 5.81 | 62.64 | 0.002 | BDL | BDL | BDL | – |
| 3 rd day | 0.01 | BDL | 0.12 | BDL | 22.06 | BDL | BDL | BDL | BDL | – |
| 4 th day | BDL | BDL | 0.91 | BDL | 11.40 | BDL | BDL | 0.002 | BDL | – |
| 5 th day | BDL | BDL | 0.51 | BDL | 1.63 | BDL | BDL | BDL | BDL | – |
| 6 th day | BDL | BDL | 0.28 | BDL | 0.25 | BDL | BDL | BDL | BDL | – |
| 7 th day | 0.01 | BDL | 0.24 | BDL | 0.92 | 0.005 | BDL | BDL | 0.023 | – |
| 8 th day | BDL | BDL | 0.22 | BDL | 0.57 | 0.004 | BDL | BDL | 0.018 | – |
| 9 th day | 0.01 | BDL | 0.18 | 0.01 | 2.16 | BDL | BDL | BDL | BDL | – |
| 10 th day | 0.03 | BDL | 0.18 | BDL | 3.23 | BDL | BDL | BDL | BDL | – |

BDL refers to below detection limit.

– refers to not measured.

| Sample 10-7 b | Pb | Cr | Ba | Zn | Fe | As | Cd | Ag | Se | Hg |
|----------------------|------|--------|------|--------|--------|-------|-------|-----|-------|----|
| 1 st day | 3.93 | 0.0592 | 6.60 | 299.98 | 503.56 | 0.013 | 0.029 | BDL | BDL | – |
| 2 nd day | 0.08 | BDL | 1.00 | 10.59 | 16.98 | BDL | BDL | BDL | BDL | – |
| 3 rd day | 0.14 | BDL | 0.24 | 5.78 | 19.92 | BDL | BDL | BDL | BDL | – |
| 4 th day | 1.23 | BDL | 2.96 | 11.41 | 19.45 | BDL | BDL | BDL | BDL | – |
| 5 th day | 0.45 | BDL | 0.23 | 3.84 | 12.97 | BDL | BDL | BDL | BDL | – |
| 6 th day | 0.48 | BDL | 0.12 | 3.24 | 24.36 | BDL | BDL | BDL | BDL | – |
| 7 th day | 0.57 | BDL | 0.11 | 3.49 | 36.57 | 0.004 | BDL | BDL | 0.019 | – |
| 8 th day | 0.40 | BDL | 0.11 | 2.93 | 34.25 | 0.004 | BDL | BDL | 0.016 | – |
| 9 th day | 0.67 | BDL | 0.09 | 4.44 | 44.23 | BDL | BDL | BDL | BDL | – |
| 10 th day | 0.24 | BDL | 0.18 | 1.30 | 17.64 | BDL | BDL | BDL | BDL | – |

BDL refers to below detection limit.

– refers to not measured.

| Sample 10-8 a | Pb | Cr | Ba | Zn | Fe | As | Cd | Ag | Se | Hg |
|----------------------|------|--------|------|--------|--------|-------|-------|-------|-------|----|
| 1 st day | 2.05 | BDL | 1.57 | 881.53 | 560.23 | BDL | 0.064 | BDL | 0.009 | – |
| 2 nd day | 0.10 | BDL | 1.22 | 45.85 | 13.74 | BDL | BDL | BDL | BDL | – |
| 3 rd day | 0.08 | BDL | 0.22 | 3.59 | 23.68 | 0.002 | BDL | BDL | BDL | – |
| 4 th day | 0.03 | BDL | 0.73 | 3.79 | 17.85 | BDL | BDL | BDL | BDL | – |
| 5 th day | 0.01 | BDL | 0.26 | 7.40 | 7.41 | BDL | BDL | BDL | BDL | – |
| 6 th day | 0.02 | BDL | 0.25 | 9.68 | 2.86 | BDL | BDL | BDL | BDL | – |
| 7 th day | 0.04 | BDL | 0.19 | 17.52 | 1.44 | 0.004 | 0.002 | BDL | 0.018 | – |
| 8 th day | 0.22 | BDL | 0.13 | 29.73 | 3.96 | 0.004 | 0.007 | BDL | 0.017 | – |
| 9 th day | 0.64 | BDL | 0.09 | 39.56 | 7.76 | BDL | 0.009 | BDL | BDL | – |
| 10 th day | 0.74 | 0.0024 | 0.13 | 21.85 | 5.70 | BDL | 0.007 | 0.001 | BDL | – |

BDL refers to below detection limit.

– refers to not measured.

| Sample 10-9 b | Pb | Cr | Ba | Zn | Fe | As | Cd | Ag | Se | Hg |
|----------------------|------|--------|------|--------|--------|-------|-------|-------|-------|----|
| 1 st day | 3.23 | 0.0304 | 0.82 | 316.26 | 430.46 | BDL | 0.019 | BDL | BDL | – |
| 2 nd day | 0.43 | BDL | 0.16 | 25.08 | 42.16 | BDL | 0.004 | BDL | BDL | – |
| 3 rd day | 0.51 | BDL | 0.14 | 10.51 | 23.82 | BDL | BDL | BDL | BDL | – |
| 4 th day | 2.00 | BDL | 1.05 | 9.82 | BDL | BDL | BDL | BDL | BDL | – |
| 5 th day | 1.10 | BDL | 0.09 | 4.54 | 25.38 | BDL | BDL | BDL | BDL | – |
| 6 th day | 1.18 | BDL | 0.05 | 3.44 | 32.57 | 0.006 | BDL | BDL | 0.022 | – |
| 7 th day | 1.15 | BDL | 0.06 | 4.25 | 26.15 | 0.004 | BDL | BDL | 0.015 | – |
| 8 th day | 1.07 | BDL | 0.05 | 4.03 | 31.94 | 0.004 | BDL | BDL | 0.016 | – |
| 9 th day | 1.08 | BDL | 0.03 | 5.78 | 50.96 | BDL | BDL | BDL | BDL | – |
| 10 th day | 1.22 | 0.0016 | 0.04 | 2.52 | 36.84 | 0.002 | BDL | 0.005 | BDL | – |

BDL refers to below detection limit.

– refers to not measured.

| Sample 11-1 e | Pb | Cr | Ba | Zn | Fe | As | Cd | Ag | Se | Hg |
|----------------------|-------|--------|------|--------|--------|-------|-------|-------|-------|----|
| 1 st day | 10.66 | 0.0638 | 0.55 | 619.87 | 295.97 | BDL | 0.009 | BDL | BDL | – |
| 2 nd day | 1.12 | BDL | 0.25 | 13.82 | 7.29 | BDL | BDL | BDL | BDL | – |
| 3 rd day | 0.05 | BDL | 0.11 | 6.01 | 1.20 | BDL | BDL | BDL | BDL | – |
| 4 th day | 0.15 | BDL | 0.10 | 6.91 | 7.75 | BDL | BDL | BDL | BDL | – |
| 5 th day | 0.40 | BDL | 0.08 | 9.37 | 21.68 | BDL | BDL | BDL | BDL | – |
| 6 th day | 0.25 | BDL | 0.10 | 4.13 | 9.67 | BDL | BDL | 0.001 | BDL | – |
| 7 th day | 0.23 | BDL | 0.11 | 2.87 | 5.00 | 0.007 | BDL | BDL | BDL | – |
| 8 th day | 0.45 | BDL | 0.10 | 3.53 | 10.31 | BDL | BDL | BDL | 0.012 | – |
| 9 th day | 0.77 | 0.0101 | 0.10 | 3.38 | 13.15 | BDL | BDL | BDL | BDL | – |
| 10 th day | 0.74 | BDL | 0.09 | 3.04 | 18.26 | BDL | BDL | BDL | BDL | – |

BDL refers to below detection limit.

– refers to not measured.

| Sample 11-2 a | Pb | Cr | Ba | Zn | Fe | As | Cd | Ag | Se | Hg |
|----------------------|-------|--------|------|--------|--------|-----|-------|-------|-----|----|
| 1 st day | 22.64 | 0.0048 | 1.29 | 116.59 | 678.10 | BDL | 0.016 | BDL | BDL | – |
| 2 nd day | 0.07 | BDL | 0.41 | 1.57 | 47.47 | BDL | BDL | BDL | BDL | – |
| 3 rd day | 0.10 | BDL | 0.29 | 0.90 | 23.36 | BDL | BDL | BDL | BDL | – |
| 4 th day | 0.13 | BDL | 0.26 | 1.19 | 16.09 | BDL | BDL | BDL | BDL | – |
| 5 th day | 0.63 | BDL | 0.14 | 1.92 | 31.93 | BDL | BDL | BDL | BDL | – |
| 6 th day | 0.67 | 0.0023 | 0.15 | 1.14 | 25.11 | BDL | BDL | 0.002 | BDL | – |
| 7 th day | 0.22 | BDL | 0.14 | 0.63 | 23.87 | BDL | BDL | BDL | BDL | – |
| 8 th day | 2.04 | 0.0403 | 0.32 | 0.51 | 10.19 | BDL | BDL | BDL | BDL | – |
| 9 th day | 0.30 | BDL | 0.26 | 0.13 | 2.02 | BDL | BDL | BDL | BDL | – |
| 10 th day | 0.71 | BDL | 0.18 | 0.31 | 13.73 | BDL | BDL | BDL | BDL | – |

BDL refers to below detection limit.

– refers to not measured.

Appendix B

Material Safety Data Sheet for steel grit used in Region 10

MATERIAL SAFETY DATA SHEET



| | | |
|---|--------------------------|--|
| ERVIN INDUSTRIES, INC. 3893 RESEARCH PARK DRIVE ANN ARBOR, MI 48108-2217 | | TELEPHONE: (734) 769-4600 FAX: (734) 663-0136 |
| Revision Date: 12/5/2012 | Replaces Date: 12/9/2009 | Revision Level: T |
| PREPARED BY: Mark Hash | | Ervin Industries |


| SECTION I | PRODUCT IDENTIFICATION | |
|---------------|------------------------|---------|
| Product Name | Chemical Family | |
| AMASTEEL SHOT | AMABRASIVE | FERROUS |
| AMASTEEL GRIT | (SHOT / GRIT MIX) | |

| SECTION II | COMPOSITION / INGREDIENTS | | | |
|--|---------------------------|----------|--|--|
| Chemical Name | CAS Registry No | % Weight | ACGIH - TLV (mg/m ³) | OSHA - PEL (mg/m ³) |
| Iron - Fe Oxide fume as Fe | 7439-89-6 | >96 | 5 | 10 |
| Carbon - C | 7440-44-0 | <1.2 | none estab. | none estab. |
| Manganese - Mn Elemental, Inorganic Compounds as Mn Fume as Mn | 7439-96-5 | <1.3 | 0.2 none estab. | 5 (ceiling) 5 (ceiling) |
| Silicon - Si as total dust Respirable fraction | 7440-21-3 | <1.2 | 10 none estab. | 15 5 |
| Chromium - Cr Elemental, Inorganic Compounds as Cr metal Cr II compounds - as Cr Cr III compounds - as Cr Cr VI compounds - water soluble Cr VI compounds - insoluble Chromic Acid and Chromates as CrO ₃ Cr VI (hexavalent chromium) in product as shipped | 7440-47-3 | <0.25 | 0.5 none estab. 0.5 0.05 0.01 none estab. | 1 0.5 0.5 5 ug 5 ug 0.1 (ceiling) |
| Copper - Cu Fume Dust & mists | 7440-50-8 | <0.25 | 0.2 1 | 0.1 1 |
| Nickel - Ni Elemental metal Insoluble as Ni Soluble compounds as Ni | 7440-02-0 | <0.20 | 1.5 0.1 0.2 | 1 1 |

| SECTION III | PHYSICAL DATA | |
|--|-------------------------------------|--|
| Cast steel shot and grit are non-hazardous as received. Fine metallic dust is generated as the abrasive breaks down from impact and wear during normal use. Since the ferrous content is >96%, dust or fumes will consist mainly of iron or iron oxide. In addition, the fine steel dust created can be a mild explosion hazard (see section V). | | |
| Boiling Point - 2850-3150 Degrees C | Melting Point - 1371-1483 Degrees C | |
| Specific Gravity (at 60 Degrees F) >7.6 | Vapor Pressure - Not Applicable | |
| % Volatile by Volume - Not Applicable | pH - Not Applicable | |
| Appearance and Odor - Spherical - no odor | Percent Solid by Weight - 100% | |

| SECTION IV | REACTIVITY DATA | |
|---|---|---|
| Stability – Stable | Hazardous decomposition products – None | Hazardous Polymerization - will not occur |
| Shot will break down into progressively smaller particles and dust during normal use. | | |

MATERIAL SAFETY DATA SHEET

| | |
|--|--|
| SECTION V | FIRE AND EXPLOSION HAZARD DATA |
| Flash Point - Not Applicable | Auto Ignition Temperature (solid iron exposed to Oxygen) -930 degree C |
| Flammability Limits - Not Applicable | Cast steel shot will not burn or explode |
| A mild fire or explosion hazard situation may be created from fine metal dust. Fire Extinguishing method for dust created due to use - use Class D extinguishing agents or dry sand to exclude air. Do not use water or other liquids, or foam. | |
|  <p>NFPA Hazard Rating: 0 = Insignificant 1 = Slight 2 = Moderate 3 = High 4 = Extreme</p> <p>Health (blue) = 0 Flammability (red) = 0 Reactivity (yellow) = 0 Special (colorless)</p> | |

| | |
|---|---------------------------|
| SECTION VI | HEALTH HAZARD DATA |
| <p>Emergency and First Aid Procedure - If inhaled, move out of area into fresh air. Flush eyes with running water, have any remaining particles removed from eyes by a qualified medical person; call 911 for immediate medical assistance.</p> <p>The end user should have an industrial hygiene evaluation to determine the proper personal protective equipment for each application or blasting operation. Threshold Limit Values - Permissible Exposure Limits - see Section II</p> <p>Primary Routes of entry - inhalation of dust or dust particles in eyes. Target Organs - Lung for chromium and lung & nasal for Nickel. Metallic Nickel is reasonably anticipated to be a human carcinogen.</p> <p>Over exposure to dust and fumes may cause mouth, eye, and nose irritation. Prolonged overexposure to manganese dust or fume affects the central nervous system. Prolonged overexposure to iron oxide fume can cause siderosis, or "iron pigmentation" of the lung. It can be seen on a chest x-ray but causes little or no disability.</p> <p>Fumes generated by welding or flame cutting a surface containing new or used abrasive or the dust created by use of the abrasive may convert a small portion of chromium to hexavalent chromium. IARC reports welding fumes are possibly carcinogenic to humans.</p> | |

| | |
|--|--|
| SECTION VII | PERSONAL PROTECTION INFORMATION |
| Ventilation - General ventilation and local exhaust should be provided to keep the dust levels below the limits shown in Section II. | |
| Respiratory protection - If an industrial hygiene evaluation shows dust exceeds OSHA PEL's indicated in Section II, a NIOSH approved respirator with appropriate filters should be worn as determined by the end user. | |
| Eye protection - Approved safety glasses w/side shields should always be worn. Other protective equipment determined by the end user. | |

| | |
|--|--|
| SECTION VIII | SPILL / LEAK PROCEDURES AND WASTE DETERMINATION |
| Shot spilled or leaked onto floors can create hazardous walking conditions. When cleaning up quantities of dust; if exceeding OSHA permissible exposure limits, an approved respirator with appropriate filters should be used. | |
| Dust from blasting or peening operations always contain contaminants. The dust must be tested to determine if it is hazardous or non-hazardous waste. After such determination, the dust must be disposed of according to appropriate local, State or Federal regulations. | |

| | |
|---|----------------------------|
| SECTION IX | SPECIAL PRECAUTIONS |
| Precautions to be taken in handling and storing - Keep dry to reduce rusting. Observe maximum floor loading limitations. | |

| | |
|---|----------------------------|
| SECTION X | TRANSPORTATION |
| DOT Classification - Not a regulated material | Proper Shipping Name - N/A |
| DOT ID # - Not regulated | |

| | |
|--|---|
| SECTION XI | REGULATORY |
| a) CERCLA Hazardous Substance | _____ yes <input checked="" type="checkbox"/> no |
| b) SARA, Title III, Extremely Hazardous Substance | _____ yes <input checked="" type="checkbox"/> no |
| c) Toxic Chemical Release Report | <input checked="" type="checkbox"/> yes _____ no |
| Nickel & Manganese are subject to requirements of Section 313 of the Community Right-to-know Act of 1986 & 40CFR Part 372. | |

The information presented here has been compiled from sources considered to be reliable and accurate to the best of our knowledge and belief, but is not guaranteed to be so.

Appendix C

Solubility and speciation of RCRA metals as well as Fe and Zn

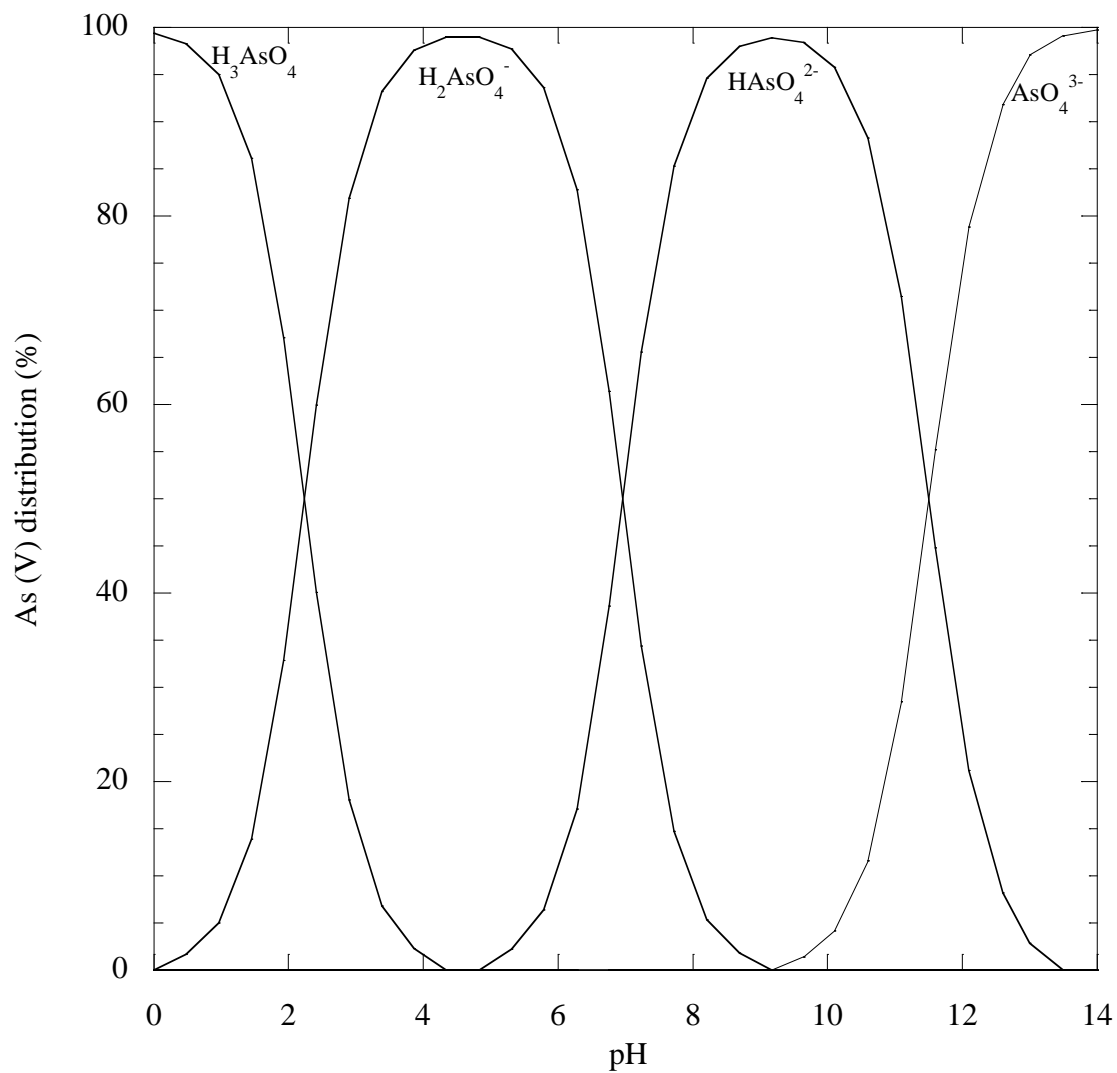


Figure C1. As (III) speciation in the leaching studies of paint waste, CH_3COOH at 0.1 M, 298 K and open to atmosphere. All the speciation was computed using MINEQL⁺. The total concentration of As leached was 8.9×10^{-6} M.

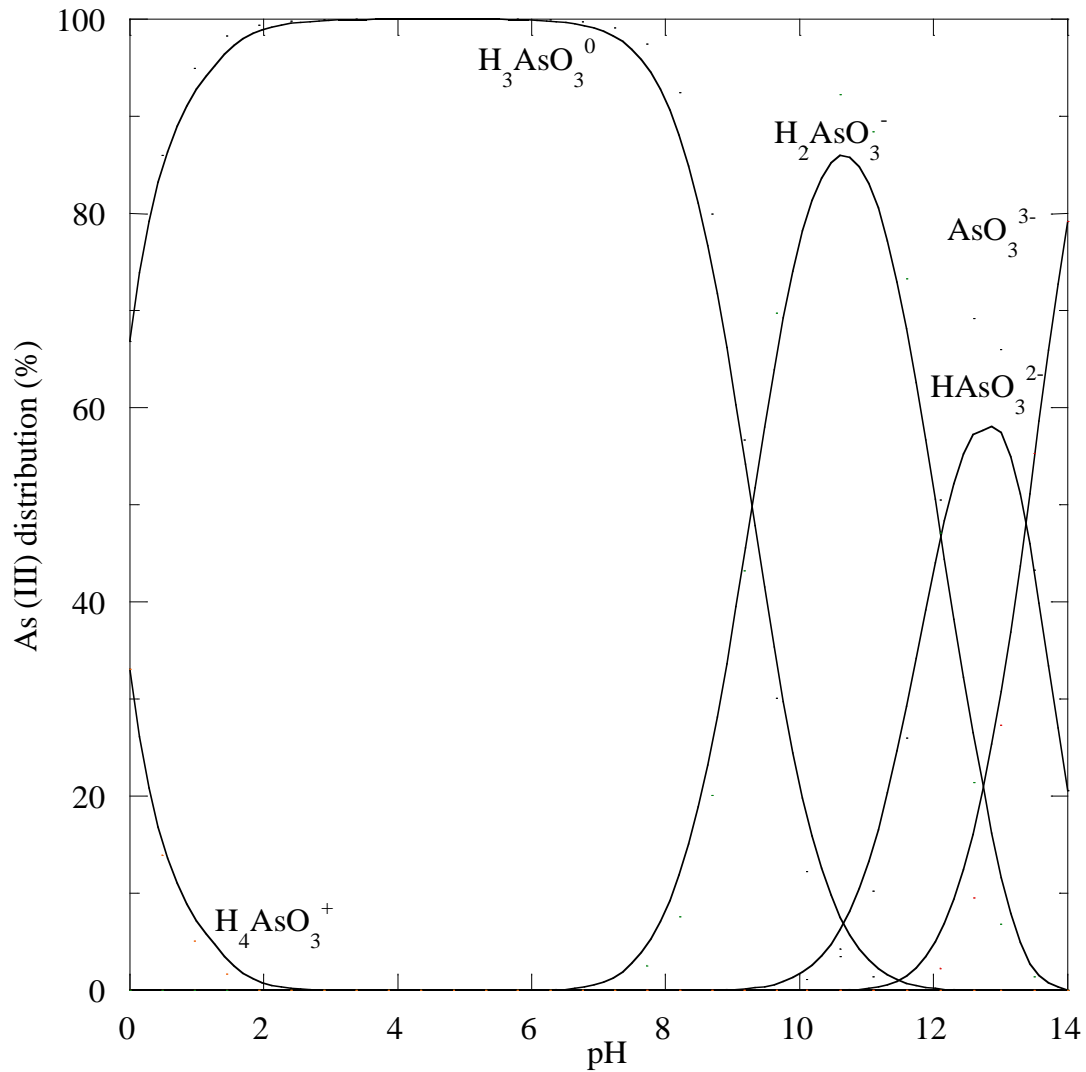


Figure C2. As (VI) speciation in the leaching studies of paint waste, CH_3COOH at 0.1 M, 298 K and open to atmosphere. All the speciation was computed using MINEQL⁺. The total concentration of As leached was 8.9×10^{-6} M.

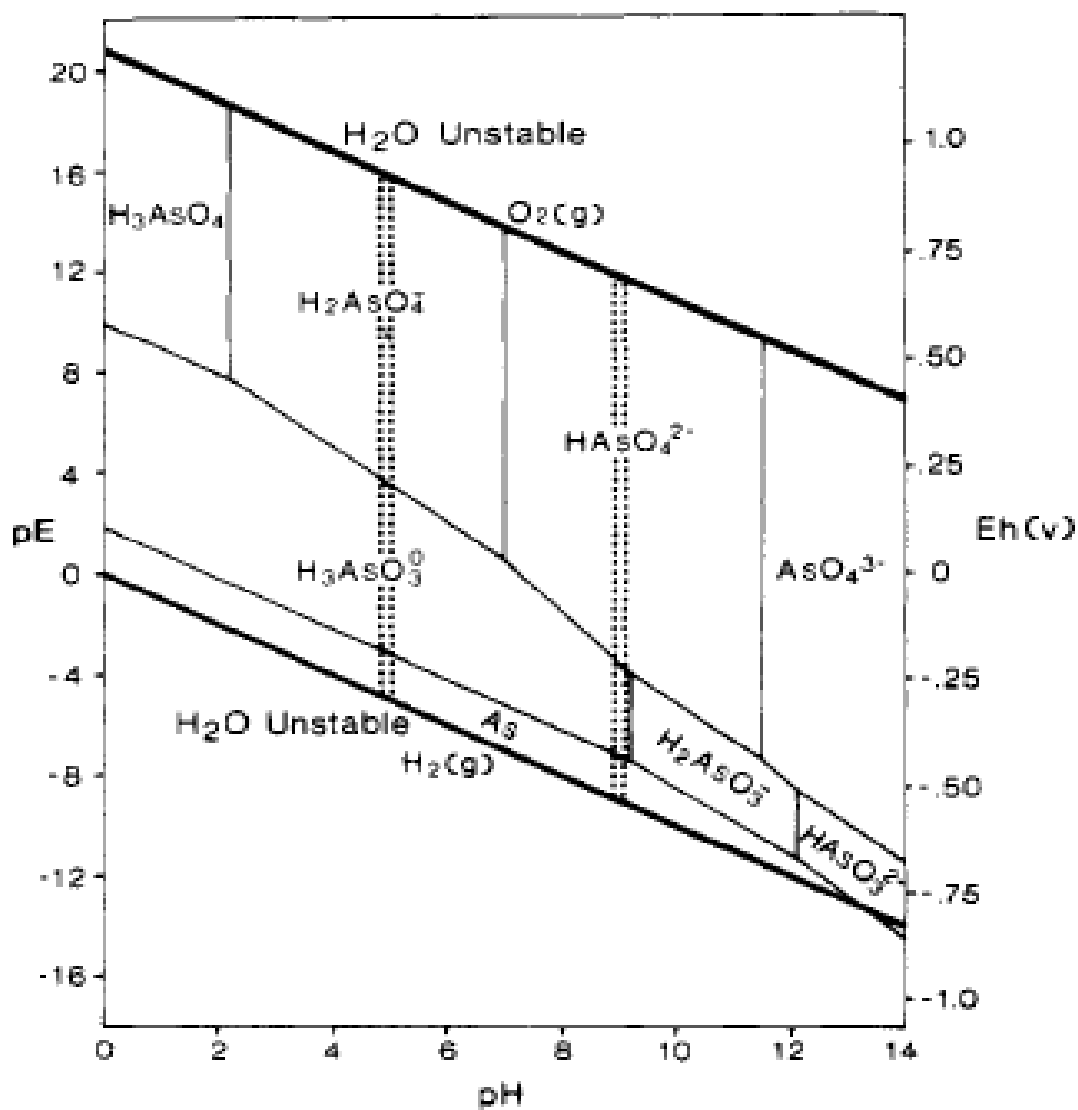


Figure C3. The pE–pH diagram for As at 298 K, in an open system with total As 5.0×10^{-8} M from Cullen and Reimer (1989).

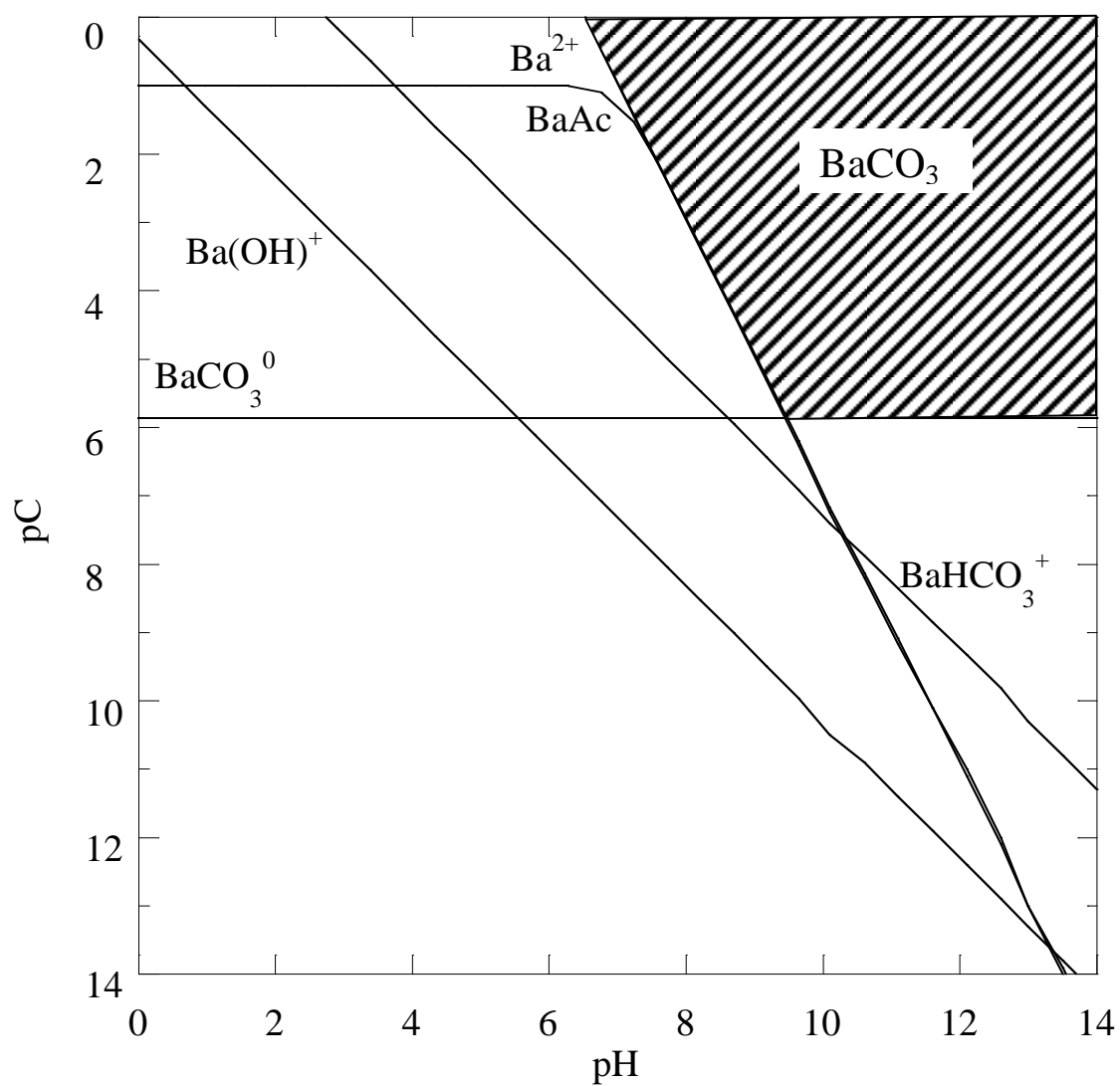


Figure C4. Ba solubility in equilibrium with BaCO_3 , CH_3COOH at 0.1 M, 298 K and open to atmosphere. All the speciation was computed using MINEQL⁺.

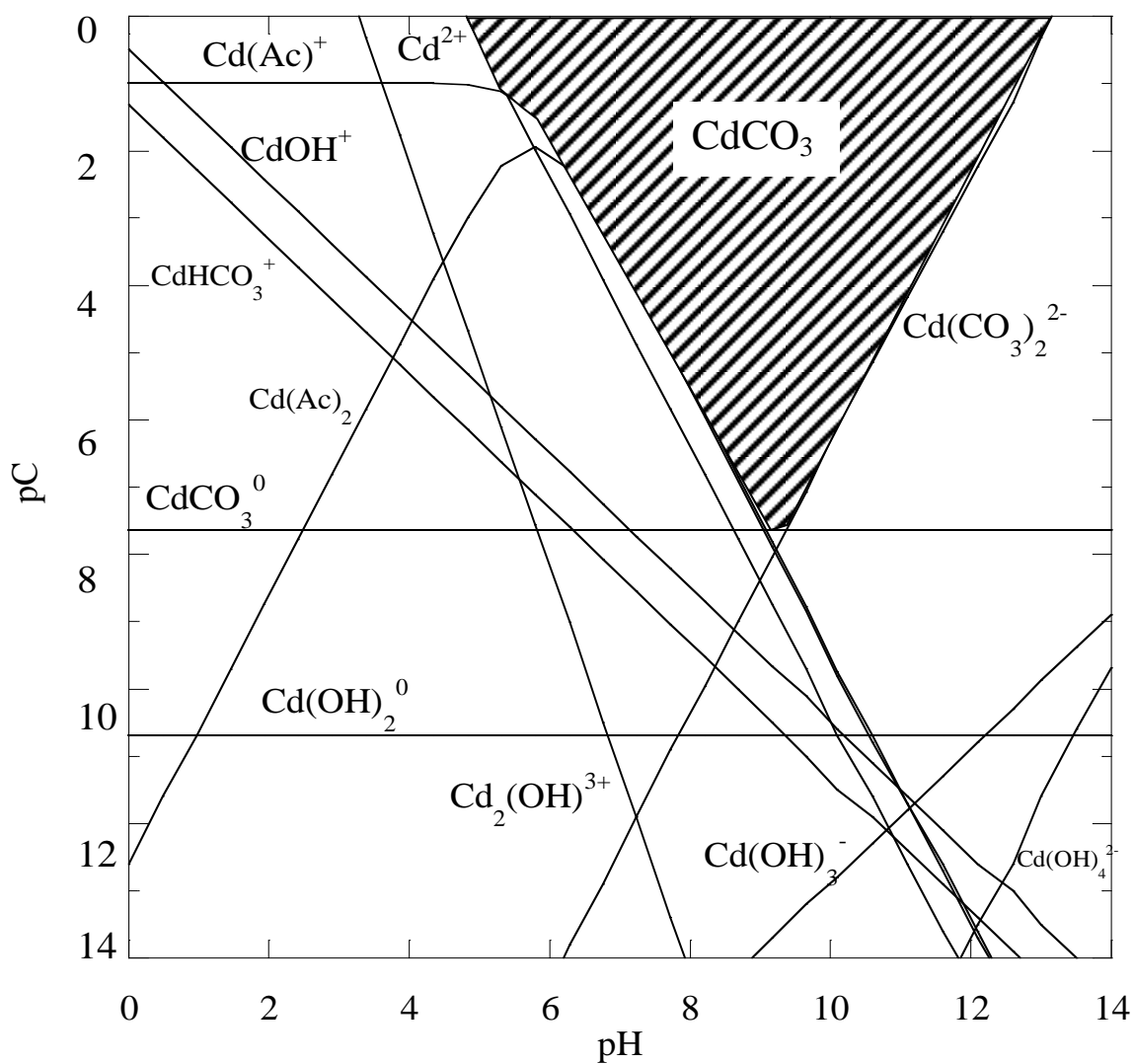


Figure C5. Cd solubility in equilibrium with CdCO_3 , CH_3COOH at 0.1 M, 298 K and open to atmosphere. All the speciation was computed using MINEQL⁺.

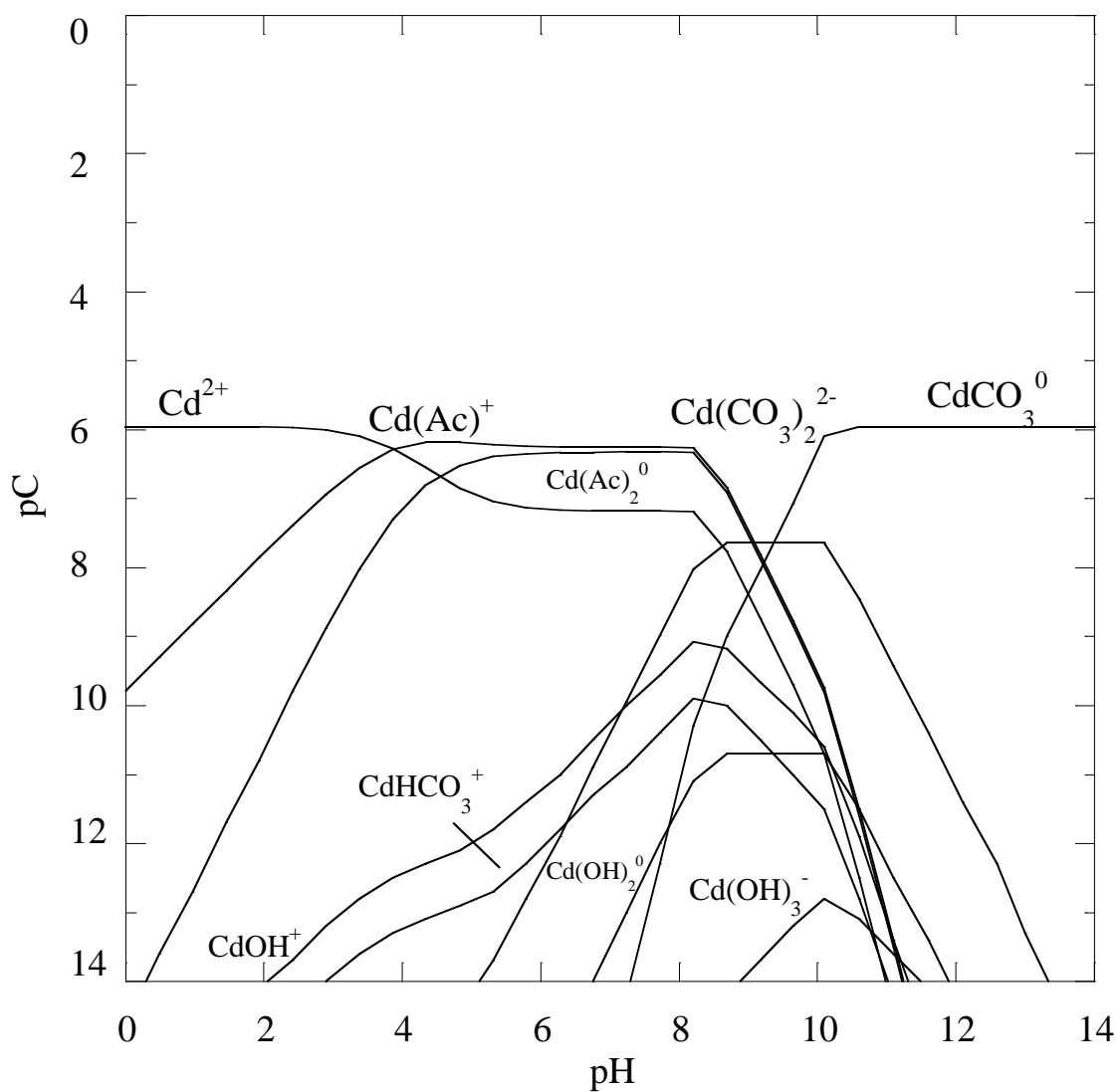


Figure C6. Cd speciation in the leaching studies of paint waste, CH_3COOH at 0.1 M, 298 K and open to atmosphere. All the speciation was computed using MINEQL⁺. The total concentration of Cd leached was 1.1×10^{-6} M.

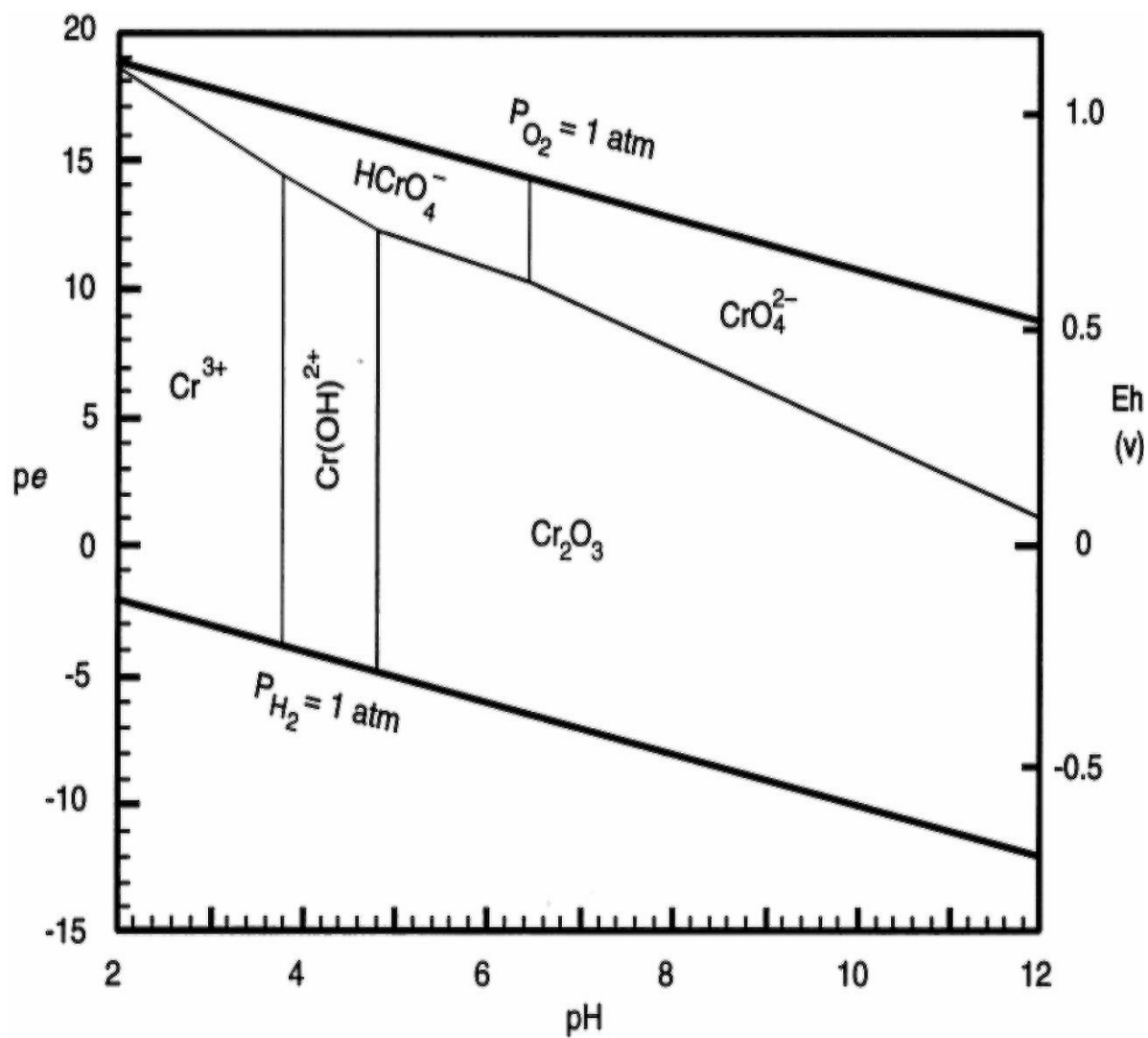


Figure C7. The pE–pH diagram for Cr at 298 K, in an open system with total Cr 1.0×10^{-6} M from Rai et al. (1989).

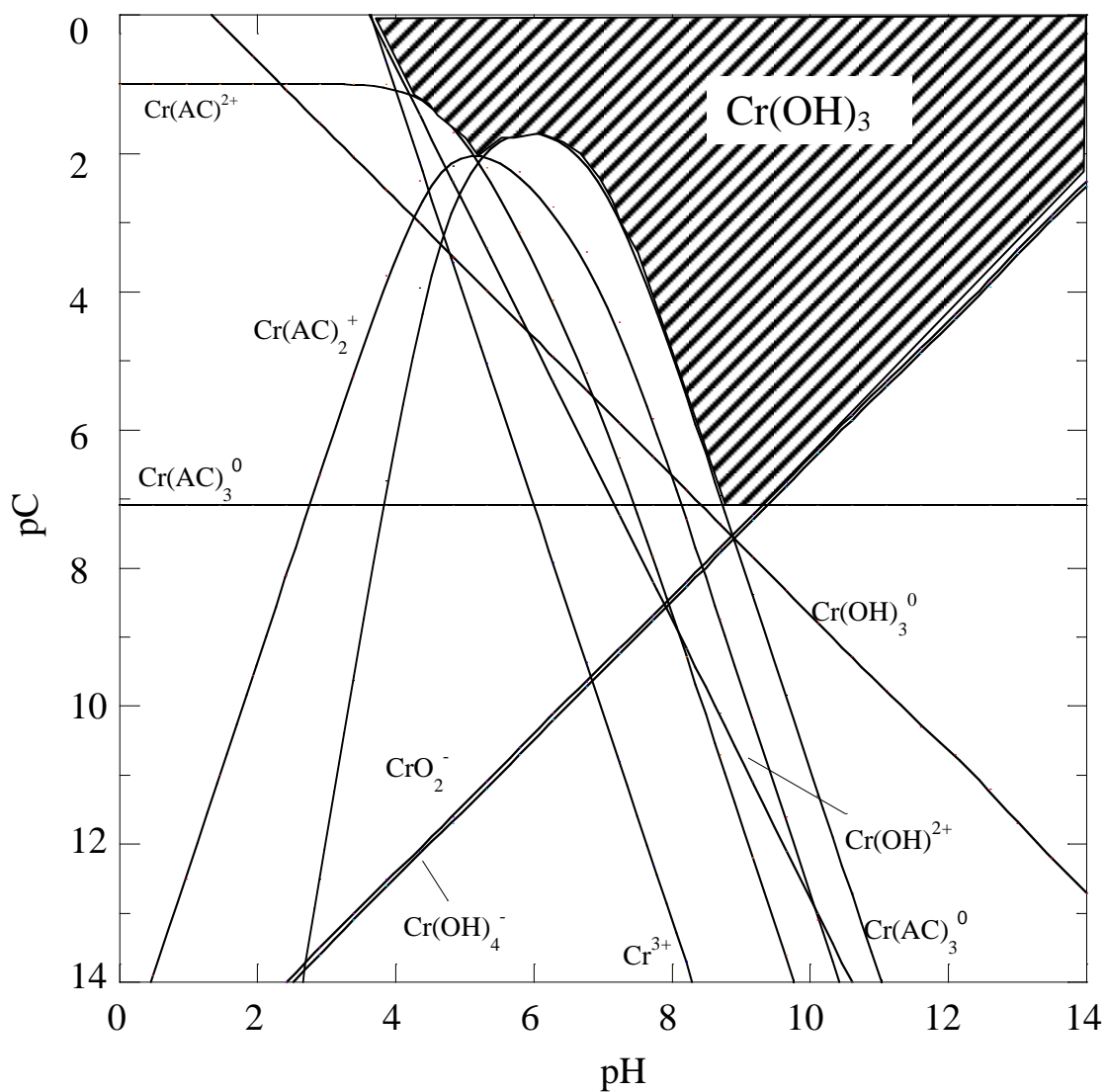


Figure C8. Cr (III) solubility in equilibrium with Cr(OH)_3 , CH_3COOH at 0.1 M, 298 K and open to atmosphere. All the speciation was computed using MINEQL⁺.

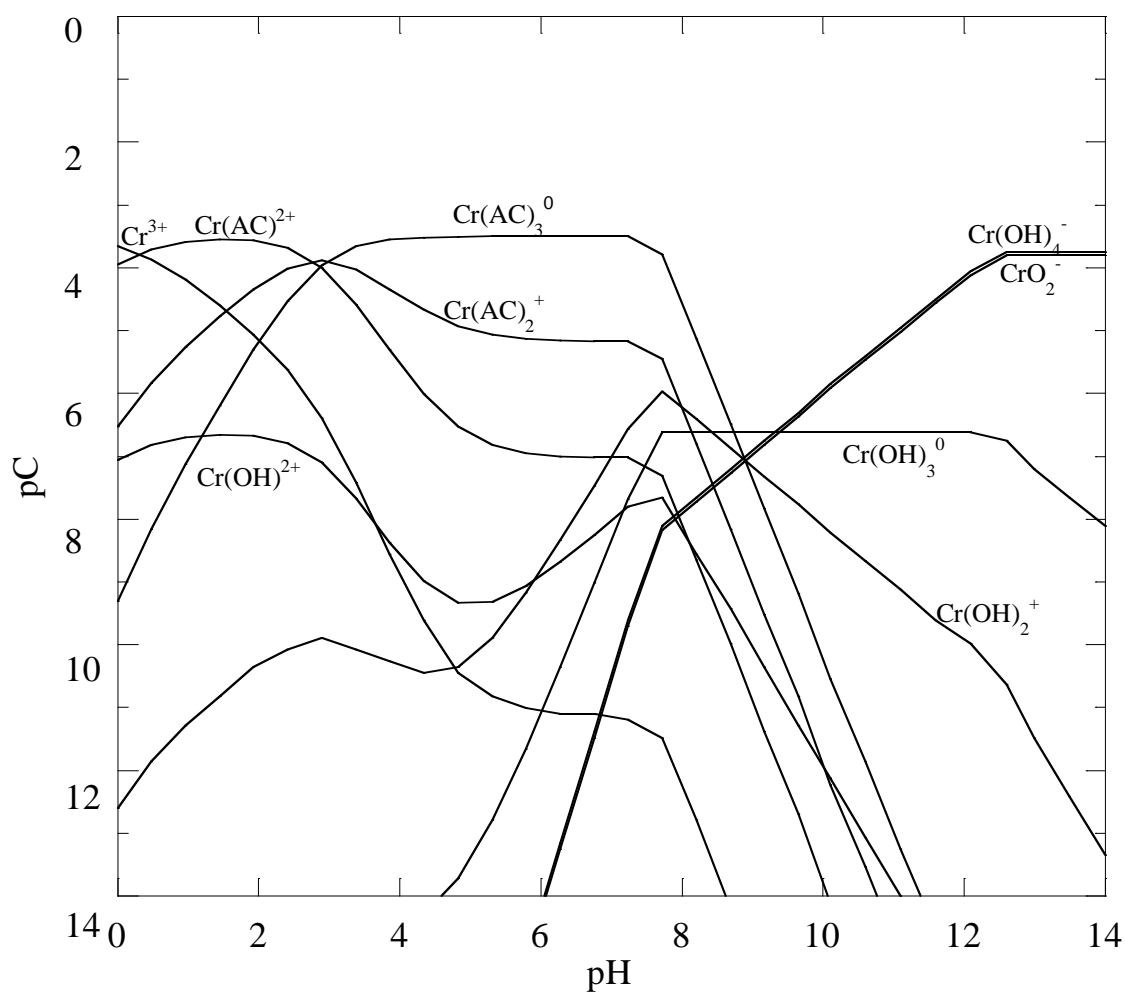


Figure C9. Cr(III) speciation in the leaching studies of paint waste, CH_3COOH at 0.1 M, 298 K and open to atmosphere. All the speciation was computed using MINEQL⁺. The total concentration of Cr leached was 1.8×10^{-4} M.

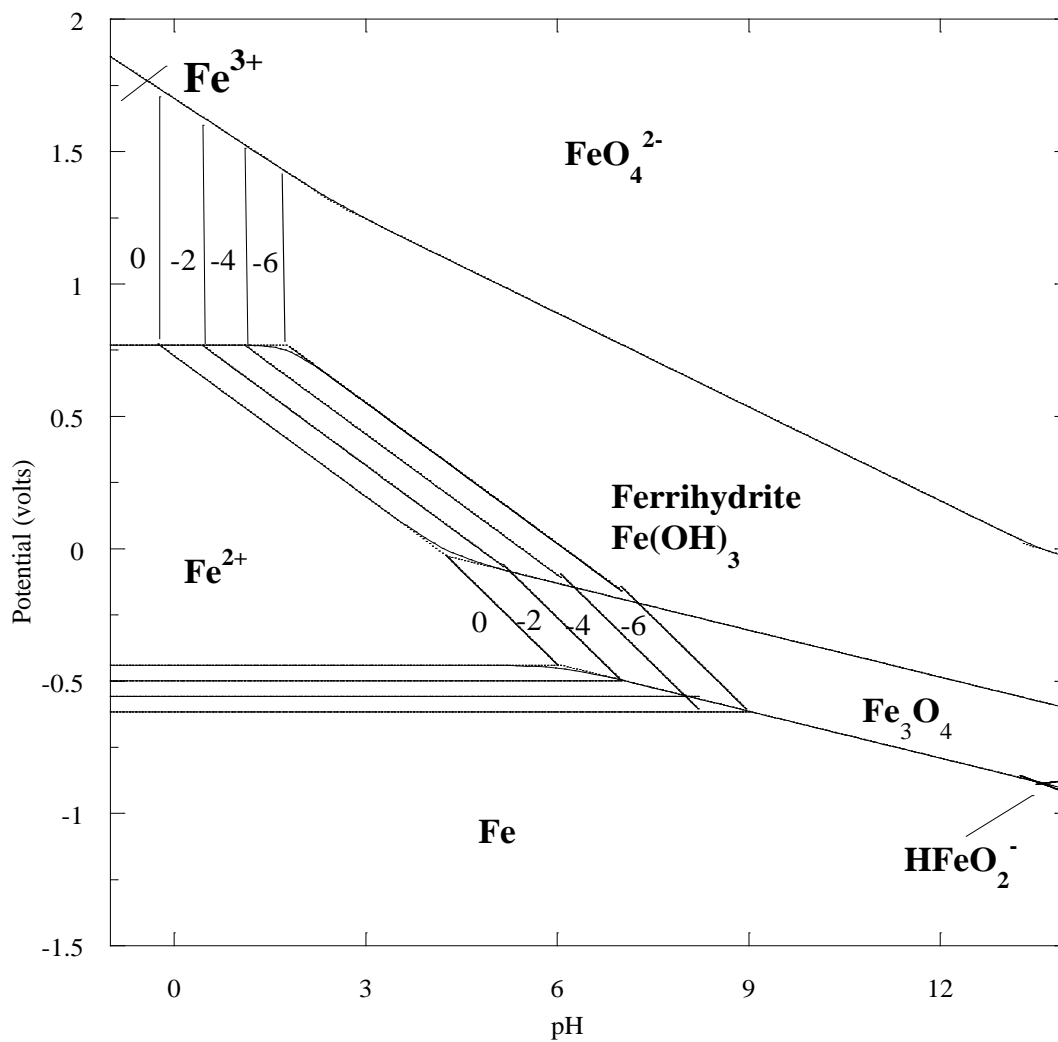


Figure C10. Potential – pH equilibrium diagram of iron or steel considering four concentrations of soluble species (10^0 , 10^{-2} , 10^{-4} , 10^{-6} M), four soluble species (Fe^{3+} , Fe^{2+} , FeO_4^{2-} , HFeO_2^-), and corrosion material ferrihydrite [$\text{Fe}(\text{OH})_3$] at 298 K.

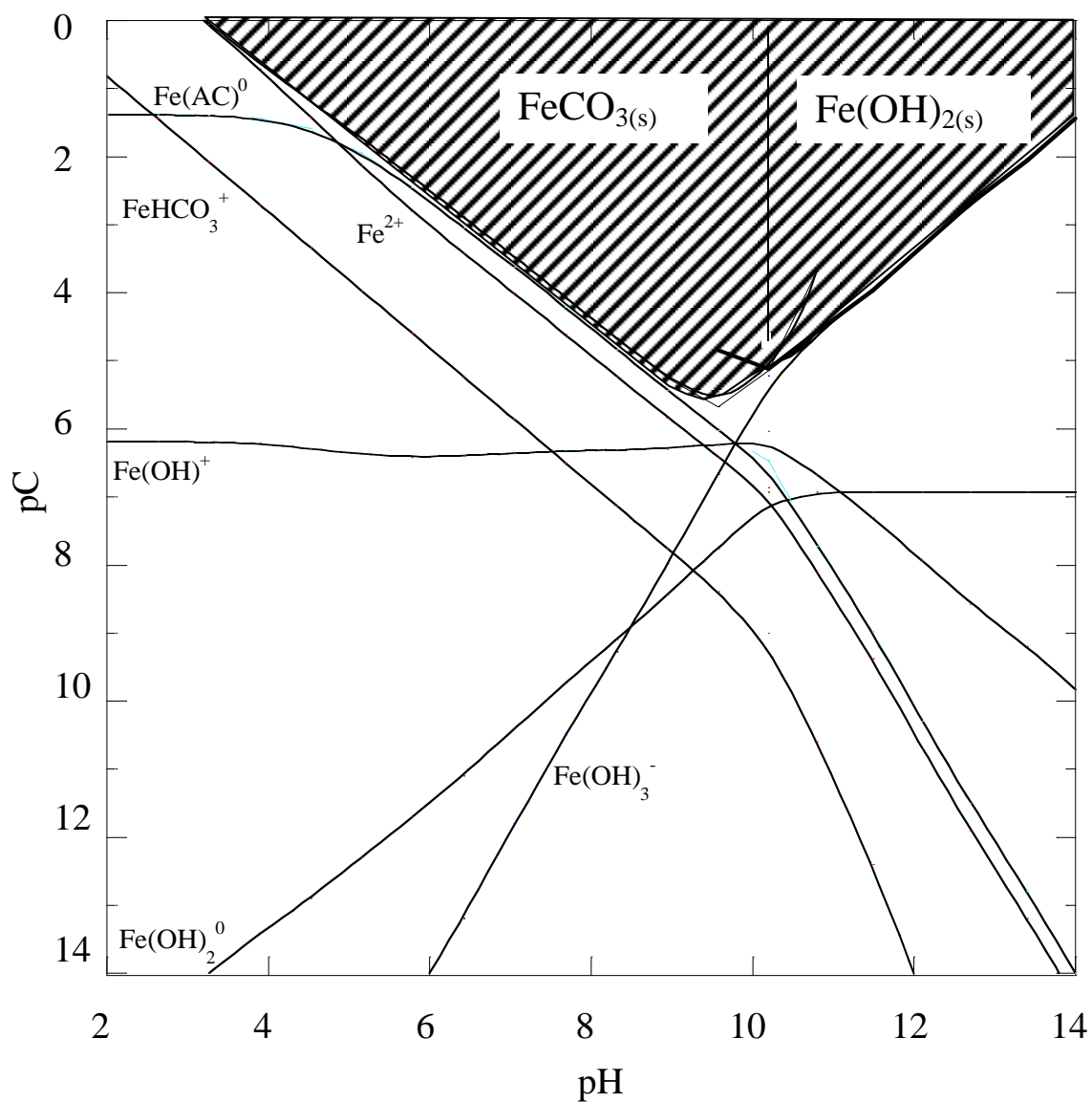


Figure C11. Fe^{2+} solubility in equilibrium with $\text{Fe}(\text{OH})_2$ and FeCO_3 , CH_3COOH at 0.1 M, 298 K and open to atmosphere. All the speciation was computed using MINEQL⁺.

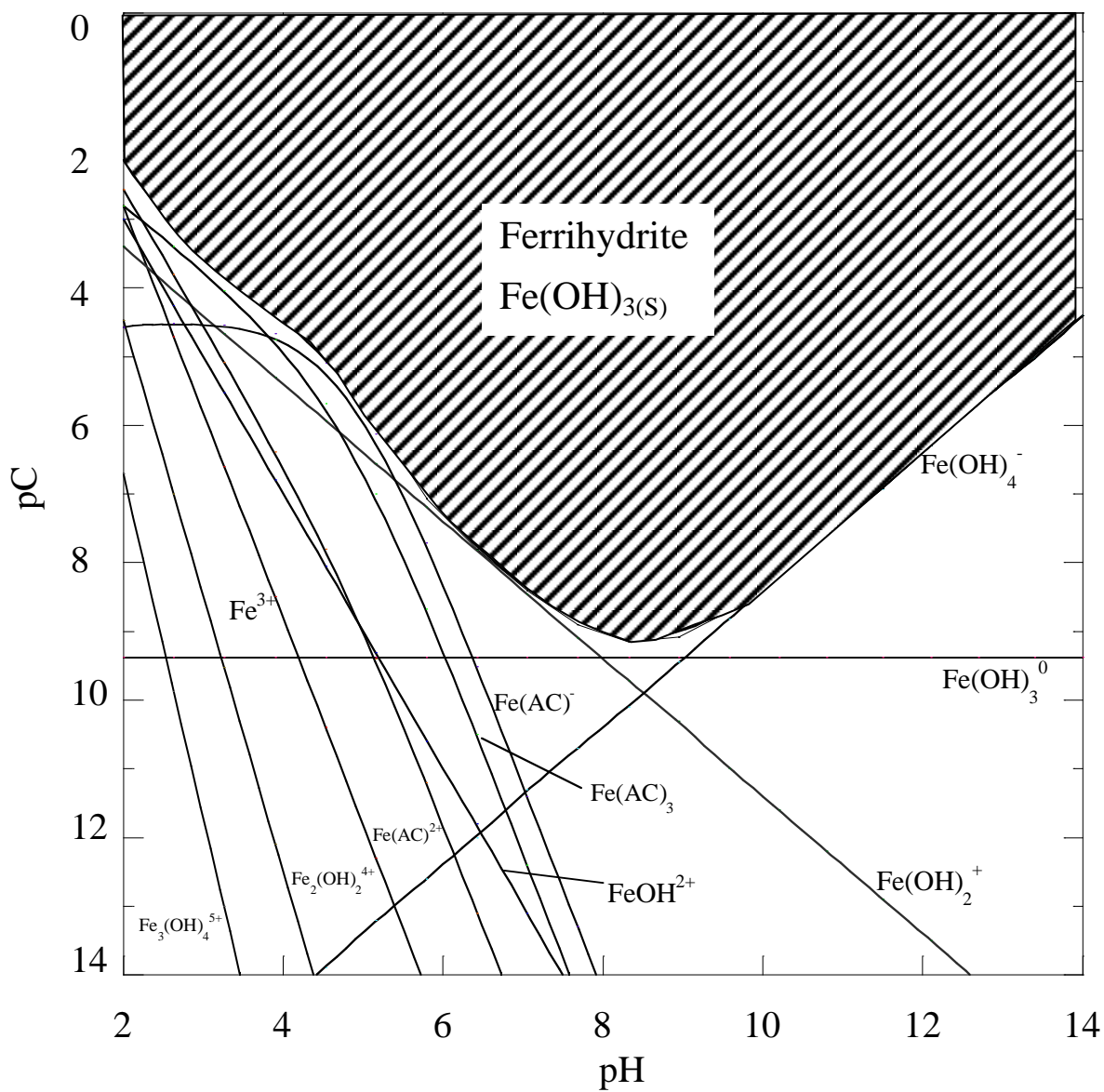


Figure C12. Fe^{3+} solubility in equilibrium with Ferrihydrite [$\text{Fe}(\text{OH})_3$], CH_3COOH at 0.1 M, 298 K and open to atmosphere. All the speciation was computed using MINEQL⁺.

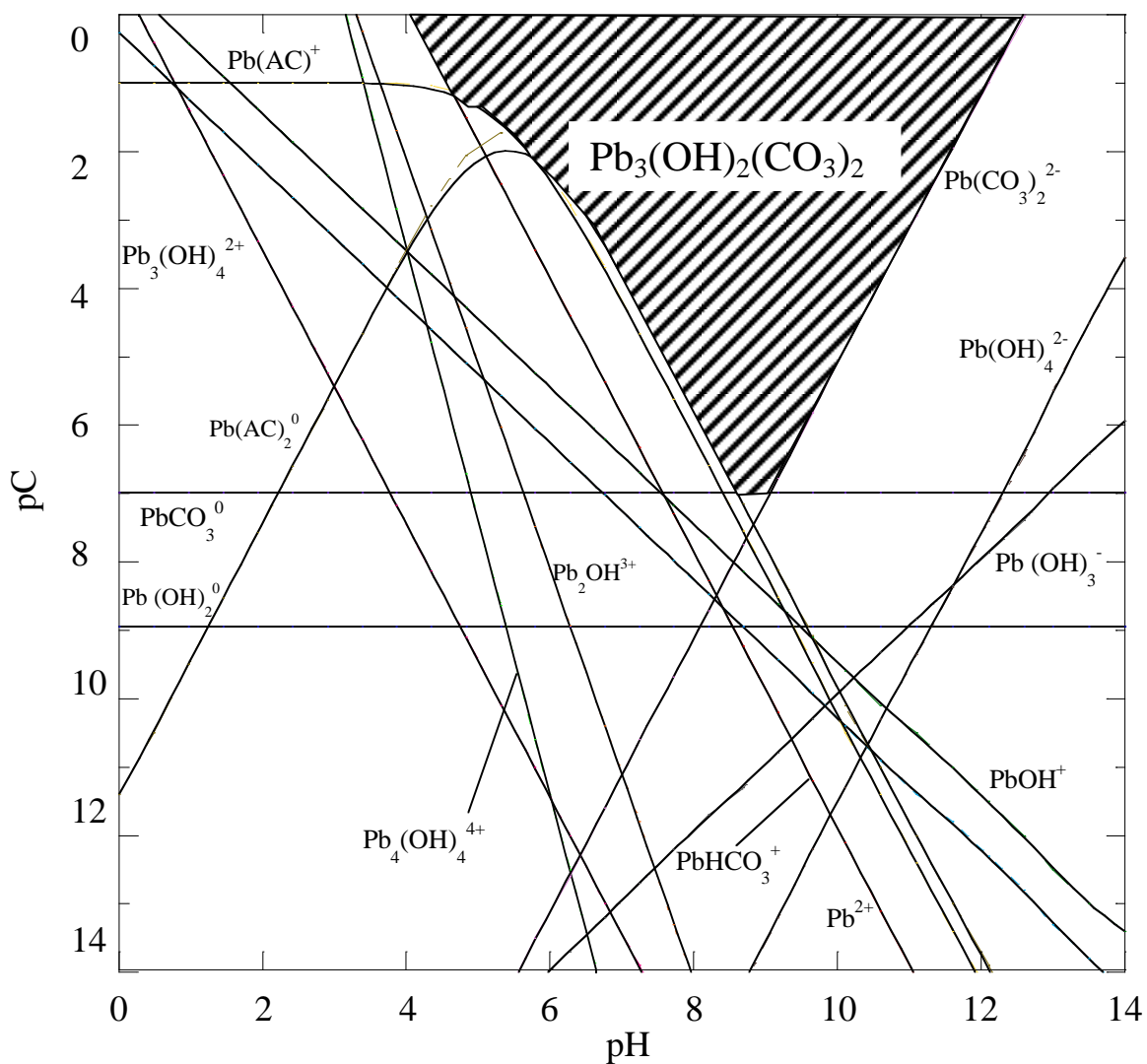


Figure C13. Pb solubility in equilibrium with $\text{Pb}_3(\text{OH})_2(\text{CO}_3)_2$, CH_3COOH at 0.1 M, 298 K and open to atmosphere. All the speciation was computed using MINEQL⁺.

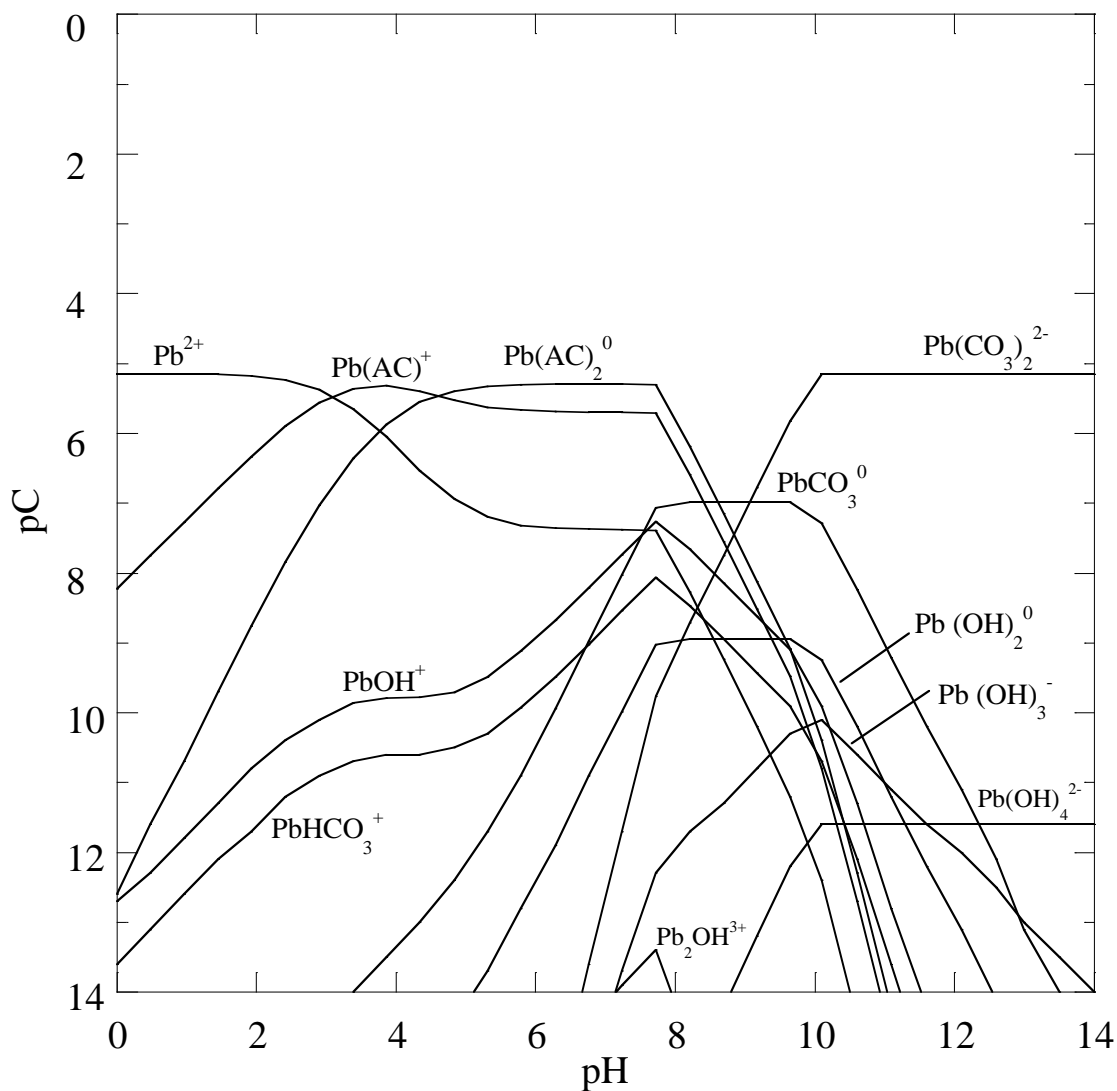


Figure C14. Pb speciation in the leaching studies of paint waste, CH_3COOH at 0.1 M, 298 K and open to atmosphere. All the speciation was computed using MINEQL⁺. The total concentration of Pb leached was 7.1×10^{-6} M.

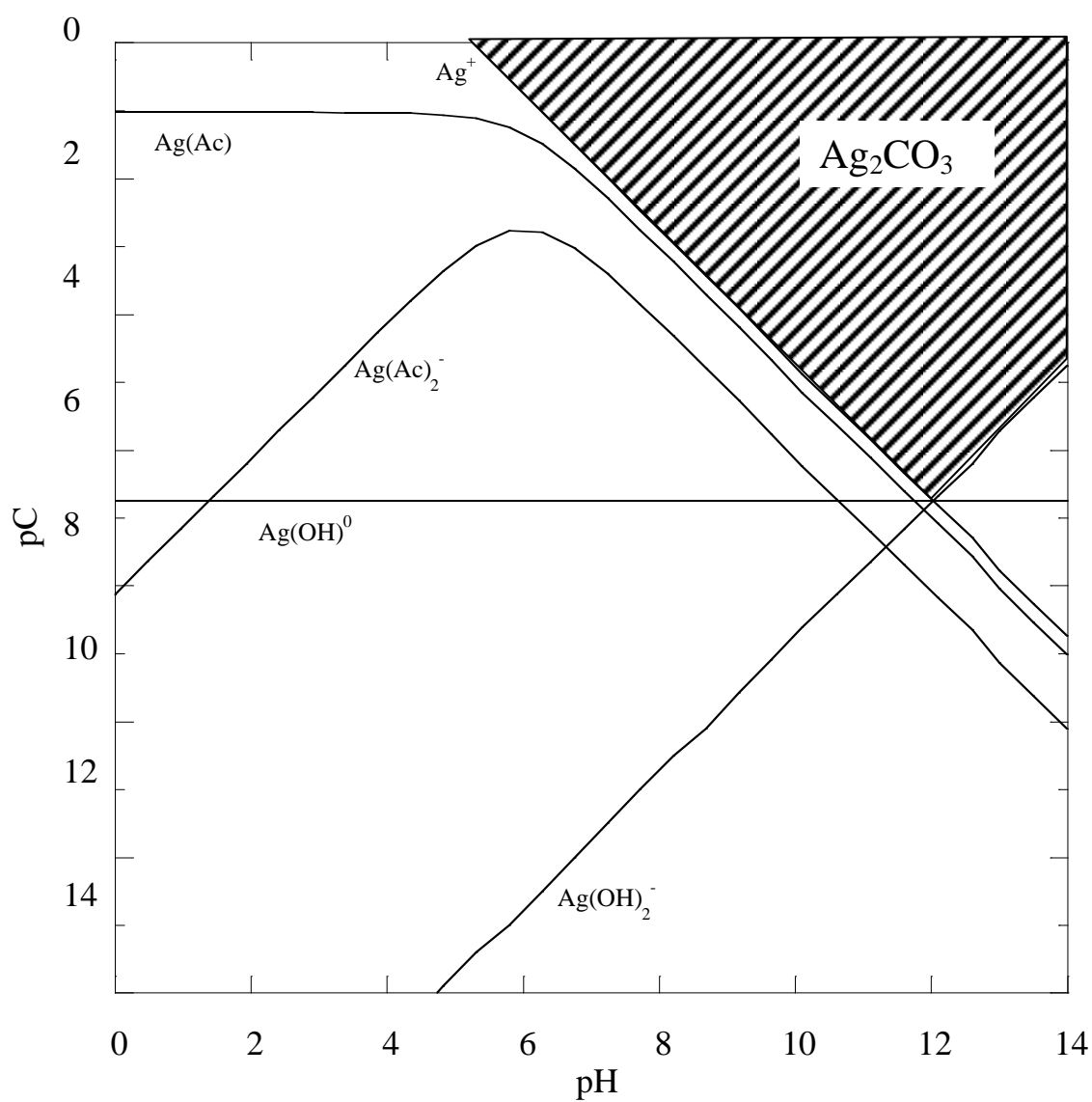


Figure C15. Ag solubility in equilibrium with Ag_2CO_3 , CH_3COOH at 0.1 M, 298 K and open to atmosphere. All the speciation was computed using MINEQL⁺.

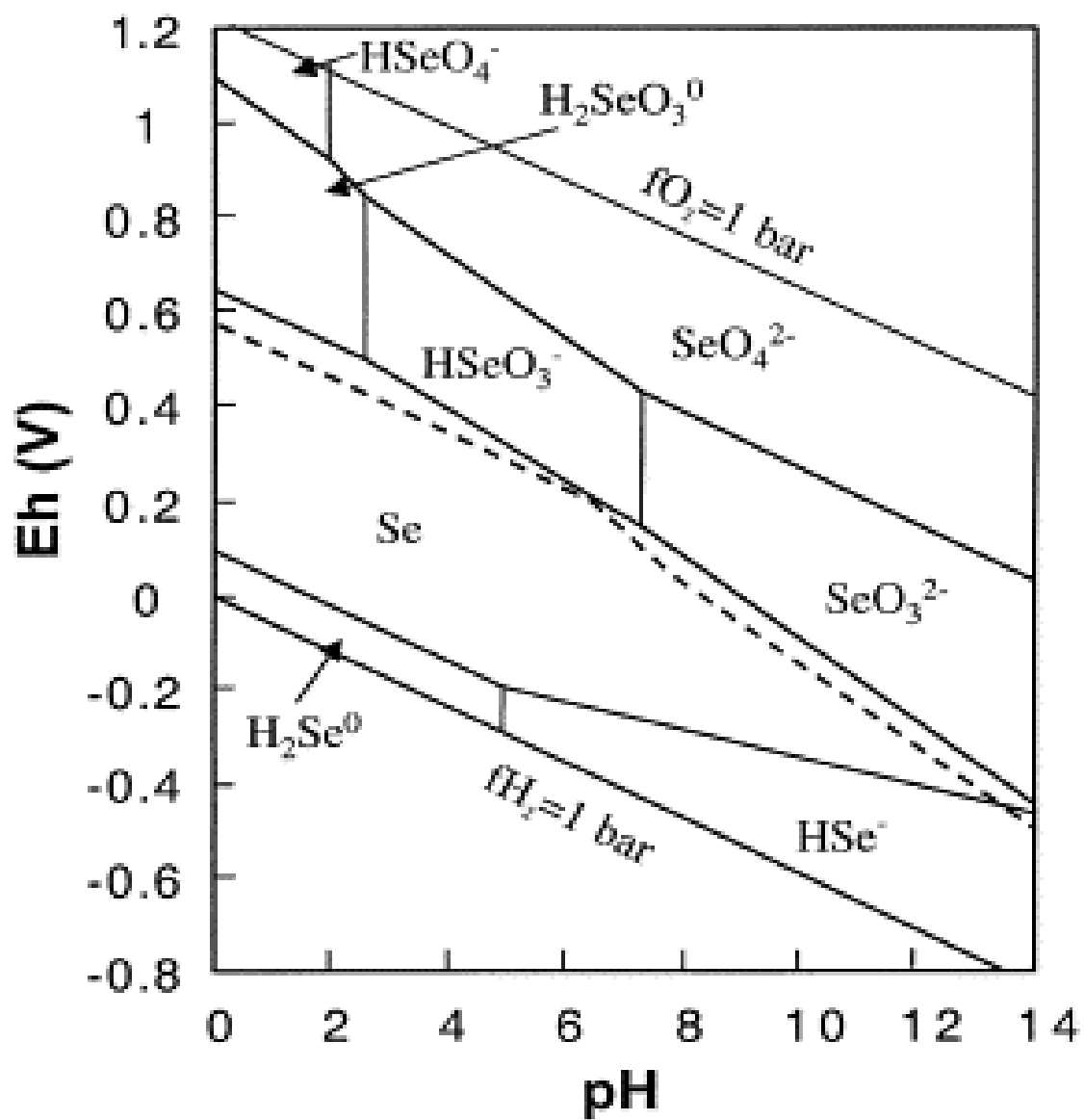


Figure C16. The pE–pH diagram for Se at 298 K, in an open system with total Se 1.0×10^{-6} M from Wagman et al. (1982).

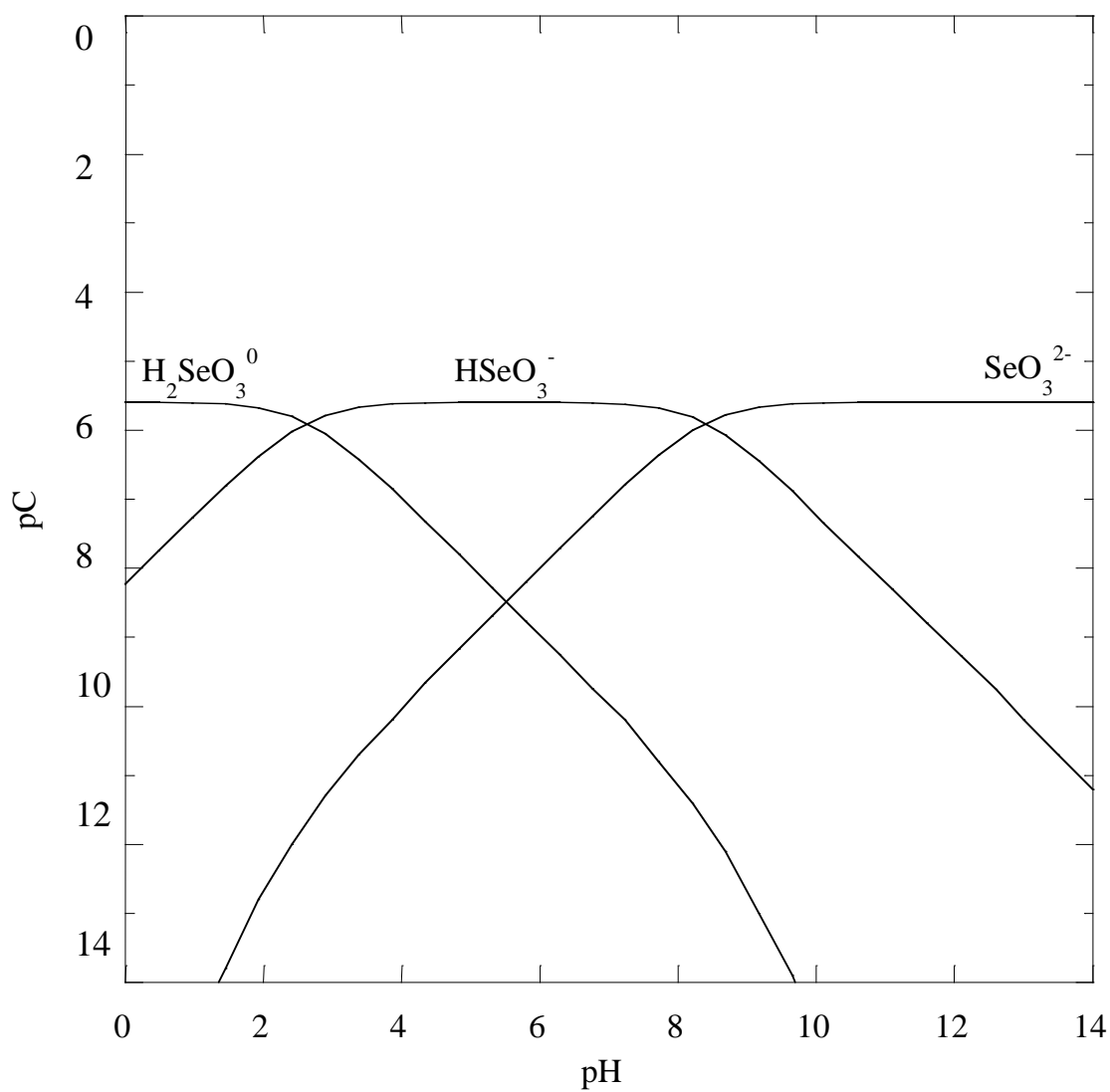


Figure C17. Se(IV) speciation in the leaching studies of paint waste, CH_3COOH at 0.1 M, 298 K and open to atmosphere. All the speciation was computed using MINEQL⁺. The total concentration of Se leached was 2.5×10^{-6} M.

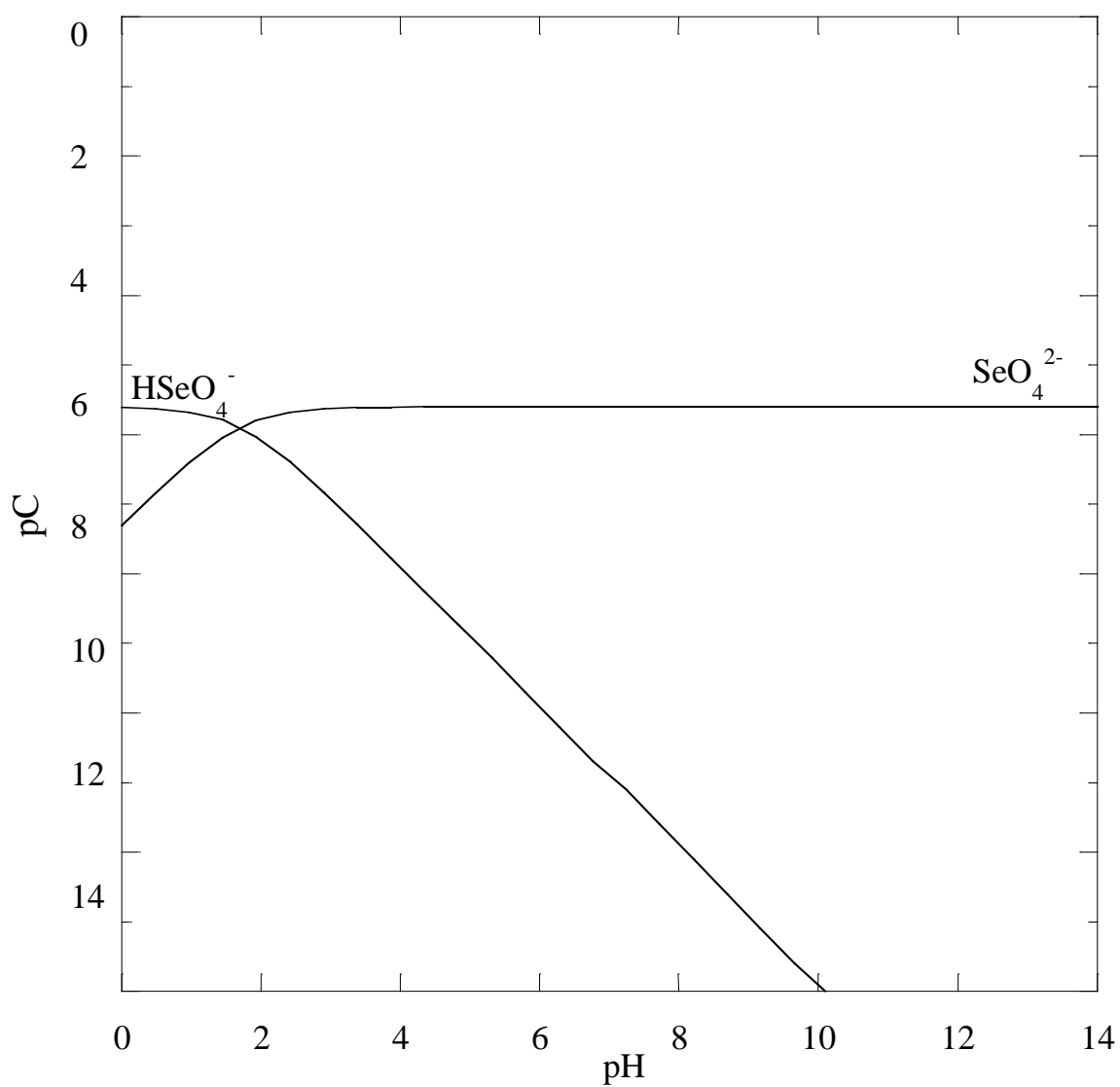


Figure C18. Se(VI) speciation in the leaching studies of paint waste, CH_3COOH at 0.1 M, 298 K and open to atmosphere. All the speciation was computed using MINEQL⁺. The total concentration of Se leached was 2.5×10^{-6} M.

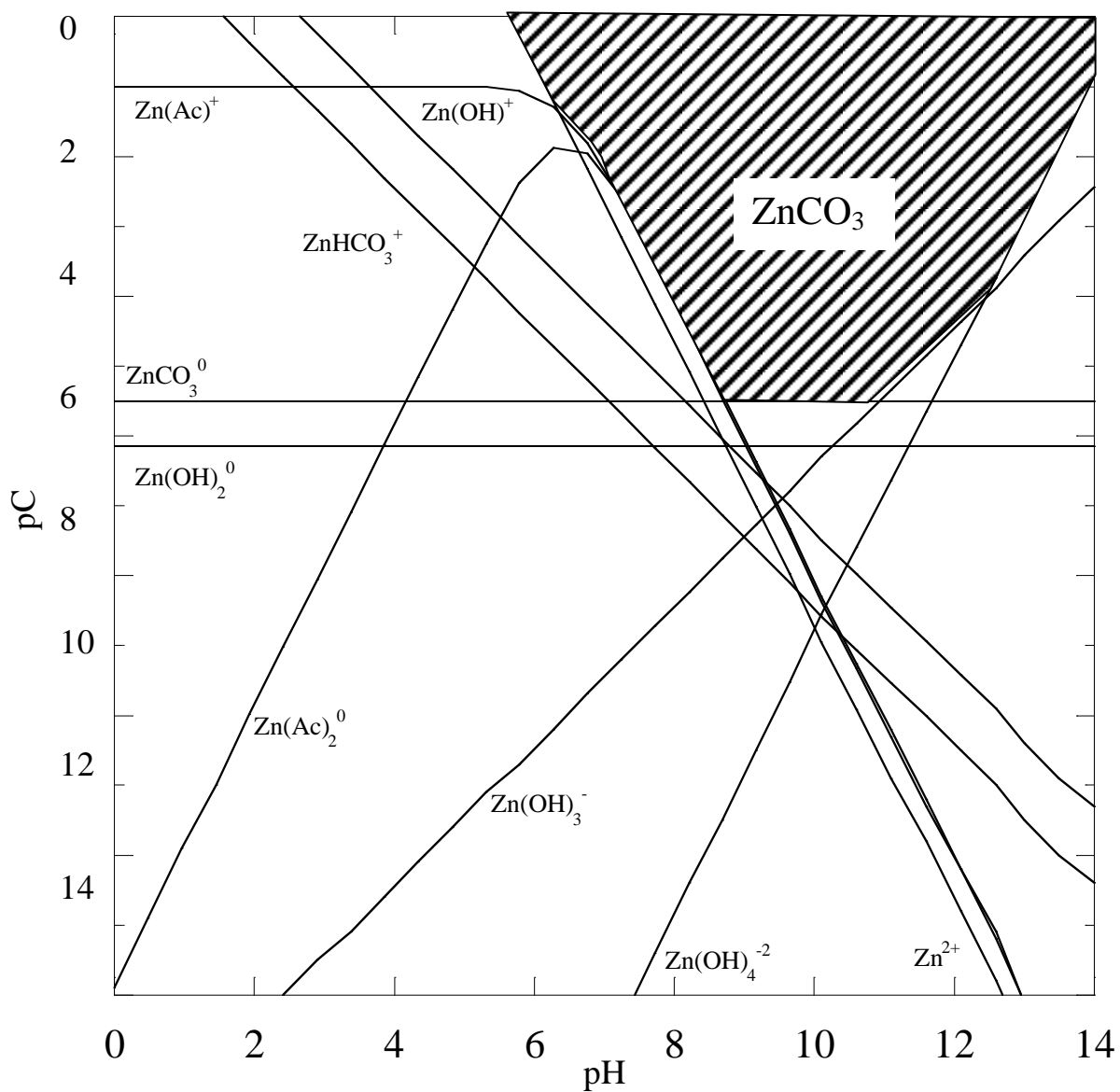


Figure C19. Zn solubility in equilibrium with ZnCO_3 , CH_3COOH at 0.1 M, 298 K and open to atmosphere. All the speciation was computed using MINEQL⁺.

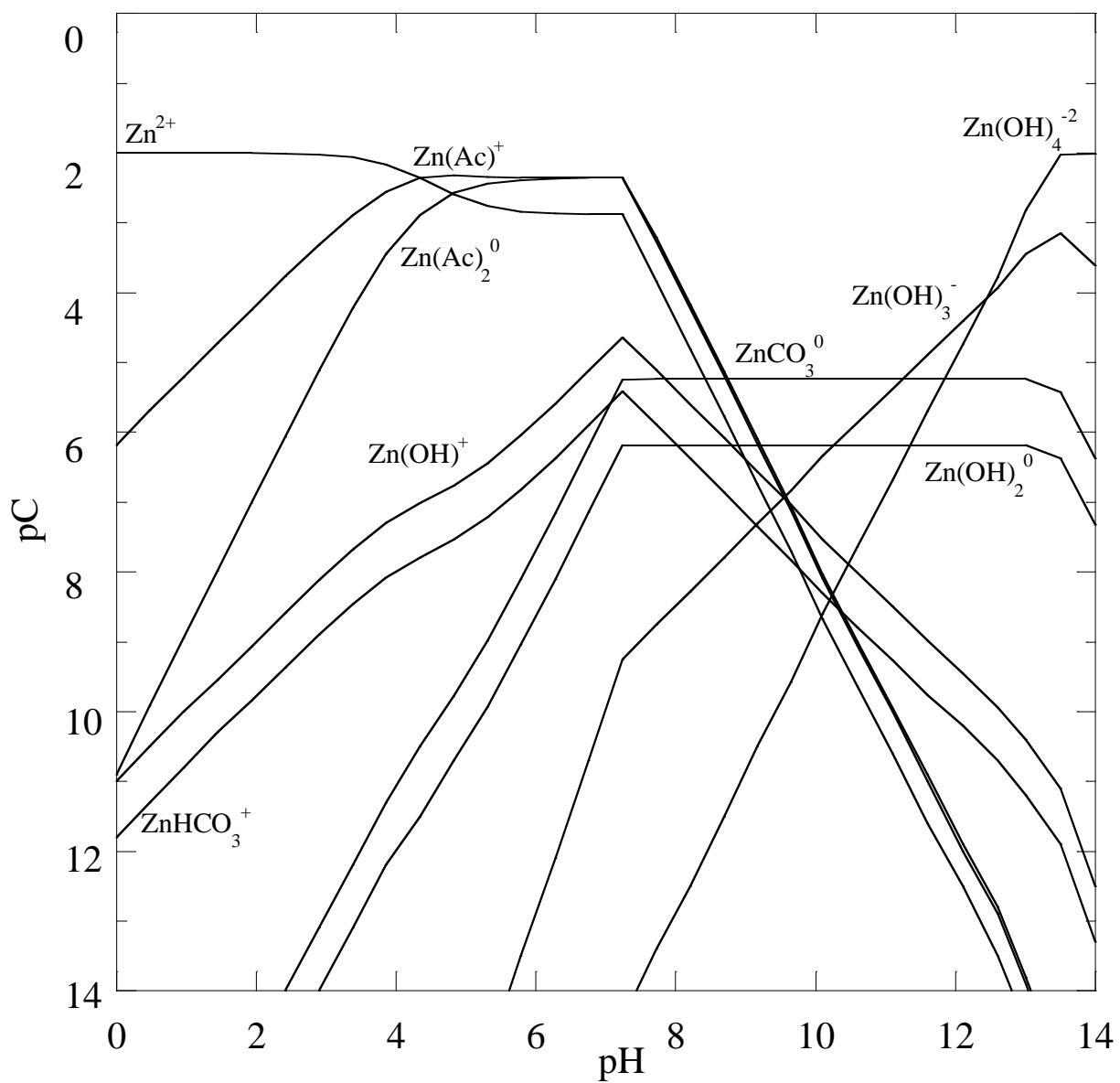


Figure C20. Zn speciation in the leaching studies of paint waste, CH_3COOH at 0.1 M, 298 K and open to atmosphere. All the speciation was computed using MINEQL⁺. The total concentration of Zn leached was 0.02 M.

Appendix D

XRD analysis data

Table D1. Standard XRD patterns for minerals in the paint samples.

| XRF detected elements | Results measured in XRD | Relative Intensity 2θ (°) | | | | | |
|-----------------------|--|------------------------------|--------------|--|--|--|--|
| | | 100% ~ 91% | 90% ~ 81% | 80% ~ 61% | 60% ~ 41% | 40% ~ 21% | 20% ~ 10% |
| Pb | lead tetroxide [Pb ₃ O ₄] | 26.4 (100%) | | | 32.1 (45%) | 52.0(26%) 34.0 (27%) | |
| | Pb ₂ (CrO ₄)O | 26.3 (99.9%) | 29.9 (87.3%) | | | 31.5 (34.5%) 31.0 (22.2%) | 48.7 (19.7%) 44.0 (20.0%) |
| Cr | Cr ₂ O ₃ | 33.6 (99.9%) | 36.2 (82.3%) | 54.9 (63.1%) | 24.5 (56.2%) | 65.2 (28.0%) 50.3 (33.7%) | |
| Zn | Zinc [Zn] | 43.2 (99.9%) | | | | 39.0 (23.4%) 36.3 (38.9%) | 70.1 (15.6%) |
| | Zinc oxide [ZnO] | 36.6 (99.9%) | | | 31.8 (57.7%) 34.4 (44.6%) | 56.6 (30.9%) 62.9 (25.6%) 47.6 (22.6%) 68.0 (22.2%) | |
| Fe | Fe | 44.7 (99.9%) | | | | | 82.3 (17.9%) 65.0 (11.7%) |
| | Ferrihydrite | 36.2 (99.9%) | | 34.3 (79%) 26.1 (77%) 36.0 (76%) | 62.4 (57%) 62.3 (55%) 56.1 (42%) | 19.5 (36%) 40.2 (36%) | |
| | Magnetite [Fe ₃ O ₄] | 35.4 (99.9%) | 35.5 (81.8%) | | 62.6 (41.6%) | 57.0 (21.7%) 43.1 (34.1%) 30.1 (35.7%) | |
| | goethite [FeO(OH)] | 21.3 (99.9%) | | | | 36.6 (36.8%) 33.3 (26.7%) | 53.3 (18.0%) 34.6 (14.5%) |
| | hematite [Fe ₂ O ₃] | 33.1 (100%) | | 35.6 (70%) | | 54.0 (36%) 49.4 (31%) 24.1 (33%) | |
| NA | Al | 38.4 (99.9%) | | | 44.6 (45.6%) | 65.0 (23.8%) 78.1 (23.5%) | |
| NA | Silica [SiO ₂] | 26.6 (99.9%) | | | | 20.8 (21%) | 50.1 (10.7%) |
| Ti | Rutile [TiO ₂] | 27.4 (99.9%) | | | 36.0 (44.3%) 54.2 (47.2%) | 41.2 (17.1%) 56.5 (13.9%) 68.8 (14.7%) | |
| Ca | CaCO ₃ | 29.3 (99.9%) | | | | 48.4 (20.5%) | 35.9 (13.9%) 39.3 (19.5%) 43.1 (14.5%) 47.4 (18.8%) |

NA: not applicable

Table D2. Possible minerals in paint samples measured by XRD

| XRF elements | Results measured in XRD | 2-1b | 2-2 e | 3-2 e | 5-1 b | 5-1 c | 5-2 a | 5-2 d | 5-4 c | 5-5 c | 5-5 d | 10-7b | 10-9b | 11-2 a | 11-2 e |
|--------------|--|------|-------|-------|-------|-------|-------|-------|-------|-------|-------|-------|-------|--------|--------|
| Pb | lead tetroxide [Pb ₃ O ₄] | | | √ | | | | | | | | | | | |
| | Pb ₂ (CrO ₄)O | | | | | | | | | | | √ | √ | √ | √ |
| Cr | Cr ₂ O ₃ | | | | | | | | | | | | | √ | √ |
| Zn | Zinc [Zn] | √ | √ | | | | | √ | √ | √ | √ | √ | | | |
| | Zinc oxide [ZnO] | √ | | | | | | | | | | | | | |
| Fe | Fe | √ | √ | √ | √ | √ | √ | √ | √ | √ | √ | | | | √ |
| | Magnetite [Fe ₃ O ₄] | | | √ | | √ | √ | √ | √ | √ | √ | | | | |
| | goothite [FeO(OH)] | | | | | | | | | | √ | | | | |
| | hematite [Fe ₂ O ₃] | | | | √ | | | √ | | | | | | | |
| NA | Al | √ | √ | √ | √ | √ | √ | √ | √ | √ | √ | √ | √ | | √ |
| NA | Silica [SiO ₂] | √ | √ | √ | √ | √ | √ | √ | √ | √ | √ | √ | √ | √ | √ |
| Ti | Rutile [TiO ₂] | √ | √ | | | | | √ | | | √ | √ | √ | √ | |
| Ca | CaCO ₃ | √ | √ | √ | √ | √ | √ | | √ | √ | | | √ | | √ |

Table D3. XRD analysis of iron and iron oxide in paint waste samples.

| Paint sample ID | Results measured in XRD | | | | | | | | | | | | | | | |
|-----------------|------------------------------|---------------------------------|--------------------------|--------------------------------------|---|------------------------|-------------------|----------------------------|--------------------------------------|---|---------------------------------|--|--|-------------------------------|--------------------------|--------------------------------------|
| | Fe | | | | Magnetite [Fe ₃ O ₄] | | | | Goethite [FeO(OH)] | | | | Hematite [Fe ₂ O ₃] | | | |
| | 2θ (°) | Relative Intensity | hkl planes | FWHM °2θ | 2θ (°) | RI | hkl planes | FWHM °2θ | 2θ (°) | RI | hkl planes | FWHM °2θ | 2θ (°) | RI | hkl planes | FWHM °2θ |
| 5-1 b | 44.5 64.9 82.3 | 100.00 11.20 1.61 | 110 200 211 | 0.1535 0.1023 0.4093 | | | | | | | | | 24.1 33.1 35.6 54.0 | 4.39 13.88 8.50 5.11 | 012 104 110 116 | 0.1535 0.1535 0.2047 0.0936 |
| 5-2 d | 44.6 65.0 82.2 99.1 | 100.00 23.67 4.29 4.60 | 110 200 211 220 | 0.1535 0.1023 0.6140 0.5117 | 35.6 43.2 | 11.90 55.26 | 103 004 | 0.1535 0.0624 | | | | | 33.1 41.0 54.3 | 18.69 3.63 16.16 | 104 113 116 | 0.1023 0.6140 0.0768 |
| 5-4 c | 44.5 64.9 82.2 99.1 | 82.14 26.10 5.36 3.09 | 110 200 211 220 | 0.2047 0.1279 0.4093 0.6140 | 30.1 35.5 43.2 | 6.55 19.95 81.71 | 220 311 400 | 0.2558 0.2558 0.0512 | | | | | | | | |
| 5-5 d | 44.6 64.9 82.2 98.9 | 100.00 31.47 7.73 4.54 | 110 200 211 220 | 0.2047 0.1023 0.5117 0.8187 | 35.3 43.2 | 12.11 77.22 | 103 004 | 0.4093 0.0768 | 21.2 26.6 36.3 39.0 54.3 | 10.06 46.07 35.39 18.22 14.69 | 101 201 111 002 402 | 0.6140 0.1023 0.1023 0.1279 0.0768 | | | | |

RI: Relative Intensity

Table D4. XRD analysis of Pb and Cr in paint waste samples.

| Paint sample ID | Results measured in XRD | | | | | | | | | | | |
|-----------------|--|--------------------|------------|----------|--------------------------------------|--------------------|------------|----------|--------------------------------|--------------------|------------|----------|
| | lead tetroxide [Pb ₃ O ₄] | | | | Pb ₂ (CrO ₄)O | | | | Cr ₂ O ₃ | | | |
| | 2θ (°) | Relative Intensity | hkl planes | FWHM °2θ | 2θ (°) | Relative Intensity | hkl planes | FWHM °2θ | 2θ (°) | Relative Intensity | hkl planes | FWHM °2θ |
| 3-2 e | 26.3480 | 11.47 | 211 | 0.1279 | | | | | | | | |
| | 30.8516 | 2.67 | 112 | 0.3070 | | | | | | | | |
| | 33.1330 | 1.88 | 310 | 0.3070 | | | | | | | | |
| | 47.4525 | 2.53 | 213 | 0.4093 | | | | | | | | |
| 10-7b | | | | | 26.2 | 29.23 | 310 | 0.1279 | | | | |
| | | | | | 29.8 | 23.16 | -112 | 0.1535 | | | | |
| | | | | | 31.4 | 8.71 | 020 | 0.1791 | | | | |
| 10-9b | | | | | 26.2 | 11.41 | 310 | 0.1279 | | | | |
| | | | | | 29.9 | 7.59 | -112 | 0.1535 | | | | |
| | | | | | 31.4 | 3.50 | 020 | 0.1535 | | | | |
| 11-2 a | | | | | 26.3 | 36.01 | 310 | 0.1279 | 33.7 | 4.42 | 104 | 0.1023 |
| | | | | | 29.9 | 23.21 | -112 | 0.1535 | 36.3 | 10.99 | 110 | 0.2047 |
| | | | | | 31.5 | 9.91 | 020 | 0.1791 | 50.2 | 11.18 | 024 | 0.0768 |
| | | | | | | | | | 54.9 | 7.50 | 116 | 0.1023 |
| 11-2 e | | | | | 26.2 | 26.67 | 310 | 0.1279 | 33.6 | 3.27 | 104 | 0.1535 |
| | | | | | 27.4 | 20.05 | 002 | 0.1279 | 36.3 | 10.69 | 110 | 0.1535 |
| | | | | | 29.9 | 18.18 | -112 | 0.1791 | 50.1 | 9.91 | 024 | 0.0768 |
| | | | | | 31.4 | 6.21 | 020 | 0.1535 | 54.8 | 4.79 | 116 | 0.1023 |
| | | | | | | | | | 64.9 | 17.61 | 300 | 0.1279 |

Deliverable for Task 7:
Correlation, Comparison, and Interpretation of
Field and Laboratory Data

Submitted

to

Carl Kochersberger
Environmental Science Bureau
Hazardous Materials and Asbestos Unit
Pod 4-1
New York State Department of Transportation
50 Wolf Road
Albany, NY 12232

October 2013

ABSTRACT

The removal of paint from bridges and other structures is a significant issue facing transportation agencies because of the presence and potential for release of lead and other contaminants upon disposal. A large percentage of the bridges are reaching a critical level of deterioration, resulting in management issues for paint waste. The New York State Department of Transportation (NYSDOT) applies a conservative approach by assuming all paint waste generated from painted steel bridges built before 1989 is hazardous. Therefore, an approach that provides accurate in-situ characterization of the waste classification would be beneficial. The goal of this project was to apply data from the field-portable X-ray fluorescence (FP-XRF) analysis and relate it to leaching for classifying waste as hazardous or not. Initially, mechanistic models were invoked for leaching and desorption in an effort to understand key variables needed for a statistical model. Surface complexation along with precipitation/dissolution modeling were applied given the elevated iron concentration and the paint composition. Results indicated that both adsorption and precipitation are important processes that support predictive mechanistic leaching from the waste. Subsequently, principle component analysis (PCA) was invoked to address and support the analysis of significant variables. The statistical models developed for metal leaching demonstrated 96 percent of the data fall within the 95% confidence level for Pb (R^2 0.6 – 0.9, $p \leq 0.01$), Ba (R^2 0.6 – 0.7, $p \leq 0.1$), and Zn (R^2 0.6 – 0.7, $p \leq 0.01$). However, the regression model obtained for Cr leaching was not significant (R^2 0.5 – 0.7, $p \leq 0.75$). Given an understanding of mechanistic processes along with a demonstrated analysis of variables through PCA, statistically-based models for leaching from paint waste were developed. A practical advantage in applying models developed is the ability to estimate contaminant leaching from paint waste without additional laboratory studies including the U.S. EPA toxicity characteristic leaching procedure (TCLP).

TABLE OF CONTENTS

| | |
|--|----|
| ABSTRACT | II |
| 1. Introduction | 1 |
| 2. Theory and Rationale | 2 |
| 3. Methodology | 8 |
| 3.1 Data collected | 8 |
| 3.2 Surface complexation model | 8 |
| 3.3 Principle component analysis (PCA) | 11 |
| 3.4 Modeling of metal leaching | 11 |
| 4. Results | 12 |
| 4.1 Metal adsorption to the iron oxide | 12 |
| 4.2 Principle component analysis | 19 |
| 4.3 Leaching model | 23 |
| 5. Conclusion | 34 |
| 6. References | 36 |
| Appendix A Leached metal as a function of total metal concentrations | 40 |
| Appendix B Modeling results for metal leaching | 45 |

TABLE OF FIGURES

| | |
|---|----|
| Figure 1. Classification of adsorption isotherms (Bradl and Hubbard, 2002; Bradl, 2004) | 4 |
| Figure 2. Desorbed Pb (A) and Cr (B) in the presence of steel grit associated with paint waste as a function of pH 0 to 14 after 18 hours using the TCLP. $Pb_T = 1.1 \times 10^{-3}$ M, $Cr_T = 1.2 \times 10^{-4}$ M, $Fe_T = 0.07$ M, ionic strength = 0.5 M, surface area = 600 m ² /g, $K_{MePb} = 10^{4.65}$, $K_{soPb} = 10^{-18.77}$. $K_{MeCr} = 10^{2.11}$, $K_{soCr} = 10^{-1.335}$ | 13 |
| Figure 3. Desorbed Pb (A) and Cr (B), and Ba in the presence of steel grit associated with paint waste as a function of pH 4.5 to 7 after 18 hours using the TCLP. $Pb_T = 1.1 \times 10^{-3}$ M, $Cr_T = 1.2 \times 10^{-4}$ M, $Ba_T = 3.2 \times 10^{-5}$, $Fe_T = 0.07$ M, ionic strength = 0.5 M, surface area = 600 m ² /g, $K_{MePb} = 10^{4.65}$, $K_{soPb} = 10^{-18.77}$. $K_{MeCr} = 10^{2.11}$, $K_{soCr} = 10^{-1.335}$, $K_{MeBa} = 10^{5.46}$, $K_{soBa} = 10^{-8.57}$. The dash line represents the 95% prediction interval. | 14 |
| Figure 4. Desorbed Ba (A) and Zn (B) in the presence of steel grit associated with paint waste as a function of pH 0 to 14 after 18 hours using the TCLP. $Ba_T = 3.2 \times 10^{-5}$, $Zn_T = 0.02$, $Fe_T = 0.07$ M, ionic strength = 0.5 M, surface area = 600 m ² /g, $K_{MePb} = 10^{4.65}$, $K_{MeZn} = 10^{3.49}$, $K_{soBa} = 10^{-8.57}$. $K_{soZn} = 10^{-11.33}$ | 17 |
| Figure 5. Desorbed Ba (A, B) and Zn (C) in the presence of steel grit associated with paint waste as a function of pH 4.5 to 7 after 18 hours using the TCLP. $Ba_T = 3.2 \times 10^{-5}$, $Zn_T = 0.02$, $Fe_T = 0.07$ M, ionic strength = 0.5 M, surface area = 600 m ² /g, $K_{MePb} = 10^{4.65}$, $K_{MeZn} = 10^{3.49}$, $K_{soBa} = 10^{-8.57}$. $K_{soZn} = 10^{-11.33}$. The dash line represents the 95% prediction interval. | 18 |
| Figure 6. Leached Pb concentrations are shown as a function of total Fe (% wt) concentrations in paint waste. The dash line represents the cut off used in this study. | 25 |
| Figure 7. Comparison of the results from predicted and observed leached Pb concentrations. The samples represent the TCLP and first day of the MEP extraction conducted on the paint waste | |

samples. Bridges were blasted to (A) surface preparation SSPC 6 with total Fe concentration greater than 24% (%wt), sample number N = 19 for TCLP and N = 8 for MEP studies; (B) SSPC 6 with total Fe concentration less than 24% (%wt). N = 19 for TCLP and N = 9 for MEP; (C) SSPC 10. N = 13 for TCLP and N = 7 for MEP. Toxicity characteristic (TC) level for Pb is 5 mg L⁻¹. The dash line represents the 95% prediction interval. 30

Figure 8. Comparison of the results from predicted and observed leached Ba concentrations. The samples represent the TCLP and first day of the MEP extraction conducted on the paint waste samples. Bridges were blasted to (A) surface preparation SSPC 6 with total Fe greater than 24% (%wt), sample number N = 19 for TCLP and N = 8 for MEP studies; (B) SSPC 6 with total Fe less than 24% (%wt). N = 19 for TCLP and N = 9 for MEP; (C) SSPC 10. N = 13 for TCLP and N = 7 for MEP. Toxicity characteristic (TC) level for Ba is 100 mg L⁻¹. The dash line represents the 95% prediction interval. 31

Figure 9. Comparison of the results from predicted and observed leached Cr concentrations. The samples represent the TCLP and first day of the MEP extraction conducted on the paint waste samples. Bridges were blasted to (A) surface preparation SSPC 6 with total Fe greater than 24% (%wt), sample number N = 19 for TCLP and N = 8 for MEP studies; (B) SSPC 6 with total Fe less than 24% (%wt). N = 19 for TCLP and N = 9 for MEP; (C) SSPC 10. N = 13 for TCLP and N = 7 for MEP. Toxicity characteristic (TC) level for Cr is 5 mg L⁻¹. The dash line represents the 95% prediction interval. 32

Figure 10. Comparison of the results from predicted and observed leached Zn concentrations. The samples represent the TCLP and first day of the MEP extraction conducted on the paint waste samples. Bridges were blasted to (A) surface preparation SSPC 6 with total Fe greater than 24% (%wt), sample number N = 19 for TCLP and N = 8 for MEP studies; (B) SSPC 6 with total Fe less than 24% (%wt). N = 19 for TCLP and N = 9 for MEP; (C) SSPC 10. N = 13 for TCLP and N = 7 for MEP. The dash line represents the 95% prediction interval. 33

LIST OF TABLES

| | |
|--|----|
| Table 1. Samples collected and studied with TCLP and MEP | 9 |
| Table 2. Total concentration, boundary conditions, and leached concentrations used in surface complexation modeling..... | 10 |
| Table 3. Principal component loadings of total metals and pH in the paint waste samples. | 21 |
| Table 4. Sample sorted with respected to surface preparation standard and Fe concentrations. .. | 24 |
| Table 5. Statistical analysis results from multivariate regression of the leached metal concentrations for Pb and Cr (mg L ⁻¹) | 27 |
| Table 6. Statistical analysis results from multivariate regression of the leached metal concentrations for Pb and Cr (mg L ⁻¹) | 28 |

1. Introduction

The removal of paint from bridges and other structures is a significant issue facing transportation agencies because of the presence and potential for release of lead and other contaminants, and the consequent impacts to human health and the environment. Although the hazards of lead paint removal from bridges have been largely identified and advances have been made in worker protection, there is still a need to identify rapid and cost-effective methods for field detection that can provide an accurate characterization of waste classification. Currently, the New York State Department of Transportation (NYSDOT) uses a conservative approach of classifying all paint waste as hazardous from bridges undergoing rehabilitation and that were constructed before 1989 (NYSDOT, 1988). This practice stems from the fact that there is no approved reliable, fast, and efficient method for classifying paint waste in situ as non hazardous.

Paint waste removed from the bridges is generally stored in 55 gallon drums or roll-off containers in the field. Because the waste will not be pretreated before shipping for disposal, the field portable X-ray fluorescence (FP-XRF) analysis was conducted on the collected paint waste samples as well as through direct analysis of paint on the bridge. The main objective of this study is to develop a model that can predict the leachability of metals in paint waste generated during bridge rehabilitation. Data from FP-XRF analysis of metals were compiled and related to the associated leaching results to better understand key variables required in developing statistical models. Mechanistic modeling further supported variables required to predict metal leaching processes. The statistical models formulated in this work are based exclusively on data collected from bridges undergoing rehabilitation where steel grit was used as the blasting material. Therefore, for other state DOTs working with similar structures and rehabilitation procedures, this research may be beneficial in supporting a field analysis for waste classification.

This report includes background on the approach and rationale for the methodology developed. Initially, mechanistic models involving adsorption and precipitation were invoked as trace metals have a high affinity for iron oxides, which form on the steel grit used as blasting material. Furthermore, based on the paint composition and metal concentrations, groups of metals were identified as playing important roles in metal mobility and leaching from the paint waste. However, the model required needs to be based exclusively on variables that can be measured in the field. Therefore, mechanistic modeling is used to support principle component analysis (PCA) of data obtained with FP-XRF. The methodology is reviewed and followed by results. The report concludes with a summary of the results and recommendations for NYSDOT.

2. Modeling Rationale

Because steel grit is applied as a blasting agent during the paint removal procedure, elevated iron concentrations were observed in the paint waste (49,367 to 799,210 mg kg⁻¹) (Shu and Axe, 2013). Using sequential extraction, X-ray diffraction (XRD), and field emission scanning electron microscopy (FESEM), iron oxides were observed to be important surfaces for controlling the degree of metal leaching from the paint waste (Shu and Axe, 2013). In fact, metal leaching from waste occurs primarily by two mechanisms (a) surface reactions (adsorption/desorption and/or surface precipitation) from the associated matrix, and (b) precipitation/dissolution. A number of researchers have demonstrated that the metal sorption to the Fe and Mn oxides is the rate limiting step for metal leaching from soil and cement-based solidified wastes (e.g., Tiruta-barna et al., 2001; Karanalids and Coudrias, 2008; Dijkstra et al., 2009). To consider whether surface complexation or precipitation contributes significantly to metal leaching, the diffuse layer model (DLM) (Dzombak and Morel, 1990) is applied to describe the surface interactions of metals with iron-based materials (Jing et al., 2006;

Karamalidis and Coudrias, 2008). Bidentate surface complexes are assumed in this study, where FeOH^0 represents a surface hydroxyl group and the surface reaction for Pb^{2+} , $\text{Cr}(\text{OH})^{2+}$, or Ba^{2+} (Me) on HFO is the following:



Mechanistic models provide a mathematical form of the equilibrium reaction based on mass balances of the species present and surface charge effects (Bradl, 2004). However, because this approach requires water chemistry conditions and species present, mechanistic models in general are more complex. Therefore, given that field data will be used to classify waste, empirical modeling is introduced into this study, and is useful for describing experimental data (e.g., Sauvé et al., 2000; Lofts et al., 2004). The empirical model is a posteriori form observed from adsorption data. For determining a good fit of experimental data a mathematical form is chosen that is as simple as possible and the number of adjustable parameters is kept at a minimum. Simple empirical models may be extended by considering additional mechanisms such as competition for sorption sites or heterogeneity of solid phase (Bradl, 2004). A number of researchers have used the theoretically-based Langmuir (e.g., Pierce and Moore, 1980; Padmanabham, 1983; Jackson and Inch, 1989; Kooner, 1993; Kanungo, 1994; Lee et al., 1996; 1998; Sauvé et al., 2000) and empirical Freundlich models (e.g., Dzombak and Morel, 1986; Mishra and Tiwary, 1995; 1998; Mishra et al., 1997; Christophi and Axe, 2000; Vaishya and Gupta, 2004) to describe equilibrium adsorption (Figure 1).

Because of the heterogeneity of the paint waste, one approach considered is based on the Freundlich isotherm (Eq. (1)):

$$(\text{adsorbed metal}) = K (\text{dissolved metal})^n \quad (1)$$

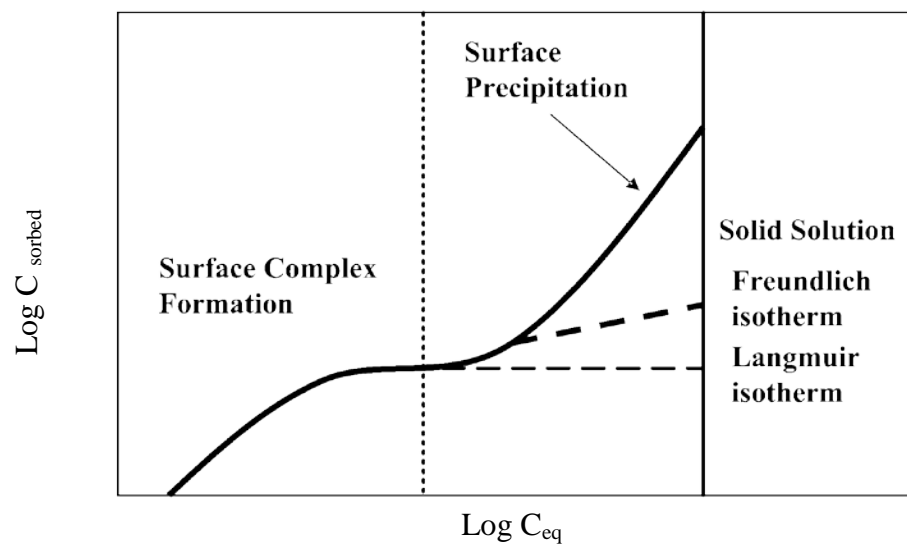


Figure 1. Classification of adsorption isotherms (Bradl and Hubbard, 2002; Bradl, 2004)

Where K is a function of adsorption energy and temperature and is a measure of adsorptive capacity; n determines intensity of adsorption. Several studies (Mcbride et al, 1997; Sauve et al., 2000; Lofts et al., 2004) have introduced multivariate regression equations to predict Freundlich parameters K and dissolved concentrations from bulk soil properties. Buchter et al. (1989) measured Freundlich parameters (K and n) for 11 different soils and 15 trace elements. They also explored the correlation of Freundlich parameters with select soil properties and found that pH, cation-exchange capacity (CEC), and iron/aluminum oxide concentrations were the most important factors correlated to K. Sauve et al. (2000) modeled the dissolved concentration of Cd, Cu, Ni, Pb, and Zn in soil solutions from a variety of contaminated soils. They found that K was dependent on pH, total metal concentrations (for Zn and Pb) (Eq. (2)), and soil organic material (for Cd, Cu, and Ni) (Eq. (3)). They further developed the model (Eq. (4)) for system studied. However, in these models, Sauve et al. (2000) did not include the specific oxides or clays in the soil.

$$\text{Log } K = a + b \cdot \text{pH} + c \cdot \log(\text{total metal}) \quad (2)$$

$$\text{or Log } K = a + b \cdot \text{pH} + c \cdot \log(\text{soil organic material}) \quad (3)$$

$$\text{Log (dissolved metal)} = a + b \cdot \text{pH} + c \cdot \log(\text{total metal}) + d \cdot \log(\text{soil organic material}) \quad (4)$$

Necessary variables in such regressions are the soil pH and the geochemically active species, which involves exchange with the soil solution and hence controls the dissolved concentration. The following general expression highlights important conditions:

$$\text{Log (dissolved metal)} = a + b \cdot \text{pH} + c \cdot \log(\text{total metal}) + d \cdot \log(\text{binding sites}) \quad (4)$$

The objective of this study is to use metal concentrations obtained with the FP-XRF to predict metal leaching and namely waste classification for the paint waste. From the earlier studies (Shu and Axe, 2013), iron oxides in the paint waste were observed to be important

surfaces for controlling the degree of metal leaching from the paint waste. Therefore, total Fe is applied and reflects the presence of iron oxide in the model. A fraction of metal was also observed to be associated with carbonates in the paint waste, which may be due to the application of calcite (CaCO_3) (12 wt% in the paint waste; Shu and Axe, 2013) as an extender (supplementary pigments) in the paint. In fact, the dissolution of calcite (CaCO_3) will also affect the pH of the system during the leaching procedure. Consequently, total Ca is expected to be an important variable in the model. Other groups of metals such as Zn and Ti present at elevated concentrations in the paint waste may be important variables in the model accounting for their potential influence on metal leaching in competitive adsorption and their function as binding site.

Based on the above discussion, metal leaching (the release of trace metal cations or anions into the aqueous phase) is expected to depend on a number of variables including (a) total metal concentration; (b) CaCO_3 ; (c) Fe concentration; and, (d) other groups of metals such as Zn and Ti present at elevated concentrations. The modeling approach to predict trace metal leaching in paint waste will involve a statistical analysis as follows:

- (i) Multivariate regression is tested in the first step of modeling.

$$\text{Leached metal} = a + b \cdot (\text{total Ca}) + c \cdot (\text{total metal}) + d \cdot (\text{total Fe}) + e \cdot (\text{Me}_{1, \text{ total}}) + \dots + n \cdot (\text{Me}_{n, \text{ total}})$$

- (ii) Box-Cox transformation (Sakia, 1992) is applied according to the residual analysis if necessary, where leached metal y is transformed to y^λ :

$$(\text{Leached metal})^\lambda = a + b \cdot (\text{total Ca}) + c \cdot (\text{total metal}) + d \cdot (\text{total Fe}) + e \cdot (\text{Me}_{1, \text{ total}}) + \dots + n \cdot (\text{Me}_{n, \text{ total}})$$

- (iii) Transformed models:

$$\text{Log (leached metal)} = a + b \cdot \log(\text{total Ca}) + c \cdot \log(\text{total metal}) + d \cdot \log(\text{total Fe}) + e \cdot \log(\text{Me}_{1, \text{ total}}) + \dots + n \cdot \log(\text{Me}_{n, \text{ total}})$$

where leached metal is in mg L^{-1} , a-n are coefficients determined using regression with appropriate data sets, and total metal is in mg kg^{-1} based on FP-XRF. The adsorption capacity is a function of iron oxides in the paint waste, which is represented by total Fe in the equation. Total Ca represents the calcite (CaCO_3) applied in the paint, which may also affect the pH (and alkalinity) during leaching, and $\text{Me}_{i, \text{ total}}$ represents the other groups of metals in the paint waste that may affect the metal leaching.

However, if all the potential variables are considered, there will be more than ten variables in the model. Therefore, it is necessary to sort the samples based on the factors that affect the metal leaching significantly. In this study, PCA was applied to identify the important factors and the potential variables in the model. PCA is a classical technique based on linear algebra. The analysis involves a mathematical procedure that transforms a number of possible correlated variables into a smaller number of uncorrelated variables called principal components (PCs) (Torrecilla et al., 2009), which are linear combinations of the original variables. The principal components account for as much of the variability in the data as possible, and each succeeding component accounts for as much of the remaining variability as possible. PCA is mainly used for key factors that explain the majority of variation within the data.

In summary, modeling metal leaching and mobility have traditionally involved mechanistic models, such as the equilibrium model DLM applied when iron oxides are significant. Other theoretical and empirical models have also been invoked in a number of studies. Because of the need to use field-based data in addressing waste classification, a statistical model using data from the FP-XRF is applied with PCA. In the next section, the methodology is presented and followed

by the associated results and discussion.

3. Methodology

3.1 Data collected

A total of 117 paint waste samples from 24 bridges in NYS were analyzed with FP-XRF for RCRA metals (i.e., As, Ba, Cr, Cd, Pb, Hg, Ag, Se) as well as Zn and Fe. Other elements such as Ca and Ti were also obtained from XRF results. The samples analyzed for toxicity characteristic leaching procedure (TCLP) (U.S. EPA, 1992) were based on the product of the select sample number from each bridge and the number of bridges, with each being conducted in triplicate (Table 1). The sample with the greatest lead concentration was further studied in duplicate with the multiple extraction procedure (MEP) analysis for each of the 24 bridges. Leaching results from the first day of the extraction were used in this study as leaching was most significant in the first 24 hours (Shu and Axe, 2013).

3.2 Surface complexation model

The DLM (Dzombak and Morel, 1992) was applied to describe surface adsorption/desorption of metals Pb, Cr, and Ba to hydrous ferric oxide (HFO) formed on the steel grit surfaces present in the paint waste (49,367 to 799,210 mg kg⁻¹). From earlier studies (Shu and Axe, 2013), XRD analysis revealed the presence of ferrihydrite (also known as HFO), magnetite, hematite, and goethite in the paint waste samples. To simplify the modeling approach for a complex system, ferrihydrite was assumed to be the dominant surface oxide on the steel grit; this surface has been demonstrated to dominate given its large surface area and high affinity for trace metals (Shu and Axe, 2013). Because leaching from the samples may be attributed to exchangeable and adsorbed forms in the paint waste (Shu and Axe, 2013), these fractions of metals were calculated (Table 2) based on the XRF and sequential extraction results.

Table 1. Samples collected and studied with TCLP and MEP

| Region | Bridge number | TCLP Sample numbers | MEP Sample numbers |
|--------|---------------|---------------------|--------------------|
| 1 | 1 | 1 | 1 |
| 2 | 2 | 2 | 2 |
| 3 | 3 | 12 | 3 |
| 5 | 5 | 11 | 5 |
| 7 | 2 | 3 | 2 |
| 10 | 9 | 12 | 9 |
| 11 | 2 | 10 | 2 |
| Total | 24 | 51 in triplicate | 24 in duplicate |

Table 2. Total concentration, boundary conditions, and leached concentrations used in surface complexation modeling

| | Pb | | | Cr | | | Ba | | | Zn | | |
|--|----------------------|------------------|----------------------|----------------------|---------|----------------------|----------------------|---------|----------------------|---------------------|----------------------|---------------------|
| | mean | minimum | maximum | mean | minimum | maximum | mean | minimum | maximum | mean | minimum | maximum |
| Total Concentrations in the paint (mg/kg) ^a | 4.6×10 ⁴ | 5 | 1.7×10 ⁵ | 3,018 | 21 | 1×10 ⁴ | 6,600 | 228 | 1.6×10 ⁴ | 1.3×10 ⁵ | 1.3×10 ⁴ | 1.1×10 ⁶ |
| Leached concentrations over TCLP procedure (M or mol/L) | 1.4×10 ⁻⁶ | BDL ^b | 1.0×10 ⁻⁵ | 1.5×10 ⁻⁵ | BDL | 1.8×10 ⁻⁴ | 1.0×10 ⁻⁵ | BDL | 7.1×10 ⁻⁵ | 0.0066 | 3.1×10 ⁻⁴ | 0.02 |
| Desorbed metal concentrations over TCLP procedure (% of total metal) | 0.011 | BDL | 0.048 | 0.62 | BDL | 3.7 | 0.55 | BDL | 2.1 | 11.72 | 0.41 | 53.5 |

a: The values are based on results from XRF.

b: BDL refers to below detection limit.

The HFO surface has low-affinity and high-affinity adsorption sites (Dzombak and Morel, 1990), where the $\text{Fe}^{\text{W}}\text{OH}$ and $\text{Fe}^{\text{S}}\text{OH}$ represent the weak-affinity and high-affinity surface hydroxyl sites, respectively. The weak-affinity site density of 0.2 mol/mol Fe and the high-affinity site density of 0.005 mol/mol Fe were used in this study (Dzombak and Morel, 1990; Meima and Comans, 1997; Apul et al., 2005). Pb, Cr, and Ba adsorption to iron oxide results in surface complexes FeOPb^+ , FeOCrOH^+ , and FeOHBa^{2+} , respectively. Surface acid–base reactions and equilibrium constants used in the DLM are from a number of references (Dzombak and Morel, 1990; Kendall, 2003; Jing et al., 2006). All reactions in this study were modeled using MINEQL⁺. Inputs for the model such as background analytes, adsorbate, and sorbent concentrations were obtained from TCLP leaching experiments, XRF analyses, and sequential extraction results (Shu and Axe, 2012; 2013).

3.3 Principle component analysis (PCA)

In PCA, eigenvalues are used to determine the percentage as well as cumulative percentage of variances. The purpose of PCA in this study is to identify the important factors and the potential variables in the model. PCA was applied for statistically analyzing the effect of variables, namely total metal concentrations (i.e., As, Ba, Cr, Cd, Fe, Pb, Hg, Ag, Se, Zn, Ti, and Ca), in the paint waste samples.

3.4 Modeling of metal leaching

Based on the PCA analysis, leaching data were subjected to multivariate statistical analyses to evaluate the effect of statistically significant variables on metal leaching. Multivariate statistical approaches such as multiple linear regression analysis (MLRA) are used to determine the significance of specific parameters among the datasets. The total metal concentrations from

FP-XRF analysis are applied as inputs in the leaching models. The coefficients a-n in the model were determined by the significance of the p-value for each coefficient.

4. Results

4.1 Metal adsorption to the iron oxide

Mechanistic models were invoked for leaching and desorption in an effort to understand key variables needed for a statistical model. Iron oxide was observed to be an important surface for the cations and anions in the paint waste. The mechanistic equilibrium model, DLM, was applied in this study, and precipitation model was used as well. The surface charge of an iron oxide is a function of pH, with an increasingly net negative charge as the pH increases above the zero point of charge, and becomes more positively charged as pH decreases. Cations desorb as the pH decreases and anions are released as the pH increases.

In this study, metal leaching varied over two orders of magnitude for the pH range of 4.5 to 7 (Shu and Axe, 2013). Based on the precipitation model, $\text{Pb}_3(\text{OH})_2(\text{CO}_3)_2$ precipitation could decrease the dissolved Pb for pH greater than 6. However, adsorption modeling may reduce the dissolved Pb to a much lower level for pH 4.5 to 7 (e. g., Pb and Cr; Figures 2 and 3). These results suggested that the observed leaching behavior is a result of adsorption. In this study, adsorption model captured 90% of the leaching data within 95% prediction interval. The importance of the oxide surface in Pb leaching was expected because of the high affinity of Pb for iron oxides (Dzombak and Morel, 1990). Other forms of Pb (PbCrO_4 and Pb_3O_4) observed from XRD (Shu and Axe, 2013) are likely associated with residual and oxide phases.

Based on the XRD results from earlier studies (Shu and Axe, 2013), chromium hydroxide ($\text{Cr}(\text{OH})_3$ or Cr_2O_3) is considered as the dominant phase in paint waste. Given its solubility,

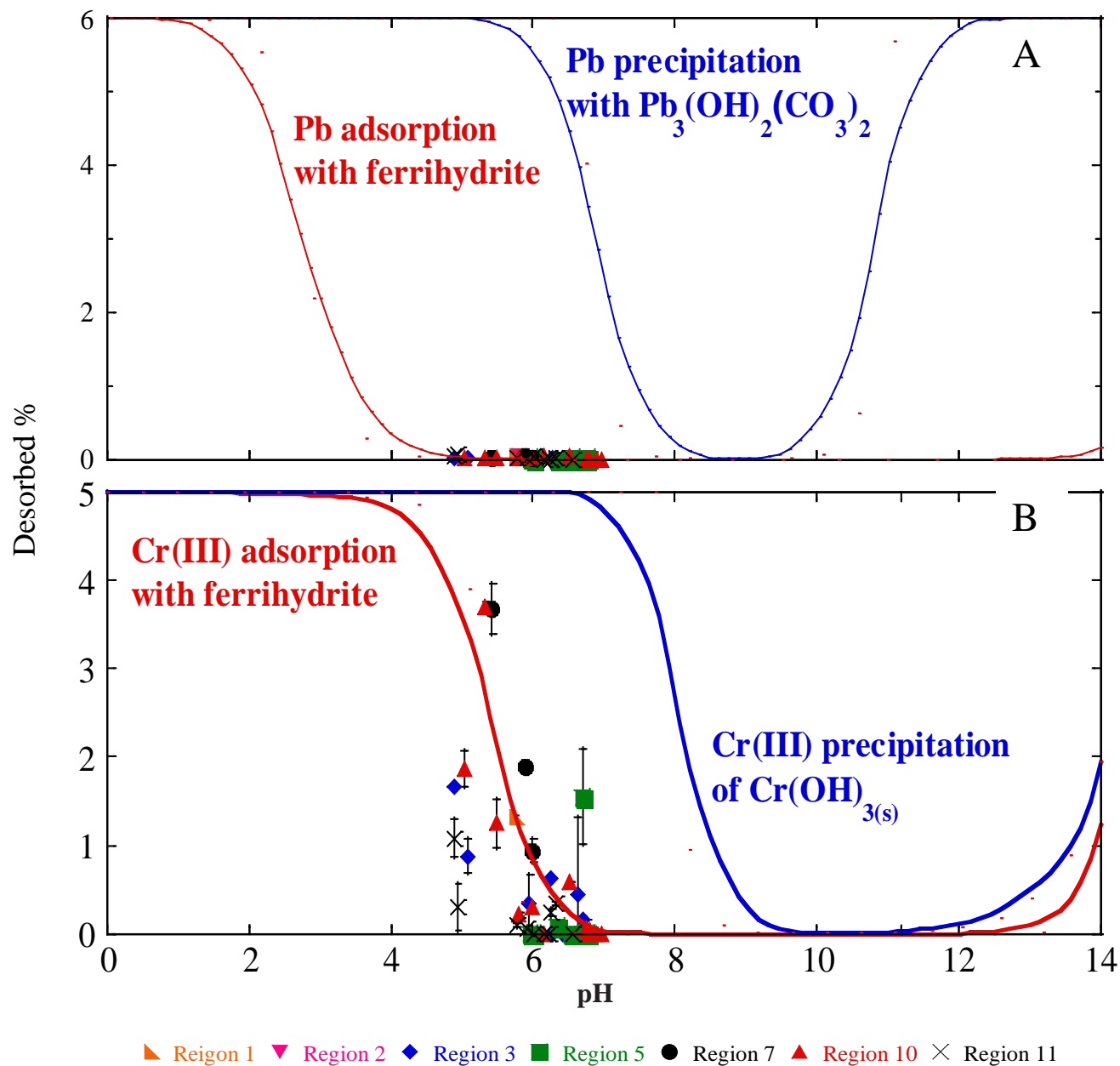


Figure 2. Desorbed Pb (A) and Cr (B) in the presence of steel grit associated with paint waste as a function of pH 0 to 14 after 18 hours using the TCLP. $Pb_T = 1.1 \times 10^{-3} M$, $Cr_T = 1.2 \times 10^{-4} M$, $Fe_T = 0.07 M$, ionic strength = 0.5 M, surface area = 600 m²/g, $K_{MePb} = 10^{4.65}$, $K_{soPb} = 10^{-18.77}$. $K_{MeCr} = 10^{2.11}$, $K_{soCr} = 10^{-1.335}$.

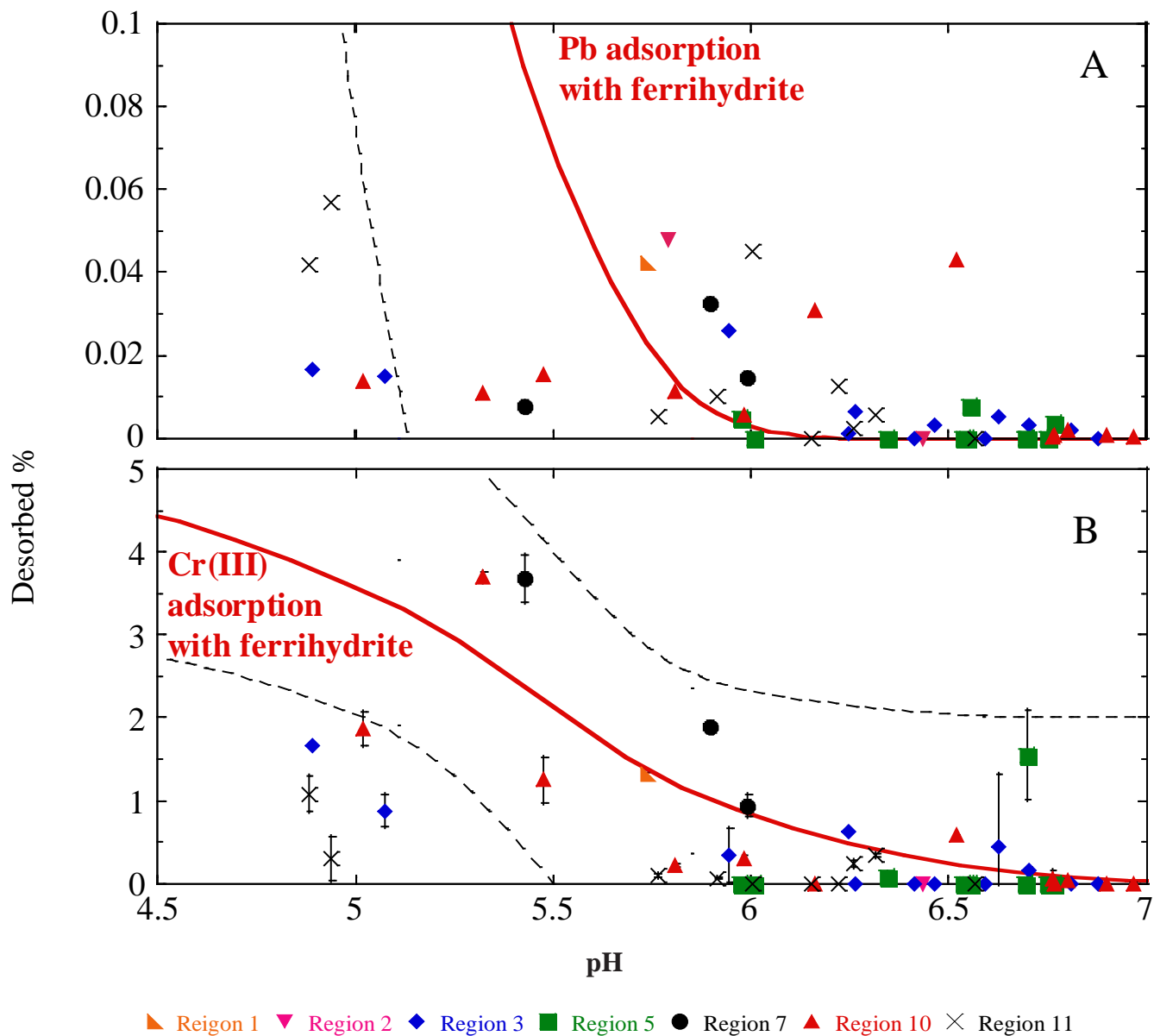


Figure 3. Desorbed Pb (A) and Cr (B), and Ba in the presence of steel grit associated with paint waste as a function of pH 4.5 to 7 after 18hours using the TCLP. $Pb_T = 1.1 \times 10^{-3}$ M, $Cr_T = 1.2 \times 10^{-4}$ M, $Ba_T = 3.2 \times 10^{-5}$, $Fe_T = 0.07$ M, ionic strength = 0.5 M, surface area = 600 m²/g, $K_{MePb} = 10^{4.65}$, $K_{soPb} = 10^{-18.77}$. $K_{MeCr} = 10^{2.11}$, $K_{soCr} = 10^{-1.335}$. The dash line represents the 95% prediction interval.

Cr(OH)₃ may influence metal leaching for pH greater than 6.8 (Figures 2 and 3). Similar with the Pb work, precipitation modeling of Cr leaching overestimated the dissolved concentration in the system. Other forms of Cr (such as PbCrO₄) observed are likely associated with the residual or oxides phases in the paint waste. The desorbed Cr decreased as pH increased from 4.5 to 7 and adsorption simulation captured 90% of the leaching data within 95% prediction interval. The DLM model adequately predicted the observed leaching (Figure 3) in the paint waste suggesting adsorption/desorption from the iron oxide surface as the dominant process. In this study, Cr(III) is expected to be the dominant species, although a small fraction of Cr(VI) maybe exist in the leachate. Cr is introduced in as both Cr₂O₃ and CrO₄²⁻ in paint (Lambourne and Strivens, 1999). A number of studies (e.g., Weng et al., 1996; Peterson et al., 1996; 1997; Bidoglio et al., 1993; Deng et al., 1996; Roskovic et al., 2011; Du et al., 2012) have been conducted to investigate Cr speciation in the presence of Fe(II) or zero valent iron in soil and solid waste. Reduction of Cr(VI) to Cr(III) was observed under acidic conditions (pH < 7) (Weng et al., 1996; 2001) as well as with reducing agents Fe(II) or zero valent iron (Peterson et al., 1996; 1997; Du et al., 2012). Weng et al. (1996; 2001) evaluated interactions between Cr(VI) and concrete particles in synthetic groundwater. The removal of Cr(VI) and Fe(II) along with the presence of Cr(III) and Fe(III) were observed under acidic conditions. Peterson et al. (1996) investigated the redox reaction between aqueous Cr and magnetite using X-ray absorption spectroscopy (XAS) using both the fine structure to provide molecular-level information on Cr adsorption and the near edge spectra for the redox reactions. Cr(VI) reacted with freshly-synthesized magnetite with a surface coverage of 4.5 mol/m² where it was observed to be reduced to Cr(III), as evidenced by the Cr absorption edge position and by the absence of a 1s → 3d pre-edge peak. Peterson et al. (1997) further used synchrotron-based XAS to investigate the reduction of aqueous Cr(VI) to Cr(III) in

magnetite-bearing soils from Cr-contaminated sites. Results indicated that mixed-valence Cr(III/VI) was reduced to Cr(III) in the presence of magnetite ($\text{Cr}^{6+} + 3\text{Fe}^{2+} \rightarrow \text{Cr}^{3+} + 3\text{Fe}^{3+}$). A recent study conducted by Du et al. (2012) reviewed reduction and immobilization of chromate in chromite ore processing residue (COPR). They found that COPR and nanoscale zero-valent iron (ZVI) with greater than 27% water (by mass) could result in nearly complete Cr(VI) reduction with less than 0.1 mg L^{-1} Cr(VI) in the (TCLP) leachate. Therefore, in this work Cr(III) is expected to be the dominant form in the leaching studies.

Generally, the leaching behavior of Pb and Cr is adequately predicted by the DLM model (Figures 2 and 3); adsorption to iron oxide formed on the steel grit surface appears to be the dominant mechanism responsible for the metal leaching over pH 4.5 to 7. These results are consistent with the other similar studies (e.g. Kendall, 2003), where metal adsorption (e.g. Pb and Cu) to iron oxides was observed to control metal leaching from the brass foundry waste over pH 5 to 7.

Ba has been used as an extender (Lambourne and Strivens, 1999), and BaSO_4 is the primary form applied in paint. XRD results demonstrated that barite (BaSO_4) is the dominant form in the system (Shu and Axe, 2013). Although the adsorption model captures more leaching data than the precipitation model, the system presented lower desorbed Ba than expected (Figures 4 and 5). This result is likely attributed to coprecipitation of the Ba mineral occurring on the steel grit surface, which is in agreement with previous studies of modeling the leaching behavior of Ba in soils (e.g., Dijkstra et al., 2009). Therefore, both sorption (including adsorption and coprecipitation) and precipitation are important processes that affect Ba leaching from the waste.

Although sorption of Zn also occurs on the steel grit iron oxide surface, because of the relatively greater concentrations of Zn in the paint waste (Shu and Axe, 2013; Figure 4),

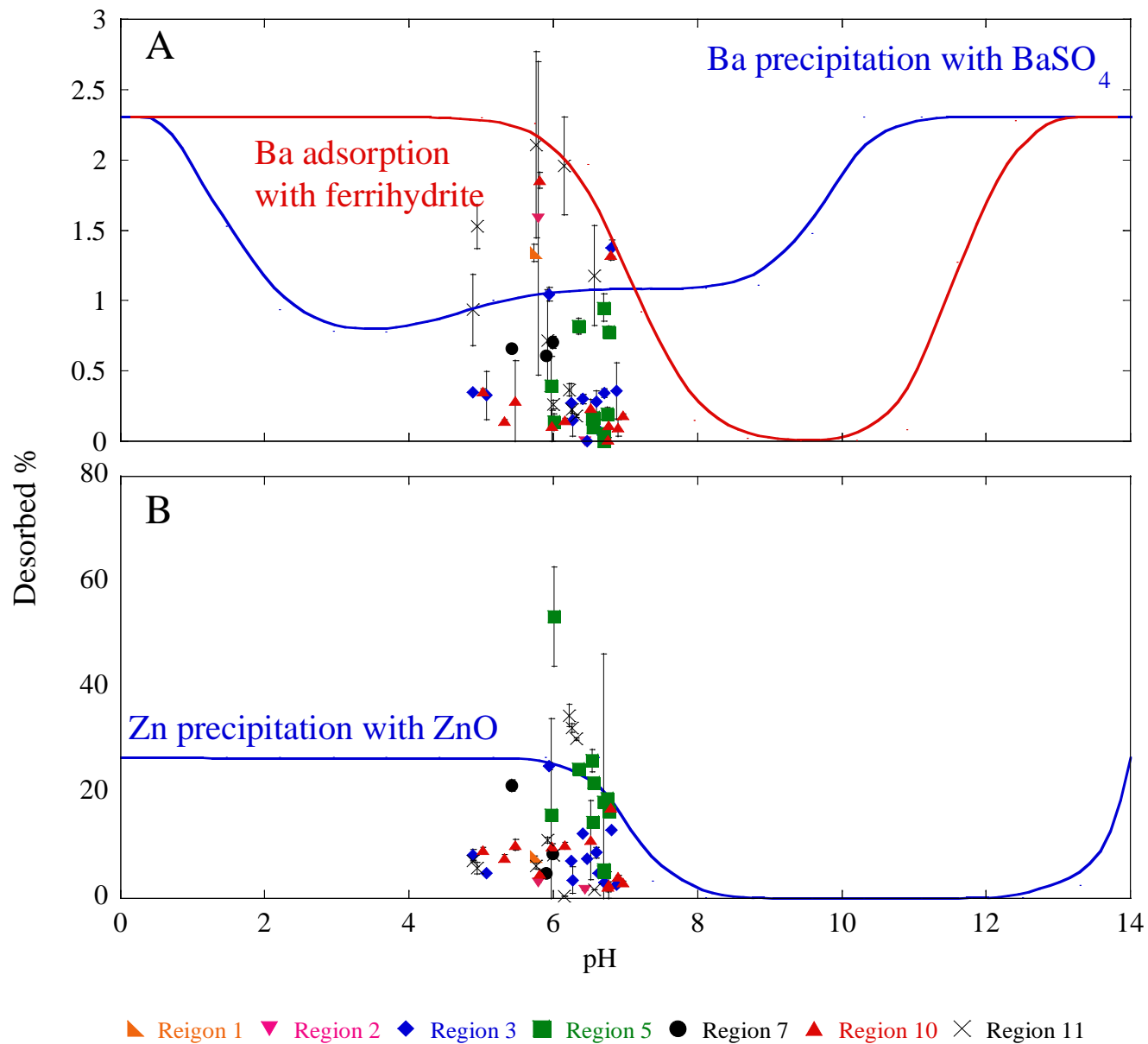


Figure 4. Desorbed Ba (A) and Zn (B) in the presence of steel grit associated with paint waste as a function of pH 0 to 14 after 18 hours using the TCLP. $Ba_T = 3.2 \times 10^{-5}$, $Zn_T = 0.02$, $Fe_T = 0.07$ M, ionic strength = 0.5 M, surface area = 600 m²/g, $K_{MeBa} = 10^{5.46}$, $K_{MeZn} = 10^{3.49}$, $K_{soBa} = 10^{-8.57}$, $K_{soZn} = 10^{-11.33}$.

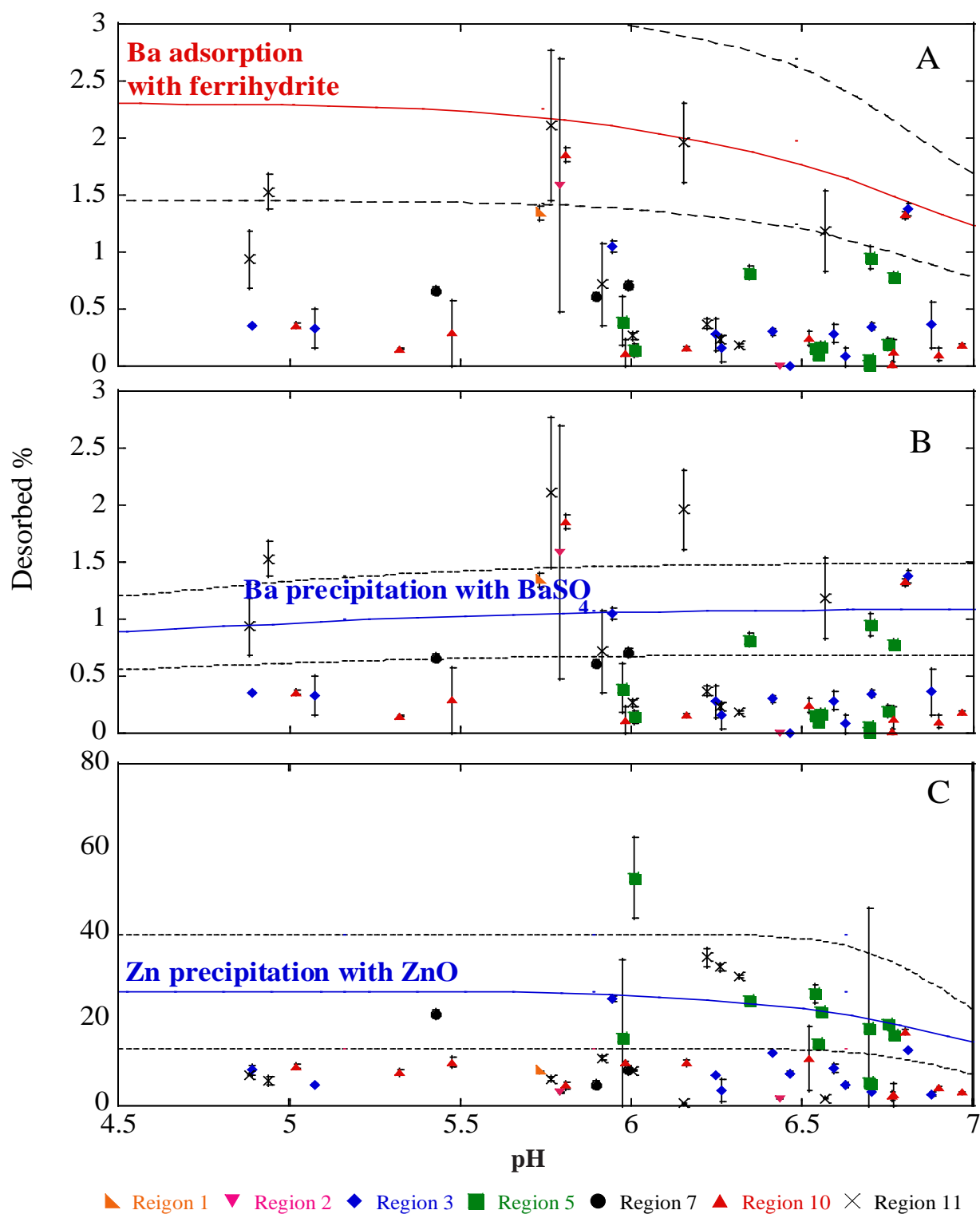


Figure 5. Desorbed Ba (A, B) and Zn (C) in the presence of steel grit associated with paint waste as a function of pH 4.5 to 7 after 18 hours using the TCLP. $Ba_T = 3.2 \times 10^{-5}$, $Zn_T = 0.02$, $Fe_T = 0.07$ M, ionic strength = 0.5 M, surface area = 600 m²/g, $K_{MeBa} = 10^{5.46}$, $K_{MeZn} = 10^{3.49}$, $K_{soBa} = 10^{-8.57}$, $K_{soZn} = 10^{-11.33}$. The dash line represents the 95% prediction interval.

precipitation plays a more important role in the system (Figures 4 and 5). In this study, Zn leaching was observed as great as 50% of the total Zn in the paint waste (Table 2). This result is attributed to the precipitated form of Zn in the paint waste, which was observed as ZnO by XRD (Shu and Axe, 2013). Other forms of zinc (Zn [synthetic]) are likely associated with the residual phase in the paint waste (Shu and Axe, 2013). Therefore, precipitation/dissolution provides a better prediction of Zn leaching (Figure 5).

Overall, based on the above discussion, results indicate that both adsorption and precipitation are important processes supporting predictive mechanistic leaching from the waste. In addition to iron oxide, other minerals and phases in paint waste may also affect leaching, such as ZnO. Therefore, a number of factors may affect metal leaching behavior including total metal concentrations in the paint waste, dominant sorbents present, competing metal ions, and the pH of the system. To develop a practical model that can be used for in-situ characterization, Fe along with other minerals (metals) present at elevated concentration in the paint waste samples are expected to play important roles in the statistical model accounting for their potential influence on metal leaching. To further investigate these variables and their effect on metal leaching, PCA was applied.

4.2 Principle component analysis

PCA is used to identify and reduce the dimensionality of data, from which a model is developed to predict metal leaching and therefore waste classification of the paint waste. The simplest and the most common method used to solve the number of principal components is the eigenvalue-one criterion also known as the Kaiser criterion (Kaiser, 1960), where the principal components (PC) with eigenvalue greater than 1 are selected. The eigenvalues reflect the quality of the projection from the N-dimensional initial table to a lower number of dimensions. The PC

with the highest eigenvalue is considered as the most significant and subsequently the PCs are introduced into the statistical model one after the other. Each eigenvalue corresponds to a factor, and each factor to one dimension. A factor is a linear combination of the initial variables, and all factors are un-correlated ($r = 0$). The eigenvalues and the corresponding factors are sorted by descending order to the degree which the initial variability is represented (converted to %).

In this study, applying PCA to the raw data showed essentially three main constituent axes with eigenvalues greater than 1 (Table 3), together explaining 85% of the data variance. The first eigenvalue equals 6.63 and represents 55.3% of the total variability. This means that if the data were represented on only one axis, 55.3% of the total variability of the data were obtained. Eighty five percent of the variance was explained by the paint properties classified under three principal components. Correlations greater than 0.66 (Table 3) are considered to demonstrate significant influence (Pradhan, et al., 2010). The first PC revealed strong relationships with the associated total concentration present in the waste; Relationships with total concentrations of Hg, Se, and Zn were observed as well. These results between the total metals in first PC are attributed to the surface preparation standard applied to the bridges. Surface preparation standard SSPC (The Society for Protective Coatings) SP-6 (Commercial Blast Cleaning) (NYSDOT, 2008) has been applied to bridges in New York State before 2006, where paint and rust from steel were removed to a remaining residual of 33% of the total removal area. After 2006, SSPC SP-10 (Near White Blast Cleaning) was required in the blasting procedure (NYSDOT, 2008) for all regions in NY. SP-10 restricts the visible residues remaining on the bridge surface to 5% of the total removal area. In this study, elevated total concentrations of As, Cd, Cr, Pb, and Ag were observed from bridges in Regions 1, 3, 7, 10, and 11, where the SSPC SP-6 blasting standard was applied.

Table 3. Principal component loadings of total metals in the paint waste samples.

| Variable | PC 1 | PC 2 | PC 3 |
|------------|--------|--------|--------|
| As | 0.829 | -0.433 | -0.22 |
| Ba | 0.658 | 0.429 | 0.19 |
| Ca | 0.655 | -0.165 | 0.672 |
| Cd | 0.877 | -0.342 | -0.243 |
| Cr | 0.854 | -0.432 | 0.004 |
| Fe | 0.375 | 0.705 | -0.437 |
| Pb | 0.863 | -0.448 | -0.027 |
| Hg | -0.698 | -0.477 | -0.191 |
| Ag | 0.886 | -0.358 | -0.228 |
| Se | -0.787 | -0.518 | -0.127 |
| Ti | 0.297 | 0.665 | -0.156 |
| Zn | -0.851 | -0.418 | -0.034 |
| Eigenvalue | 6.63 | 2.64 | 1.00 |
| Proportion | 0.553 | 0.22 | 0.076 |
| Cumulative | 0.553 | 0.773 | 0.849 |

Correlation value greater than 0.66 are highlighted

Greater concentrations of total Hg, Se, and Zn were related with the bridges in Regions 2 and 5, which were blasted with surface preparation standard SSPC SP-10 (Margrey, 2012) during rehabilitation. With the first PC, fifty-five percent of the total variability can be explained.

The second PC in PCA revealed the influence of Fe in the paint waste demonstrating that Fe is an important factor impacting model variability in paint waste. This result is attributed to the iron oxide formed on the steel grit surface, which provides a highly reactive surface for metal sorption in the system and further controls the degree of metal leaching from the paint waste. In addition to Fe, Ti was also observed to be an important factor in the paint waste based on PC2 (Table 3). This result is somewhat attributed to the application of TiO_2 as extenders in paint, which may provide sorption surface for trace metals as well. The third PC exhibited the effect of Ca in the paint waste. The observed behavior of Ca is consistent with Andra et al. (2011), where Ca was an important factor in the mobilization of Pb from alkaline soils in San Antonio, TX. The observed Ca is attributed to the application of calcite (CaCO_3) (12 wt% in paint waste, Shu and Axe, 2013) as an extender (supplementary pigments) in the paint (Lambourne and Strivens, 1999). The release of the CaCO_3 from paint waste does not directly affect the metal leaching. However, the dissolution of the CaCO_3 results in an increase in pH during the leaching procedure. Because metal leaching is a function of pH, dissolution of the CaCO_3 reflects this pH change and hence metal leaching. Therefore, CaCO_3 is expected to be an important factor in the leaching model.

Using the PCA analysis, the most important factors accounting for total variability in the paint waste are the surface preparation standard and surface complexation (iron oxide). Other factors such as Ti and Ca, also impact the variability in paint waste, because of the competitive sorption surface and their effect on the pH and alkalinity of leachate. Therefore, metal leaching

(the release of trace metal cation or anion to the water phase) depends on (a) total metal concentrations; (b) CaCO_3 affecting the pH and alkalinity; (c) Fe oxides providing a highly reactive surface for metal sorption; and, (d) other groups of metals such as Zn and Ti in the paint waste.

To address the best-fit model of experimental data, the mathematical form should be chosen to be as simple as possible with the number of adjustable parameters at a minimum. Therefore, multiple regression analysis was applied in this study.

4.3 Leaching model

Given an understanding of mechanistic processes along with a demonstrated analysis of variables through PCA, statistically-based models for leaching from paint waste are developed. In this study, multiple linear regression analysis (MLRA) was applied to establish a single correlation between a dependent and several independent variables. Metal leaching is the dependent variable and the metal concentrations from PCA are independent variables. The primary objective of this analysis was to use independent variables capable of predicting the dependent variable leached metal concentration. Results from leaching studies (TCLP and MEP) (Shu and Axe, 2013) were used to assess predicted values. Because the surface preparation standard was observed to be an important factor in PCA analysis, leaching results were sorted into groups with respect to the two methods: SSPC 6 and SSPC 10 (Table 4). The surface preparation methods mentioned here refer to the ones applied in the previous rehabilitation, which determined the residual waste remaining on the bridge.

The results were also divided based on Fe concentration ($\leq 24\%$ or $> 24\%$ by % wt) in the paint waste, where leaching followed unique trends (Figure 6). A modeling approach to predict trace metal leaching was derived from statistical analysis as follows:

Table 4. Sample sorted with respected to surface preparation standard and Fe concentrations.

| Region | Bridges | SSPC 6 | | SSPC 10 |
|-----------|---------|-----------------------|--------------------|------------------------------|
| | | $\text{Fe} \leq 24\%$ | $\text{Fe} > 24\%$ | $7 \leq \text{Fe} \leq 80\%$ |
| Region 1` | 1-1 | | √ | |
| Region 2 | 2-1 | | | √ |
| | 2-2 | | | √ |
| Region 3 | 3-1 | | √ | |
| | 3-2 | | √ | |
| | 3-3* | √ | √ | |
| Region 5 | 5-1 | | | √ |
| | 5-2 | | | √ |
| | 5-3 | | | √ |
| | 5-4 | | | √ |
| | 5-5 | | | √ |
| Region 7 | 7-1* | √ | √ | |
| | 7-2 | √ | | |
| Region 10 | 10-1* | √ | √ | |
| | 10-2 | | √ | |
| | 10-3 | √ | | |
| | 10-4 | | √ | |
| | 10-5 | √ | | |
| | 10-6 | √ | | |
| | 10-7 | √ | | |
| | 10-8 | | √ | |
| | 10-9 | √ | | |
| Region 11 | 11-1* | √ | √ | |
| | 11-2* | √ | √ | |

* Great variability of Fe concentrations were observed in different sampling locations.

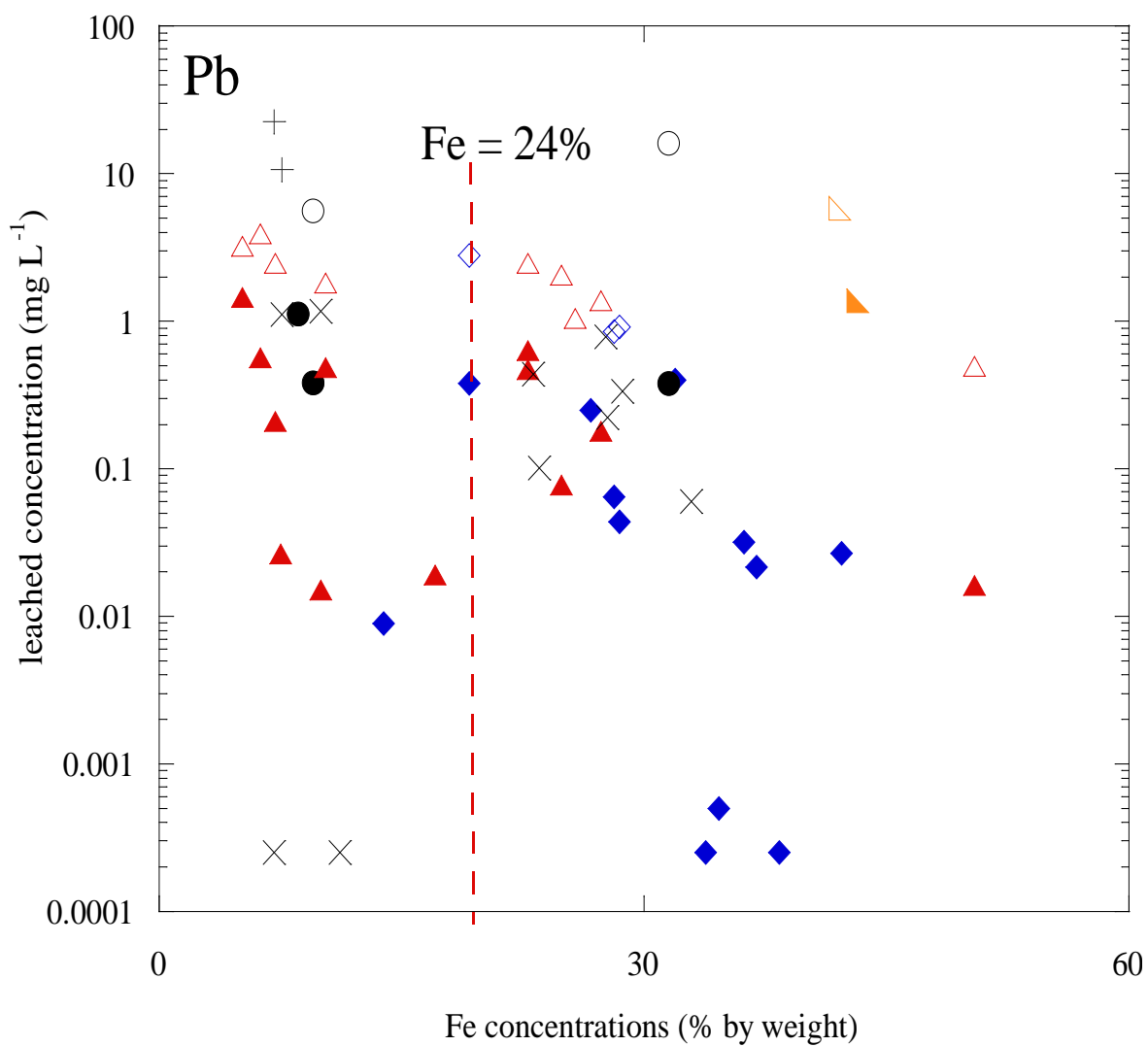


Figure 6. Leached Pb concentrations are shown as a function of total Fe (% wt) concentrations in paint waste. The dash line represents the cut off used in this study.

(i) Multivariate regression is tested in the first step of modeling.

$$\text{Leached metal} = a + b \cdot (\text{total Ca}) + c \cdot (\text{total metal}) + d \cdot (\text{total Fe}) + e \cdot (\text{Me}_{1, \text{ total}}) + \dots + n \cdot (\text{Me}_{n, \text{ total}})$$

(ii) Box-Cox transformation (Sakia, 1992) is applied according to the residual analysis if necessary, where leached metal y is transformed to y^λ :

$$(\text{Leached metal})^\lambda = a + b \cdot (\text{total Ca}) + c \cdot (\text{total metal}) + d \cdot (\text{total Fe}) + e \cdot (\text{Me}_{1, \text{ total}}) + \dots + n \cdot (\text{Me}_{n, \text{ total}})$$

(iii) Log-transformation is also tested:

$$\text{Log (leached metal)} = a + b \cdot \log(\text{total Ca}) + c \cdot \log(\text{total metal}) + d \cdot \log(\text{total Fe}) + e \cdot \log(\text{Me}_{1, \text{ total}}) + \dots + n \cdot \log(\text{Me}_{n, \text{ total}})$$

where leached metal concentrations are in mg L^{-1} , a - n are coefficients determined using regression with appropriate data sets, and total metal is in mg kg^{-1} based on FP-XRF. The adsorption capacity is a function of iron oxides in the paint waste, which is represented by total Fe in the equation. Total Ca represents the calcite (CaCO_3) applied in the paint, which may also affect the pH (and alkalinity) during leaching. $\text{Me}_{i, \text{ total}}$ represents other total metals in the paint waste that may affect the metal leaching. This last variable may be an artifact of the waste composition where a number of metals were observed to be present. For example, concentrations of Pb, As, Cd, Cr, and Ag follow similar trends, while concentration trends of Zn, Hg, and Se are consistent. These observations and trends were throughout all the regions in New York State, demonstrating consistent use of specific pigment formulations in paint (Shu and Axe, 2013).

The coefficient of determination, R^2 (Tables 5 and 6), is an estimate of the model fit in predicting observed leaching. The % variation of the data is explained by the best fit.

$$R^2 = \text{sum of squares (regression)} / \text{sum of squares (total)}$$

Table 5. Statistical analysis results from multivariate regression of the leached metal concentrations for Pb and Cr (mg L⁻¹)

| Metal | Surface preparation | Model used for prediction | R ² | Sample number | statistical significance |
|-------|---------------------|---|----------------|---------------|--------------------------|
| Pb | SSPC 6; Fe ≤ 24% | TCLP Pb (mg L ⁻¹) = 10 ^ [26.6 – 3.24 log total Ba (mg Kg ⁻¹) - 0.1 log total Fe (mg Kg ⁻¹) – 2.26 log total Cr (mg Kg ⁻¹) + 4.28 log total Pb (mg Kg ⁻¹) – 7.83 log total Ca (mg Kg ⁻¹) + 3.13 log total Ti (mg Kg ⁻¹) - 3.09 log total Ag (mg Kg ⁻¹)] | 0.6 | 28 | P = 0.01 |
| | SSPC 6; Fe > 24% | TCLP Pb (mg L ⁻¹) = 10 ^ [-19.63 – 3.72 log total Fe (mg Kg ⁻¹) - 3.03 log total Cr (mg Kg ⁻¹) + 5.28 log total Pb (mg Kg ⁻¹) + 1.92 log total Ti (mg Kg ⁻¹) + 1.64 log total Ag (mg Kg ⁻¹) - 0.74 log total Se (mg Kg ⁻¹) + 2.93 log total Zn (mg Kg ⁻¹)] | 0.7 | 27 | P =0.001 |
| | SSPC SP 10 | TCLP Pb (mg L ⁻¹) = 10 ^ [-3.20 + 1.34×10 ⁻⁶ Fe mg/kg + 0.00022 total Pb (mg Kg ⁻¹) + 2.55×10 ⁻⁵ total Ca (mg Kg ⁻¹) – 3.63×10 ⁻⁵ total Ti (mg Kg ⁻¹)] | 0.9 | 20 | P = 0.005 |
| Cr | SSPC 6; Fe ≤ 24% | TCLP Cr (mg L ⁻¹) = -12.2 + 0.00051 total Ba (mg Kg ⁻¹) + 0.000019 total Fe (mg Kg ⁻¹) - 0.00068 total Cr (mg Kg ⁻¹) + 0.000063 total Pb (mg Kg ⁻¹) + 0.00013 total Ca (mg Kg ⁻¹) + 0.00011 total Ti (mg Kg ⁻¹) | 0.6 | 28 | P = 0.003 |
| | SSPC 6; Fe > 24% | TCLP Cr (mg L ⁻¹) = - 0.80 + 0.000006 total Fe (mg Kg ⁻¹) - 0.00048 total Cr (mg Kg ⁻¹) - 0.000019 total Ca (mg Kg ⁻¹) + 0.0417 Se + 0.0062 total Cd (mg Kg ⁻¹) + 0.00013 total As (mg Kg ⁻¹) | 0.6 | 27 | P = 0.003 |
| | SSPC SP 10 | TCLP Cr (mg L ⁻¹) = 12.4 - 0.000022 total Zn (mg Kg ⁻¹) - 0.000032 total Fe (mg Kg ⁻¹) + 0.0077 total Cr (mg Kg ⁻¹) + 0.000053 total Pb (mg Kg ⁻¹) - 0.00020 total Ca (mg Kg ⁻¹) - 0.000038 total Ti (mg Kg ⁻¹) | 0.5 | 20 | P = 0.75 |

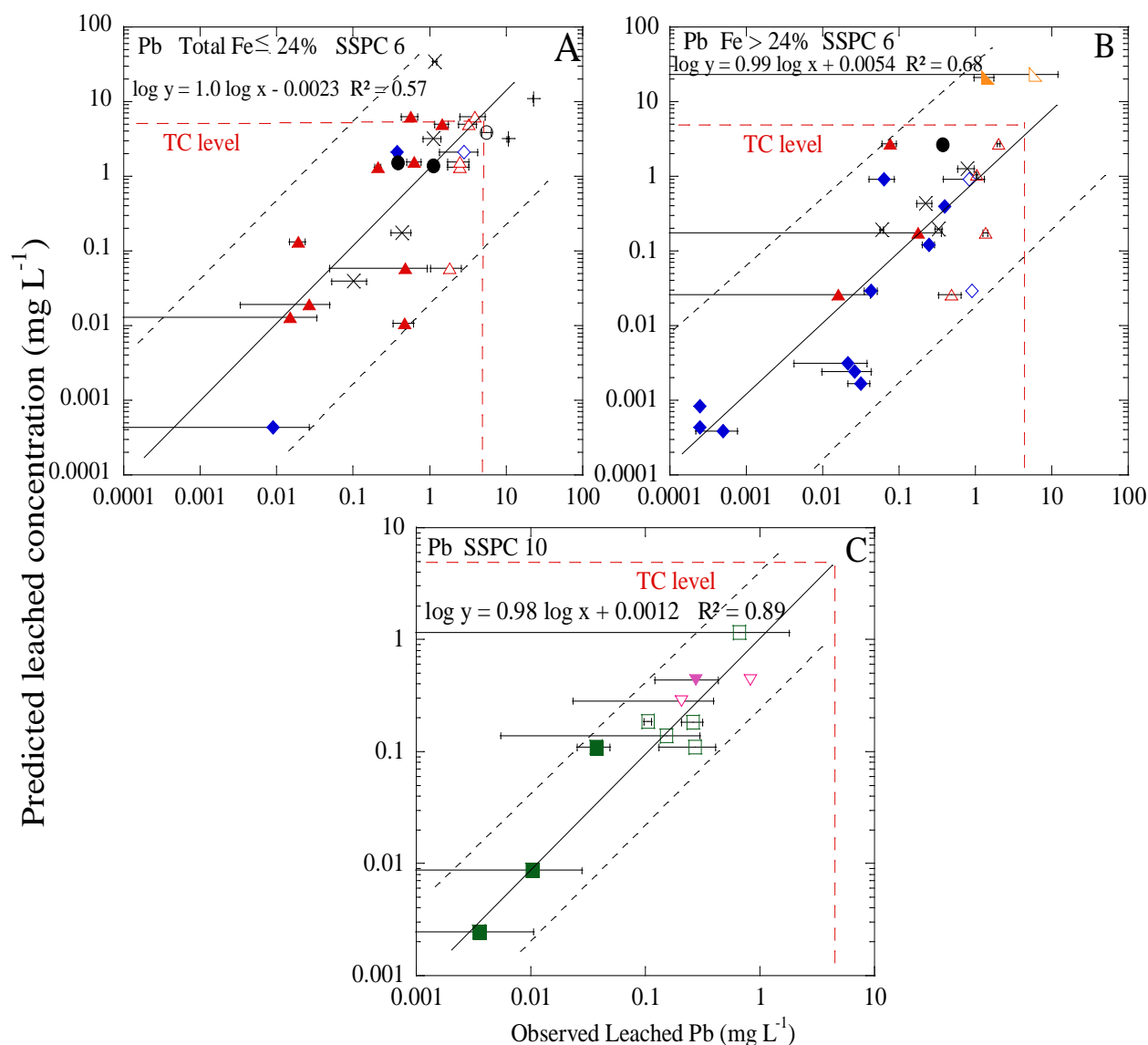
Table 6. Statistical analysis results from multivariate regression of the leached metal concentrations for Ba and Zn (mg L⁻¹)

| Metal | Surface preparation | Model used for prediction | R ² | Sample number | statistical significance |
|-------|---------------------|--|----------------|---------------|--------------------------|
| Ba | SSPC 6; Fe ≤ 24% | $\text{TCLP Ba (mg L}^{-1}\text{)} = \{[1.92 - 1.91 \times 10^{-6} \text{ total Fe (mg Kg}^{-1}\text{)} - 3.57 \times 10^{-6} \text{ total Pb (mg Kg}^{-1}\text{)} - 1.81 \times 10^{-5} \text{ total Ca (mg Kg}^{-1}\text{)} + 2.46 \times 10^{-5} \text{ total Ti (mg Kg}^{-1}\text{)} + 0.023 \text{ total Ag (mg Kg}^{-1}\text{)} - 0.013 \text{ total Se (mg Kg}^{-1}\text{)} - 0.014 \text{ total Cd (mg Kg}^{-1}\text{)}]^{1/0.23} - 0.37\}/0.45$ | 0.6 | 28 | P < 0.0001 |
| | SSPC 6; Fe > 24% | $\text{TCLP Ba (mg L}^{-1}\text{)} = 4.98 - 0.00018 \text{ total Ba (mg Kg}^{-1}\text{)} - 0.000070 \text{ Cr (mg Kg}^{-1}\text{)} - 0.000074 \text{ total Ca (mg Kg}^{-1}\text{)} - 0.000056 \text{ total Ti (mg Kg}^{-1}\text{)} - 0.039 \text{ total Ag (mg Kg}^{-1}\text{)} + 0.011 \text{ total Se (mg Kg}^{-1}\text{)} + 0.033 \text{ total Cd (mg Kg}^{-1}\text{)} - 0.000086 \text{ total As (mg Kg}^{-1}\text{)}$ | 0.6 | 27 | P = 0.1 |
| | SSPC SP 10 | $\text{TCLP Ba (mg L}^{-1}\text{)} = \{[-0.66 - 2.18 \times 10^{-5} \text{ total Ba (mg Kg}^{-1}\text{)} + 2.63 \times 10^{-6} \text{ total Zn (mg Kg}^{-1}\text{)} + 3.37 \times 10^{-6} \text{ total Fe (mg Kg}^{-1}\text{)} + 0.00011 \text{ total Pb (mg Kg}^{-1}\text{)} - 1.14 \times 10^{-5} \text{ total Ca (mg Kg}^{-1}\text{)} - 0.0014 \text{ total As (mg Kg}^{-1}\text{)}]^{0.5} - 0.14\}/0.64$ | 0.7 | 20 | P = 0.01 |
| Zn | SSPC 6; Fe ≤ 24% | $\text{Zn TCLP (mg L}^{-1}\text{)} = 436 + 0.0014 \text{ total Zn (mg Kg}^{-1}\text{)} - 0.16 \text{ total Cr (mg Kg}^{-1}\text{)} - 0.011 \text{ total Pb (mg Kg}^{-1}\text{)} + 0.046 \text{ total Ti (mg Kg}^{-1}\text{)} - 6.17 \text{ total Ag (mg Kg}^{-1}\text{)} - 17.1 \text{ total Se (mg Kg}^{-1}\text{)} + 0.27 \text{ total As (mg Kg}^{-1}\text{)}$ | 0.7 | 28 | P < 0.0001 |
| | SSPC 6; Fe > 24% | $\text{Zn TCLP (mg L}^{-1}\text{)} = 10^{\wedge} [8.65 + 0.864 \log \text{ total Zn (mg Kg}^{-1}\text{)} - 1.58 \log \text{ total Fe (mg Kg}^{-1}\text{)} - 0.653 \log \text{ total Cr (mg Kg}^{-1}\text{)} - 0.347 \log \text{ total Ca (mg Kg}^{-1}\text{)} + 0.358 \log \text{ total Ti (mg Kg}^{-1}\text{)} + 0.443 \log \text{ total Cd (mg Kg}^{-1}\text{)}]$ | 0.6 | 27 | P = 0.001 |
| | SSPC SP 10 | $\text{Zn TCLP (mg L}^{-1}\text{)} = \{[0.40 - 0.00050 \text{ total Ba (mg Kg}^{-1}\text{)} + 5.27 \times 10^{-5} \text{ total Zn (mg Kg}^{-1}\text{)} + 4.79 \text{ total Ag (mg Kg}^{-1}\text{)} - 0.015 \text{ total As (mg Kg}^{-1}\text{)}]^2 + 178.59\}/0.70$ | 0.7 | 20 | P = 0.001 |

A P value of 5% or less is generally accepted as the point at which there is a 5% chance that the results would have been observed in a random distribution. In other words, the model is specified correctly with a 95% probability.

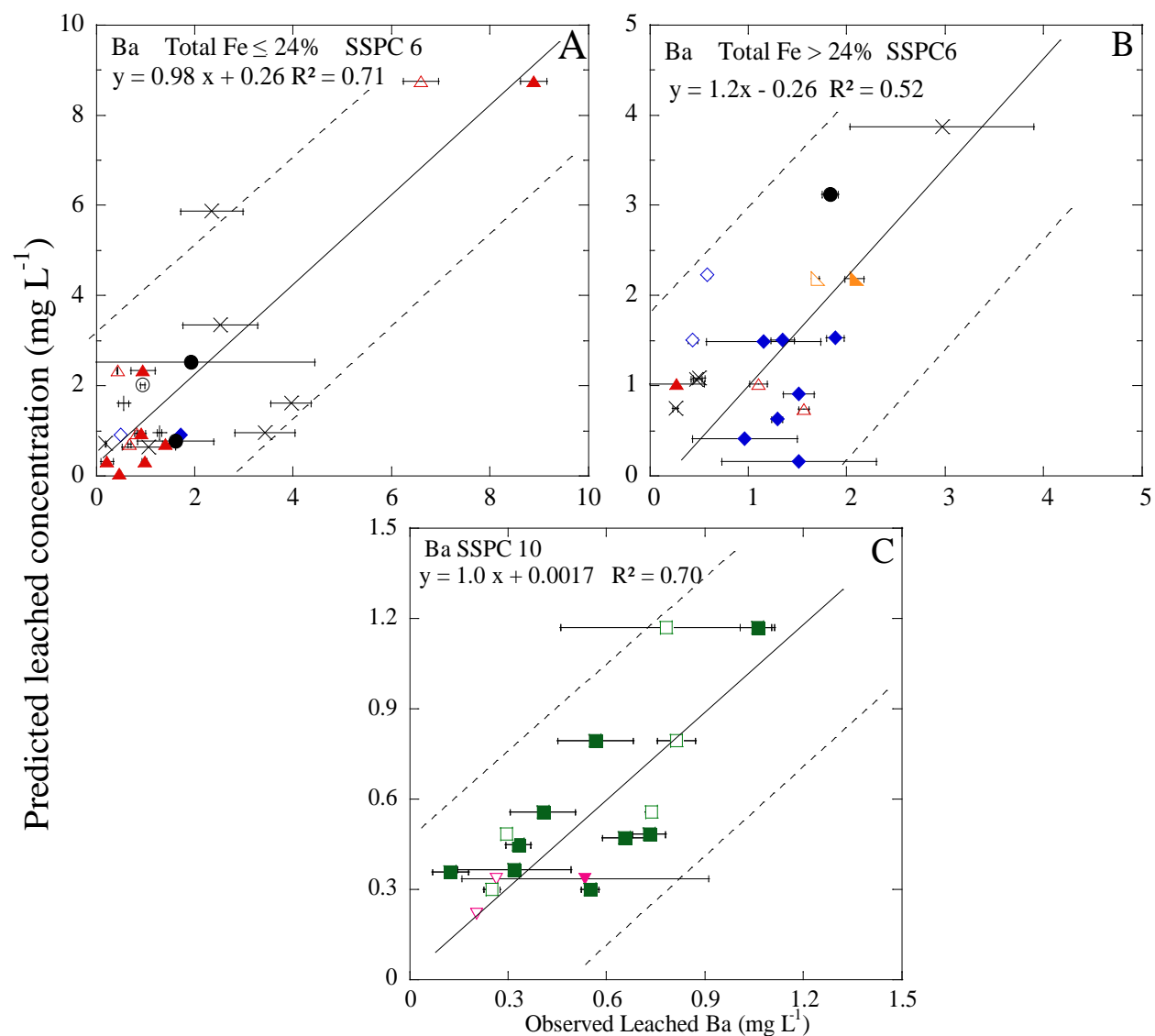
The statistical models developed for metal leaching demonstrated 96 percent of the data fall within the 95% confidence level for Pb (R^2 0.6 – 0.9, $p \leq 0.01$), Ba (R^2 0.6 – 0.7, $p \leq 0.1$), and Zn (R^2 0.6 – 0.7, $p \leq 0.01$) (Tables 5 and 6) (Figures 7 to 10). However, the regression model obtained for Cr leaching was not significant (R^2 0.5 – 0.7, $p \leq 0.75$) (Table 5) as the p value was observed as great as 0.75, suggesting the regression is not significant for Cr. Good correlations were observed between predicted and observed metal leaching for bridge samples blasted with SSPC 10 preparation ($R^2 = 0.60$ for Pb, $R^2 = 0.74$ for Ba, and $R^2 = 0.72$ for Zn) (Figures 7 to 10).

Compared to the bridges cleaned with SSPC 6, the bridges blasted using SSPC 10 revealed less leached metal concentrations. For example, leached Pb concentrations varied from less than 0.0005 (detection limit) to 0.67 mg L⁻¹, which are less than TC level of 5 mg L⁻¹. Similarly, these samples revealed less than 0.0007 (detection limit) to 0.43 mg L⁻¹ for Cr, and less than 0.0004 (detection limit) to 0.81 mg L⁻¹ for Ba; these fall below the TC level of 5 mg L⁻¹ for Cr and 100 mg L⁻¹ for Ba. Results indicate that the paint waste from bridges cleaned with SSPC 10 is classified as non-hazardous material. For bridges cleaned with SSPC 6, 9% of the samples exhibited leached Pb concentrations greater than TC level of 5 mg L⁻¹ (Figure 7), while 5% of the samples revealed leached Cr concentrations greater than TC level of 5 mg L⁻¹ (Figure 9). Overall, 14% of the samples revealed metal leaching greater than TC levels, suggesting the hazardous nature for these samples. Most of the leaching data can be described adequately over a wide range of total metal concentrations. In contrast to the metals discussed above (Pb, Cr, and Ba), the bridge samples blasted using SSPC 10 revealed greater leached Zn concentrations (from



TCLP samples: ▲ Region 1 ▼ Region 2 ◆ Region 3 ■ Region 5 ● Region 7 ▲ Region 10 × Region 11
MEP samples: △ Region 1 ▽ Region 2 ◇ Region 3 □ Region 5 ○ Region 7 △ Region 10 + Region 11

Figure 7. Comparison of the results from predicted and observed leached Pb concentrations. The samples represent the TCLP and first day of the MEP extraction conducted on the paint waste samples. Bridges were blasted to (A) surface preparation SSPC 6 with total Fe concentration greater than 24% (%wt), sample number N = 19 for TCLP and N = 8 for MEP studies; (B) SSPC 6 with total Fe concentration less than 24% (%wt). N = 19 for TCLP and N = 9 for MEP; (C) SSPC 10. N = 13 for TCLP and N = 7 for MEP. Toxicity characteristic (TC) level for Pb is 5 mg L⁻¹. The dash line represents the 95% prediction interval.



TCLP samples: ▲ Region 1 ▼ Region 2 ◆ Region 3 ■ Region 5 ● Region 7 ▲ Region 10 × Region 11
 MEP samples: △ Region 1 ▽ Region 2 ◇ Region 3 □ Region 5 ○ Region 7 △ Region 10 + Region 11

Figure 8. Comparison of the results from predicted and observed leached Ba concentrations. The samples represent the TCLP and first day of the MEP extraction conducted on the paint waste samples. Bridges were blasted to (A) surface preparation SSPC 6 with total Fe greater than 24% (%wt), sample number N = 19 for TCLP and N = 8 for MEP studies; (B) SSPC 6 with total Fe less than 24% (%wt). N = 19 for TCLP and N = 9 for MEP; (C) SSPC 10. N = 13 for TCLP and N = 7 for MEP. Toxicity characteristic (TC) level for Ba is 100 mg L⁻¹. The dash line represents the 95% prediction interval.

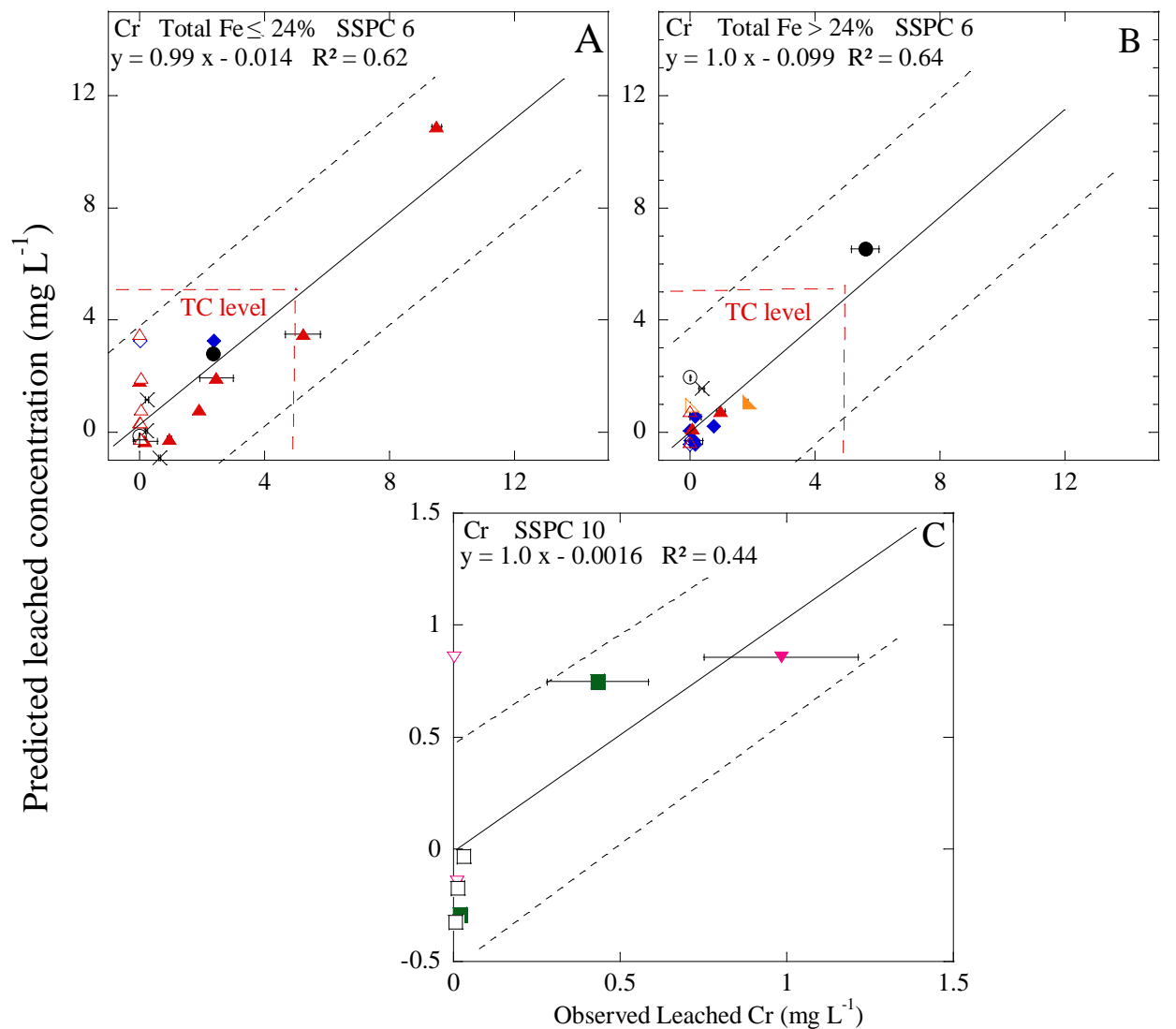
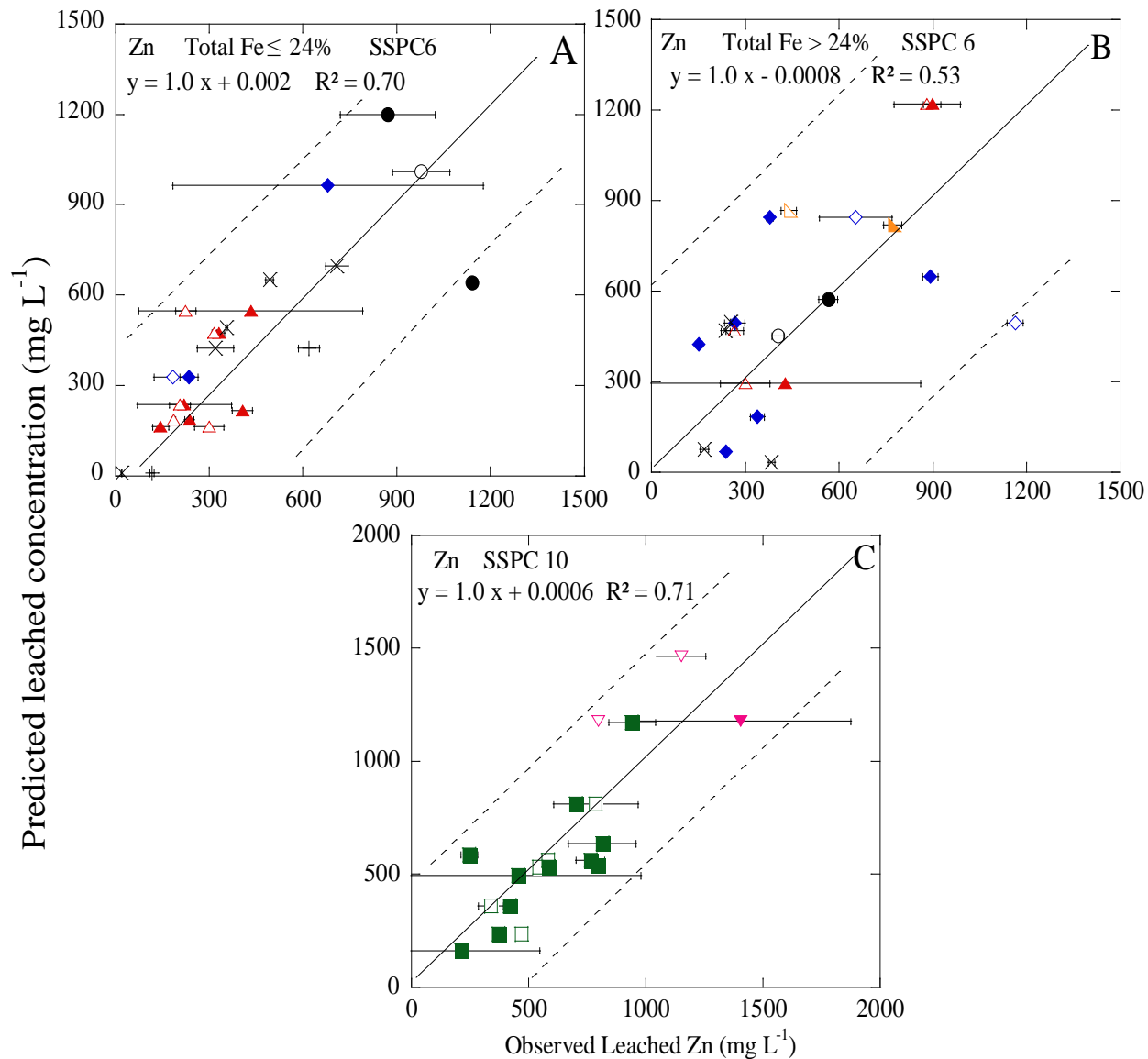


Figure 9. Comparison of the results from predicted and observed leached Cr concentrations. The samples represent the TCLP and first day of the MEP extraction conducted on the paint waste samples. Bridges were blasted to (A) surface preparation SSPC 6 with total Fe greater than 24% (%wt), sample number N = 19 for TCLP and N = 8 for MEP studies; (B) SSPC 6 with total Fe less than 24% (%wt). N = 19 for TCLP and N = 9 for MEP; (C) SSPC 10. N = 13 for TCLP and N = 7 for MEP. Toxicity characteristic (TC) level for Cr is 5 mg L^{-1} . The dash line represents the 95% prediction interval.



TCLP samples: ▲ Reigon 1 ▼ Region 2 ◆ Region 3 ■ Region 5 ● Region 7 ▲ Region 10 × Region 11
 MEP samples: △ Region 1 ▽ Region 2 ◇ Region 3 □ Region 5 ○ Region 7 △ Region 10 + Region 11

Figure 10. Comparison of the results from predicted and observed leached Zn concentrations. The samples represent the TCLP and first day of the MEP extraction conducted on the paint waste samples. Bridges were blasted to (A) surface preparation SSPC 6 with total Fe greater than 24% (%wt), sample number N = 19 for TCLP and N = 8 for MEP studies; (B) SSPC 6 with total Fe less than 24% (%wt). N = 19 for TCLP and N = 9 for MEP; (C) SSPC 10. N = 13 for TCLP and N = 7 for MEP. The dash line represents the 95% prediction interval

216 mg L⁻¹ to 1405 mg L⁻¹) than the samples cleaned with SSPC 6 (129 mg L⁻¹ to 1163 mg L⁻¹). These results are consistent with the increasing usage of zinc primer (ZnO, Zn₃(PO₄)₂·2H₂O, and epoxy zinc rich primer) (80% zinc content dry) in bridges blasted using SSPC 10.

On the other hand, metal leaching is affected by total Fe concentrations in the paint waste, where iron oxide forms on the steel grit surface providing a reactive surface for metal sorption. In this study, metal leaching increased with decreasing Fe ($\leq 24\%$ by weight) compared to that observed with relatively greater Fe concentrations ($> 24\%$). This effect is supported by the model developed as well. A negative correlation was obtained between metal leaching (including Pb and Ba) and total Fe concentrations in the paint: metal leaching decreased as total Fe concentration increased in the samples (Tables 5 and 6). These results are consistent with the well-recognized importance of iron oxide in surface complexation with trace metals.

Negative prediction values may be obtained at lower metal concentrations for Cr and Ba (Figure 8 and 9). This result occurs when metal leaching is less than the detection level. Therefore, the false negative results would not affect the characterization of the waste classification. For this project, an Excel template for collecting the FP-XRF data with linked formula will be provided for predicting metal leaching and classifying waste. Validation of this approach is recommended.

5. Conclusion

In this study, the characterization of waste classification was conducted on the collected waste samples. Data from the FP-XRF were applied to predict leaching and therefore waste classification. Mechanistic models were initially invoked for leaching and desorption in an effort to understand key variables needed for a statistical model. Surface complexation and precipitation/dissolution modeling were found to accurately depict leaching given the elevated

iron concentrations and the paint composition. Results indicated that both processes, adsorption and precipitation, are important in predicting metal leaching from the waste. Subsequently, PCA was invoked to address and support the analysis of significant variables. The statistical models developed for metal leaching demonstrated 96 percent of the data falling within the 95% confidence level for Pb (R^2 0.6 – 0.9, $p \leq 0.01$), Ba (R^2 0.6 – 0.7, $p \leq 0.1$), and Zn (R^2 0.6 – 0.7, $p \leq 0.01$). However, the regression model obtained for Cr leaching is not significant (R^2 0.5 – 0.7, $p \leq 0.75$). Given an understanding of mechanistic processes along with a demonstrated analysis of variables through PCA, statistically-based models for leaching from paint waste were developed. The results in this study indicated that the paint waste from bridges cleaned with SSPC 10 may be for the most part classified as non-hazardous material, while 14% of the sample set would be classified as hazardous for the bridges blasted using SSPC 6. A practical advantage in applying models developed is the ability to estimate contaminant leaching from paint waste without additional laboratory studies including TCLP. Therefore, the statistically-based models developed are a powerful approach for predicting metal leaching and therefore waste classification. Furthermore, this work supports the use of FP-XRF as a strong tool for in-situ characterization.

One recommendation from this study is the need for model validation in the field. Because the models developed in this study are based on the collected samples from the 24 bridges in seven regions of NYS, bridge samples collected from other regions are suggested for model validation. The simplicity of verifying a waste to be hazardous or nonhazardous using FP-XRF and the model has significant benefits that substantiate its continued use as SSPC 10 is applied.

6. References

- Andra, S.S., Datta, R., Reddy, R., Saminathan, S.K., Sarkar, D. (2011) Antioxidant Enzymes Response in Vetiver Grass: A Greenhouse Study for Chelant-Assisted Phytoremediation of Lead-Contaminated Residential Soils. *CLEAN–Soil, Air, Water* 39, 428-436.
- Apul, D.S., Gardner, K.H., Eighmy, T.T., Fällman, A.-M., Comans, R.N. (2005) Simultaneous application of dissolution/precipitation and surface complexation/surface precipitation modeling to contaminant leaching. *Environmental Science & Technology* 39, 5736-5741.
- Barnes, G.L., Davis, A.P. (1996) Dissolution of lead paint in aqueous solutions. *Journal of Environmental Engineering* 122, 663-666.
- Bidoglio, G., Gibson, P., O'Gorman, M., Roberts, K. (1993) X-ray absorption spectroscopy investigation of surface redox transformations of thallium and chromium on colloidal mineral oxides. *Geochimica et Cosmochimica Acta* 57, 2389-2394.
- Bradl, H.B. (2004) Adsorption of heavy metal ions on soils and soils constituents. *Journal of Colloid and Interface Science* 277, 1-18.
- Christophi, C.A., Axe, L. (2000) Competition of Cd, Cu, and Pb adsorption on goethite. *Journal of Environmental Engineering* 126, 66-74.
- Deng, Y., Stjernström, M., Banwart, S. (1996) Accumulation and remobilization of aqueous chromium (VI) at iron oxide surfaces: Application of a thin-film continuous flow-through reactor. *Journal of contaminant hydrology* 21, 141-151.
- Dijkstra, J.J., Meeussen, J.C., Comans, R.N. (2009) Evaluation of a generic multisurface sorption model for inorganic soil contaminants. *Environmental Science & Technology* 43, 6196-6201.
- Du, J., Lu, J., Wu, Q., Jing, C. (2012) Reduction and immobilization of chromate in chromite ore processing residue with nanoscale zero-valent iron. *Journal of hazardous materials* 215, 152-158.
- Dzombak, D.A., Morel, F.M. (1986) Sorption of cadmium on hydrous ferric oxide at high sorbate/sorbent ratios: Equilibrium, kinetics, and modeling. *Journal of Colloid and Interface Science* 112, 588-598.
- Dzombak, D.A., Morel, F.M. (1990) Surface complexation modeling: hydrous ferric oxide. Wiley New York.

- Groenenberg, J., Römkens, P., Comans, R., Luster, J., Pampura, T., Shotbolt, L., Tipping, E., De Vries, W. (2010) Transfer functions for solid-solution partitioning of cadmium, copper, nickel, lead and zinc in soils: derivation of relationships for free metal ion activities and validation with independent data. *European Journal of Soil Science* 61, 58-73.
- Jackson, R., Inch, K. (1989) The in-situ adsorption of ^{90}Sr in a sand aquifer at the Chalk River Nuclear Laboratories. *Journal of contaminant hydrology* 4, 27-50.
- Jing, C., Liu, S., Korfiatis, G.P., Meng, X. (2006) Leaching behavior of Cr (III) in stabilized/solidified soil. *Chemosphere* 64, 379-385.
- Kaiser, H.F. (1960) The application of electronic computers to factor analysis. *Educational and psychological measurement*.
- Kanungo, S.B. (1994) Adsorption of cations on hydrous oxides of iron: II. Adsorption of Mn, Co, Ni, and Zn onto amorphous FeOOH from simple electrolyte solutions as well as from a complex electrolyte solution resembling seawater in major ion content. *Journal of Colloid and Interface Science* 162, 93-102.
- Karamalidis, A.K., Voudrias, E.A. (2008) Anion leaching from refinery oily sludge and ash from incineration of oily sludge stabilized/solidified with cement. Part II. Modeling. *Environmental Science & Technology* 42, 6124-6130.
- Kendall, D.S. (2003) Toxicity characteristic leaching procedure and iron treatment of brass foundry waste. *Environmental Science & Technology* 37, 367-371.
- Kooner, Z. (1993) Comparative study of adsorption behavior of copper, lead, and zinc onto goethite in aqueous systems. *Environmental Geology* 21, 242-250.
- Lofts, S., Spurgeon, D.J., Svendsen, C., Tipping, E. (2004) Deriving soil critical limits for Cu, Zn, Cd, and Pb: A method based on free ion concentrations. *Environmental Science & Technology* 38, 3623-3631.
- Margrey, K.W., Riese, J.B. Email on February 24th 2012.
- McBride, M., Sauve, S., Hendershot, W. (1997) Solubility control of Cu, Zn, Cd and Pb in contaminated soils. *European Journal of Soil Science* 48, 337-346.

Meima, J.A., Comans, R.N. (1997) Geochemical modeling of weathering reactions in municipal solid waste incinerator bottom ash. *Environmental Science & Technology* 31, 1269-1276.

Mishra, S.P., Tiwari, D., Dubey, R. (1997) The uptake behaviour of rice (Jaya) husk in the removal of Zn (II) ions—A radiotracer study. *Applied radiation and isotopes* 48, 877-882.

Mishra, S.P., Tiwari, D. (1999) Ion exchangers in radioactive waste management. Part XI.

New York State Department of Transportation, (1988) Specification for bridges – removal of lead based paints – new department paint system for structural steel. Engineering instruction EI 88-36

New York State Department of Transportation, (2008) Standard Specification.

Removal of barium and strontium ions from aqueous solutions by hydrous ferric oxide. *Applied radiation and isotopes* 51, 359-366.

Padmanabham, M. (1983) Comparative study of the adsorption-desorption behaviour of copper (II), zinc (II), cobalt (II) and lead (II) at the goethite solution interface. *Soil Research* 21, 515-525.

Peterson, M.L., Brown, G.E., Parks, G.A. (1996) Direct XAFS evidence for heterogeneous redox reaction at the aqueous chromium/magnetite interface. *Colloids and Surfaces A: Physicochemical and Engineering Aspects* 107, 77-88.

Peterson, M.L., Brown, G.E., Parks, G.A., Stein, C.L. (1997) Differential redox and sorption of Cr (III/VI) on natural silicate and oxide minerals: EXAFS and XANES results. *Geochimica et Cosmochimica Acta* 61, 3399-3412.

Pierce, M.L., Moore, C.B. (1980) Adsorption of arsenite on amorphous iron hydroxide from dilute aqueous solution. *Environmental Science & Technology* 14, 214-216.

Pradhan, D., Mishra, D., Kim, D.J., Ahn, J.G., Chaudhury, G.R., Lee, S.W. (2010) Bioleaching kinetics and multivariate analysis of spent petroleum catalyst dissolution using two acidophiles. *Journal of hazardous materials* 175, 267-273.

Roskovic, R., Stipanovic Oslakovic, I., Radic, J., Serdar, M. (2011) Effects of chromium (VI) reducing agents in cement on corrosion of reinforcing steel. *Cement and Concrete Composites* 33, 1020-1025.

Sakia, R.M. (1992) The Box-Cox Transformation Technique: A Review. *Journal of the Royal Statistical Society. Series D (The Statistician)* 41, 169-178.

Sauve, S., Hendershot, W., Allen, H.E. (2000) Solid-solution partitioning of metals in contaminated soils: dependence on pH, total metal burden, and organic matter. *Environmental Science & Technology* 34, 1125-1131.

Sauvé, S., Norvell, W.A., McBride, M., Hendershot, W. (2000) Speciation and complexation of cadmium in extracted soil solutions. *Environmental Science & Technology* 34, 291-296.

Shu, Z., Axe, L. (2013) Report Submitted to New York State Department of Transportation, Deliverable for Task 6: Collection of samples for laboratory analyses.

Strivens, T., Lambourne, R. (1999) *Paint and surface coatings: theory and practice*. Woodhead.

Tiruta-Barna, L.R., Barna, R., Moszkowicz, P. (2001) Modeling of solid/liquid/gas mass transfer for environmental evaluation of cement-based solidified waste. *Environmental Science & Technology* 35, 149-156.

Torrecilla, J.S., García, J., Rojo, E., Rodríguez, F. (2009) Estimation of toxicity of ionic liquids in Leukemia Rat Cell Line and Acetylcholinesterase enzyme by principal component analysis, neural networks and multiple lineal regressions. *Journal of hazardous materials* 164, 182-194.

Vaishya, R.C., Gupta, S.K. (2004) Batch kinetic modeling of arsenic removal from water by mixed oxide coated sand (mocs). *Journal of environmental science & engineering* 46, 123-136.

Weng, C., Huang, C., Allen, H.E., Leavens, P.B., Sanders, P.F. (1996) Chemical interactions between Cr (VI) and hydrous concrete particles. *Environmental Science & Technology* 30, 371-376.

Weng, C.-H., Huang, C., Allen, H., Sanders, P.F. (2001) Cr (VI) adsorption onto hydrous concrete particles from groundwater. *Journal of Environmental Engineering* 127, 1124-1131.

Appendix A

Leached metal as a function of total metal concentrations

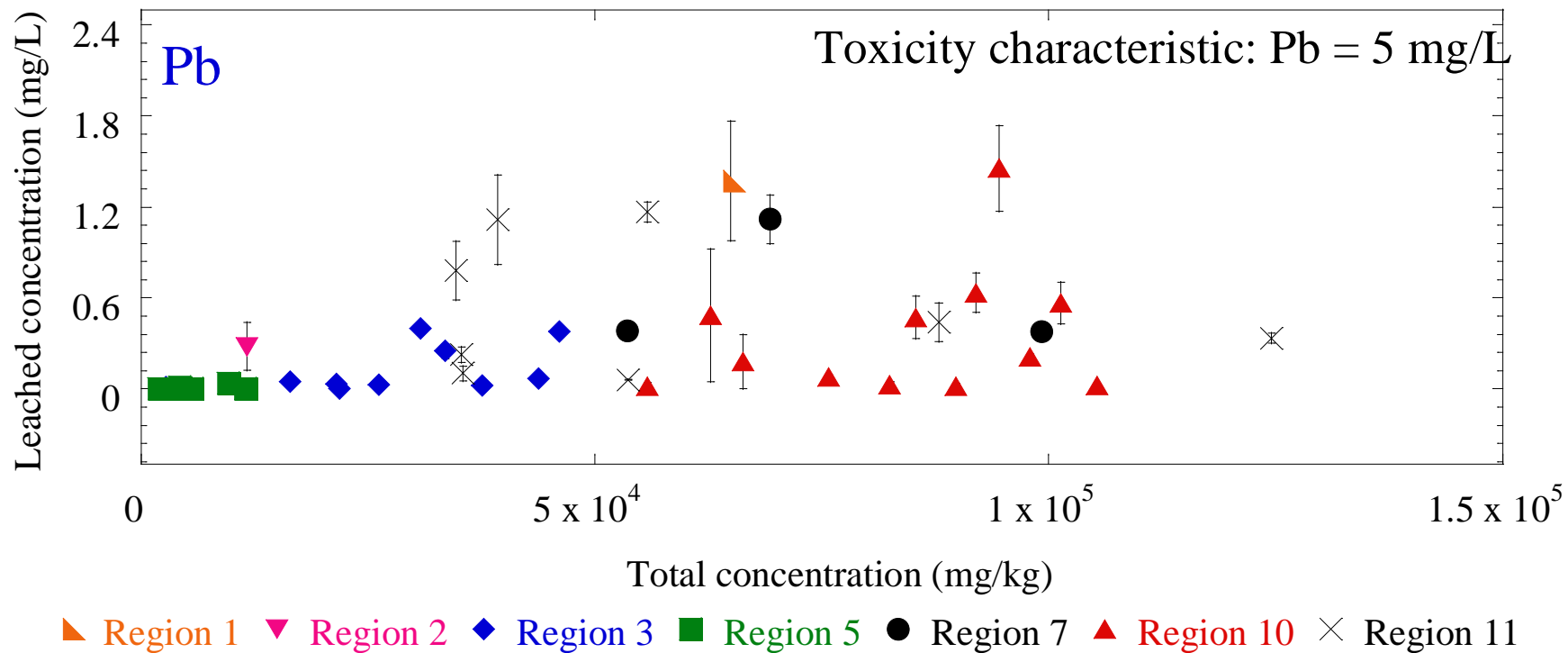


Figure A1. Leaching results from TCLP for Pb as a function of XRF results. Samples are extracted using Fluid #1 (0.1 N acetic acid, which has been adjusted with NaOH to an initial pH of 4.93 ± 0.05) or Fluid #2 (0.1 N acetic acid, which has an initial pH of 2.88 ± 0.05) based on the alkalinity of the waste material.

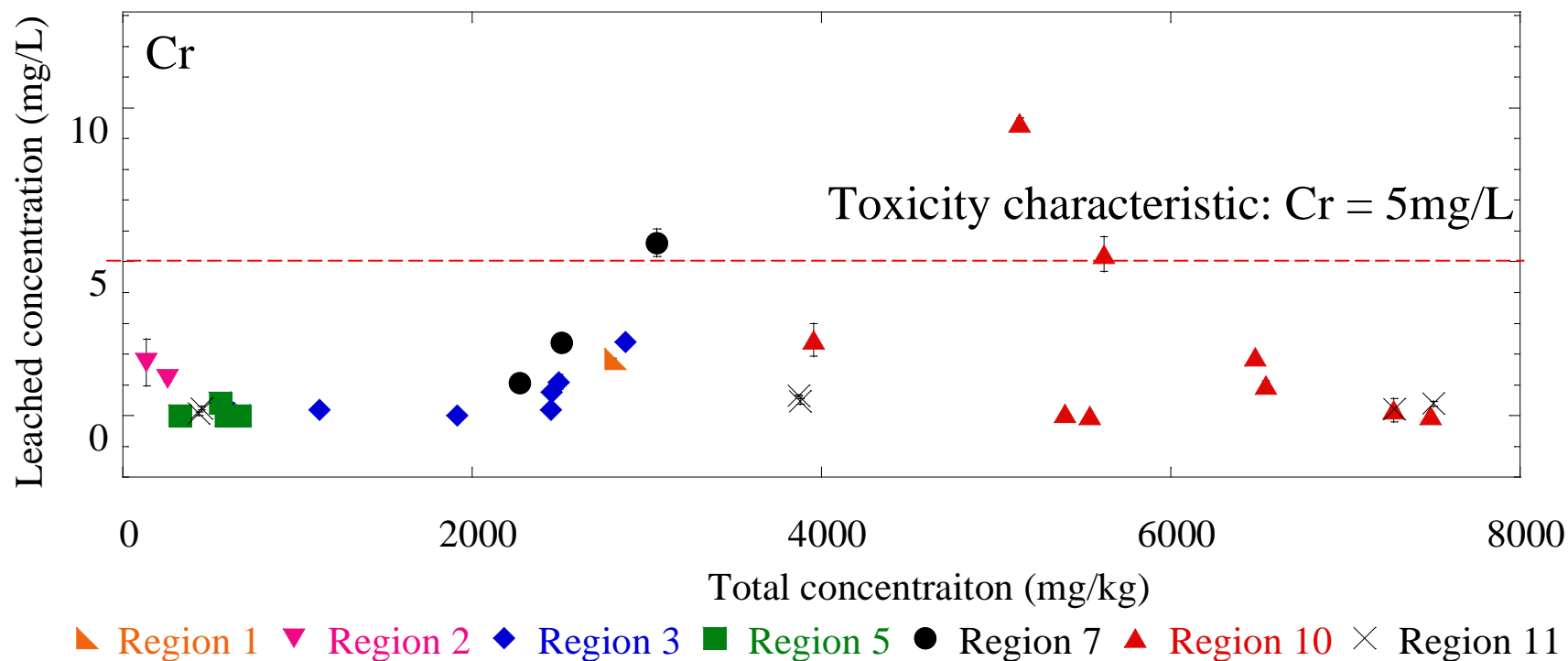


Figure A2. Leaching results from TCLP for Cr as a function of XRF results. Samples are extracted using Fluid #1 (0.1 N acetic acid, which has been adjusted with NaOH to an initial pH of 4.93 ± 0.05) or Fluid #2 (0.1 N acetic acid, which has an initial pH of 2.88 ± 0.05) based on the alkalinity of the waste material.

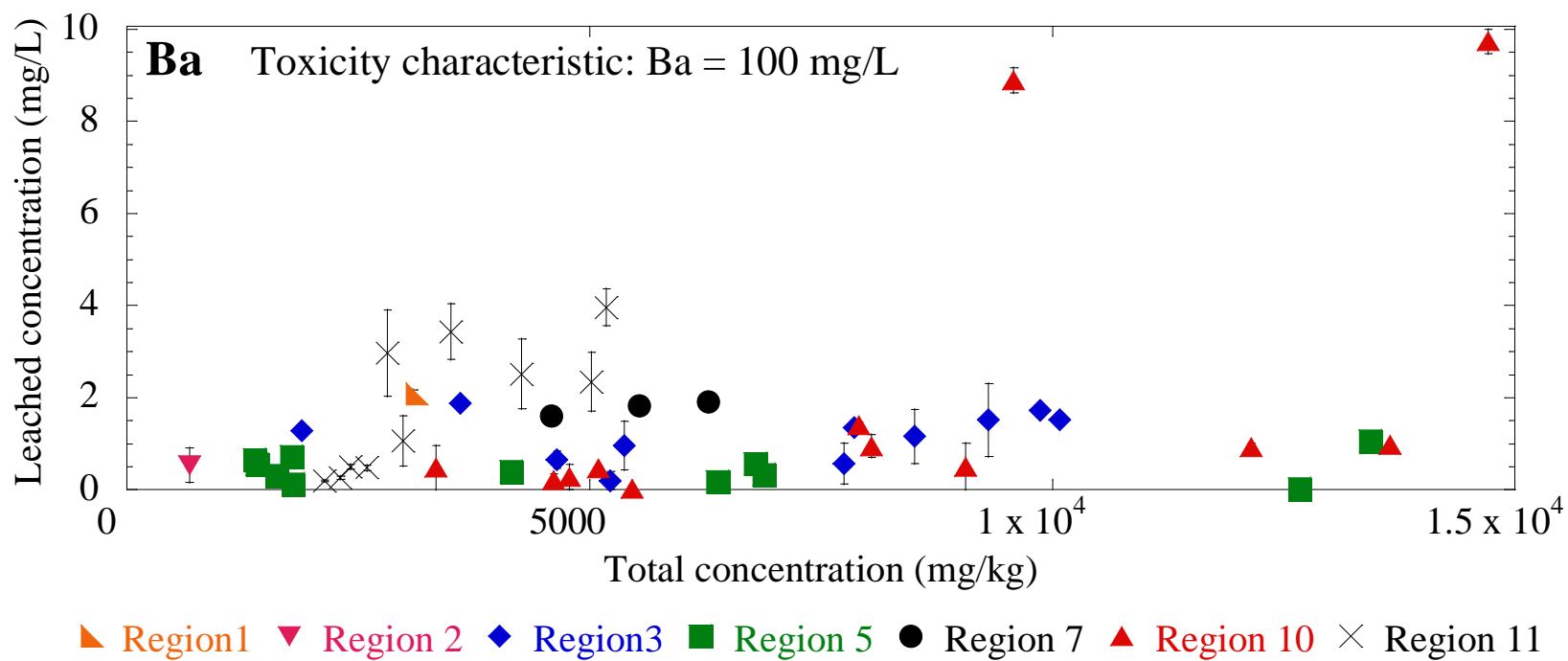


Figure A3. Leaching results from TCLP for Ba as a function of XRF results. Samples are extracted using Fluid #1 (0.1 N acetic acid, which has been adjusted with NaOH to an initial pH of 4.93 ± 0.05) or Fluid #2 (0.1 N acetic acid, which has an initial pH of 2.88 ± 0.05) based on the alkalinity of the waste material.

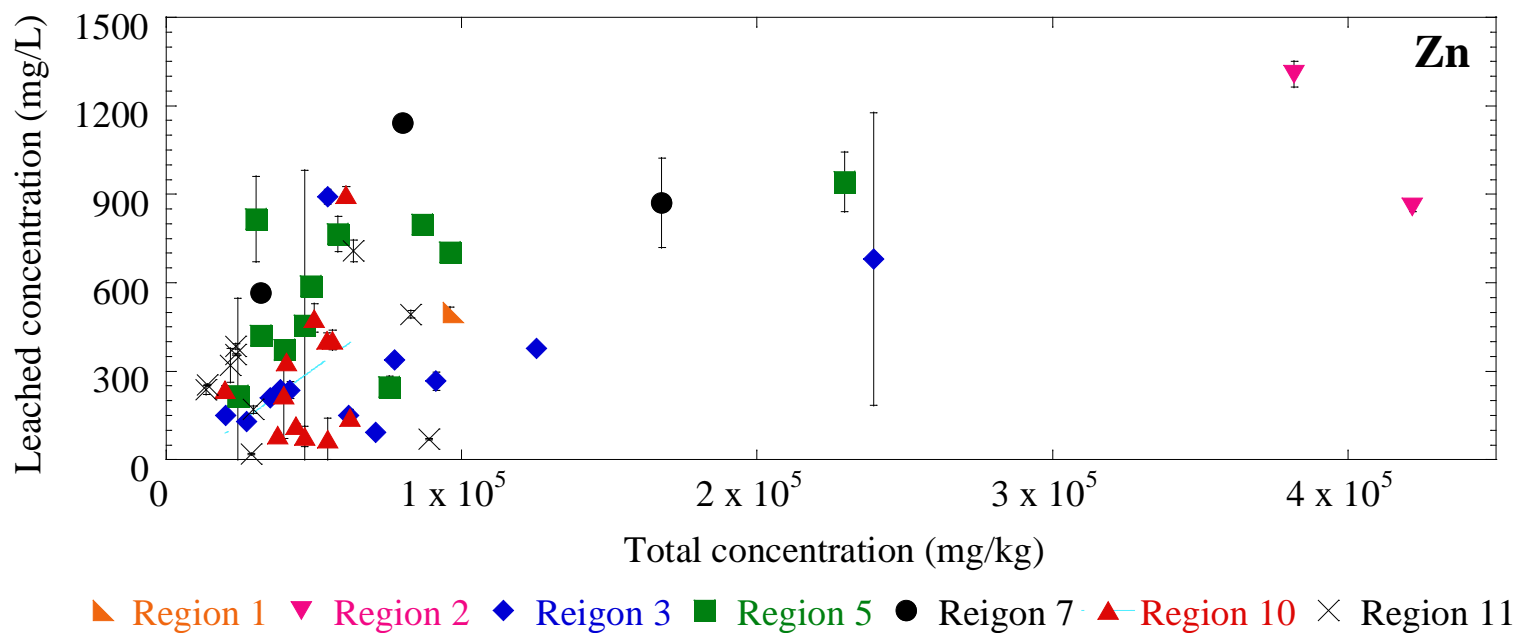


Figure A4. Leaching results from TCLP for Zn as a function of XRF results. Samples are extracted using Fluid #1 (0.1 N acetic acid, which has been adjusted with NaOH to an initial pH of 4.93 ± 0.05) or Fluid #2 (0.1 N acetic acid, which has an initial pH of 2.88 ± 0.05) based on the alkalinity of the waste material.

Appendix B

Modeling results for metal leaching

Pb; SSPC 6; Fe ≤24%

Regression Analysis: log Pb TCLP versus log Ba XRF, log Fe mg/Kg, ...

- * log Hg is (essentially) constant
- * log Hg has been removed from the equation.

The regression equation is

$$\begin{aligned}\log \text{ Pb TCLP mean} = & 14.0 - 1.72 \log \text{ Ba XRF} - 0.053 \log \text{ Fe mg/Kg} \\ & - 1.20 \log \text{ Cr XRF mean} + 2.27 \log \text{ mining and Soil mode Pb mea} \\ & - 4.15 \log \text{ Ca mean} + 1.66 \log \text{ Ti} - 1.64 \log \text{ Ag}\end{aligned}$$

| Predictor | Coef | SE Coef | T | P |
|---------------------------------|---------|---------|-------|-------|
| Constant | 13.97 | 12.31 | 1.13 | 0.270 |
| log Ba XRF | -1.7168 | 0.9883 | -1.74 | 0.098 |
| log Fe mg/Kg | -0.0531 | 0.6558 | -0.08 | 0.936 |
| log Cr XRF mean | -1.2022 | 0.5768 | -2.08 | 0.050 |
| log mining and Soil mode Pb mea | 2.2713 | 0.8164 | 2.78 | 0.011 |
| log Ca mean | -4.154 | 1.513 | -2.75 | 0.012 |
| log Ti | 1.664 | 1.159 | 1.44 | 0.167 |
| log Ag | -1.6403 | 0.8278 | -1.98 | 0.061 |

S = 0.657136 R-Sq = 54.5% R-Sq(adj) = 38.5%

Analysis of Variance

| Source | DF | SS | MS | F | P |
|----------------|----|---------|--------|------|-------|
| Regression | 7 | 10.3280 | 1.4754 | 3.42 | 0.014 |
| Residual Error | 20 | 8.6365 | 0.4318 | | |
| Total | 27 | 18.9646 | | | |

| Source | DF | Seq SS |
|---------------------------------|----|--------|
| log Ba XRF | 1 | 0.1512 |
| log Fe mg/Kg | 1 | 1.6015 |
| log Cr XRF mean | 1 | 0.0055 |
| log mining and Soil mode Pb mea | 1 | 4.4678 |
| log Ca mean | 1 | 2.1142 |
| log Ti | 1 | 0.2923 |
| log Ag | 1 | 1.6955 |

Unusual Observations

| | log Ba | log Pb | | | | |
|-----|--------|-----------|--------|--------|----------|----------|
| Obs | XRF | TCLP mean | Fit | SE Fit | Residual | St Resid |
| 20 | 3.89 | -2.051 | -1.894 | 0.611 | -0.157 | -0.65 X |
| 24 | 4.14 | -0.327 | -1.157 | 0.522 | 0.830 | 2.08R |

R denotes an observation with a large standardized residual.

X denotes an observation whose X value gives it large leverage.

Pb; SSPC 6; Fe >24%

Regression Analysis: log Pb TCLP versus log Fe mg/Kg, log Cr XRF m, ...

* log Hg is (essentially) constant
* log Hg has been removed from the equation.

The regression equation is

log Pb TCLP mean = - 13.2 - 2.68 log Fe mg/Kg - 2.18 log Cr XRF mean
+ 3.80 log mining and Soil mode Pb mea + 1.38 log Ti
+ 1.18 log Ag - 0.535 log Se + 2.11 log Soil & mining Zn ppm

| Predictor | Coef | SE Coef | T | P |
|---------------------------------|---------|---------|-------|-------|
| Constant | -13.24 | 13.71 | -0.97 | 0.346 |
| log Fe mg/Kg | -2.681 | 2.361 | -1.14 | 0.270 |
| log Cr XRF mean | -2.1836 | 0.6997 | -3.12 | 0.006 |
| log mining and Soil mode Pb mea | 3.797 | 1.883 | 2.02 | 0.058 |
| log Ti | 1.3829 | 0.7130 | 1.94 | 0.067 |
| log Ag | 1.178 | 1.076 | 1.09 | 0.287 |
| log Se | -0.5351 | 0.5659 | -0.95 | 0.356 |
| log Soil & mining Zn ppm | 2.1149 | 0.8013 | 2.64 | 0.016 |

S = 0.791618 R-Sq = 68.6% R-Sq(adj) = 57.0%

Analysis of Variance

| Source | DF | SS | MS | F | P |
|----------------|----|---------|--------|------|-------|
| Regression | 7 | 25.9617 | 3.7088 | 5.92 | 0.001 |
| Residual Error | 19 | 11.9065 | 0.6267 | | |
| Total | 26 | 37.8682 | | | |

| Source | DF | Seq SS |
|---------------------------------|----|---------|
| log Fe mg/Kg | 1 | 2.4669 |
| log Cr XRF mean | 1 | 0.9397 |
| log mining and Soil mode Pb mea | 1 | 14.5018 |
| log Ti | 1 | 0.5017 |
| log Ag | 1 | 0.0700 |
| log Se | 1 | 3.1160 |
| log Soil & mining Zn ppm | 1 | 4.3656 |

Unusual Observations

| | log Fe mg/Kg | log Pb TCLP mean | Fit | SE Fit | Residual | St Resid |
|--------|-----------------|---------------------|--------|--------|----------|----------|
| Obs 22 | 5.58 | -3.602 | -2.434 | 0.550 | -1.168 | -2.05R |

R denotes an observation with a large standardized residual.

* NOTE * All values in column are identical.

Pb; SSPC 10

General Regression Analysis: Pb TCLP mean versus Fe mg/kg, mining and S, ...

Box-Cox transformation of the response with rounded lambda = 0
The 95% CI for lambda is (-0.405, 0.355)

Regression Equation

$\ln(\text{Pb TCLP mean}) = -6.45868 + 2.78346\text{e-}006 \text{ Fe mg/kg} + 0.000460326 \text{ mining and Soil mode Pb mean pp} + 5.28451\text{e-}005 \text{ Ca mean} - 7.52988\text{e-}005 \text{ Ti mean}$

11 cases used, 9 cases contain missing values

Coefficients

| Term | Coef | SE Coef | T | P |
|---------------------------------|----------|---------|----------|-------|
| Constant | -6.45868 | 1.41240 | -4.57283 | 0.004 |
| Fe mg/kg | 0.00000 | 0.00000 | 1.31715 | 0.236 |
| mining and Soil mode Pb mean pp | 0.00046 | 0.00009 | 5.06752 | 0.002 |
| Ca mean | 0.00005 | 0.00002 | 2.15276 | 0.075 |
| Ti mean | -0.00008 | 0.00002 | -3.54014 | 0.012 |

Summary of Model

S = 0.738499 R-Sq = 88.67% R-Sq(adj) = 81.11%
PRESS = 14.7180 R-Sq(pred) = 49.03%

Analysis of Variance

| Source | DF | Seq SS | Adj SS | Adj MS | F |
|---------------------------------|----|---------|---------|---------|---------|
| Regression | 4 | 25.6058 | 25.6058 | 6.4015 | 11.7376 |
| Fe mg/kg | 1 | 2.8231 | 0.9462 | 0.9462 | 1.7349 |
| mining and Soil mode Pb mean pp | 1 | 14.6456 | 14.0053 | 14.0053 | 25.6798 |
| Ca mean | 1 | 1.3021 | 2.5275 | 2.5275 | 4.6344 |
| Ti mean | 1 | 6.8350 | 6.8350 | 6.8350 | 12.5326 |
| Error | 6 | 3.2723 | 3.2723 | 0.5454 | |
| Lack-of-Fit | 4 | 0.6984 | 0.6984 | 0.1746 | 0.1357 |
| Pure Error | 2 | 2.5739 | 2.5739 | 1.2869 | |
| Total | 10 | 28.8781 | | | |

| Source | P |
|---------------------------------|----------|
| Regression | 0.005325 |
| Fe mg/kg | 0.235854 |
| mining and Soil mode Pb mean pp | 0.002294 |
| Ca mean | 0.074820 |
| Ti mean | 0.012217 |
| Error | |
| Lack-of-Fit | 0.954444 |
| Pure Error | |
| Total | |

Fits and Diagnostics for Unusual Observations for Transformed Response

$\ln(\text{Pb})$

| | TCLP | | SE | | St |
|-----|-------|-----|-----|----------|-------|
| Obs | mean) | Fit | Fit | Residual | Resid |

Fits for Unusual Observations for Original Response

| | Pb | | |
|-----|------|-----------|---|
| | TCLP | | |
| Obs | mean | Fit | |
| 2 | * | 0.0048054 | X |

X denotes an observation whose X value gives it large leverage.

Cr; SSPC 6; Fe ≤24%

Regression Analysis: Cr TCLP versus Ba XRF, Fe mg/kg, ...

- * Hg is (essentially) constant
- * Hg has been removed from the equation.

The regression equation is

$$\begin{aligned}\text{Cr TCLP} = & -12.2 + 0.000510 \text{ Ba XRF} + 0.000019 \text{ Fe mg/kg} - 0.000681 \text{ Cr XRF mean} \\ & + 0.000063 \text{ mining and Soil mode Pb mean pp} + 0.000125 \text{ Ca mean} \\ & + 0.000109 \text{ Ti mean}\end{aligned}$$

| Predictor | Coef | SE Coef | T | P |
|---------------------------------|------------|------------|-------|-------|
| Constant | -12.214 | 3.009 | -4.06 | 0.001 |
| Ba XRF | 0.0005099 | 0.0001243 | 4.10 | 0.001 |
| Fe mg/kg | 0.00001922 | 0.00000501 | 3.83 | 0.001 |
| Cr XRF mean | -0.0006814 | 0.0002556 | -2.67 | 0.014 |
| mining and Soil mode Pb mean pp | 0.00006323 | 0.00002145 | 2.95 | 0.008 |
| Ca mean | 0.00012508 | 0.00004153 | 3.01 | 0.007 |
| Ti mean | 0.00010923 | 0.00006443 | 1.70 | 0.105 |

S = 1.49824 R-Sq = 58.8% R-Sq(adj) = 47.1%

Analysis of Variance

| Source | DF | SS | MS | F | P |
|----------------|----|---------|--------|------|-------|
| Regression | 6 | 67.374 | 11.229 | 5.00 | 0.003 |
| Residual Error | 21 | 47.139 | 2.245 | | |
| Total | 27 | 114.513 | | | |

| Source | DF | Seq SS |
|---------------------------------|----|--------|
| Ba XRF | 1 | 19.643 |
| Fe mg/kg | 1 | 20.652 |
| Cr XRF mean | 1 | 0.001 |
| mining and Soil mode Pb mean pp | 1 | 4.440 |
| Ca mean | 1 | 16.187 |
| Ti mean | 1 | 6.451 |

Unusual Observations

| Obs | Ba XRF | Cr TCLP | Fit | SE Fit | Residual | St Resid |
|-----|--------|---------|-------|--------|----------|----------|
| 24 | 13656 | 9.516 | 6.858 | 1.134 | 2.658 | 2.71R |
| 25 | 7908 | 5.241 | 2.548 | 0.677 | 2.694 | 2.02R |

R denotes an observation with a large standardized residual.

Cr; SSPC 6; Fe >24%

Residual Plots for Cr TCLP

* NOTE * All values in column are identical.

Regression Analysis: Cr TCLP versus Fe mg/kg, Cr XRF mean, ...

* Hg is (essentially) constant

* Hg has been removed from the equation.

The regression equation is

$$\text{Cr TCLP} = -0.80 + 0.000006 \text{ Fe mg/kg} - 0.000480 \text{ Cr XRF mean} - 0.000019 \text{ Ca mean} \\ + 0.0417 \text{ Se} + 0.00621 \text{ Cd} + 0.000128 \text{ As}$$

| Predictor | Coef | SE Coef | T | P |
|-------------|-------------|------------|-------|-------|
| Constant | -0.801 | 1.037 | -0.77 | 0.449 |
| Fe mg/kg | 0.00000587 | 0.00000264 | 2.22 | 0.038 |
| Cr XRF mean | -0.0004803 | 0.0001314 | -3.65 | 0.002 |
| Ca mean | -0.00001922 | 0.00001536 | -1.25 | 0.225 |
| Se | 0.04169 | 0.01256 | 3.32 | 0.003 |
| Cd | 0.006209 | 0.007916 | 0.78 | 0.442 |
| As | 0.0001281 | 0.0001057 | 1.21 | 0.239 |

S = 0.815234 R-Sq = 59.8% R-Sq(adj) = 47.7%

Analysis of Variance

| Source | DF | SS | MS | F | P |
|----------------|----|---------|--------|------|-------|
| Regression | 6 | 19.7734 | 3.2956 | 4.96 | 0.003 |
| Residual Error | 20 | 13.2921 | 0.6646 | | |
| Total | 26 | 33.0655 | | | |

| Source | DF | Seq SS |
|-------------|----|---------|
| Fe mg/kg | 1 | 0.0082 |
| Cr XRF mean | 1 | 0.0144 |
| Ca mean | 1 | 3.9491 |
| Se | 1 | 13.5526 |
| Cd | 1 | 1.2721 |
| As | 1 | 0.9769 |

Unusual Observations

| Obs | Fe mg/kg | Cr TCLP | Fit | SE Fit | Residual | St Resid |
|-----|----------|---------|--------|--------|----------|----------|
| 4 | 267060 | 1.096 | -0.600 | 0.373 | 1.695 | 2.34R |
| 14 | 315263 | 5.625 | 4.086 | 0.702 | 1.539 | 3.72R |

R denotes an observation with a large standardized residual.

Cr; SSPC 10

Regression Analysis: Cr TCLP versus Soil & mining Zn ppm, Fe mg/kg, ...

- * Ag is highly correlated with other X variables
- * Ag has been removed from the equation.

The regression equation is

$$\begin{aligned} \text{Cr TCLP} = & 12.4 - 0.000022 \text{ Soil \& mining Zn ppm} - 0.000032 \text{ Fe mg/kg} \\ & + 0.0077 \text{ Cr XRF mean} + 0.000053 \text{ mining and Soil mode Pb mean pp} \\ & - 0.000198 \text{ Ca mean} - 0.000038 \text{ Ti mean} \end{aligned}$$

8 cases used, 12 cases contain missing values

| Predictor | Coef | SE Coef | T | P |
|---------------------------------|-------------|------------|-------|-------|
| Constant | 12.38 | 19.46 | 0.64 | 0.639 |
| Soil & mining Zn ppm | -0.00002232 | 0.00003736 | -0.60 | 0.657 |
| Fe mg/kg | -0.00003236 | 0.00005264 | -0.61 | 0.649 |
| Cr XRF mean | 0.00771 | 0.01276 | 0.60 | 0.654 |
| mining and Soil mode Pb mean pp | 0.0000529 | 0.0001667 | 0.32 | 0.804 |
| Ca mean | -0.0001983 | 0.0003084 | -0.64 | 0.636 |
| Ti mean | -0.00003833 | 0.00007606 | -0.50 | 0.703 |

S = 0.694055 R-Sq = 44.9% R-Sq(adj) = 0.0%

Analysis of Variance

| Source | DF | SS | MS | F | P |
|----------------|----|--------|--------|------|-------|
| Regression | 6 | 0.3929 | 0.0655 | 0.14 | 0.965 |
| Residual Error | 1 | 0.4817 | 0.4817 | | |
| Total | 7 | 0.8746 | | | |

| Source | DF | Seq SS |
|---------------------------------|----|--------|
| Soil & mining Zn ppm | 1 | 0.0900 |
| Fe mg/kg | 1 | 0.0003 |
| Cr XRF mean | 1 | 0.0387 |
| mining and Soil mode Pb mean pp | 1 | 0.0425 |
| Ca mean | 1 | 0.0991 |
| Ti mean | 1 | 0.1223 |

Unusual Observations

| Obs | Soil & mining Zn ppm | Cr TCLP | Fit | SE Fit | Residual | St Resid |
|-----|----------------------|---------|--------|--------|----------|----------|
| 3 | 46847 | * | -0.325 | 1.125 | * | * X |
| 4 | 24237 | * | -4.383 | 7.585 | * | * X |
| 5 | 40033 | * | 0.014 | 0.694 | * | * X |
| 6 | 229523 | * | -6.478 | 11.168 | * | * X |
| 7 | 30363 | * | -5.193 | 8.690 | * | * X |
| 8 | 75547 | 0.433 | 0.433 | 0.694 | -0.000 | * X |
| 9 | 48987 | * | 0.008 | 0.694 | * | * X |
| 10 | 86590 | * | -3.494 | 6.417 | * | * X |
| 11 | 32043 | 0.020 | 0.020 | 0.694 | -0.000 | * X |
| 12 | 58217 | * | -6.851 | 11.296 | * | * X |

| | | | | | | |
|----|--------|-------|--------|--------|--------|-----|
| 13 | 96237 | * | 0.033 | 0.694 | * | * X |
| 15 | 425507 | 0.012 | 0.012 | 0.694 | 0.000 | * X |
| 16 | 40033 | 0.014 | 0.014 | 0.694 | -0.000 | * X |
| 17 | 48987 | 0.008 | 0.008 | 0.694 | -0.000 | * X |
| 18 | 32043 | * | 0.020 | 0.694 | * | * X |
| 19 | 58217 | * | -6.851 | 11.296 | * | * X |
| 20 | 96237 | 0.033 | 0.033 | 0.694 | -0.000 | * X |

X denotes an observation whose X value gives it large leverage.

Ba; SSPC 6; Fe ≤24%

Residual Plots for Ba TCLP

General Regression Analysis: Ba TCLP versus Fe mg/kg, mining and S, ...

* NOTE * Hg cannot be estimated and has been removed.

Box-Cox transformation of the response with rounded lambda = 0.225200
The 95% CI for lambda is (0.005, 0.465)

Regression Equation

Ba TCLP^{0.2252} = 1.92329 - 1.89806e-006 Fe mg/kg - 3.56777e-006 mining and
Soil mode Pb mean pp - 1.81219e-005 Ca mean + 2.45514e-005
Ti mean + 0.0232546 Ag - 0.0127287 Se - 0.0136753 Cd

Coefficients

| Term | Coef | SE Coef | T | P |
|---------------------------------|----------|----------|----------|-------|
| Constant | 1.92329 | 0.305617 | 6.29313 | 0.000 |
| Fe mg/kg | -0.00000 | 0.000001 | -2.51207 | 0.021 |
| mining and Soil mode Pb mean pp | -0.00000 | 0.000003 | -1.37978 | 0.183 |
| Ca mean | -0.00002 | 0.000005 | -3.91766 | 0.001 |
| Ti mean | 0.00002 | 0.000009 | 2.64555 | 0.016 |
| Ag | 0.02325 | 0.009242 | 2.51608 | 0.021 |
| Se | -0.01273 | 0.005501 | -2.31394 | 0.031 |
| Cd | -0.01368 | 0.004915 | -2.78211 | 0.012 |

Summary of Model

S = 0.192262 R-Sq = 56.46% R-Sq(adj) = 41.23%
PRESS = 1.69019 R-Sq(pred) = 0.47%

Analysis of Variance

| Source | DF | Seq SS | Adj SS | Adj MS | F |
|---------------------------------|----|---------|----------|----------|---------|
| Regression | 7 | 0.95885 | 0.958848 | 0.136978 | 3.7057 |
| Fe mg/kg | 1 | 0.11949 | 0.233265 | 0.233265 | 6.3105 |
| mining and Soil mode Pb mean pp | 1 | 0.03814 | 0.070372 | 0.070372 | 1.9038 |
| Ca mean | 1 | 0.32986 | 0.567333 | 0.567333 | 15.3480 |
| Ti mean | 1 | 0.13513 | 0.258713 | 0.258713 | 6.9990 |
| Ag | 1 | 0.00400 | 0.234009 | 0.234009 | 6.3306 |
| Se | 1 | 0.04612 | 0.197920 | 0.197920 | 5.3543 |
| Cd | 1 | 0.28611 | 0.286112 | 0.286112 | 7.7402 |
| Error | 20 | 0.73929 | 0.739292 | 0.036965 | |
| Lack-of-Fit | 12 | 0.51592 | 0.515922 | 0.042994 | 1.5398 |
| Pure Error | 8 | 0.22337 | 0.223369 | 0.027921 | |
| Total | 27 | 1.69814 | | | |

| Source | P |
|---------------------------------|----------|
| Regression | 0.009912 |
| Fe mg/kg | 0.020693 |
| mining and Soil mode Pb mean pp | 0.182888 |
| Ca mean | 0.000853 |
| Ti mean | 0.015516 |
| Ag | 0.020516 |

| | |
|-------------|----------|
| Se | 0.031425 |
| Cd | 0.011503 |
| Error | |
| Lack-of-Fit | 0.275250 |
| Pure Error | |
| Total | |

Fits and Diagnostics for Unusual Observations for Transformed Response

| | Ba | | | | | |
|-----|------------------------|----------|----------|-----------|----------|---|
| Obs | TCLP ^{0.2252} | Fit | SE Fit | Residual | St Resid | |
| 28 | 0.690386 | 0.968790 | 0.138065 | -0.278404 | -2.08073 | R |

Fits for Unusual Observations for Original Response

| Obs | Ba TCLP | Fit | |
|-----|---------|----------|---|
| 28 | 0.19297 | 0.868665 | R |

R denotes an observation with a large standardized residual.

Ba; SSPC 6; Fe >24%

Regression Analysis: Ba TCLP versus Ba XRF, Cr XRF mean, ...

- * Hg is (essentially) constant
- * Hg has been removed from the equation.

The regression equation is

$$\text{Ba TCLP} = 2.69 - 0.000079 \text{ Ba XRF} - 0.000030 \text{ Cr XRF mean} - 0.000032 \text{ Ca mean} \\ - 0.000024 \text{ Ti mean} - 0.0167 \text{ Ag} + 0.0049 \text{ Se} + 0.0140 \text{ Cd} - 0.000037 \text{ As}$$

| Predictor | Coef | SE Coef | T | P |
|-------------|-------------|------------|-------|-------|
| Constant | 2.685 | 1.106 | 2.43 | 0.026 |
| Ba XRF | -0.00007926 | 0.00006155 | -1.29 | 0.214 |
| Cr XRF mean | -0.0000299 | 0.0001358 | -0.22 | 0.828 |
| Ca mean | -0.00003193 | 0.00001654 | -1.93 | 0.069 |
| Ti mean | -0.00002425 | 0.00002422 | -1.00 | 0.330 |
| Ag | -0.01671 | 0.03646 | -0.46 | 0.652 |
| Se | 0.00492 | 0.01156 | 0.43 | 0.675 |
| Cd | 0.01399 | 0.02327 | 0.60 | 0.555 |
| As | -0.0000365 | 0.0001100 | -0.33 | 0.744 |

S = 0.664481 R-Sq = 43.4% R-Sq(adj) = 18.3%

Analysis of Variance

| Source | DF | SS | MS | F | P |
|----------------|----|---------|--------|------|-------|
| Regression | 8 | 6.0973 | 0.7622 | 1.73 | 0.160 |
| Residual Error | 18 | 7.9476 | 0.4415 | | |
| Total | 26 | 14.0449 | | | |

| Source | DF | Seq SS |
|-------------|----|--------|
| Ba XRF | 1 | 0.5918 |
| Cr XRF mean | 1 | 0.4345 |
| Ca mean | 1 | 4.3894 |
| Ti mean | 1 | 0.2954 |
| Ag | 1 | 0.0710 |
| Se | 1 | 0.1121 |
| Cd | 1 | 0.1543 |
| As | 1 | 0.0487 |

Ba; SSPC 10;

General Regression Analysis: Ba TCLP versus Ba XRF, Soil & minin, Fe mg/kg, ...

Box-Cox transformation of the response with rounded lambda = 0.5
The 95% CI for lambda is (-0.075, 1.015)

Regression Equation

Ba TCLP^{0.5} = -0.662387 - 2.17667e-005 Ba XRF + 2.62614e-006 Soil & mining Zn ppm + 3.36626e-006 Fe mg/kg + 0.000111838 mining and Soil mode Pb mean pp - 1.14467e-005 Ca mean - 0.00140021 As

19 cases used, 1 cases contain missing values

Coefficients

| Term | Coef | SE Coef | T | P |
|---------------------------------|-----------|----------|----------|-------|
| Constant | -0.662387 | 0.510234 | -1.29820 | 0.219 |
| Ba XRF | -0.000022 | 0.000010 | -2.11097 | 0.056 |
| Soil & mining Zn ppm | 0.000003 | 0.000001 | 1.84907 | 0.089 |
| Fe mg/kg | 0.000003 | 0.000001 | 2.90043 | 0.013 |
| mining and Soil mode Pb mean pp | 0.000112 | 0.000028 | 4.02088 | 0.002 |
| Ca mean | -0.000011 | 0.000005 | -2.15883 | 0.052 |
| As | -0.001400 | 0.000561 | -2.49721 | 0.028 |

Summary of Model

S = 0.151198 R-Sq = 69.72% R-Sq(adj) = 54.58%
PRESS = 0.737005 R-Sq(pred) = 18.65%

Analysis of Variance

| Source | DF | Seq SS | Adj SS | Adj MS | F |
|---------------------------------|----|----------|----------|----------|---------|
| Regression | 6 | 0.631592 | 0.631592 | 0.105265 | 4.6046 |
| Ba XRF | 1 | 0.024745 | 0.101872 | 0.101872 | 4.4562 |
| Soil & mining Zn ppm | 1 | 0.009376 | 0.078163 | 0.078163 | 3.4191 |
| Fe mg/kg | 1 | 0.010538 | 0.192317 | 0.192317 | 8.4125 |
| mining and Soil mode Pb mean pp | 1 | 0.419774 | 0.369603 | 0.369603 | 16.1675 |
| Ca mean | 1 | 0.024597 | 0.106544 | 0.106544 | 4.6606 |
| As | 1 | 0.142562 | 0.142562 | 0.142562 | 6.2360 |
| Error | 12 | 0.274331 | 0.274331 | 0.022861 | |
| Lack-of-Fit | 6 | 0.127487 | 0.127487 | 0.021248 | 0.8682 |
| Pure Error | 6 | 0.146844 | 0.146844 | 0.024474 | |
| Total | 18 | 0.905923 | | | |

| Source | P |
|---------------------------------|----------|
| Regression | 0.011867 |
| Ba XRF | 0.056434 |
| Soil & mining Zn ppm | 0.089222 |
| Fe mg/kg | 0.013316 |
| mining and Soil mode Pb mean pp | 0.001697 |
| Ca mean | 0.051819 |
| As | 0.028059 |
| Error | |
| Lack-of-Fit | 0.565933 |
| Pure Error | |

Total

Fits and Diagnostics for Unusual Observations for Transformed Response

No unusual observations

Zn; SSPC 6; Fe ≤24%

Regression Analysis: Zn TCLP versus Soil & mining Zn, Cr XRF mean, ...

- * Hg is (essentially) constant
- * Hg has been removed from the equation.

The regression equation is

$$\begin{aligned}\text{Zn TCLP} = & 436 + 0.00143 \text{ Soil \& mining Zn ppm} - 0.164 \text{ Cr XRF mean} \\ & - 0.0108 \text{ mining and Soil mode Pb mean pp} + 0.0460 \text{ Ti mean} - 6.17 \text{ Ag} \\ & - 17.1 \text{ Se} + 0.268 \text{ As}\end{aligned}$$

| Predictor | Coef | SE Coef | T | P |
|---------------------------------|-----------|----------|-------|-------|
| Constant | 435.7 | 140.9 | 3.09 | 0.006 |
| Soil & mining Zn ppm | 0.001431 | 0.001069 | 1.34 | 0.196 |
| Cr XRF mean | -0.16398 | 0.04095 | -4.00 | 0.001 |
| mining and Soil mode Pb mean pp | -0.010841 | 0.003396 | -3.19 | 0.005 |
| Ti mean | 0.04604 | 0.01214 | 3.79 | 0.001 |
| Ag | -6.175 | 3.953 | -1.56 | 0.134 |
| Se | -17.084 | 6.536 | -2.61 | 0.017 |
| As | 0.26752 | 0.07670 | 3.49 | 0.002 |

S = 185.033 R-Sq = 69.6% R-Sq(adj) = 59.0%

Analysis of Variance

| Source | DF | SS | MS | F | P |
|----------------|----|---------|--------|------|-------|
| Regression | 7 | 1568061 | 224009 | 6.54 | 0.000 |
| Residual Error | 20 | 684748 | 34237 | | |
| Total | 27 | 2252808 | | | |

| Source | DF | Seq SS |
|---------------------------------|----|--------|
| Soil & mining Zn ppm | 1 | 583115 |
| Cr XRF mean | 1 | 247783 |
| mining and Soil mode Pb mean pp | 1 | 3481 |
| Ti mean | 1 | 190321 |
| Ag | 1 | 118284 |
| Se | 1 | 8572 |
| As | 1 | 416503 |

Unusual Observations

| | | Soil & mining | | | | | |
|-----|--------|---------------|-------|--------|----------|----------|--|
| Obs | Zn ppm | Zn TCLP | Fit | SE Fit | Residual | St Resid | |
| 13 | 80200 | 1141.3 | 558.9 | 51.4 | 582.5 | 3.28R | |

R denotes an observation with a large standardized residual.

Zn; SSPC 6; Fe >24%

Regression Analysis: log Zn TCLP versus log Soil & m, log Fe mg/Kg, ...

* log Hg is (essentially) constant
* log Hg has been removed from the equation.

The regression equation is

log Zn TCLP = 8.65 + 0.864 log Soil & mining Zn ppm - 1.58 log Fe mg/Kg
- 0.653 log Cr XRF mean - 0.347 log Ca mean + 0.358 log Ti
+ 0.443 log Cd

| Predictor | Coef | SE Coef | T | P |
|--------------------------|---------|---------|-------|-------|
| Constant | 8.651 | 3.054 | 2.83 | 0.010 |
| log Soil & mining Zn ppm | 0.8643 | 0.2170 | 3.98 | 0.001 |
| log Fe mg/Kg | -1.5802 | 0.5279 | -2.99 | 0.007 |
| log Cr XRF mean | -0.6534 | 0.1833 | -3.57 | 0.002 |
| log Ca mean | -0.3471 | 0.2321 | -1.50 | 0.150 |
| log Ti | 0.3581 | 0.1905 | 1.88 | 0.075 |
| log Cd | 0.4428 | 0.1755 | 2.52 | 0.020 |

S = 0.225197 R-Sq = 66.3% R-Sq(adj) = 56.1%

Analysis of Variance

| Source | DF | SS | MS | F | P |
|----------------|----|---------|---------|------|-------|
| Regression | 6 | 1.99212 | 0.33202 | 6.55 | 0.001 |
| Residual Error | 20 | 1.01428 | 0.05071 | | |
| Total | 26 | 3.00640 | | | |

| Source | DF | Seq SS |
|--------------------------|----|---------|
| log Soil & mining Zn ppm | 1 | 0.28592 |
| log Fe mg/Kg | 1 | 0.77527 |
| log Cr XRF mean | 1 | 0.04424 |
| log Ca mean | 1 | 0.38373 |
| log Ti | 1 | 0.18025 |
| log Cd | 1 | 0.32272 |

Unusual Observations

| Obs | log Soil & mining Zn ppm | log Zn TCLP | Fit | SE Fit | Residual | St Resid |
|-----|--------------------------------|----------------|--------|--------|----------|----------|
| 12 | 4.96 | 3.0658 | 2.6155 | 0.1201 | 0.4503 | 2.36R |

R denotes an observation with a large standardized residual.

Zn; SSPC 10

General Regression Analysis: Zn TCLP versus Ba XRF, Soil & mining Zn, Ag, As

Box-Cox transformation of the response with rounded lambda = 0.5
The 95% CI for lambda is (-0.125, 1.325)

Regression Equation

Zn TCLP^{0.5} = 0.396622 - 0.00049622 Ba XRF + 5.25726e-005 Soil & mining Zn ppm + 4.79214 Ag - 0.0145836 As

19 cases used, 1 cases contain missing values

Coefficients

| Term | Coef | SE Coef | T | P |
|----------------------|----------|---------|----------|-------|
| Constant | 0.39662 | 7.75561 | 0.05114 | 0.960 |
| Ba XRF | -0.00050 | 0.00034 | -1.46689 | 0.165 |
| Soil & mining Zn ppm | 0.00005 | 0.00001 | 4.16802 | 0.001 |
| Ag | 4.79214 | 1.82091 | 2.63173 | 0.020 |
| As | -0.01458 | 0.00667 | -2.18574 | 0.046 |

Summary of Model

S = 3.71799 R-Sq = 69.60% R-Sq(adj) = 60.91%
PRESS = 340.591 R-Sq(pred) = 46.50%

Analysis of Variance

| Source | DF | Seq SS | Adj SS | Adj MS | F | P |
|----------------------|----|---------|---------|---------|---------|----------|
| Regression | 4 | 443.077 | 443.077 | 110.769 | 8.0131 | 0.001409 |
| Ba XRF | 1 | 12.650 | 29.745 | 29.745 | 2.1518 | 0.164507 |
| Soil & mining Zn ppm | 1 | 331.923 | 240.147 | 240.147 | 17.3724 | 0.000948 |
| Ag | 1 | 32.463 | 95.741 | 95.741 | 6.9260 | 0.019720 |
| As | 1 | 66.041 | 66.041 | 66.041 | 4.7775 | 0.046321 |
| Error | 14 | 193.528 | 193.528 | 13.823 | | |
| Lack-of-Fit | 8 | 138.422 | 138.422 | 17.303 | 1.8839 | 0.227975 |
| Pure Error | 6 | 55.107 | 55.107 | 9.184 | | |
| Total | 18 | 636.606 | | | | |

Fits and Diagnostics for Unusual Observations for Transformed Response

| Obs | Zn TCLP ^{0.5} | Fit | SE Fit | Residual | St Resid |
|-----|------------------------|---------|---------|----------|----------|
| 8 | 15.7395 | 24.3687 | 1.32052 | -8.62916 | -2.48279 |

R

Fits for Unusual Observations for Original Response

| Obs | Zn TCLP | Fit |
|-----|---------|---------|
| 8 | 247.733 | 593.834 |

R

R denotes an observation with a large standardized residual.

Deliverable for Task 8: Project Presentations and Outreach

**Submitted
to
Carl Kochersberger
Environmental Science Bureau
Hazardous Materials and Asbestos Unit
Pod 4-1
New York State Department of Transportation
50 Wolf Road
Albany, NY 12232**

December 2013

Project Presentations and Outreach

The findings and outreach for this project were conveyed through in person meetings, conference calls, and reports. From November 2009 to December 2013, nine task deliverables have been submitted to New York State Department of Transportation (NYSDOT). During this period, the Lisa Axe and Zhan Shu from NJIT have met with the NYSDOT Project Manager, Technical Working Group (TWG), and other interested parties, at prescheduled meetings to present project findings and provide overall outreach:

- May 10th, 2010, XRF training was provided for NYSDOT personnel (Task 3).
- September 2nd, 2010, a conference call was set up with Region 8 construction personnel. The sampling plan and approach was further discussed (Task 1).
- August 9th, 2011, a preliminary report on the sampling effort was submitted and the preliminary results were discussed through a conference call with NYSDOT personnel. Because of the presence of iron, which is common in bridge paint waste, impacted metal leaching, additional analyses were identified for inclusion in the study. Specifically, multiple extraction procedure (MEP) and sequential extraction (SE) were proposed to investigate long-term mobility of the trace metals in paint waste (Tasks 2, 4 and 5).
- April 12th, 2012, a conference call was set up with NYSDOT to discuss the findings and the obtain input for Tasks 4 and 5.
- January 25th, 2013, the Lisa Axe and Zhan Shu from NJIT visited the NYSDOT and UTRC Team to present the status of the project on work being conducted and obtain input on Tasks 1 through 5.

- June 20th, 2013, the content of the Task 6 was discussed with the project manager through a conference call and a presentation with an overview of the results. The status of the project was also discussed and input was received.
- October 4th, 2013, the drafts for Tasks 7 and 9 were submitted to the project manager. The tasks were discussed with the project manager through a conference call and a presentation with an overview of the results. The status of the project was also discussed and input was received.
- December 4th, 2013, the final report presentation was provided to NYSDOT personnel to present project findings and receive input (Appendix A).



UTRC/NYSDOT project final report: Field Methods for Determining Lead Content in Bridge Paint Removal Waste

Zhan Shu¹, Lisa Axe¹, Kauser Jahan² and Kandalam V. Ramanujachary³

¹Department of Civil and Environmental Engineering
New Jersey Institute of Technology, Newark, NJ

²Department of Civil and Environmental Engineering,

³Department of Chemistry and Biochemistry,
Rowan University, Glassboro, NJ

December 2013



Outline

- Background & Motivation
- Objectives
- Sampling Approach
- Methods
- Results
- Conclusion
- Recommendation
- Accomplishments



Background & Motivation

- The majority of the steel bridges in the interstate system were constructed between 1950 and 1980. All steel bridges were protected from corrosion by paint coatings containing lead and chromate.
- Other elemental compounds of arsenic, barium, cadmium, mercury, selenium, and silver were used in paint as pigments and preservatives as well.
- In New York state, lead-based paint has been prohibited from commercial use since 1989.
- As the use of lead paint declined, substantial zinc-based paint has been applied for corrosion protection.



Background & Motivation

- Paint removal from bridges is a significant issue because of the potential release of contaminants, and the consequent impact to human health and the environment.
- The New York State Department of Transportation (NYSDOT) has previously used a conservative approach of classifying all paint waste as hazardous.
- There is no rapid and cost-effective method for classifying paint waste in situ.





Objectives

- Evaluate the effectiveness of the field-portable X-ray fluorescence (FP-XRF) to reliably characterize the hazardous nature of the paint waste.
- Use the Hach field portable spectrophotometer to detect the lead levels in bridge wash water.
- Investigate the mechanism responsible for metal leaching.
- Understand key variables needed for a statistical model.
- Develop a model that can predict the leachability of metals in paint waste generated during bridge rehabilitation.



Sampling Approach

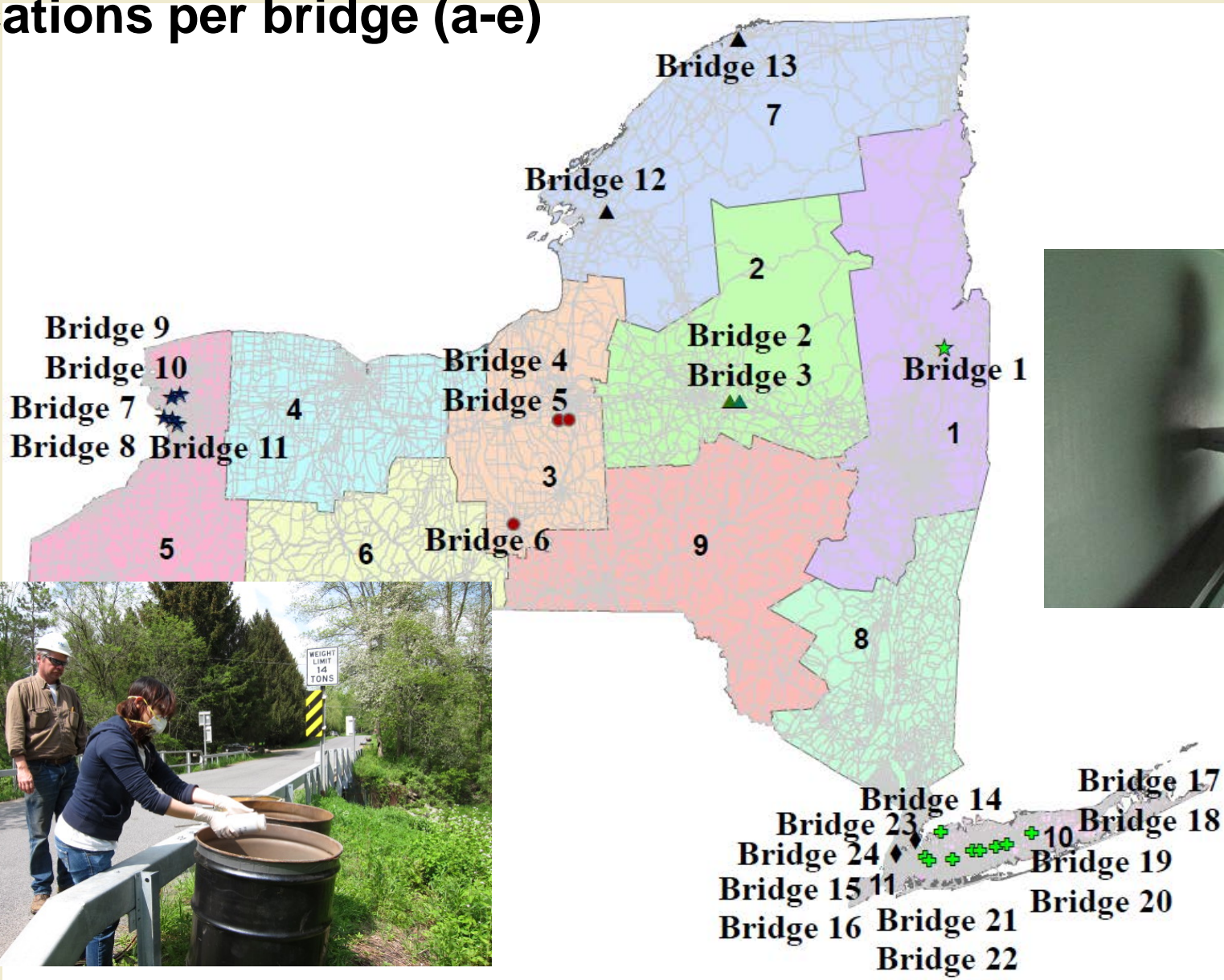
- Bridges in NY repainted after 1989 are tested with a one-sided t-test:
 - $H_0: \mu_0 < 5 \text{ mg/L}$
 - $H_1: \mu_0 \geq 5 \text{ mg/L}$
- Power = $P(\text{rejecting } H_0 \mid H_0 \text{ is false})$

$$= P(t > t_\alpha - \frac{\Delta}{\sigma/\sqrt{n}})$$

$$\alpha = 0.95$$
- A sample size is needed to control the probability that a correct action will be taken.
- Based on sample size estimation, 24 bridges were randomly selected from those repainted after 1989.



NY Bridges Sampled in the Study: 24 bridges and 5 sample locations per bridge (a-e)





Methods

Paint Analysis

- NITON XLp-300 FP-XRF analyzer
- NITON XL3t-600 FP-XRF analyzer



Leaching Experiments

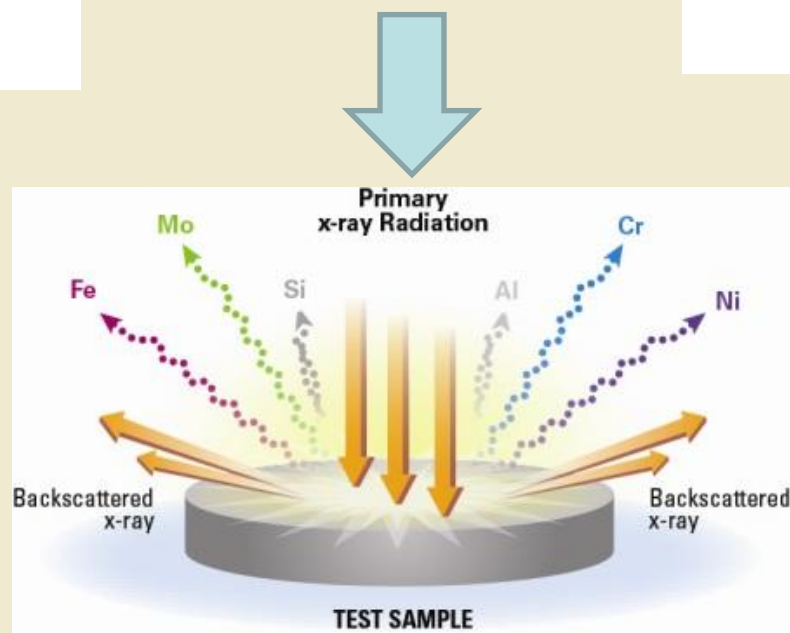
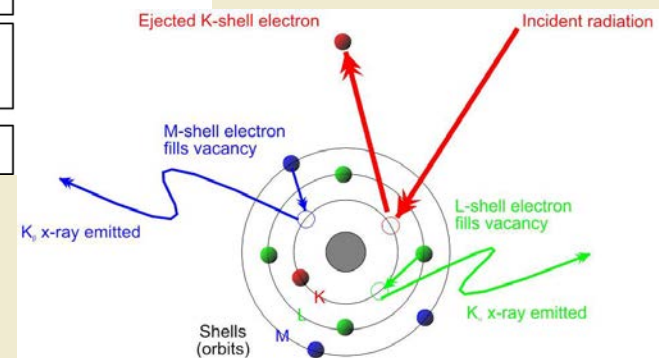
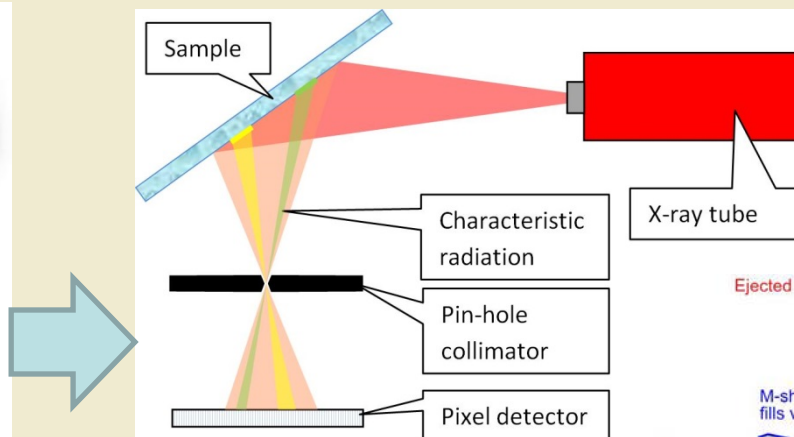
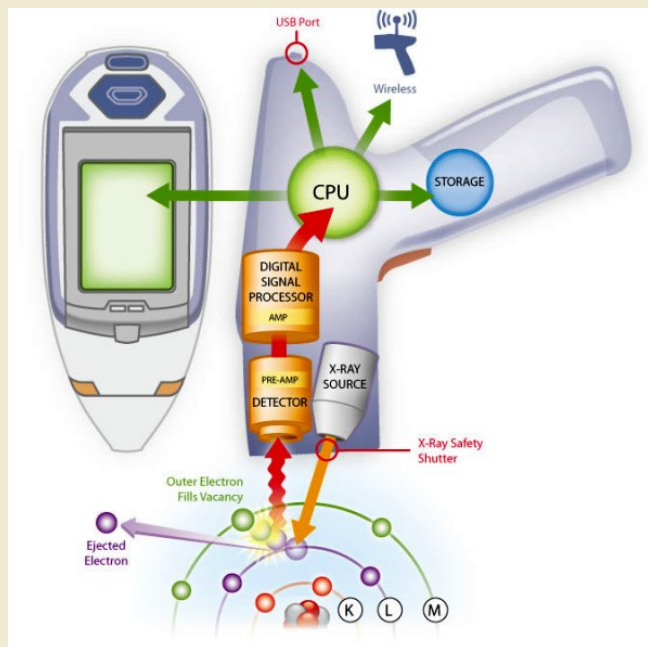
- Toxicity Characteristic Leaching Procedure (TCLP) U.S. EPA Method 1311
- Multiple Extraction Procedure (MEP) Methods 1310B and 1320 of the U.S. EPA SW-846
- Sequential Extraction Procedure (SE)

Mineralogy and Morphology

- PANalytical Empyrean x-ray diffraction (XRD) system
- Field emission scanning electron microscopy (FE-SEM) along with the energy dispersive X-ray micro analyzer (EDX)

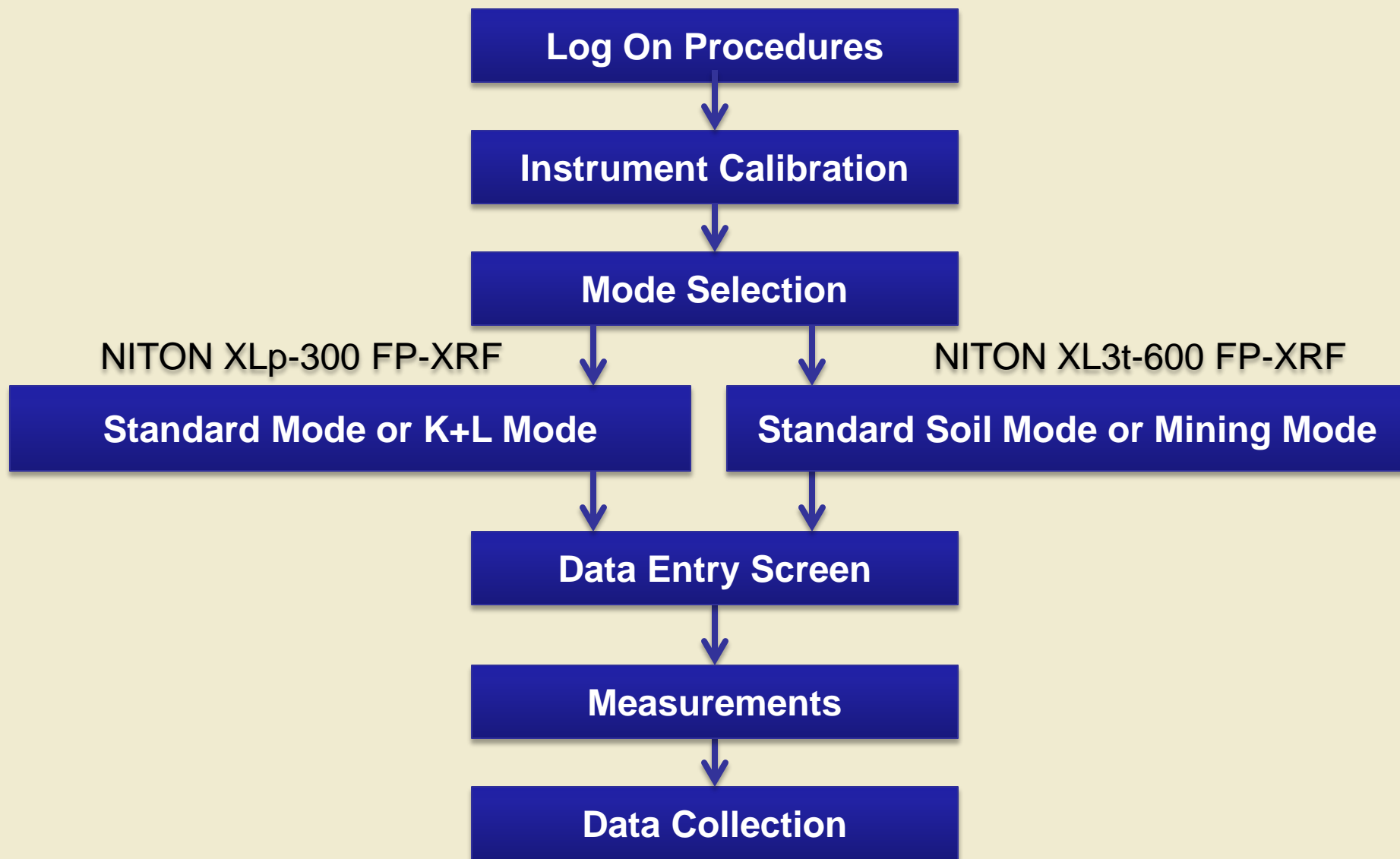


FP-XRF analysis





Standard operating procedure (SOP) for FP-XRF

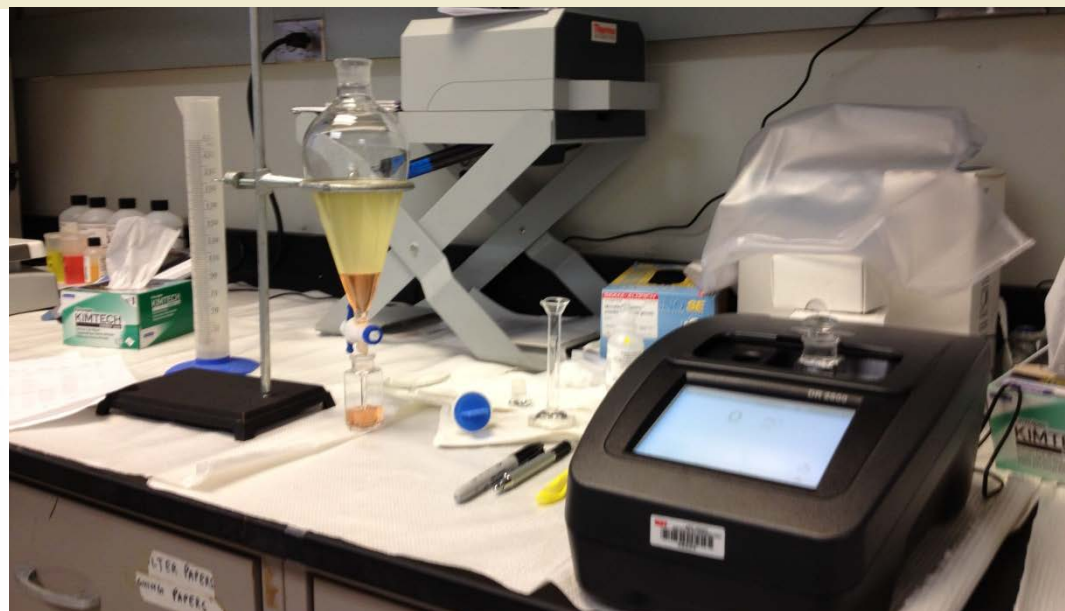




Methods (continued)

Wash Water Analysis

- Dissolved lead analysis: Hach field spectrophotometer Method 8033
- Total lead analysis: digestion with EPA SW-846 Method 3010A followed by analysis with the Hach field spectrophotometer





Methods (continued)

Mechanistic Modeling

- The diffuse layer model (DLM) was used to describe the metal adsorption over the pH of 4.5 to 7.
- Ferrihydrite (hydrous ferric oxide, HFO) is dominant iron oxide coating on the steel grit surface.
- The HFO surface has low-affinity and high-affinity adsorption sites.
- PbCO_3 ($\text{pK}_{\text{so}} = 13.13$), $\text{Pb}_3(\text{OH})_2(\text{CO}_3)_2$ ($\text{pK}_{\text{so}} = 45.46$) (Barnes and Davis, 1996), $\text{Cr}(\text{OH})_3$ (or Cr_2O_3) ($\text{pK}_{\text{so}} = 33.13$) (Jing et al., 2006), BaSO_4 ($\text{pK}_{\text{so}} = 8.29$), and ZnO ($\text{pK}_{\text{so}} = 6.12$) were determined as the dominant phases in the system .



Methods (continued)

- **Principal Component Analysis (PCA)**

- Address and support the analysis of significant variables.

- **Statistical Modeling of Metal Leaching**

- Multivariate regression:

- $$\text{Leached metal} = a + b \cdot (\text{total Ca}) + c \cdot (\text{total metal}) + d \cdot (\text{total Fe}) + e \cdot (\text{Me}_{1, \text{ total}}) + \dots + n \cdot (\text{Me}_{n, \text{ total}})$$

- Box-Cox transformation:

- $$(\text{Leached metal})^\lambda = a + b \cdot (\text{total Ca}) + c \cdot (\text{total metal}) + d \cdot (\text{total Fe}) + e \cdot (\text{Me}_{1, \text{ total}}) + \dots + n \cdot (\text{Me}_{n, \text{ total}})$$

- Transformed models:

- $$\text{Log (leached metal)} = a + b \cdot \log(\text{total Ca}) + c \cdot \log(\text{total metal}) + d \cdot \log(\text{total Fe}) + e \cdot \log(\text{Me}_{1, \text{ total}}) + \dots + n \cdot \log(\text{Me}_{n, \text{ total}})$$

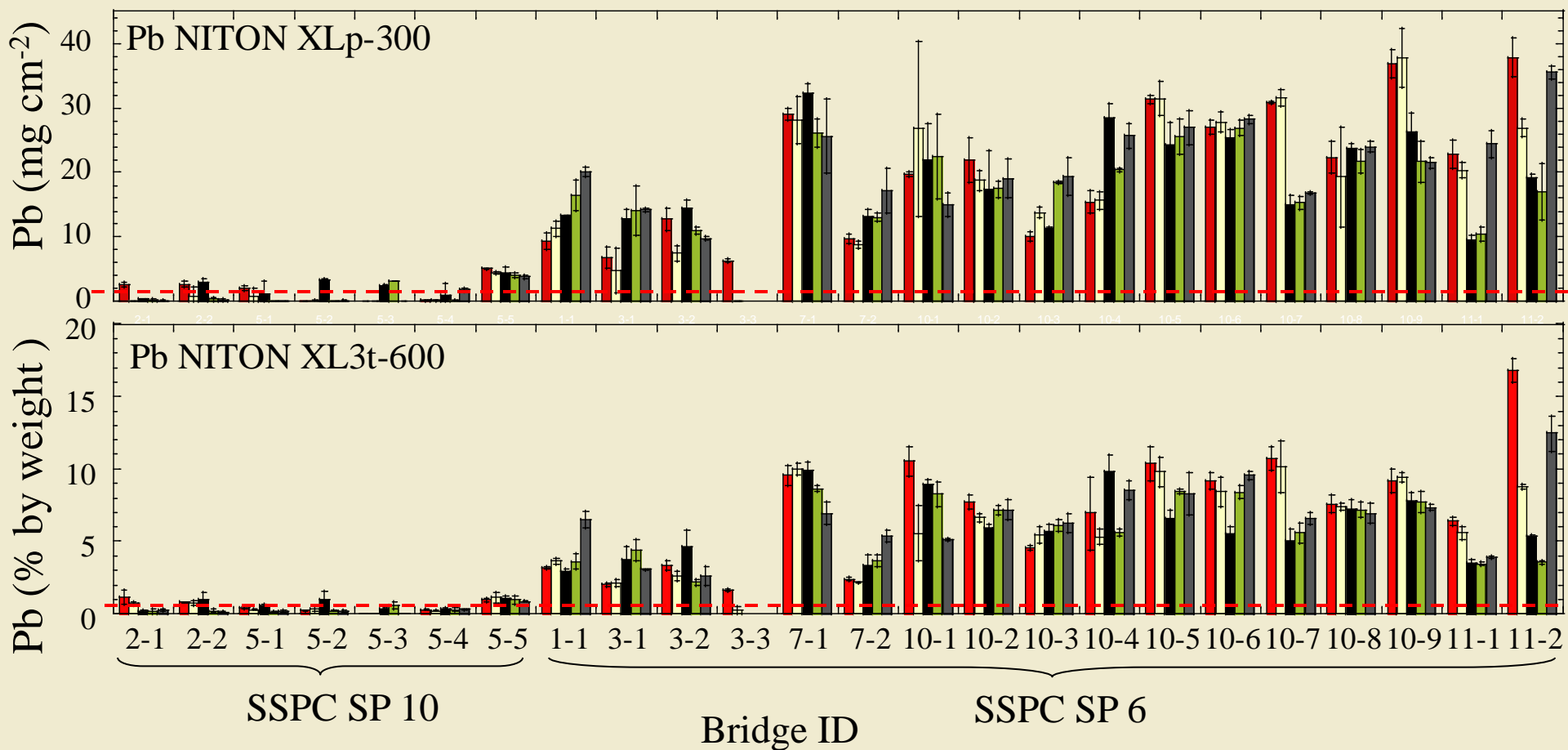


Results

Total Metal Concentrations

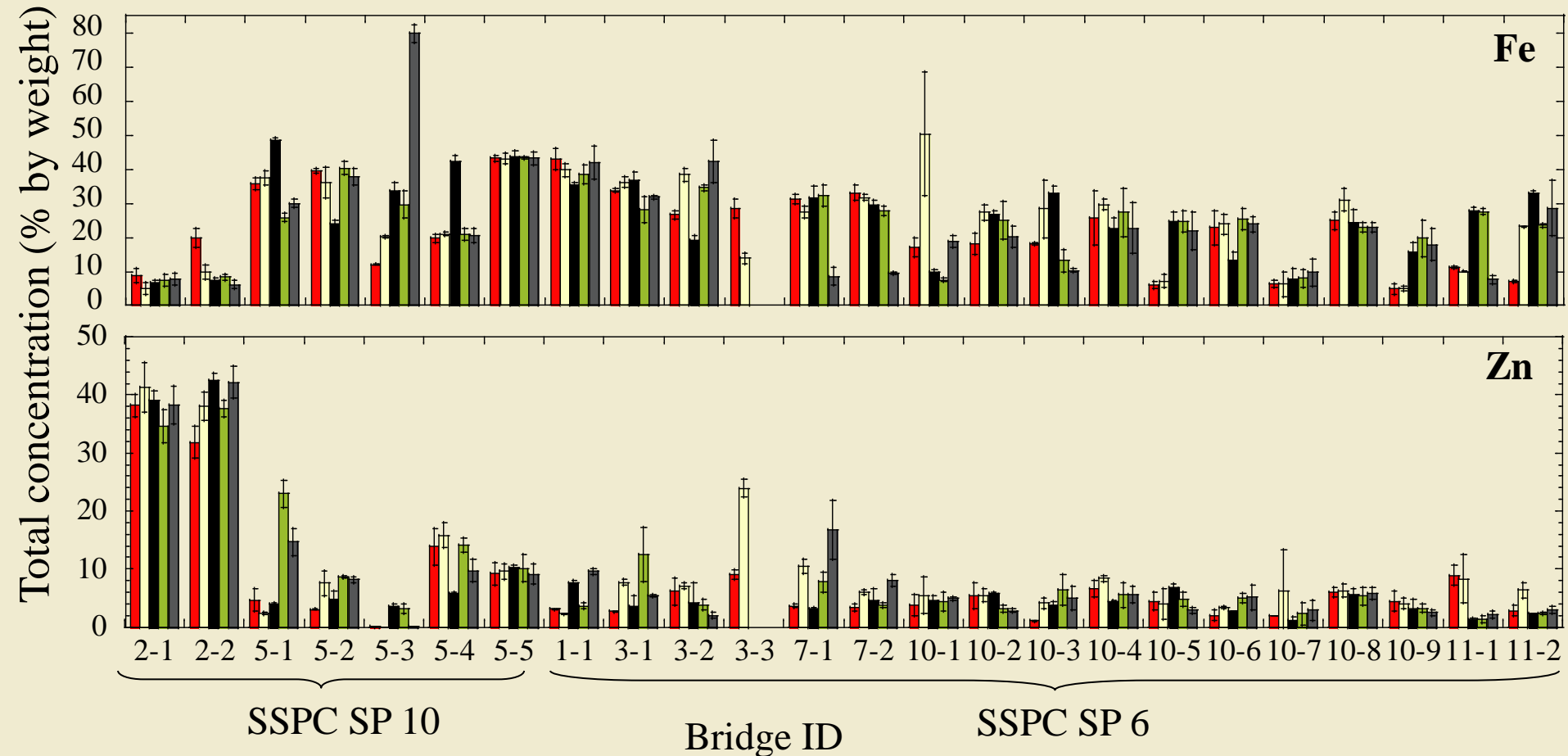


Pb concentrations in paint as a function of 24 bridges. Lead-based paint > 1 mg/cm² or 0.5% by weight (5000 mg/kg).



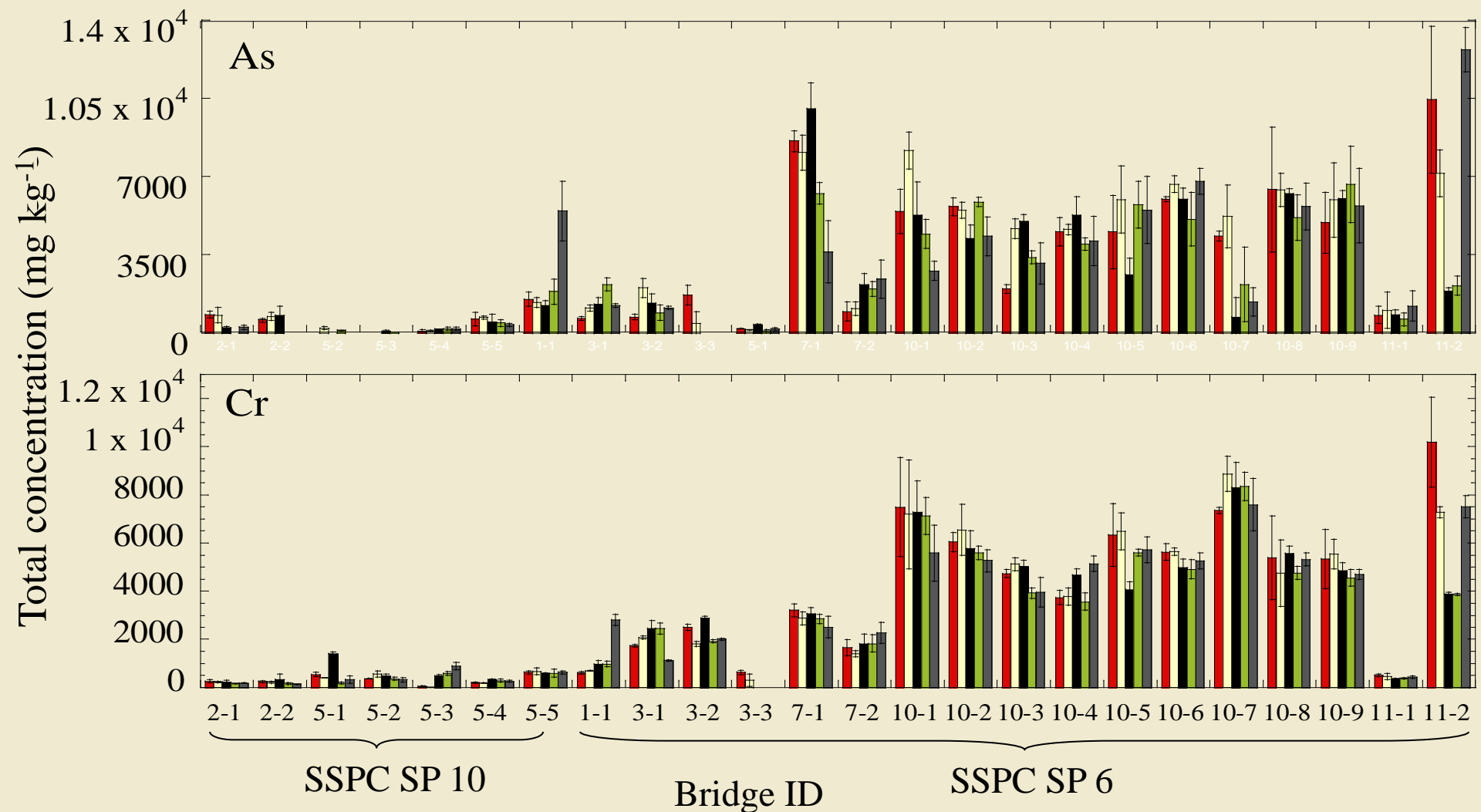


Fe and Zn concentrations analyzed with FP-XRF. Fe, ranging from 5% to 80%, is from applying steel grit blasting abrasive material.





As and Cr concentrations analyzed with FP-XRF.

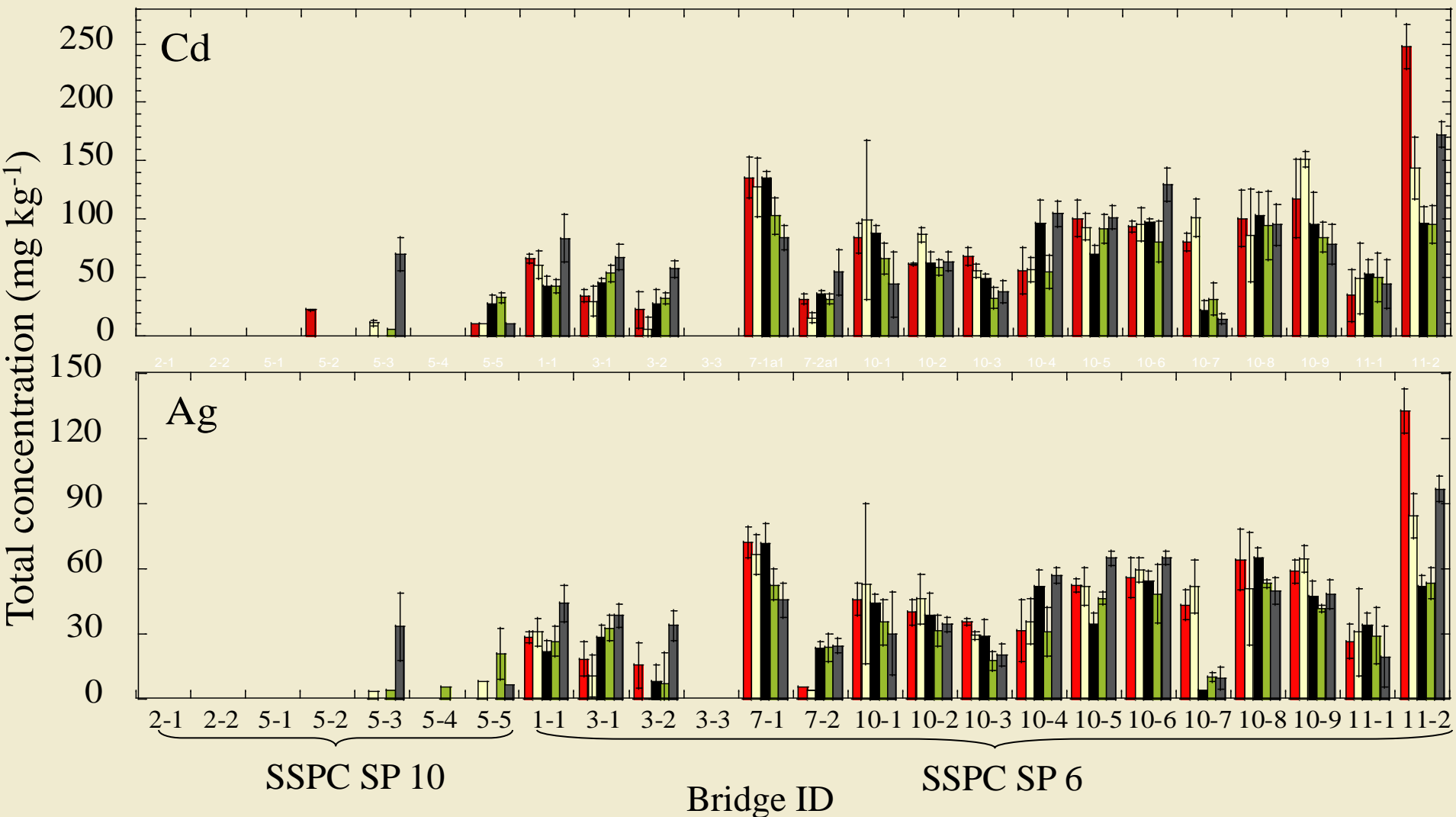


Five samples:



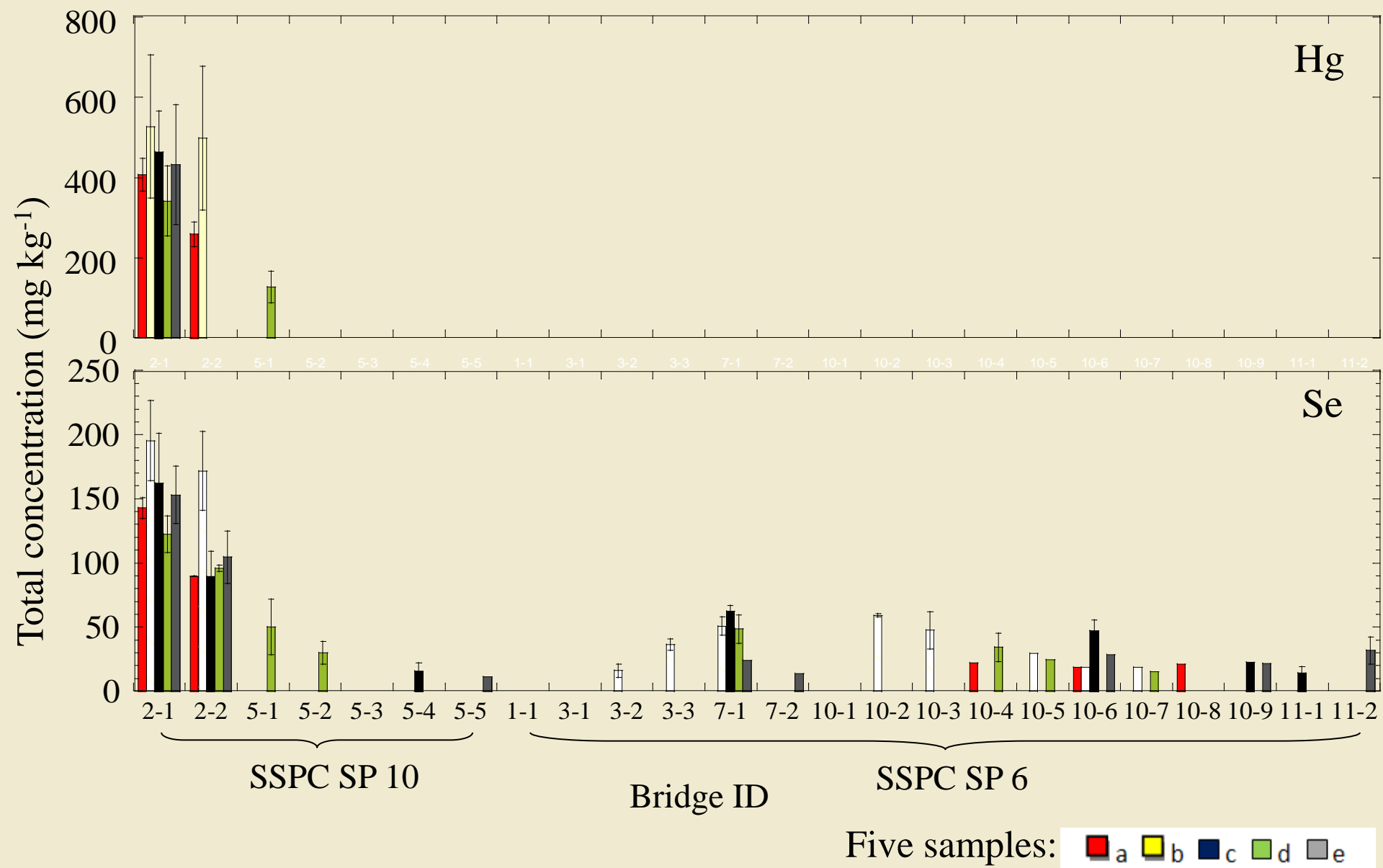


Cd and Ag concentrations analyzed with FP-XRF.



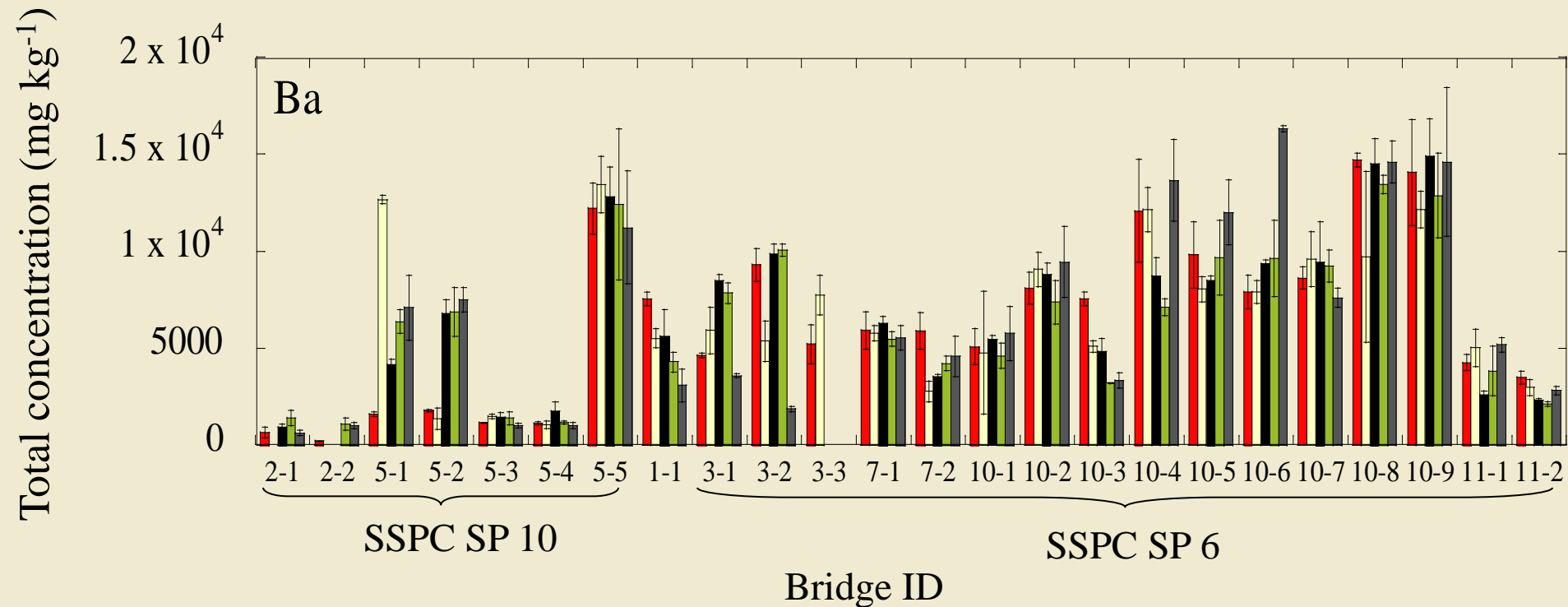


Hg and Se concentrations analyzed with FP-XRF.





Ba concentration analyzed with FP-XRF.



Five samples: ■ a ■ b ■ c ■ d ■ e



Coefficient of determination (R^2) for RCRA metals, iron as well as zinc.

| | Pb | Ba | Cr | Cd | Ag | Hg | Se | As | Fe | Zn |
|----|-------|--------|-------|-------|--------|------|------|-------|-------|-----|
| Pb | 1.0 | | | | | | | | | |
| Ba | 0.17 | 1.0 | | | | | | | | |
| Cr | 0.73 | 0.17 | 1.0 | | | | | | | |
| Cd | 0.68 | 0.02 | 0.33 | 1.0 | | | | | | |
| Ag | 0.67 | 0.03 | 0.31 | 0.95 | 1.0 | | | | | |
| Hg | 0.11 | 0.60 | 0.07 | 0.0 | 0.0 | 1.0 | | | | |
| Se | 0.33 | 0.40 | 0.30 | 0.10 | 0.085 | 0.99 | 1.0 | | | |
| As | 0.78 | 0.10 | 0.56 | 0.72 | 0.72 | 0.28 | 0.17 | 1.0 | | |
| Fe | 0.056 | 0.0004 | 0.091 | 0.063 | 0.033 | 0.82 | 0.29 | 0.024 | 1.0 | |
| Zn | 0.14 | 0.10 | 0.18 | 0.011 | 0.0082 | 0.94 | 0.76 | 0.11 | 0.086 | 1.0 |

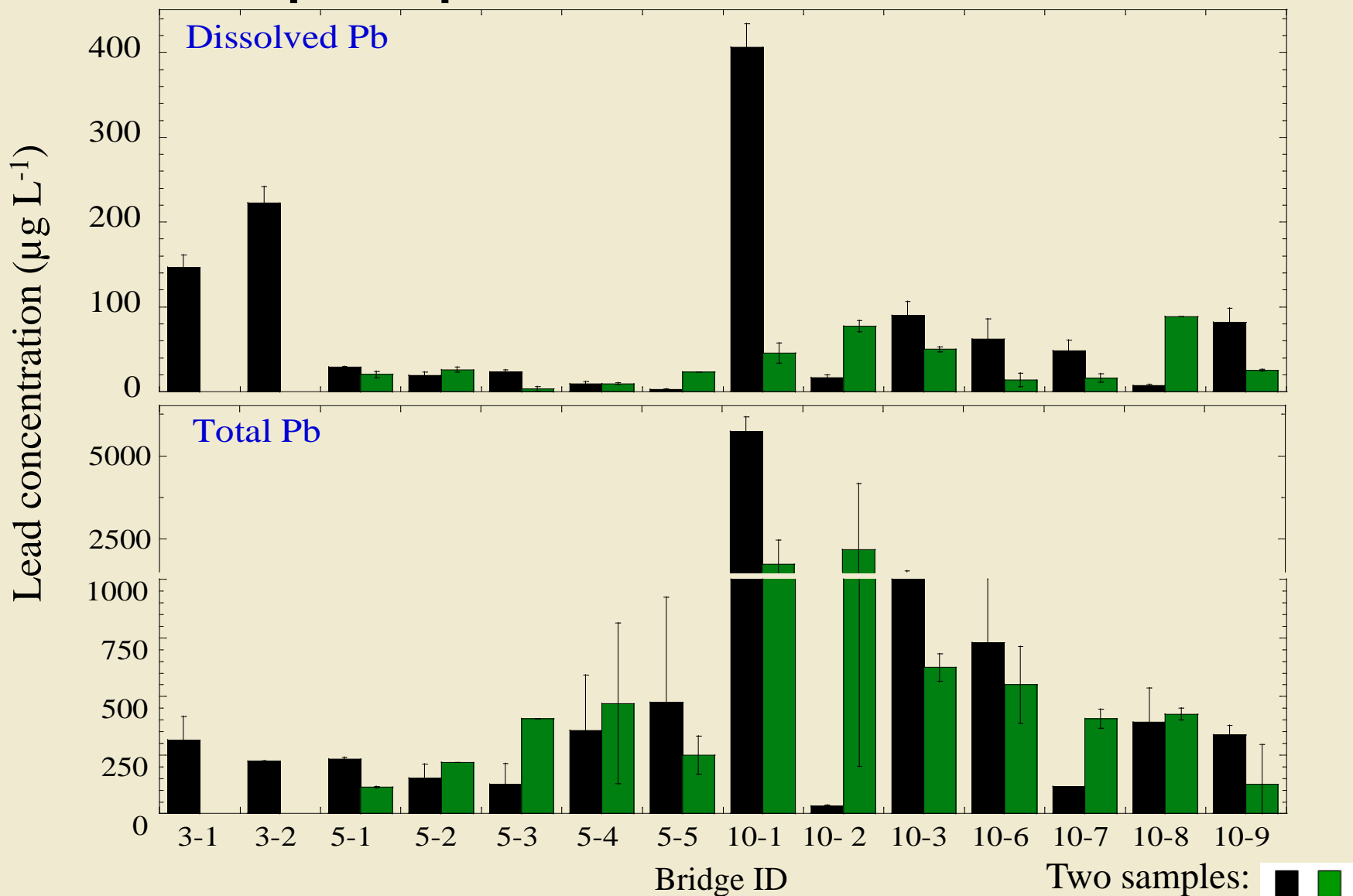


Results

Lead in Wash Water



Dissolved and total lead sampled at 14 bridges using the Hach field spectrophotometer.



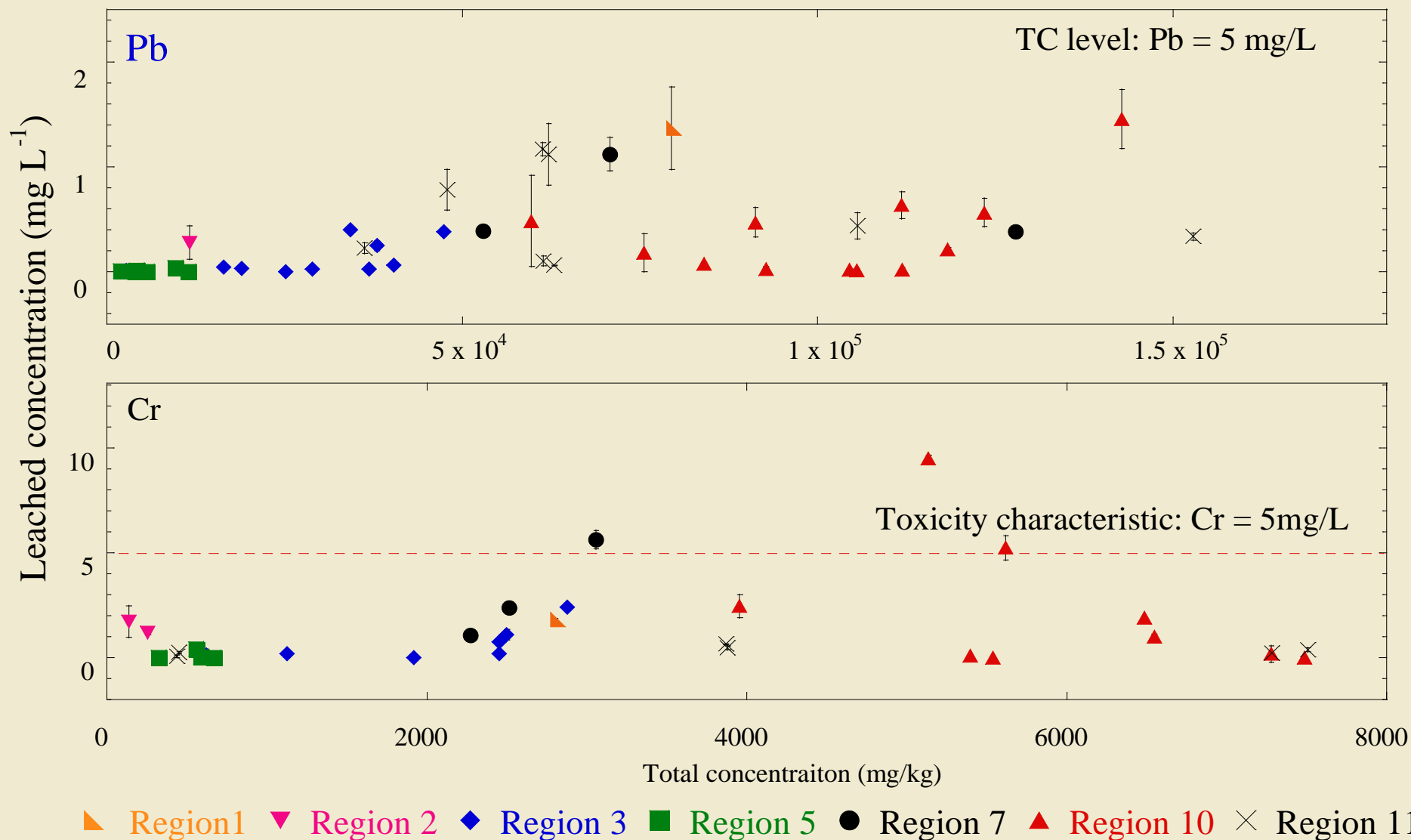


Results

Leaching Results

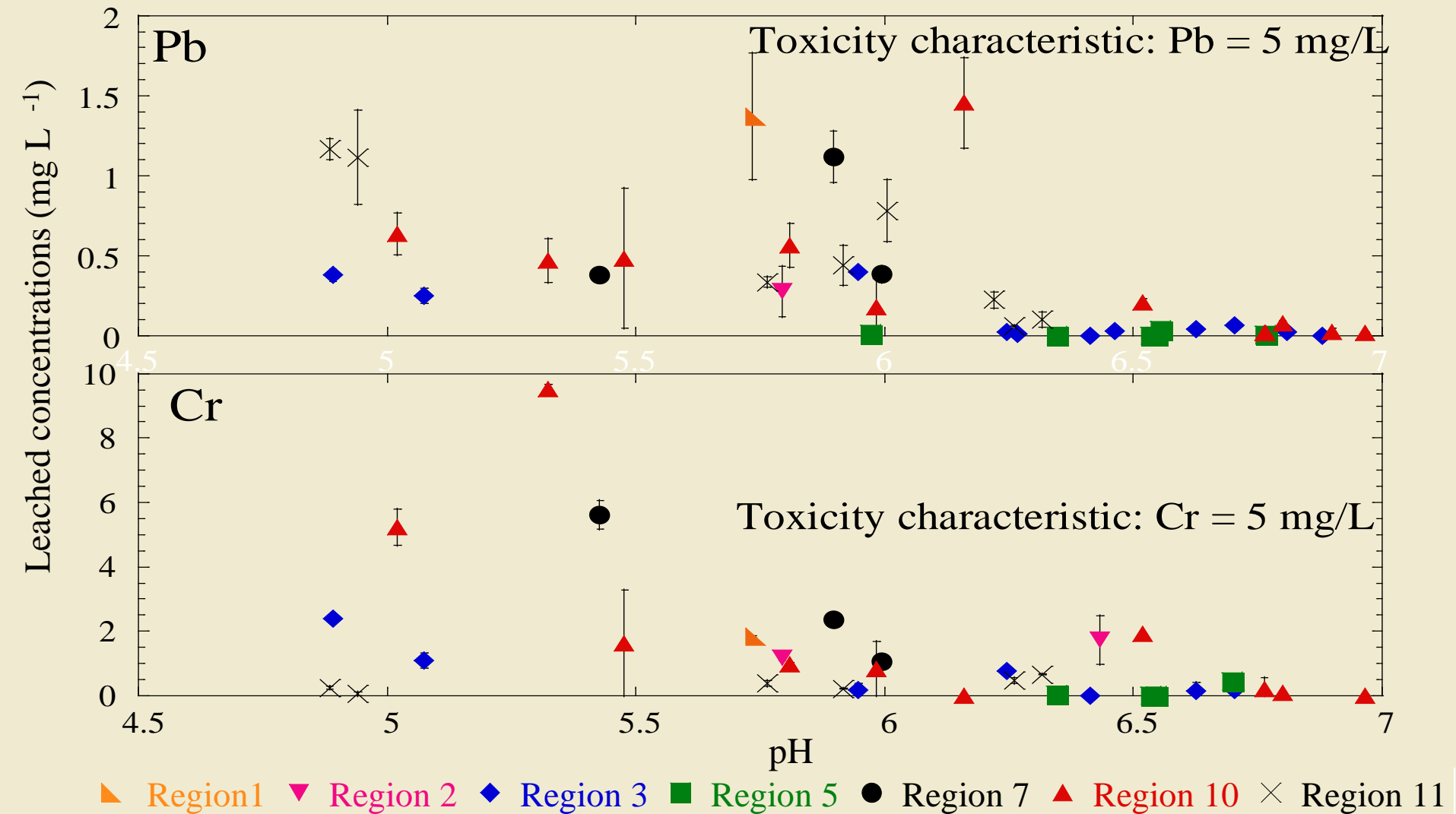


TCLP results for Pb and Cr are shown as a function of the total concentrations in the paint waste.



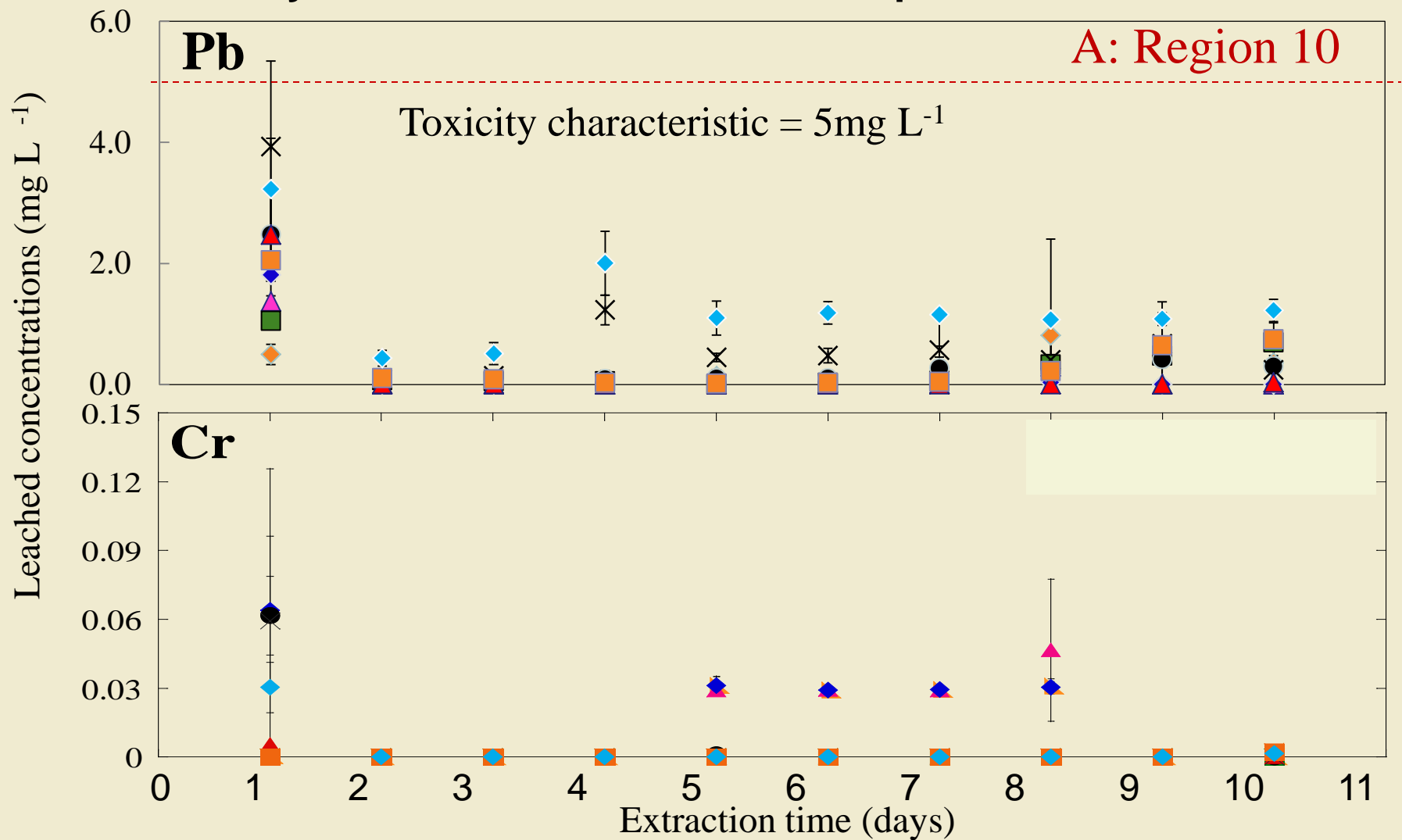


Leaching results from TCLP for Pb and Cr as a function of pH after 18 hours extraction with 0.1 ionic strength and $P_{CO_2} = 10^{-3.5}$ atm.





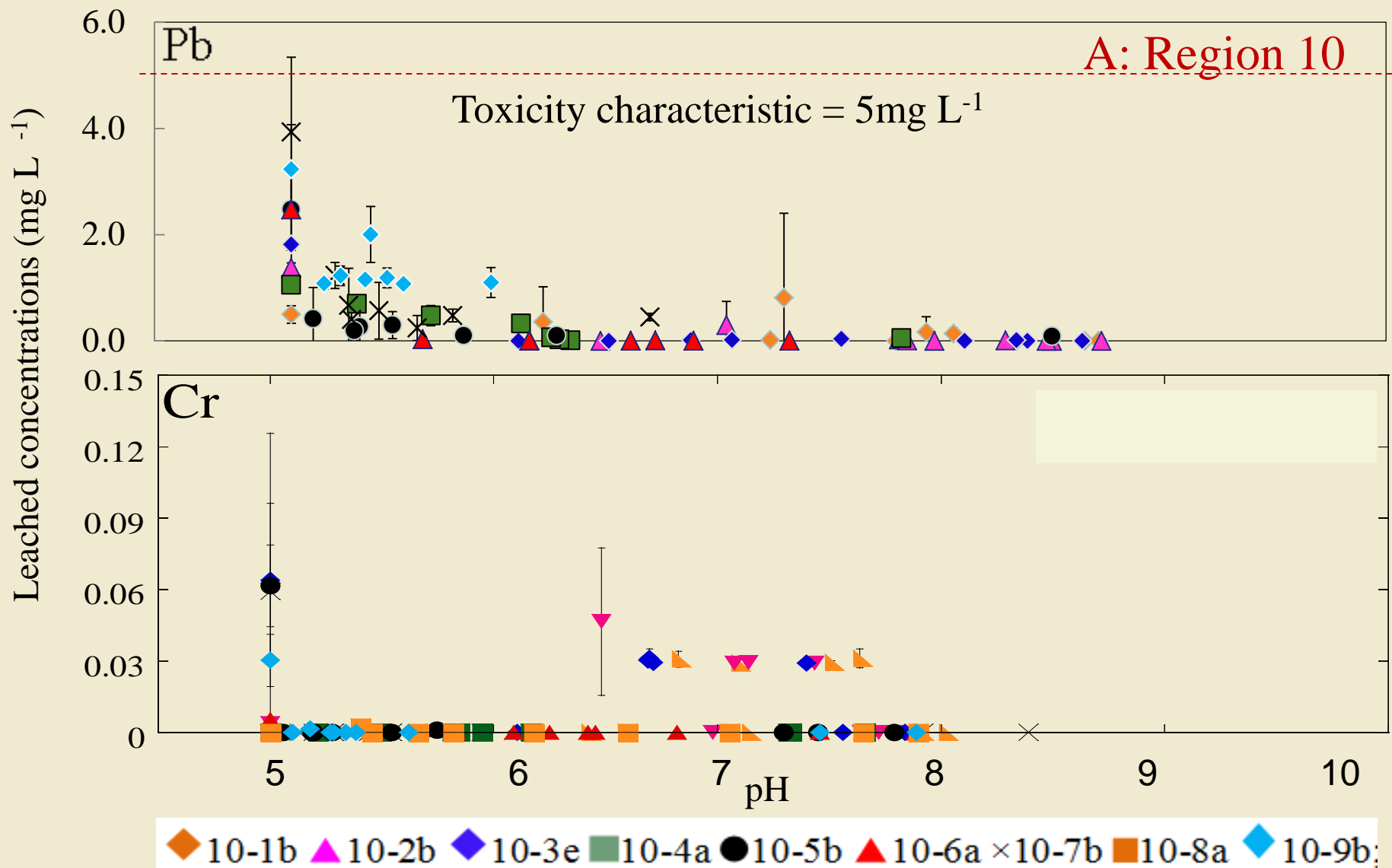
Leaching results from MEP for Pb and Cr as a function of times after 10 days of extraction with the initial pH of 3.0 ± 0.2 .



◆ 10-1b
 ▲ 10-2b
 ◆ 10-3e
 ■ 10-4a
 ● 10-5b
 ▲ 10-6a
 × 10-7b
 ■ 10-8a
 ◆ 10-9b

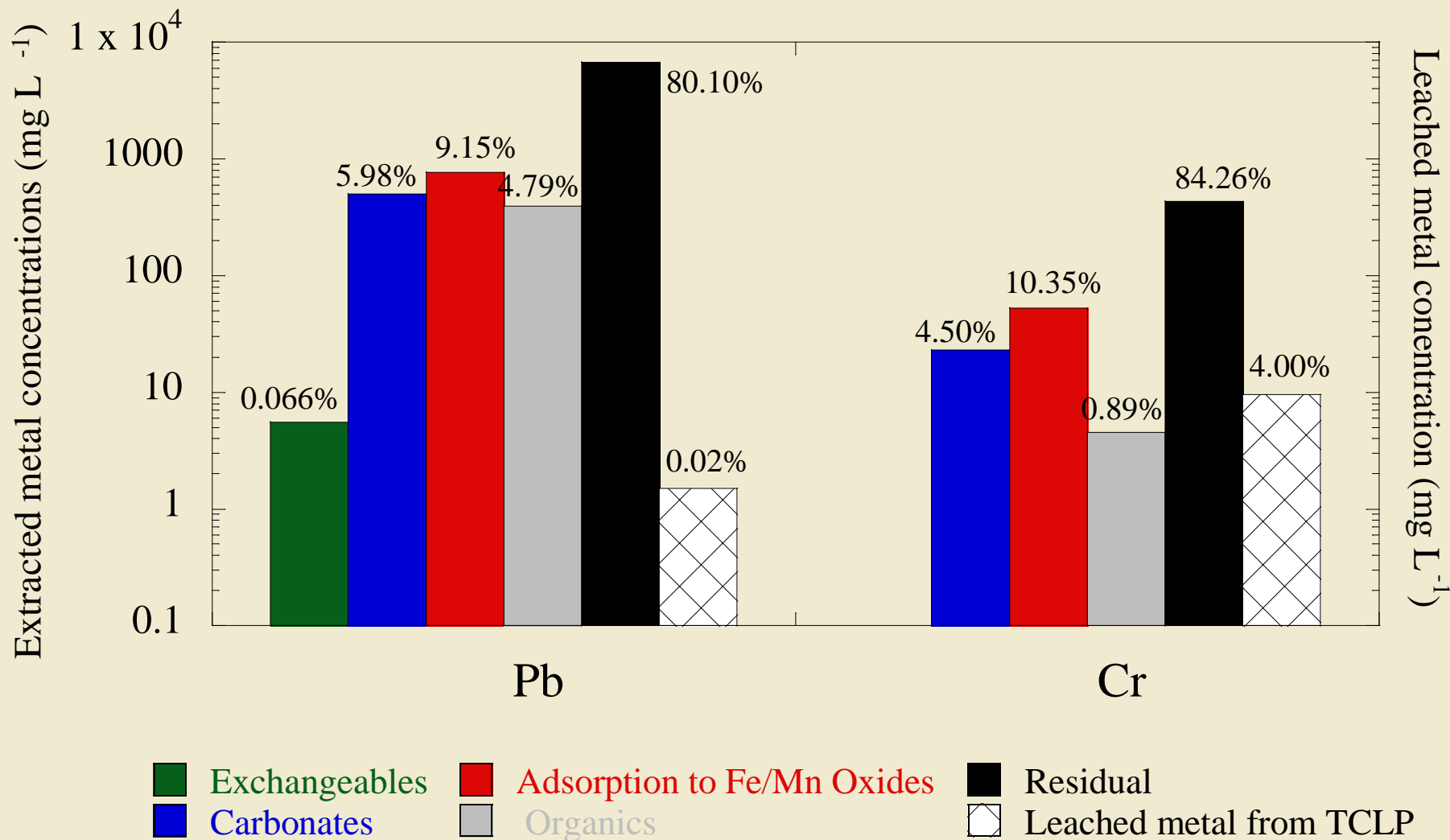


Leaching results from MEP for Cr as a function of pH after 10 days of extraction with the initial pH of 3.0 ± 0.2 .



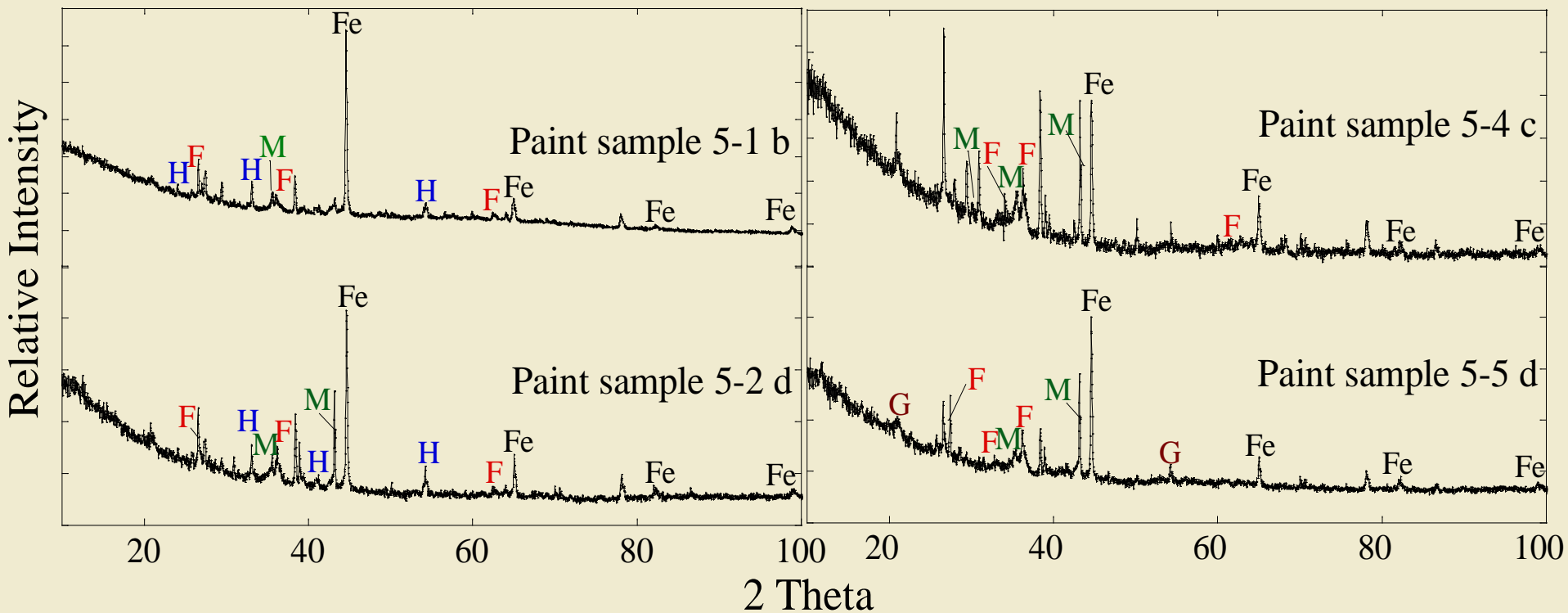


Phases Pb and Cr are associated with in paint waste samples along with the leached metal from the TCLP procedure.





XRD patterns of iron and iron oxides in paint waste where ferrihydrite is the dominant oxide in the waste.



Fe – Fe

M – magnetite [Fe_3O_4] (7.1%)

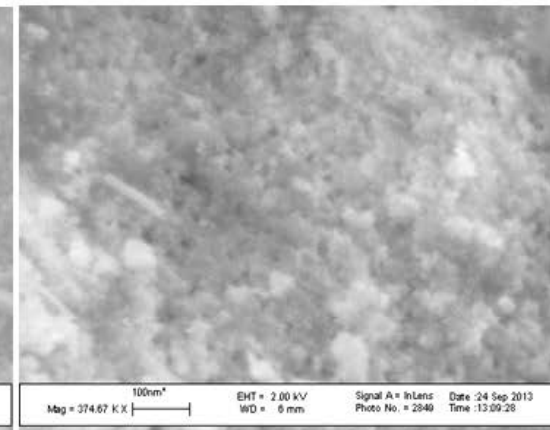
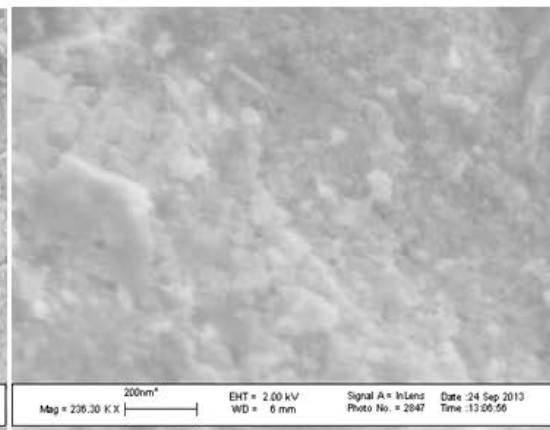
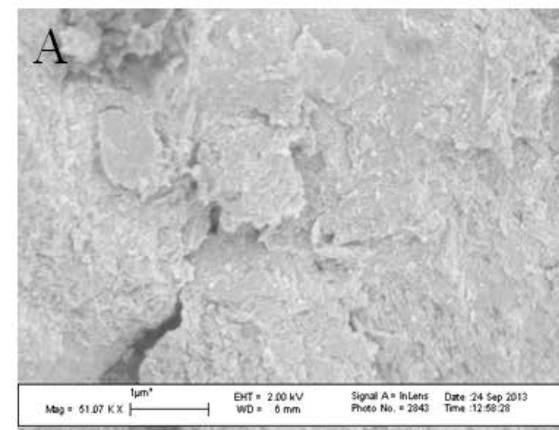
G – goethite [$\text{FeO}(\text{OH})$] (22%)

F – ferrihydrite ($\text{Fe}_2\text{O}_3 \cdot 0.5\text{H}_2\text{O}$) (60%)

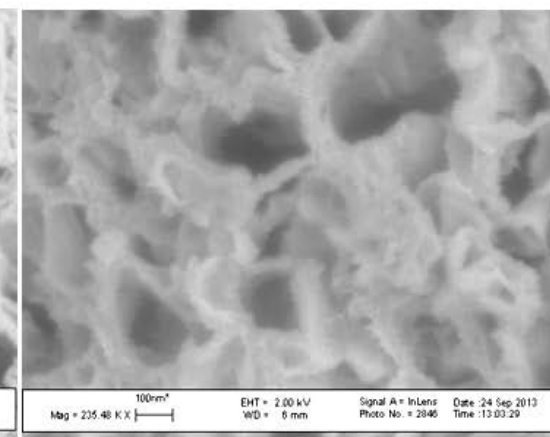
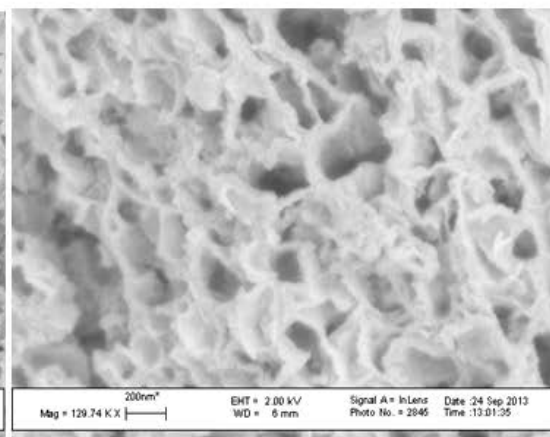
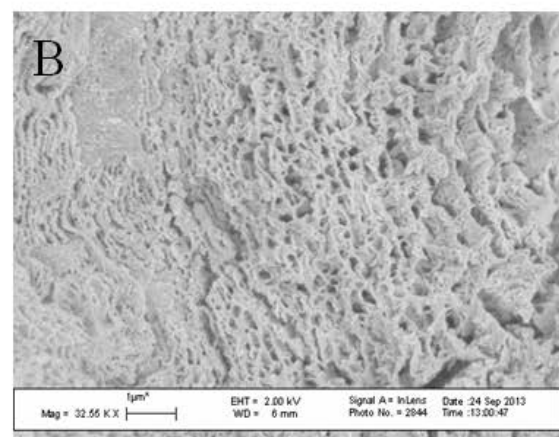
H – hematite [Fe_2O_3] (11%)



Nanostructured, microporous iron oxide coatings were observed on the steel grit surface using FE-SEM.



| Element | Wt% |
|---------|-------|
| Fe | 70.91 |
| O | 23.79 |
| Si | 1.46 |
| Cl | 0.93 |
| Mn | 0.67 |
| Ca | 0.57 |
| Al | 0.57 |
| Mg | 0.53 |
| S | 0.31 |
| Pb | 0.09 |
| Cr | 0.08 |
| Ba | 0.08 |





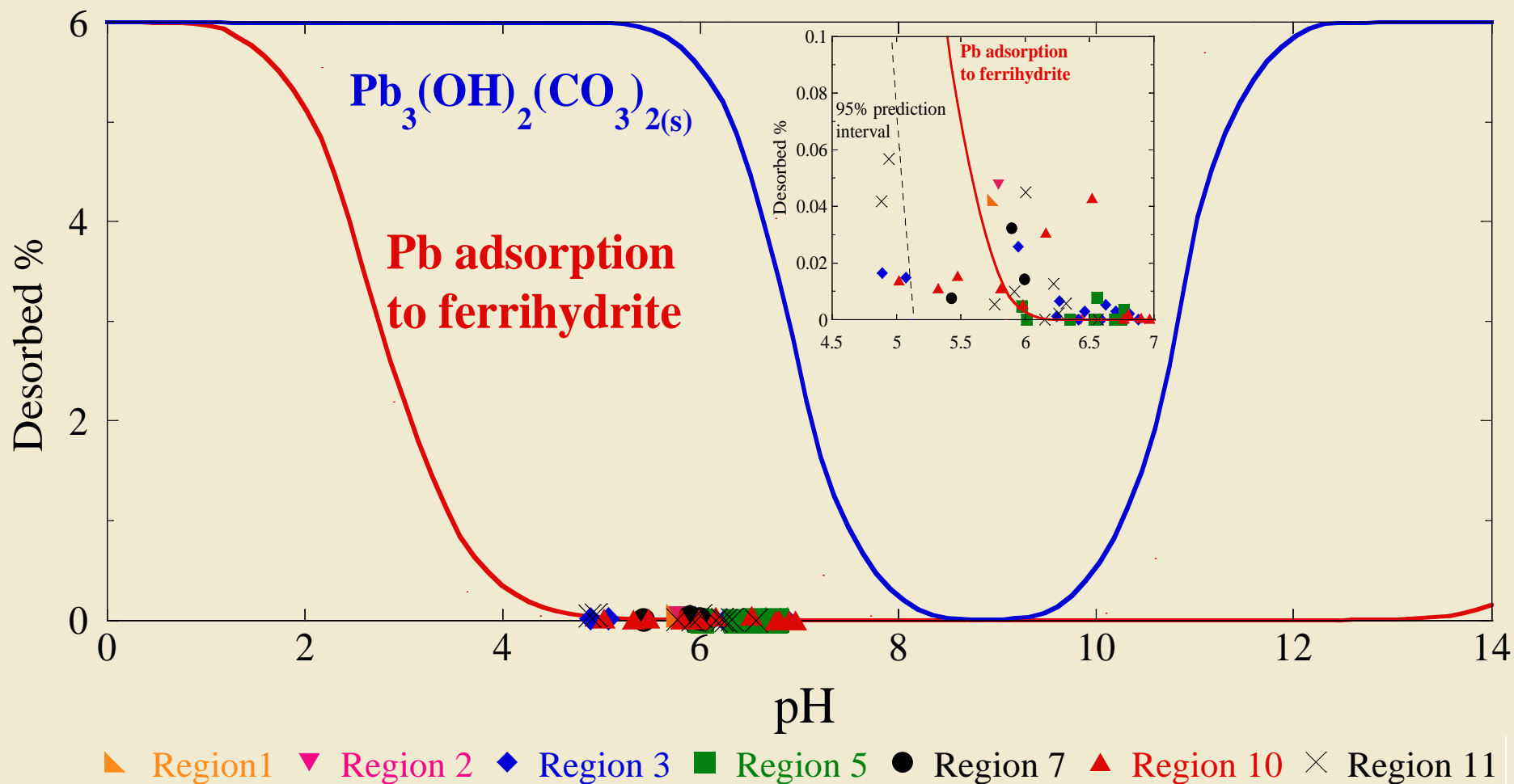
Results

Modeling



Desorbed Pb in the presence of steel grit associated with paint waste as a function of pH after 18 hours using the TCLP.

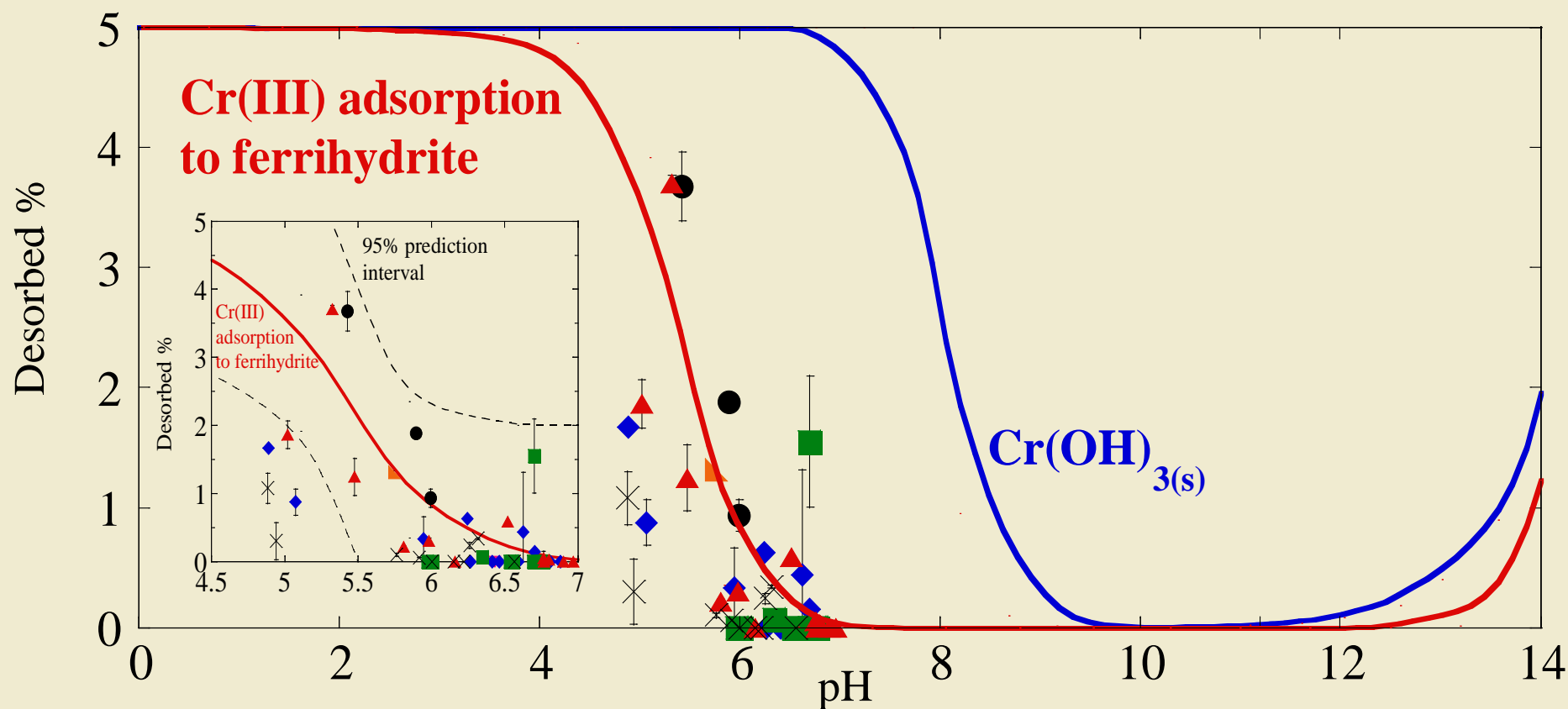
$Pb_T = 1.0 \times 10^{-5} \text{ M}$, $Fe_T = 0.07 \text{ M}$, ionic strength = 0.1 M , surface area = $600 \text{ m}^2/\text{g}$, $K_{MePb} = 10^{4.65}$, $K_{soPbCO_3} = 10^{-13.13}$, and $K_{so Pb_3(OH)_2(CO_3)_2} = 10^{-45.46}$





Desorbed Cr in the presence of steel grit associated with paint waste as a function of pH after 18 hours using the TCLP.

$\text{Cr}_T = 1.8 \times 10^{-4} \text{ M}$, $\text{Fe}_T = 0.07 \text{ M}$, ionic strength = 0.1 M, surface area = 600 m²/g, $K_{\text{MeCr(III)}} = 10^{2.11}$, and $K_{\text{soCr}_2\text{O}_3} = 10^{-33.13}$.

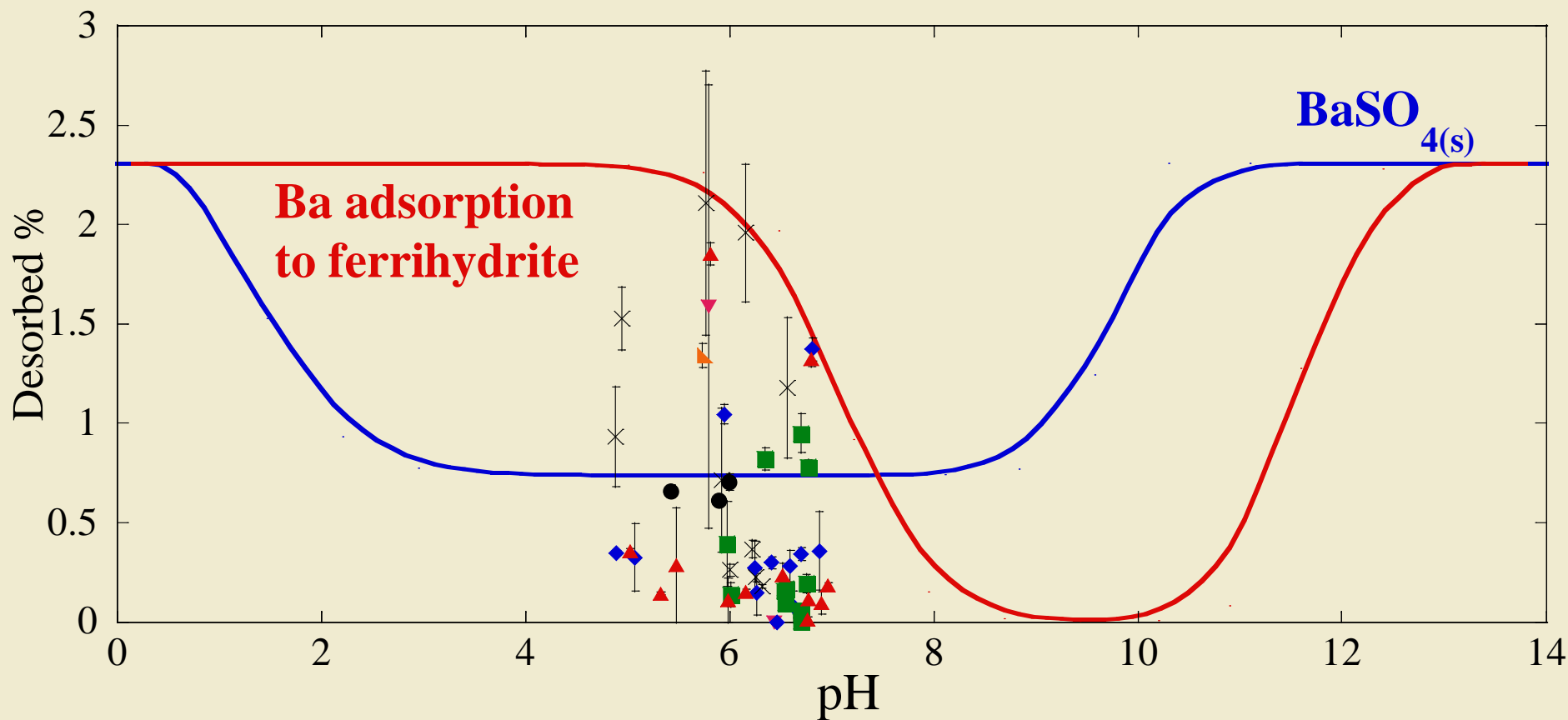


▲ Region 1
 ▼ Region 2
 ◆ Region 3
 ■ Region 5
 ● Region 7
 ▲ Region 10
 × Region 11



Desorbed Ba in the presence of steel grit associated with paint waste as a function of pH after 18 hours using the TCLP.

$Ba_T = 3.2 \times 10^{-5} \text{ M}$, $Fe_T = 0.07 \text{ M}$, ionic strength = 0.1 M , surface area = $600 \text{ m}^2/\text{g}$, $K_{MeBa} = 10^{5.46}$, and $K_{soBaSO_4} = 10^{-9.86}$.

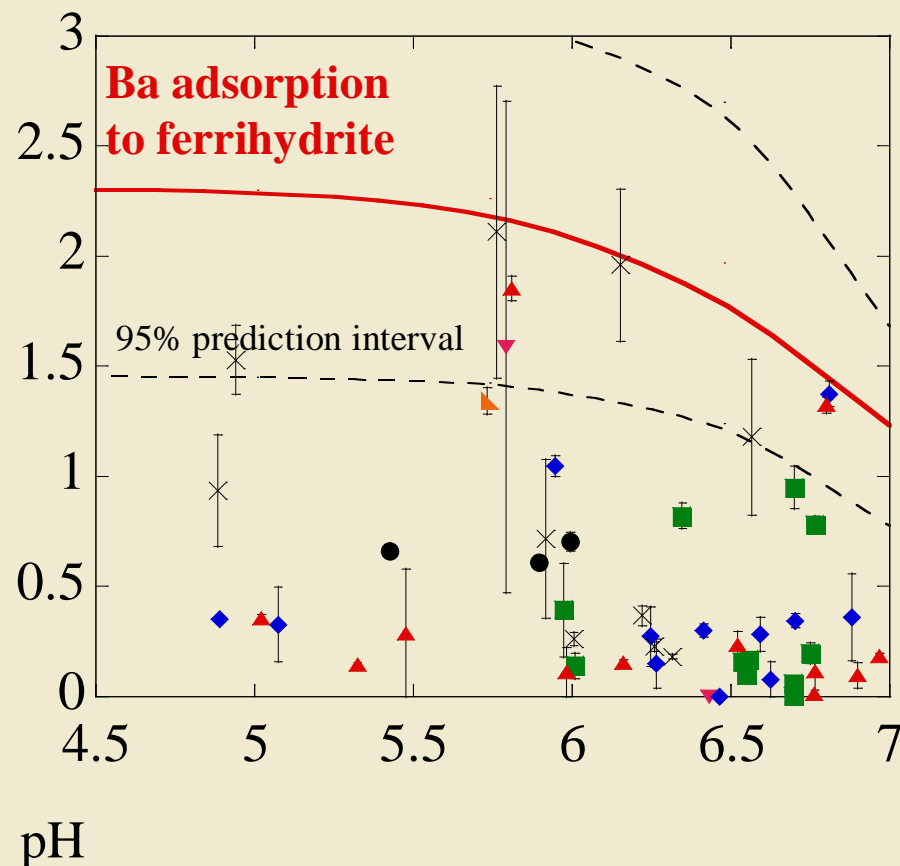
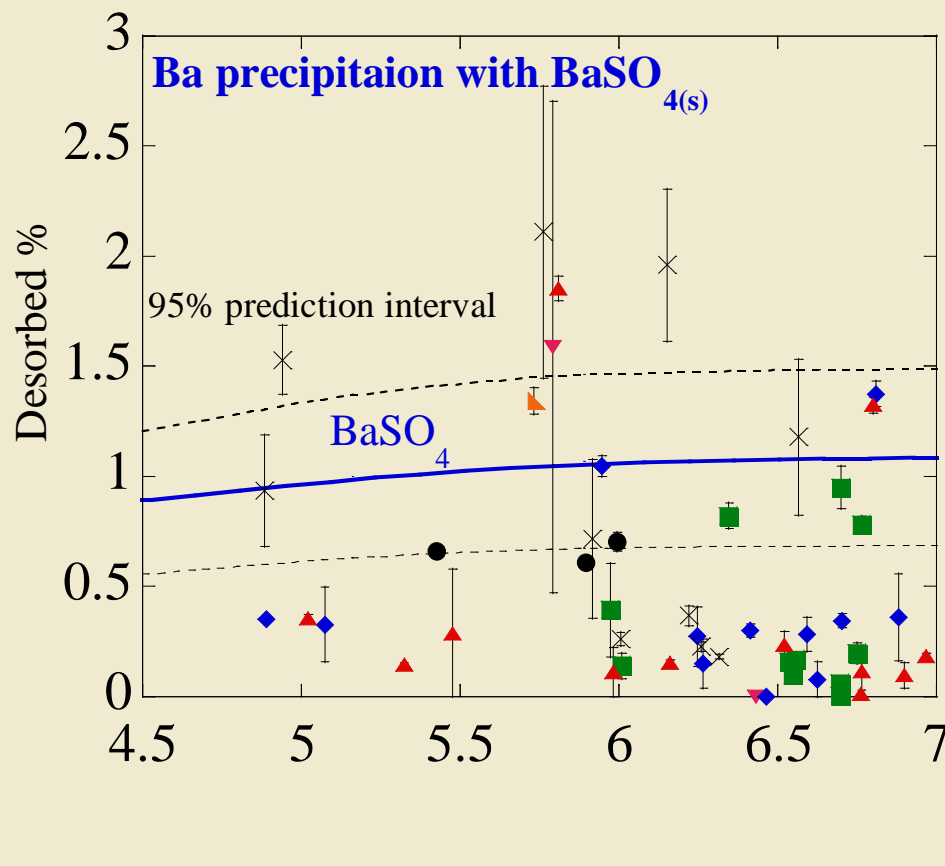


▲ Region 1
 ▼ Region 2
 ◆ Region 3
 ■ Region 5
 ● Region 7
 ▲ Region 10
 × Region 11



Desorbed Ba in the presence of steel grit associated with paint waste as a function of pH after 18 hours using the TCLP.

$Ba_T = 3.2 \times 10^{-5} \text{ M}$, $Fe_T = 0.07 \text{ M}$, ionic strength = 0.1 M , surface area = $600 \text{ m}^2/\text{g}$, $K_{MeBa} = 10^{5.46}$, and $K_{soBaSO_4} = 10^{-9.86}$.

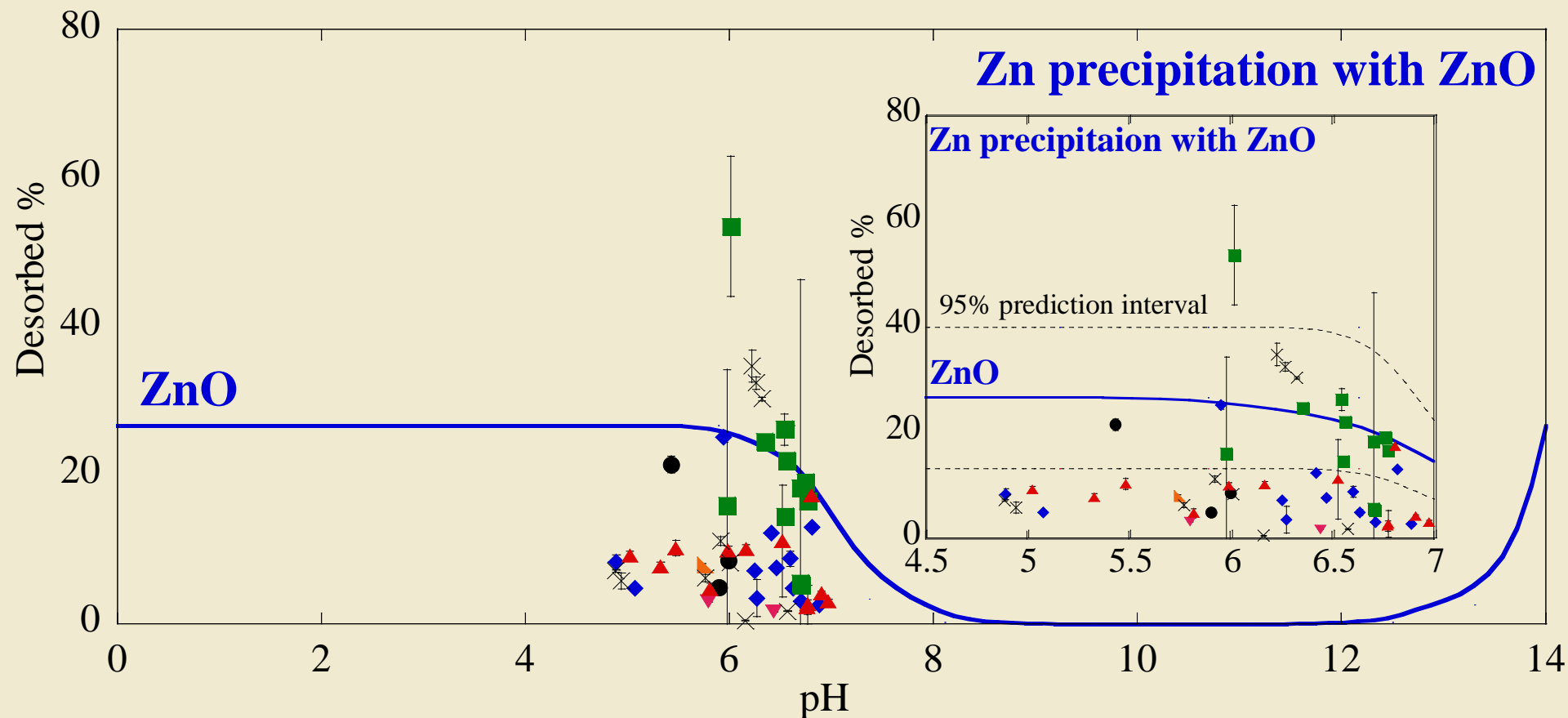


▴ Region 1
 ▾ Region 2
 ◆ Region 3
 ■ Region 5
 ● Region 7
 ▴ Region 10
 × Region 11



Desorbed Zn in the presence of steel grit associated with paint waste as a function of pH after 18 hours using the TCLP.

$Zn_T = 0.02$ M, $Fe_T = 0.07$ M, ionic strength = 0.1 M, surface area = 600 m²/g, $K_{MeZn} = 10^{3.49}$, and $K_{soZnO} = 10^{-16.12}$.



▲ Region 1
 ▼ Region 2
 ◆ Region 3
 ■ Region 5
 ● Region 7
 ▲ Region 10
 × Region 11



Mechanistic Model Summary

- Overall, based on the above discussion, both adsorption and precipitation are important processes supporting predictive mechanistic leaching from the waste.
- A number of factors may affect metal leaching behavior including
 - Total metal concentrations in the paint waste,
 - Dominant sorbents present (such as iron oxides),
 - Competing metal ions, and
 - The pH of the system.



Principal Component Analysis (PCA)

- PCA is a classical technique based on linear algebra.
 - The analysis involves a mathematical procedure that transforms a number of possible correlated variables into a smaller number of uncorrelated variables called principal components (PCs)
 - The PCs are linear combinations of the original variables.
 - The PCs account for as much of the variability in the data as possible, and
 - Each succeeding PC accounts for as much of the remaining variability as possible.
- The eigenvalues reflect the quality of the projection from the N-dimensional initial table to a lower number of dimensions.
 - The eigenvalues and the corresponding factors are sorted by descending order to the degree which the initial variability is represented (converted to %).
 - Correlations greater than 0.66 are considered to demonstrate significant influence.



Principal component loadings of total metals in the paint waste samples.

| Variable | PC 1 | PC 2 | PC 3 |
|------------|--------------|--------------|--------------|
| As | 0.829 | -0.433 | -0.22 |
| Ba | 0.658 | 0.429 | 0.19 |
| Ca | 0.655 | -0.165 | 0.672 |
| Cd | 0.877 | -0.342 | -0.243 |
| Cr | 0.854 | -0.432 | 0.004 |
| Fe | 0.375 | 0.705 | -0.437 |
| Pb | 0.863 | -0.448 | -0.027 |
| Hg | -0.698 | -0.477 | -0.191 |
| Ag | 0.886 | -0.358 | -0.228 |
| Se | -0.787 | -0.518 | -0.127 |
| Ti | 0.297 | 0.665 | -0.156 |
| Zn | -0.851 | -0.418 | -0.034 |
| Eigenvalue | 6.63 | 2.64 | 1.00 |
| Proportion | 0.553 | 0.22 | 0.076 |
| Cumulative | 0.553 | 0.773 | 0.849 |

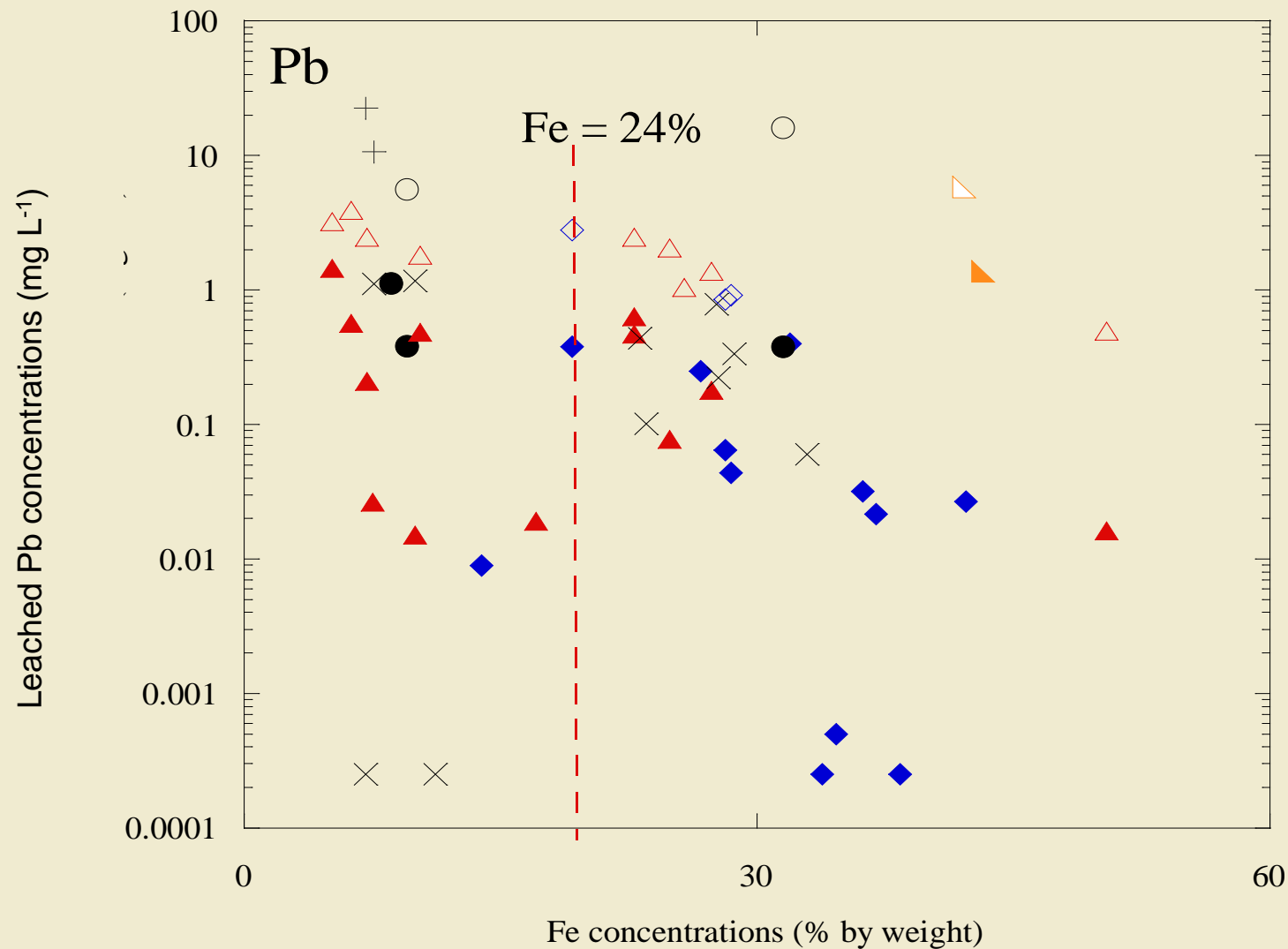


Principal Component Analysis Summary

- Using the PCA analysis, the most important factors accounting for total variability in the paint waste are
 - The surface preparation standard (reflected in PC 1)
 - Surface complexation (iron oxide) (reflected in PC 2) and
 - CaCO_3 (reflected in PC 3)
- Therefore, metal leaching depends on
 - Total metal concentrations;
 - CaCO_3 affecting the pH and alkalinity;
 - Fe oxides providing a highly reactive surface for metal sorption; and,
 - Other groups of metals such as Zn and Ti in the paint waste.



Leached Pb concentrations are shown as a function of total Fe (wt%) concentrations in paint waste.



TCLP samples: ▲ Region 1 ▼ Region 2 ◆ Region 3 ■ Region 5 ● Region 7 ▲ Region 10 × Region 11

MEP samples: ▢ Region 1 ▽ Region 2 ◇ Region 3 □ Region 5 ○ Region 7 △ Region 10 + Region 11



Surface Preparation Standard

- The basic standards for preparing metal substrates are a joint effort between the Society for Protective Coatings (SSPC) and the National Association of Corrosion Engineers International (NACE).
- SSPC surface preparation standard (SP)-6 (Commercial Blast Cleaning) has been applied to bridges in NYS before 2006, where
 - Paint and rust from steel were removed to a remaining residual of 33% of the total removal area.
- After 2006, SSPC SP-10 (Near White Blast Cleaning) was required in the blasting procedure for all regions in NY.
 - SP-10 restricts the visible residues remaining on the bridge surface to 5% of the total removal area.



Samples sorted with respected to surface preparation standard and Fe concentrations.

| Region | Bridges | SSPC 6 | | SSPC 10 |
|-----------|---------|---------------|----------|------------------------|
| | | Fe \leq 24% | Fe > 24% | 7 \leq Fe \leq 80% |
| Region 1 | 1-1 | | √ | |
| Region 2 | 2-1 | | | √ |
| | 2-2 | | | √ |
| Region 3 | 3-1 | | √ | |
| | 3-2 | | √ | |
| | 3-3* | √ | √ | |
| Region 5 | 5-1 | | | √ |
| | 5-2 | | | √ |
| | 5-3 | | | √ |
| | 5-4 | | | √ |
| | 5-5 | | | √ |
| Region 7 | 7-1* | √ | √ | |
| | 7-2 | √ | | |
| Region 10 | 10-1* | √ | √ | |
| | 10-2 | | √ | |
| | 10-3 | √ | | |
| | 10-4 | | √ | |
| | 10-5 | √ | | |
| | 10-6 | √ | | |
| | 10-7 | √ | | |
| | 10-8 | | √ | |
| | 10-9 | √ | | |
| Region 11 | 11-1* | √ | √ | |
| | 11-2* | √ | √ | |



Statistical analysis results from multivariate regression of the leached metal concentrations for Pb and Cr (mg L⁻¹)

| Metal | Surface preparation | Model used for prediction | R ² | Sample Number | Statistical Significance |
|-------|---------------------|---|----------------|---------------|--------------------------|
| Pb | SSPC 6; Fe ≤ 24% | TCLP Pb (mg L ⁻¹) = 10 ^ [26.6 – 3.24 log total Ba (mg Kg ⁻¹) - 0.1 log total Fe (mg Kg ⁻¹) – 2.26 log total Cr (mg Kg ⁻¹) + 4.28 log total Pb (mg Kg ⁻¹) – 7.83 log total Ca (mg Kg ⁻¹) + 3.13 log total Ti (mg Kg ⁻¹) - 3.09 log total Ag (mg Kg ⁻¹)] | 0.6 | 28 | P = 0.01 |
| | SSPC 6; Fe > 24% | TCLP Pb (mg L ⁻¹) = 10 ^ [-19.63 – 3.72 log total Fe (mg Kg ⁻¹)- 3.03 log total Cr (mg Kg ⁻¹) + 5.28 log total Pb (mg Kg ⁻¹)+ 1.92 log total Ti (mg Kg ⁻¹) + 1.64 log total Ag (mg Kg ⁻¹) - 0.74 log Se + 2.93 log total Zn (mg Kg ⁻¹)] | 0.7 | 27 | P =0.001 |
| | SSPC SP 10 | TCLP Pb (mg L ⁻¹) = 10 ^ [-3.20 + 1.34×10 ⁻⁶ Fe mg/kg + 0.00022 total Pb (mg Kg ⁻¹) + 2.55×10 ⁻⁵ total Ca (mg Kg ⁻¹) – 3.63×10 ⁻⁵ total Ti (mg Kg ⁻¹)] | 0.9 | 20 | P = 0.005 |
| Cr | SSPC 6; Fe ≤ 24% | TCLP Cr (mg L ⁻¹) = -12.2 + 0.00051 total Ba (mg Kg ⁻¹) + 0.000019 total Fe (mg Kg ⁻¹) - 0.00068 total Cr (mg Kg ⁻¹) + 0.000063 total Pb (mg Kg ⁻¹) + 0.00013 total Ca (mg Kg ⁻¹) + 0.00011 total Ti (mg Kg ⁻¹) | 0.6 | 28 | P = 0.003 |
| | SSPC 6; Fe > 24% | TCLP Cr (mg L ⁻¹) = - 0.80 + 0.000006 total Fe (mg Kg ⁻¹) - 0.00048 total Cr (mg Kg ⁻¹) - 0.000019 total Ca (mg Kg ⁻¹) + 0.0417 Se + 0.0062 total Cd (mg Kg ⁻¹) + 0.00013 total As (mg Kg ⁻¹) | 0.6 | 27 | P = 0.003 |
| | SSPC SP 10 | TCLP Cr (mg L ⁻¹) = 12.4 - 0.000022 total Zn (mg Kg ⁻¹) - 0.000032 total Fe (mg Kg ⁻¹) + 0.0077 total Cr (mg Kg ⁻¹) + 0.000053 total Pb (mg Kg ⁻¹) - 0.00020 total Ca (mg Kg ⁻¹) - 0.000038 total Ti (mg Kg ⁻¹) | 0.5 | 20 | P = 0.75 |



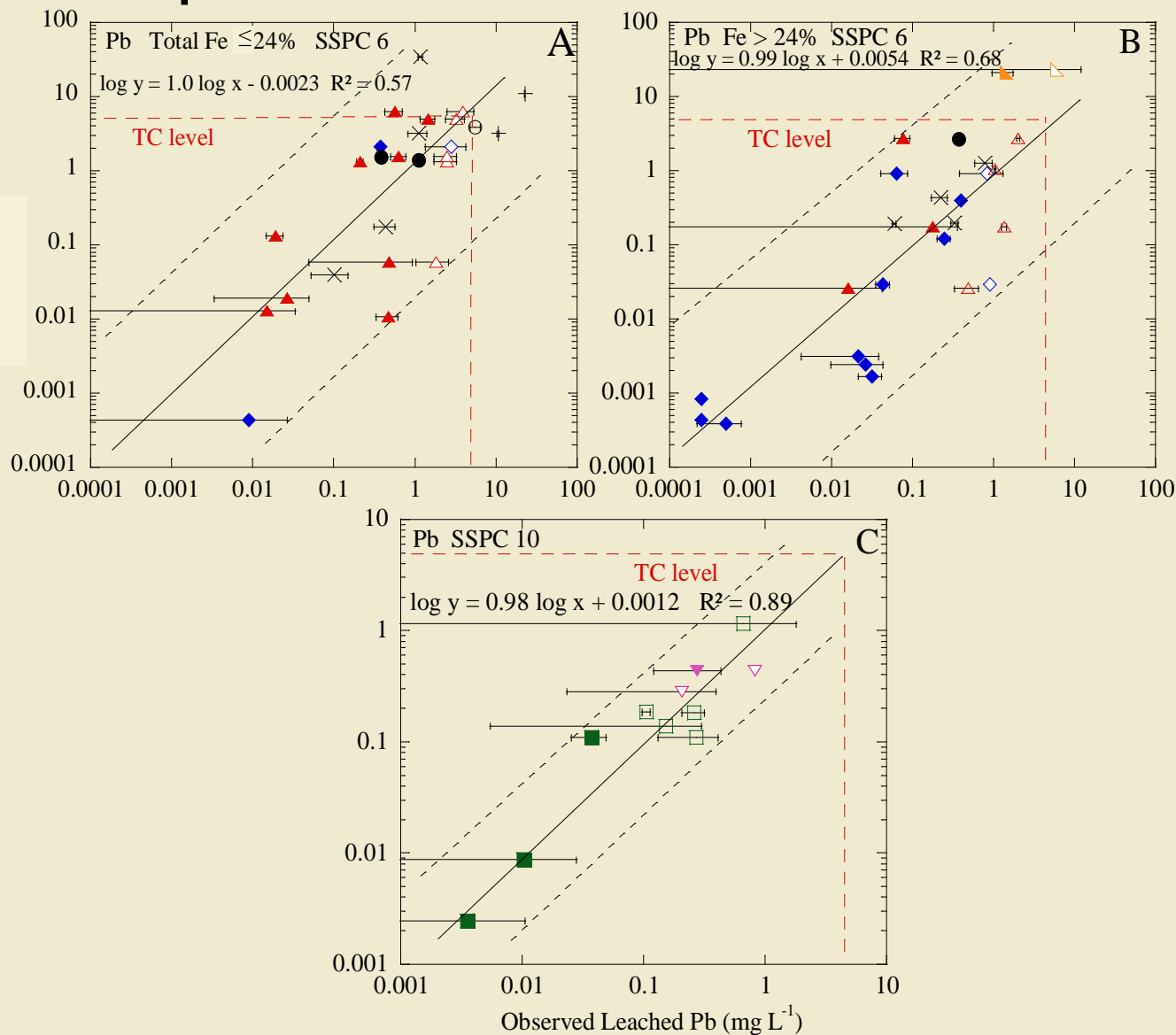
Statistical analysis results from multivariate regression of the leached metal concentrations for Ba and Zn (mg L⁻¹)

| Metal | Surface preparation | Model used for prediction | R ² | Sample Number | Statistical Significance |
|-------|---------------------|--|----------------|---------------|--------------------------|
| Ba | SSPC 6; Fe ≤ 24% | TCLP Ba (mg L ⁻¹) = {[1.92 - 1.91 × 10 ⁻⁶ total Fe (mg Kg ⁻¹) - 3.57 × 10 ⁻⁶ total Pb (mg Kg ⁻¹) - 1.81 × 10 ⁻⁵ total Ca (mg Kg ⁻¹) + 2.46 × 10 ⁻⁵ total Ti (mg Kg ⁻¹) + 0.023 total Ag (mg Kg ⁻¹) - 0.013 total Se (mg Kg ⁻¹) - 0.014 total Cd (mg Kg ⁻¹)] ^{1/0.23} - 0.37}/0.45 | 0.6 | 28 | P < 0.0001 |
| | SSPC 6; Fe > 24% | TCLP Ba (mg L ⁻¹) = 4.98 - 0.00018 total Ba (mg Kg ⁻¹) - 0.000070 Cr (mg Kg ⁻¹) - 0.000074 total Ca (mg Kg ⁻¹) - 0.000056 total Ti (mg Kg ⁻¹) - 0.039 total Ag (mg Kg ⁻¹) + 0.011 total Se (mg Kg ⁻¹) + 0.033 total Cd (mg Kg ⁻¹) - 0.000086 total As (mg Kg ⁻¹) | 0.6 | 27 | P = 0.1 |
| | SSPC SP 10 | TCLP Ba (mg L ⁻¹) = {[-0.66 - 2.18 × 10 ⁻⁵ total Ba (mg Kg ⁻¹) + 2.63 × 10 ⁻⁶ total Zn (mg Kg ⁻¹) + 3.37 × 10 ⁻⁶ total Fe (mg Kg ⁻¹) + 0.00011 total Pb (mg Kg ⁻¹) - 1.14 × 10 ⁻⁵ total Ca (mg Kg ⁻¹) - 0.0014 total As (mg Kg ⁻¹)] ^{0.5} - 0.14}/0.64 | 0.7 | 20 | P = 0.01 |
| Zn | SSPC 6; Fe ≤ 24% | Zn TCLP (mg L ⁻¹) = 436 + 0.0014 total Zn (mg Kg ⁻¹) - 0.16 total Cr (mg Kg ⁻¹) - 0.011 total Pb (mg Kg ⁻¹) + 0.046 total Ti (mg Kg ⁻¹) - 6.17 total Ag (mg Kg ⁻¹) - 17.1 total Se (mg Kg ⁻¹) + 0.27 total As (mg Kg ⁻¹) | 0.7 | 28 | P < 0.0001 |
| | SSPC 6; Fe > 24% | Zn TCLP (mg L ⁻¹) = 10 ^ [8.65 + 0.864 log total Zn (mg Kg ⁻¹) - 1.58 log total Fe (mg Kg ⁻¹) - 0.653 log total Cr (mg Kg ⁻¹) - 0.347 log total Ca (mg Kg ⁻¹) mean + 0.358 log total Ti (mg Kg ⁻¹) + 0.443 log total Cd (mg Kg ⁻¹)] | 0.6 | 27 | P = 0.001 |
| | SSPC SP 10 | Zn TCLP (mg L ⁻¹) = {[0.40 - 0.00050 total Ba (mg Kg ⁻¹) + 5.27 × 10 ⁻⁵ total Zn (mg Kg ⁻¹) + 4.79 total Ag (mg Kg ⁻¹) - 0.015 total As (mg Kg ⁻¹)] ² + 178.59}/0.70 | 0.7 | 20 | P = 0.001 |



Comparison of predicted and observed leached Pb concentrations.

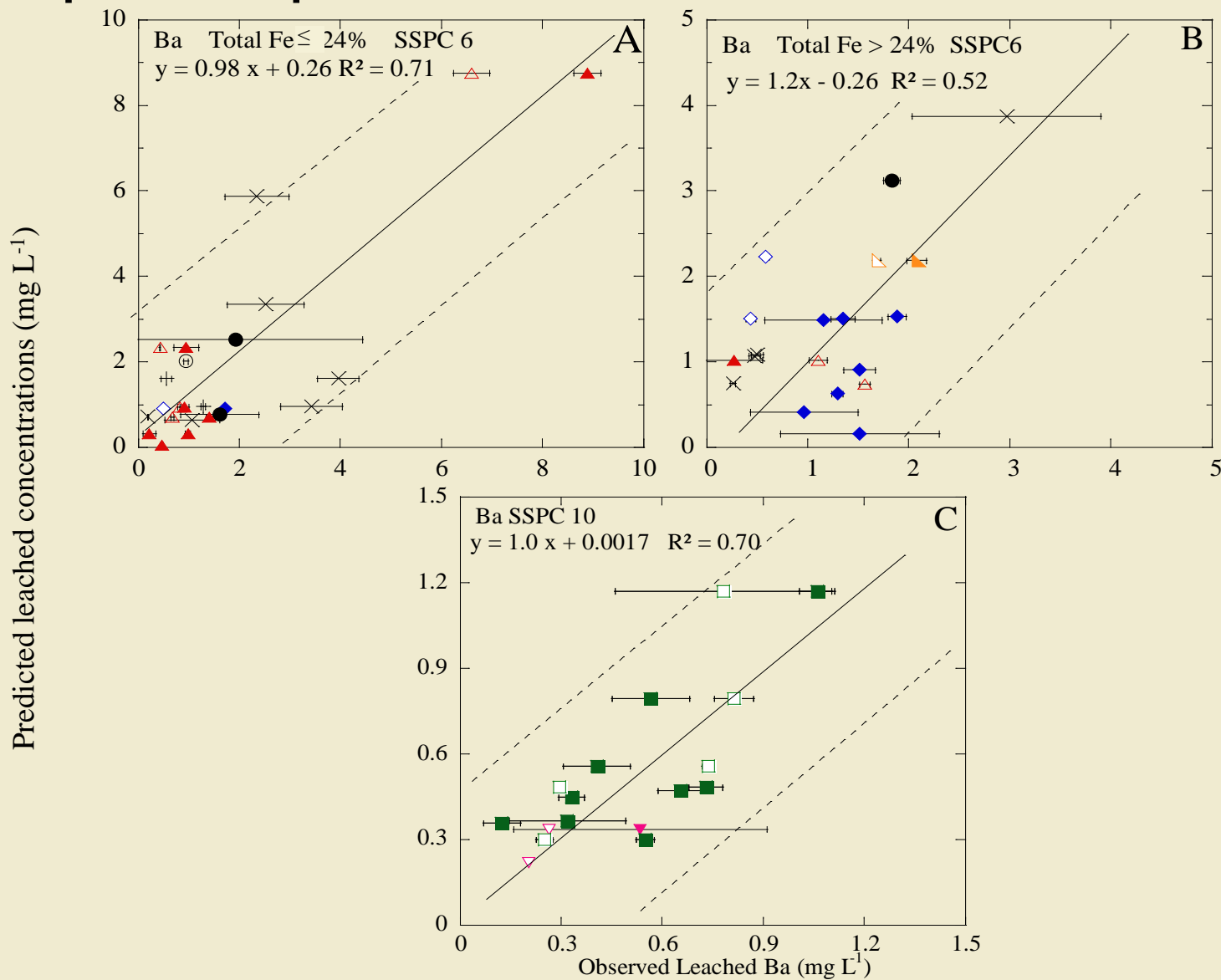
Predicted leached concentrations (mg L⁻¹)



TCLP samples: ▲ Region 1 ▼ Region 2 ◆ Region 3 ■ Region 5 ● Region 7 ▲ Region 10 × Region 11
 MEP samples: ▢ Region 1 ▽ Region 2 ◇ Region 3 □ Region 5 ○ Region 7 △ Region 10 + Region 11



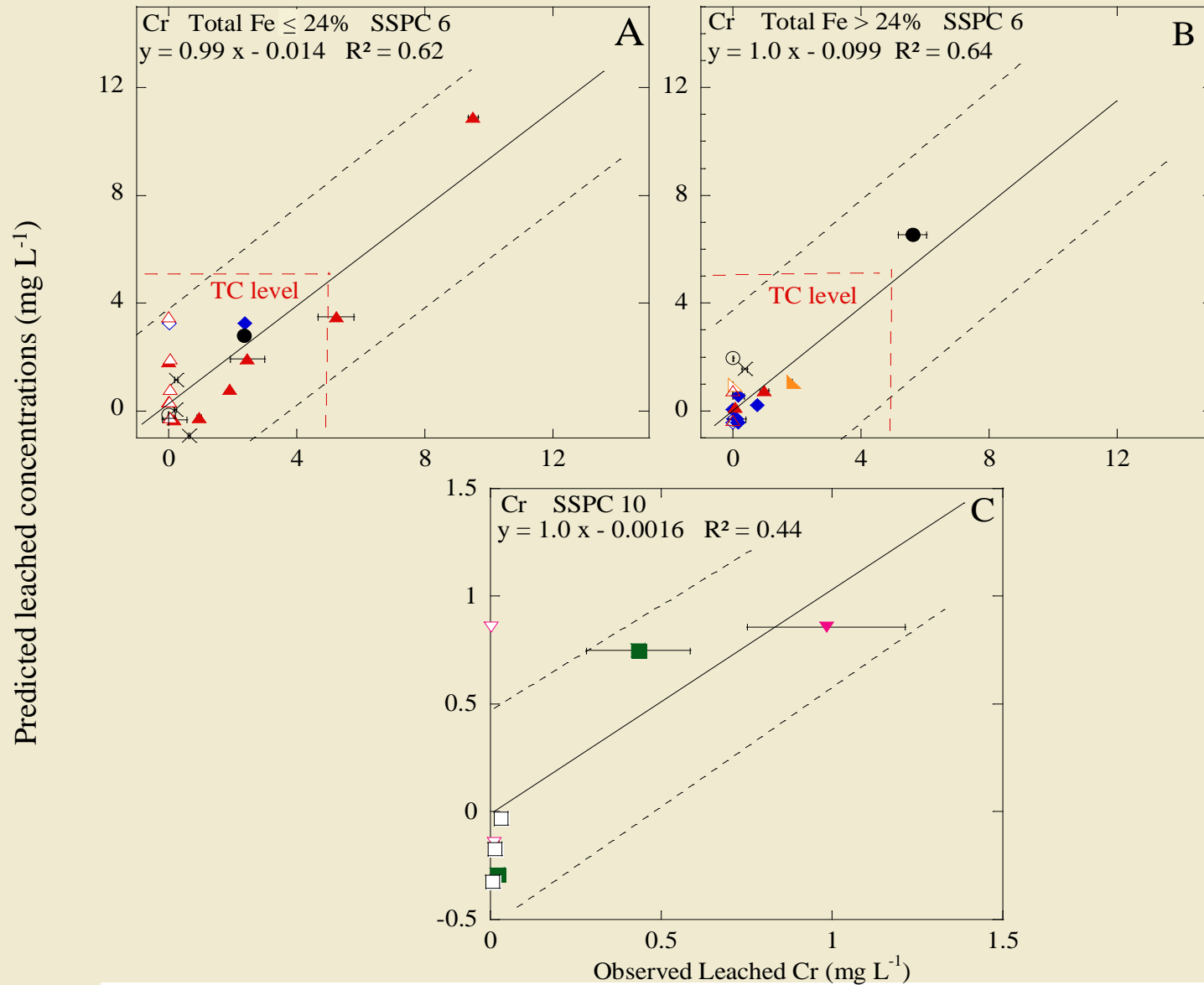
Comparison of predicted and observed leached Ba concentrations.



TCLP samples: ▲ Region 1 ▼ Region 2 ◆ Region 3 ■ Region 5 ● Region 7 ▲ Region 10 × Region 11
MEP samples: ▢ Region 1 ▽ Region 2 ◇ Region 3 □ Region 5 ○ Region 7 △ Region 10 + Region 11



Comparison of predicted and observed leached Cr concentrations.

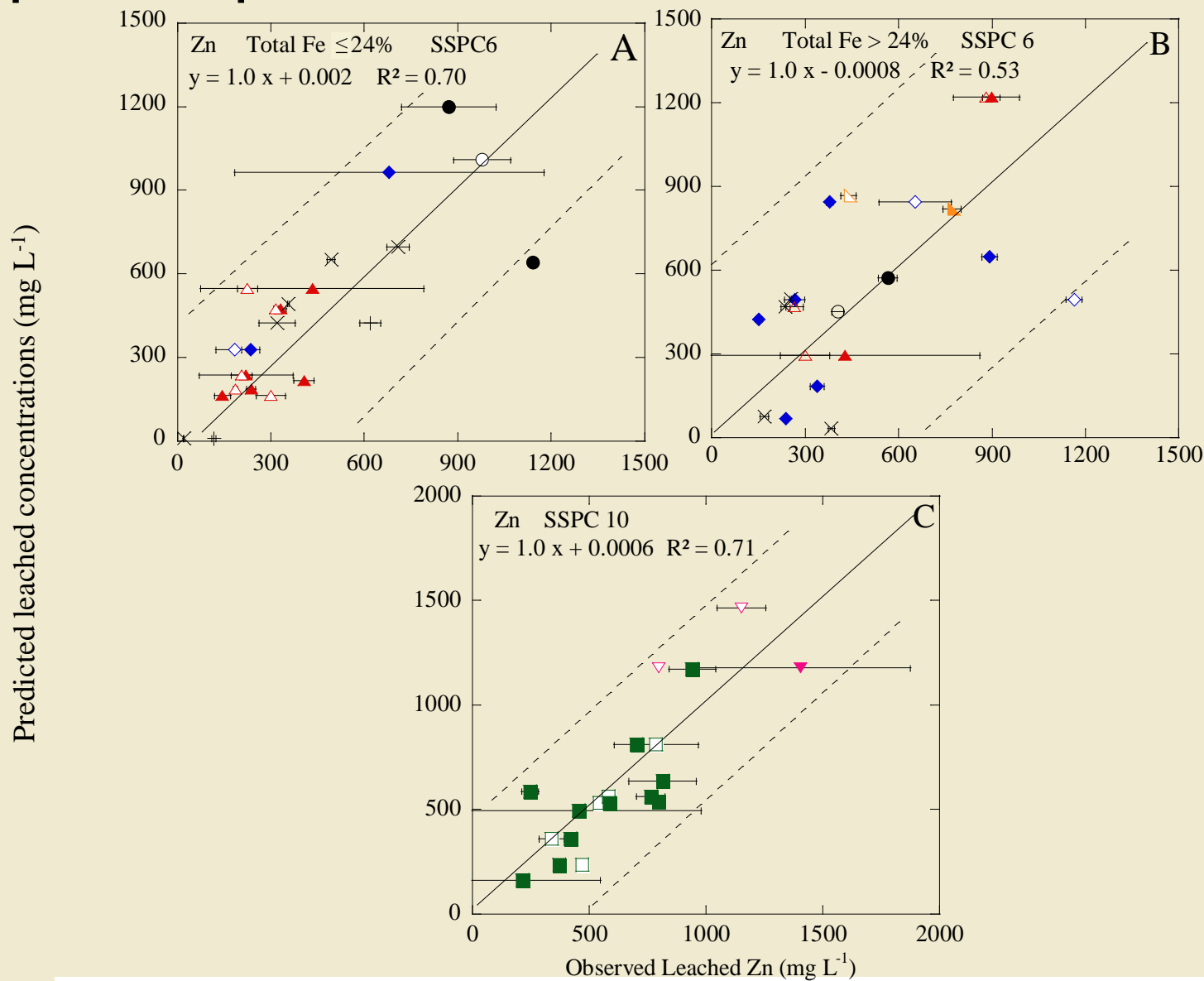


TCLP samples: ▲ Region 1 ▼ Region 2 ◆ Region 3 ■ Region 5 ● Region 7 ▲ Region 10 × Region 11

MEP samples: ◀ Region 1 ▽ Region 2 ◊ Region 3 □ Region 5 ○ Region 7 △ Region 10 + Region 11



Comparison of predicted and observed leached Zn concentrations.



TCLP samples: ▲ Region 1 ▼ Region 2 ◆ Region 3 ■ Region 5 ● Region 7 ▲ Region 10 × Region 11

MEP samples: ◻ Region 1 ▽ Region 2 ◇ Region 3 □ Region 5 ○ Region 7 △ Region 10 + Region 11



Conclusions

- A suite of analyses were applied to develop statistically-based models to predict leaching:
 - Total metals – FP-XRF
 - Mineralogy – XRD
 - Morphology and surface composition – FE-SEM/EDX
 - Metal mobility:
 - TCLP – simulates landfill conditions
 - MEP– simulates 1,000 years of freeze and thaw cycles and prolonged exposure to a leaching medium
 - SEP – identifies phases metals are associated with
 - Modeling
 - Mechanistic – adsorption vs. precipitation
 - PCA – statistically-based leaching model



Conclusions (continued)

- The use of corrosion inhibitors has resulted in elevated concentrations of Pb and Zn on bridge structures and in the paint waste.
- The elevated iron concentrations observed are due to the steel grit applied as a blasting abrasive.
- Although elevated Pb (5 to 168,090 mg kg⁻¹) and other metal concentrations were observed in the paint samples, leached Pb from the TCLP study was only up to 1.46 mg L⁻¹.
- Paint waste with elevated Fe concentrations (and consequent iron oxides) revealed lower metal leaching suggesting trace metals were sequestered through interactions with iron oxide coatings formed on the steel grit surface.



Conclusions (continued)

- MEP results revealed greater lead concentrations (up to 22.6 mg L^{-1}) in the leachate than in the TCLP; five of the 24 bridge paint samples exhibited Pb greater than the TC level of 5 mg L^{-1} .
- This long-term leaching study (MEP) indicated that trace metal sorption (including adsorption and coprecipitation) to the iron oxide surface is likely the mechanism responsible for the reduced leaching observed.
- Through SEP, the greatest fraction of mobilized metals (as great as 15% by wt) was associated with the iron oxide phase.
- XRD and FE-SEM further corroborated the presence of ferrihydrite coatings on the steel grit surface.
- Ferrihydrite, the dominant phase on the steel grit surface, provides abundant binding sites for trace metals. Surface sorption and coprecipitation may lead to structural incorporation of sorbed metals.



Conclusions (continued)

- The statistically-based model indicated that 96 percent of the data falling within the 95% prediction interval for Pb (R^2 0.6 – 0.9, $p \leq 0.01$), Ba (R^2 0.6 – 0.7, $p \leq 0.1$), and Zn (R^2 0.6 – 0.7, $p \leq 0.01$). However, the regression model obtained for Cr leaching is not significant (R^2 0.5 – 0.7, $p \leq 0.75$).
- The paint waste from bridges cleaned with SSPC 10 may be for the most part classified as non-hazardous waste, while 14% of the samples from the bridges blasted using SSPC 6 would be classified as hazardous waste.
- A practical advantage in applying models developed is the ability to estimate contaminant leaching from paint waste without additional laboratory studies including TCLP.



Recommendation

- Because the models developed in this study are based on the collected samples from the 24 bridges in seven regions of NYS, bridge samples collected from other regions are suggested for model validation.



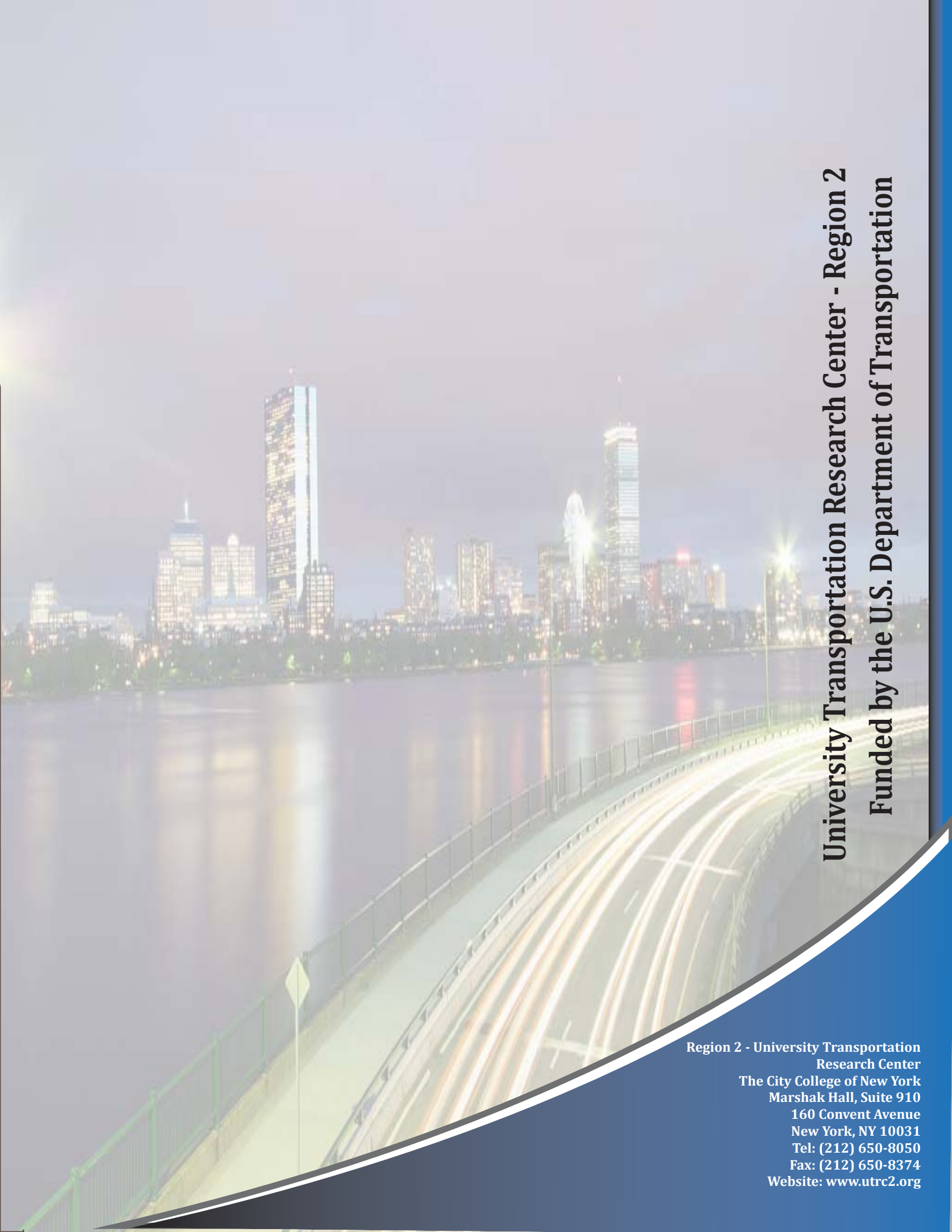
Accomplishments

1. Shu, Z., Axe, L. Jahan, K. Ramanujachary, K. V., Field Methods for Rapidly Characterizing Paint Waste during Bridge Rehabilitation (manuscript in preparation).
2. Shu, Z., Axe, L. Jahan, K. Ramanujachary, K. V., Trace Metal Leaching Mechanisms from Bridge Paint Waste in the Presence of Steel Grit (submitted to Environmental Science and Technology).
3. Shu, Z., Axe, L. Jahan, K. Ramanujachary, K. V., Metal Leaching from the Bridge Paint Waste in the Presence of Steel Grit (submitted to Chemosphere).
4. Shu, Z., Axe, L. Jahan, K. Ramanujachary, K. V., Metal Concentrations and Distribution in Paint Waste Generated during Bridge Rehabilitation in New York State (submitted to Environmental Engineering Science).
5. Shu, Z., Axe, L. Jahan, K. Ramanujachary, K. V., Rapid On-site Waste Characterization Tool for Managing Paint Waste from Bridge Rehabilitation", **New Jersey Department of Transportation (NJDOT) 15th Annual Research Showcase**, West Windsor, New Jersey, October 23, 2013.



Accomplishments (Continued)

6. Shu, Z., Axe, L. Jahan, K. Ramanujachary, K. V., Trace metal leaching from bridge paint waste in the presence of iron oxide surfaces, Division of Colloid and Surface Chemistry, **246th American Chemical Society (ACS) National Meeting**, Indianapolis, Indiana, September 8-12, 2013.
7. Shu, Z., Axe, L. Jahan, K. Ramanujachary, K. V., Leaching Behavior of Lead and Chromium from Bridge Paint Waste in the Presence of Steel Grit, Session of Steel Bridges Committee, **Transportation Research Board 92nd Annual Meeting**, Washington, D.C., January 13-17, 2013.
8. Shu, Z., Axe, L. Jahan, K. Ramanujachary, K. V., Leaching behavior of lead and other metals in the presence of steel grit, Session of Environmental Chemistry of Fe-Oxides and Fe-Hydroxides, **244rd American Chemical Society (ACS) National Meeting**, Philadelphia, Pennsylvania, August 19-23, 2012.
9. Shu, Z., Axe, L. Jahan, K. Ramanujachary, K. V., Field methods for rapidly characterizing paint waste during bridge rehabilitation, Session of Environmental chemistry for a sustainable world, **243rd American Chemical Society (ACS) National Meeting**, San Diego, California, March 25-29, 2012.



University Transportation Research Center - Region 2

Funded by the U.S. Department of Transportation

Region 2 - University Transportation
Research Center
The City College of New York
Marshak Hall, Suite 910
160 Convent Avenue
New York, NY 10031
Tel: (212) 650-8050
Fax: (212) 650-8374
Website: www.utrc2.org